Palaeoecology and Palaeodiet: reconstructing adaptations in the Middle and Late Pleistocene Ursidae through dental microwear and geochemistry

Spyridoula Pappa

Royal Holloway,

University of London

Degree of PhD

Declaration of Authorship

I _____ hereby declare that this thesis and the work presented in it is entirely my own. Where I have consulted the work of others, this is always clearly stated,

Signed:

Date:

Abstract

Large carnivores are of particular relevance to our understanding of the impact of palaeoclimatic changes on the contemporary fauna, since they occupied a wide range of environments and demonstrate contrasting feeding strategies. In this respect, the modern and fossil Ursidae are a remarkably diverse group, characterized by significant differences in dental and cranial morphology between species, reflecting a range of dietary adaptations from hypercarnivory, through various omnivory strategies and into herbivory.

The thesis explores the palaeodietary ecology and physiology of Middle and Late Pleistocene bears, in order to understand ursid dietary flexibility in response to changing environments. The research combines innovative techniques such as dental microwear analysis with geochemical analysis (trace elements and high-resolution Sr/Ca, Ba/Ca and Zn/Ca intra-tooth profiles) via LA-ICP-MS.

The study focuses on Britain and encompasses the cave bear species *Ursus deningeri*, as well as the brown bear, *Ursus arctos*, complemented by study of the cave bear *Ursus ingressus*, from Greece. The study presents a new detailed dental microwear database for modern ursids, establishing a preferred methodology and revealing consistent separation into different parts of dietary ecospace for the eight extant species and also between modern brown bears from different latitudes. The extant database is then applied to British and Greek fossil bear specimens for the first time, in order to shed light on differences between cave bears and brown bears, and contrasting evidence from brown bears from different glacial and interglacials.

The Late Pleistocene site of Tornewton Cave is examined in further detail. A pilot study into the geochemistry of bear teeth, as well as those of other carnivores and herbivores from the site, has revealed potential weaning and hibernation signals in bears, as well as seasonal dietary changes in both bears and some herbivores.

Acknowledgments

I am indebted to my supervisor Danielle Schreve for her continuous support, for the invaluable discussions and her excellent supervision. I would like also to thank her for funding my participation in 74th SVP meeting and my travel costs for my visit in Natural History Museum Berlin. I am also grateful for the support on the chemical analysis of my second supervisors Christina Manning and Matthew Thirlwall. I especially would like to thank Christina Manning for her help and discussions on the chemical data.

Kind thanks to Florent Rivals for being like my supervisor. I was very fortunate to work with him and I had the opportunity to learn the microwear technique under his guidance. I feel honored that he shared his knowledge with me. I enjoyed the discussions we had and made my two visits in Institut Català de Paleoecologia Humana i Evolució Social (IPHES), Tarragona, Spain) a real pleasure. Many thanks in this respect to IPHES institute that kindly provided the hospitality and facilities.

I am also grateful to Royal Holloway University of London (RHUL) and both Geography and Earth Sciences Departments that provided material, room and utilities, as well as to Geography Department that funded this PhD. I would like also to thank many colleagues and friends from both departments who one way or the other helped and supported me during this project. Wolfagang Müller introduced me into the technique of enamel analysis through LA-ICP-MS and provided with literature and important training regarding the chemical analysis. Viola Warter gave me access to IGOR (iolite) and shared with me her experience on using it. Adrian Palmer, Claire Mayers and Neil Holloway helped with the laboratory work. I would like also to thank Ian Candy, Lucy Flower, Melissa Marr, Jenni Sherriff, Paul Lincoln, Jacob Bendle, Rhys Timms, Pierre Schreve and Iñaki Valcarcel for their support and enjoyable discussions.

Many visits of different museums and institutes around Britain and Europe were carried out during the course of this study. I would like to thank all of the staff who assisted me and gave me access to the respective collections and granted loans: Andy Currant (NHMLondon), Pip Brewer (NHML), Emma Bernard (NHML), Zoe Hughes (NHML), Roberto Portela-Miguez (NHML), John Cooper (Brighton Booth Museum),

Eliza Howlett (Oxford University NHM), Juliet Hay(Oxford University NHM), Malgosia Nowak-Kemp (Oxford University NHM), Dennis Parsons (Somerset County Heritage Centre Museum, Taunton), Barry Chandler (Torquay Museum, Devon), Frank Zachos (NHMVienna), Alexander Bibl (NHMV), Celine Bens (NHMParis), Géraldine Veron (NHMP), Christian Funk (NHMBerlin), Gernot Rabeder (Institut für Palaontologie, Universität Wien), Christos Vlachos (AUTHGreece), Evangelia Tsoukala (AUTHG) and Chris Collins (NHML), Efstratia Ververiotou (NHML) who helped with the laboratory work. I would like to thank especially my colleagues in Natural History Museum Pip Brewer and Martha Richter who were of great help during the last four months of my thesis. It is a great honour for me to work with such a great people.

I would like also to thank for invaluable discussions Andy Currant (NHML), Adrian Lister (NHML), Jerry Hooker (NHML), Louise Humphrey (NHML), Doris Nagel (University Vienna), Gernot Rabeder (University Vienna), Martina Pacher (University Vienna), Katherina Bastl (University Vienna), Nina Kowalik (Polish Academy of Science), Katerina Vasileiadou (NHMLesvos Petrified Forest), Evangelos Vlachos (AUTHGreece) and for provided literature I thank Martina Pacher (University Vienna), Nina Kowalik (Polish Academy of Science) and Katerina Chatzopoulou (AUTHGreece). For provided accommodation during my visits I would like to thank my friends Gertrud Benedikt and Alexandros Xafis and my uncle Sakis and my aunt Rosa.

I gratefully acknowledge the support of the Quaternary Research Association for funding travel expenses within Britain with the New Research Workers Award and University of London Grants for PGR Study Costs.

Finally, I would like to express my gratitude to my family. I owe my deepest thanks to my father and mother who they supported me my whole life. I am grateful to my sister, aunt Lena and uncle Panos, they believed in me and cared lovingly for me. I would also like to thank Litsa and Xenofon, they supported and encouraged me continuously. Especially, Xenofon impressed me by being an amassing person and our discussions gave me strength.

Contents

Title	1
Declaration of Authorship	2
Abstract	3
Acknowledgements	4
Contents	6
List of Figures	13
List of Tables	35
Chapter 1. Introduction	46
1.1. Introduction	46
1.2. Aims and Objectives	49
1.2.1. Aims	49
1.2.2. Objectives	49
1.3. Site description and palaeonviromental summary	51
1.4. Mammal teeth: structure and function	62
1.5. Structure of the thesis	66
Chapter 2. The Ursidae: evolution, ecology and extinction	68
2.1. Introduction	68
2.2. Systematics and the early evolution of the Ursidae	68
2.3. The Pleistocene evolution of the Ursidae	76
2.4. Size change, palaeodiet and palaeoecology in Pleistocene brown bear and cave bear species	85
2.4.1. Size change	85
2.4.2. Palaeodiet	86
2.5. Molecular phylogenies of the Ursidae	90
2.6. Quaternary extinctions and the Ursidae	92
2.7. The Ursidae today	94
2.7.1. *Helarctos malayanus Raffles, 1821, sun bear or honey bear*	94
2.7.2. *Melursus ursinus Shaw, 1791, sloth bear*	96
2.7.3.*Tremarctos ornatus F. G. Cuvier, 1825, spectacled or Andean bear*	97
2.7.4. *Ailuropoda melanoleuca David, 1869, giant panda*	99

2.7.5. *Ursus maritimus Phipps, 1774, polar bear* 100
2.7.6. *Ursus americanus Pallas, 1780, American black bear* 102
2.7.7. *Ursus thibetanus Cuvier, 1823, Asian black bear* 104
2.7.8. *Ursus arctos Linnnaeus, 1758, brown bear* 105
2.8. Diets of extant bears 107
Chapter 3. Dental Microwear Analysis – Extant Species 111
3.1. Introduction to Dental Microwear Analysis (DMA) 111
3.2. Literature Review 111
3.2.1. The application of DMA in palaeontology 111
3.2.2. DMA applications in carnivores 117
3.2.3. Applications to the Ursidae 121
3.3. DMA materials and methods 125
3.3.1. Material from extant species 125
3.3.2. DMA methodology 126
3.3.3. Additional DMA approaches – advantages of stereomicroscopy 130
3.3.4. Description of microscopic scars 132
3.3.5. Non-microwear features observed on Ursidae 135
3.3.6. Statistical method used for DMA 139
3.4. Results of the Dental Microwear Analysis from the reference data set of extant Ursidae 140
3.4.1. Results from facet and non-facet surfaces of enamel 140
3.4.2. Results on grinding (talonid) and slicing (trigonid) areas of extant Ursidae based on Bivariate analysis 144
3.4.3. Statistical tests 154
3.4.3.1. Statistical analysis of the grinding area 155
3.4.3.2. Statistical analysis of the slicing area 160
3.4.4. Results of the Principal Component Analysis (PCA) on extant ursid species 165
3.4.4.1. PCA - Results on the grinding (talonid) area of m1s on extant species 166
3.4.4.2. PCA - Results on the slicing (trigonid) area of m1s on extant species 172

3.5. Discussion 175

Chapter 4. Dental Microwear Analysis – Pleistocene Extinct species 182

4.1. Introduction 182

4.2. Material 182

4.3. Results of the Dental Microwear Analysis (DMA) on the extinct Ursidae from Britain 183

4.3.1. Results Dental Microwear Analysis (DMA) from Westbury-sub-Mendip (MIS 13) 183

4.3.1.1. Bivariate Analysis results from Westbury – sub - Mendip (MIS 13) 183

4.3.1.2. Principal Component Analysis (PCA) results from Westbury – sub - Mendip (MIS 13) 186

4.3.2. Results Dental Microwear Analysis (DMA) from Kents Cavern (breccias layer) (early Middle Pleistocene) 188

4.3.2.1. Bivariate Analysis results from Kents Cavern (breccias) (early Middle Pleistocene) 188

4.3.2.2. PCA results from Kents Cavern (breccias) (early Middle Pleistocene) 191

4.3.3. Results Dental Microwear Analysis (DMA) from Grays Thurrock (MIS 9) 193

4.3.3.1.Bivariate Analysis results from Grays Thurrock (MIS 9) 193

4.3.3.2. PCA results from Grays Thurrock (MIS 9) 196

4.3.4. Results Dental Microwear Analysis (DMA) from Tornewton Cave (MIS 5e) 198

4.3.4.1. Bivariate Analysis results from Tornewton Cave (MIS 5e) 198

4.3.4.2. PCA results from Tornewton Cave (MIS 5e) 201

4.3.5. Results Dental Microwear Analysis (DMA) from Banwell Bone Cave (MIS 5a) 203

4.3.5.1. Bivariate Analysis results from Banwell Bone Cave (MIS 5a) 203

4.3.5.2. PCA results from Banwell Bone Cave (MIS 5a) 206

4.3.6. Results Dental Microwear Analysis (DMA) from Kents Cavern 208

(cave earth) (MIS 3)
4.3.6.1. Bivariate Analysis results from Kents Cavern (cave earth) (MIS 3) 208
4.3.6.2. PCA results from Kents Cavern (cave earth) (MIS 3) 211
4.3.7. Results Dental Microwear Analysis (DMA) from Sandford Hill (MIS 3) 213
4.3.7.1. Bivariate Analysis results from Sandford Hill (MIS 3) 213
4.3.7.2. PCA results from Sandford Hill (MIS 3) 216
4.3.8. Results Dental Microwear Analysis (DMA) from Cow Cave (Holocene?) 218
4.3.8.1. Bivariate Analysis results from Cow Cave (Holocene?) 218
4.3.8.2. PCA results from Cow Cave (Holocene?) 221
4.3.9. Statistical tests for all sites from Britain in comparison with extant species 223
4.4. Results on extinct Ursidae from the European mainland: the example of Loutra Arideas Cave (Late Pleistocene) from Greece 229
4.4.1. Dental Microwear Analysis (DMA) results from Loutra Arideas Cave (LAC) 229
4.4.2. PCA results from Loutra Arideas Cave (LAC) 232
4.5. Discussion 234
Chapter 5. Geochemical Analysis 244
5.1. Introduction 244
5.2. Geochemical Analysis Literature Review 245
5.2.1. Tooth histology with emphasis to enamel tissue 246
5.2.1.1. Incremental features of enamel 250
5.2.1.2. Amelogenesis – Enamel formation 251
5.2.2. Sampling strategies 254
5.2.3. Trace elements - Sr/Ca and Ba/Ca ratios in food webs 256
5.2.4. Diagenesis 261
5.3. Ecology and dental development in modern analogue taxa 265
5.3.1. Bears 265
5.3.1.1. Ecology 265

5.3.1.2. Dental Development 265
5.3.1.3. Hibernation 268
5.3.2. *Crocuta crocuta* (Spotted hyaena) Erxlebon, 1777 271
5.3.2.1. Ecology 271
5.3.2.2. Dental Development 275
5.3.3. *Cervus elaphus* (Red deer) 277
5.3.3.1. Ecology 277
5.3.3.2. Dental Development 278
5.3.4. *Equus* (Horse) 280
5.3.4.1. Ecology 280
5.3.4.2. Dental Development 281
5.4. Materials and Methods 283
5.4.1. Case study: Tornewton Cave, Devon, UK 283
5.4.1.1. Site History – stratigraphy and palaeoenviromental summary 283
5.4.1.2. Site geology 289
5.4.1.3. Material 290
5.4.2. Methodology 292
5.4.2.1. Sample preparation 292
5.4.2.2. Analytical methodology 294
5.5. Results of the Geochemical Analyses 299
5.5.1. Precision and accuracy of trace element analysis 299
5.5.2. Results high - resolution of trace element analysis for each species from Tornewton Cave 306
5.5.2.1. Results of *U. arctos* teeth 306
5.5.2.1.1. Element profiles of *U. arctos* samples 306
5.5.2.1.2. Examination of diagenesis on *U. arctos* samples through comparison with modern published data 319
5.5.2.2. Results of *C. crocuta* teeth 321
5.5.2.2.1. Element profiles of *C. crocuta* samples 321
5.5.2.2.2. Examination of diagenesis in *C. crocuta* samples through comparison with modern published data 326

5.5.2.3. Results of *C. elaphus* samples 329
5.5.2.3.1. Element profiles of *C. elaphus* samples 329
5.5.2.3.2. Examination of diagenesis on *C. elaphus* samples through comparison with modern published data 334
5.5.2.4. Results of the *Equus* sample 336
5.5.2.4.1. Element profiles of the *Equus* sample 336
5.5.2.4.2. Examination of diagenesis in the *Equus* sample through comparison with modern published data 339
5.6. Discussion 342
5.6.1. Sr/Ca, Ba/Ca and Zn/Ca ratios of *U. arctos* samples 343
5.6.2. Sr/Ca, Ba/Ca and Zn/Ca ratios of *C. crocuta* samples 351
5.6.3. Sr/Ca, Ba/Ca and Zn/Ca ratios of *C. elaphus* samples 354
5.6.4. Sr/Ca, Ba/Ca and Zn/Ca ratios of *Equus* samples 358
5.6.5. Average Sr/Ca and Ba/Ca in food web from Tornewton Cave 360
Chapter 6. Conclusions 364
6.1. Dental Microwear Analysis method and database of extant bear specimens 365
6.2. Palaeodietary and palaeocological niches of extinct bear species 371
6.3. Palaeodietary and physiological remarks on carnivore and herbivore species from Tornewton Cave 375
6.4. Future work 379
Bibliography 382
Appendices 439
IA. Table 1. Microwear features raw results for extant bear species on the grinding area 439
IA. Table 2. Microwear features raw results for extant bear species on the slicing area 443
IB. Table 1. PCA score results for extant bear species on the grinding area 447
IB. Table 2. PCA score results for extant bear species on the slicing area 450
IC. Table 1. Microwear features raw results for extinct species from Britain and Greece on the grinding area 453
IIA. Geochemical Analysis. LOB values 456

IIB. Geochemical Analysis. Video 1 LA-ICPMS running procedure. CD folder 1.

IIB. Geochemical Analysis. Results for each specimen in excel document. CD folder 2.

List of Figures

Figure 1.1. Maps showing the location of each site including additional information regarding the species of Ursidae present and the stratigraphical position of the studied material where known. The marine oxygen isotope stratigraphy is shown on the left as a climatic yardstick (modified from Walker and Lowe, 2007). 59

Figure 1.2. Detail of the Middle and Late last cold stage, based on the NorthGRIP $\delta^{18}O$ record according to GICC05 (modified from Svensson *et al*. [2008]). 60

Figure 1.3. Tooth structure and components, based on human teeth (modified from Hillson [1986]). 63

Figure 1.4. Structure and orientation in mammalian teeth. A. Cross-section of a first lower molar in a domestic dog (*Canis familiaris*), showing the enamel dentine junction (EDJ) and cement dentine junction (CDJ). B. Orientation terminology for upper and lower teeth of crab-eating macaque (*Macaca fascicularis*) (modified from Ungar [2010]). 65

Figure 1.5. Cheek-tooth form in various mammals. All are upper teeth with both the buccal view (left) and occlusal view (right). A. Secodont (shearing) carnassials of lion (*Panthera leo*). B. Plagiaulacoid (blade-like) molar of musky rat kangaroo (*Hypsiprymnodon moschatus*). C. Bilophodont (two-lophed) molar of Malayan tapir (*Tapirus indicus*). D. Bunodont (low, rounded) molar of babirusa (*Babyrousa babyroussa*), showing the position of the four key cusps. E. Ptychodont (folded) molar of North American beaver (*Castor canadensis*). F. Selenodont (crescent-shaped lophs) molar of cow (*Bos taurus*). 66

Figure 2.1. Schematic reconstruction of the evolutionary history of the cave, brown and black bear lineages (after Kurtén [1969]). 75

Figure 2.2. Left: Comparison of skulls of extant brown bear *U. arctos* (NHM UK Life Sciences department registered number: 52.1575) (A) and cave bear *U. spelaeus* from Petralona (specimen from AUTh registered number PEC 1000) (photo modified from Baryshnikov and Tsoukala [2010]). Right: Icons representing brown bear and cave bear specimens in this study. Several distinctive characteristics can be observed on the cave bear skull, including its large size, the extended diastema between canines and cheek teeth, the curve of the mandibular ramus, the doming of the forehead and the retraction of the nasal bridge. 83

Figure 2.3. A. Map showing the Late Pleistocene geographical distribution of cave bear *U. spelaeus* (modified from Kahlke [1994]). B. Map showing European sites where *U. spelaeus* and *U. ingressus* remains have been identified (modified from Baca *et al*. [2014]). 84

Figure 2.4. $\delta^{13}C$ and $\delta^{15}N$ values of brown bears. Left: In eastern Beringia before and after the extinction of the giant short-faced bear. Right: In Europe before and after the extinction of cave bears (after Bocherens [2015] and references therein). 89

Figure 2.5. Phylogeny of extant and fossil bears (modified from Kraus *et al*. [2008] with an update of polar bear origination from Miller *et al*. [2012]) (extant species photos modified from Wikipedia). 91

Figure 2.6. Summary information for *H. malayanus* including geographical distribution (map from Fredriksson *et al*. [2008]), the skull and mandible (lateral view) and additional biological details. 95

Figure 2.7. Summary information for *M. ursinus* including geographical distribution (map from Gashelis *et al*. [2008b]), the skull and 97

mandible (lateral view) and additional biological details.

Figure 2.8. Summary information for *T. ornatus* including geographical distribution (map from Goldstein *et al.* [2008]), the skull and mandible (lateral view) and additional biological details. 98

Figure 2.9. Summary information for *A. melanoleuca* including geographical distribution (map from Lü *et al*. [2008]), the skull and mandible (lateral view) and additional biological details. 100

Figure 2.10. Summary information for *U. maritimus* including geographical distribution (map from Wiig *et al*. [2015]), the skull and mandible (lateral view) and additional biological details. 102

Figure 2.11. Summary information for *U. americanus* including geographical distribution (map from Garshelis *et al*. [2008a]), the skull and mandible (lateral view) and additional biological details. 103

Figure 2.12. Summary information for *U. thibetanus* including geographical distribution (map from Garshelis and Steinmetz [2008]), the skull and mandible (lateral view) and additional biological details. 105

Figure 2.13. Summary information for *U. arctos* including geographical distribution (map from McLellan *et al*. [2008]), the skull and mandible (lateral view) and additional biological details. 107

Figure 3.1. **A**: *U. arctos* reconstruction. **B**: Example of extant *U. arctos* skull and mandibles (specimen from NHM London,registered number: NHM 52.1575. **C**: Tooth morphology of first lower carnassials (m1), including areas indicated on the buccal side on which observations were focused for the microwear analysis. 127

Figure 3.2. Dental Microwear Analysis moulding and casting procedure. **A**. Selection of tooth samples from the collections. **B**. Cleaning process of teeth surface with acetone and then with 96%

alcohol. **C.** Silicon applicator gun used to mould teeth using high-resolution silicone. **D.** Teeth of a bear skull covered with silicone. **E.** Lab putty. **F.** Bear teeth covered with putty. **G.** Final silicone mould (negative part). **H.** Filling procedure with clear epoxy resin in the laboratory. **I.** Final resin cast (positive part). 129

Figure 3.3. Dental Microwear Analysis. Stereolight microscope. **A**. Zeiss Stemi 2000C stereomicroscope used in Spain (IPHES). **B**. An ocular reticle with a square area of 0.16 mm^2 used in the quantification of the microwear features. 130

Figure 3.4. Microwear features observed on m1 samples (buccal side of hypoconid) under stereolight-microscope with x35 magnification including all the different features observed on bear samples (small pits, large pits, gouges, puncture pits, fine scratches, coarse scratches, hypercoarse scratches, cross-scratches). 134

Figure 3.5. Dental Microwear Analysis. Non-microwear features observed on bear teeth (together with one example of wolverine). A. Fresh scratches. B. Fresh scratches and resin bubble. C. Wave like pattern. D1. Wave like pattern along the cusp. D2. Schematic drawing of Hunter-Schreger bands (HSB) (image modified from Stefen [2001]). E - G. Wave pattern starting from the tip of the cusp. 137

Figure 3.6. Dental Microwear Analysis. Non-microwear features observed on samples of the Ursidae. **A - C.** Exaggerated morphology on the buccal side of teeth from the cave bear group. 138

Figure 3.7. Photomicrographs of specimens at x25 magnification with facet and non-facet enamel surfaces. **A.** *U. maritimus* from Greenland (NHM Vienna: 14657); **B.** *U. deningeri* from Westbury-sub-Mendip (MIS 13) (NHM London: M92445). 141

Figure 3.8. Comparison of total number of scratches and pits between observations on **facet** and **non-facet** enamel surfaces on the grinding (talonid) area of m1s in extant *U. maritimus* and extinct *U. deningeri*. **Graph A**: *U. maritimus* comparison of total number of **scratches** on facet and non-facet surfaces. **Graph B**: *U. maritimus* comparison of total number of **pits** on facet and non-facet surfaces. **Graph C**: *U. deningeri* comparison of total number of **scratches** on facet and non-facet surfaces**. Graph D**: *U. deningeri* comparison of total number of **pits** on facet and non-facet surfaces. 142

Figure 3.9. Extant species plot of raw data of total number of pits versus scratches. **A.** Analysis on grinding (talonid) area. **B.** Analysis on slicing (trigonid) area. (For the total number of each species, see table 3.2). 147

Figure 3.10. Plot of raw data for extant species of the total number of large versus small pits. **A.** Analysis on grinding (talonid) area. **B.** Analysis on slicing (trigonid) area. For the total number of each species, see table 3.2. 150

Figure 3.11. Bivariate plot for extant species based on microwear signatures (average number of pits versus scratches). Error bars represent the standard deviation of pits and scratches. **A.** Analysis on grinding (talonid) area. **B.** Analysis on slicing (trigonid) area. For the total number of each species please see table 3.2. 152

Figure 3.12. Box and whisker plot showing the values for pits from each extant species. The boxes represent 25^{th} – 75^{th} percentiles, the medians (black lines) and the whiskers show maximum and minimum values. 154

Figure 3.13. PCA plots for extant bear species on the **grinding** (talonid) area. **A**. Graph component 1 versus 2. **B.** Graph component 1 versus

3. For details of symbols, see key. Symbols of Variables as follow: NS: number of scratches; NP: number of pits; NfineS: number of fine scratches; NcoarseS: number of coarse scratches; NLP: number of large pits; NsP: number of small pits; Ngouge: number of gouges; Npp: number of puncture pits; SWS: score of wide scratches. 170

Figure 3.14. Photomicrographs of extant bear species' tooth enamel on the **grinding** (talonid) area at 35 times magnification. **A**. *A. melanoleuca*, **B.** *U. maritimus*, **C.** *H. malayanus*, **D.** *U. americanus*, **E.** *M. ursinus* and **F.** *U. thibetanus*. 171

Figure 3.15. Photomicrographs of *U. arctos* (from different geographical regions) tooth enamel on the grinding (talonid) area at 35 times magnification. **A**. *U. arctos,* Kamchatka, Russia; **B.** *U. arctos,* Slovakia, central Europe and **C.** *U. arctos,* Finland, Northern Europe. 172

Figure 3.16. PCA plots for extant bear species on the **slicing** (trigonid) area. **A**. Graph component 1 versus 2. **B.** Graph component 1 versus 3. For details of symbols, see key. Symbols of Variables as follow: NS: number of scratches; NP: number of pits; NfineS: number of fine scratches; NcoarseS: number of coarse scratches; NLP: number of large pits; NsP: number of small pits; Ngouge: number of gouges; Npp: number of puncture pits; SWS: scratches width score. 174

Figure 4.1. Bivariate diagrams for bears from Westbury-sub-Mendip (MIS 13), UK, in comparison with the extant bear microwear database. **A.** Plot of average number of pits versus scratches. Error bars represent the standard deviation of pits and scratches. **B.** Plot of raw data of the total number of large versus small pits. 185

Figure 4.2. PCA plots for Westbury-sub-Mendip (MIS 13), UK in comparison with extant bear species. **A**. Graph component 1 versus 2. **B.** Graph component 1 versus 3. The shaded polygon indicates the position of the specimens from Westbury-sub-Mendip. For details of symbols, see key. Symbols of variables as follows: NS: number of scratches; NP: number of pits; NfineS: number of fine scratches; NcoarseS: number of coarse scratches; NLP: number of large pits; NsP: number of small pits; Ngouge: number of gouges; Npp: number of puncture pits; SWS: scratches width score. 187

Figure 4.3. Bivariate diagrams for bears from Kents Cavern (breccias) (early Middle Pleistocene), UK, in comparison with extant bear database. **A.** Plot of average number of pits versus scratches. Error bars represent the standard deviation of pits and scratches. **B.** Plot of raw data of the total number of large versus small pits. 190

Figure 4.4. PCA plots for Kents Cavern (breccias) (early Middle Pleistocene), UK, in comparison with extant bear species. **A**. Graph component 1 versus 2. The shaded polygon indicates the position of the specimens from Kents Cavern (breccias). **B.** Graph component 1 versus 3. For details of symbols, see key. Symbols of Variable as follows: NS: number of scratches; NP: number of pits; NfineS: number of fine scratches; NcoarseS: number of coarse scratches; NLP: number of large pits; NsP: number of small pits; Ngouge: number of gouges; Npp: number of puncture pits; SWS: scratches width score. 192

Figure 4.5. Bivariate diagrams for bears from Grays Thurrock (MIS 9), UK in comparison with the extant bear database. **A.** Plot of average number of pits versus scratches. Error bars represent the standard deviation of pits and scratches. **B.** Plot of raw data of

the total number of large versus small pits. 195

Figure 4.6. PCA plots for Grays Thurrock (MIS 9), UK, in comparison with extant bear species. **A**. Graph component 1 versus 2. The shaded polygon indicates the position of the specimens from Grays Thurrock. **B.** Graph component 1 versus 3. For details of symbols, see key. Symbols of Variable as follows: NS: number of scratches; NP: number of pits; NfineS: number of fine scratches; NcoarseS: number of coarse scratches; NLP: number of large pits; NsP: number of small pits; Ngouge: number of gouges; Npp: number of puncture pits; SWS: scratches width score. 197

Figure 4.7. Bivariate diagrams for bears from Tornewton Cave (MIS 5e), UK, in comparison with the extant bear database. **A.** Plot of average number of pits versus scratches. Error bars represent the standard deviation of pits and scratches. **B.** Plot of raw data of the total number of large versus small pits. 200

Figure 4.8. PCA plots for Tornewton Cave (MIS 5e), UK, in comparison with extant bear species. **A**. Graph component 1 versus 2. The shaded polygon indicates the position of the specimens from Tornewton Cave. **B.** Graph component 1 versus 3. For details of symbols, see key. Symbols of Variable as follows: NS: number of scratches; NP: number of pits; NfineS: number of fine scratches; NcoarseS: number of coarse scratches; NLP: number of large pits; NsP: number of small pits; Ngouge: number of gouges; Npp: number of puncture pits; SWS: scratches width score. 202

Figure 4.9. Bivariate diagrams for bears from Banwell Bone Cave (MIS 5a), UK, in comparison with the extant bear database. **A.** Plot of average number of pits versus scratches. Error bars represent the standard deviation of pits and scratches. **B.** Plot of raw data of the total number of large versus small pits. 205

Figure 4.10. PCA plots for Banwell Bone Cave (MIS 5a), UK, in comparison with extant bear species. **A**. Graph component 1 versus 2. The shaded polygon indicates the position of the specimens from Banwell Bone Cave. **B.** Graph component 1 versus 3. For details of symbols, see key. Symbols of Variable as follows: NS: number of scratches; NP: number of pits; NfineS: number of fine scratches; NcoarseS: number of coarse scratches; NLP: number of large pits; NsP: number of small pits; Ngouge: number of gouges; Npp: number of puncture pits; SWS: scratches width score. 207

Figure 4.11. Bivariate diagrams for bears from Kents Cavern (cave earth) (MIS 3), UK, in comparison with the extant bear database. **A.** Plot of average number of pits versus scratches. Error bars represent the standard deviation of pits and scratches. **B.** Plot of raw data of the total number of large versus small pits. 210

Figure 4.12. PCA plots for Kents Cavern (MIS 3), UK, in comparison with extant bear species. **A**. Graph component 1 versus 2. The shaded polygon indicates the position of the specimens from Kents Cavern (cave earth). **B.** Graph component 1 versus 3. For details of symbols, see key. Symbols of Variable as follows: NS: number of scratches; NP: number of pits; NfineS: number of fine scratches; NcoarseS: number of coarse scratches; NLP: number of large pits; NsP: number of small pits; Ngouge: number of gouges; Npp: number of puncture pits; SWS: scratches width score. 212

Figure 4.13. Bivariate diagrams for bears from Sandford (MIS 3), UK, in comparison with extant bear database. **A.** Plot of average number of pits versus scratches. Error bars represent the standard deviation of pits and scratches. **B.** Plot of raw data of

the total number of large versus small pits. 215

Figure 4.14. PCA plots for Sandford Hill (MIS 3), UK, in comparison with extant bear species. **A**. Graph component 1 versus 2. The shaded polygon indicates the position of the specimens from Sandford Hill. **B.** Graph component 1 versus 3. For details of symbols, see key. Symbols of Variable as follows: NS: number of scratches; NP: number of pits; NfineS: number of fine scratches; NcoarseS: number of coarse scratches; NLP: number of large pits; NsP: number of small pits; Ngouge: number of gouges; Npp: number of puncture pits; SWS: scratches width score. 217

Figure 4.15. Bivariate diagrams for bears from Cow Cave (Holocene?), UK, in comparison with the extant bear database. **A.** Plot of average number of pits versus scratches. Error bars represent the standard deviation of pits and scratches. **B.** Plot of raw data of the total number of large versus small pits. 220

Figure 4.16. PCA plots for Cow Cave (Holocene?), UK, in comparison with extant bear species. **A**. Graph component 1 versus 2. The shaded polygon indicates the position of the specimens from Cow Cave. **B.** Graph component 1 versus 3. Details of symbols see key. Symbols of Variable as follows: NS: number of scratches; NP: number of pits; NfineS: number of fine scratches; NcoarseS: number of coarse scratches; NLP: number of large pits; NsP: number of small pits; Ngouge: number of gouges; Npp: number of puncture pits; SWS: scratches width score. 222

Figure 4.17. Bivariate diagrams for bears from Loutra Arideas Cave (LAC) (Late Pleistocene), Greece, in comparison with the extant bear database. **A.** Plot of average number of pits versus scratches. Error bars represent the standard deviation of pits and scratches. **B.** Plot of raw data of the total number of large versus

small pits. 231

Figure 4.18. PCA plots for Loutra Arideas Cave (LAC) (Late Pleistocene), Greece, in comparison with extant bear species. **A**. Graph component 1 versus 2. The shaded polygon indicates the position of the specimens from Loutra Arideas Cave. **B.** Graph component 1 versus 3. Details of symbols see key. Symbols of Variable as follows: NS: number of scratches; NP: number of pits; NfineS: number of fine scratches; NcoarseS: number of coarse scratches; NLP: number of large pits; NsP: number of small pits; Ngouge: number of gouges; Npp: number of puncture pits; SWS: scratches width score. 233

Figure 4.19. Photomicrographs of extinct bear species tooth enamel on grinding (talonid) area at 35 times magnification. **A.** *U. deningeri* from Westbury-sub-Mendip (MIS 13). **B.** *U. deningeri* from Kents Cavern (breccias) (early Middle Pleistocene). **C.** *U. arctos* from Grays Thurrock (MIS 9). **D.** *U. arctos* from Tornewton Cave (MIS 5e). **E.** *U. arctos* from Banwell Bone Cave (MIS 5a). **F.** *U. arctos* from Kents Cavern (Cave earth) (MIS 3). **G.** *U. arctos* from Sandford Hill (MIS 3). 242

Figure 5.1. The components and elements of dentine and enamel and their potential applications (from Smith and Tafforeau, 2008). 246

Figure 5.2. The composition by weight % of water, organic material and mineral for bone, dentine and enamel in humans (from Pasteris *et al*. [2008]). 247

Figure 5.3. Three contrasting enamel prism patterns (after Hillson [1986]). 248

Figure 5.4. SEM micrographs showing enamel prisms for different species. **A.** *Canis lupus familiaris*. **B.** *Otaria bryonia*. **C.** *Ursus arctos* (image modified from Stefen [1997]). 249

Figure 5.5. Cross-sectioned molar of chimpanzee showing incremental features in enamel. **A.** Long time periods, reflected by Retzius lines, are shown by white arrows. Diurnal cross-striations are shown in the white bracket. **B.** Blue dotted lines illustrate the perikymata of the outer layer of enamel. **C.** Molar section with enamel features under transmitted light microscopy (image modified from Smith and Tafforeau [2008]). 251

Figure 5.6. A mammalian ameloblast. **Left:** the secretory stage. **Right:** Ruffle-ended, maturation stage ameloblasts (images modified from Moss-Salentijn *et al*. [1997]). 252

Figure 5.7. High resolution microtomographic figures showing enamel mineralisation and microstructure on a third lower molar fragment of *Rhinoceros sondaicus*. Mineral density ($g_{HA}cm^{-3}$) of enamel in cross section (red shows the densest and blue the least dense enamel) (from Tafforeau *et al*. [2007]). 254

Figure 5.8. Schematic reconstruction of the *intra*-tooth sampling method. Horizontal samples were taken from the enamel cusp to the cervix of tooth (image from Balasse [2002]). 255

Figure 5.9. Trophic pyramid with respect to deposition of Sr by percentage of retention at each level (data from Radosevich [1993] and image from Odum and Barrett [2005]). 257

Figure 5.10. Trace element discrimination study of a terrestrial grazing ecosystem in North America. The plant-vole-marten curves illustrate the reduction in Sr/Ca and Ba/Ca at each stage of the trophic pyramid (from Elias *et al.* [1982]). 257

Figure 5.11. Fossil primate tooth images with monochromatic absorption synchrotron micro-CT showing examples of diagenetic patterns. **A.** Modern human tooth with normal (homogenous) tissue. **B.** Pleistocene human tooth demonstrating slight tissue

heterogeneity. **C.** Miocene hominoid tooth (slight heterogeneity). **D.** Miocene hominoid tooth with good preservation of enamel but poor preservation of dentine. **E.** Eocene primate with inverse contrast between tissues. **F.** Pleistocene hominin tooth with strong alteration of both enamel and dentine. **G.** Same tooth as F with moderate contrast of tissues. **H.** Miocene hominoid with de-mineralised enamel. **I.** Eocene primate with no tissue contrast and metallic oxides (image and information from Smith and Tafforeau [2008]). 264

Figure 5.12. *Ursus arctos* dentition (NHM, London, Life Sciences collections 1851.10.27.1). Top: Upper left side dentition with near complete dentition (missing 2nd and 3rd premolars). Below: Lower right side with complete dentition. Upper case denotes upper teeth, lower case denotes lower teeth. ^{s} denotes superior (upper), ^{i} denotes inferior (lower). 266

Figure 5.13. Cranium and mandible of a four month old individual of *Ursus arctos* from the Pyrenees. The upper image shows an X-ray photograph of the cranium, deciduous and partially-erupted permanent dentition and the lower image present a schematic illustration (modified after Debeljak [1996]). 267

Figure 5.14. Systematics and geographic distribution, biology and body size in *Crocuta crocuta*. Image from http://images.fineartamerica.com/images-medium-large/spotted-hyena-crocuta-crocuta-portrait-pete-oxford.jpg 273

Figure 5.15. Cranium and mandible of spotted hyaena **A**. Lateral view (left side) of cranium and mandible ramus. **B.** Ventral view of cranium. **C.** Dorsal view of cranium. Scale 10cm (image modified from Pales and Lambert [1971]). 274

Figure 5.16. Systematics and geographic distribution, biology and body size

in *Cervus elaphus*. Image from http://fc04.deviantart.net/fs23/f/2007/339/9/d/Red_Deer___Stock_by_Sassy_Stock.jpg 278

Figure 5.17. Systematics and geographic distribution, biology and body size in *Equus przewalskii*. Image from http://animaldiversity.org/accounts/Equus_caballus_przewalskii/pictures/ 281

Figure 5.18. **A.** Permanent and deciduous right upper dentition (after Hillson [1986]). **B.** Timing and sequence of tooth eruption and mineralization (modified from Hillson [1986]; Bryant *et al*. [1996b]). 282

Figure 5.19. Tornewton Cave top: plan of the cave and below: projected elevation of the cave (after Proctor [1994]). 284

Figure 5.20. Tornewton Cave stratigraphical profile with dates where available (modified from Sutcliffe and Zeuner [1962]) (see also table 5.6 and 5.7 and text for supplementary information). 286

Figure 5.21. Map with Tornewton Cave and additional geological map (simplified) (A) for Devon and Cornwall (after Charman and Newnham [1996]). 289

Figure 5.22. Photographs of the teeth from Tornewton Cave that were sampled by LA-ICP-MS (see also table 5.8 for supplementary information). 292

Figure 5.23. Specimen preparation for the LA-ICP-MS (see also text for supplementary information). 294

Figure 5.24. Photo of laser ablation unit A. (ICP-MS not shown) showing photograph B. and schematic C. details of Laurin two-volume laser–ablation cell (modified from Müller *et al*. [2009]). D. Details of sample holder showing sample (M41530, *C. elaphus*,

m2)), NIST 610 and 612 and STDP3-5, STDP3-150 and STDP3-1500 (see also text for supplementary information and appendix IIB folder 1 video 1 showing an example of the running procedure). 296

Figure 5.25. Accuracy of the ICP-MS demonstrated through average values of all element concentrations included in the **STDP3-1500** phosphate glass across different days and times of analysis, compared to average published values of elements from Klemme *et al*. (2008). 301

Figure 5.26. Accuracy of the ICP-MS demonstrated through average values of all element concentrations included in the **STDP3-150** phosphate glass across different days and times of analysis, compared to average published values of elements from Klemme *et al*. (2008). 302

Figure 5.27. Accuracy of the ICP-MS demonstrated through average values of all element concentrations included in the **STDP3-5** phosphate glass across different days and times of analysis, compared to average published values of elements from Klemme *et al*. (2008). 303

Figure 5.28. Representative laser ablation tracks marked with green or blue lines on each of three bear tooth samples from Tornewton Cave (NHM specimens). The start and end of each profile are located close to the EDJ. 307

Figure 5.29. **Sr, Ba** and **Zn** concentrations (in ppm) from laser ablation profiles in Tornewton Cave bear samples, shown against distance (in mm) down the profile. 0 on the X –axis marks the oldest enamel and the starting point for analysis. 311

Figure 5.30. **Mg** and **U** concentrations (in ppm) from laser ablation profiles in Tornewton Cave bear samples, shown against distance (in mm)

down the profile. 0 on the X –axis marks the oldest enamel and the starting point for analysis. 313

Figure 5.31. **Al**, **U**, **Mn**, **Pb** and **REE** concentrations (in ppm) from laser ablation profiles of M 40750 (A1 & A2), M 92414 (B1 & B2), M 92417 (C1 & C2) and M 41097 (D1 & D2) bear teeth from Tornewton Cave, shown against the distance (in mm) down the profile. 0 on the X –axis marks the oldest enamel and the starting point for analysis. Sectioned teeth and laser ablation tracks are also shown. 316

Figure 5.32. **Al**, **U**, **Mn**, **Pb** and **REE** concentrations (in ppm) from laser ablation profiles of M 41397 (A1 & A2), M 41389 (B1 & B2), M 40646 (C1 & C2) and M 40688 (D1 & D2) bear teeth from Tornewton Cave, shown against distance (in mm) down the profile. 0 on the X –axis marks the oldest enamel and the starting point for analysis. Sectioned teeth and laser ablation tracks are also shown. 318

Figure 5.33. Box plots showing **Ce, Nd** (top) and **U** (below) concentrations (in ppm) data for bear samples from Tornewton Cave in comparison with concentrations reported for extant black bear teeth (1st box plot on each graph) (Kohn *et al*., 2013). The pink rectangles represent concentration ranges reported on modern enamel (Kohn *et al*., 1999). The boxes represent 1st and 3nd quartiles, the medians (horizontal line), averages are represented by diamonds and the whiskers show the 90th and 10th percentiles. 320

Figure 5.34. Box plots showing **Al** (top) and **Mn** (below) concentrations (in ppm) data for each bear sample from Tornewton Cave in comparison with concentrations reported for extant black bear teeth (1st box plot on each graph) (Kohn *et al*., 2013). The pink

rectangles represent concentration ranges reported on modern enamel (Kohn *et al*., 1999). The boxes represent 1st and 3nd quartiles, the medians (horizontal line), averages are represented by diamonds and the whiskers show the 90th and 10th percentiles. 321

Figure 5.35. Laser ablation tracks marked with blue lines on each hyaena tooth sampled from Tornewton Cave (NHM specimens). The start and end of each profile are located close to the EDJ. 322

Figure 5.36. **Sr**, **Ba**, **Zn** (A.1 & B.1); **Mg** and **U** (A.2 & B.2); **Al**, **U**, **Mn**, **Pb** (A.3 & B.3) and **REE** (A.4 & B.4) concentrations (in ppm) from laser ablation profiles of M92410 (A1 - A4) and M38994 (B1 – B4) hyaena teeth from Tornewton Cave, shown against distance (in mm) down the profile. 0 on the X –axis marks the oldest enamel and the starting point for analysis. Sectioned teeth and laser ablation tracks are also shown. 325

Figure 5.37. Box plots showing **Ce, Nd** (top) and **U** (below) concentrations (in ppm) for each hyaena sample from Tornewton Cave in comparison with concentrations reported for extant carnivore teeth (1st box plot on each graph) (Kohn *et al*., 2013). The pink rectangles represent concentration ranges reported on modern enamel (Kohn *et al*., 1999). The boxes represent 1st and 3nd quartiles, the medians (horizontal line), averages are represented by diamonds and the whiskers show the 90th and 10th percentiles. 327

Figure 5.38. Box plots showing **Al** (top) and **Mn** (below) concentrations (in ppm) for each hyaena sample from Tornewton Cave in comparison with concentrations reported on carnivore teeth (1st box plot on each graph) (Kohn *et al*., 2013). The pink rectangles represent concentration ranges reported on modern enamel

(Kohn *et al*., 1999). The boxes represent 1st and 3nd quartiles, the medians (horizontal line), averages are represented by diamonds and the whiskers show the 90th and 10th percentiles. 328

Figure 5.39. Laser ablation tracks marked with blue lines on each of three red dear tooth samples from Tornewton Cave (NHM specimens). The start and end of each profile are located close to the EDJ. In m1 (A), part of the enamel at the end of the profile was covered with resin, thus this profile is expected to be shorter than the other two teeth (m2 and m3, B and C respectively). 329

Figure 5.40. **Ba**, **Zn** (A.1, B.1 & C.1); **Al**, **U**, **Mn**, **Pb** (A.2, B.2 &C.2) and **REE** (A.3, B.3 & C.3) concentrations (in ppm) from laser ablation profiles of M 41530 m1 (A.1 – A.3), M41530 m2 (B.1 – B.3) and M41530 m3 (C.1 – C.3) red deer teeth from Tornewton Cave, shown against distance (in mm) down the profile. 0 on the X – axis marks the oldest enamel and the starting point for analysis. Sectioned teeth and laser ablation tracks are also shown. 332

Figure 5.41. **Mg** and **U** (A.1, B.1 & C.1) concentrations (in ppm) from laser ablation profiles of red deer teeth from Tornewton Cave, shown against distance (in mm) down the profile. 0 on the X –axis marks the oldest enamel and the starting point for analysis. 333

Figure 5.42. Box plots showing **Ce, Nd** (top) and **U** (below) concentrations (in ppm) data of each red deer tooth from Tornewton Cave in comparison with concentrations reported on extant herbivore teeth (1st box plot on each graph) (Kohn *et al*., 2013). The pink rectangles represent concentration ranges reported on modern enamel (Kohn *et al*., 1999). The boxes represent 1st and 3nd quartiles, the medians (horizontal line), averages are represented by diamonds and the whiskers show the 90th and

10th percentiles. 335

Figure 5.43. Box plots showing **Al** (top) and **Mn** (below) concentrations (in ppm) data of each red deer tooth from Tornewton Cave in comparison with concentrations reported on extant herbivore teeth (1st box plot on each graph) (Kohn *et al*., 2013). The pink rectangles represent concentration ranges reported on modern enamel (Kohn *et al*., 1999). The boxes represent 1st and 3nd quartiles, the medians (horizontal line), averages are represented by diamonds and the whiskers show the 90th and 10th percentiles. 335

Figure 5.44. Laser ablation track marked with a blue line on the horse tooth sample from Tornewton Cave (NHM specimen). The start and end of each profile are located close to the EDJ. 336

Figure 5.45. **Sr**, **Ba**, **Zn** (A.1); **Al**, **U**, **Mn**, **Pb** (A.2) and **REE** (A.3) concentrations (in ppm) from the laser ablation profile of M92408 horse tooth from Tornewton Cave, shown against distance (in mm) down the profile. 0 on the X –axis marks the oldest enamel and the starting point for analysis. The sectioned tooth and laser ablation track are also shown. 338

Figure 5.46. **Mg** and **U** (A.1) concentrations (in ppm) from the laser ablation profile of M92408 horse tooth from Tornewton Cave, shown against distance (in mm) down the profile. 0 on the X –axis marks the oldest enamel and the starting point for analysis. 339

Figure 5.47. Box plots showing **Ce, Nd** (top) and **U** (below) concentrations (in ppm) of the horse tooth from Tornewton Cave in comparison with concentrations reported on extant herbivore teeth (1st box plot on each graph) (Kohn *et al*., 2013). The pink rectangles represent concentration ranges reported on modern enamel (Kohn *et al*., 1999). The boxes represent 1st and 3nd quartiles,

the medians (horizontal line), averages are represented by diamonds and the whiskers show the 90th and 10th percentiles. 340

Figure 5.48. Box plots showing **Al** (top) and **Mn** (below) concentrations (in ppm) in the horse tooth from Tornewton Cave in comparison with concentrations reported on extant herbivore teeth (1st box plot on each graph) (Kohn *et al*., 2013). The pink rectangles represent concentration ranges reported on modern enamel (Kohn *et al*., 1999). The boxes represent 1st and 3nd quartiles, the medians (horizontal line), averages are represented by diamonds and the whiskers show the 90th and 10th percentiles. 341

Figure 5.49. Graphs showing high resolution **Sr/Ca and Ba/Ca** (A.1, B.1, C.1) and **Zn/Ca ratios and U-concentrations** (A.2, B.2, C.2) of bear m1s from Tornewton Cave, shown against distance (in mm). The oldest enamel is at the cusp of the tooth (0 on the X -axis), whilst the youngest is at the end of profile. Sectioned teeth and laser ablation tracks are also shown. Red and blue lines mark the Sr/Ca and Ba/Ca areas that most probably represent unaltered dietary signals and were used for the calculation of average values (see section 5.6.5). The different dietary stages according to Humphrey *et al*. (2008b) are also indicated (arrows mark the start of each stage). 346

Figure 5.50. Graphs showing high resolution **Sr/Ca and Ba/Ca** (A.1, B.1) and **Zn/Ca ratios and U-concentrations** (A.2, B.2) of bear canine teeth from Tornewton Cave, shown against distance (in mm). The oldest enamel is at the cusp of the tooth (0 on the X -axis), whilst the youngest is at the end of profile. Sectioned teeth and laser ablation tracks are also shown. Red and blue lines mark the Sr/Ca and Ba/Ca areas that most probably represent unaltered dietary signals and were used for the calculation of average values (see section 5.6.5). The different dietary stages according

to Humphrey *et al*. (2008b) are also indicated (arrows mark the start of each stage). 348

Figure 5.51. Graphs showing high resolution **Sr/Ca and Ba/Ca** (A.1, B.1, C.1) and **Zn/Ca ratios and U-concentrations** (A.2, B.2, C.2) of bear m3 teeth from Tornewton Cave, shown against distance (in mm). The oldest enamel is at the cusp of the tooth (0 on the X -axis), whilst the youngest is at the end of profile. Sectioned teeth and laser ablation tracks are also shown. Red and blue lines mark the Sr/Ca and Ba/Ca areas that most probably represent unaltered dietary signals and were used for the calculation of average values (see section 5.6.5). The different dietary stages according to Humphrey *et al*. (2008b) are also indicated (arrows mark the start of each stage). 350

Figure 5.52. Graphs showing high resolution **Sr/Ca and Ba/Ca** (A.1 and B.1) and **Zn/Ca ratios and U-concentrations** (A.2 and B.2) in m1 hyaena teeth from Tornewton Cave, shown against distance (in mm). The oldest enamel is at the cusp of the tooth (0 on the X -axis), whilst the youngest is at the end of the profile. Sectioned teeth and laser ablation tracks are also shown. Red and blue lines mark the Sr/Ca and Ba/Ca areas that most probably represent unaltered dietary signals and were used for the calculation of average values (see section 5.6.5). The different dietary stages according to Humphrey *et al*. (2008b) are also indicated (arrows mark the start of each stage). 354

Figure 5.53. Graphs showing the high resolution **Sr/Ca and Ba/Ca** (A.1, B.1, C.1) and **Zn/Ca ratios and U-concentrations** (A.2, B.2, C.2) of M41530 m1 (A.1 and A.2), M41530 m2 (B.1 and B.2) and M41530 m3 (C.1 and C.2) red deer teeth from Tornewton Cave, shown against distance (in mm). The oldest enamel is at the cusp of the tooth (0 on the X -axis), whilst the youngest is at the

end of the profile. Sectioned teeth and laser ablation tracks are also shown. Red and blue lines mark the Sr/Ca and Ba/Ca areas that most probably represent unaltered dietary signals and were used for the calculation of average values (see section 5.6.5). The different dietary stages according to Humphrey *et al*. (2008b) are also indicated (arrows mark the start of each stage). 357

Figure 5.54. Graphs showing high-resolution **Sr/Ca and Ba/Ca** (A.1) and **Zn/Ca ratios and U-concentrations** (A.2) in a horse m3 from Tornewton Cave, shown against distance (in mm). The oldest enamel is at the cusp of the tooth (0 on the X -axis), whilst the youngest is at the end of the profile. Sectioned teeth and laser ablation tracks are also shown. Red and blue lines mark the Sr/Ca and Ba/Ca areas that most probably represent unaltered dietary signals and were used for the calculation of average values (see section 5.6.5). The different dietary stages according to Humphrey *et al*. (2008b) are also indicated (arrows mark the start of each stage). 359

Figure 5.55. Graph showing the average **Sr/Ca and Ba/Ca** ratios from each tooth from Tornewton Cave. Errors denote 2 standard deviations. 362

List of Tables

Table 1.1. Age and key associated faunal elements of the study sites (see also Fig. 1.1 and text for supplementary information). 60

Table 2.1. Taxonomic designations for extant bears (after Krause *et al*. [2008]) 92

Table 2.2. Dietary groupings of food items consumed by each extant bear species used in this study. Bold type denotes the predominant food types. 109

Table 3.1. t-tests for inequality of surface means for scratches and pits on both *U. maritimus* and *U. deningeri* individuals. 143

Table 3.2. Extant bear species, additional information such as: mean, standard deviation and 95% Confidence interval (CL) for each species are presented for both Grinding (talonid) and Slicing (trigonid) area. 144

Table 3.3. Extant bear species, analysis on Grinding (G), (talonid) and Slicing (S), (trigonid) area. Information for pits includes 1st quartile, minimum, median, maximum and 3rd quartile. 148

Table 3.4. ANOVA results for extant species on the **grinding** area. Summary of the results from all features that were measured in each species, compared and tested between and within groups. Abbreviations as follows: Sum of sqrs is the sum of squares due to features; df is the degree of freedom in the features; Mean sqrs is the mean sum of squares due to features; F is the *F*-statistic and p is the p-value. 155

Table 3.5. Results from **Tukey's test for scratches** on the grinding area between the following extant species: **1:** A*. melanoleuca* (n: 4); **2:** *H. malayanus* (n: 17); **3:** *M. ursinus* (n: 4); **4:** *U. americanus* (n:

9); **5:** *U. maritimus* (n: 14); **6:** *U. thibetanus* (n: 6); **7:** *U. arctos*, Greece (n: 4); **8:** *U. arctos*, Central Europe (n: 10); **9:** *U. arctos*, USA (n: 8); **10:** *U. arctos*, Russia (n: 23); **11:** *U. arctos*, North Europe (n: 9). Values below the diagonal are the results of Tukey's test and those above are the p-values. 156

Table 3.6. Results from **Tukey's test for pits** on the grinding area between the following extant species: **1:** A*. melanoleuca* (n: 4); **2:** *H. malayanus* (n: 17); **3:** *M. ursinus* (n: 4); **4:** *U. americanus* (n: 9); **5:** *U. maritimus* (n: 14); **6:** *U. thibetanus* (n: 6); **7:** *U. arctos*, Greece (n: 4); **8:** *U. arctos*, Central Europe (n: 10); **9:** *U. arctos*, USA (n: 8); **10:** *U. arctos*, Russia (n: 23); **11:** *U. arctos*, North Europe (n: 9). Values below the diagonal are the results of Tukey's test and those above are the p-values. Significant inter-species differences are marked in pink. 157

Table 3.7. Results from **Tukey's test for fine scratches** on the grinding area between the following extant species: **1:** *A. melanoleuca* (n: 4); **2:** *H. malayanus* (n: 17); **3:** *M. ursinus* (n: 4); **4:** *U. americanus* (n: 9); **5:** *U. maritimus* (n: 14); **6:** *U. thibetanus* (n: 6); **7:** *U. arctos*, Greece (n: 4); **8:** *U. arctos*, Central Europe (n: 10); **9:** *U. arctos*, USA (n: 8); **10:** *U. arctos*, Russia (n: 23); **11:** *U. arctos*, North Europe (n: 9). Values below the diagonal are the results of Tukey's test and those above are the p-values. Significant inter-species differences are marked in pink. 157

Table 3.8. Results from **Tukey's test for coarse scratches** features on grinding area between the following extant species: **2:** *H. malayanus* (n: 17); **3:** *M. ursinus* (n: 4); **4:** *U. americanus* (n:9); **5:** *U. maritimus* (n: 14); **6:** *U. thibetanus* (n: 6); **7:** *U. arctos*, Greece (n: 4); **8:** *U. arctos*, Central Europe (n: 10); **9:** *U. arctos*, USA (n: 8); **10:** *U. arctos*, Russia (n: 23); **11:** *U. arctos*, North Europe (n: 9). Values below the diagonal are the results of Tukey's test and

those above are the p-values. Significant inter-species differences are marked in pink. 158

Table 3.9. Results from **Tukey's test for large pits** features on grinding area between the following extant species: **1:** A*. melanoleuca* (n: 4); **2:** *H. malayanus* (n: 17); **3:** *M. ursinus* (n: 4); **4:** *U. americanus* (n: 9); **5:** *U. maritimus* (n: 14); **6:** *U. thibetanus* (n: 6); **7:** *U. arctos*, Greece (n: 4); **8:** *U. arctos*, Central Europe (n: 10); **9:** *U. arctos*, USA (n: 8); **10:** *U. arctos*, Russia (n: 23); **11:** *U. arctos*, North Europe (n: 9). Values below the diagonal are the results of Tukey's test and those above are the p-values. Significant inter-species differences are marked in pink. 158

Table 3.10. Results from **Tukey's test for small pits** on the grinding area between the following extant species: **1:** A*. melanoleuca* (n: 4); **2:** *H. malayanus* (n: 17); **3:** *M. ursinus* (n: 4); **4:** *U. americanus* (n: 9); **5:** *U. maritimus* (n: 14); **6:** *U. thibetanus* (n: 6); **7:** *U. arctos*, Greece (n: 4); **8:** *U. arctos*, Central Europe (n: 10); **9:** *U. arctos*, USA (n: 8); **10:** *U. arctos*, Russia (n: 23); **11:** *U. arctos*, North Europe (n: 9). Values below the diagonal are the results of Tukey's test and those above are the p-values. Significant inter-species differences are marked in pink. 159

Table 3.11. Results from **Tukey's test for gouges** on the grinding area between the following extant species: **2:** *H. malayanus* (n: 17); **3:** *M. ursinus* (n: 4); **5:** *U. maritimus* (n:14); **6:** *U. thibetanus* (n: 6); **7:** *U. arctos*, Greece (n: 4); **8:** *U. arctos*, Central Europe (n: 10); **9:** *U. arctos*, USA (n: 8); **10:** *U. arctos*, Russia (n: 23); **11:** *U. arctos*, North Europe (n: 9). Values below the diagonal are the results of Tukey's test and those above are the p-values. Significant inter-species differences are marked in pink. 159

Table 3.12. Results from **Tukey's test for puncture pits** on the grinding area

between the following extant species: **2:** *H. malayanus* (n: 17); **3:** *M. ursinus* (n: 4); **4:** *U. americanus* (n: 9); **5:** *U. maritimus* (n: 14); **7:** *U. arctos*, Greece (n: 4); **8:** *U. arctos*, Central Europe (n: 10); **9:** *U. arctos*, USA (n: 8); **10:** *U. arctos*, Russia (n: 23); **11:** *U. arctos*, North Europe (n: 9). Values below the diagonal are the results of Tukey's test and those above are the p-values. Significant inter-species differences are marked in pink. 160

Table 3.13. ANOVA results for extant species on the **slicing** area. Summary of the results from all features that were measured in each species, compared and tested between and within groups. Abbreviations as follows: Sum of sqrs is the sum of squares due to features; df is the degree of freedom in the features; Mean sqrs is the mean sum of squares due to features; F is the *F*-statistic and p is the p-value. 161

Table 3.14. Results from **Tukey's test for scratches** on the slicing area between the following extant species: **1:** *A. melanoleuca* (n: 3); **2:** *H. malayanus* (n: 11); **3:** *M. ursinus* (n: 4); **4:** *U. americanus* (n: 9); **5:** *U. maritimus* (n: 14); **6:** *U. thibetanus* (n: 4); **7:** *U. arctos*, Greece (n: 4); **8:** *U. arctos*, Central Europe (n: 8); **9:** *U. arctos*, USA (n: 3); **10:** *U. arctos*, Russia (n: 21). Values below the diagonal are the results of Tukey's test and those above are the p-values. Significant inter-species differences are marked in pink. 162

Table 3.15. Results from **Tukey's test for pits** on the slicing area between the following extant species: **1:** *A. melanoleuca* (n: 3); **2:** *H. malayanus* (n: 11); **3:** *M. ursinus* (n: 4); **4:** *U. americanus* (n: 9); **5:** *U. maritimus* (n: 14); **6:** *U. thibetanus* (n: 4); **7:** *U. arctos*, Greece (n: 4); **8:** *U. arctos*, Central Europe (n: 8); **9:** *U. arctos*, USA (n: 3); **10:** *U. arctos*, Russia (n: 21). Values below the diagonal are the results of Tukey's test and those above are the

p-values. Significant inter-species differences are marked in pink. 162

Table 3.16. Results from **Tukey's test for fine scratches** on the slicing area between the following extant species: **1:** *A. melanoleuca* (n: 3); **2:** *H. malayanus* (n: 11); **3:** *M. ursinus* (n: 4); **4:** *U. americanus* (n: 9); **5:** *U. maritimus* (n: 14); **6:** *U. thibetanus* (n: 4); **7:** *U. arctos*, Greece (n: 4); **8:** *U. arctos*, Central Europe (n: 8); **9:** *U. arctos*, USA (n: 3); **10:** *U. arctos*, Russia (n: 21). Values below the diagonal are the results of Tukey's test and those above are the p-values. Significant inter-species differences are marked in pink. 163

Table 3.17. Results from **Tukey's test for coarse scratches** on the slicing area between the following extant species: **2:** *H. malayanus* (n: 11); **3:** *M. ursinus* (n: 4); **4:** *U. americanus* (n:9); **5:** *U. maritimus* (n:14); **6:** *U. thibetanus* (n:4); **7:** *U. arctos*, Greece (n:4); **8:** *U. arctos*, Central Europe (n:8); **9:** *U. arctos*, USA (n:3); **10:** *U. arctos*, Russia (n:21). Values below the diagonal are the results of Tukey's test and those above are the p-values. Significant inter-species differences are marked in pink. 163

Table 3.18. Results from **Tukey's test for large pits** on the slicing area between the following extant species: **1:** A*. melanoleuca* (n: 3); **2:** *H. malayanus* (n: 11); **3:** *M. ursinus* (n: 4); **4:** *U. americanus* (n:9); **5:** *U. maritimus* (n:14); **6:** *U. thibetanus* (n:4); **7:** *U. arctos*, Greece (n:4); **8:** *U. arctos*, Central Europe (n:8); **9:** *U. arctos*, USA (n:3); **10:** *U. arctos*, Russia (n:21). Values below the diagonal are the results of Tukey's test and those above are the p-values. 164

Table 3.19. Results from **Tukey's test for small pits** on the slicing area between the following extant species: **1:** A*. melanoleuca* (n: 3); **2:** *H. malayanus* (n: 11); **3:** *M. ursinus* (n: 4); **4:** *U. americanus*

(n:9); **5:** *U. maritimus* (n:14); **6:** *U. thibetanus* (n:4); **7:** *U. arctos*, Greece (n:4); **8:** *U. arctos*, Central Europe (n:8); **9:** *U. arctos*, USA (n:3); **10:** *U. arctos*, Russia (n:21). Values below the diagonal are the results of Tukey's test and those above are the p-values. Significant inter-species differences are marked in pink. 164

Table 3.20. Results from **Tukey's test for puncture pits** on the slicing area between the following extant species: **2:** *H. malayanus* (n: 11); **3:** *M. ursinus* (n: 4); **4:** *U. americanus* (n: 9); **5:** *U. maritimus* (n: 14); **6:** *U. thibetanus* (n: 4); **8:** *U. arctos*, Central Europe (n: 8); **9:** *U. arctos*, USA (n: 3); **10:** *U. arctos*, Russia (n: 21). Values below the diagonal are the results of Tukey's test and those above are the p-values. Significant inter-species differences are marked in pink. 165

Table 3.21. Extant species, analysis on the **grinding** (talonid) area. Summary of Principal Component Analysis (PCA). 166

Table 3.22. Extant species, analysis on **grinding** (talonid) area. Loadings of each variable of the PCA on the components. 167

Table 3.23. Extant species, analysis on the **slicing** (trigonid) area. Summary of Principal Component Analysis (PCA). 173

Table 3.24. Extant species, analysis on **slicing** (trigonid) area. Loadings of each variable of the PCA on the components. 173

Table 4.1. Westbury-sub-Mendip (MIS 13), UK (n: 15) statistical summary of eight microwear features. Mean, standard deviation (SD), 95% Confidence interval (CL), 1st and 3rd quartile, minimum, maximum and median values are given. 184

Table 4.2. Kents Cavern bear (breccias), UK (n: 6) statistical summary of eight microwear features. Mean, standard deviation (SD), 95% Confidence interval (CL), 1st and 3rd quartile, minimum,

maximum and median values are given. 189

Table 4.3. Grays Thurrock (MIS 9), UK (n: 10) statistical summary of eight microwear features. Mean, standard deviation (SD), 95% Confidence interval (CL), 1st and 3rd quartile, minimum, maximum and median values are given. 194

Table 4.4. Tornewton Cave bear (MIS 5e), UK (n: 21) statistical summary of eight microwear features. Mean, standard deviation (SD), 95% Confidence interval (CL), 1st and 3rd quartile, minimum, maximum and median values are given. 199

Table 4.5. Banwell Bone bear (MIS 5a), UK (n: 4) statistical summary of eight microwear features. Mean, standard deviation (SD), 95% Confidence interval (CL), 1st and 3rd quartile, minimum, maximum and median values are given. 204

Table 4.6. Kents Cavern bear (MIS 3), (n: 12) UK statistical summary of eight microwear features. Mean, standard deviation (SD), 95% Confidence interval (CL), 1st and 3rd quartile, minimum, maximum and median values are given. 209

Table 4.7. Sandford Hill bears (MIS 3), UK (n: 4) statistical summary of eight microwear features. Mean, standard deviation (SD), 95% Confidence interval (CL), 1st and 3rd quartile, minimum, maximum and median values are given. 214

Table 4.8. Cow Cave (Holocene?), UK (n: 8) statistical summary of eight microwear features. Mean, standard deviation (SD), 95% Confidence interval (CL), 1st and 3rd quartile, minimum, maximum and median values. 219

Table 4.9. ANOVA results for extinct species from Britain and extant species on the **grinding** area. A summary is given of the results from all the different features that were measured in each

species and compared and tested between and within groups. Abbreviations as follows: Sum of sqrs is the sum of squares due to features; df is the degree of freedom in the features; Mean sqrs is the mean sum of squares duet to features; F is the *F*-statistic and p is the p-value.

224

Table 4.10. **A.** Results from **Tukey's test for scratches** for extinct UK species including extant species. **B.** Results from **Tukey's test for pits** for extinct UK species including extant species. Numbers linked with the following species **1:** *A. melanoleuca*; **2:** *H. malayanus*; **3:** *M. ursinus*; **4:** *U. americanus*; **5:** *U. maritimus*; **6:** *U. thibetanus*; **7:** *U. arctos*, Greece; **8:** *U. arctos*, Central Europe; **9:** *U. arctos*, USA; **10:** *U. arctos*, Russia; **11:** *U. arctos*, North Europe; **12:** Westbury-sub-Mendip (MIS 13); **13:** Kents Cavern (breccias); **14:** Grays Thurrock (MIS 9); **15:** Tornewton Cave (MIS 5e); **16:** Banwell Bone Cave (MIS 5a); **17:** Kents Cavern (MIS 3); **18:** Sandford Hill (MIS 3); **19:** Cow Cave (Holocene?). Values below the diagonal are the results of Tukey's test and those above are the p-values.

225

Table 4.11. **A.** Results from **Tukey's test for fine scratches** for extinct UK species including extant species. **B.** Results from **Tukey's test for coarse scratches** for extinct UK species including extant species. Numbers linked with the following species **1:** *A. melanoleuca*; **2:** *H. malayanus*; **3:** *M. ursinus*; **4:** *U. americanus*; **5:** *U. maritimus*; **6:** *U. thibetanus*; **7:** *U. arctos*, Greece; **8:** *U. arctos*, Central Europe; **9:** *U. arctos*, USA; **10:** *U. arctos*, Russia; **11:** *U. arctos*, North Europe; **12:** Westbury-sub-Mendip (MIS 13); **13:** Kents Cavern (breccias); **14:** Grays Thurrock (MIS 9); **15:** Tornewton Cave (MIS 5e); **16:** Banwell Bone Cave (MIS 5a); **17:** Kents Cavern (MIS 3); **18:** Sandford Hill (MIS 3); **19:** Cow Cave (Holocene?). Values below the diagonal are the results of

Tukey's test and those above are the p-values. 226

Table 4.12. **A.** Results from **Tukey's test for large pits** for extinct UK species including extant species. **B.** Results from **Tukey's test for small pits** for extinct UK species including extant species. Numbers linked with the following species **1:** *A. melanoleuca*; **2:** *H. malayanus*; **3:** *M. ursinus*; **4:** *U. americanus*; **5:** *U. maritimus*; **6:** *U. thibetanus*; **7:** *U. arctos*, Greece; **8:** *U. arctos*, Central Europe; **9:** *U. arctos*, USA; **10:** *U. arctos*, Russia; **11:** *U. arctos*, North Europe; **12:** Westbury-sub-Mendip (MIS 13); **13:** Kents Cavern (breccias); **14:** Grays Thurrock (MIS 9); **15:** Tornewton Cave (MIS 5e); **16:** Banwell Bone Cave (MIS 5a); **17:** Kents Cavern (MIS 3); **18:** Sandford Hill (MIS 3); **19:** Cow Cave (Holocene?). Values below the diagonal are the results of Tukey's test and those above are the p-values. 227

Table 4.13. **A.** Results from **Tukey's test for gouges** for extinct UK species including extant species. **B.** Results from **Tukey's test for puncture pits** for extinct UK species including extant species. Numbers linked with the following species **2:** *H. malayanus*; **3:** *M. ursinus*; **4:** *U. americanus*; **7:** *U. arctos*, Greece; **8:** *U. arctos*, Central Europe; **9:** *U. arctos*, USA; **10:** *U. arctos*, Russia; **11:** *U. arctos*, North Europe; **12:** Westbury-sub-Mendip (MIS 13); **13:** Kents Cavern (breccias); **14:** Grays Thurrock (MIS 9); **15:** Tornewton Cave (MIS 5e); **16:** Banwell Bone Cave (MIS 5a); **17:** Kents Cavern (MIS 3); **18:** Sandford Hill (MIS 3); **19:** Cow Cave (Holocene?). Values below the diagonal are the results of Tukey's test and those above are the p-values. 228

Table 4.14. Loutra Arideas Cave (LAC) (Late Pleistocene), Greece (n: 10) statistical summary of eight microwear features. Mean, standard deviation (SD), 95% Confidence interval (CL), 1st and 3rd

quartile, minimum, maximum and median values. 230

Table 5.1. Elements in teeth and their uses with information regarding their concentrations (data from Kohn *et al*. [1999] and Kohn *et al*. [2013]). C and I in brackets indicate respectively concentration and isotope composition and the application of each element. 258

Table 5.2. Weaning and tooth eruption times (in months) from black and brown bear (from Dittrich [1960]; Rausch [1961]; Marks and Erickson [1966]; Ewer [1973]; Debeljak [1996]). I = incisors, Ci = canine initial eruption, Cf = canine final eruption, P = premolars, M = molars. 268

Table 5.3. Timing of birth and tooth eruption sequence in months of *Canis lupus* and *Panthera leo* (from Kohn and McKay [2012]). I = incisors, Ci = canine initial eruption, Cf = canine final eruption, P = premolars, M = molars, X = normally absent. 276

Table 5.4. Eruption sequence and age (in months) of permanent dentition of *Cervus elaphus* (adjusted from Hillson [1986], Brown and Chapman [1991a] and Azorit *et al*. [2002]). 279

Table 5.5. Eruption sequence (gingival emergence) in fallow deer (*Dama dama*) (from Brown and Chapman [1991a]). 279

Table 5.6. Stratigraphy of Tornewton Cave (after Sutcliffe and Zeuner [1962]; Currant in Roberts [1996]). Description from base upwards (see also Fig. 5.20 and table 5.7 and text for supplementary information and details regarding the Otter Stratum). 285

Table 5.7. Age and associated mammalian elements of the fossiliferous horizons (Units) from Tornewton Cave (see also Fig. 5.20 and text for supplementary information). 288

Table 5.8. Specimens from Tornewton Cave included in the present geochemical analysis (lower case letters denote lower teeth and upper case denote upper teeth) (see also photographs Fig. 5.22). 291

Table 5.9. Rationale for selection of the LA-ICPMS technique. 295

Table 5.10. Details of the settings used for the LA-ICPMS. 297

Table 5.11. Details of the steps used to calculate the distance on each sample (in mm). 298

Table 5.12. Precision of ICP-MS for the three phosphate glasses analysed (STDP3-1500, STDP3-150, STDP3-5) in comparison with the relative two standard deviations (2 RSD and average) data from Klemme *et al*. (2008). In bold black type are all values within accepted and published values and in red bold type, those that are slightly higher. 304

Table 5.13. Precision of ICP-MS of MACs-3 element values (average and standard deviation [STDEV]) analysed in comparison with average and standard deviations (STDEV) element values from Jochum *et al*. (2012). 305

Table 5.14. Sr/Ca and Ba/Ca averages from each tooth from Tornewton Cave. 360

Table 6.1. Similarities and overlaps between extinct bear population dietary ecospaces (from PCA) and extant species ecospaces. 375

Chapter 1. Introduction

1.1. Introduction

The rapid climatic fluctuations of the Middle and Late Pleistocene produced major changes in the palaeobiogeography and community structure of European mammalian populations, as a result of repeated environmental and vegetation changes (e.g. Barnosky *et al*., 2004; Hofreiter and Stewart, 2009; Stuart and Lister, 2007; Kahlke *et al*., 2011; Stuart and Lister, 2012). Large carnivores are of particular relevance to our understanding of the impact of these changes on the contemporary fauna, since they occupied a wide range of environments, they are less tied to particular biotopes than herbivores and they demonstrate contrasting feeding strategies. The fact that these animals can adapt their modes of life and to their role as assorted predators underlines the diversity present within the Order Carnivora (e.g. Ewer, 1973; Turner, and Antón, 1997; 2004). This remarkable diversity is clearly seen in the Family Ursidae, today represented by eight species with each adapted to a particular environment and mode of life.

Many bear species are omnivorous and can adjust their diet according to food availability in different habitats. The most extreme example of behavioural flexibility in the Ursidae is that of the brown bear (*Ursus arctos* Linnaeus, 1758), which not only occupies a wider range of habitats in the Palearctic (except Africa) and Nearctic, but also demonstrates greater dietary variability than any other species of bear (McLellan *et al*., 2008; Bojarska and Selva, 2012). In terms of the composition of bear diet, several different factors need to be considered, the most important of which are temperature and snow cover. In arctic and alpine regions, modern brown bear exhibit dietary extremes characterised respectively by large volumes of meat (including large concentrations of spawning salmon) and roots (Mattson, 1998). In these areas, the density of brown bears is high (Miller *et al*., 1997) and according to Hilderbrand *et al*. (1999), most carnivorous brown bears, such as those living in coastal areas of North America, have also the most productive populations. In addition, this more carnivorous tendency in North America brown bears differentiates them from, and reduces

potential dietary overlaps with another bear species on the same continent, namely the black bear (*Ursus americanus* Pallas, 1780). The black bear is generally referred to as omnivorous but apparently consumes more plant and fruit matter than salmon (Fortin *et al*., 2007). Another important example of adaptability to a particular environment and different dietary preferences within the brown bear is the fact that northern European brown bear are more carnivorous than their southern counterparts, based on the proportion of ungulates in their diet during all seasons (except during winter hibernation) (Persson *et al*., 2001; Bojarska and Selva, 2012). These examples and those from bears more widely can therefore serve as a proxy for understanding their European Pleistocene counterparts, in particular the evidence of adaptation to different diets in northern populations as a function of climate, environment and latitude.

In contrast to the more carnivorous northern European brown bears, populations found in the deciduous and mixed forests of continental central and eastern Europe (e.g. the Dinaric and Carpathian mountain ranges) exploit a large variety of soft mast, such as fleshy fruits, together with hard mast items (i.e. fruits and seeds with a hard outer covering or exocarp, nuts and acorns and pine seeds) (Bojarska and Selva, 2012). The brown bears of Greece represent the most southerly distribution in Europe of the species (Karamanlidis *et al*., 2015). In this brown bear population, green vegetation and soft mast are the predominant foods (Giannakos, 1997; Vlachos *et al*., 2000). The brown bears from these more temperate environments can therefore serve as appropriate analogues for Pleistocene bear species during interglacial periods. Finally, the Ursidae include three extant species, the polar bear (*Ursus maritimus* Phipps, 1774), giant panda (*Ailuropoda melanoleuca* David, 1869) and sloth bear (*Melursus ursinus* Shaw, 1791*)*, which have highly specialised diets, representing hypercarnivory, herbivory and insectivory/frugivory respectively (Joshi *et al*., 1997; Derocher *et al*., 2002; Macdonald, 2009).

Although the complexities of individual ecosystems and the dietary flexibility of the Ursidae (despite their carnivorous morphological features) can make interpretation of their feeding ecology difficult (Robbins *et al*., 2004; Sacco and Van Valkenburgh, 2004),

the availability of innovative techniques such as molecular, dental histological, isotopic and microwear analyses has made it possible to explore the palaeoecology and palaeodiet even in extinct species.

This study focuses on the examination of changing Middle and Late Pleistocene palaeoecology and niche differentiation in British fossil ursids. Bears were extremely common carnivores in the Pleistocene fossil record, found in both cold- and temperate-climate deposits (Schreve and Currant, 2003) and their study therefore has potential to shed light on the palaeoecology of this climatically-complex period. Although British fossil material forms the core of this project, bear specimens from a single Greek locality are also included in order to provide comparison with the dietary behaviour of a different species from the cave bear group, *Ursus ingressus* Rabeder *et al*., 2004a (Rabeder *et al*., 2004a).

In order to understand better large carnivore responses to palaeoclimatic and palaeoenvironmental change during the Pleistocene, a key element of this study has been the utilisation of dental microwear techniques by deploying stereolight microscopy on British and Greek fossil bear teeth for the first time. This has been complemented by the establishment of a novel and comprehensive reference database of modern bear teeth representing different species with different diets, which can serve as analogues for the Pleistocene specimens. Finally, Laser Ablation Inductively Coupled Plasma Mass Spectrometry (LA-ICP-MS, quadrupole) was utilised to extract a high-resolution signal from the highly mineralised enamel layer, both in fossil bear teeth and those of other taxa recovered from Tornewton Cave, Devon, in order to explore patterns linked with seasonal dietary variability and with animal physiology (e.g. periods of suckling, hibernation, weaning signal) in the Pleistocene mammalian ecosystem.

1.2. Aims and Objectives

1.2.1. Aims

As stated above, the overarching aim of this thesis is **to investigate the palaeodietary and palaeoecological niches, together with aspects of the physiology, of different fossil bears in the Middle to Late Pleistocene in Britain and Greece**. Within this overall aim, a number of subsidiary aims can be identified:

1. To develop a robust methodology for the application of dental microwear to modern and fossil bear teeth, including assessment of the appropriateness of particular areas of the tooth, or individual facets, for this type of study.
2. To develop and validate a complete database of different food types related to microwear features for extant Ursidae.
3. To reconstruct, using the extant database, the palaeodietary adaptations of various fossil bear species (*Ursus deningeri* von Reichenau, 1906, *U*. *arctos*) from Britain, and of *U*. *ingressus* from Greece.
4. To explore potential dietary differentiation between fossil bears from different warm- and cold-climate episodes in Britain, with a particular focus on the Late Pleistocene and including examination of stadial-interstadial variation during Marine Oxygen Isotope Stage (MIS) 3.
5. To document the different dietary and physiological parameters preserved within the dental enamel of carnivore and herbivore teeth, including an evaluation of post-depositional diagenesis, variation in elemental concentration across the teeth, and enamel histological evidence for potential hibernation behaviour.

1.2.2. Objectives

In order to accomplish the aims of this study the following objectives must be met:

1. To test, statistically, the microwear observations from selected samples and species (one extant and one extinct) on both facet and non-facet tooth surfaces

in order to reveal the importance of enamel surface selection in Dental Microwear Analysis (DMA) (Aim 1).

2. To compare the microwear features observed on the trigonid and talonid areas of the first lower molar (m1) in extant bear specimens in order to establish the most appropriate area for DMA selection and effective differentiation of species ecospaces (Aim 1).
3. To undertake a DMA using stereo light microscopy on modern bear species to explore dietary variability *between* species, and on brown bear (*U. arctos*) specimens from different geographical regions (northern Europe, Russia, Greece, central Europe and USA) in order examine variability *within* an individual species (Aim 2).
4. To reconstruct, through Principal Component Analyses (PCA), the different dietary ecospace that each extant bear species occupies (Aim 2).
5. To undertake a DMA of fossil British and Greek bear specimens representing different species and from different time periods and to compare the results with those from the modern reference database in order to reconstruct inter- and intra-specific palaeodietary trends, highlighting adaptations to changing environments, climates and carnivore guild composition (Aims 3 and 4).
6. To produce element concentration profiles from tooth enamel of Late Pleistocene mammals via LA-ICP-MS from a pilot study site at Tornewton Cave (Devon, UK), including concentrations of alteration indicators (such as Mn, Al, Pb, U and Rare Earth Elements [REE]) present in each tooth in order to identify changes that may linked with the diagenetic alteration of tooth chemistry in the burial environment (Aim 5).
7. To generate high resolution *intra*-tooth Strontium (Sr)/Calcium (Ca) and Barium (Ba)/Ca profiles from tooth enamel of Late Pleistocene mammals via LA-ICP-MS from Tornewton Cave, and to use these to make observations on the physiology of each species and to identify potential indicators of hibernation in bears (Aim 5).
8. To use the average values calculated from Sr/Ca and Ba/Ca profiles of each animal to determine the trophic level of each species represented and its palaeodietary implications (Aims 3, 4 and 5).

1.3. Site description and palaeonviromental summary

In order to achieve the objectives of this thesis, sites with ursid remains representing different interglacial and glacial climatic conditions during the early Middle to Late Pleistocene were examined (Fig. 1.1). A particular emphasis was placed on the study of localities representing the last cold stage (Devensian, MIS 5d-2), where numerous abrupt climate changes have been recorded, for example by the $\delta^{18}O$ Greenland ice-core stratigraphy (Svensson *et al*., 2008; Blockley *et al*., 2014) (See also Fig. 1.2). For example, the Middle Devensian (MIS 3) represents a period of elevated climatic warmth when compared with MIS 4 and MIS 2 but is characterised by multiple millennial to sub-millenial-scale climate oscillations between stadials and interstadials (Walker and Lowe, 2007) (see also Fig. 1.2). These fluctuations have been linked to Heinrich events (Dansgaard *et al*., 1993) and to the variable strength of thermohaline circulation in the North Atlantic (Bond *et al*., 1997). However, during MIS 3, the relatively arid environment and the development of rich soils gave rise to fertile open grasslands that supported enormous herbivore biomass (Guthrie, 2001). During the full glacial conditions of MIS 2 (the Late Devensian), an ice sheet extended across much of Britain and had profound effects on the environment (Bowen *et al*., 2002). The terminal Pleistocene is characterised by the abrupt warming of the Lateglacial Interstadial (14,692 BP), after which the Younger Dryas stadial marks a return to intense cold-climatic conditions from 12,896 to 11,703 BP (Rasmussen *et al*., 2006). These major changes in climate would have had an impact on vegetation patterns and therefore, a direct effect on mammalian populations at that time.

The eight sites for the DMA were deliberately selected to cover different extinct bear species from various time periods. In the early Middle Pleistocene in Britain, only one species has traditionally been recognised, the cave bear *U. deningeri*, as exemplified at Westbury-sub-Mendip, Somerset (Bishop, 1974, 1975) and Kents Cavern, Devon (breccia horizon) (Procter *et al*., 2005), both of which were examined as part of this thesis. *U. deningeri* is replaced after MIS 12 by *Ursus spelaeus* Rosenmüller and

Heinroth, 1794 (Schreve, 2001), although remains are rare in Britain compared to the continental mainland where this species persists until the end of the Pleistocene (Pacher and Stuart, 2009). The only dental material available in Britain from *U. spelaeus* comes from the MIS 11 interglacial site of Swanscombe, Kent. However, the two crania represented both belong to very old individuals and the advanced wear stage of the teeth unfortunately proved unsuitable for the purposes of the DMA study. In order, therefore, to include a representative from the cave bear group, material of *U*. *ingressus* was included from the Greek site of Loutra Almopia Cave. The sole bear species in Britain from MIS 9 onwards is the brown bear, *U*. *arctos* (Schreve, 2001). From Britain, six sites with *U. arctos* were accordingly investigated (see also Fig. 1.1 and Table 1.1.). Background information, together with a chronological and palaeoenvironmental summary, is presented below for each of the study sites.

Westbury-sub-Mendip, Somerset, UK

The site, henceforth referred to as Westbury, is located in the Mendip hills of Somerset, south of Bristol (Fig 1.1.A) and was discovered in 1969 during limestone quarrying when many fossil animal bones came to light (Bishop, 1974, 1975, 1982). Extensive excavations were subsequently carried out by the Natural History Museum from 1976-1984 (Andrews *et al*., 1999) with reports on the microfaunal remains by Currant (1986) and Andrews (1990) and the large mammals by Stringer *et al*. (1999), Gentry (1999) and Turner (1999). The stratigraphy of the cave is very complex and includes nineteen units containing sixty sub-units (Schreve *et al*., 1999), although the deposits can be grouped into two main Members, the Early Pleistocene Siliceous Member and the early Middle Pleistocene Calcareous Member, which has yielded the majority of the fossil mammalian remains (Bishop, 1982; Stuart, 1982) and is the basis for the investigations presented here. The Calcareous Member can be further subdivided into an assemblage from the main chamber and a “rodent earth” assemblage composed of many thousands of small mammal remains (Stringer *et al*., 1999).

Table 1.1 presents a list of the large carnivores found within the cave deposits. All bear specimens examined here are from the Calcareous Member (see Fig. 1.1. for details).

The number of specimens of cave bear *U*. *deningeri* is remarkable and the abundance of young and neonate individuals indicates that the cave was occupied by females with cubs (Andrews and Turner, 1992). The faunal assemblage from the Calcareous Member is characteristic of the early Middle Pleistocene Cromerian Complex (Stuart and Lister, 2001) and the presence of *Arvicola terrestris cantiana*, a water vole that evolved from *Mimomys savini* (Sutcliffe and Kowalski, 1979), indicates an age late within this period, possibly correlated with Cromerian Interglacial IV or MIS 13 (Schreve *et al*., 1999). The palaeoenvironmental conditions inferred for the Calcareous Group were described in detail by Andrews and Stringer (1999) and consist predominantly of open grassland (Andrews and Cook, 1999; Schreve *et al*., 1999). The climate was temperate, as indicated by the high percentage of woodland rodents (Agusti and Anton, 2002), with an intervening cool oscillation.

Kents Cavern, Devon, UK

Kents Cavern is a significant historical and palaeontological site containing one of the most important Pleistocene sequences in Britain (Campbell and Sampson, 1971; Proctor, 1996; Keen, 1998). The cave is located in southwest England, 2km east of Torquay (Fig. 1.1.A) and contains a long sequence of sediments with fossil mammal remains and artefacts covering both a part of the early Middle Pleistocene and the Late Pleistocene Middle Devensian (Proctor, 1996). Excavations in the cave started in 1825 by J. MacEnery (Campbell and Sampson, 1971), followed by more systematic investigations between 1865 and 1880 by W. Pengelly (Pengelly, 1884). Subsequent reviews were carried out by Campbell and Sampson (1971) of the lithic industries and fauna, as well as Pengelly's notes on the stratigraphy, and of aspects of the fauna by Lister (1987). A schematic section through the deposits was provided by Proctor (1996) who also summarised the main lithostratigraphic units. Fossil mammalian remains have been found in two of the five units. The oldest material occurs in cemented limestone breccias (cobbles and gravel in an over-consolidated clayey matrix), comprising abundant remains of the spelaeoid bear, *U. deningeri*. The deposits have been widely interpreted as dating from the late Cromerian Complex and the assemblage is characteristic of a temperate climate (Proctor, 1996; Proctor *et al*.,

2005). Dating by Uranium-series (U-series) and ESR by Proctor (1994, 1996) for the breccia deposits has suggested ages of 300 to 400ka BP (MIS 9 or 11), although this is at the limit of the U-series method. Most recently, McFarlane *et al*. (2011) have dated the deposits to MIS 12 or early MIS 11 age, although caution is required since the precise age of this unit remains uncertain.

The second unit at Kents Cavern is referred to as the 'cave earth' deposit, correlated with MIS 3 by Currant and Jacobi (1997, 2001, 2011) on account of its characteristic suite of mammals including *Crocuta crocuta*, *Mammuthus primigenius*, *Equus ferus* and *Coelodonta antiquitatis*, which these authors attribute to their Middle Devensian Pin Hole Mammal Assemblage-Zone (MAZ) (see also table 1.1). This has been upheld by Accelerator Mass Spectrometry (AMS) radiocarbon dates using ultrafiltered collagen, which have attributed the assemblage to the Middle Devensian (Jacobi *et al*., 2006; 2009). The Middle Devensian is characterised by an open, cool steppic grassland and by multiple stadial-interstadial oscillations (Keen, 1998) (see also Fig. 1.2). Studies on coleopteran and chironomid assemblages from other MIS 3 sites suggest that the mean summer temperatures in Britain during this period were around +8 to +11°C and -16 to -22°C in winter (Schreve *et al*., 2013).

Grays Thurrock, Essex, UK

One of the best preserved late Middle Pleistocene mammalian assemblages in Britain is that of Grays Thurrock in Essex, 32km to the east of London and located on the north bank of the River Thames (Fig. 1.1.A). During the 19th century, a variety of fossil mammalian remains came to light from this open site during the extraction of clay ("brickearth") from the three main pits (Western, Central and Eastern) present (Schreve, 1997). The stratigraphy and the sediments of the site were first examined by Morris (1836) and most of the remains were collected between 1845 and 1850. The fossiliferous beds comprise laminated clays with sand and gravel layers, overlain by a shell bed (Schreve, 1997). Complete study of the assemblage was carried out by Schreve (1997); the site has been attributed to the MIS 9 interglacial and the mammalian assemblage assigned to the Purfleet MAZ (Schreve, 2001). A predominance of woodland species indicates fully temperate environmental

conditions with a climate possibly warmer than at present (Schreve, 1997). The key mammalian faunal elements are listed in Table 1.1. Beetle assemblages from other MIS 9 sites indicate that the climate was warmer than today with mean summer temperatures between 17 and 16 °C and winter temperatures between -11 and +13 °C (Coope, 2010).

Tornewton Cave, Devon, UK

Tornewton Cave contains one of the most complete late Middle and Late Pleistocene sequences in Britain. The cave is part of the Torbryan Caves group located on the south-west side of the Torbryan Valley in Devon (southwest England) approximately 27Km to the southwest of Exeter (Fig. 1.1.A). The site forms the basis of a pilot case study to investigate the geochemistry of bear and other mammalian teeth (see Chapter 5) and for this reason, a detailed description of site's history, stratigraphy and geology will be presented in section 5.4. of Chapter 5. The present section will therefore be restricted to palaeoenviromental observations regarding the beds that have yielded abundant bear remains. According to Gilmour *et al*. (2007), the deposits of both the "Bear Stratum" and overlying "Hyaena Stratum" should be attributed to the first two temperate substages of MIS 5, MIS 5e (Ipswichian Interglacial) and MIS 5c (early Devensian) respectively. The Last Interglacial was characterised by the development of mixed oak woodland, elevated summer temperatures (> 17°C) compared to today and mild winters (> 0°C) (Candy *et al*., 2010).

It is worth noting, however, that Gilmour *et al*. (2007) suspected that the "Bear Stratum" contained material of different ages and that both cave bear (*U*. *spelaeus*) and *U. arctos* were present, albeit from different chronological horizons. However, based on a preliminary morphometrical study, Pappa *et al.* (2013) found no significant differences between the bear remains from the different layers and all bear specimens from Tornewton Cave were attributed to *U. arctos*.

Banwell Bone Cave, Somerset, UK

Banwell Bone Cave is located at the western end of Banwell Hill in western Mendip, Somerset (Fig. 1.1.A). The cave was discovered in 1824 and explored and excavated by

W. Beard, who recovered many thousands of predominantly large and complete mammal bones (Currant, 2000, 2004). The assemblage is dominated by remains of bison (*Bison priscus* Bojanus, 1827) and reindeer (*Rangifer tarandus* Linnaeus, 1758), while brown bear and wolf (*Canis lupus* Linnaeus, 1758) are the principle carnivores represented. The bear remains are especially notable for their large size (Currant and Jacobi, 2001; Currant, 2004), whereas the heavily worn wolf teeth suggest that this carnivore specialised in rapid flesh slicing and to some extent bone consumption (Flower and Schreve, 2014). According to Turner (2009), during this stage, the carnivore guild seems to have been temporarily restricted to these two species, together with a reduced prey of bison and reindeer. The faunal list from Banwell Bone Cave is presented in Table 1.1.

The Banwell Bone Cave assemblage forms the type Mammal Assemblage-Zone for the Early Devensian of Currant and Jacobi, 2001, 2011) and has been correlated with MIS 5a on the basis of U-series dating (Gilmour *et al*., 2007; Currant and Jacobi, 2011). The climate was cold and the environment open tundra (Currant and Jacobi, 2001; 2011). Based on beetle assemblages from sites of equivalent age, the palaeotemperatures have been reconstructed as mean summer values of 7 to 11°C and winter values of -10 to -30°C (Maddy *et al*., 1998).

Sandford Hill, Somerset, UK

Sandford Hill cave (or caves) is located in western Mendip, Somerset (Fig. 1.1.A). Very little is known from the literature about the exact history and discovery of this site, although the main collector was W. Beard of Banwell fame (Currant, 2000). According to Currant (2000), who reviewed the mammalian collection from the site, there are two distinct faunal groups from this site that can be separated on the basis of bone preservation, one being better mineralised than the other. In addition, one group is composed mainly of remains of spotted hyaena and bones with gnaw marks, while the other has abundant reindeer remains, together with those of lion and woolly rhinoceros (see table 1.1) that are less well-mineralised and bear no trace of any modification (Currant, 2000). The group with abundant spotted hyaena has been described as similar to that of the Kents Cavern ‘cave earth’ and has been attributed to

the Pin Hole MAZ of the Middle Devensian (Currant and Jacobi 2001; 2011). The mammalian remains suggest that Sandford Hill was characterised by a cool climate steppe grassland palaeoenvironment at the time of deposition (Currant, 2004), with similar palaeotemperatures to those reconstructed for Kents Cavern (see above).

Loutra Almopia Cave (LAC), Greece

Loutra Almopia Cave (LAC) is one of the richest sites for cave bear, *U*. *ingressus* (Rabeder *et al*., 2004a) and was the first site in Greece where this species was described (Tsoukala and Rabeder, 2005; Tsoukala *et al*., 2006). This Late Pleistocene site is situated on the northern slope of the Nicolaou Rema gorge, on the slopes of the Voras Mountain (at 2524m, the third highest mountain in Greece) and close to the border with Macedonia (FYROM) (Fig. 1.1.B). The cave comprises two fossiliferous horizons, one within the sediments of the cave floor across all five chambers present, referred to as LAC I, II, III, Ib and Ic. The second (younger) horizon, LAC 1a, is situated 5m above the cave floor. The first fossiliferous horizon (in all chambers except LAC 1a) has yielded thousands specimens of *U. ingressus* as well as other large mammalian fauna (Tsoukala, 1994; 2006; Tsoukala and Rabeder, 2005; Tsoukala *et al*., 1998; 2001; 2006) (see table 1.1). The abundance of small mammalian remains in LAC is also remarkable, including insectivores, rodents, lagomorphs and bats (Chatzopoulou *et al*., 2001; Chatzopoulou 2003; 2005; Tsoukala *et al*., 2006). In LAC Ia (second fossiliferous horizon), which has been dated to 14 000-13 000 years BP, only small mammals were found (Chatzopoulou, 2014).

Absolute dating of a *U. ingressus* femur from chamber LAC I has revealed that bears occupied the cave at least during the Middle Weichselian (42 500 BP) (Rabeder *et al*., 2006; Frischauf *et al*., in press). The radiocarbon dates and associated fauna (including the presence of small mammals that are indicators of temperate climate and a Mediterranean flora) confirm that the animals were living during a relatively mild climatic phase during the last Ice Age. Climatic conditions were less severe in Greece and for many mammals, southeast Europe served as a refuge during the Weichselian (Tsoukala *et al*., 2006; Chatzopoulou, 2014). The climate appears to be drier than that

of today, while the palaeoenvironmental reconstruction based on the species present suggests the presence of minor glaciers on the peaks of the Voras Mountains, adjacent coniferous and deciduous forests, local waterbodies in the form of rivers and streams and extensive grassland in the vicinity (Tsoukala *et al*., 2006; Chatzopoulou, 2014).

Cow Cave, Devon, UK

Cow Cave is part of a system of 20 caves located in Chercombe Bridge Limestone around the village of Chudleigh in Devon (Campbell and Collcutt, 1998) (Fig. 1.1.A). The Chudleigh Caves and nearby Pixie's Hole have played an important role in Pleistocene mammalian faunal studies, however Cow Cave received relatively little attention until Beynon's investigations in 1931 (Campbell and Collcutt, 1998). Little is known regarding the stratigraphical positions of the mammal remains, which are listed by these authors as bear, wolf, fox, hyaena, deer, wild cat, giant deer and ox. Moreover eight unstratified flint implements were also recorded (Campbell and Collcutt, 1998). The first stratigraphical descriptions were made by Simons (1963) (in Campbell and Collcutt, 1998) and Rosenfeld (1969), with the former reporting six horizons yielding bone remains. The age of the mammalian remains is uncertain, although a Holocene age has been proposed, however, the artefacts have been assigned a date late in the Devensian (Campbell and Collcutt, 1998) and it is possible that some of the mammalian material also dates to this period.

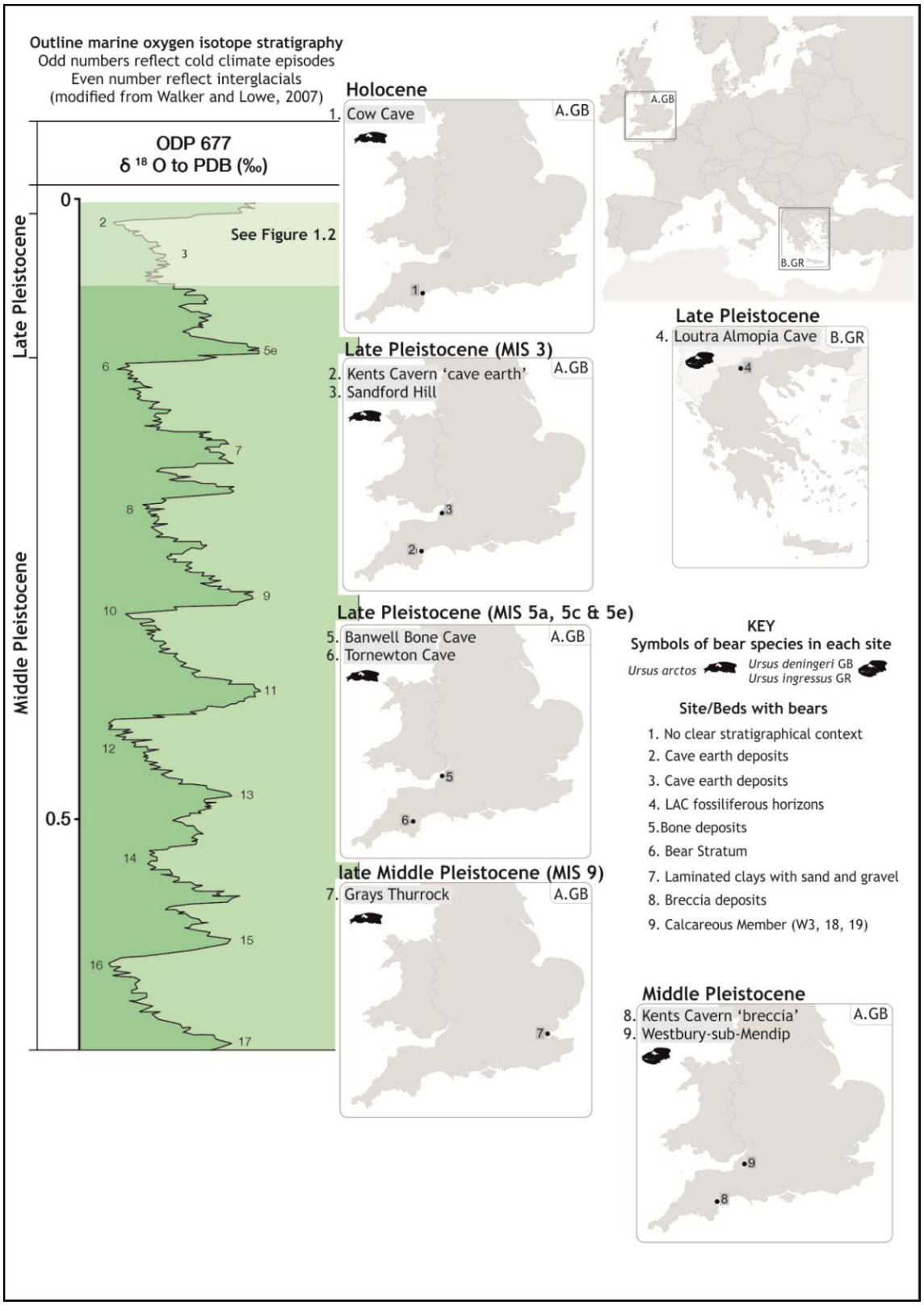

Figure 1.1. Maps showing the location of each site including additional information regarding the species of Ursidae present and the stratigraphical position of the studied material where known. The marine oxygen isotope stratigraphy is shown on the left as a climatic yardstick (modified from Walker and Lowe, 2007).

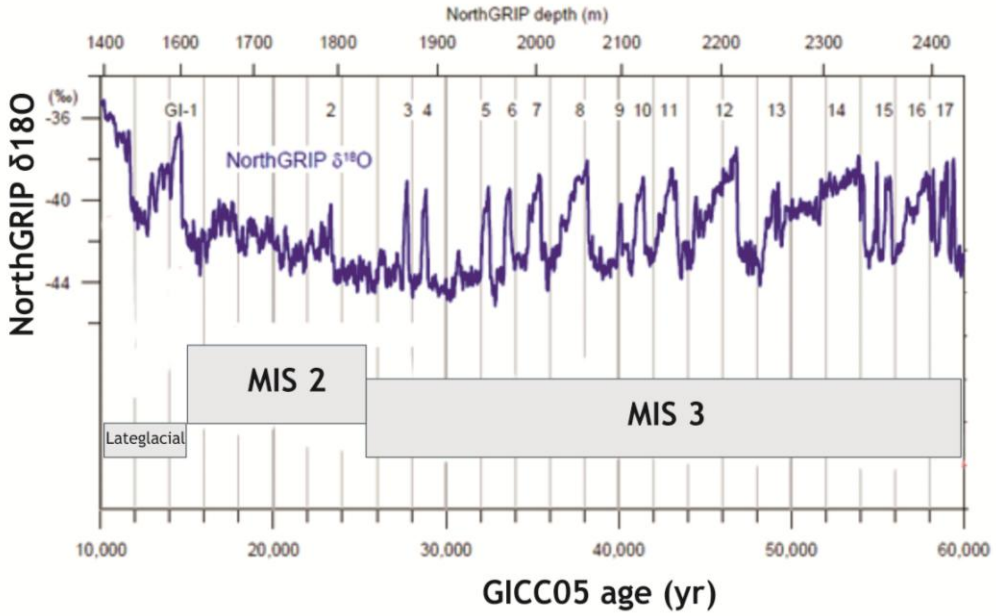

Figure 1.2. Detail of the Middle and Late last cold stage, based on the NorthGRIP $\delta^{18}O$ record according to GICC05 (modified from Svensson *et al*. [2008]).

Table 1.1. Age and key associated faunal elements of the study sites (see also Fig. 1.1 and text for supplementary information).

Site	Age	Associated Fauna	References
Westbury-sub-Mendip, Somerset, UK	**early Middle Pleistocene (late Cromerian Complex)** (MIS 13?)	**Only Carnivores** *Homotherium latidens* *Panthera leo* *Panthera gombaszoegensis* *Canis lupus mosbachensis* *Canis (Xenocyon) lycaonoides* *Ursus deningeri* *Crocuta crocuta* *Pachycrocuta brevirostris*	Bishop, 1974; 1982; Schreve *et al*., 1999; Turner, 1999
Kents Cavern, Devon, UK	**early Middle Pleistocene (late Cromerian Complex)** (MIS 13?) "breccia" horizon	*Ursus deningeri* *Panthera leo* *Arvicola terrestris cantiana* *Microtus oeconomus*	Keen, 1998; Proctor *et al*., 2005
	Middle Devensian MIS 3 "cave earth" horizon	*Canis lupus* *Vulpes vulpes* *Ursus arctos* *Crocuta crocuta* *Mammuthus primigenius* *Equus ferus* *Coelodonta antiquitatis* *Megaloceros giganteus* *Cervus elaphus* *Rangifer tarandus*	Proctor, 1996; Currant and Jacobi, 1997; 2001; Keen, 1998;
Grays Thurrock, Essex, UK	**late Middle Pleistocene MIS 9** Purfleet MAZ	*Canis lupus* *Vulpes vulpes* *Crocuta crocuta* *Ursus arctos* *Palaeoloxodon antiquus* *Equus ferus* *Stephanorhinus hemitoechus* *Stephanorhinus kirchbergensis* *Sus scrofa* *Cervus elaphus*	Schreve, 1997; 2001

		Dama dama *Capreolus capreolus* *Megaloceros giganteus* *Bos primigenius*	
Tornewton Cave, Devon, UK	**Ipswichian Interglacial MIS 5e and early Devensian (MIS 5c)**	*Canis lupus* *Vulpes vulpes* *Ursus arctos* *Crocuta crocuta* *Panthera leo* *Stephanorhinus hemitoechus* *Dama dama* *Cervus elaphus*	Currant, 1996; 1998
Banwell Bone Cave, Somerset, UK	**Early Devensian, MIS 5a** Banwell Bone Cave MAZ	*Lepus timidus* *Microtus oeconomus* *Canis lupus* *Vulpes vulpes* *Vulpes lagopus* *Ursus arctos* *Gulo gulo* *Rangifer tarandus* *Bison priscus*	Currant and Jacobi, 1997; 2001; Currant, 2004; Gilmour *et al*., 2007
Sandford Hill, Somerset, UK	**Middle Devensian, MIS 3** Pin Hole MAZ	*Lepus timidus* *Panthera leo* *Canis lupus* *Crocuta crocuta* *Ursus arctos* *Equus ferus* *Coelodonta antiquitatis* *Rangifer tarandus* *Cervus elaphus* *Bison priscus*	Currant, 2000; 2004
Loutra Almopias Cave, GR	**Late Pleistocene, MIS 3** LAC fossiliferous horizons with *U. ingressus*	*Crocuta crocuta spelaea* *Panthera leo spelaea* *Panthera pardus* *Vulpes vulpes* *Canis lupus* *Meles meles* mustelids *Bos primigenius* *Capra ibex* *Cervus elaphus* *Dama dama*	Rabeder *et al*., 2006; Tsoukala and Rabeder, 2005; Tsoukala *et al*., 2006.
Cow Cave, Devon, UK	**Holocene, MIS 1 (possibly mixed with Devensian)**	*Crocuta crocuta* *Panthera leo* *Ursus arctos* *Cervus elaphus* *Capreolus capreolus* *Rangifer tarandus* *Bison priscus* *Microtus nivalis* *Arvicola amphibious* *Lepus*	Campbell and Collcutt, 1998

1.4. Mammal teeth: structure and function

Mammalian teeth comprise a fundamental element of the body, since through the process of chewing, animals consume food and generate energy. In mammals, the connections between endothermy, metabolism and mastication are therefore vital for survival (Ungar, 2010). Among the many particular attributes of teeth, one of the most important is that they provide an indication of the feeding habits of each species (Hillson, 1986) and therefore directly relate to the environment in which they are present (Ungar, 2010).

Teeth come in many shapes and sizes. They are highly diagnostic and from a single isolated tooth, it is possible to identify its exact position in the dentition and to establish the genus or even the species of animal to which it belongs. Another important aspect of teeth is that they are formed of enamel, one of the hardest biological materials known and which, once formed, cannot be substantially modified except by ion exchange within the mouth (Ungar, 2010). From the perspective of preservation of chemical information, enamel is an ideal material for isotopic studies, since due to its low porosity, it has excellent potential to record faithfully an original isotopic signature (Lee-Thorp and Van der Merwe, 1991; Wang and Cerling, 1994). Thus, researchers benefit from the extremely resistant structure of the tooth, which limits the effect of diagenesis and therefore facilitates chemical studies (see also Chapter 5 for further details).

Although the chemical signature of enamel is relatively resistant to change, the enamel surface of the tooth can change shape during food consumption. In these cases, information can be recorded regarding dental micro-abrasion or microwear and the direction of chewing action, which can further be used as a tool to establish food preferences (Ungar, 2015) (see also Chapter 3 and 4). In addition to tooth wear a well established analytical technique such as mesowear has been also used. Mesowear begins with the observation that attrition, caused by tooth-to-tooth contact, tends to form facets, whereas abrasion, caused by tooth-to-food contact, tends to obliterate them (Fortelius and Solounias, 2000). Moreover, the thickness of enamel has been used in many studies to separate hard object feeding mammals from soft feeders (Kay, 1981;

Dumont, 1995). Researchers have also focused on the analysis of enamel microstructure, since many mammals show some specialization in this regard. This can not only inform about dietary choices but microstructure information can also be linked to aspects of mammalian physiology and to chemical analysis (Koenigswald, 1992; Koenigswald *et al*., 1997; Koenigswald *et al*., 2010; Lucas *et al*., 2008; Smith and Tafforeau, 2008) (see also Chapter 5).

A tooth is composed of two main parts, namely the crown and the root; these parts consist of organic and inorganic components that are described further in Chapter 5. The root is completely encased in the bony socket of the jaw and is covered with a bone-like material, the cement layer (Fig. 1.3.B). The crown is the part of the tooth that projects into the mouth and consists of three layers, from inside to outside the pulp, the dentine and finally, the enamel (Ungar, 2010) (Fig. 1.3.B).

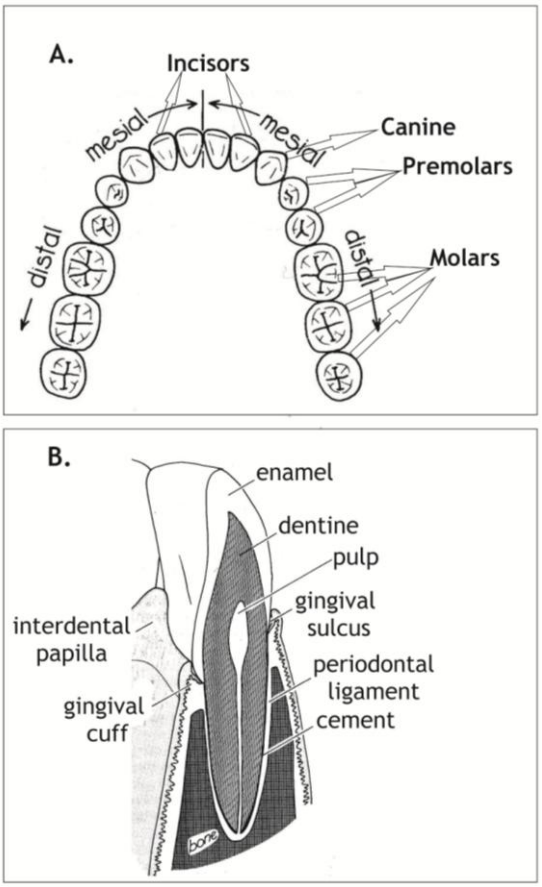

Figure 1.3. Tooth structure and components, based on human teeth (modified from Hillson [1986]).

Two important junctions or demarcations are present within the tooth structure. The first separates the enamel from the dentine and is referred to as the enamel dentine junction (EDJ) and the second is between the cement and the dentine (the cement dentine junction, CDJ) (Hillson, 1986) (see Fig. 1.4.A). All mammalian teeth follow the same construction. In terms of the tooth position in the mouth, the most anterior teeth are the incisors, followed by the canines, both of which have single cusps. These are followed further along the jaws by the premolars and molars (Fig. 1.3.A). Premolars and molars have the most complex occlusal surfaces with both principal and secondary cusps, depending on diet and the evolutionary history of the species concerned. These posterior teeth are employed for shearing, slicing, crushing and grinding of food and have morphological adaptations for particular diets (Ungar, 2010). For example, Wright *et al*. (1991) showed that bats that consume tough insects have longer shearing crests on their posterior teeth, whereas those that feed on pulpy fruits have better-developed crushing and grinding surfaces. In addition, omnivorous bears and raccoons have larger crushing surfaces on their cheek teeth whereas carnivorous cats have larger shearing surfaces (see Ungar 2015 and references therein). Finally, observed masticatory movements have also been shown to link clearly to individual diets (Ungar, 2015).

Each tooth is characterised by posterior and anterior parts according to the direction in which it is facing (forward or backward). The descriptions “buccal” and “lingual” refer to the position of the tooth surface, either facing the cheek or the tongue respectively (Fig. 1.4.B).

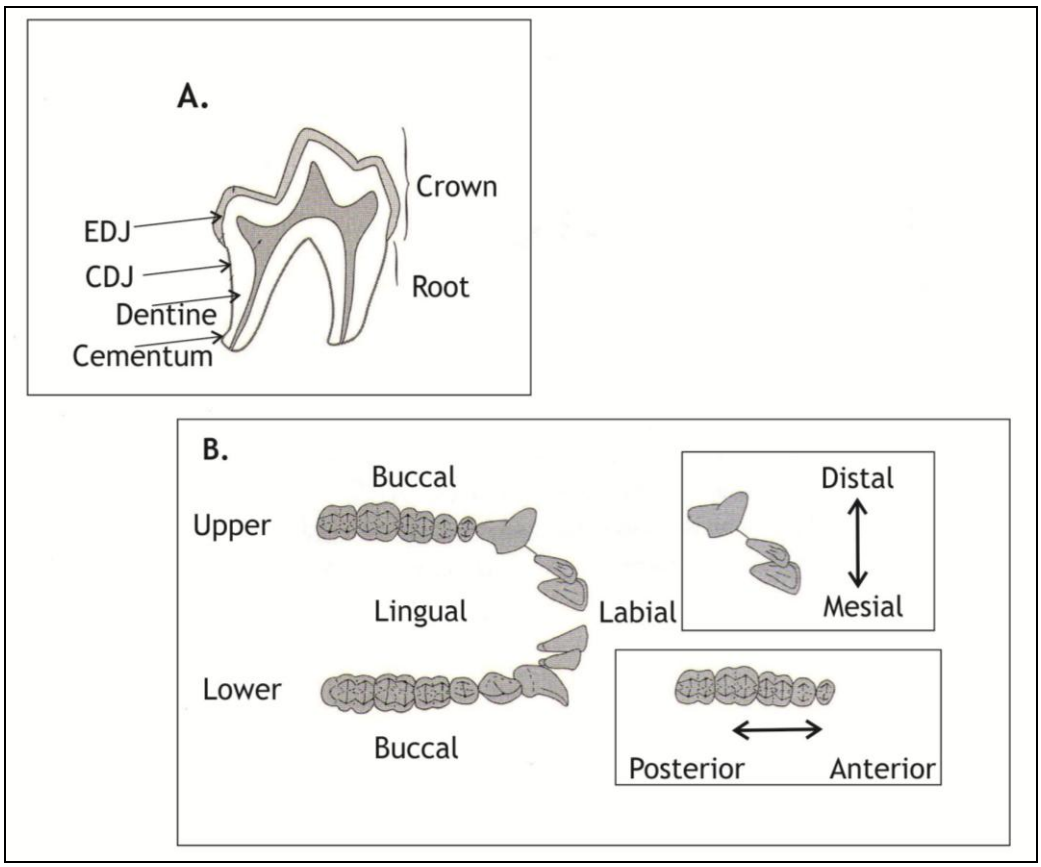

Figure 1.4. Structure and orientation in mammalian teeth. **A.** Cross-section of a first lower molar in a domestic dog (*Canis familiaris*), showing the enamel dentine junction (EDJ) and cement dentine junction (CDJ). **B.** Orientation terminology for upper and lower teeth of crab-eating macaque (*Macaca fascicularis*) (modified from Ungar [2010]).

Hillson (1986) divided mammals into three groups based on observations of their cheek teeth features: (1) those with teeth bearing sharp, shearing edges, (2) those with flattened occlusal surfaces, and (3) those with complex infoldings. Sometimes, species may have elements of two or even all three of these categories. Figure 1.5. illustrates six examples of cheek tooth forms in six different mammals. A further important separation of teeth may be made according to the high of the crown. High-crowned teeth are referred to as hypsodont, whereas low-crowned teeth are referred to as brachyodont. The degree of hypsodonty can also strongly reflect diet, since mammals with an abrasive diet, such as grazers that consume silica-rich grasses, have the most hypsodont teeth (Ungar, 2010).

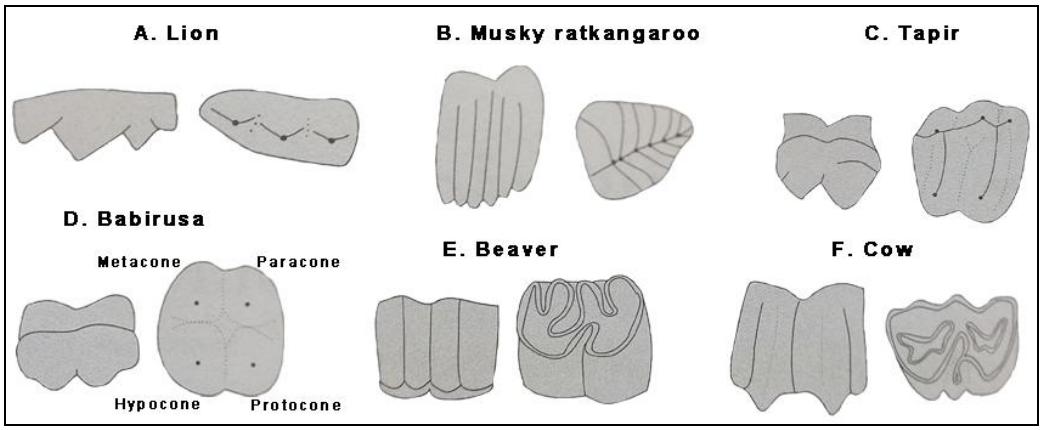

Figure 1.5. Cheek-tooth form in various mammals. All are upper teeth with both the buccal view (left) and occlusal view (right). **A.** Secodont (shearing) carnassials of lion (*Panthera leo*). **B.** Plagiaulacoid (blade-like) molar of musky rat kangaroo (*Hypsiprymnodon moschatus*). **C.** Bilophodont (two-lophed) molar of Malayan tapir (*Tapirus indicus*). **D.** Bunodont (low, rounded) molar of babirusa (*Babyrousa babyroussa*), showing the position of the four key cusps. **E.** Ptychodont (folded) molar of North American beaver (*Castor canadensis*). **F.** Selenodont (crescent-shaped lophs) molar of cow (*Bos taurus*) (modified from Ungar [2010]).

From a palaeontological and zooarchaeological point of view, teeth are very common finds and typically form the majority of museum collections. This allows the study of feeding mechanisms and other palaeobiological aspects even in extinct species.

1.5. Structure of the thesis

The present thesis consists of six Chapters. Following the Introduction, aims and objectives (Chapter 1), Chapter 2 provides a literature review of the Ursidae in terms of their evolution, fossil and recent history in Britain, modern distribution and extinction, as well as presenting some of the key ecological and biological aspects of living bears. Chapter 3 presents an overview of Dental Microwear Analysis (DMA) and establishes a methodology, which is subsequently applied throughout the thesis. This Chapter then presents the results of DMA on specimens of living bear species in order to establish a reference database of dental microwear characteristics, before discussing the results in terms of known species diets in modern bears.

Chapter 4 presents the results of DMA on extinct bear species from Middle and Late Pleistocene sites in Britain, together with the results from extinct bear specimens from

the Late Pleistocene of Greece. These are further interpreted in terms of the inferred dietary preferences and ecological niches of the fossil forms.

Chapter 5 presents a pilot geochemical study on mammalian remains (including brown bears) from the Late Pleistocene site of Tornewton Cave, designed to complement the DMA studies above. A literature review describes the development of such studies to infer palaeodiet, with a particular focus on Strontium/Calcium (Sr/Ca) and Barium/Calcium (Ba/Ca) ratios, before the history and context of the site is outlined. The methodology is then developed, the results presented and the implications discussed for the reconstruction of mammalian physiology and trophic level in past populations.

The key findings and conclusions of the thesis are presented in Chapter 6, with respect to methodological considerations and implications for palaeodietary and behavioural reconstructions in fossil bears. Finally the initial aims of the thesis are reviewed and limitations and areas for future development are rehearsed.

Chapter 2. The Ursidae: evolution, ecology and extinction

2.1. Introduction

This Chapter focuses on the Ursidae family. More specifically, information is provided regarding the bear systematics, evolution and for the Pleistocene species, details such as dietary habits and body size (in 2.2-2.4). Sections 2.5 and 2.6 include present molecular phylogenies and information on Quaternary extinctions, while Sections 2.7 and 2.8 are devoted to ursids today including information about geographical distribution, general biological details and diets.

2.2. Systematics and the early evolution of the Ursidae

The systematic position of the bears is given below. Where genera are discussed further in the text, all species in that genus are listed, both fossil and living. Where genera are not discussed further in the text, the species are not elaborated. † denotes extinct form.

Kingdom: Animalia

Class: Mammalia

Order: Carnivora Bowdich, 1821

Sub-Order: Caniformia Kretzoi, 1938

Family: Ursidae Fischer de Waldheim, 1817 (Synonyms: Ursinidae Gray, 1821; Ailuropodidae Pocock, 1916)

Sub-Family: Ailuropodinae Grevé, 1894

Genus: *Agriarctos*† Kretzoi, 1942

Genus: *Ailurarctos*† Qiu & Qi, 1989

Genus: *Ailuropoda* Grevé, 1894

Species: *baconi*† (Woodward, 1915)

melanoleuca (David, 1869)

microta† Pei, 1962

minor† Pei, 1962

wulingshanensis† Wang *et al*. 1982

Genus: *Kretzoiarctos* Abella *et al*., 2012

Sub-Family: Ursinae Viret, 1955

Genus: *Helarctos* Horsfield 1825

Species: *malayanus* Raffles, 1821

Genus: *Indarctos*† Pilgrim, 1913

Genus: *Melursus* Meyer, 1793

Species: *ursinus* Shaw, 1791

Genus: *Ursus* Linnaeus, 1758

Species: *abstrusus*† Bjork, 1970

americanus Pallas, 1780 (= *Euarctos americanus* Thenius, 1979)

arctos Linnaeus, 1758 (Synonyms: *U. prearctos*† Boule, 1919; *U. arctos fossilis*† Goldfuss, 1821, *U. priscus*† Cuvier, 1823)

deningeri† von Reichenau, 1904

dolinesis† Garcia & Arsuaga, 2001

eremus† Rabeder *et al.,* 2004

etruscus† Cuvier, 1823 (Synonyms: *U. cultridens* Cuvier, 1824)

ingressus† Rabeder *et al*., 2004

ladinicus† Rabeder *et al*., 2004

maritimus Phipps, 1774 (= *Thalarctos maritimus* Gromov & Baranova, 1981)

minimus† (Synonyms: *U. arvernensis* Croizet & Jobert, 1828; *U. ruscinensis* Depéret, 1890, *U. boecki* Schlosser, 1899)

praepriscus† Mottl, 1951

rodei† Musil, 2001

rossicus† Borissiak 1930

sackdillingensis† Heller, 1956

savini† Andrews, 1922

spelaeus† Rosenmüller, 1794

suessenbornensis† Soergel, 1926

thibetanus Cuvier, 1823 (Synonyms: *Selenarctos thibetanus* Gromov &

Baranova, 1981; *U. scherzi* Dehm, 1943; *U. mediterraneus* Major, 1873; *Plionarctos (stehlini* Kretzoi, 1941; *U. (Plionarctos) telonensis* Bonifay, 1971; *U. (Selenarctos) karabach* Vereschagin & Tikhonov, 1994)

Genus: *Ursavus*† Schlosser, 1899

Species: *brevirhinus*† Hofmann, 1887

depereti† Fraile, 1997 (Synonyms: *Kretzoiarctos beatrix* Abella *et al*., 2011; *Agriarctos beatrix* Abella *et al*., 2011; *U. primaevus* Álvarez Sierra, 2003)

ehrenbergi† *Thenius, 1947*

elmensis† Stehlin, 1917

orientalis† Qiul *et al*.,1985

pawniensis† Frick, 1926

primaevus† Gaillard

tedfordi† Qiu *et al*., 2014

Sub-Family: Tremarctinae Merriam & Stock, 1925

Genus: *Arctodus*† Leidy, 1854

Species: *brasiliensis*† Lund, 1838

pampariensis† Kurtén, 1967

pristinus† Leidy, 1854

simus† Cope, 1879

Genus: *Arctotherium*† Bravard, 1857

Species: *angustidens*† Gervais & Ameghino, 1880

vetustum† Ameghino, 1902

bonariense† Gervais, 1852

tarijense† Ameghino, 1902

wingei† Ameghino, 1902

Genus: *Plionarctos*† Frick, 1926

Genus :*Tremarctos* Gervais, 1855

Species: *floridianus*† Gidley, 1928

ornatus Cuvier, 1825

Sub-Family: Agriotheriinae† Kretzoi (1929)

Genus: *Agriotherium*† Wagner, 1837

Species: *africanum*† Hendey, 1972

inexpectans† Qiu *et al*., 1991

insigne† Gervais, 1853

myanmarensis† Ogino *et al*., 2011

gregoryi† Frick, 1926

schneideri† Sellards, 1916

sivalensis† Cautley & Falconer, 1836

The bears are members of the Order Carnivora, one of the most fascinating orders in the Class Mammalia. The Latin origins of the name Carnivora highlight the distinguishing features of its members: *caro* signifying "meat or flesh" and *vorare* "to devour". Of particular evolutionary importance are the carnassial teeth, namely the fourth upper premolar (P4) and first lower molar (m1), which have scissor-like blades and are adapted to shear through flesh (Ewer, 1973). Nevertheless, despite these morphological adaptations towards meat-eating, there is extreme diversification in diet (with concomitant modifications to the dentition), as demonstrated most particularly by the bears. Bears are diphyodont and heterodont animals, generally with three incisors on each side top and bottom (there are some exceptions, which are outlined in the dental formulae given below). Bears also have large canines that enable them to break branches, tear apart logs in search of insects, and subdue and kill animal prey (Macdonald, 2009). Body size is highly variable (see 2.7. below). The sun bear and the sloth bear are the smallest forms, followed by the Asian black bear and the spectacled bear. The largest forms are the American black bear and the grizzly bear, with the polar bear being the largest member of the Family while the pandas are about the size of an American black bear (Macdonald, 2009).

Bears have a heavily-built skeleton so they depend on their strength rather than on speed. They are primarily adapted for movement across rough uplands and forests

(although the polar bear can also traverse ice) and have a plantigrade posture, whereby the entire sole of their posterior feet touches the ground and supports their weight, also allowing them to stand bipedally (Macdonald, 2009). This way of walking dictates the morphology of the limb bones, metapodials and digits. In plantigrade species, the limb bones are shorter and heavier and there is greater lateral mobility at the wrist and ankle than in digitigrades or unguligrades; the metapodials are shorter and more divergent and the digits are arranged fanwise (Ewer, 1973). The anterior feet, depending on the species concerned, are not entirely plantigrade but rise partially from the ground (pasemidigitigrade) (Macdonald, 2009).

Within the Carnivora, the bears form part of the sub-Order Caniformia, which comprises the Families Canidae (wolves and dogs), Ursidae (the bears), Mustelidae (badger, otters and their relatives), Procyonidae (raccoons, coatis and their relatives), Otariidae (sea lions), Odobenidae (walruses), Phocidae (seals), Mephitidae (skunks and stink badgers) and the Ailuridae (red panda). These are distinct from the second sub-Order within the Carnivora, the Feliformia Kretzoi, 1945, which comprises the Families Felidae (cats), Herpestidae (mongooses), Hyaenidae (hyaenas), Viverridae (civets), Eupleridae (fossas and their relatives) and Nandiniidae (African palm civet) (Wilson and Reeder, 2005). There are two main differences between the sub-Orders. In the Feliformia, the ethmo-turbinal is long and extends to the anterior part of the nasal chamber, whereas in the Caniformia, it is short and does not reach the front of the nasal chamber (Ewer, 1973). The second difference concerns the auditory bullae; in the Caniformia, the bulla is formed by a single tympanic bone with no separate entotympanic element, whereas in the Feliformia, the bulla is formed from both the ecto– and entotympanic bones and is divided by a partition where the two meet (Ewer, 1973).

The phylogeny of the Caniformia has been subject to various revisions. For example, the giant panda genus *Ailuropoda* has alternately been considered part of the Ursidae (e.g. Talbot and Shields, 1996) and as a separate Family (e.g. Zhang and Shi, 1991). Each Family within the Caniformia (excepting the Ailuridae and Odobenidae, which are today represented by a single species each) includes a range of species with different body shapes, sizes and habits. For many of these species, plant food makes an important contribution to their diet. This is particularly the case for the Ursidae, where

many representatives of the Family include plant food in their diet. Characteristics of the Ursidae include large cheek teeth adapted for crushing, wide and laterally-flattened crowns with large, low and sub-equal cusps that lack noticeable cutting edges, a heavy form and large size, plantigrade feet and five digits in each foot.

The evolutionary history of the Ursidae Family is more recent than that of other carnivores. It can be traced back to the early Miocene (Kurtén, 1968), when the ancestral members evolved from early canids (McLellan and Reiner, 1994). The small-bodied *Ursavus* Schlosser, 1899 is considered to be the first genus within the Ursidae (Kurtén, 1968), believed to have evolved from the hemicyonid carnivore genus *Cephalogale* (Erdbrink, 1953; Argant and Philippe, 1997). Based on remains found in Miocene deposits in Styria (Austria), in Silesia (Poland) and at La Grive-St-Alban (France), *Ursavus* was similar in size to a modern wolf and possessed characteristic fine vertical wrinkles on the enamel of its teeth (Erdbrink, 1953). The most basal species recognised is *Ursavus elmensis* Stehlin 1917, the remains of which were found during the excavation of a railway tunnel excavation at Elm, between Frankfurt and Fulda (Germany), within Burdigalian (early Miocene) age deposits (Erdbrink, 1953). This species lived under relatively stable and sub-tropical climates in Europe during the early Miocene (McLellan and Reiner, 1994). *U. elmensis* had all its premolars, which were adapted for slicing, while its molars show the beginning of the expansion of chewing surface that was to characterise the bear teeth of later times (Kurtén, 1976).

Major disagreements exist regarding the systematic subdivision of the Ursidae. In the literature, the number of subfamilies recognised within the Ursidae varies from three to five (e.g. McLellan and Reiner, 1994; Quiles, 2003). McLellan and Reiner (1994) discussed five sub-Families, the Hemicyoninae, Agriotheriinae, Tremarctinae, Ursinae and Ailuropodidae but most recently, only three sub-Families have been accepted, the Ursinae, Tremarctinae and extinct Agriotheriinae (Fulton and Strobeck, 2006), a position that is followed here. With respect to the Tremarctinae, the only living representative is the spectacled bear, *Tremarctos ornatus* Cuvier, 1825, although the extinct tremarctine genus of short-faced bears, *Arctodus* Leidy, 1854 is well known from the Pleistocene fossil record of North and South America (Kurtén, 1969; Schubert *et al*., 2010 and references therein). The largest member of the Carnivora was the Early Pleistocene species *Arctotherium angustidens* Gervais and Ameghino, 1880 with a

body mass between 1588 and 1749 kg from which remains were found in Ensenadan sediments in La Plata City, Buenos Aires Provinae, Pampean Region in Argentina (South America) (Soibelzon and Schubert, 2011). According to the authors this is the earliest, largest and most carnivorous member of the genus. The second largest member in size was the Pleistocene species *Arctodus simus* Cope, 1897 with a body mass of 700 kg or more (some males close to 1000kg) (Christiansen, 1999a) from which scattered remains were found within cave deposits and open sites from both western and eastern North America (Kurtén, 1969).

Kurtén (1966) proposed that the sub-Family Agriotheriinae may have evolved from *Ursavus*. One of the best-known representatives, the "hyaena bear" *Agriotherium insigne* Gervais, 1853, which survived until the earliest Villafranchian (Late Pliocene, European Land Mammal Age MN 16) in Europe, has been described as a very large ancestral form of bear but with a dentition retaining some dog-like characters (Kurtén, 1968; Kahlke, 1999).

According to molecular data (see 2.5 below), the radiation of the Ursinae sub-Family, which is of principal interest to the present thesis, occurred around 5.39Ma (Krause *et al*., 2008; Miller *et al*., 2012), at the Miocene-Pliocene boundary. This transition was marked by a global drop in temperatures and by increased seasonality (Zachos *et al*., 2001), with the replacement of forest by open C4 grassland habitats, especially at low latitude (Cerling *et al*., 1997).

It is generally accepted that the genus *Ursus* first appeared in Europe, at the French site of Montpellier (MN 14), in the Early Pliocene (5.05Ma) (Krause *et al*., 2008), in the form of the small-bodied bear *Ursus minimus* Devèze and Bouillet, 1827. This species is typical of Ruscinian to Early Villafranchian faunal assemblages (Kurtén, 1968; Kahlke, 1999). The weight of *U. minimus* has been reconstructed as approximately 50kg (Stirling and Derocher, 1990), similar to the maximum size of extant male *Helarctos malayanus* Raffles, 1821. Anatomically, this species had many similarities with living Asian black bears (*U. thibetanus* Cuvier, 1823) (Kurtén, 1968; Baryshnikov and Lavrov, 2013), including thin and sharp canines and enlarged molars, better adapted to consume vegetation (Kurtén, 1976). The Late Pliocene was marked by relatively dry climatic conditions and the widespread development of savanna and steppe grasslands

(Kurtén, 1968; Stirling and Derocher, 1990). *U. minimus* gave rise to *U. etruscus*, which was also initially small and most probably gave rise to the extinct cave bear lineage as well as to brown bears of Eurasia and north America, and to extant Asiatic and American black bears (McLellan and Reiner, 1994; Baryshnikov, 2007) (see also Figure 2.1).

Ursine bears are also known from other, younger Early Pleistocene sites across Europe, including the Kuchurganian beds in Ukraine (Korotkevich, 1967), Barót-Köpecz in Romania (Maier von Mayerfels, 1929), Alcoy in Spain (Montoya *et al*., 2006) and Dorkovo in Bulgaria (Delson *et al*., 2005). Attribution to *U. boecki* Schlosser, 1899 has been suggested by Wagner (2010), although other authors (e.g. Baryshnikov, 2007) have proposed conspecificity with *U. minimus*. From MN 15b (late Ruscinian), black bears generally attributed to *U. minimus* therefore become a regular (although never abundant) component of European faunal assemblages, occurring from the Caucasus to France and from the UK to Spain (Wagner, 2010).

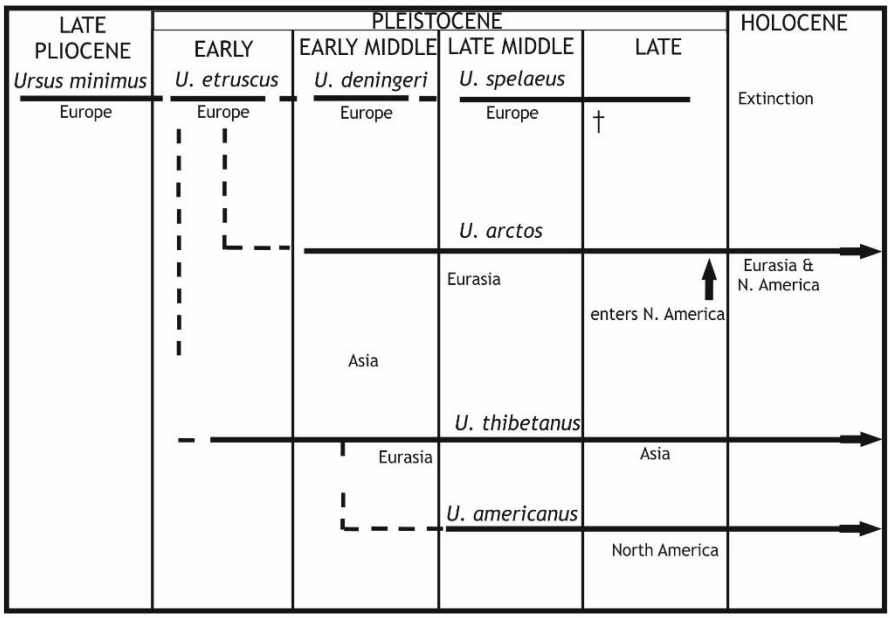

Figure 2.1. Schematic reconstruction of the evolutionary history of the cave, brown and black bear lineages (after Kurtén [1969]).

2.3. The Pleistocene evolution of the Ursidae

Many Pleistocene deposits have proved to be rich in ursid remains, leading to the recognition of multiple new bear species and sub-species, and related phylogenetic studies (e.g. Erdbrink, 1953; Kurtén, 1968; 1969; Mazza and Rustioni, 1994; Argant and Philippe, 1997).

U. minimus fossils record a progressive increase in size, evolving by the Early Pleistocene (MN 17) into *Ursus etruscus* Cuvier, 1823 (= *Ursus* aff. *etruscus* Mazza and Rustioni, 1992), although some authors view *U. etruscus* as representing an entirely separate new lineage of perhaps Asiatic origin (Rustioni and Mazza, 1993). The type specimen is from the Early Pleistocene site of Figline in the Upper Valdarno of Italy and the species subsequently became widespread in Europe (Mazza and Rustioni, 1992; Wagner, 2010) and North Africa (Geraads, 1997), with some closely related forms reportedly known from China (Kurtén, 1968) and central Asia (Baryshnikov, 2007). Early *U. etruscus* were small-bodied (similar to modern *U. thibetanus*), increasing in size until terminal forms approached the size of extant large brown bear (Kurtén, 1968; Mazza and Rustioni, 1992). In addition, significant changes occurred through time in *U. etruscus* dentition, revealing an increasing importance of herbivory (Kahlke, 1999). This is highlighted by the elongation of the molars and the development of a tuberculated occlusal surface, whereas the carnassial function of the teeth became reduced and the anterior premolars dwindled to small pegs (Kurtén, 1968; Mazza and Rustioni, 1992). All the premolars, however, were preserved in the Etruscan bear and it was not until the Middle Pleistocene that the *Ursus* line began to lose these teeth (Erdbrink, 1953). These changes in size and morphology in *U. etruscus* may be connected to the climatic fluctuations of the Pleistocene and associated palaeoenvironmental change. According to Erdbrink (1953), both brown and cave bears descended from *U. etruscus*, which explains the occurrence of features that are both *arctos*-like (e.g. specimens from Early Pleistocene deposits at Tegelen, the Netherlands) and *spelaeus*-like (e.g. specimens from the Valdarno, Italy). Some of the arctoid-like features, which are also present in *U. etruscus*, include the slender horizontal ramus with straight ventral profile, a narrow and elliptical fourth lower premolar (p4) with a massive and prominent protoconid, a slender lower first molar (m1), a rectangular second molar (m2) without medial constrictions, a triangular fourth upper premolar (P4) with simple, pointed cusps, a

quadrangular to rectangular upper first molar (M1) lacking central constriction and an upper second molar (M2) lacking torsion (no twisting) (García, 2004).

Despite the commonly-held position that *U. etruscus* was the common ancestor of the brown bear, cave bear and American and Asiatic black bear lineages (Kurtén, 1976; Rabeder *et al*., 2000; Argant, 2001) (see also Figure 2.1), Mazza and Rustioni (1994) have proposed that the black bear group (*Ursus minimus-thibetanus*) is ancestral to the other bear groups.

The brown bear was the first species to be described scientifically, by Carl von Linné, under the name *Ursus arctos* (Systema Naturae, 1, Ed. 10, p. 47, Holmiae, 1758) (cited in Erdbrink 1953). The type locality was most probably in Sweden although there is no known holotype (Miller, 1912) (for additional information on morphology and biology see 2.7.8). The wide morphological diversity of the species has created taxonomic confusion in the past and continues to do so today (Erdbrink, 1953; Pacher, 2007), a typical example being the extensive list published by the former, which contains 232 recent and 39 fossil species and subspecies.

A number of late Early Pleistocene and early Middle Pleistocene arctoid species have been proposed, although again, the taxonomic position remains controversial. These include *U. prearctos* Boule, 1919, *U. praepriscus* Mottl, 1951, *U. rodei* Musil, 2001 (from the Epivillafranchian site of Untermaßfeld in Germany) and *U. dolinensis* Garcia and Arsuaga, 2001 (from the late Early Pleistocene levels in the Sierra de Atapuerca, northern Spain and from Le Vallonnet, southern France (Rustioni and Mazza, 1993, but see Baryshnikov 2007 for a re-identification). Considerable disagreement remains in the literature regarding the timing of the appearance of the first true brown bears in Europe. According to a study of material from Bad Deutch-Altenburg in Austria, brown bears were already present in Europe at the end of the Early Pleistocene (Rabeder and Withalm, 2006; Rabeder *et al*., 2010), whereas other authors do not recognise their existence until the Last Interglacial, for example at Taubach and Ehringsdorf, Germany and Vence, France (Argant, 1996; Koenigswald and Heinrich, 1999).

In China, fossil brown bear material has been described from early Middle Pleistocene cave deposits at Choukoutien (Pei, 1934) and the species has a continuous record from this period until the present day in East Asia (Kurtén, 1968). According to Kurtén

(1959), the growth of the Scandinavian and Alpine ice sheets during the Elsterian glaciation (Marine Oxygen Isotope Stage [MIS] 12) caused the eastern and western bear populations to become separated from one other. Kurtén (1959) further proposed that the eastern population gave rise to *U. arctos*, whereas the western population evolved to *Ursus spelaeus* Rosenmüller, 1794 (and not Rosenmüller and Heinroth, 1794 - see Rosendahl and Kempe 2005). Records of *U. arctos* from Heppenloch, Germany (Kurtén, 1959) and Lunel-Viel, France (Kurtén, 1968) demonstrate that the species was certainly present in Europe by the late Middle Pleistocene. However, although the former has previously been attributed to the Holsteinian interglacial (MIS 11) (e.g. Adam, 1975), its age has not been recently reviewed, whereas the latter site is now considered to be possibly of younger, MIS 9 age (e.g. van Asperen and references therein). Of equal note is that the brown bear is absent from uncontested Holsteinian sites such as Steinheim-an-der-Murr in Germany (Kurtén, 1959; Schreve and Bridgland, 2002) and is also absent from Britain during the equivalent interglacial, the Hoxnian (Schreve, 2001). *U. arctos* consequently first makes an appearance in Britain during MIS 9 (Schreve, 1997; Schreve, 2001).

Finds of Late Pleistocene brown bears are not only common in Britain (e.g. Reynolds, 1906; Currant and Jacobi, 2001) but also in southern Europe (e.g. Marra, 2003), although remains have been less abundant in central Europe (e.g. Lebel *et al*., 2001; Sabol, 2001; Guérin, 2002). According to Döppes and Pacher (2005), the first evidence of brown bear in the Alpine area after the Last Glacial Maximum is from the southern Alpine site of Grotte Ernesto (Italy) and from northern Alpine site of Neue-Laubenstein – Bärenhöhle (Germany). Suggestions that both brown bear and cave bear co-existed, for example in Central Europe, have been based mainly on uncertain stratigraphical evidence and potential conflation of Late Glacial/Holocene brown bear remains with older Late Pleistocene finds (Pacher, 2007; Pacher and Stuart, 2007). Careful attention is therefore needed in the study of bear material in order to establish the true nature of this proposed coexistence.

As well as cave bears (see below), the brown bear shared its western and southern European range during the Middle Pleistocene with the Himalayan black bear (*U. thibetanus* = *Ursus scherzo* Dehm, 1943) (Schreve and Currant, 2003). Remains of *U.*

thibetanus are not common but have been recovered from sites in France (Argant, 1991; Crégut-Bonnoure, 1996), Spain (Torres Perez Hidalgo, 1988), Greece (Kurtén and Poulianos, 1977) and in Germany (Kurtén, 1975; Turner, 2000) but not in Britain. Multiple synonyms for these black bears have been proposed, together with a number of subspecies, of which only two, *U. t. permjak* in the Urals and *U. t. mediterraneus* in the rest of the range in Caucasus and Europe are considered valid (Baryshnikov, 2007; Wagner, 2010).

The earliest representatives of spelaeoid bears occur in Europe at approximately the same time as the arctoid ones, with the appearance of *U. deningeri* von Reichenau, 1904. As with brown bears, the considerable variability apparent in morphology and size has led to the description of numerous subspecies of dubious validity. These are reviewed by Grandal d'Anglade and Vidal Romani (1997), based on Torres Perez Hidalgo (1988) and Torres Perez Hidalgo (1992), and by Wagner (2010). The nominotypical subspecies *U. deningeri deningeri* was described from the locality of Mosbach 2 in Germany by von Reichenau (1904). Early Middle Pleistocene forms such as *Ursus suessenbornensis* Soergel, 1926, have also been widely regarded as an early spelaeoid bear or subspecies of *U. deningeri* (Kurtén, 1969; Kahlke, 1999; Baryshnikov, 2007), although this species has equally been synonymized with *U. arctos* (Mazza and Rustioni, 1994; Rabeder *et al*., 2010). The Süßenborn bear combines some primitive (arctoid) limb proportions with larger body dimensions, which Kahlke (1999) suggested reflect a steppic adaptation during the European early Middle Pleistocene. The earliest *U. deningeri* was very probably the direct ancestor of the Late Pleistocene cave bear *U. spelaeus* and is known from many different sites of early Middle Pleistocene age in the Czech Republic, Poland, Hungary, France, Italy, Spain, Greece, Moldova, Turkey and the UK (e.g. Reichenau, 1906; Kurtén and Poulianos, 1981; Bishop, 1982; Tsoukala, 1991; Stuart, 1996; Stiner, 1998; Stiner *et al*., 1998; Koenigswald and Heinrich, 1999; Argant and Argant, 2002; García, 2003). A particular site of note for early *U. deningeri* is Le Vallonet cave in southern France (e.g. Baryshnikov, 2007; Argant, 2009; Wagner, 2010), although the identification of this material was challenged by García (2003), who referred it instead to the arctoid *U. dolinensis* while recognising some spelaeoid features.

In Britain, the replacement of *U. deningeri* by *U. spelaeus* has traditionally been placed during the Anglian (Elsterian) glaciation (e.g. Schreve, 2001). However, the boundary between these two species is somewhat subjective and a much later transition, at the beginning of the last Interglacial, has been proposed by Rabeder *et al*. (2000). Some researchers have proposed intermediate or transitional taxa such as *U. spelaeus deningeroides* (Mottl, 1964; Argant, 1991), whereas other authors consider both *U. deningeri* and *U. spelaeus* to be a single species but demonstrating variability through time (Kurtén, 1968; Mazza and Rustioni, 1994). Baryshnikov and Foronova (2001) have yet a third opinion, placing both species in the subgenus *Spelearctos* together with *Ursus rossicus* Borissiak 1930 and the late Early Pleistocene *Ursus savini* Andrews, 1922 (= *U. deningeri hundsheimensis* Zapfe, 1946) from West Runton, Norfolk (UK).

U. rossicus was a small continental form that was widely distributed during the Middle and Late Pleistocene in Eastern Europe, southern parts of western Siberia, in Kazakhstan and in the Ural Mountains (see Baryshnikov and Foronova 2001 and references therein). *U. savini* was a small form with relatively short face, identified from a type specimen at Bacton (Norfolk, UK) and from others at Hundsheim (Austria) (Kahlke, 1999). Regarding *U. savini*'s phylogenetic position, three models are currently in use (summarised from Wagner and Cermák, 2012): 1. *U. savini* is an ancestor of *U. deningeri* (or its earliest subspecies) and as such, represents an early spelaeoid form (e.g. Kurtén, 1968; 1976; García and Arsuaga, 2001); 2. *U. savini* is synonymous with *U. deningeri*, possible one of its subspecies (e.g. Torres Perez Hidalo, 1992; Mazza and Rustioni, 1994; Argant and Crégut-Bonnoure, 1996; Grandal d'Anglade and López-González, 2004; Rabeder *et al*., 2010); and 3. *U. savini* is a representative of an independent lineage of small spelaeoid bears (continuing until the Late Pleistocene) and representing a sister clade to the main *U. deningeri-U. spelaeus* lineage (e.g. Baryshnikov, 2006; 2007). According to Wagner (2010), this species belongs to the *deningeri* group and most probably represents an endemic local race that has no direct descendents.

As stated above, in Britain, *U. spelaeus* is documented as a distinct species for the first (and only) time in the Hoxnian interglacial, MIS 11 (Schreve, 2001; Schreve and

Currant, 2003). However, no evidence of *U. spelaeus* is present in Britain from MIS 9 onwards (Schreve, 2001), an observation corroborated by Pacher and Stuart (2009), who reported no confirmed evidence of the Late Pleistocene cave bear in Britain. Thus, *U. arctos* was the sole species in Britain from MIS 9 onwards and occurred in both interglacial and glacial stages. Furthermore, at some sites, such as Grays Thurrock in Essex, brown bear is apparently the dominant large carnivore (Schreve, 1997). This succession is in marked contrast to what is known on the European mainland where multiple species of cave bear apparently co-existed and *U. spelaeus* persisted until its extinction in the Late Pleistocene (e.g. Rabeder *et al*., 2004a; Pacher and Stuart, 2009).

The cave bear *U. spelaeus* was first described by Rosenmüller in his doctoral thesis and the oft-cited attribution of Rosenmüller and Heinroth, 1794 is therefore no longer valid (Kempe *et al*., 2005; Rosendahl and Kempe 2005). This species is a characteristic element of the last "Ice Age" and its remains have been found by the thousand in many European caves, such as the celebrated Drachenhöhle near Mixnitz in Styria (Austria) (Kahlke, 1999). The species evolved from *U. deningeri* and irrespective of the timing of the transition, there are some apparent morphological differences between them. For example, *U. spelaeus* has a larger body size than *U. deningeri* (Kurtén, 1969), while its cheek teeth show progressive modification of the occlusal surface during the Pleistocene (Rabeder and Tsoukala, 1990; Rabeder, 1999). In addition, *U. spelaeus* loses the anterior premolars and the molars become enlarged over time (Kurtén, 1969; Kahlke, 1999). The skull of *U. spelaeus* is very large and is characterised by the well-defined sagittal crest and the stepped profile of the forehead in lateral view (this is also a clear distinction from the skull of *U. arctos*) (Kurtén, 1968; 1976; Torres Perez Hidalgo, 1988; Mazza and Rustioni, 1994) (see Figure 2.2). Recently, studies using CT scanning and 3D modeling of the cranial traits of *U. deningeri* have confirmed that in this species, the stepped forehead does not reach the level of development observed in *U. spelaeus* (García *et al*., 2006; Santos *et al*., 2014). The limb bones and, most particularly, the tibia, metapodials and third phalanges are shorter and more robust in *U. spelaeus* compared to *U. arctos* (Reynolds, 1906; Kurtén, 1959, 1968, 1976; Kahlke, 1999).

As with other bears, *U. spelaeus* remains show high *intra*-specific variability, which has again resulted in the description of a number of subspecies (not all of them valid);

these are reviewed by Grandal d' Anglade and Vidal Romani (1997). The differences between different geographical populations have been expressed in various ways, for example by examination of morphometric variation in cheek teeth (e.g. Grandal d'Anglade, 1993; Rabeder, 1983; 1989; Paunovic, 1988; Rabeder and Tsoukala, 1990). Rabeder (1983) developed a statistical method of morphometric analysis of the occlusal features of cave bear teeth with the aim of quantifying evolutionary trends, using the fourth upper and fourth lower premolars, and then expanding to consider the rest of the dentition, including molars and incisors (Rabeder, 1999). Nagel and Rabeder (1997) further demonstrated that this method of morphodynamic analysis can tested and corroborated by radiometric dating. However this approach is open to criticism as it is somewhat subjective and by prioritising only certain features of the tooth (e.g. measurements or structure), potentially informative data may have been discarded. As mentioned above, *U. spelaeus* had a strong tendency to split into local 'races' (Kurtén, 1968). Accordingly, several caves in high mountain areas of the Alps (e.g. in the Totes Gebirge of Austria) were described as yielding 'pygmy' or 'high-alpine small forms' (Ehrenberg, 1929). According to Rabeder (1983), the high plateaux of the Calcareous Alps were occupied by these forms during a relatively warm part of the last glaciation. The dentition of these forms was described by him as developed beyond the level of Middle Pleistocene *U. deningeri* but not to the level of that seen in contemporaneous cave bears from the lowlands. The idea that these small forms could represent more than one cave bear species that lived in Alps between 50-40 ka B.P. (Rabeder, 1995) was ultimately supported by ancient DNA analyses (Hofreiter *et al*., 2004a; Rabeder and Hofreiter, 2004; Rabeder *et al*., 2004a) and as a result, three new species were described (Rabeder *et al*., 2004a). These are *Ursus eremus* Rabeder *et al*., 2004a (holotype from Ramesch bone cave in Totes Gebirge, Austria), *Ursus ladinicus* Rabeder *et al*., 2004a (holotype from Conturines cave in Italy) and *Ursus ingressus* Rabeder *et al*., 2004a (holotype from Gamssulzen cave in Totes Gebirge Austria).

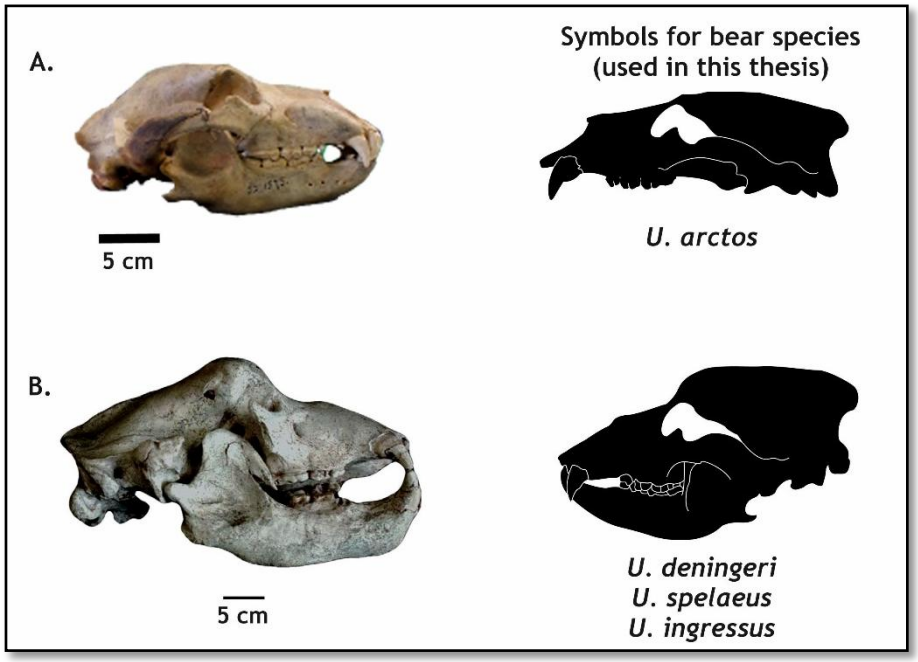

Figure 2.2. Left: Comparison of skulls of extant brown bear *U. arctos* (NHM UK Life Science department registered number: 52.1575) (A) and cave bear *U. spelaeus* from Petralona (specimen from AUTh registered number PEC 1000) (photo modified from Baryshnikov and Tsoukala [2010]). Right: Icons representing brown bear and cave bear specimens in this study. Several distinctive characteristics can be observed on the cave bear skull, including its large size, the extended diastema between canines and cheek teeth, the curve of the mandibular ramus, the doming of the forehead and the retraction of the nasal bridge.

A combination of radiometric and DNA analyses has suggested that around 50 ka B.P., a very large-bodied bear migrated into the Alps (*U. ingressus*), which had been formerly inhabited by *U. eremus* and probably *U. ladinicus* since 80ka B.P. (Hofreiter *et al*., 2004a; Rabeder and Hofreiter, 2004; Rabeder *et al*., 2004a). Interestingly, *U. ingressus* and *U. eremus* apparently coexisted sympatrically for approximately 15ka without any detectable gene flow between the two populations, leading Hofreiter *et al*. (2004a) and Rabeder *et al*., (2004a) to propose that a behavioural mechanism existed that prevented these two cave bear species from interbreeding. Currently, it is widely accepted that during the terminal Late Pleistocene, Europe was inhabited by *U. spelaeus* and *U. ingressus* (Rabeder *et al*., 2004a; 2004b; Rabeder and Hofreiter, 2004; Hofreiter *et al*., 2004a; Figure 2.3), although debate remains regarding the taxonomical position of these forms, with some authors regarding them as separate species (Rabeder *et al*., 2004a; 2004b; Rabeder and Hofreiter, 2004; Hofreiter *et al*., 2004a) and others as sub-species of *U. spelaeus* (Baryshnikov and Puzachenko, 2011).

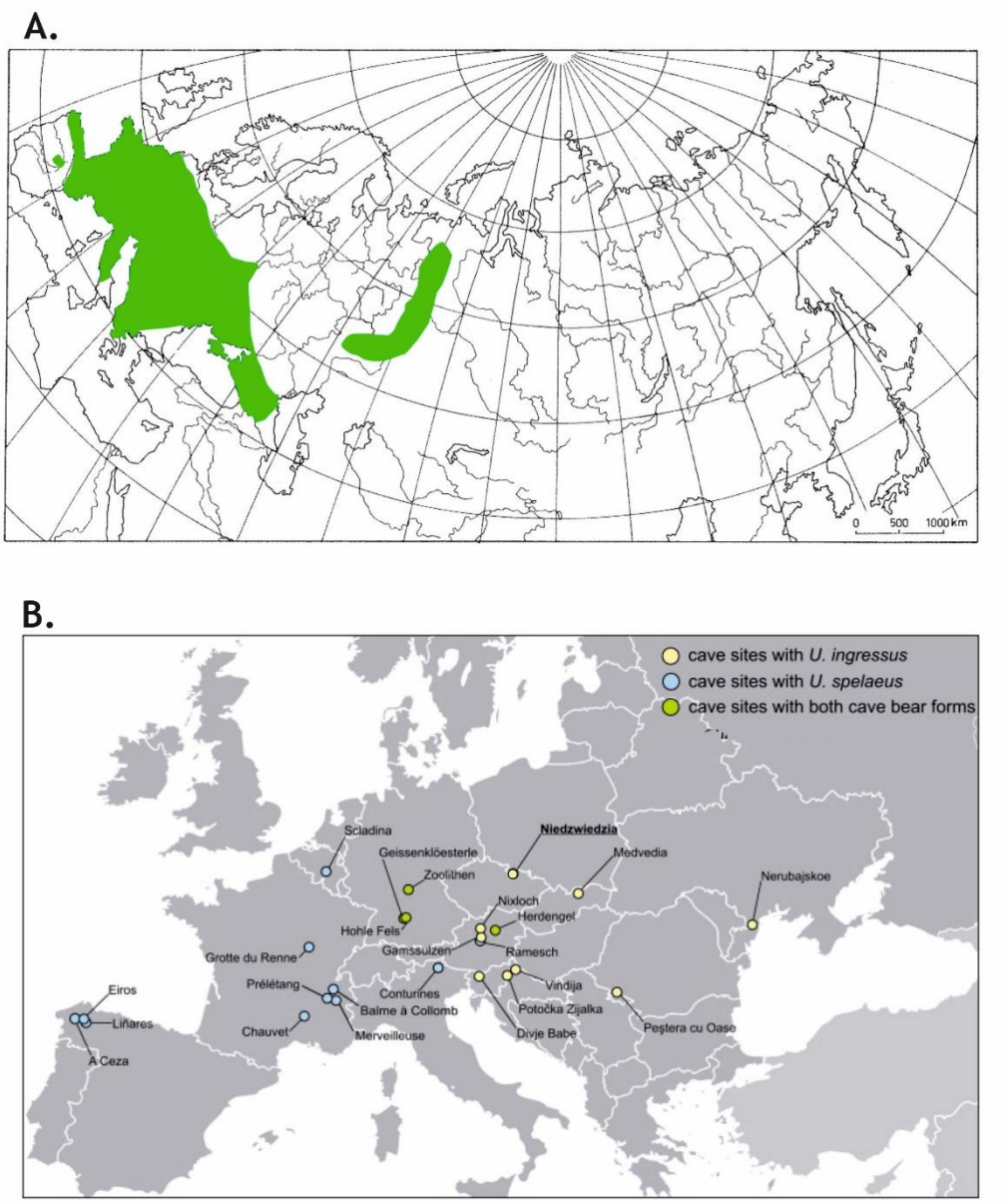

Figure 2.3. A. Map showing the Late Pleistocene geographical distribution of cave bear *U. spelaeus* (modified from Kahlke [1994]). **B.** Map showing European sites where *U. spelaeus* and *U. ingressus* remains have been identified (modified from Baca *et al*. [2014]).

Further revision has been undertaken of cave bears formerly identified as *U. spelaeus* from Greece, with material from Loutra Almopia Cave now re-assigned to *U. ingressus* (Rabeder *et al*., 2006; Tsoukala *et al*., 2006). Baca *et al*. (2014) recently suggested an earlier appearance of *U. ingressus* in the Sudeten mountains of central Europe, around 80ka B.P. based on findings from Niedźwiedzia Cave in Poland. This would imply that immigration of the species in this region occurred earlier than the colonisation of the Alps and Swabian Jura.

The geographical distribution of the cave bear group extends eastwards from northwest Spain across central Europe to the Urals and from Belgium and the Harz region of Germany in the north to Italy and Greece in the south and the Crimea in the southeast (Figure 2.3A). Figure 2.3.B illustrates the distribution of *U. spelaeus* and *U. ingressus* from sites where these species have been confirmed on the basis of molecular studies.

2.4. Size change, palaeodiet and palaeoecology in Pleistocene brown bear and cave bear species

2.4.1. Size change

It is immediately apparent that one of the most common characteristics in bears is their high *intra*-specific variability and in particular, extreme variation in body size. Although an increase in size has been a key factor in bear evolution from the Pliocene to the Pleistocene (Stirling and Derocher, 1990), the subsequent variability in size makes comparisons within and between different fossil assemblages difficult, leading to the description of many new subspecies. However, such fluctuation in size may more naturally be linked to the climatic oscillations that took place during the Pleistocene (Erdbrink, 1953; Kurtén, 1958; 1959). According to body mass calculations based on different skeletal elements, the maximum weight reconstructed for a male cave bear was around 1000kg (Kurtén, 1976; Vereshchagin and Baryshnikov, 1983, Rabeder *et al*., 2000). In general, the body size of brown bear is smaller than that of cave bear, although remains from the last glaciations are notably large (Kurtén, 1959). A particularly characteristic example is the massive brown bear noted in the Banwell Bone Cave Mammal Assemblage-Zone of the Early Devensian in Britain, correlated with MIS 5a (Currant and Jacobi, 2001; Currant, 2004).

Today, the largest bears in existence are the polar and the Kodiak bears. The males of these species can reach up to 800kg but the average is between 400 to 600kg and females are usually smaller (Christiansen, 1999a) (for ranges in size of extant brown bears see 2.7.8). It is important to mention here that the very large brown bears from Kodiak Island in Alaska (USA) have been isolated from the mainland for approximately

10,000 years and have grown to an exceptional size (males average 680 – 815kg) (Macdonald, 2009).

Within the Pleistocene bears, there are the aforementioned examples of small forms such as the Alpine cave bear species and there is also evidence that brown bears experienced a reduction in body size of up to 20% during the Late Pleistocene (Kurtén, 1960). A further important factor to be taken into consideration is sexual dimorphism. Brown bears show pronounced sexual dimorphism with a male:female weight ratio of approximately 1.5:2.0 (Silva and Downing, 1995). Sexual dimorphism was equally apparent in cave bears with evidence from both *U. deningeri* and *U. spelaeus,* with certain males significantly larger (e.g. Kurtén, 1955; Stiner, 1998; Stiner *et al*., 1998; Weinstock, 2000; Baryshnikov *et al*., 2003; Pacher, 2004; Quiles *et al*., 2005).

2.4.2. Palaeodiet

A key question related to the palaeoecology (and indeed to the extinction) of fossil bears concerns their diet. Numerous lines of evidence can be used to reconstruct past dietary habits, including dental morphology, morphometrical analysis of both cranial and postcranial elements, geochemistry and dental microwear.

Based on their dental morphology, most researchers have concluded that all species of cave bear were predominantly vegetarian, much more so than brown bears or other ursids (Erdbrink, 1953; Kurtén, 1976; Mattson, 1998; Rabeder *et al*., 2000; Grandal d'Anglade and López-González, 2005). The degree of tooth wear (the tooth enamel stage) in cave bears is usually associated with tough and abrasive food items and has further been used to reconstruct age profiles in cave bear populations (e.g. Stiner, 1998). Nevertheless, examples of occasional scavenging behaviour of cave bear remains by other cave bears have been recognised from tooth marks on bones (e.g. Pacher, 2000), while it has even been proposed at some sites that cave bears systematically exploited the carcasses of other cave bears (Pinto Llona and Andrews, 2003; Pinto Llona *et al*., 2005). However, as regards the latter behaviour, Pacher and Stuart (2009) have pointed out the difficulties in identifying not only the nature of the

damage on the remains but also in excluding the possibility that it was produced by other carnivorous species.

The largely herbivorous status of the cave bear species has been further strengthened by the fact that almost all remains of these animals have been found in caves, used by the animals for giving birth and for winter hibernation (e.g. Stiner, 1998; Stiner *et al*., 1998; Tsoukala *et al*., 2006), the latter linked to a diet of seasonally available plants and invertebrates. Caves were equally used as dens by the more omnivorous brown bear in Britain but this behaviour is rare in continental European sites (Kurtén and Anderson, 1980). The diet of modern brown bear (see Chapter 1 and below 2.8) shows some strongly seasonal and regional variability; some individuals are largely vegetarian whereas others include more than 50% meat or fish in their diet (Hilderbrand *et al*., 1998).

In recent years, researchers have developed the use of isotopic proxies to reveal information on both palaeodiet of bears and their palaeoenvironment (e.g. Bocherens *et al*., 1994a; Hilderbrand *et al*., 1996; Reinhard *et al*., 1996; Stiner *et al*., 1998; Bocherens *et al*., 2004; Richards *et al*., 2008b; Bocherens *et al*., 2011a; Dotsika *et al*., 2011). Particular attention has been given to cave bear assemblages from different sites, since aspects of their palaecology has been much debated. Bocherens *et al*. (1994a), Fernández Mosquera *et al*. (2001) and Münzel *et al*. (2011) have suggested that cave bears were herbivorous species with a diet based mainly on C3 plants. Studies on bone collagen of cave bear samples using carbon ($\delta^{13}C$) and nitrogen ($\delta^{15}N$) analysis have upheld the dental morphological conclusions that these animals were much more vegetarian than their brown bear relatives (e.g. Bocherens *et al*., 2006; 2011a). Furthermore, Bocherens *et al*. (2011a) were able to suggest ecological differentiation between two genetically distinct cave bear species, *U.* eremus and *U. ingressus*, as well as *U. arctos* from Austria. Both cave bear species were purely herbivorous but apparently consumed different plant types, whereas brown bears also included some animal protein in their diet.

In contrast, Hilderbrand *et al*. (1996), Richards *et al*. (2008b), Stiller *et al*. (2010) and Dotsika *et al*. (2011) have demonstrated that some cave bear populations showed $\delta^{15}N$ values similar to those of many modern bears such as *U. arctos* and *U. americanus,*

suggesting omnivorous to carnivorous tendencies. However, Bocherens (1998) stressed the potential for error when comparing modern specimens (usually hair and serum), which represent a short period of time, and fossil bones and teeth, which represent a much longer period of an individual's life but where the isotopic values will be time-averaged.

Richards *et al*. (2008b) identified higher $\delta^{15}N$ values in the majority of cave bears from Peštera cu Oase in Romania when compared to herbivores from the same site. Possible explanations for these differences might be the inclusion of fish into the bears' diet (Richards *et al*., 2008b; Stiller *et al*., 2010), hibernation process and/or the inclusion of different plant species in the diet (Grandal d' Anglade and Fernández Mosquera, 2008; Pérez-Rama *et al*., 2011b; Bocherens *et al*., 2011a; Grandal d' Anglade *et al*., 2011). Studies on *U. deningeri* have suggested that the isotopic signature is similar to that of *U. spelaeus* (Bocherens *et al*., 1994a; García García *et al*., 2009), whereas Stiner *et al*. (1998) has invoked a more omnivorous diet for this species.

In contrast, studies of fossil brown bears have consistently identified differences in diet compared to cave bears, largely through the consumption of more protein (Bocherens *et al.*, 1997; Stiner *et al*., 1998; Bocherens *et al*., 2011a). Perhaps unexpectedly, given the environmental constraints in operation, *U. arctos* appear to have been more carnivorous in Europe and more herbivorous in Alaska. This suggests that dietary adaptations are equally influenced by competition with other species, respectively cave bears and giant short-faced bears in those two regions (Münzel *et al*., 2011; Bocherens, 2015). Isotopic analysis on *A. simus* remains has revealed that these bears were hyper-carnivorous and consumed meat such as reindeer and muskoxen (Bocherens, 2015). Figure 2.4. presents $\delta^{13}C$ and $\delta^{15}N$ values of brown bears in eastern Beringia before and after the extinction of the giant short-faced bear and in Europe, before and after the extinction of the cave bear (from Bocherens, 2015), in order to reveal the effects of changing inter-specific competition. The $\delta^{15}N$ values for most *U. arctos* before 20ka in Beringia are subdued compared to those of *A. simus*, suggesting that the former was out-competed for meat resources by the latter and forced to adopt a more herbivorous diet, a pattern that is reversed from 20ka onwards, after the extinction of *A. simus*. For the European brown bear, $\delta^{15}N$ values in samples older than 25ka are higher than those in contemporary cave bears, indicating a more meat-based

diet, whereas younger brown bear samples show lower values, indicating a switch towards a more omnivorous diet following the extinction of the herbivorous cave bear (data from Matheus [1995], Barnes *et al*. [2002], Bocherens [2015] and references therein).

It is worth mentioning that decreasing $\delta^{15}N$ values can result not only from reduced consumption of animal protein in the diet but also from variation in soil $\delta^{15}N$ values due to climatic conditions linked with vegetation cover (Rosendahl and Grupe, 2001; Bocherens *et al.,* 2006) or by a higher amount of nitrogen-fixing plants in the animal's diet. According to Vila Yaboada *et al*. (2001), $\delta^{15}N$ values in nitrogen-fixing plants are lower than in plants that do not fix nitrogen. Geochemical studies that referred to bears physiology and/or hibernation are discussed in 5.2. and 5.3.1.3 (Chapter 5) respectively. Additionally, a separate session on available references regarding dental microwear analysis on ursids follows in Chapter 3 (in 3.2.3).

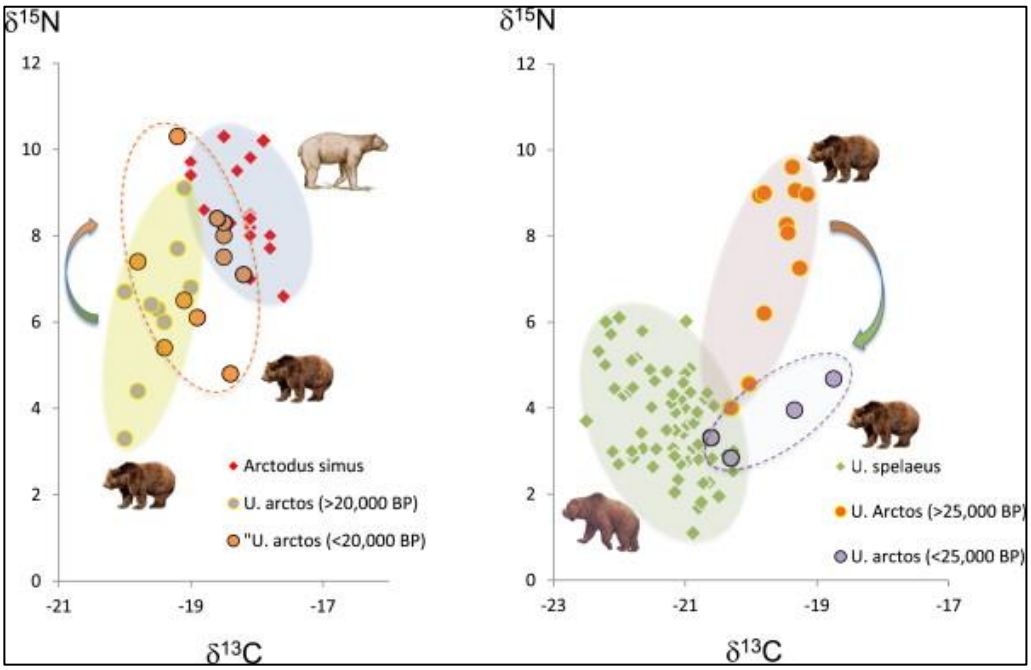

Figure 2.4. $\delta^{13}C$ and $\delta^{15}N$ values of brown bears. Left: In eastern Beringia before and after the extinction of the giant short-faced bear. Right: In Europe before and after the extinction of cave bears (after Bocherens [2015] and references therein).

2.5. Molecular phylogenies of the Ursidae

The development of molecular studies as a tool for establishing evolutionary relationships has been one of the most innovative and important developments in palaeontology.

Key divergence events within the wider Ursidae were investigated by Krause *et al*. (2008) using mitochondrial DNA (mtDNA). Figure 2.5 illustrates the resulting ursid phylogeny (with updates where applicable) and highlights the importance of the Miocene-Pliocene boundary in species diversification. According to Krause *et al*. (2008), the posterior mean of the divergence time between bears and harbor seal was estimated at 36Ma and the divergence between the giant panda and the rest of the bears has been calculated between 22.1-17.9Ma (Figure 2.5). Further studies, using not only mitochondrial but also nuclear DNA from modern bears, has recently upheld the basal position of the giant panda and the spectacled bear in the ursid evolutionary tree (Talbot and Shields, 1996a; Waits *et al*., 1999; Yu *et al*., 2007). The next divergence event is that of the spectacled bear group from the main bear lineage, which occurred between 15.6-12.4Ma, with a further split between the extant spectacled bear and the extinct American giant short-faced bear 7-5.3Ma. Between 5.4 and 4.1Ma, five modern bear lineages further diversified, the sloth bears, brown bears, American black bears, Asian black bears and sun bears (Krause *et al*., 2008). These authors also dated the divergence event between the cave and the brown bears around 3.1-2.4Ma.

MtDNA, in combination with fossil evidence, has also been used to investigate further the relationship between polar bear and brown bear, revealing the two to be sister species (Miller *et al*., 2012; Hirata *et al*., 2013). Despite the fact that the two bears are regarded as distinct species and their home ranges do not usually overlap, evidence of interbreeding (exacerbated by climate change bringing the two into contact) is increasingly noted (e.g. Doupe *et al*., 2006).

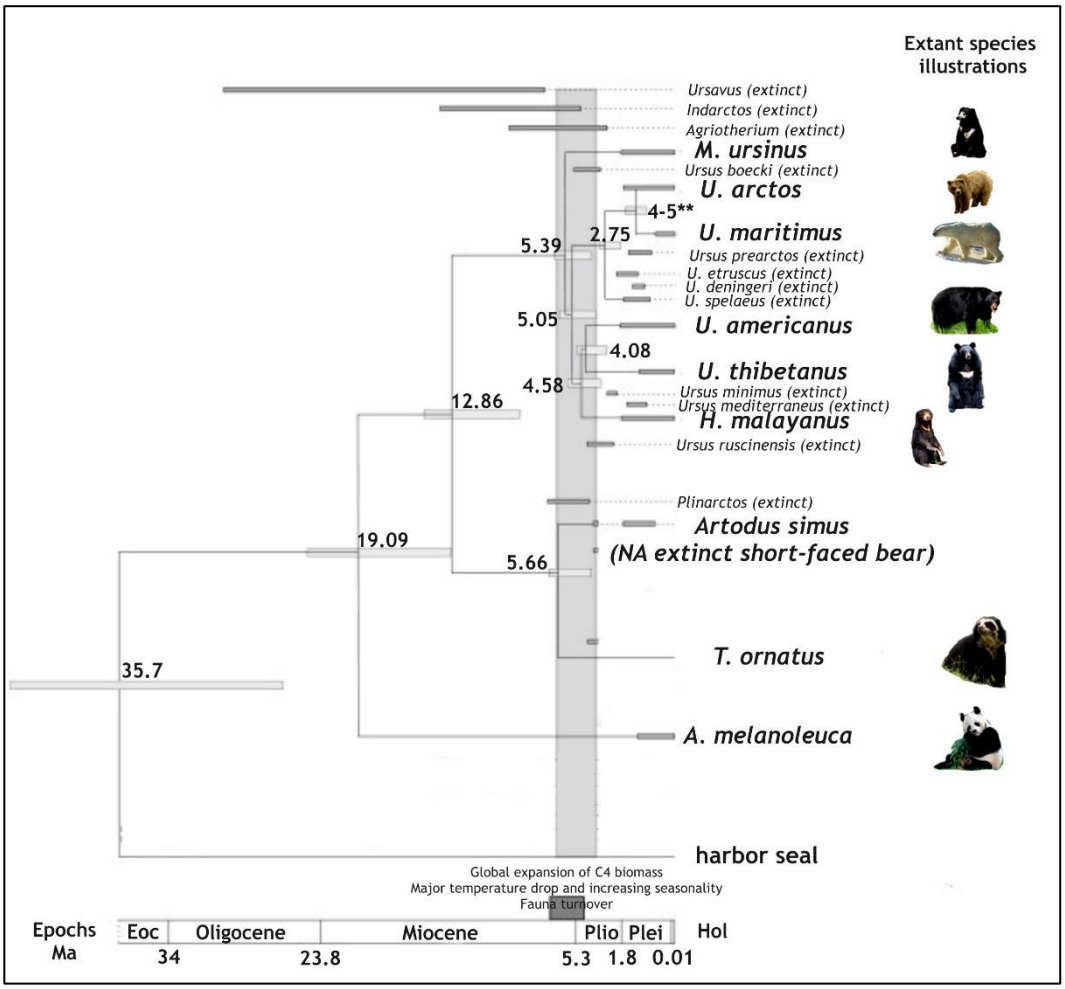

Figure 2.5. Phylogeny of extant and fossil bears (modified from Kraus *et al.* [2008] with an update of polar bear origination from **Miller *et al*. [2012]) (extant species photos modified from Wikipedia).

As well as wider genus-level definition, the Family Ursidae is a very good example in which to investigate complex speciation and rapid evolution of distinct phenotypes (Miller *et al*., 2012). Taberlet and Bouvet (1994) were the first to identify two main lineages in European brown bears, an eastern and a western one, based on partial MtDNA control region analyses. The eastern lineage is characterised by large populations, whereas the latter comprises only small fragmented populations (Taberlet and Bouvet, 1994). Studies on these geographically distinct mtDNA clades were further developed by Leonard *et al*. (2000), Barnes *et al*. (2002) and Miller *et al*. (2006). The eastern lineage is widespread across the Eurasian continent, from northeastern Europe to far eastern Russia, whereas the western lineage comprises two clades, an Iberian one and a Balkan/Italian one (Hirata *et al*., 2013 and references therein). In addition, in North America, four clades among the extant brown bears have been identified (Talbot and Shields, 1996a). As might be expected, polar bear was

not only found to be embedded within the brown bear clade but was also revealed to be closely related to clade 2a from North America, which is currently distributed in the Admiralty, Baranof and Chichagof island group of southeastern Alaska (Talbot and Shields, 1996a; Lindqvist *et al*., 2010; Miller *et al*., 2012).

Genetic analysis of fossil bear samples has revealed a number of extinct clades and subclades for both ancient brown bears (Barnes *et al*., 2002; Valdiosera *et al*., 2008) and, as mentioned, for cave bears (Hofreiter *et al*., 2004a; b; Knapp *et al*., 2009; Baca *et al*., 2014).

According to morphological and molecular data, five genera are recognized today: *Melursus*, *Ursus, Helarctos, Tremarctos* and *Ailuropoda* (after Krause *et al*. [2008]). These are presented below in Table 2.1. Nomenclature in this thesis follows Wozencraft (1989).

Table 2.1. Taxonomic designations for extant bears (after Krause *et al*. [2008])

Common name	**Wozencraft (1989) (this study)**	**Eisenburg (1981)**	**Ewer (1973)**	**Nowak (1991)**
Giant panda	*Ailuropoda melanoleuca*	*A. melanoleuca*	*A. melanoleuca*	*A. melanoleuca*
Spectacled bear	*Tremarctos ornatus*	*T. ornatus*	*T. ornatus*	*T. ornatus*
Asian black bear	*Ursus thibetanus*	*Selenarctos thibetanus*	*S. thibetanus*	*U. thibetanus*
Sloth bear	*Melursus ursinus*	*M. ursinus*	*M. ursinus*	*Ursus ursinus*
Sun bear	*Helarctos malayanus*	*H. malayanus*	*H. malayanus*	*Ursus malayanus*
Polar bear	*Ursus maritimus*	*Thalarctos maritimus*	*T. maritimus*	*Ursus maritimus*
American black bear	*Ursus americanus*	*U. americanus*	*Euarctos americanus*	*Ursus americanus*
Brown bear	*Ursus arctos*	*U. arctos*	*U. arctos*	*Ursus arctos*

2.6. Quaternary extinctions and the Ursidae

The topic of megafaunal extinctions has been the subject of intensive research for many years (e.g. Barnosky *et al*., 2004; Stuart *et al*., 2004; Stuart, 2005; Stuart and Lister, 2007), although the causes are still much debated and worldwide, clear differences are apparent between the pattern of extinction and the population dynamics of different species.

Cave bear extinction from northern Eurasia took place during the last Glacial-Interglacial transition (Barnosky *et al*., 2004). Kurtén (1976) suggested that the species survived the Last Glacial Maximum (LGM) and according to Pacher and Stuart (2009), it became extinct from central Europe at about 27,800cal yr BP. The disappearance of the cave bear from central Europe coincides fairly closely with the cooling climate and vegetational changes around the LGM (Pacher and Stuart, 2009).

As already explained in 2.4.2, cave bears appear to have been predominantly vegetarian and most probably heavily reliant on high-quality plant food; thus they would have been vulnerable to deteriorating vegetational productivity and quality (Pacher and Stuart, 2009). In addition, in contrast to brown bears, which during the Late Pleistocene had a wide geographical range, cave bears had a much more restricted range. As Pacher and Stuart (2009) pointed out, this fact in combination with a more herbivorous diet, may have made this species more vulnerable to extinction in the facing of climatic deterioration.

Furthermore, due to their large size, cave bears were also more vulnerable to extinction and as with all large animals, they existed in smaller populations than smaller mammal and had much slower reproduction rate, both factors that counted against them (Lister and Bahn, 2007).

The theory that humans may have been involved in cave bear extinction has little evidence to support it (e.g. Pacher, 1997; 2002). In addition, investigations in several Alpine cave sites reported that cave bears and humans used particular caves at different times (e.g. Pacher, 2000; 2004).

Brown bears were, however, exterminated from many western European countries in 18th and 19th centuries due to intensive persecution by humans and the species went extinct in many countries (Enserink and Vogel, 2006; Hofreiter and Stewart, 2009). Nevertheless, brown bears survived in many other areas across the eastern Palaearctic after the end of Weichselian period (Kurtén, 1968).

In Britain, brown bears survived into the Holocene and numerous records are known, for example, from the Fens of eastern England and from Mesolithic sites such as Star Carr, Yorkshire. However, there is no evidence that the species survived into the post-

glacial period in Ireland (Schreve and Currant, 2003). It has been suggested that brown bears had become extinct in Britain by the 10th Century AD, even though there is little evidence for their survival much beyond the Roman period (Yalden, 1999). Two of the most recent archaeological examples with ^{14}C dates come from a Bronze age site at Ratfyn, Wiltshire (at 3500 b.p.) and the other from northern Scotland (at 2673 b.p.) (Schreve and Currant, 2003 and references therein).

2.7. The Ursidae today

All modern bears except *Tremarctos ornatus* and *Ursus maritimus* (in part) inhabit Eurasia. The following sections describe each extant species in terms of its morphology, range and ecology.

2.7.1. *Helarctos malayanus* Raffles, 1821, sun bear or honey bear

H. malayanus today occupies Southeast Asia (Figure 2.6.), coexisting with two other bear species, *U. thibetanus* and *M. ursinus* throughout Asia and eastern India respectively (Macdonald, 2009). The type locality of the species is Sumatra in Indonesia (Wilson and Reeder, 2005). The main habitat for this species is the tropical rain forest (encompassing a great variety of forest types), although some groups have also been observed in ecosystems that have a long dry season (Fredriksson *et al*., 2008). The altitudinal range occupied varies from sea level to over 2,100 m, although lower altitudes seem to be preferred (Fredriksson *et al*., 2008).

This species is one of the smallest in size amongst modern bears. Body size ranges and other biological information, including the dental formula and reproduction, are presented in Figure 2.6. Since the sun bear has access to food year round, it does not hibernate (Fredriksson *et al*., 2008). *H. malayanus* is a largely arboreal animal, usually nesting in trees for sleeping (Macdonald, 2009). The most remarkable characteristics of the sun bear's appearance are the 'necklace-like' mark on the chest, which forms a white circle or semicircle shape on the dark coat, and its long tongue (up to 25cm), which is used for consuming insects and honey (Augeri, 2005; Fredriksson *et al*., 2006). Further details of the diet of this species are given in 2.8. As a skilled climber of trees, it

descends from the trees hind feet first (Erdbrink, 1953). The forelimbs are turned inward (Augeri, 2005) and very strong and sharp claws are present on both fore and hind feet. These are strongly recurved and laterally flattened; the size of the claws is remarkably large compared to the rest of the body (Erdbrink, 1953).

Erdbrink (1953) further remarked on the breadth and shortness of the skull in this species, the broadness of the nasal cavity, the short, thick mandible and the very high (near vertical) symphysis. The total number of teeth is 40, however some reduction in the number of the premolars has been observed (Figure 2.6).

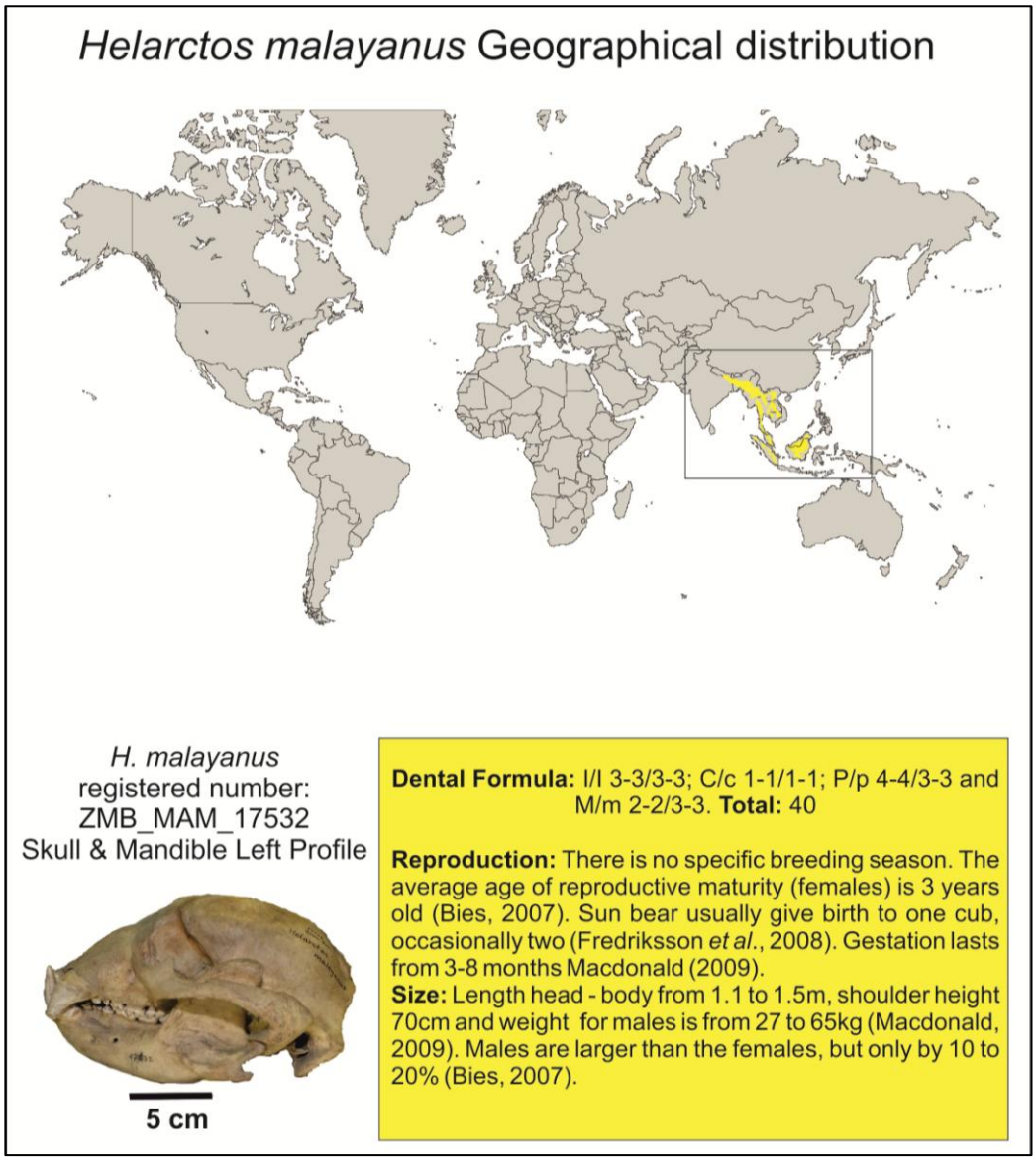

Figure 2.6. Summary information for *H. malayanus* including geographical distribution (map from Fredriksson *et al*. [2008]), the skull and mandible (lateral view) and additional biological details.

2.7.2. *Melursus ursinus* Shaw, 1791, sloth bear

M. ursinus lacks the first upper incisors, a feature shared with modern sloths and from where its name derives (Erdbrink, 1953). Sloth bears are found in India, Nepal, Sri Lanka and Bhutan (Gashelis *et al*., 2008b). Body size ranges and other biological information, including the dental formula and reproduction, are presented in Figure 2.7.

M. ursinus inhabits lowland ecosystems including wet or dry tropical forests, savannas, scrublands and grassland (Garshelis *et al*., 2008b and references therein; Macdonald, 2009) and does not hibernate. By nature, they are solitary animals except for the mating period and when females are with their cubs (Stirling, 1993). According to Akhtar *et al*. (2007), sloth bears deliver their cubs in "day dens", which are used as a shelter after nocturnal foraging. This species will also climb trees in order to find honeycomb (Macdonald, 2009). Further details of the diet of this species are given in 2.8.

In appearance, the sloth bear has a long, mealy-coloured snout and a white or yellowish V or Y-shaped chest mark on an otherwise dark coat, hook-like claws adapted for digging and protuberant lips and tongue (Erdbrink, 1953). The sloth bear has no post-canine biting space as seen in other ursids. It has a broad palate that facilitates sucking, the premolars are always present, the M1 (upper first molar) has a rectangular-shaped crown roughly equal in size to that of the M2 (upper second molar) and the five digital pads on the hind feet are aligned (Erdbrink, 1953). According to Figueirido *et al*. (2009), this insectivorous bear has a more developed symphyseal region, more outwardly-directed canines and reduced post-carnassial molars. Although similar in body mass to *U. americanus* and *U. thibetanus*, the skull of the sloth bear is considerably longer (average length from premaxilla to occipital condyles: 287.47mm) and can sometimes reach the length of that seen in the largest brown bears (Christiansen, 2007).

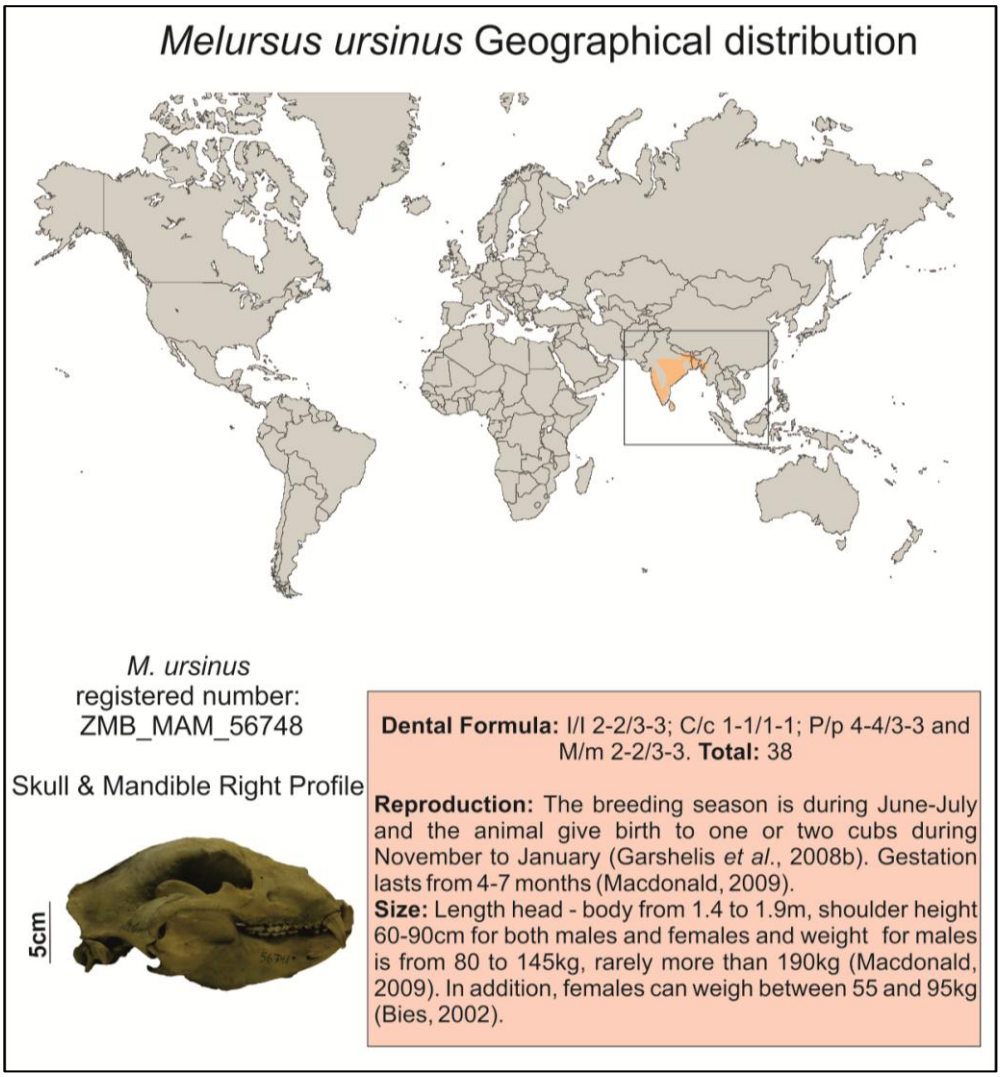

Figure 2.7. Summary information for *M. ursinus* including geographical distribution (map from Gashelis *et al*. [2008b]), the skull and mandible (lateral view) and additional biological details.

2.7.3. *Tremarctos ornatus* F. G. Cuvier, 1825, spectacled or Andean bear

T. ornatus is the only modern bear species to inhabit South America, where it is the second largest land mammal (Macdonald, 2009). The name spectacled bear derives from the distinctive circular or semicircular almost white markings around the eyes. Body size ranges and other biological information, including the dental formula and reproduction, are presented in Figure 2.8. *T. ornatus* is non-hibernatory, since it can find food throughout the year, and its activity pattern ranges from diurnal to mixed diurnal and nocturnal (Goldstein *et al.*, 2008). They are versatile animals and occupy a great variety of habitats, from desert scrub to forests to high altitude grasslands ranging in elevation from 250 to 4,750m above sea level (Goldstein *et al*. 2008).

Although most bears are tree climbers, this skill is essential in *T. ornatus* in its arboreal habitat, from where it sources all its food. Further details of the diet of this species are given in 2.8. Its vegetarian diet is highlighted by the morphology of the skull and mandible, in particular the presence of a short and concave mandible, a deep horizontal ramus, a large masseter and temporalis muscle and large lower post-carnassial molars (Christiansen, 2007; Figueirido *et al*., 2009).

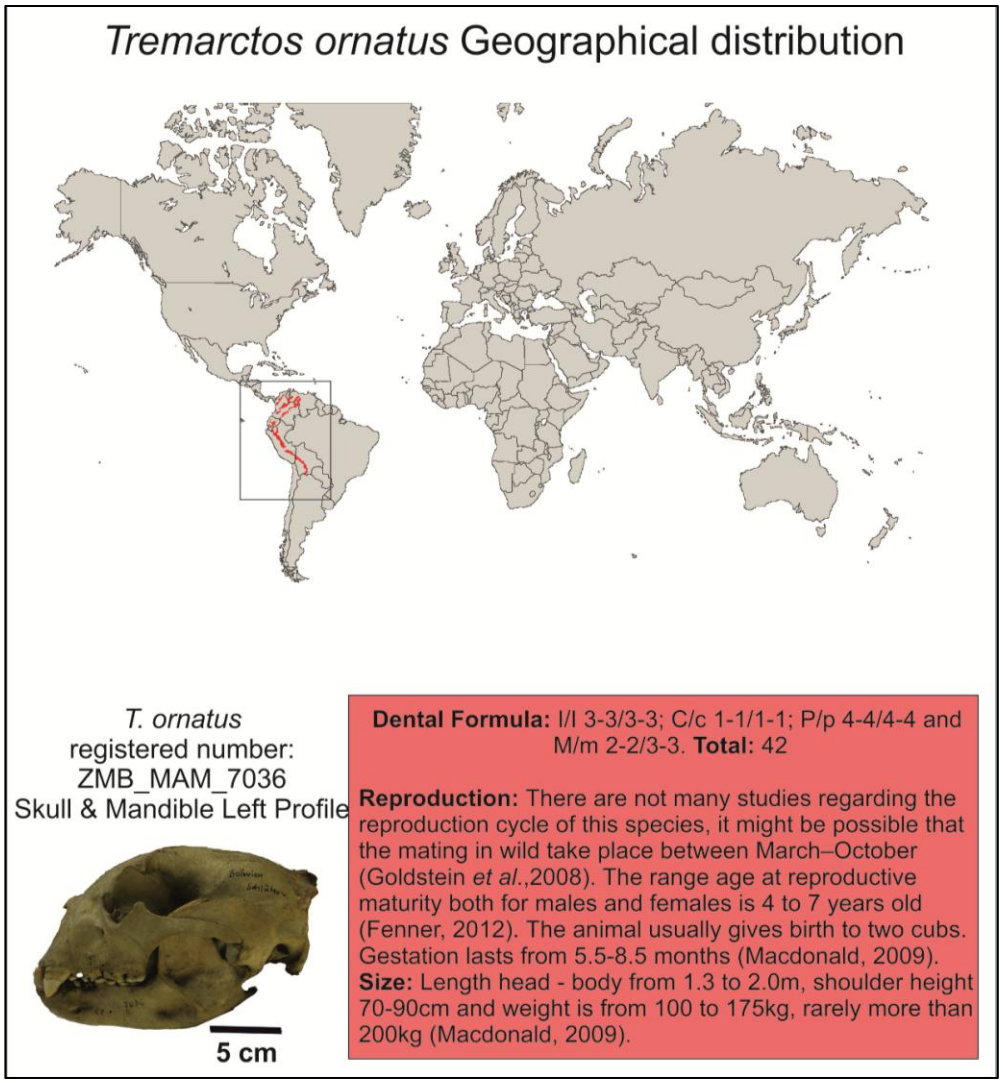

Figure 2.8. Summary information for *T. ornatus* including geographical distribution (map from Goldstein *et al.* [2008]), the skull and mandible (lateral view) and additional biological details.

2.7.4. *Ailuropoda melanoleuca* David, 1869, giant panda

A. melanoleuca is a distinctive species with black and white fur and very characteristic black patches on the eyes and ears. Giant pandas are restricted to south-central China (Figure 2.9). Body size ranges and other biological information, including the dental formula and reproduction, are presented in Figure 2.9.

The giant panda occupies temperate montane forests with dense bamboo vegetation, ranging in altitude from 1,200 to 4,100m above sea level (Lü *et al*., 2008). Pandas do not hibernate but in order to find sufficient food during the winter period, they move below 1,950m elevation, returning in summer to sites above 2,160m (Liu *et al*., 2002). In order to facilitate handling of the bamboo stems on which they depend, the species has evolved one of its wrist bones into a "pseudo thumb" (Davis, 1964; MacDonald, 2009). Further details of the diet of this species are given in 2.8. According to Christiansen (2007), the giant panda has a higher bite force in comparison to its body size and a more specialised craniodental morphology than any other bear species.

The giant panda fore foot is short and powerful and the digital pads are elliptical in outline with the fifth toe being slightly smaller from the rest (Davis, 1964). The hind foot is slightly narrower than the fore foot and the claws are strongly compressed and narrow, tapering from a wide base to a sharp tip (Davis, 1964). This species has a short tail (as in all bear species) but longer than that of the other ursids.

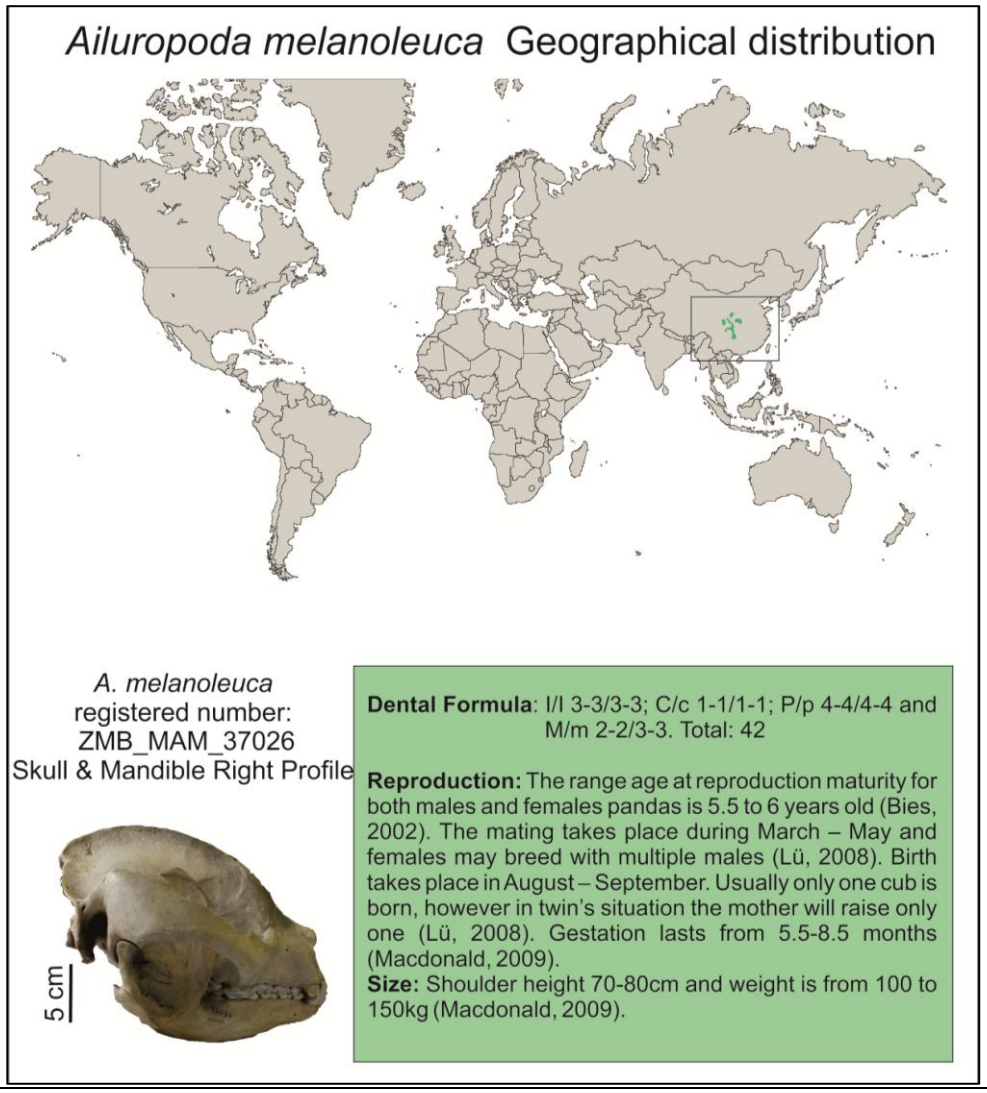

Figure 2.9. Summary information for *A. melanoleuca* including geographical distribution (map from Lü *et al*. [2008]), the skull and mandible (lateral view) and additional biological details.

2.7.5. *Ursus maritimus* Phipps, 1774, polar bear

U. maritimus is the largest of the world's bear species. It has a distinctive white coat (sometimes yellowish in summer) for camouflage in its Arctic habitat (Miller, 1912; Macdonald, 2009). Polar bears have a circumpolar distribution in the northern hemisphere, occurring in Asia, Europe and North America (see Figure 2.10) and they make long-distance annual migrations from their traditional winter ranges to remnant high-latitude summer sea ice (Durner *et al*., 2009). Body size ranges and other biological information, including the dental formula and reproduction, are presented in Figure 2.10.

U. maritimus has a unique metabolism adapted to living in cold conditions, which can be switched from a normal state to a slow, hibernation-like condition at any time of the year (Nelson *et al*., 1983; Macdonald, 2009). Polar bear premolars and molars are sharper than the flat grinding teeth of other ursids, indicating a more carnivorous diet (Macdonald, 2009). Further details of the diet of this species are given in 2.8.

According to Sacco and Van Valkenburgh (2004), carnivorous bears such as polar bear exhibit reduced molar grinding areas, as well as having relatively small carnassial blades (as seen in omnivorous canids), believed to reflect relative prey size, relative prey vulnerability and seasonal variation in diet. For example, the low leverage (the operation of most skeletal muscles involves leverage) of polar bear signifies that they hunt animals much smaller than themselves, relying on their muscular strength rather than on craniodental adaptations (Sacco and Van Valkenburgh, 2004). Polar bears have reduced moment arms on the masticatory muscles, a deeper rostrum and a longer diastema between canines and cheek teeth compared to other bears (Figueirido *et al*., 2009). *U. maritimus* is a great swimmer. The fore paws are large and oar-like with slightly webbed toes; the hind feet serve only as rudders (Macdonald, 2009).

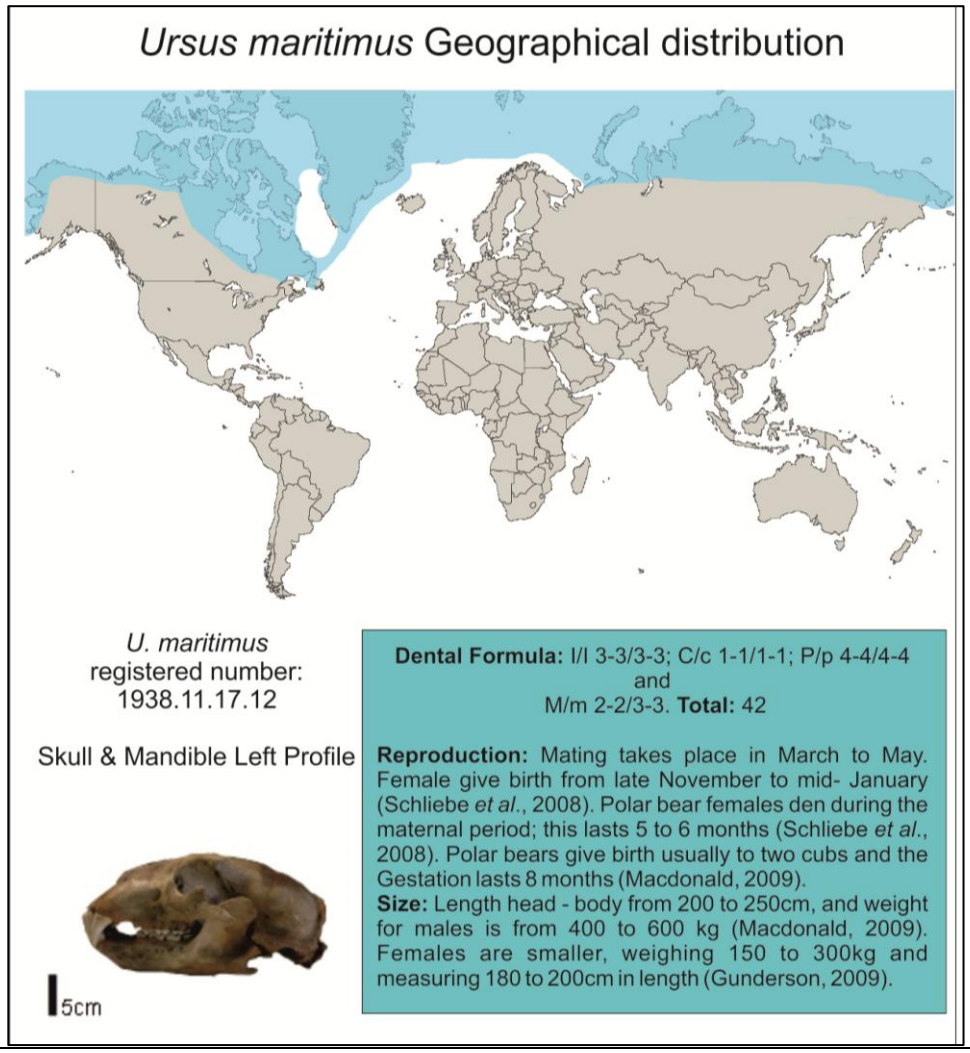

Figure 2.10. Summary information for *U. maritimus* including geographical distribution (map from Wiig *et al*. [2015]), the skull and mandible (lateral view) and additional biological details.

2.7.6. *Ursus americanus* Pallas, 1780, American black bear

The American black bear is so named after its fur colour, despite the coat varying from light cinnamon to dark charcoal, variation that may be related to the different geographical areas that the species occupies (Macdonald, 2009). Today, 16 subspecies are recognized (Wilson and Reeder, 2005) extending across North America from Canada to Mexico (Dobey *et al*., 2005; Garshelis *et al*., 2008a; Frary *et al*., 2011) (Figure 2.11.) and broadly overlapping in range with the North American grizzly bear, *U. arctos horribilis*. The species is also very common, twice as numerous as all other bears put together (Macdonald, 2009). Body size ranges and other biological information, including the dental formula and reproduction, are presented in Figure 2.11.

American black bears hibernate and follow the same four physiological stages (see also 5.3.1.3 [Chapter 5]) as the brown bear (Nelson *et al*., 1983). Although they are a primarily temperate and boreal forest species, they are very adaptable and they also occur in subtropical areas and rainforests, subarctic zones and tundra, and dry scrub forests (Garshelis *et al*., 2008a), ranging in altitude from sea level to 3,500m above sea level. In order to acquire food, black bears are adapted to climb trees, although they have smaller claws than other bear species (Macdonald, 2009). Further details of the diet of this species are given in 2.8. The skull of *U. americanus* is relatively small and straight in profile (Figure 2.11) and their lower bite force compared to, for example, the sloth bear or Asian black bear, highlights their omnivorous diet (Christiansen, 2007).

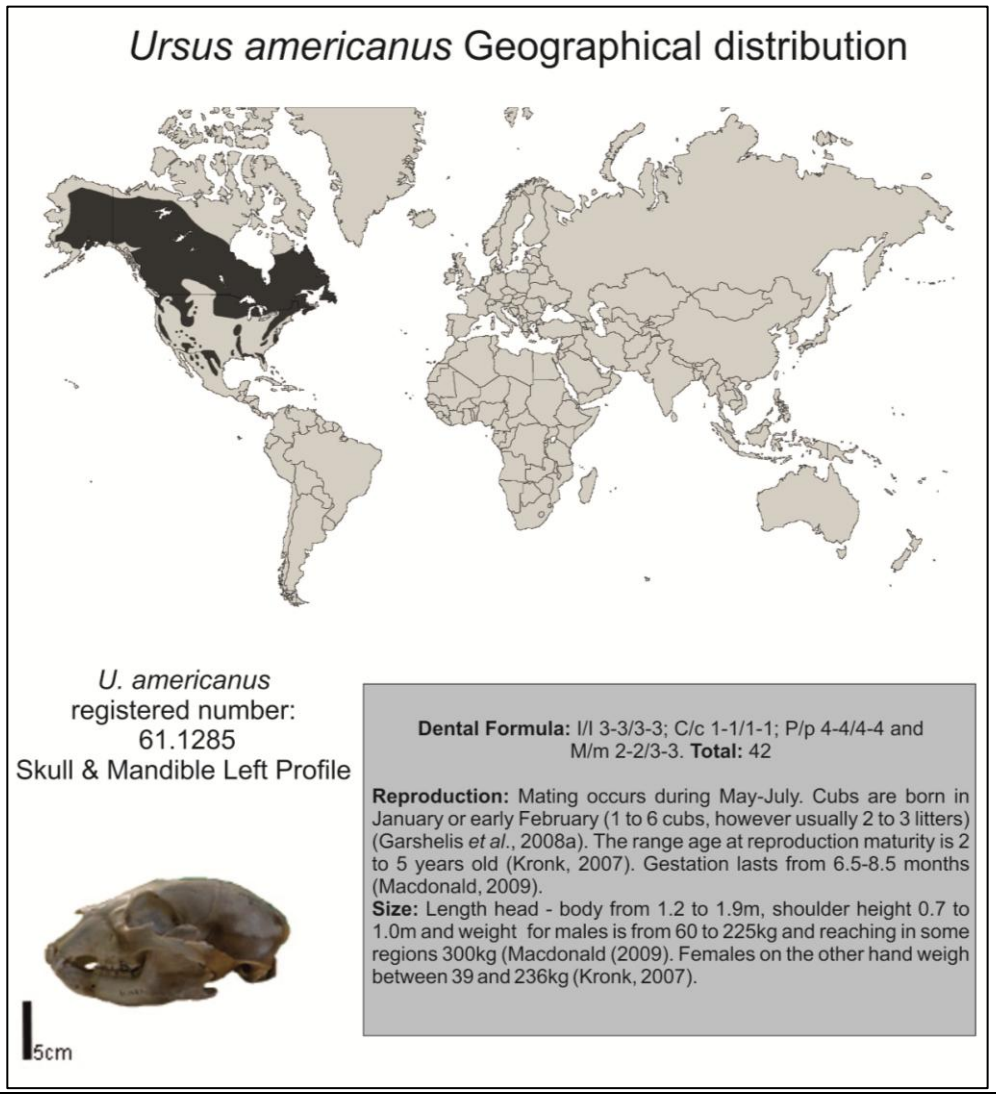

Figure 2.11. Summary information for *U. americanus* including geographical distribution (map from Garshelis *et al*. [2008a]), the skull and mandible (lateral view) and additional biological details.

2.7.7. *Ursus thibetanus* Cuvier, 1823, Asian black bear

U. thibetanus is similar in size and skull morphology to *U. americanus*. Today, seven subspecies are recognized (Wilson and Reeder, 2005). The main characteristic of *U. thibetanus* is the white crescent-shaped mark on its chest, against an otherwise black coat. This distinctive feature has given rise to its other name of "moon bear" (Macdonald, 2009). The species can be found in Iran, Afghanistan and Pakistan, across Southeast Asia, China and Korea (Garshelis and Steinmetz, 2008) (Figure 2.12). Body size ranges and other biological information, including the dental formula and reproduction, are presented in Figure 2.12.

Asian black bears inhabit a variety of forest habitats, including coniferous, temperate broad-leaved, subtropical and tropical (Garshelis and Steinmetz, 2008; Macdonald, 2009). In mountainous regions, they range as high as 4,300m above sea level during summer and in winter to about 1,500m or lower (Garshelis and Steinmetz, 2008). Further details of the diet of this species are given in 2.8.

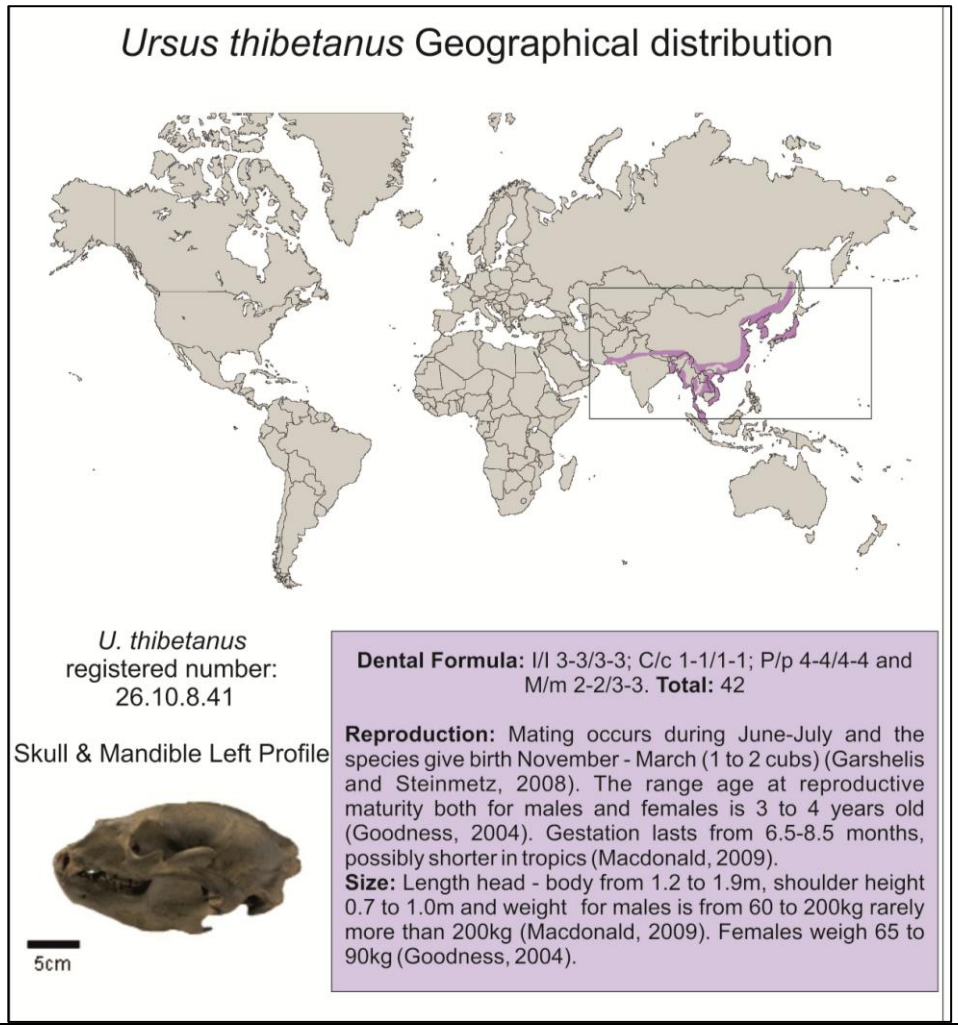

Figure 2.12. Summary information for *U. thibetanus* including geographical distribution (map from Garshelis and Steinmetz [2008]), the skull and mandible (lateral view) and additional biological details.

2.7.8. *Ursus arctos* Linnnaeus, 1758, brown bear

U. arctos is globally the most widely distributed bear species. Sixteen subspecies of brown bear are recognised today (Wilson and Reeder, 2005), including the grizzly bears in N. America (*U. a. horribilis* Ord, 1815), the Himalayan brown bear (*U. a. isabellinus* Horsfield, 1826) and the Kamchatka brown bear (*U. a. beringianus* Middendorff, 1851), the last being one of the largest forms of brown bear at present. The body size and the diet of *U. arctos* vary greatly according to their geographical distribution and the different habitats occupied (Figure 2.13). Body size ranges and other biological information, including the dental formula and reproduction, are presented in Figure 2.13, while diet is outlined in 2.8 below (see also Chapter 1).

The largest populations are found in North America and Europe at the present day and the species is relatively abundant in Canada, Alaska and Russia (Miller *et al*., 1997; McLellan *et al*., 2008). Smaller populations are found scattered across Asia, in the Himalayas, Mongolia, India, Japan and China, in the southern regions of North America and in southern Europe (McLellan *et al*., 2008). This wide distribution reflects the diverse range of habitats that the species occupies including temperate forests, rain forests, Arctic shrub lands to open alpine tundra, dry Asian steppes and even desert or semi desert (McLellan *et al*., 2008; Macdonald, 2009). Some populations overlap with *U. americanus*, *U. thibetanus* and *U.maritimus*.

In appearance, *U. arctos* has a variable brown or buff colour with the legs and feet being usually darker. The skull is rather robust, the rostrum moderately long, the brain case deep but not unusually wide, the profile nearly straight and ventral profile faintly and evenly concave throughout and the mandible is robust with a broad coronoid process (Miller, 1912). According to Christiansen (2007), *U. arctos* has a relatively tall and thick mandibular symphysis with a moderate bite force.

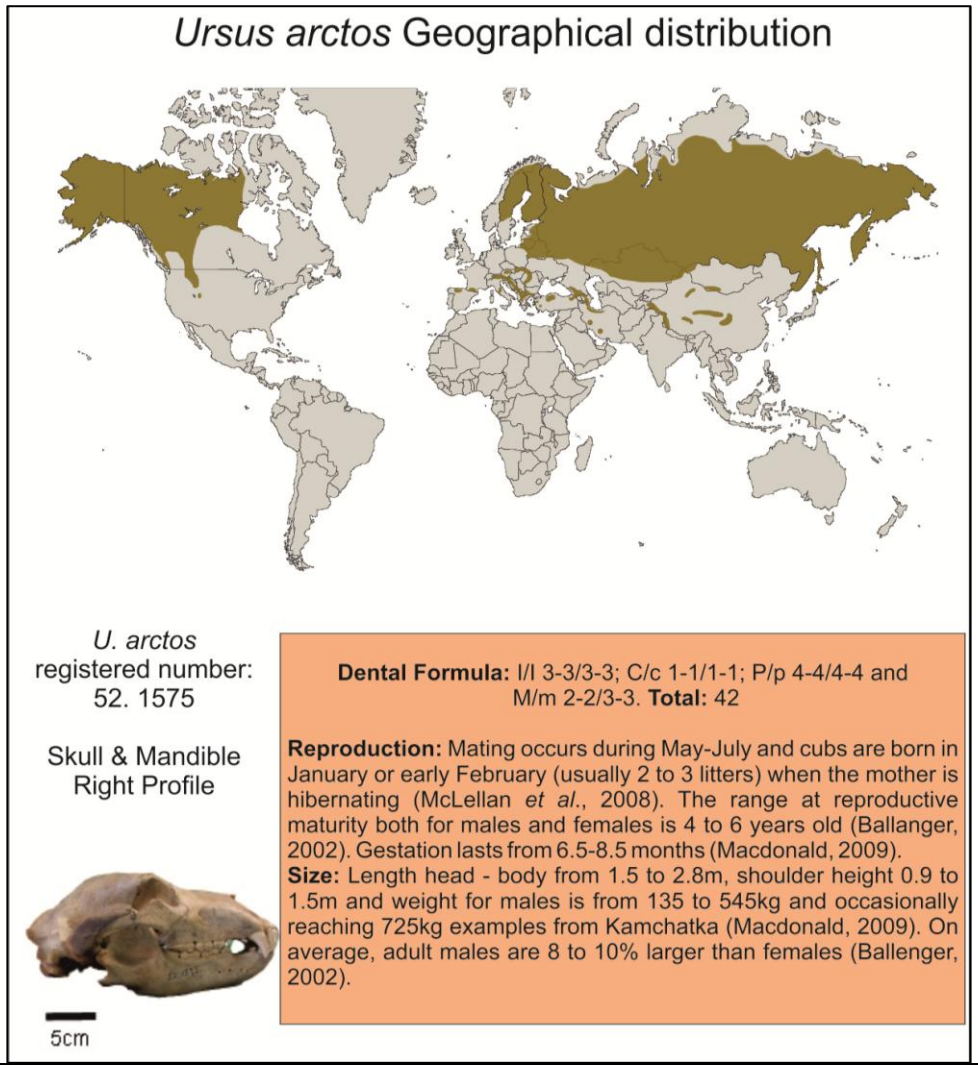

Figure 2.13. Summary information for *U. arctos* including geographical distribution (map from McLellan *et al.* [2008]), the skull and mandible (lateral view) and additional biological details.

2.8. Diets of extant bears

The large variation in modern bear diet has previously been referred to in Chapter 1. Table 2.2 summarises the dietary preferences of the extant species that have been included in this study, with the most commonly-consumed items marked in bold. The term "hard mast" refers to fruits and seeds with a hard protective covering (including both acorns and pine nuts) and "soft mast" refers to fleshy fruits, strobili and leaves (after Mattson, 1998).

A. melanoleuca is a herbivore and subsists almost exclusively on bamboo shoots, stalks and leaves and very occasionally scavenging and rodent predation (Davis, 1964; MacDonald, 2009).

T. ornatus. Although the diet of the spectacled bear varies according to habitat, it consists predominantly of vegetable material including fruits, plants, cactuses and, very occasionally, meat (Peyton 1980; Goldstein *et al*., 2008; Macdonald, 2009). The most prevalent food is soft mast, although hard mast and invertebrates may also be consumed (Peyton 1980; Goldstein *et al*., 2008).

U. thibetanus consumes leaves, shoots, insects, a variety of fruits, nuts and, in some areas, meat. Diet varies seasonally but the predominant food is hard mast (Huygens *et al*., 2003; Garshelis and Steinmetz, 2008; Koike *et al*., 2012).

M. ursinus has a rather specialised insectivorous diet, feeding mainly on termites and ants (Joshi *et al*., 1997), the only bear to do so (see also table 2.2).

H. malayanus consumes fruit, insects, honey and occasionally meat (Ewer, 1973), with variation on a seasonal basis (Fredriksson *et al*., 2006). The predominant food is insects with a component of soft mast (Augeri, 2005; Fredriksson *et al*., 2006).

U. maritimus has a highly specialised hypercarnivorous diet, preying almost exclusively on seals (Derocher *et al*., 2002) but with occasional fish, sea birds and their eggs and carrion (Ewer, 1973).

U. americanus feeds on a wide range of food, including nuts, fruits, roots, insects, vertebrates and fish. Their diet varies seasonally and regionally (Bennett *et al*., 1943; Garshelis et al., 2008a; Macdonald, 2009; Frary *et al*., 2011) but the predominant food type is soft mast (Cottam *et al*., 1939; Hilderbrand *et al*., 1999; Fortin *et al*., 2007).

U. arctos consumes a wide range of fleshy fruits, nuts, fish and vertebrates depending on season, region and probably competition with other bear species (see also Chapter 1). The predominant foods are marked in Table 2.2. (after Mattson, 1998; Vulla *et al*., 2009; Bojarska and Selva, 2012), although it should be noted that for North American *U. arctos*, both soft mast and vertebrates are highlighted because these bears consume more of the former than other brown bear populations (Bojarska and Selva, 2012). Overall, brown bears are substantially more carnivorous when compared with *U. americanus* (Mattson, 1998).

Table 2.2. Dietary groupings of food items consumed by each extant bear species used in this study. Bold type denotes the predominant food types.

	Dietary Grouping			
Species	**Term-Group**	**Symbols**	**Description**	**References**
A. melanoleuca	**Foliage**		Exclusively bamboo	(Davis, 1964; Mattson, 1998)
T. ornatus	Hard mast		Fruits, insects and berries	(Peyton, 1980)
	Soft mast			
	Invertebrates			
U. thibetanus	**Hard mast**		Insects, fruits with seeds and flesh	(Mattson, 1998; Huygens *et al*., 2003)
	Soft mast			
	Invertebrates			
	Vertebrates			
M. ursinus	**Invertebrates**		Mainly termites but also ants, bees and beetles.	(Joshi *et al*., 1997; Bargali *et al*., 2004; Ramesh *et al*., 2009)
	Soft mast			
H. malayanus	Soft mast		Fibrous food (leaves and flowers) as well as fruits and insects	(Augeri, 2005; Fredriksson *et al*., 2006)
	Invertebrates			
U. maritimus	**Vertebrates**	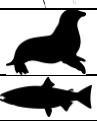	Mainly seals but also fish	(Rugh and Shelden, 1993; Derocher *et al*., 2002)
U. americanus	**Soft mast**		Mostly fibrous food (leaves and flowers) as well as soft fruits and occasionally fish	(Cottam *et al*., 1939; Bennett *et al*., 1943; Mattson, 1998; Hilderbrand *et al*., 1999; Fortin *et al*., 2007)
	Vertebrates			
U. arctos, Greece	**Soft mast**		Mainly fleshy fruits and green vegetation	(Vlachos *et al*., 2000; Paralikidis *et al*., 2010; Bojarska and Selva, 2012)
U. arctos, central Europe	**Hard mast**		Fleshy fruits, nuts, fish and vertebrates	(Rigg and Gorman, 2005; Bojarska and Selva, 2012)
	Soft mast			
	Vertebrates			
U. arctos, USA	**Vertebrates**		Fleshy fruits, nuts, fish and vertebrates	(Mattson, 1998; Mowat and Heard, 2006; Fortin *et al*., 2007; Bojarska and Selva, 2012)
	Soft mast			
	Hard mast			
U. arctos, Russia	**Vertebrates**	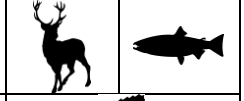	Fleshy fruits, nuts, fish and vertebrates	(Bergman, 1936; Kistchinski, 1972; Krechmar, 1995; Bojarska and Selva, 2012)
	Soft mast			

	Hard mast			
U. arctos, North Europe	Invertebrates		Fleshy fruits, invertebrate and vertebrates (more carnivorous tendencies than southern counterparts)	(Elgmork and Kaasa, 1992;Persson *et al*., 2001; Vulla *et al*., 2009; Bojarska and Selva, 2012)
	Soft mast			
	Vertebrates			

Chapter 3. Dental Microwear Analysis – Extant Species

3.1. Introduction to Dental Microwear Analysis (DMA)

One of the key questions to be addressed in this study regards the nature of Pleistocene ursid diet and the respective niches of the various species in the palaeoecosystem, in order to understand better Pleistocene palaeoecology and palaeoenvironmental change.

As outlined in Chapter 2, most modern bear species have developed an omnivorous strategy that allows them to adjust their dietary habits according to food availability in their environment. Thus, geographical and environmental variables (eg. temperature, precipitation, length of the plant-growing season, seasonality and inter-specific interactions, especially competition with other carnivores) should be taken into consideration when attempting to reconstruct the palaeodietary patterns of these animals.

This Chapter presents information on the development and general application of the Dental Microwear Analysis (DMA) technique to recent and fossil organisms, before outlining the methodologies applicable to DMA analysis of both extant (this Chapter) and extinct (Chapter 4) bear species. Dental microwear observations were first completed on specimens of extant bear species in order to produce, for the first time, a complete reference database of food types for living Ursidae. This information is then applied in Chapter 4 of this thesis to extinct bears from a range of Pleistocene sites in Britain and from a single locality in Greece, in order to derive new, quantifiable palaeodietary information for these animals

3.2. Literature Review

3.2.1. The application of DMA in palaeontology

DMA entails the study of the microscopic scars that appear on a tooth's enamel surface as a consequence of mastication. Variation in dental microwear patterns

reflects the properties of food consumed by extinct (and indeed living) mammals, thereby directly shedding light on their palaeodietary ecology.

Analysis of dental micro-abrasion or microwear of teeth is therefore a complementary method to infer primarily the diet of fossil taxa (e.g. Walker *et al*., 1978; Solounias *et al*., 1988; Solounias and Semprebon, 2002; Rivals and Deniaux, 2003; Merceron *et al*., 2004a, 2005a; Semprebon and Rivals, 2006; Semprebon and Rivals, 2007; Rivals and Athanassiou, 2008; Semprebon and Rivals, 2010) and secondly, to reconstruct jaw movements from the microwear pattern and orientation (e.g. Ryan, 1979; Gordon, 1984a, b; Charles *et al*., 2007; Williams *et al*., 2009). The method therefore adds to established vertebrate palaeontology analytical techniques such as dental mesowear and cranio-dental morphological studies.

Investigation into the dental microwear of living mammals demonstrates that marks on the occlusal surface relating to food consumption renew every few days or weeks in life, so at the point of death, the microwear patterns recorded will illustrate the final weeks of diet of the animal (Grine, 1986).

Different factors such as facet type, tooth type and instrument settings must be considered before employing DMA as these may influence the microwear pattern obtained (Ungar, 2015).

Various methods have been employed in the examination of dental microwear by researchers and a review of these studies is presented in 3.3.3. below. In order to elucidate the dietary preferences of extinct species, it is essential to establish first a comprehensive database of dental micro-features from extant species with a range of diets, against which features from extinct taxa can be compared.

Various studies have adopted this procedure, for example the microwear analytical study that was first employed on modern wild primate teeth in order to reconstruct their diet by Teaford and Walker (1984). Since it was very difficult to know exactly what each individual consumed in life, these authors selected species with distinctive diets, such as mangabey and capuchin monkeys that consumed hard objects including nuts, bark and palm fronds, colobus and howler monkeys and gorillas that ate leaves

and other tough, fibrous foods, and chimpanzees and orang-utans with broad diets but a preference for soft sugary fruits. The general observation made for primates was that hard object feeders had higher proportions of pits, the tough food consumers had more scratches, whereas the broad-diet frugivores exhibited intermediate ratios of pits and scratches (Teaford and Walker, 1984). Further studies on primate dental microwear provided further insights as to the palaeodiet and palaeoecology of some species. For example, Grine (1981) and (1986) suggested that among South African early hominins, *Australopithecus africanus* molars had more striated occlusal facets, whereas *Paranthropus robustus* molars had more heavily pitted surfaces. According to Grine, this suggested that the former ate softer foods such as fruits and immature leaves whereas the latter consumed small, hard objects such as nuts. Further studies identified even *intra*-specific differences in microwear patterns in the wedge-capped capuchin, *Cebus olivaceus* (Teaford and Robinson, 1989) and the mantled howler, *Allouatta palliata* (Teaford and Glander, 1991), reflecting seasonal and ecological zone differences in diet.

Ungar (1998) and Ungar and Lucas (2010) confirmed that primates consuming hard and brittle foods such as nuts and palm fronds have microwear surfaces dominated by pits, created by opposing teeth approaching one another to crush these items. In contrast, the consumption of tough and abrasive foods such as leaves and insect exoskeletons creates parallel microwear scratches on the enamel surface, as a result of the teeth shearing past one another in a cutting action.

Semprebon *et al*. (2004) further employed DMA on primates with known diets, as well as extant and extinct ungulates. However, instead of scanning electron microscopy (SEM), they used standard reflective light microscopy. These authors not only proved that low-magnification stereomicroscopy can reveal dietary information but also demonstrated that microwear analysis can effectively distinguish among graminivores, folivores and frugivores, as well as identifying seed predators and hard-object feeders. This study also saw the introduction of new descriptors for microwear features such as “hypercoarse” scratches and “puncture” pits (see 3.3.4).

Using DMA, researchers have consequently explored dietary regimes in various mammalian taxa and successfully used the dietary patterns revealed by specimens of extant species in order to reconstruct both palaeodiet in their fossil relatives and to explore palaeoenvironmental changes (Solounias and Semprebon, 2002; Merceron *et al*., 2004b; 2005a; b). Notably, Solounias and Semprebon (2002) produced a comprehensive database of microwear features in extant ungulates that can be used for comparison with extinct species. In the same study, the authors further demonstrated that discrete microwear features can be associated with either browsers or grazers, with the former having more pits than the latter, and the latter having more scratches than the former.

These observations can be summarised through the "Microwear Index" (MI), a ratio involving the total number of scratches divided by the total number of pits that was firstly calculated by MacFadden *et al*. (1999) and computed on SEM data. According to this index, when observations are made in a very specific enamel area such as a 0.5mm X 0.5mm square, a MI lower than 1.5 indicates a browsing diet and above 1.5, a grazing diet. Furthermore, Solounias and Semprebon (2002) showed that grazing signatures can be separated into C3 (usually with fine scratches) and C4 (usually with coarse scratches) grass-dominated diets, that browsing patterns can be distinguished between leaf and fruit feeders and finally, that mixed feeders can be divided into two types: the seasonal or regional and "meal-by-meal". According to these authors, seasonal mixed feeder ungulates vary their diets according to rainfall and seasonal variations in vegetation and when they migrate, they may alter their diet according to the availability of browse or grass. It was suggested that when these ungulate species browse, they demonstrate microwear features similar to those seen in obligate browsers, however when the same taxa graze, their results differ from those of obligate grazers by having more pits than seen in the latter (Solounias and Semprebon, 2002). In contrast, within the "meal-by-meal" mixed feeders, no discernible browsing or grazing subgroups are apparent; these mixed feeders show microwear features that lie close to the obligate grazers and to other species that display a high level of abrasion on the tooth surface (Solounias and Semprebon, 2002).

Subsequent studies on ungulates were frequently used to test, for example, the dietary plasticity of fossil species compared with their modern relatives (e.g. Merceron *et al*., 2005a; Rivals *et al*., 2007; Rivals and Semprebon, 2011). For example, a DMA study of modern North American and extinct bison revealed considerable dietary flexibility in these ungulates during the Late Pleistocene when compared to living bison and made the point that the ecology of modern relatives does not always reflect accurately the ecology of an extinct species (Rivals and Semprebon, 2011). Microwear studies have also been combined with stable isotope analyses in order to reveal palaeoenvironmental conditions. For example, Merceron *et al*. (2006) studied the permanent molars of fossil bovids from two Late Miocene localities in Bulgaria. These authors concluded that southwestern Bulgaria was dominated by open wooded landscapes where C3 graminoids grew in abundance among the herbaceous layer, while the microwear results suggested that the proportion of dicotyledons such as forbs, bushes or shrubs was probably higher in the local vegetation of one of the localities (Kalimantsi), compared to the other (Hadjidimovo-1).

Semprebon and Rivals (2007, 2010) used the same method to generate new perspectives on consumption patterns in the Artiodactyla (Camelidae and Antilocapridae families), demonstrating that the same species may feed differently depending on geographical area. In both studies, the authors suggested that it is possible through microwear analysis to identify the influence of dust and grit, which is ingested if the animals feed either close to the ground or on leaves, especially in arid and more open environments.

Regarding the etiology of microwear, previous studies have attempted to examine the relative influence of phytoliths (endogenous plant silicates) and exogenous grit from soil (Baker *et al*., 1959) on dental microwear. Walker *et al*. (1978) compared the microwear pattern of the bush hyrax (*Heterohyrax brucei*), which is a browser on trees and shrubs, with that of the rock hyrax (*Procavia* johnstoni), a seasonal grazer that consumes mostly grass, especially during the rainy season. These authors found that the rock hyraxes had more microwear striations on their teeth in the wet season than either rock hyraxes sampled during the dry season or bush hyraxes. However, dust particles were present in the faecal pellets of both species, hence as it is clear that

phytoliths were ingested in quantity by *P. Johnstoni*, it seems very likely that these silicified plant cells, rather the dust particles, were the cause of the microscratches (Walker *et al*., 1978).

Microwear analysis has also been successfully used to explore dietary patterns in proboscideans (Green *et al*., 2005; Palombo *et al*., 2005; Todd *et al*., 2007; Rivals *et al*., 2010; Rivals *et al*., 2012). Green *et al*. (2005) studied Pleistocene mastodon (*Mammut americanum*) from Florida and reconstructed a similar dietary profile to that the extant black rhinoceros (*Diceros bicornis*), a well-established browser that uses its prehensile lips for gathering leaves and twigs. Most recently, a detailed study of Pleistocene *Mammuthus* (mammoth), *Palaeoloxodon* (straight-tusked elephant) and *Mammut* specimens from Europe and North America has similarly revealed extensive dietary plasticity in these three lineages (Rivals *et al*., 2012).

Microwear features have also been used by Nelson *et al*. (2005) to infer the diets of extant squirrels. These authors successfully demonstrated differences in the association of microwear scars linking with differences in the known diets of modern squirrels; this approach is very promising for future studies using the ecomorphology of small mammal fossils. More recently, Purnell *et al*. (2013) tested the hypothesis that dental microwear should differ within a guild of small-bodied insectivores through 3D analysis of microwear textures, focussing on the greater horseshoe bat (*Rhinolophus ferrumequinum*), a mixed feeder that includes more 'hard' prey such as Coleoptera in its diet, the soprano pipistrelle (*Pipistrellus pygmaeus*), a dipteral specialist, mainly consuming 'softer' prey, the common pipistrelle (*Pipistrellus pipistrellus*), which consumes both soft Diptera and some 'hard' species, and the common long-eared bat (*Plecotus auritus*), a 'soft' prey consumer specialising on Lepidoptera. According to the results, the four bat species occupy largely non-overlapping dietary ecospaces, with a clear separation between the species that consume the 'hardest' prey (*R. ferrumequinum*) and the 'soft' prey specialist (*P. auritus*).

Aside from mammalian herbivores, DMA has been attempted with aquatic vertebrates in order to explore trophic ecology in fish (Purnell *et al*., 2006). It has further been

applied to dinosaurs (hadrosaurid ornithopods, the dominant terrestrial herbivores of the Late Cretaceous) and has proved to be a very promising method for further exploring jaw movements and dietary preferences in reptiles (Williams *et al*., 2009). More specifically, Williams *et al*. (2009) demonstrated that *Edmontosaurus* teeth preserved four distinct sets of scratches aligned in different orientations, indicating an isognathic, near vertical, postero-dorsal power stroke during feeding and suggesting that this genus was a grazer rather than a browser.

One of the most recent microwear studies published has been undertaken on conodont specimens, where DMA was combined with finite element, occlusal and microstructural analyses (Martínez-Pérez *et al*., 2014). The microwear results from this study revealed that on conodont tips, both sides of the denticles exhibit polishing, suggesting either contact occurred between elements in the absence of food or contact occurred with nonabrasive food.

3.2.2. DMA applications in carnivores

In terms of application to mammals, it can therefore be seen that DMA has been successfully applied to primates and to a wide variety of herbivores, including ungulates and proboscideans. In addition, the technique has also been applied to living and fossil carnivores, however, in a rather less comprehensive way than in herbivores. Van Valkenburgh *et al*. (1990) carried out a key study on carnivores, in order to explore the feeding behaviour of the sabretooth cat, *Smilodon fatalis.* In this study, microwear analysis was conducted on the first lower molar (m1) using SEM at x250 magnification. Information from living carnivores was used to ascertain the microwear patterns created as a consequence of large bone consumption, with spotted hyaenas (*Crocuta crocuta*) at one end of the range representing an extreme bone feeder, and cheetahs (*Acinonyx jubatus*) at the other as exclusive flesh consumers (Van Valkenburgh *et al*., 1990). These authors reported that hyaenas exhibited a higher percentage of pits than scratches, that cheetahs possessed few pits but an abundance of narrow scratches and that the microwear features on the other species were found in intermediate

densities, thereby reflecting their intermediate dietary preferences between hyaena and cheetah (Van Valkenburgh *et al*., 1990). As a result, the presence of long, narrow scratches and a limited number of pits on *S. fatalis* teeth indicates that this animal avoided bone while feeding (Van Valkenburgh *et al*., 1990).

An alternative microwear approach on large carnivores was published by Anyonge (1996), however this time, the author concentrated on the analysis of microwear features in the upper canines, linking them with killing and feeding behaviour. According to this study, the canines of *S. fatalis* were similar to those of living felids, with relatively few microwear features apparent; however, these specimens had relatively more pits when compared to cheetahs and African lions (*Panthera leo*). Anyonge (1996) interpreted the presence of these few microwear features as a result of killing and feeding behaviour, also confirming that *S. fatalis* avoided contact with bone during these activities.

Subsequent studies have focused on palaeodietary reconstruction of diverse extinct taxa. For example, Dewar (2004) examined the palaeodiet of fossil miacids, condylarths, creodonts and other fossil carnivores by applying the low magnification stereomicrowear technique (after Solounias and Semprebon, 2002) and comparing the data with those generated from a sample of extant *Ursus, Canis, Lycaon*, *Otocyon, Urocyon* and *Ailuropoda* genera. He focused on examination of the M1 (first upper molar) and particularly on the paracone, concluding that pits distinguished the consumption of meat better than scratches.

Goillot *et al*. (2009) applied microwear analysis on both slicing and grinding facets of M1 and m1 teeth of carnivores, modifying the Solounias and Semprebon (2002) low–magnification method and analysing the surfaces through an image software package developed by Merceron *et al*. (2004a; 2005b). More specifically, Goillot *et al*. (2009) used some extant species from the following carnivore families: Ursidae, Ailuridae, Hyaenidae, Mustelidae, Eupleridae, Herpestidae, Felidae, Procyonidae and Canidae in order to explore the dietary habits of the extinct amphicyonid, *Amphicyon major*. These authors agreed that microwear analysis using optical stereomicroscopy could be applied to most carnivores and in particular, they highlighted the importance of the

slicing facet of the carnassial teeth in facilitating palaeodietary interpretation. They concluded that the microwear features on the slicing area of *A. major* carnassials suggested an omnivorous diet, although one with strong meat-eating tendencies, suggesting affinities with the diet of the modern red fox (*Vulpes vulpes*). *A. major* also possessed a high number of scratches and many broad pits, indicating that it consumed a significant proportion of plants and hard items (Goillot *et al*., 2009).

In recent years, a new approach to microwear analysis has been developed, consisting of a 3D method where microwear texture is examined (e.g. Ungar *et al*., 2003; Scott *et al*., 2006). The technique relies on a combination of scanning confocal profilometry and scale-sensitive fractal analysis (SSFA) and the terminology therefore differs to that of the 2D method. Thus, comparison between the results of 3D and 2D is only possible when the same specimen and the same surface has been analysed using both approaches. The 3D approach recognises that teeth function on multiple levels and therefore, that microwear surface textures are likely to be sensitive to scale (Ungar, 2015 and references therein). Scale-sensitive fractal analysis is based on the idea that the apparent length, area and volume of a rough surface will change according to the scale of observations, so surfaces may appear smooth at coarse scale and rough with increasing fine resolution (Ungar, 2015). Area-scale fractal complexity (Asfc) and length-scale anisotropy of relief (epLsar) are the two of the basic terms that are used to calculate 3D texture analysis. According to Ungar (2015), heavily pitted surfaces tend to have higher Asfc values than those dominated by uniform-sized scratches, while a surface dominated by striations aligned in the same direction has a higher epLsar value than one dominated by pits, or one with scratches lacking a preferred orientation.

The first to employ this technique, on the carnassial wear facets of three carnivores showing different degrees of bone consumption (cheetah, African lion and spotted hyaena), were Schubert *et al*. (2010). These authors identified three key textural features that indicate an increase in durophagy (ie. the consumption of hard materials such as invertebrate exoskeletons or bone) in these taxa: (1) an increase in microwear complexity, (2) an increase in the size of microwear features and (3) a decrease in uniform orientation of the features. According to these observations, cheetahs lie at

one end of the spectrum (low durophagy) and spotted hyaenas at the other (high durophagy), since the latter had the highest overall average complexity of features (Schubert *et al*. 2010). Ungar *et al*. (2010) used the same method to examine microwear texture on the shearing facet of m1 and m2 in *Canis latrans* (coyote) and *Lycaon pictus* (African wild dog) and compared them with both large felids and hyaenas. Although these authors found some similarities between the patterns in wild dog and cheetah, these were not consistent when compared across different teeth, forcing them to conclude that texture patterns may not, in fact, be the result of dietary habits. This implies that shearing facets may not be suitable for comparison across different carnivores (Ungar *et al*., 2010).

Stynder *et al*. (2012) subsequently compared microwear patterns in m1 carnassials from Mio-Pliocene hyaenas by applying microwear texture analysis, using Schubert *et al*.'s (2010) database on feliforms for comparison. They found that the microwear textures in fossil hyaenas were similar to those seen in *Panthera leo*, a species that occasionally includes bone in its diet. These authors therefore determined that the Mio-Pliocene hyaenas were low consumers of bone, agreeing with the suggestion that most Mio-Pliocene hyaenas were active predators, only developing a bone-cracking ability (and exploitation of the scavenging niche) during the Plio-Pleistocene (Stynder *et al*., 2012).

DeSantis *et al*. (2012) also employed microwear texture analysis and showed, in contrast to Van Valkenburgh *et al*. (1990), that *S. fatalis* possessed microwear features indicating bone consumption. These authors used microwear texture analysis to interpret the dietary niches of extinct carnivores from the Late Pleistocene tarpits site of Rancho La Brea (California, USA). They found no evidence for bone crushing features in the American lion, *Panthera atrox*, and accordingly compared its dietary habits to those of extant cheetah. No significant differences were found in microwear patterns through the sequence, suggesting that the various predators did not change their diets over time (DeSantis *et al*., 2012).

Bastl *et al*. (2012) applied the low magnification microwear technique (after Solounias and Semprebon, 2002), using an extant sample of carnivores (Hyaenidae, Felidae,

Canidae, Viverridae and Nandiniidae) with different dietary habits in order to elucidate the microwear patterns for bone/meat, meat/bone, meat, mixed carnivorous (meat/plant matter) and fruit-based diets, and to compare these against a fossil hyaenodont. Based on their microwear observations and enamel microstructure results, *Hyaenodon* teeth were judged to exhibit heavy gouging and extensive pitting and scratching of the enamel, indicating the consumption of tough foods such as bone. Analogies were drawn with the features on extant striped hyaena (*Hyaena hyaena*) and spotted hyaena, thereby implying similar dietary behaviour(Bastl *et al*., 2012).

3.2.3. Applications to the Ursidae

Studies on enamel wear patterns in the Ursidae began in 2001 when Pinto-Llona and Andrews (2001) compared modes and degrees of tooth wear between brown (*Ursus arctos*) and cave bears (*Ursus spelaeus*) from northern Spain in order to establish whether cave bears were consuming (plant) foods with a high grit content. Both macroscopic and microscopic observations were made, and although the methodology is not very clear regarding the microscopic parts, the authors concluded that the cave bears from this geographical region did not ingest gritty foods. Later, Pinto-Llona (2006) further developed the methodology regarding the microwear features on *U. arctos* and *U. spelaeus*, by analysing two facets on the m1, the distal facet of the protoconid and the lingual facet of the hypoconid, using SEM, before digitising the features and analysing the images using bespoke microwear software (after Ungar *et al*., 1991). According to this study, cave bears possessed the highest proportion of pits relative to scratches in both facets and the greatest density of microwear features. In contrast, brown bears had a large concentration of scratches on both facets, which was interpreted as the result of grass consumption (Pinto-Llona, 2006). Moreover, Pinto-Llona (2006) suggested that the preferred orientation in microwear features seen in cave bears (which interestingly is not replicated in brown bears) is a function of both the chewing dynamic and nature of the food consumed.

The first detailed study of ursid palaeodiet was carried out by Peigne *et al*. (2009), using Goillot *et al*.'s (2009) database and the low-magnification microwear technique

(after Merceron *et al*., 2004b), to examine a large sample of Late Pleistocene *U. spelaeus* from Goyet in Belgium. The analysis was concentrated on the labial facet of the paraconid of the m1 and the conclusion was drawn that these bears had an omnivorous diet, since they presented an intermediate number of small and large pits, revealing a different pattern to both piscivores and herbivores (Peigne *et al*., 2009). However, these conclusions must be treated as tentative on account of the limitations of the study. Given the wide dietary diversity seen in modern bears, it would be necessary to include other similar species (eg. *U. arctos,* American black bear *Ursus americanus* and Himalayan black bear *Ursus thibetanus*) in order to make a fully effective comparison (see Bocherens, 2009).

Most recently, Pinto-Llona (2013) used SEM to undertake microwear studies (following the methodology of Ungar *et al*., 1991) on bears from northern Spain, including extant and extinct brown bears and cave bears from the same region. Her results identified variations in wear patterns between the species, which can be summarised as follows: *U. spelaeus* had a larger number of marks (pits and scratches) than both fossil and extant *U. arctos*; extinct *U. arctos* had the highest percentage of scratches compared to pits and *U. spelaeus* the lowest. This may reflect a greater level of grass consumption by brown bears in this region and also suggests that cave bears, in contrast, consumed neither grass nor food soiled with grit. The large number of pits observed in cave bears from northern Spain may, on the other hand, indicate bone consumption (Pinto-Llona, 2013). Pinto-Llona (2013) further reported the difficulties of studying bears using dental microwear because of potential highly seasonal preferences in diet. Nevertheless, both in this study and in Pinto-Llona (2006), these conclusions must be treated with caution as Münzel *et al*. (2014) pointed out because without direct information about the position of the individual bear in a food web, it is not possible to draw conclusions about the diets of either brown or cave bears.

Donohue *et al*. (2013) examined the buccal facet of the m1 protoconid and the mesial facet of the m2 hypoconulid in the extinct short-face bear, *Arctodus simus*, using a comparative dataset of living ursids, including *U. americanus*, the polar bear *Ursus maritimus*, the panda *Ailuropoda melanoleuca*, the sun bear *Helarctos malayanus* and the spectacled bear *Tremarctos ornatus*. These authors used dental microwear

textures analysis (after Ungar *et al*., 2003) and reported that the m2 served as a better recorder of diet than the m1. However, it is not explained why the authors focussed on the talonid area of the m2 instead of the same area in the m1.

Donohue *et al*. (2013) further showed that in extant bears, carnivores and omnivores (*U. maritimus* and *U. americanus*) have significantly higher and more variable complexity (Asfc) (as previously mentioned, this can be translated, according to Ungar [2015], as reflecting with heavily pitted surfaces) than the more herbivorous species (*A. melanoleuca*, *T. ornatus*, *U. malayanus*). However it must be stressed that first, these authors have a major gap in their database by omitting *U. arctos* from it, and second, both the black bear and the sun bear feed on a wide range of fruits, although the latter consumes more insects, (e.g. Hilderbrand *et al*., 1999; Fortin *et al*., 2007 [for black bear] Fredriksson *et al*., 2006 [for sun bear]), so some level of overlap between the two species would be expected. In addition Donohue *et al*. (2013) demonstrated that *A. melanoleuca* is different from *U. maritimus* and *U. americanus* by having higher and more variable anisotropy (epLsar) values (i.e. that the enamel surface is dominated by striations that are aligned in the same direction [Ungar, 2015]). Their conclusions concerning the extinct *A. simus* were that it exhibits wear structure similar to the living *T. ornatus,* which is inconsistent with the consumption of hard objects (e.g. bone) (Donohue *et al*., 2013).

Most recently, Münzel *et al*. (2014) applied both stable isotope and dental microwear analyses in order to explore the palaeoecology of different cave bear species from two sites in the Swabian Jura (SW Germany) Geißenklösterle and Hohle Fels (with *U. ingressus*) and two sites from the Totes Gebirge (Austria), the Gamssulzen (with *U. ingressus*) and the Ramesch (with *Ursus eremus*). Their reference dataset was relatively small, including specimens of black bear, brown bear, polar bear and panda and fossil brown bear (pre-LGM). They used the low magnification microwear technique (after Solounias and Semprebon, 2002). Based on their microwear observations of the reference bears, the authors suggested that the brown bear demonstrated the entire range of diversity encountered with relation of pits to scratches, namely a high number of pits combined with a low number of scratches and *vice versa*.

In addition, these authors found a high density of scratches both on the carnivorous polar bear and on the herbivorous, grass-eating panda in the reference database. However, the bear specimens from SW Germany exhibited differences to the reference specimens, although the microwear pattern was similar across the two sites. It suggested that the German cave bears had a herbivorous diet but one that involved negligible amounts of grass. In contrast, Münzel *et al*. (2014) found considerable differences between the microwear patterns of *U. ingressus* (from Gamssulzen) and *U. eremus* (from Ramesch) from the Totes Gebirge area and although there were similarities to the cave bears from SW Germany, there was a much wider range of feeding specialisms apparent within their herbivorous niche. These authors confirmed that the prevalence of pits over scratches is considered to be a typical microwear pattern in herbivorous bears (Münzel *et al*., 2014).

The above review establishes the potential for microwear analysis of recent and fossil Ursidae, suggesting that discrete microwear features can be identified within the members of this Family, which in turn can highlight different dietary patterns. More specifically, the studies of Peigne *et al*. (2009) and Goillot *et al*. (2009) have demonstrated that low-magnification microwear studies can be carried out successfully on recent and fossil specimens, although both these investigations were hampered by the use of modern databases that excluded some of the most common bear species, namely *U. arctos*, *U. americanus* and *U. thibetanus*. Donohue *et al*. (2013) subsequently were the first to apply dental microwear texture analysis with confocal microscopy (a technique still very much under development in this regard) on ursids and although the authors did include black bear in their reference database, they excluded *U. arctos* and *U. thibetanus*, again limiting the full potential of their study. The most recent publication by Münzel *et al*. (2014), which included different cave bear groups from two different regions, again highlighted the exceptional potential of microwear analysis to elucidate palaeodiet but this study employed only a small reference database from extant species and further development of method and analysis is needed.

3.3. DMA materials and methods

3.3.1. Material from extant species

The reference bears for this study were selected from eight different museum and university collections around Europe, including the Natural History Museum in Vienna, Austria (NHMV), the Natural History Museum in Paris, France (NHMP) (Department of Comparative Anatomy), the Natural History Museum in Berlin, Germany (NHMB), the Aristotle University of Thessaloniki (Geology Department) (AUThG) and Aristotle University of Thessaloniki (Laboratory of Wildlife and freshwater Fisheries of the School of Forestry and Natural Environment) (AUThW), Greece (see also Appendix I.A). Only wild-caught, adult specimens were used. A set of 168 specimens representing all eight present-day species of ursids was initially collected. After exclusion of specimens with obvious *post mortem* damage, pathologies or poor preservation, 110 samples from modern bears were ultimately included in the microwear analysis. These include *Ailuropoda melanoleuca* (n: 4), *Helarctos malayanus* (n: 17), *Melursus ursinus* (n: 4), *Tremarctos ornatus* (n: 2), *Ursus americanus* (n: 9), *Ursus maritimus* (n: 14) and *Ursus thibetanus* (n: 6). Since the omnivorous *Ursus arctos* today has a large geographical range, samples were targeted from different regions, in order to capture the full potential dietary variability *within* an individual species. These include *U. arctos*, Greece (n: 4); *U. arctos*, central Europe (n: 10); *U. arctos*, USA (n: 8); *U. arctos*, Russia (n: 10) and *U. arctos*, northern Europe (n: 9).

Microwear observations must be calibrated against the known diets of modern bears. This information has been drawn from extensive published research (e.g. Davis, 1964; Joshi *et al*., 1997; Mattson, 1998; Hilderbrand *et al*., 1999; Derocher *et al*., 2002; Augeri, 2005; Bojarska and Selva, 2012) through different approaches (e.g. faecal samples analysis, daily observations, and chemical analysis). This enabled the categorisation of bears into dietary groups (as presented in 2.8.). Based on the most consumed food items, the dietary preferences of bear species can be summarised as follows:

A. melanoleuca (Foliage - Herbivore)

H.malayanus (Invertebrates-Omnivore)

M. ursinus (Invertebrates-Insectivore)

T. ornatus (Soft mast-Omnivore)

U. americanus (Soft mast-Omnivore)

U.maritimus (Vertebrates-Hypercarnivore)

U. thibetanus (Hard mast-Omnivore)

U. arctos, Greece (Soft mast-Omnivore)

U. arctos, central Europe (Hard mast-Omnivore)

U. arctos, USA (Vertebrates-Omnivore)

U. arctos, Russia (Vertebrates-Omnivore)

U. arctos, northern Europe (Soft mast-Omnivore)

3.3.2. DMA methodology

For the stereomicrowear analysis, it was necessary first to produce moulds of the teeth to be studied. Thus, in each collection examined, the first lower molars (m1, carnassials) with an occlusal surface wear indicative of prime adults (categories IV, V and VI of Stiner, 1998) were selected for study (Fig. 3.1). This tooth combines bunodont cusps and a corresponding basin (talonid area) associated with crushing actions, with shearing blades (trigonid with protoconid and paraconid cusps) that are linked with slicing actions (Fig. 3.1.C). Where this tooth was unavailable or poorly preserved, the upper fourth premolar (P4) and the upper first molar (M1), which are present in the corresponding part of the upper jaw, were chosen.

On all m1 specimens, microwear analysis was conducted both on the buccal part of the protoconid or paraconid (slicing area) and on the buccal area of hypoconid (grinding area) (Fig. 3.1.C), with the purpose of revealing potential differentiation on the microwear pattern of each area.

Moreover, on each area of the same tooth, initial observations of microwear features were conducted on two surfaces, the “wear” facet and the “unworn” non-facet

surfaces of the enamel, in order to check if either the wear stage present on the tooth and the surface selected for by the observer influenced the subsequent analysis.

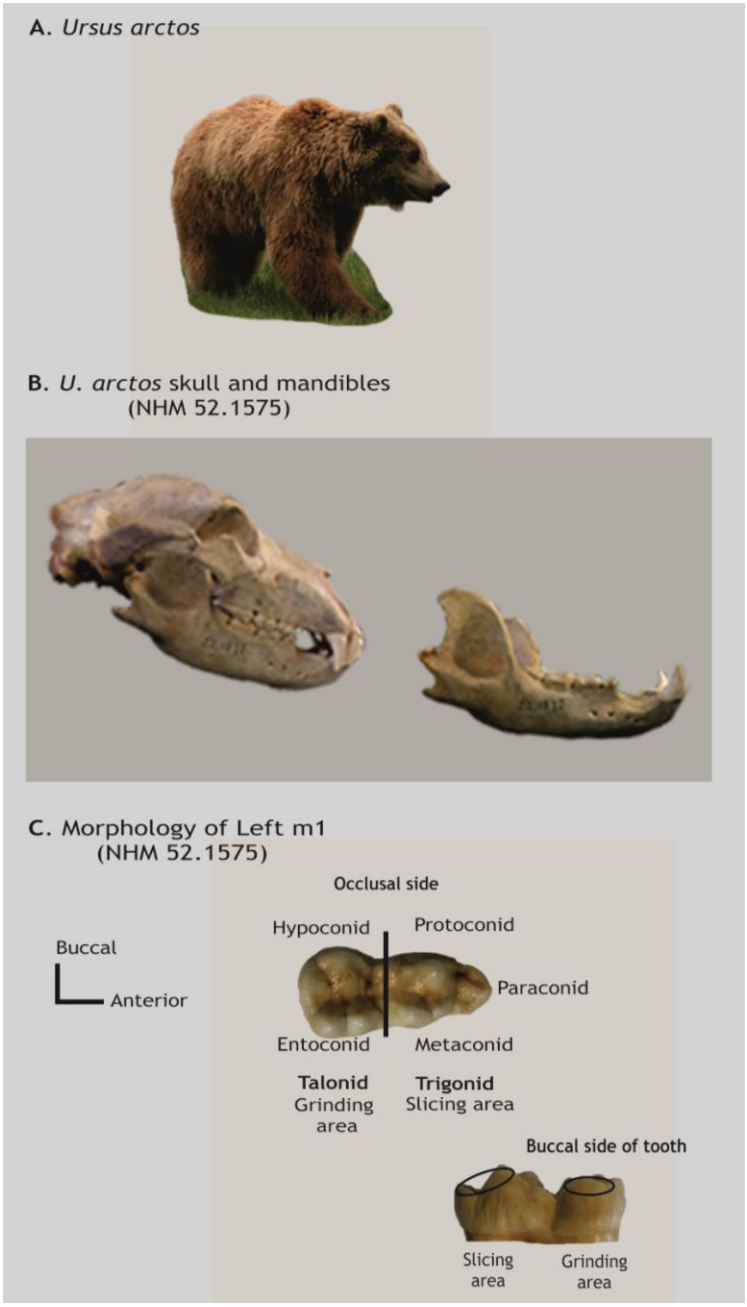

Figure 3.1. A: *U. arctos* reconstruction. **B**: Example of extant *U. arctos* skull and mandibles (specimen from NHM London, Life Sciences collections registered number: NHM 52.1575. **C**: Tooth morphology of first lower carnassials (m1), including areas indicated on the buccal side on which observations were focused for the microwear analysis.

Enamel microwear features were assessed via standard light stereomicroscopy at low magnification (x35) to evaluate microwear features on high-resolution epoxy casts of

teeth, following the cleaning, moulding, casting and examination protocol developed by Solounias and Semprebon (2002) and Semprebon *et al*., (2004). The following steps were completed:

Following the successful obtaining of destructive sampling permission from the various research institutions, well-preserved samples from various collections were selected for analysis (Fig. 3.2 A). The occlusal surface of each specimen was first carefully cleaned with a cotton stick using acetone to remove any consolidants or varnish from the occlusal surface of the tooth. The surface was then cleaned with a cotton swab and 96% alcohol to remove the acetone residues that can be left on the surface (Fig. 3.2 B).

The tooth surface must be totally dry prior to the moulding phase. Once dry, the moulding substance, a high-resolution dental silicone suitable for microwear analysis (President Plus Regular Body; Coltene whaledent, REF. 4627) (Goodall *et al*., 2015), was applied with a gun (mixed with the hardener in its single-use tip), directly on to the tooth (Fig. 3.2 C and D). Once the silicone was completely dry, which required a waiting time of 5 to 10 minutes in order to ensure the best moulding results, a wall of Lab Putty (President fast Coltene whaledent; REF. 4632) was formed around the mould (Fig. 3.2 E, F and G). Subsequently, this mould was further processed at the Department of Geography (Royal Holloway University of London) by being filled with clear epoxy resin (Fig. 3.2 H). After 24 hours, the resin was hard enough to remove the tooth casts from the moulds (Fig. 3.2 I).

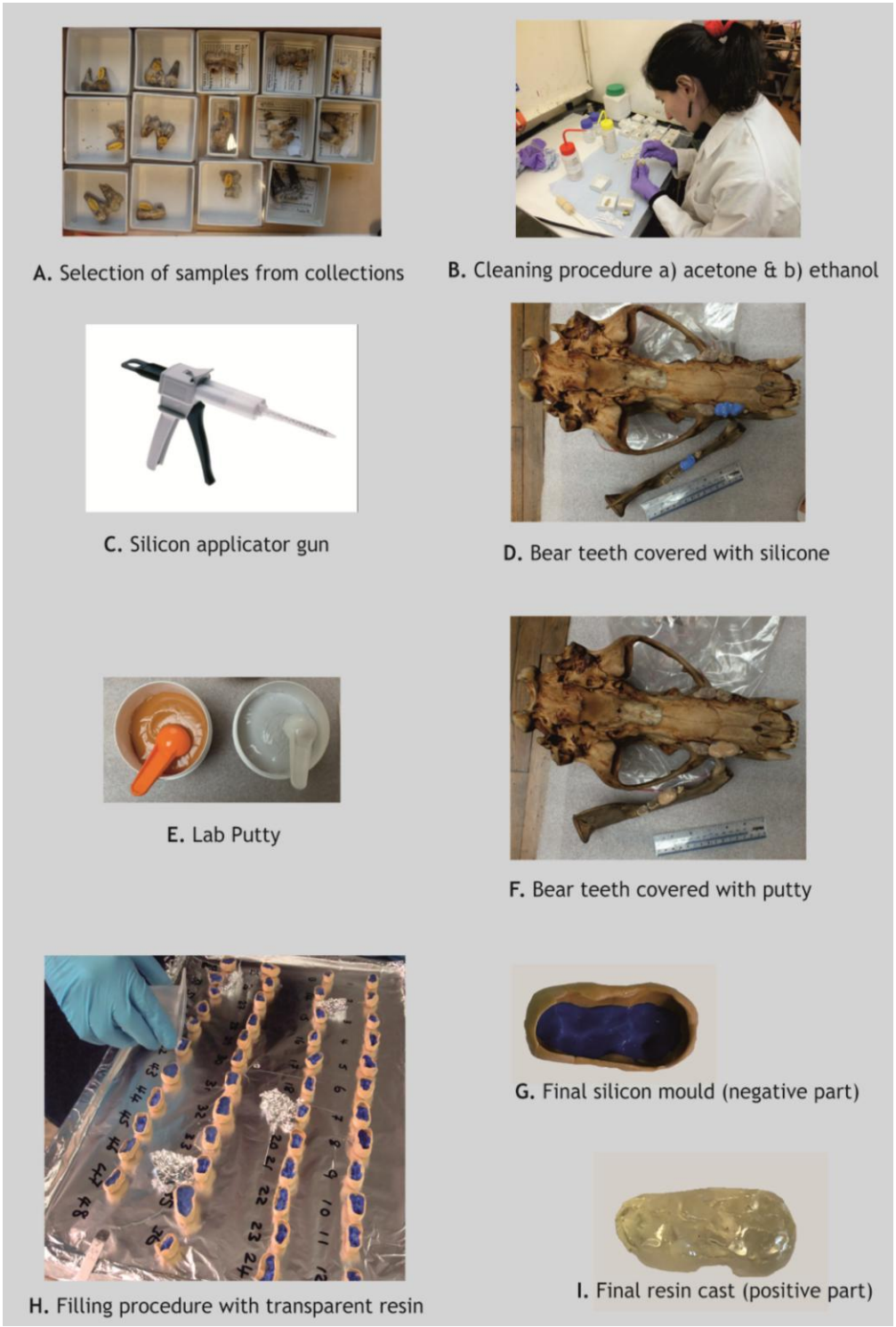

Figure 3.2. Dental Microwear Analysis moulding and casting procedure. **A**. Selection of tooth samples from the collections. **B**. Cleaning process of teeth surface with acetone and then with 96% alcohol. **C.** Silicon applicator gun used to mould teeth using high-resolution silicone. **D.** Teeth of a bear skull covered with silicone. **E.** Lab putty. **F.** Bear teeth covered with putty. **G.** Final silicone mould (negative part). **H.** Filling procedure with clear epoxy resin in the laboratory. **I.** Final resin cast (positive part).

The resin casts were then examined under a light microscope. Those with bad preservation or other taphonomical marks (including any marks produced by excavation process, storage in the collection and, more rarely, by the cleaning procedure) were excluded from the subsequent analysis. The specimens were studied both in the Geography Department of Royal Holloway University of London with an Olympus SZ51 with WHSZ 10x –H/22 stereomicroscope at x35 magnification and at the Institutit Català de Paleoecologia Humana i Evolució Social (IPHES) in Spain, using a Zeiss Stemi 2000C stereomicroscope at x35 magnification (Fig. 3.3 A). The use of a different brand of stereomicroscope does not influence the results (F. Rivals, pers. comm.). External (and where required, internal) lights on the microscopes were used to reveal the microfeatures on the enamel surface of the samples. Microwear features were quantified in a square area of 0.16 mm^2 by using an ocular reticle (Fig. 3.3 B).

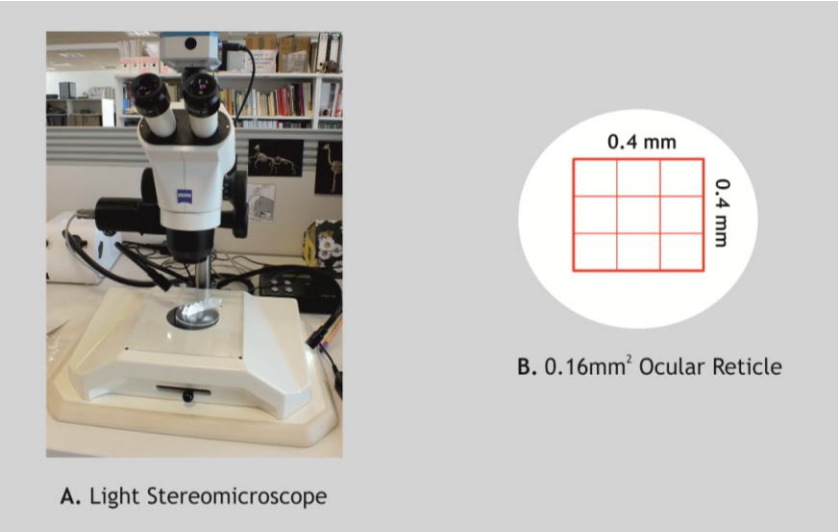

Figure 3.3. Dental Microwear Analysis. Stereolight microscope. **A**. Zeiss Stemi 2000C stereomicroscope used in Spain (IPHES). **B**. An ocular reticle with a square area of 0.16 mm^2 used in the quantification of the microwear features.

3.3.3. Additional DMA approaches – advantages of light stereomicroscopy

Various methods have been employed by researchers in the examination of dental microwear, for example the use of different microscopes for the observations of microscopic scars. Initially, a scanning electron microscope (SEM) was employed for

microwear studies (Walker *et al*., 1978; Ryan, 1979). The SEM method was later used by other researchers who analysed the micro-features with different image software such as Microwear 2.1 or 4.0 (Ungar, 1996; El-Zaatari *et al*., 2005; Valli and Palombo, 2008). However, other methods have subsequently been developed, including the use of light microscopy such as confocal microscopic techniques.

Confocal microscopy has been used to reconstruct the diets of extinct hominins (dental microwear texture analysis [DMTA]) (Scott *et al*., 2005, 2006; 2009 Ungar *et al*., 2010), whereas stereomicroscopic methodologies (light microscopy for dental microwear [LDM]) (Solounias and Semprebon, 2002; Merceron *et al*., 2004a; b;) have become common in recent years since they have the advantage of being simpler, quicker and less expensive to use.

As already explained in 3.3.2, microwear features on dental enamel were examined by using stereomicroscope (light microscopy for dental microwear [LDM]) and following the examination protocol developed by Solounias and Semprebon (2002) and Semprebon *et al*. (2004). Semprebon *et al*. (in press) have outlined in detail the strengths and weaknesses of each method, stressing that in all microwear approaches, care must be given to: 1) the potential error involved in the analyses and 2) causal factors producing microwear scars.

SEM and LDM (used in this thesis) rely on observer measurements, whilst DMTA employs an automated approach. Different researchers have attempted to identify and quantify both the inter- and *intra*-observer errors involved in each approach (e.g. Grine *et al*., 2002; Galbany *et al*., 2005; DeSantis *et al*., 2012; Williams and Geissler, 2014). Although these studies have provided some important insights into potential errors inherent in microwear studies, it is important not to generalise across methods and errors can be greatly controlled by following the correct methodological protocols (Semprebon *et al*., in press).

The methodology developed by Solounias and Semprebon (2002) and used here follows the same standard microscope calibration and systematic counting method employed every day in diagnostic medicine and life science research to count accurately substances such as blood cells (Semprebon *et al*., in press). In addition, the

use of a calibrated ocular reticle sub-divided into nine sub-squares greatly reduced the risk of losing track of features during counting. The user must be well trained and be aware that the features are counted following a strict protocol that guarantees that features are not skipped or counted twice (Semprebon *et al*., in press). Replication should also be undertaken to limit errors introduced due to potential variable scar distribution. When the above steps are followed and protocols are correctly observed, both inter- and *intra*-observer error have been proved to be low (Semprebon *et al*., 2004).

On the other hand, DMTA is a fully automated approach and although it has been developed in order to reduce subjectivity and inter-observer error (e.g. Ungar *et al*., 2003), as correctly pointed out by Semprebon *et al*. (in press), this approach reduces inter-observer error only when the exact same location on the same tooth surface is scanned twice, since results obtained on the same tooth and same facet may be quite different when different regions of that tooth and facet are scanned. Its useful application may therefore be limited.

3.3.4. Description of microscopic scars

The microscopic scars that appear on the tooth are variable and before starting the DMA, it is important to differentiate and to categorise these features. Solounias and Hayek (1993) first instituted a set of categories regarding microwear features. Later Solounias and Semprebon (2002) introduced four more variables, in addition to the traditionally-counted number of scratch scars (elongated microfeatures with straight parallel sides) and pits scars (circular or sub-circular microfeatures with approximately similar widths and lengths), namely the classification of pits as small or large and scratches as fine and coarse. Subsequently, Semprebon *et al*. (2004) added new type of scratches and pits in terms of their texture, describing both “hypercoarse” scratches and “puncture” pits.

This study follows the classification of microwear features based on Solounias and Semprebon (2002) and Semprebon *et al*. (2004). Hence, the following features were identified on bear samples, reflecting the masticatory actions of the animals involved:

1. Pits are microwear features that are circular or subcircular in outline. Pits can be separated into the following categories:

- **Small pits**. These are bright white in colour under the microscope and have a very regular appearance with sharp, distinct and circular borders (Fig. 3.4 A and B).

- **Large pits**. These are deeper than the small pits and dark in colour. They are at least double the size of the small pits and often have somewhat less regular outlines, albeit retaining a circular form (Fig. 3.4 A and C).

2. Gouges (G) are microfeatures that are both larger and deeper than large pits and with irregular edges. Usually the surface of enamel has the appearance of being "chipped" away (Fig. 3.4 A and C).

3. Punctures (P) vary in size; they can be as small as small pits but can also be much larger. The key to their identification is their depth, since they are very deep (usually deepest at their centre) and symmetrical, with regular margins, (Fig. 3.4 A and C).

4. Scratches (S) are elongated microwear features that are straight and have parallel sides. Scratches can be divided into the following categories:

- Fine scratches, which are narrow and relatively shallow (Fig. 3.4 B and D).

- Coarse scratches, which are wider and relatively deep, usually with a high refractivity (Fig. 3.4 B and D) (after Semprebon *et al*. [2004]).

- Hypercoarse scratches, which are wider than coarse scratches and with a dark colour (Fig. 3.4 B) (after Semprebon *et al*. [2004]).

- Cross scratches, which are oriented more-or-less perpendicular to the majority of scratches on the enamel surface (Fig. 3.4 C and D).

5. A **Scratch Width Score** (SWS) is assigned, depending on the level of scratches observed. A score of zero (0) is given when only fine scratches are present, one (1) when there is a mixture of fine and coarse scratches on the surface, two (2) when predominantly coarse scratches are present and three (3) when the surface has also hypercoarse scratches.

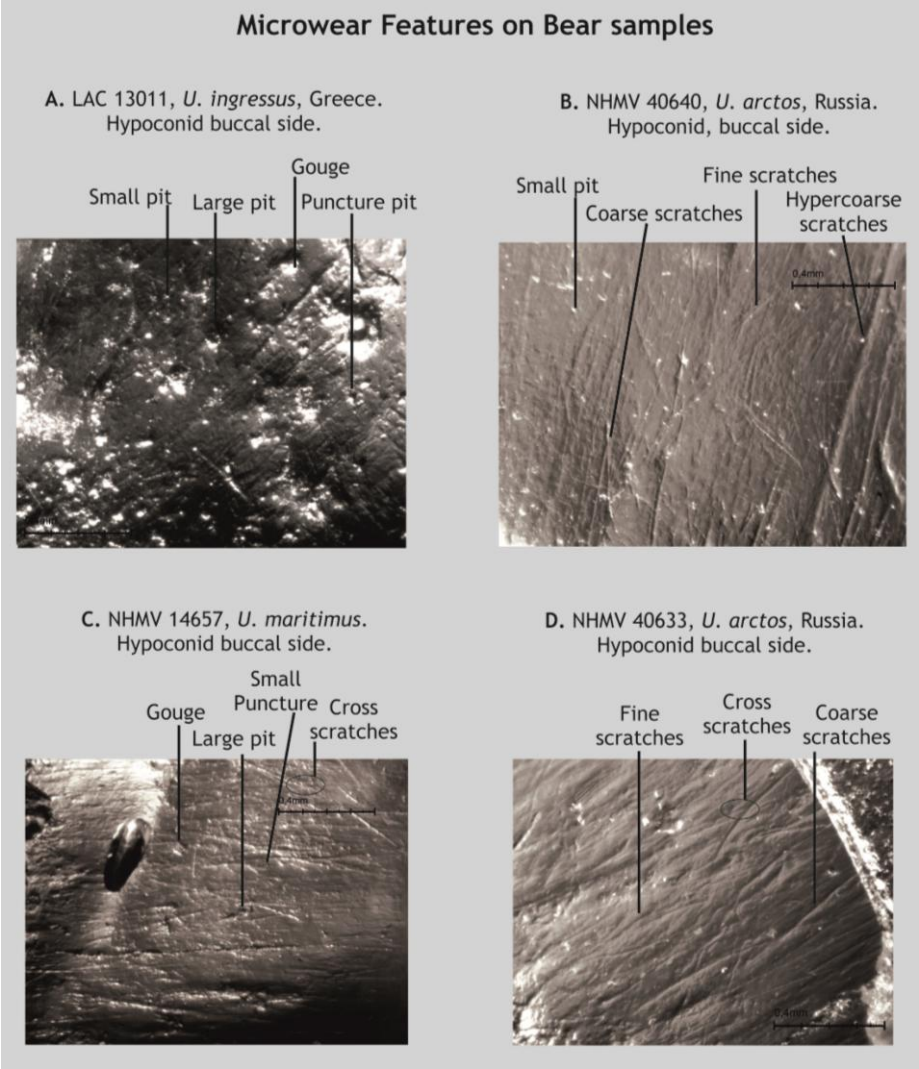

Figure 3.4. Microwear features observed on m1 samples (buccal side of hypoconid) under stereolight-microscope with x35 magnification including all the different features observed on bear samples (small pits, large pits, gouges, puncture pits, fine scratches, coarse scratches, hypercoarse scratches, cross-scratches).

3.3.5. Non-microwear features observed on Ursidae

It is well known that after death, a number of factors have the potential to cause damage to the enamel and to produce new marks or obscure microwear scars by processes not related to mastication, especially when fossil samples are examined (e.g. Shipman, 1981; King *et al*., 1999). In addition, other aspects should also be considered such as dental erosion, which may be caused by a variety of reasons (e.g. health issues or ingestion of acidic food). Different experiments that mimic taphonomic procedures have been undertaken in order to document the effect on tooth enamel and to understand how they may affect microwear features (e.g. Gordon, 1984c and King *et al*., 1999), as with enamel erosion (e.g. Meurman and Frank, 1991a; b). Thus, different taphonomic aspects that have the potential to alter the "original" nature of the microwear features need to be taken into consideration during dental microwear studies.

During this study, as well as previously-noted non-microwear features, new features were found that are described for the first time below. Again, this highlights the importance of detailed understanding of different aspects of tooth morphology and enamel structure within each species under consideration. Throughout the analysis, all the non-microwear features identified below were excluded.

Some established non-microwear features that were observed on many extinct bear samples can be described as "fresh scratches", usually produced during excavation of the specimen, storage in the collection and/or the sample cleaning procedure (Fig. 3.5 A and B), as well as resin bubbles (Fig. 3.5 B), which were found in casts of both extant and extinct samples and usually produced during the moulding resin procedure.

Furthermore, three additional non-microwear features were observed on the samples studied here. The first is potentially linked to the enamel structure and was observed both on samples of the cave bear group (*U. deningeri*) and on samples of modern *U. maritimus*. The features consist of a wave-like pattern of lines that are sometimes continuous and are preserved along the entire length of the cusp crown (Fig. 3.5 D1

and D2), while at other times, they appear only in some parts of the enamel surface (Fig. 3.5 C).

A further interesting non-microwear feature observed here is a second type of wave pattern that this time starts from the tip of the cusp and then goes around the cusp, producing deep lines that sometimes give the impression of hypercoarse scratches, especially under x35 magnification (Fig. 3.5 E, F and G). This is a pattern that was observed on *A. melanoleuca* and on the cave bear group (specifically *U. spelaeus* and *U. ingressus*).

The origin of these features is most probably linked to enamel structure and more particularly, to different types of Hunter-Schreger bands (HSB) or to perikymata (external ridges and troughs encircling the tooth crown that are formed by Retzius lines as they reach the enamel surface [Smith and Tafforeau, 2008]). HSB are an optical phenomenon produced by refraction of light due to the internal structure of enamel, however the term was also used for the underlying structure of layers of descussating prisms (Koenigswald *et al*., 2010) (see 5.2.1 for further details).

Different studies have focused on the analysis of HSB patterns in relation to diet and/or to evolutionary patterns on different taxa (e.g. Koenigswald, 1992; Koenigswald and Clemens, 1992; Stefen, 1997a; b; 1999; 2001; Koenigswald *et al*., 2010; Tseng, 2011; 2012; Bastl *et al*., 2012). It is worth mentioning two aspects that Stefen (2001) reported after studying the enamel structure of arctoid carnivore: 1) variation in the number of zigzag HSB in different teeth could reflect different biomechanical constraints on the teeth and 2) zigzag HSB occur on the occlusal surface of the carnassials and have been assumed to render the enamel more resistant to wear.

The analysis of these features is beyond the scope of the present study and remain to be explored in more depth in future, since they may reveal new information about species' diet.

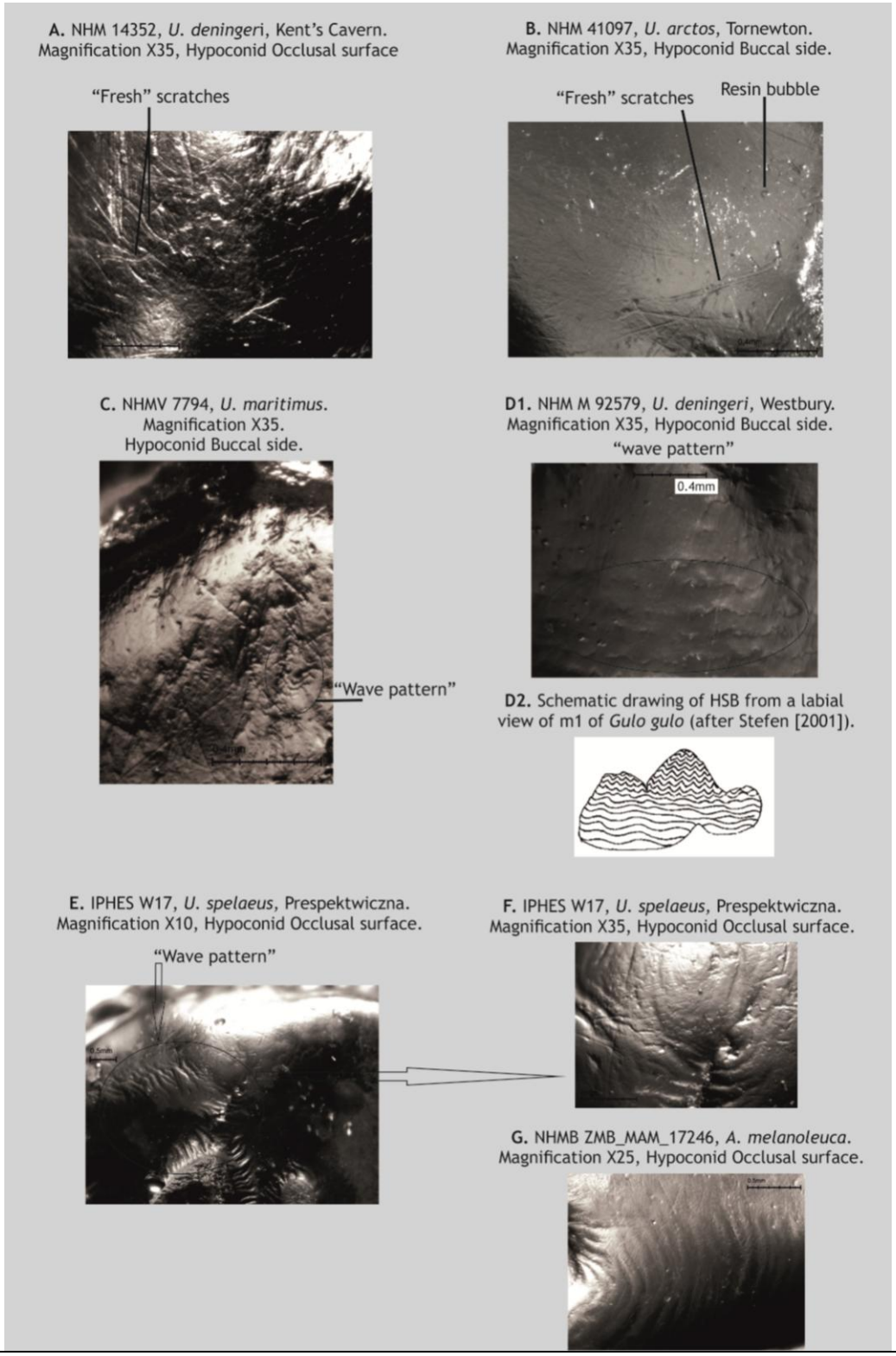

Figure 3.5. Dental Microwear Analysis. Non-microwear features observed on bear teeth (together with one example of wolverine). **A**. Fresh scratches. **B**. Fresh scratches and resin bubble. **C.** Wave like pattern. **D1.** Wave like pattern along the cusp. D2. Schematic drawing of Hunter-Schreger bands (HSB) (image modified from Stefen [2001]). **E - G.** Wave pattern starting from the tip of the cusp.

The final new non-microwear feature that was observed (mainly on the cave bear group, *U. spelaeus* and *U. ingressus*) is linked to the more complex occlusal surface that all cave bear teeth have when compared to other bear species. The complexity of their crown includes some additional small ridges (line-like features) on the buccal side of their teeth, which are developed almost vertical to the main cusp axis of the tooth. Under x35 magnification, these features resemble huge gouges or, where the tooth is slightly worn, hypercoarse scratches (Fig. 3.6 A, B and C).

Caution is therefore needed with respect to the above features, in order to avoid any potential error in the analysis and interpretation.

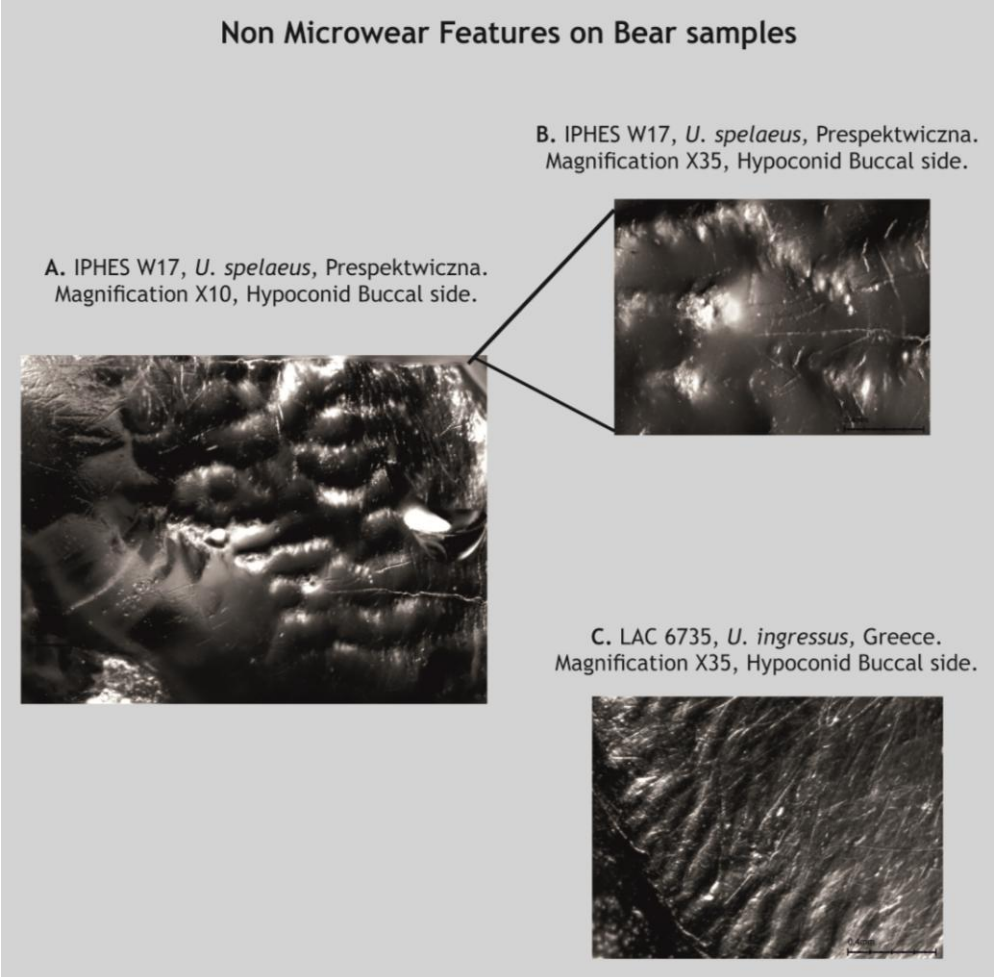

Figure 3.6. Dental Microwear Analysis. Non-microwear features observed on samples of the Ursidae. **A - C.** Exaggerated morphology on the buccal side of teeth from the cave bear group.

3.3.6. Statistical methods used for DMA

All data for the DMA were collected in Excel, before application of both Excel and PAST statistical packages.

To assess differential microwear patterning across the results of the observations in non-facet and facet enamel surfaces, Student's t-tests were performed for scratches and pit variables.

Regarding the extant species (which form the main comparative database of this study), statistical analysis was completed on the data for both the slicing and grinding areas in all 110 samples measured. The data were first examined using bivariate comparison, plotting the total number of pits against the total number of scratches, in order to test for potential differences between species. Descriptive statistics included the following for pits and scratches: minimum, maximum, mean, standard deviation and 95% confidence. In addition, box-and-whisker plots were also created to depict the distribution of pit features, showing the 1^{st} and 3^{rd} quartiles.

In order to explore which microwear traits best differentiate the species, an Analysis Of Variance (ANOVA) with a Tukey's pairwise test were used for the observations on both the grinding and slicing areas.

For the extant bear dataset, a Principal Components Analysis (PCA) was employed to identify any groupings emerging from individual scores from both grinding and slicing areas. Nine different variables were examined. For the extinct species, statistical analysis focused exclusively on the grinding area observations, since this area permitted the clearest separation into dietary ecospace in the extant (reference) bear database (see 3.4.1). Statistical analysis of extinct bear samples included bivariate comparison as well as PCA.

3.4. Results of the Dental Microwear Analysis from the reference data set of extant Ursidae

This Chapter presents the results regarding dental microwear observations on extant bear species, establishing for the first time a complete database of food types related to microwear features for the living Ursidae. This permits the exploration of dietary variability both *between* the eight different species analysed and, for *U. arctos*, variability *within* an individual species from different geographical regions (northern Europe, Russia, Greece, central Europe and USA). The purpose of the observations on living bears is to provide a dietary "benchmark", against which the dental microwear of fossil samples can be compared. As already outlined in 3.3.2, the first lower molar (m1) was examined and occlusal surfaces with wear stages indicative of prime adults [categories IV, V & VI of Stiner, 1998] were selected for study. Both the grinding (talonid) and slicing (trigonid) areas of the m1 were examined.

3.4.1. Results from facet and non-facet surfaces of enamel

Microwear features on both wear facet and "unworn" non-facet surfaces of enamel on the same tooth were initially observed, in order to ascertain whether either the wear stage present and/or the surface selected by the observer influenced the subsequent analysis. Such variability is readily apparent between facet and non-facet enamel surfaces in modern polar bear under x25 magnification (Fig. 3.7.A) as well as in fossil *Ursus deningeri* from Westbury-sub-Mendip (Fig. 3.7.B).

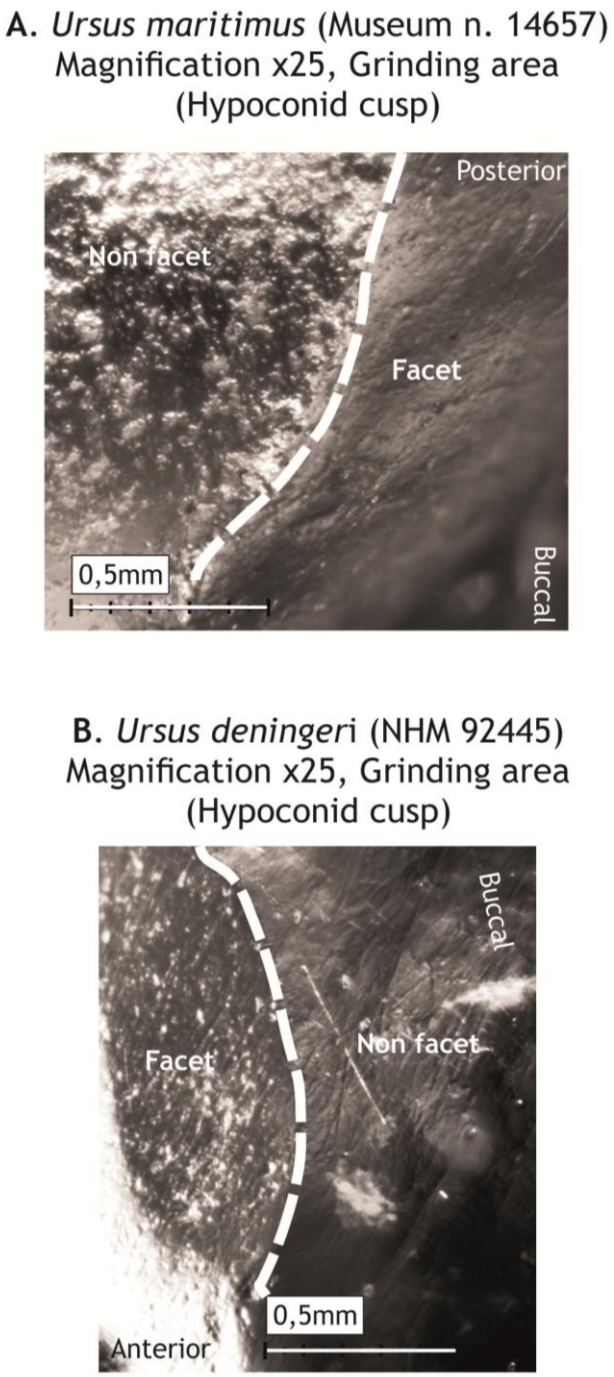

Figure 3.7. Photomicrographs of specimens at x25 magnification with facet and non-facet enamel surfaces. **A.** *U. maritimus* from Greenland (NHM Vienna: 14657); **B.** *U. deningeri* from Westbury-sub-Mendip (MIS 13) (NHM London: M92445).

In order to explore this further, molars of two species were chosen for more detailed examination: extant *Ursus maritimus* (n: 10) (Fig. 3.8. A and B) and extinct *Ursus deningeri* (n: 10) (Fig. 3.8. C and D). For all individuals, both the facet and non-facet enamel surfaces were analysed and the total number of scratches and pit features were estimated (Fig. 3.8.).

The results reveal a difference in the total number of scratches and pit features in both *U. maritimus* and *U. deningeri*, for observations on facet compared to non-facet enamel surfaces. Scratches on non-facet enamel surfaces are much more numerous (ranging from a minimum of 15 to a maximum of 30) than on facet surfaces (ranging from minimum 3 to maximum 14) and in some individuals, are almost double (Fig. 3.8. A and C). Likewise, pit features are three- to six- or even seven times more common on a facet surface (ranging from minimum 40 to maximum 85) compared to a non-facet surface (ranging from minimum 15 to maximum 30) in the same individual (Fig. 3.8. B and D).

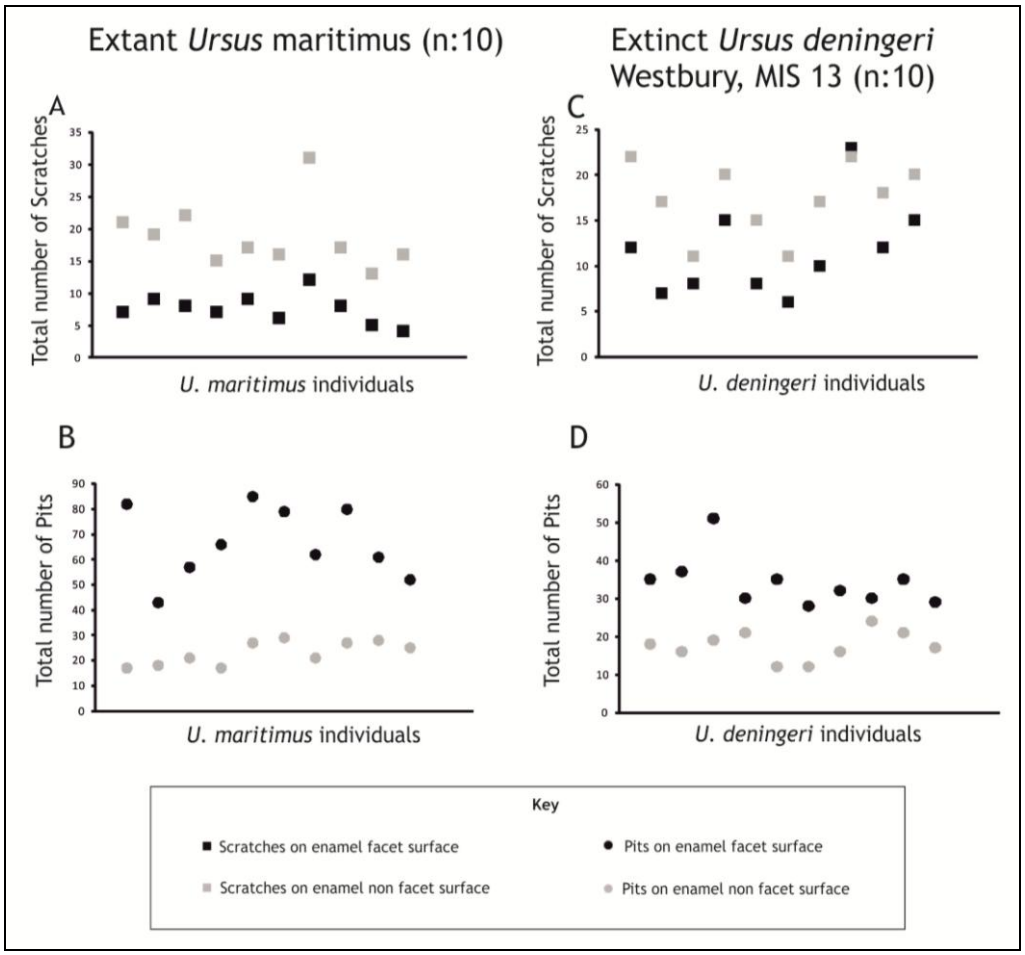

Figure 3.8. Comparison of total number of scratches and pits between observations on **facet** and **non-facet** enamel surfaces on the grinding (talonid) area of m1s in extant *U. maritimus* and extinct *U. deningeri*. **Graph A**: *U. maritimus* comparison of total number of **scratches** on facet and non-facet surfaces. **Graph B**: *U. maritimus* comparison of total number of **pits** on facet and non-facet surfaces. **Graph C**: *U. deningeri* comparison of total number of **scratches** on facet and non-facet surfaces**. Graph D**: *U. deningeri* comparison of total number of **pits** on facet and non-facet surfaces.

To establish whether there were significant differences between the results of the observations on facet and non-facet enamel surface of the two species, t-tests were performed for scratches and pit variables. Table 3.1 shows the t-test results for inequality of surface means for scratches and pit features in both *U. maritimus* and *U. deningeri* individuals. As can be seen from the p values on table 3.1, in *U. maritimus* and *U. deningeri*, scratches on the non-facet enamel surface differ significantly from on the facet enamel surface ($p<0.0001$ and $p<0.0124$ respectively). This is also the case when the pits were tested, from non-facet and facet enamel surface of both species ($p<0.0001$ for both *U. maritimus* and *U. deningeri*) (table 3.1).

Table 3.1. t-tests for inequality of surface means for scratches and pits on both *U. maritimus* and *U. deningeri* individuals.

Variable	Surface Enamel	n	Mean	Variance	t	p
Scratches (*U. arctos*)	**Non Facet**	10	18.7	26.011	-6.34	< 0.0001 ****
	Facet	10	7.5	5.1667		
Pits (*U. arctos*)	**Non Facet**	10	23	22.444	9.21	< 0.0001 ****
	Facet	10	66.7	202.68		
Scratches (*U. deningeri*)	**Non Facet**	10	17.3	16.011	-2.78	0.0124 ***
	Facet	10	11.6	26.044		
Pits (*U. deningeri*)	**Non Facet**	10	17.6	14.933	6.83	< 0.0001 ****
	Facet	10	34.2	44.178		

This indicates the importance of surface selection prior to analysis and the potential biasing effect that facet or non-facet surfaces may have on the interpretation of palaeodiet.

In this study, only the results from non-facet "unworn" enamel surfaces are presented, following also the recommended practice of other authors, such as Ungar and Teaford (1996) and Münzel *et al*. (2014).

3.4.2. Results on grinding (talonid) and slicing (trigonid) areas of extant Ursidae based on Bivariate analysis

As outlined in 3.3.2, 168 individuals of extant bear species were analysed. After exclusion of specimens with obvious *post mortem* modifications, pathologies or poor preservation, 110 specimens from modern bears were ultimately included in the microwear analysis. Table 3.2 shows the total number of individuals from each species that were analysed and the number of specimens that were analysed on the grinding (talonid) and slicing (trigonid) areas, shown against the results from both areas, including mean, standard deviation and 95% confidence interval both for pits and scratches (see also for raw data Appendix IA table 1 and table 2).

Table 3.2. Extant bear species, additional information such as: mean, standard deviation and 95% Confidence interval (CL) for each species are presented for both Grinding (talonid) and Slicing (trigonid) area.

			Pits		**Scratches**	
Species	**Observations on Grinding (G) or Slicing (S)**	**n**	**Mean, SD**	**95% CL***	**Mean, SD**	**95% CL***
A. melanoleuca	G	4	57.0; 5.9	5.8	19.3; 1.7	1.7
	S	3	53.3;11.7	13.3	18.7; 1.53	1.7
H. malayanus	G	17	25.7; 5.2	2.5	19.5; 3.1	1.5
	S	12	26.0; 3.2	1.8	19.3; 2.2	1.2
M. ursinus	G	4	36.8; 5.3	5.1	16.0; 1.6	1.6
	S	4	33.0; 9.6	9.4	14.5; 2.6	2.61
U. americanus	G	9	27.4; 6.1	4.0	16.1; 1.8	1.2
	S	9	27.2; 4.5	2.95	17.1; 2.15	1.4
U. maritimus	G	14	20.9; 3.8	2.0	16.3; 3.1	1.6
	S	14	20.4; 8.2	4.3	16.2; 2.7	1.4
U. thibetanus	G	6	20.3; 1.4	1.1	17.7; 1.8	1.4
	S	4	21.75; 2.5	2.45	15.0; 1.6	1.6
***U. arctos*, Greece**	G	4	20.0; 3.8	3.8	20.0;3.4	3.3
	S	4	16.0; 1.4	1.4	22.25; 3.3	3.24
***U. arctos* (Central Europe)**	G	10	36.2; 7.6	4.7	20.9; 3.2	2.0
	S	8	36.4; 3.8	2.6	18.0; 4.0	2.8
***U. arctos* (USA)**	G	8	28.4; 5.1	3.5	21.3; 4.8	3.3
	S	3	30.3; 4.9	5.6	18.7; 2.9	3.3
***U. arctos* (Russia)**	G	23	31.5; 5	2.0	20.0; 3.4	1.4
	S	21	29.8; 5.6	2.4	19.2; 5.45	2.3
***U. arctos* (North Europe)**	G	9	32.4; 5.7	3.8	19.6; 3.9	2.6

Comparison of microwear features was initially done by plotting the total number of pits against the total number of scratches on bivariate graphs, in order to test potential ratios of meat:plant or fruit:plant matter between species (following Donohue *et al*. [2013)]). Figures 3.9.A and 3.9.B show the variation between extant bear species based on observations of the talonid and trigonid areas respectively. These reveal that the grinding area (Fig. 3.9.A) provides a clearer separation of the living bear species into different parts of dietary ecospace than the slicing area (Fig. 3.9.B).

Furthermore, differentiation between *U. maritimus*, *A. melanoleuca, H. malayanus* and *M. ursinus* is very clear on the grinding surface (Fig. 3.9.A). The bamboo consumer *A. melanoleuca* differs from the hyper-carnivorous *U. maritimus* and the omnivorous *U. arctos* and *U. americanus* in its clearly higher numbers of pits. The mean number of pits in a standard 0.16 mm^2 area in giant panda is 57 (minimum 49 and maximum 62), in polar bear and brown bear, the mean number is 20 and in American black bear, 27 (see also table 3.2 and 3.3). *U. maritimus*, *U. arctos* from Greece and *U. thibetanus* are characterised by fewer than 25 pits. With respect to the number of scratches, most individuals in all species exhibit intermediate values between 17 and 23 scratches (see means and standard deviations in table 3.2). Some *U. maritimus* and *M. ursinus* individuals are characterised by very low numbers of scratches (as few as 13), whereas some *U. arctos* specimens from Russia and the USA have the most (up to 28) (Fig. 3.9.A).

Furthermore, differences in microwear features are evident even in *U. arctos* from different geographical regions (Fig. 3.9.A), in particular the separation of *U. arctos* from Greece compared to *U. arctos* from Russia and from central Europe. Individuals of *U. arctos* from central Europe show the highest number of pits (up to a maximum of 46) while *U. arctos* from Greece has the lowest number of pits (a maximum of 25). In contrast, both *U. arctos* from Russia and from northern Europe show intermediate values of pits (maximum numbers of 40 and 39 respectively). Moreover, differentiation is also evident when scratches are compared between groups and most *U. arctos* from northern Europe have, compared to other brown bears, the smallest number of scratches (maximum 16) (Fig. 3.9.A; see also table 3.2).

With respect to analysis of the slicing surface (Fig. 3.9.B), any patterning is harder to detect between species, since there is a large overlap between them. However, most *U. maritimus* individuals have the lowest number of pits observed in any species (fewer than 21) and these can be clearly differentiated from *A. melanoleuca*, *H. malayanus*, *M. ursinus* and *T. ornatus*. On the other hand, *A. melanoleuca* has the highest number of pits, with a maximum of 62 observed (see table 3.2). In contrast to the results from the grinding surface, the results from the slicing surface show that there is a noteworthy overlap between *U. arctos* from different geographical regions and the other species (Fig. 3.9.B), thereby precluding the identification of any individual characteristics.

It is therefore concluded that observations on the m1 trigonid produce a different picture to those made on the talonid (Fig. 3.9.B) and do not generate as clear a separation into dietary ecospace.

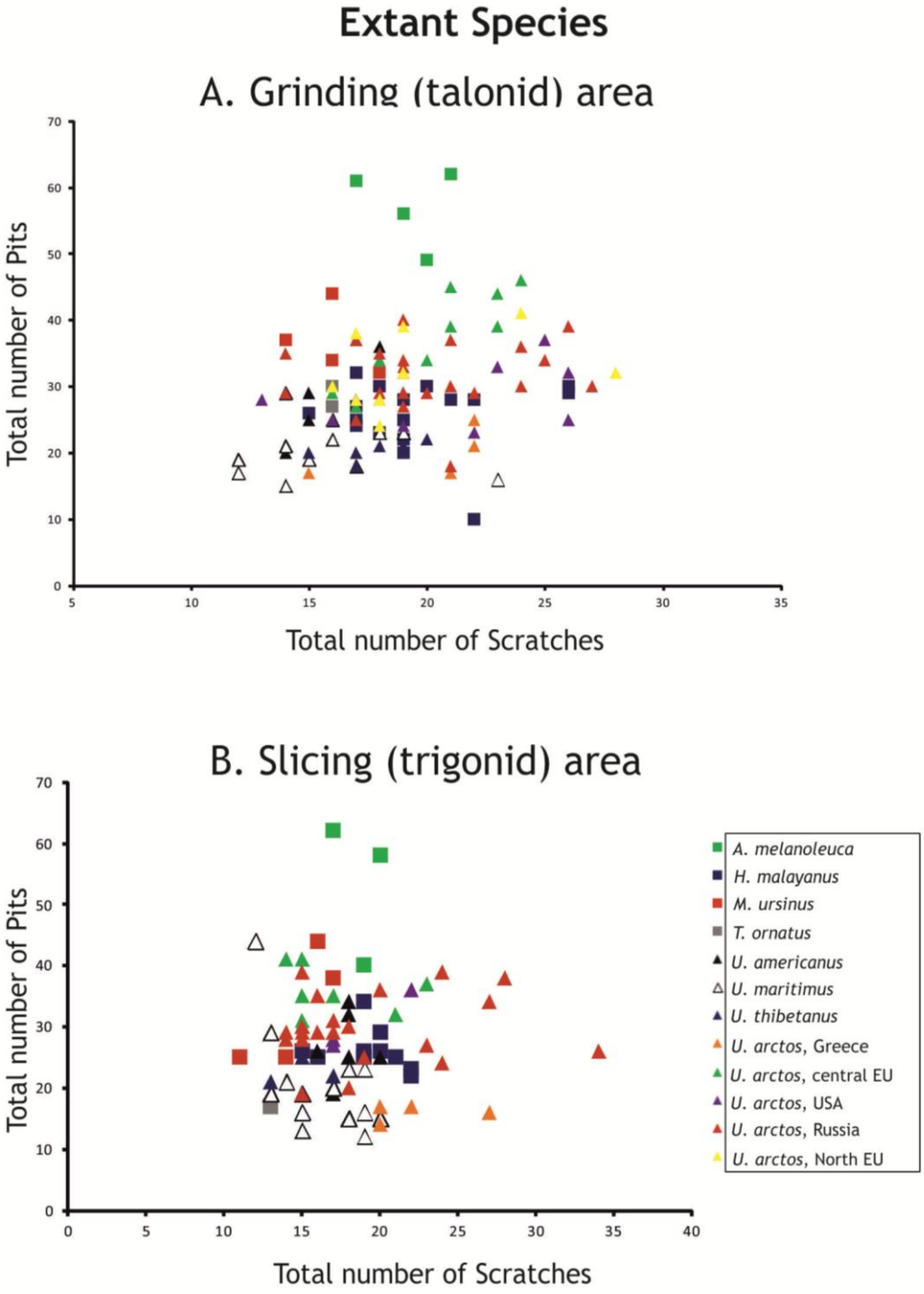

Figure 3.9. Extant species plot of raw data of total number of pits versus scratches. **A.** Analysis on grinding (talonid) area. **B.** Analysis on slicing (trigonid) area. (For the total number of each species, see table 3.2).

In carnivores, pits rather than scratches have been described as the most dietary-diagnostic features (Bastl *et al*., 2012). Thus, the total number of large pits versus small pits was plotted in Figures 3.10.A and 3.10.B for both grinding and slicing areas respectively. These figures equally reveal a separation of the extant bear species into different parts of a dietary ecospace, based on observations of the grinding (talonid) area, a distinction that is not paralleled by observations on the slicing (trigonid) area. Table 3.3 presents additional information for each species exclusively for pit features regarding the minimum, maximum, 1st and 3rd quartile and mean values.

Table 3.3. Extant bear species, analysis on Grinding (G), (talonid) and Slicing (S), (trigonid) area. Information for pits includes 1st quartile, minimum, median, maximum and 3rd quartile.

			Pits				
Species	**Observations on Grinding (G) or Slicing (S)**	**n**	**1st Quartile**	**Min**	**Median**	**Max**	**3rd Quartile**
A. melanoleuca	G	4	54.25	49	58.5	62	61.25
	S	3	-	40	58	62	-
H. malayanus	G	17	24	10	27	32	29
	S	12	-	22	25	34	-
M. ursinus	G	4	33.5	32	35.5	44	38.75
	S	4	-	25	31.5	44	-
T. ornatus	G	2	27.75	27	28.5	30	29.25
U. americanus	G	9	22	20	28	37	29
	S	9	-	19	26	34	-
U. maritimus	G	14	18.25	15	21.5	29	23
	S	14	-	12	19	44	-
U. thibetanus	G	6	20	18	20.5	22	21
	S	4	-	19	21.5	25	-
***U. arctos*, Greece**	G	4	17	17	19	25	22
	S	4	-	14	16.5	17	-
***U. arctos* (Central Europe)**	G	10	30.25	25	36.5	46	42.75
	S	8	-	31	36	41	-
***U. arctos* (USA)**	G	8	24.75	23	26.5	37	32.25
	S	3	-	27	28	36	-
***U. arctos* (Russia)**	G	23	29	18	30	40	35
	S	21	-	19	29	39	-
***U. arctos* (North Europe)**	G	9	28	24	32	41	38

The results reveal that with respect to the grinding area (Fig. 3.10.A), *U. arctos* from Greece has the lowest number of small pits (minimum 7 and maximum 11), but a relatively high number of large pits (maximum 12), which clearly differentiate it from the other *U. arctos* groups from different geographical regions (see also table 3.3). In

contrast, *U. arctos* from central Europe possess a relatively small number of large pits (fewer than 6) and an intermediate number of small pits (between 15 and 22), again differentiating it from *U. arctos* from northern Europe, which has highest number of large pits (most individuals have between 6 and 9) and small pits (between 20 and 30) (Fig. 3.10.A). Regarding the *U. arctos* from Russia, although there is an overlap of some individuals with *U. arctos* from both northern and central Europe, most have a relatively high number of large pits (between 6 and 12), closer to the ecospace occupied by *U. arctos* from Greece but with the overall number of small pits between 10 and 27 (see also table 3.3).

A. melanoleuca is readily distinguished from the other species and displays the highest number of small pits (between 20 and 30) in any of the species observed. In contrast, most individuals of *U. maritimus* have a total number of large pits lower than 6 and a total of small pits between 11 and 20 (Fig. 3.10.A).

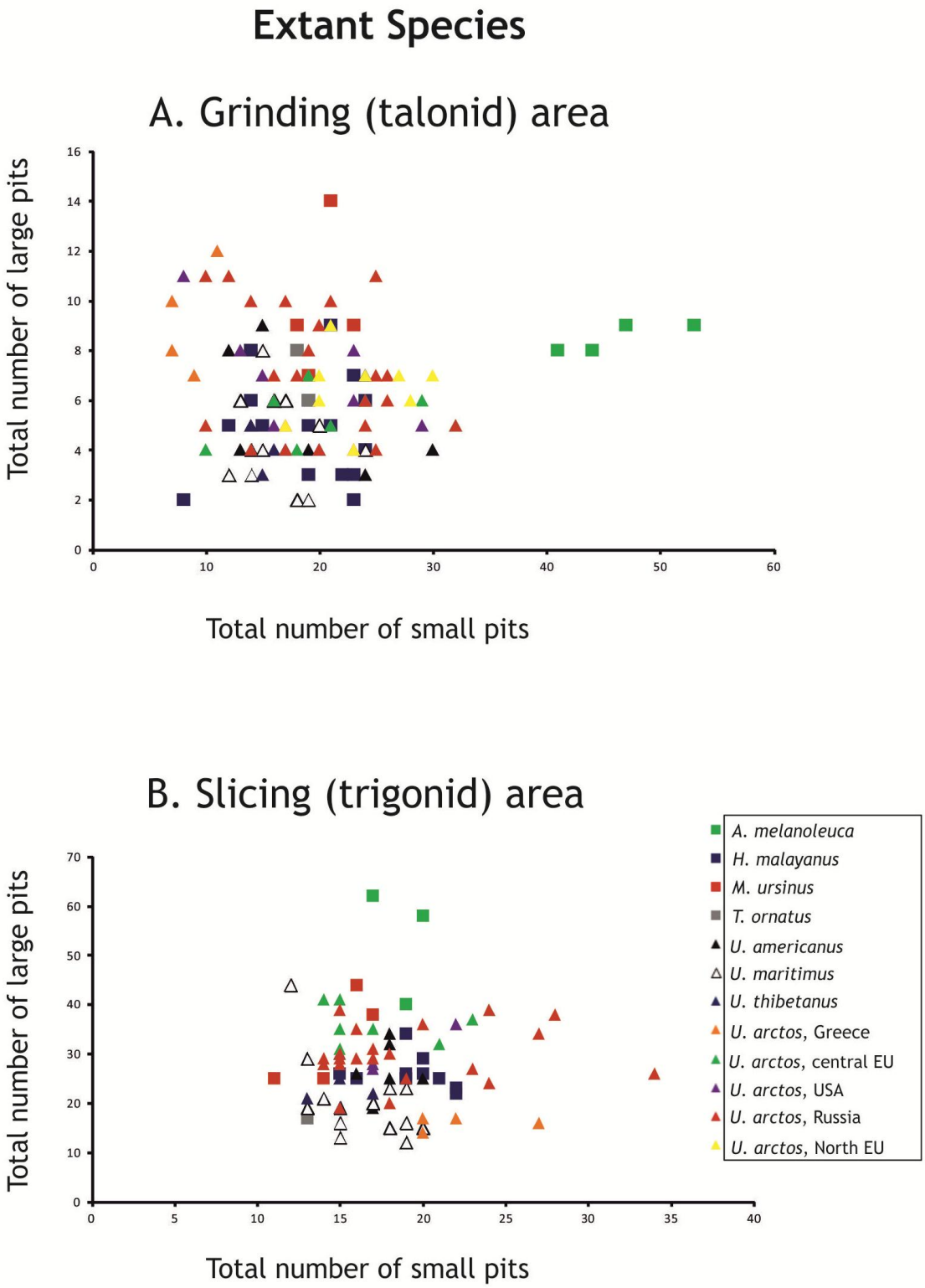

Figure 3.10. Plot of raw data for extant species of the total number of large versus small pits. **A.** Analysis on grinding (talonid) area. **B.** Analysis on slicing (trigonid) area. For the total number of each species, see table 3.2.

Figures 3.11.A and 3.11.B show the mean number of pits versus scratches for each species, and for both the grinding and slicing surfaces respectively. Again, patterns based on observations of the grinding area are more distinct, allowing clearer differentiation of the species, whereas observations made on the slicing area reveal a large overlap in standard deviation values and means in some species. Returning to the detail of the grinding area (Fig. 3.11.A), there is a clear separation between the bamboo eater *A. melanoleuca* and the hyper-carnivorous *U. maritimus*, with the former having the highest average number of pits (mean 57) and intermediate values for average number of scratches (mean 19). The same graph reveals further distinction between species with differing diets, since the insectivorous *M. ursinus* exhibits a relatively high average number of pits (mean 36.8) and the smallest average number of scratches (mean 16) compared to both *U. maritimus* and the insectivorous/frugivorous *H. malayanus*, the latter having an intermediate average number of pits (mean 25.7) and scratches (mean 19.5).

Additionally, all *U. arctos* groups are distinguished from the other species and occupy the right-hand sector of the graph, in which the total number of average values for scratches is greater than for all other species. Interestingly, even within the *U. arctos* group, it is possible to observe a separation between the individuals from different geographical regions. *U. arctos* from central Europe have the highest average number of pits (mean 36.2), *U. arctos* from Russia and northern Europe have intermediate values (mean 31.5 and 32.4 respectively), whereas *U. arctos* from Greece have the lowest average number of pits (mean 20). In contrast, the omnivorous *U. americanus* plots in the left-hand sector of the graph and is clearly differentiated from the *U. arctos* group, having a smaller average number of scratches (mean 16.1) and an intermediate average number of pits (mean 27.4) (Fig. 3.11.A).

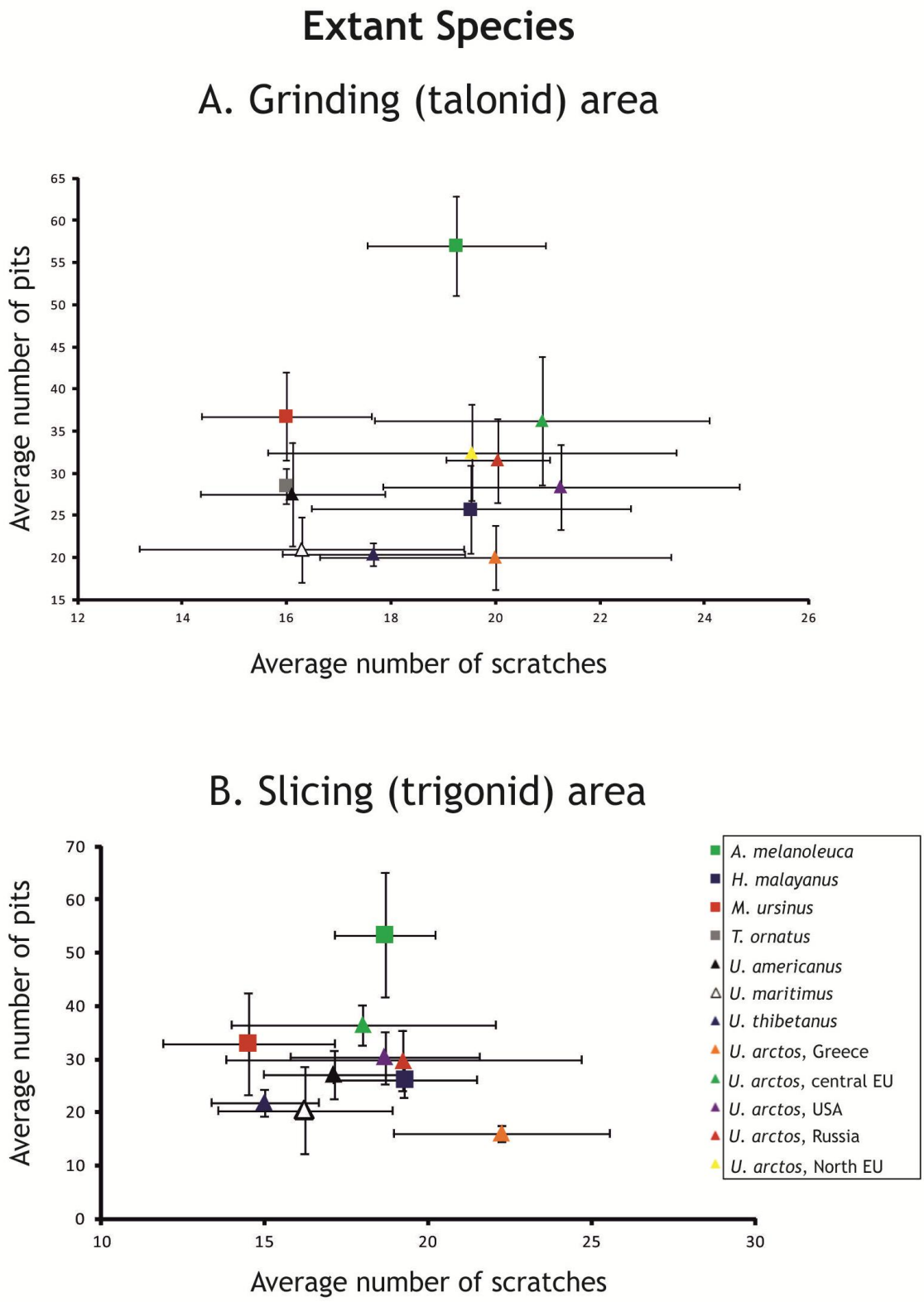

Figure 3.11. Bivariate plot for extant species based on microwear signatures (average number of pits versus scratches). Error bars represent the standard deviation of pits and scratches. **A.** Analysis on grinding (talonid) area. **B.** Analysis on slicing (trigonid) area. For the total number of each species please see table 3.2.

As stated above, pits are viewed as more important than scratches for establishing dietary differentiation. For this reason, an additional chart (Fig. 3.12) was created that shows the range of the total pit number in all species and in *U. arctos* from different geographical regions. These data again illustrate that there are some major differences between the different species. However, surprisingly, there is overlap noted between *U. maritimus* and *U. arctos* from Greece with respect to their values for the 1st and 3rd quartile, although the median values differ. Moreover, the mean values are also close between the following pairs of species: *T. ornatus* and *U. americanus*, *U. thibetanus* and *U. arctos* from Greece, and *U. arctos* from Russia and *U. arctos* from northern Europe (Fig. 3.12).

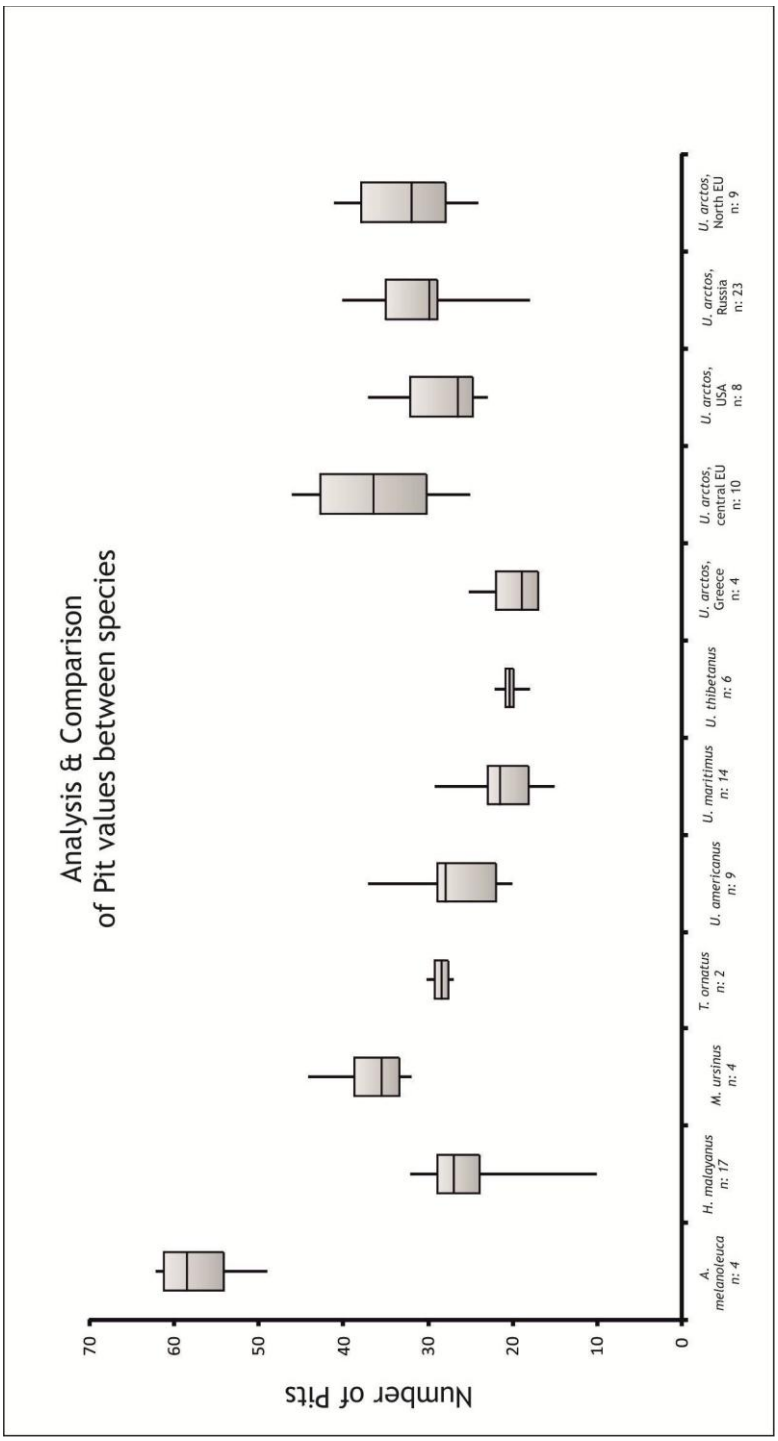

Figure 3.12. Box and whisker plot showing the values for pits from each extant species. The boxes represent 25th – 75th percentiles, the medians (black lines) and the whiskers show maximum and minimum values.

3.4.3. Statistical tests

To establish which microwear variables are significant in the differentiation of extant species, analysis of variance (ANOVA) statistical tests were performed, together

Tukey's pairwise comparison tests, for measurements of all microwear features (or variables) made on both the grinding and slicing areas from all species.

3.4.3.1. Statistical analysis of the grinding area

Table 3.4 shows the ANOVA between extant species based on the grinding area. The p-values for the following microwear features: scratches, pits, fine scratches, coarse scratches, large pits, small pits, gouges and puncture pits reveal significant ($p<0.05$) differences between the groups. This means that between any one pair of bear species, there is a significant difference in at least one of the above features. Two features, the scratch width score and the observation of cross-scratches (absence or presence) were excluded as most values were very similar between species.

Table 3.4. ANOVA results for extant species on the **grinding** area. Summary of the results from all features that were measured in each species, compared and tested between and within groups. Abbreviations as follows: Sum of sqrs is the sum of squares due to features; df is the degree of freedom in the features; Mean sqrs is the mean sum of squares due to features; F is the *F*-statistic and p is the p-value.

		Sum of sqrs	df	Mean sqrs	F	p
Scratches	**Between groups:**	338.21	10	33.8	3.275	0.001 ***
	Within groups:	1001.64	97	10.3		
	Total:	1339.85	107			
		Sum of sqrs	**df**	**Mean sqrs**	**F**	**p**
Pits	**Between groups:**	6036.54	10	603.6	21.91	< 0.0001 ****
	Within groups:	2672.2	97	27.5		
	Total:	8708.74	107			
		Sum of sqrs	**df**	**Mean sqrs**	**F**	**p**
Fine Scratches	**Between groups:**	604.91	10	60.5	5.295	< 0.0001 ****
	Within groups:	1108.05	97	11.4		
	Total:	1712.96	107			
		Sum of sqrs	**df**	**Mean sqrs**	**F**	**p**
Coarse Scratches	**Between groups:**	81.97	9	9.1	5.962	< 0.0001 ****
	Within groups:	140.55	92	1.5		
	Total:	222.52	101			
		Sum of sqrs	**df**	**Mean sqrs**	**F**	**p**
Large Pits	**Between groups:**	213.62	10	21.4	5.225	< 0.0001 ****
	Within groups:	396.57	97	4.1		
	Total:	610.19	107			
		Sum of sqrs	**df**	**Mean sqrs**	**F**	**p**

Small Pits	**Between groups:**	3844.29	10	384.4	14.62	0.0001 ****
	Within groups:	2550.71	97	26.3		
	Total:	6395	107			
		Sum of sqrs	**df**	**Mean sqrs**	**F**	**p**
Gouges	**Between groups:**	55.52	8	6.9	16.1	0.0001 ****
	Within groups:	37.07	86	0.4		
	Total:	92.59	94			
		Sum of sqrs	**df**	**Mean sqrs**	**F**	**p**
Puncture Pits	**Between groups:**	341.681	8	42.7	10.76	0.0001 ****
	Within groups:	357.229	90	3.9		
	Total:	698.909	98			

Although the ANOVA results reveal that at least one pair of bear species is significantly different with respect to the number of scratches, table 3.5. shows no significant differences between any of the bear species. However, all the other microwear features observed on the grinding area show significant differences between several bear species (see Tables 3.6 – 3.12).

Table 3.5. Results from **Tukey's test for scratches** on the grinding area between the following extant species: **1:** A. *melanoleuca* (n: 4); **2:** *H. malayanus* (n: 17); **3:** *M. ursinus* (n: 4); **4:** *U. americanus* (n: 9); **5:** *U. maritimus* (n: 14); **6:** *U. thibetanus* (n: 6); **7:** *U. arctos*, Greece (n: 4); **8:** *U. arctos*, Central Europe (n: 10); **9:** *U. arctos*, USA (n: 8); **10:** *U. arctos*, Russia (n: 23); **11:** *U. arctos*, North Europe (n: 9). Values below the diagonal are the results of Tukey's test and those above are the p-values.

	1	**2**	**3**	**4**	**5**	**6**	**7**	**8**	**9**	**10**	**11**
1		1	0.7075	0.7489	0.8085	0.9974	1	0.9963	0.9836	1	1
2	0.2326		0.5961	0.641	0.7099	0.9904	1	0.9993	0.9949	1	1
3	2.705	2.938		1	1	0.996	0.4069	0.1438	0.0871	0.391	0.585
4	2.613	2.845	0.09248		1	0.9978	0.45	0.1669	0.1027	0.433	0.631
5	2.467	2.7	0.2378	0.1453		0.9992	0.5202	0.2086	0.1317	0.503	0.7
6	1.318	1.55	1.387	1.295	1.149		0.952	0.7139	0.574	0.946	1
7	0.6243	0.3917	3.329	3.237	3.092	1.942		1	0.9997	1	1
8	1.373	1.141	4.078	3.986	3.841	2.691	0.7491		1	1	0.9
9	1.665	1.432	4.37	4.277	4.132	2.983	1.04	0.2913		1	0.9
10	0.6604	0.4279	3.366	3.273	3.128	1.978	0.0362	0.7129	1.004		1
11	0.2543	0.0218	2.959	2.867	2.722	1.572	0.3699	1.119	1.41	0.406	

Table 3.6. Results from **Tukey's test for pits** on the grinding area between the following extant species: **1:** A*. melanoleuca* (n: 4); **2:** *H. malayanus* (n: 17); **3:** *M. ursinus* (n: 4); **4:** *U. americanus* (n: 9); **5:** *U. maritimus* (n: 14); **6:** *U. thibetanus* (n: 6); **7:** *U. arctos*, Greece (n: 4); **8:** *U. arctos*, Central Europe (n: 10); **9:** *U. arctos*, USA (n: 8); **10:** *U. arctos*, Russia (n: 23); **11:** *U. arctos*, North Europe (n: 9). Values below the diagonal are the results of Tukey's test and those above are the p-values. Significant inter-species differences are marked in pink.

	1	2	3	4	5	6	7	8	9	10	11
1		0.0002	0.0001	0.0001	0.0001	0.0002	0.0002	0.0001	0.0002	0.0001	0.0001
2	15.95		0.006	0.9999	0.8209	0.6924	0.6109	0.01164	0.9966	0.583	0.360
3	10.32	5.628		0.0428	0.00018	0.0002	0.0002	1	0.1044	0.726	0.898
4	15.06	0.886	4.742		0.4109	0.2832	0.2235	0.07352	1	0.926	0.776
5	18.38	2.434	8.062	3.32		1	1	0.0002	0.2231	0.01	0.0034
6	18.69	2.738	8.366	3.624	0.3033		1	0.0002	0.1393	0.005	0.0016
7	18.85	2.908	8.536	3.794	0.4732	0.1699		0.0002	0.1044	0.003	0.0011
8	10.6	5.348	0.2803	4.462	7.782	8.086	8.255		0.1665	0.839	0.957
9	14.59	1.36	4.268	0.4742	3.795	4.098	4.268	3.988		0.988	0.9272
10	12.98	2.964	2.664	2.078	5.398	5.702	5.871	2.384	1.604		1
11	12.51	3.434	2.194	2.548	5.868	6.172	6.342	1.914	2.074	0.47	

Table 3.7. Results from **Tukey's test for fine scratches** on the grinding area between the following extant species: **1:** *A. melanoleuca* (n: 4); **2:** *H. malayanus* (n: 17); **3:** *M. ursinus* (n: 4); **4:** *U. americanus* (n: 9); **5:** *U. maritimus* (n: 14); **6:** *U. thibetanus* (n: 6); **7:** *U. arctos*, Greece (n: 4); **8:** *U. arctos*, Central Europe (n: 10); **9:** *U. arctos*, USA (n: 8); **10:** *U. arctos*, Russia (n: 23); **11:** *U. arctos*, North Europe (n: 9). Values below the diagonal are the results of Tukey's test and those above are the p-values. Significant inter-species differences are marked in pink.

	1	2	3	4	5	6	7	8	9	10	11
1		0.9905	0.01836	0.06763	0.00072	0.1934	0.0281	0.9961	1	0.834	0.688
2	1.548		0.294	0.586	0.02613	0.8532	0.3759	1	1	1	0.9988
3	5.144	3.596		1	0.9961	0.9983	1	0.2349	0.0899	0.69	0.835
4	4.506	2.959	0.6375		0.9377	1	1	0.5056	0.25	0.92	0.976
5	6.529	4.981	1.385	2.022		0.7378	0.9888	0.01836	0.0047	0.132	0.228
6	3.891	2.343	1.253	0.6155	2.638		0.9996	0.7933	0.5163	0.993	0.9992
7	4.946	3.398	0.1978	0.4396	1.583	1.055		0.3075	0.1268	0.777	0.897
8	1.385	0.1629	3.759	3.121	5.144	2.506	3.561		1	1	0.997
9	0.7914	0.7565	4.353	3.715	5.737	3.1	4.155	0.5935		0.987	0.9497
10	2.4	0.8521	2.744	2.106	4.129	1.491	2.546	1.015	1.609		1
11	2.748	1.2	2.396	1.759	3.781	1.143	2.198	1.363	1.956	0.348	

Table 3.8. Results from **Tukey's test for coarse scratches** features on grinding area between the following extant species: **2:** *H. malayanus* (n: 17); **3:** *M. ursinus* (n: 4); **4:** *U. americanus* (n:9); **5:** *U. maritimus* (n: 14); **6:** *U. thibetanus* (n: 6); **7:** *U. arctos*, Greece (n: 4); **8:** *U. arctos*, Central Europe (n: 10); **9:** *U. arctos*, USA (n: 8); **10:** *U. arctos*, Russia (n: 23); **11:** *U. arctos*, North Europe (n: 9). Values below the diagonal are the results of Tukey's test and those above are the p-values. Significant inter-species differences are marked in pink.

	2	**3**	**4**	**5**	**6**	**7**	**8**	**9**	**10**	**11**
2		0.9273	1	0.7778	0.8797	0.0002	0.8308	0.9921	0.3958	0.445
3	1.966		0.9833	1	1	0.0002	1	1	0.9957	0.998
4	0.4057	1.56		0.9114	0.9646	0.0002	0.941	0.9995	0.5886	0.641
5	2.441	0.4753	2.035		1	0.0002	1	0.9992	0.9999	1
6	2.153	0.1872	1.747	0.288		0.0002	1	0.9999	0.9987	1
7	10.39	8.425	9.985	7.95	8.238		0.0002	0.000159	0.0002	0.0002
8	2.303	0.337	1.897	0.1383	0.1498	8.088		0.9998	0.9996	1
9	1.404	0.5617	0.9985	1.037	0.7489	8.987	0.8987		0.9484	0.965
10	3.26	1.294	2.855	0.819	1.107	7.131	0.9573	1.856		1
11	3.152	1.186	2.746	0.7105	0.9985	7.239	0.8488	1.747	0.1085	

Table 3.9. Results from **Tukey's test for large pits** features on grinding area between the following extant species: **1:** A*. melanoleuca* (n: 4); **2:** *H. malayanus* (n: 17); **3:** *M. ursinus* (n: 4); **4:** *U. americanus* (n: 9); **5:** *U. maritimus* (n: 14); **6:** *U. thibetanus* (n: 6); **7:** *U. arctos*, Greece (n: 4); **8:** *U. arctos*, Central Europe (n: 10); **9:** *U. arctos*, USA (n: 8); **10:** *U. arctos*, Russia (n: 23); **11:** *U. arctos*, North Europe (n: 9). Values below the diagonal are the results of Tukey's test and those above are the p-values. Significant inter-species differences are marked in pink.

	1	**2**	**3**	**4**	**5**	**6**	**7**	**8**	**9**	**10**	**11**
1		0.071	0.9844	0.1526	0.01322	0.0132	0.9998	0.1387	0.8624	0.934	0.701
2	4.474		0.0018	1	1	1	0.0089	1	0.9072	0.822	0.976
3	1.654	6.128		0.0051	0.00034	0.0003	1	0.0045	0.1716	0.257	0.087
4	4.042	0.432	5.695		0.9984	0.9984	0.0233	1	0.9786	0.942	0.997
5	5.291	0.817	6.945	1.249		1	0.0013	0.9989	0.5771	0.444	0.766
6	5.291	0.817	6.945	1.249	0		0.0013	0.9989	0.5771	0.444	0.7662
7	0.9921	5.466	0.6614	5.034	6.283	6.283		0.0205	0.4171	0.549	0.251
8	4.101	0.373	5.754	0.05879	1.191	1.191	5.093		0.9728	0.93	0.996
9	2.315	2.159	3.968	1.727	2.976	2.976	3.307	1.786		1	1
10	2.042	2.432	3.695	2	3.25	3.25	3.034	2.059	0.2732		1
11	2.719	1.755	4.373	1.323	2.572	2.572	3.711	1.382	0.4042	0.677	

Table 3.10. Results from **Tukey's test for small pits** on the grinding area between the following extant species: **1:** A. *melanoleuca* (n: 4); **2:** *H. malayanus* (n: 17); **3:** *M. ursinus* (n: 4); **4:** *U. americanus* (n: 9); **5:** *U. maritimus* (n: 14); **6:** *U. thibetanus* (n: 6); **7:** *U. arctos*, Greece (n: 4); **8:** *U. arctos*, Central Europe (n: 10); **9:** *U. arctos*, USA (n: 8); **10:** *U. arctos*, Russia (n: 23); **11:** *U. arctos*, North Europe (n: 9). Values below the diagonal are the results of Tukey's test and those above are the p-values. Significant inter-species differences are marked in pink.

	1	2	3	4	5	6	7	8	9	10	11
1		0.0002	0.0001	0.0001	0.0001	0.0002	0.0002	0.0001	0.0002	0.0002	0.00017
2	14.46		0.9999	1	0.9988	0.9834	0.0151	0.9278	1	1	0.7935
3	13.56	0.8974		1	0.9203	0.7694	0.0018	0.999	0.9998	1	0.987
4	14.21	0.2455	0.652		0.9942	0.9566	0.0087	0.9684	1	1	0.879
5	15.67	1.208	2.105	1.453		1	0.1572	0.4303	0.9993	0.964	0.2506
6	16.13	1.667	2.564	1.912	0.4595		0.3062	0.242	0.9886	0.861	0.123
7	19.69	5.231	6.129	5.477	4.024	3.564		0.0002	0.0181	0.003	0.0002
8	12.39	2.071	1.174	1.826	3.279	3.738	7.302		0.9091	0.995	1
9	14.54	0.0805	0.978	0.326	1.127	1.586	5.151	2.152		1	0.7602
10	13.81	0.6537	0.2438	0.4082	1.861	2.321	5.885	1.417	0.7342		0.9651
11	11.95	2.506	1.608	2.26	3.713	4.173	7.737	0.4347	2.586	1.852	

Table 3.11. Results from **Tukey's test for gouges** on the grinding area between the following extant species: **2:** *H. malayanus* (n: 17); **3:** *M. ursinus* (n: 4); **5:** *U. maritimus* (n:14); **6:** *U. thibetanus* (n: 6); **7:** *U. arctos*, Greece (n: 4); **8:** *U. arctos*, Central Europe (n: 10); **9:** *U. arctos*, USA (n: 8); **10:** *U. arctos*, Russia (n: 23); **11:** *U. arctos*, North Europe (n: 9). Values below the diagonal are the results of Tukey's test and those above are the p-values. Significant inter-species differences are marked in pink.

	2	3	5	6	7	8	9	10	11
2		0.0001	1	0.9882	0.0001	0.0001	1	1	1
3	9.788		0.0001	0.0001	0.8575	0.9563	0.0001	0.0001	0.0001
5	0.4425	10.23		0.9355	0.0001	0.0001	0.9998	0.9959	1
6	1.363	8.425	1.805		0.0009	0.0004	0.998	1	0.9958
7	7.682	2.106	8.124	6.319		1	0.0002	0.0002	0.0002
8	8.103	1.685	8.546	6.74	0.4213		0.0001	0.0002	0.0001
9	0.3097	9.478	0.7522	1.053	7.372	7.793		1	1
10	0.7219	9.066	1.164	0.641	6.96	7.381	0.4121		1
11	0.1927	9.595	0.6352	1.17	7.489	7.91	0.117	0.5291	

Table 3.12. Results from **Tukey's test for puncture pits** on the grinding area between the following extant species: **2:** *H. malayanus* (n: 17); **3:** *M. ursinus* (n: 4); **4:** *U. americanus* (n: 9); **5:** *U. maritimus* (n: 14); **7:** *U. arctos*, Greece (n: 4); **8:** *U. arctos*, Central Europe (n: 10); **9:** *U. arctos*, USA (n: 8); **10:** *U. arctos*, Russia (n: 23); **11:** *U. arctos*, North Europe (n: 9). Values below the diagonal are the results of Tukey's test and those above are the p-values. Significant inter-species differences are marked in pink.

	2	3	4	5	7	8	9	10	11
2		0.4418	0.9929	0.4996	0.6223	0.0037	1	0.1639	0.9998
3	3.052		0.9388	0.0019	0.00344	0.6343	0.736	0.9998	0.8012
4	1.263	1.789		0.08772	0.1351	0.056	1	0.6795	1
5	2.928	5.98	4.191		1	0.0001	0.2396	0.0003	0.1907
7	2.673	5.725	3.936	0.2556		0.0001	0.334	0.0006	0.273
8	5.699	2.648	4.437	8.628	8.372		0.0153	0.9186	0.0215
9	0.6267	2.425	0.6361	3.555	3.3	5.073		0.3812	1
10	3.814	0.7622	2.551	6.742	6.487	1.885	3.187		0.4527
11	0.7857	2.266	0.477	3.714	3.459	4.914	0.159	3.028	

3.4.3.2. Statistical analysis of the slicing area

Table 3.13 shows the ANOVA between extant species based on the slicing area. The p-values for the following microwear features: scratches, pits, fine scratches, coarse scratches, large pits, small pits and puncture pits reveal significant ($p<0.05$) differences between groups. This means that there is for any pair of bear species, there is a significant difference in at least one of the above features. However, it must be noted that the ANOVA p-values from the slicing area features are higher than those from the grinding area (e.g. p-values from scratches, fine scratches and large pits) (tables 3.13 and 3.15, 3.16 and 3.18). Three features: the scratch width score, gouges and the observation of cross-scratches (absence or presence) were excluded, as most values were similar between species. Thus, unlike the tests on the grinding area, Tukey's pairwise tests on the slicing area revealed significant differences only between *U. arctos* (Greece) and *M. ursinus* for scratches (Tables 3.14), between *A. melanoleuca* and *M. ursinus* and *A. melanoleuca* and *U. maritimus* for fine scratches (Tables 3.16) and between *U. maritimus* and *U. arctos* (central Europe) and *U. thibetanus* and *U. arctos* (central Europe) for puncture pits (Table 3.20). Although the ANOVA results revealed that at least one pair of bear species should be significant different from each

other with respect to the number of large pits, there are no significant differences between any of the bear species in Table 3.18. The exceptions are differences based on pits, coarse scratches and small pits (Tables 3.15, 3.17 and 3.19 respectively), which reveal some more significant differences between some species.

Table 3.13. ANOVA results for extant species on the **slicing** area. Summary of the results from all features that were measured in each species, compared and tested between and within groups. Abbreviations as follows: Sum of sqrs is the sum of squares due to features; df is the degree of freedom in the features; Mean sqrs is the mean sum of squares due to features; F is the *F*-statistic and p is the p-value.

		Sum of sqrs	df	Mean sqrs	F	p
Scratches	**Between groups:**	261.63	9	29.1	2.131	0.04 *
	Within groups:	968.32	71	13.6		
	Total:	1229.95	80			
		Sum of sqrs	**df**	**Mean sqrs**	**F**	**p**
Pits	**Between groups:**	4267.41	9	474.2	13.56	< 0.0001 ****
	Within groups:	2482.54	71	34.9		
	Total:	6749.95	80			
		Sum of sqrs	**df**	**Mean sqrs**	**F**	**p**
Fine Scratches	**Between groups:**	366.65	9	40.7	3.639	0.001 ***
	Within groups:	806.05	72	11.2		
	Total:	1172.7	81			
		Sum of sqrs	**df**	**Mean sqrs**	**F**	**p**
Coarse Scratches	**Between groups:**	134.34	8	16.8	5.228	< 0.0001 ****
	Within groups:	221.62	69	3.2		
	Total:	355.96	77			
		Sum of sqrs	**df**	**Mean sqrs**	**F**	**p**
Large Pits	**Between groups:**	175.7	9	19.5	2.093	0.04 *
	Within groups:	662.4	71	9.3		
	Total:	838.11	80			
		Sum of sqrs	**df**	**Mean square**	**F**	**p**
Small Pits	**Between groups:**	2791.07	9	310.1	9.655	< 0.0001 ****
	Within groups:	2280.51	71	32.1		
	Total:	5071.58	80			
		Sum of sqrs	**df**	**Mean sqrs**	**F**	**p**
Puncture Pits	**Between groups:**	212.82	7	30.4	4.521	<0.001 ***
	Within groups:	443.85	66	6.7		
	Total:	656.66	73			

Table 3.14. Results from **Tukey's test for scratches** on the slicing area between the following extant species: **1:** *A. melanoleuca* (n: 3); **2:** *H. malayanus* (n: 11); **3:** *M. ursinus* (n: 4); **4:** *U. americanus* (n: 9); **5:** *U. maritimus* (n: 14); **6:** *U. thibetanus* (n: 4); **7:** *U. arctos*, Greece (n: 4); **8:** *U. arctos*, Central Europe (n: 8); **9:** *U. arctos*, USA (n: 3); **10:** *U. arctos*, Russia (n: 21). Values below the diagonal are the results of Tukey's test and those above are the p-values. Significant inter-species differences are marked in pink.

	1	**2**	**3**	**4**	**5**	**6**	**7**	**8**	**9**	**10**
1		1	0.7025	0.9995	0.9844	0.8306	0.8487	1	1	1
2	0.3802		0.522	0.9937	0.936	0.672	0.9455	0.9999	1	1
3	2.614	2.994		0.9763	0.9989	1	0.03122	0.8656	0.7025	0.5324
4	0.976	1.356	1.638		1	0.9947	0.4148	1	0.9995	0.9944
5	1.539	1.919	1.076	0.5627		0.9999	0.203	0.9985	0.9844	0.9402
6	2.3	2.681	0.3137	1.325	0.7618		0.05717	0.9429	0.8306	0.682
7	2.248	1.868	4.862	3.224	3.787	4.549		0.6786	0.8487	0.9416
8	0.4183	0.7985	2.196	0.5577	1.12	1.882	2.666		1	0.9999
9	0	0.3802	2.614	0.976	1.539	2.3	2.248	0.4183		1
10	0.3585	0.02173	2.973	1.334	1.897	2.659	1.89	0.7768	0.3585	

Table 3.15. Results from **Tukey's test for pits** on the slicing area between the following extant species: **1:** *A. melanoleuca* (n: 3); **2:** *H. malayanus* (n: 11); **3:** *M. ursinus* (n: 4); **4:** *U. americanus* (n: 9); **5:** *U. maritimus* (n: 14); **6:** *U. thibetanus* (n: 4); **7:** *U. arctos*, Greece (n: 4); **8:** *U. arctos*, Central Europe (n: 8); **9:** *U. arctos*, USA (n: 3); **10:** *U. arctos*, Russia (n: 21). Values below the diagonal are the results of Tukey's test and those above are the p-values. Significant inter-species differences are marked in pink.

	1	**2**	**3**	**4**	**5**	**6**	**7**	**8**	**9**	**10**
1		0.0002	0.0002	0.0002	0.0002	0.0002	0.0002	0.001	0.0002	0.0002
2	10.71		0.6428	1	0.8608	0.9735	0.1668	0.1325	0.97	0.9885
3	7.967	2.743		0.8434	0.026	0.07388	0.00061	0.9947	0.9992	0.9962
4	10.23	0.4789	2.264		0.6676	0.8812	0.07533	0.2681	0.9972	0.9994
5	12.92	2.211	4.954	2.69		1	0.9689	0.0014	0.1692	0.2345
6	12.38	1.665	4.408	2.144	0.5458		0.8471	0.0048	0.3544	0.4535
7	14.63	3.918	6.661	4.397	1.707	2.253		0.0002	0.0062	0.010
8	6.645	4.065	1.322	3.586	6.276	5.731	7.984		0.806	0.7128
9	9.012	1.698	1.045	1.219	3.909	3.363	5.616	2.367		1
10	9.236	1.474	1.269	0.9951	3.685	3.139	5.392	2.591	0.2239	

Table 3.16. Results from **Tukey's test for fine scratches** on the slicing area between the following extant species: **1:** *A. melanoleuca* (n: 3); **2:** *H. malayanus* (n: 11); **3:** *M. ursinus* (n: 4); **4:** *U. americanus* (n: 9); **5:** *U. maritimus* (n: 14); **6:** *U. thibetanus* (n: 4); **7:** *U. arctos*, Greece (n: 4); **8:** *U. arctos*, Central Europe (n: 8); **9:** *U. arctos*, USA (n: 3); **10:** *U. arctos*, Russia (n: 21). Values below the diagonal are the results of Tukey's test and those above are the p-values. Significant inter-species differences are marked in pink.

	1	2	3	4	5	6	7	8	9	10
1		0.9988	0.0056	0.6291	0.0098	0.2701	0.5736	0.4104	0.518	0.5281
2	1.092		0.0551	0.972	0.0862	0.7577	0.9573	0.8821	0.9377	0.9416
3	5.659	4.567		0.5736	1	0.8995	0.6291	0.7835	0.6834	0.6737
4	2.772	1.68	2.887		0.691	0.9999	1	1	1	1
5	5.411	4.319	0.2475	2.64		0.9517	0.7423	0.8713	0.7901	0.7817
6	3.58	2.488	2.079	0.8084	1.831		1	1	1	1
7	2.887	1.795	2.772	0.1155	2.524	0.6929		1	1	1
8	3.233	2.142	2.425	0.4619	2.178	0.3464	0.3464		1	1
9	3.003	1.911	2.656	0.231	2.409	0.5774	0.1155	0.231		1
10	2.982	1.89	2.677	0.21	2.43	0.5984	0.09448	0.252	0.021	

Table 3.17. Results from **Tukey's test for coarse scratches** on the slicing area between the following extant species: **2:** *H. malayanus* (n: 11); **3:** *M. ursinus* (n: 4); **4:** *U. americanus* (n:9); **5:** *U. maritimus* (n:14); **6:** *U. thibetanus* (n:4); **7:** *U. arctos*, Greece (n:4); **8:** *U. arctos*, Central Europe (n:8); **9:** *U. arctos*, USA (n:3); **10:** *U. arctos*, Russia (n:21). Values below the diagonal are the results of Tukey's test and those above are the p-values. Significant inter-species differences are marked in pink.

	2	3	4	5	6	7	8	9	10
2		0.7199	1	0.835	0.9998	0.00017	0.7199	0.509	0.2432
3	2.461		0.8569	1	0.9547	0.01691	1	1	0.9973
4	0.3555	2.106		0.9328	1	0.00023	0.8569	0.6769	0.3782
5	2.171	0.2901	1.816		0.9856	0.00908	1	0.9998	0.9866
6	0.7691	1.692	0.4136	1.402		0.00042	0.9547	0.8445	0.5682
7	7.537	5.076	7.181	5.366	6.768		0.01691	0.04176	0.13
8	2.461	0	2.106	0.2901	1.692	5.076		1	0.9973
9	2.912	0.4512	2.557	0.7412	2.143	4.625	0.4512		0.9999
10	3.557	1.096	3.201	1.386	2.788	3.98	1.096	0.6446	

Table 3.18. Results from **Tukey's test for large pits** on the slicing area between the following extant species: **1:** A. *melanoleuca* (n: 3); **2:** *H. malayanus* (n: 11); **3:** *M. ursinus* (n: 4); **4:** *U. americanus* (n:9); **5:** *U. maritimus* (n:14); **6:** *U. thibetanus* (n:4); **7:** *U. arctos*, Greece (n:4); **8:** *U. arctos*, Central Europe (n:8); **9:** *U. arctos*, USA (n:3); **10:** *U. arctos*, Russia (n:21). Values below the diagonal are the results of Tukey's test and those above are the p-values.

	1	**2**	**3**	**4**	**5**	**6**	**7**	**8**	**9**	**10**
1		0.6135	0.9813	0.4244	0.4108	0.473	0.473	0.6544	0.9963	1
2	2.804		0.9971	1	1	1	1	1	0.9843	0.8985
3	1.58	1.224		0.9777	0.9748	0.9859	0.9859	0.9984	1	0.9998
4	3.203	0.3984	1.622		1	1	1	1	0.9321	0.7608
5	3.233	0.4285	1.653	0.0301		1	1	1	0.9258	0.7481
6	3.097	0.2931	1.517	0.1054	0.1355		1	1	0.9513	0.8031
7	3.097	0.2931	1.517	0.1054	0.1355	0		1	0.9513	0.8031
8	2.718	0.0862	1.138	0.4846	0.5147	0.3793	0.3793		0.9895	0.9198
9	1.264	1.54	0.3161	1.939	1.969	1.833	1.833	1.454		1
10	0.7224	2.082	0.8579	2.48	2.51	2.375	2.375	1.996	0.5418	

Table 3.19. Results from **Tukey's test for small pits** on the slicing area between the following extant species: **1:** A. *melanoleuca* (n: 3); **2:** *H. malayanus* (n: 11); **3:** *M. ursinus* (n: 4); **4:** *U. americanus* (n:9); **5:** *U. maritimus* (n:14); **6:** *U. thibetanus* (n:4); **7:** *U. arctos*, Greece (n:4); **8:** *U. arctos*, Central Europe (n:8); **9:** *U. arctos*, USA (n:3); **10:** *U. arctos*, Russia (n:21). Values below the diagonal are the results of Tukey's test and those above are the p-values. Significant inter-species differences are marked in pink.

	1	**2**	**3**	**4**	**5**	**6**	**7**	**8**	**9**	**10**
1		0.0002	0.0002	0.0002	0.0002	0.0002	0.0002	0.0002	0.0002	0.0002
2	10.59		0.9923	1	0.9916	0.9888	0.378	0.9388	0.9999	1
3	9.199	1.394		0.9974	0.614	0.5859	0.04281	1	1	0.8903
4	10.4	0.19	1.204		0.9797	0.9743	0.3007	0.968	1	0.9997
5	12	1.41	2.803	1.6		1	0.94	0.3752	0.8674	1
6	12.06	1.468	2.862	1.658	0.0584		0.9503	0.3504	0.8486	0.9999
7	13.9	3.308	4.701	3.498	1.898	1.84		0.01513	0.1277	0.7137
8	8.688	1.905	0.511	1.715	3.314	3.373	5.213		0.9985	0.6984
9	9.812	0.7805	0.6132	0.5905	2.19	2.249	4.088	1.124		0.987
10	11.31	0.7185	2.112	0.9085	0.6911	0.7495	2.589	2.623	1.499	

Table 3.20. Results from **Tukey's test for puncture pits** on the slicing area between the following extant species: **2:** *H. malayanus* (n: 11); **3:** *M. ursinus* (n: 4); **4:** *U. americanus* (n: 9); **5:** *U. maritimus* (n: 14); **6:** *U. thibetanus* (n: 4); **8:** *U. arctos*, Central Europe (n: 8); **9:** *U. arctos*, USA (n: 3); **10:** *U. arctos*, Russia (n: 21). Values below the diagonal are the results of Tukey's test and those above are the p-values. Significant inter-species differences are marked in pink.

	2	**3**	**4**	**5**	**6**	**8**	**9**	**10**
2		0.9903	0.9874	0.9521	0.9667	0.1969	1	0.88
3	1.183		1	0.524	0.5725	0.6843	0.9929	0.9996
4	1.237	0.05357		0.499	0.5473	0.7081	0.9905	0.9998
5	1.572	2.755	2.809		1	0.01151	0.9422	0.2349
6	1.468	2.652	2.705	0.1033		0.01431	0.9589	0.2692
8	3.594	2.411	2.357	5.166	5.062		0.2138	0.9288
9	0.0584	1.125	1.179	1.63	1.527	3.536		0.8962
10	1.895	0.7117	0.6582	3.467	3.363	1.699	1.837	

The statistical tests confirm that observations on the grinding (m1 talonid) surface (as seen in Tables 3.5 – 3.12) reveal clearer (ie. more significant) differentiation between species for most microwear features, and also more significant pairwise differences than for observations on the slicing area (m1 trigonid) (Tables 3.14 – 3.20).

3.4.4. Results of the Principal Component Analysis (PCA) on extant ursid species

Multiple components are necessary to account for all of the significant variation observed in the microwear analysis. The results from all extant ursid species were therefore included in a Principal Component Analysis (PCA), comprising both grinding and slicing areas. Plots identifying the first three components explaining variation in grinding (in 3.4.4.1) and slicing (in 3.4.4.2) area observations were accordingly generated.

Nine variables were employed as follows: number of scratches (NS), number of pits (NP), number of fine scratches (NSfine), number of coarse scratches (NScoarse), number of large pits (NLP), number of small pits (NsP), number of gouges (Ngouges), number of puncture pits (NpP) and the scratch width score (SWS) (see in 3.3.4 for details of microscopic scar description).

3.4.4.1. PCA - Results on the grinding (talonid) area of m1s on extant species

The living bear species can be separated into different parts of dietary ecospace, as illustrated by analysis of the grinding area of the teeth. Figures 3.13 A and B show the distribution of extant species through a PCA, using nine independent variables of dental microwear representing eight extant bear species including *U. arctos* from five different geographical regions (Greece, Russia, Central Europe, North Europe and USA) (Appendix I.B table 1, score of PCA).

Table 3.21 shows the summary of the PCA with the values for each component. Abbreviations of the nine independent variables are given also in the caption of Figure 3.13.

Table 3.21. Extant species, analysis on the **grinding** (talonid) area. Summary of Principal Component Analysis (PCA).

PC	Eigenvalue	% variance
1	0.12	41.78
2	0.06	20.99
3	0.03	11.59
4	0.02	8.15
5	0.02	6.77
6	0.02	6.16
7	0.01	4.22
8	0.00	0.23
9	0.00	0.11

On the grinding area along the first axis (x), PC1 explains 41.78% of variance and along the second axis (y), PC2 accounts for 20.99% (Fig. 3.13 A) and PC3 for 11.59% (Fig. 3.13 B). PC1 is heavily influenced by a positive association with the number of puncture pits (NpP) and by a negative association with the scratch width score (SWS). Also, some high scores on other variables suggest a tendency towards a relatively high percentage of number of pits (NP) and number of large pits (NLP). The main variable that contributes positively to component PC2 is the number of coarse scratches (NScoarse) and negatively, the number of small pits (NsP); there is also a low percentage of fine scratches (NSfine) (Fig. 3.13 A). On the plot of PC1 and PC3, the y axis (component 3) is most heavily influenced by the number of large pits (NLP) and negatively, by puncture

pits (NpP). Table 3.22 shows the loadings of each variable of the PCA on the components.

Table 3.22. Extant species, analysis on **grinding** (talonid) area. Loadings of each variable of the PCA on the components.

	PC 1	PC 2	PC 3	PC 4	PC 5	PC 6	PC 7	PC 8	PC 9
NS	0.07	-0.06	0.07	0.11	-0.26	0.12	0.53	-0.15	0.77
NP	**0.22**	-0.23	**0.41**	0.16	0.20	0.06	-0.07	-0.80	-0.15
NSfine	0.12	**-0.27**	0.05	0.04	-0.38	0.19	0.61	0.12	-0.59
NScoarse	0.11	**0.79**	**0.34**	0.41	-0.23	-0.10	0.04	0.01	-0.12
NLP	**0.24**	0.11	**0.55**	-0.67	0.21	-0.23	0.20	0.20	0.04
NsP	0.06	**-0.40**	**0.47**	0.52	0.21	0.00	-0.13	0.52	0.11
Ngouges	0.15	0.18	0.09	-0.15	0.10	0.93	-0.17	0.10	0.03
NpP	**0.88**	0.03	**-0.39**	0.11	0.17	-0.12	0.01	0.08	0.02
SWS	**-0.24**	0.20	**-0.16**	0.18	0.76	0.06	0.51	-0.01	-0.09

The hyper-carnivorous *U. maritimus* is distinguished from other species by having the highest scratches width score (a score of 3, indicating that microwear characteristics in this species include fine scratches, coarse scratches and hypercoarse-scratches), as well as an absence of puncture pits. It is also the only species to reveal the presence of hypercoarse-scratches (Fig. 3.13 A and 3.14 B).

A. melanoleuca is equally separated clearly from all other species and has high number of small pits (NsP) and fine scratches; another important aspect is the absent of coarse scratches (NScoarse) (Fig. 3.13 A and 3.14 A).

On the other end of the microwear spectrum, on the central and right-hand side of the plot (Fig. 3.13 A) and, as determined by the positive association with the number of puncture pits (Npp), are most of the omnivorous species. Some of these species also have individuals that occupy the left-hand side of the microwear spectrum and not unexpectedly, there is an overlap between these individuals. Nevertheless, by looking the distribution of the majority of individuals from each group (species), a good separation can be observed (Fig. 3.13 A). More specifically, *U. arctos* from different geographical regions remain well separated. In particular, *U. arctos* from Russia and from central Europe (Fig. 3.13 A and 3.15 B) show the highest percentage of pits, as well as puncture pits, gouges and large pits. Both the *U. arctos* from Russia and from central Europe have similar number of gouges compared to other species. Furthermore, the former occupies a wide range on the graph, most likely suggesting

that diet is variable from one individual to another. The *U. arctos* from Russia and northern Europe (Fig. 3.15 B and C) are still well separated, with the latter showing the smallest percentage of puncture pits compared with the other *U. arctos* group and occupying the central part of the graph. In contrast, *U. arctos* from Greece occupies the left-hand side of the plot and is clearly separated from the other *U. arctos* grouping. *U. arctos* from the USA has individuals that overlap both with *U. americanus* (see also Fig. 3.14 D), and with *U. arctos* from northern Europe but there are also some outliers (Fig. 3.13 A). Thus, variability in food consumed is clearly apparent.

The insectivore/frugivore *H. malayanus* (Fig. 3.14 C) has a relatively high number of fine scratches (NfineS) and small pits (NsP) and a smaller percentage of number of puncture pits (NpP) when compared with *U. arctos*, Russia and central Europe. Unexpectedly, given its omnivorous diet, *U. thibetanus* (Fig. 3.14 F) is also clearly differentiated from the other omnivorous species and is relatively close to the microwear spectrum of *U. maritimus*. It is more likely that *U. thibetanus* includes a bigger amount of more abrasive items in its diet than the rest of the omnivorous species. Unfortunately, however, the relevant photomicrographs do not clearly show the microwear features (a general problem of microscopic images from bear specimens). Interestingly, *U. thibetanus* has the lowest percent of puncture pits compared with the other omnivorous species and has the highest percentage of SWS after *U. maritimus*. It is also very close to the *U. arctos* from Greece (Fig. 3.13 A).

The omnivorous *U. americanus* occupies mostly the central part of the microwear space, lying closest to and overlapping with other omnivorous individuals but clearly distinct from *U. arctos* from Russia and central Europe (Fig. 3.13 A and 3.14 D). Perhaps unsurprisingly, given their comparable diet (albeit with some slight differentiation according to region and season), there is overlap between some individuals of *U. americanus* and *U. arctos* from northern Europe (Fig. 3.13 A).

Unfortunately, the insectivorous *M. ursinus* (Fig. 3.14 E) and the frugivore/omnivore *T. ornatus* do not separate out into a clear microwear ecospace, probably due to the small number of individuals sampled (Fig. 3.13 A). The former overlaps with most of the specimens on the right-hand side of the plot, while the latter has one individual

that lies within the identified ecospace of *U. americanus* and one in that of *H. malayanus*. However, both species are clearly differentiated from the hypercarnivorous *U. maritimus* and the herbivorous *A. melanoleuca*.

Species differentiation is equally apparent on Fig. 3.13 B, where components 1 and 3 are combined, although this is less clearly visible than in components 1 and 2 (Fig. 3.13 A). Here, both *A. melanoleuca* and *U. maritimus* are well separated from the other bear species, however differentiation amongst the remainder of the species is not obvious.

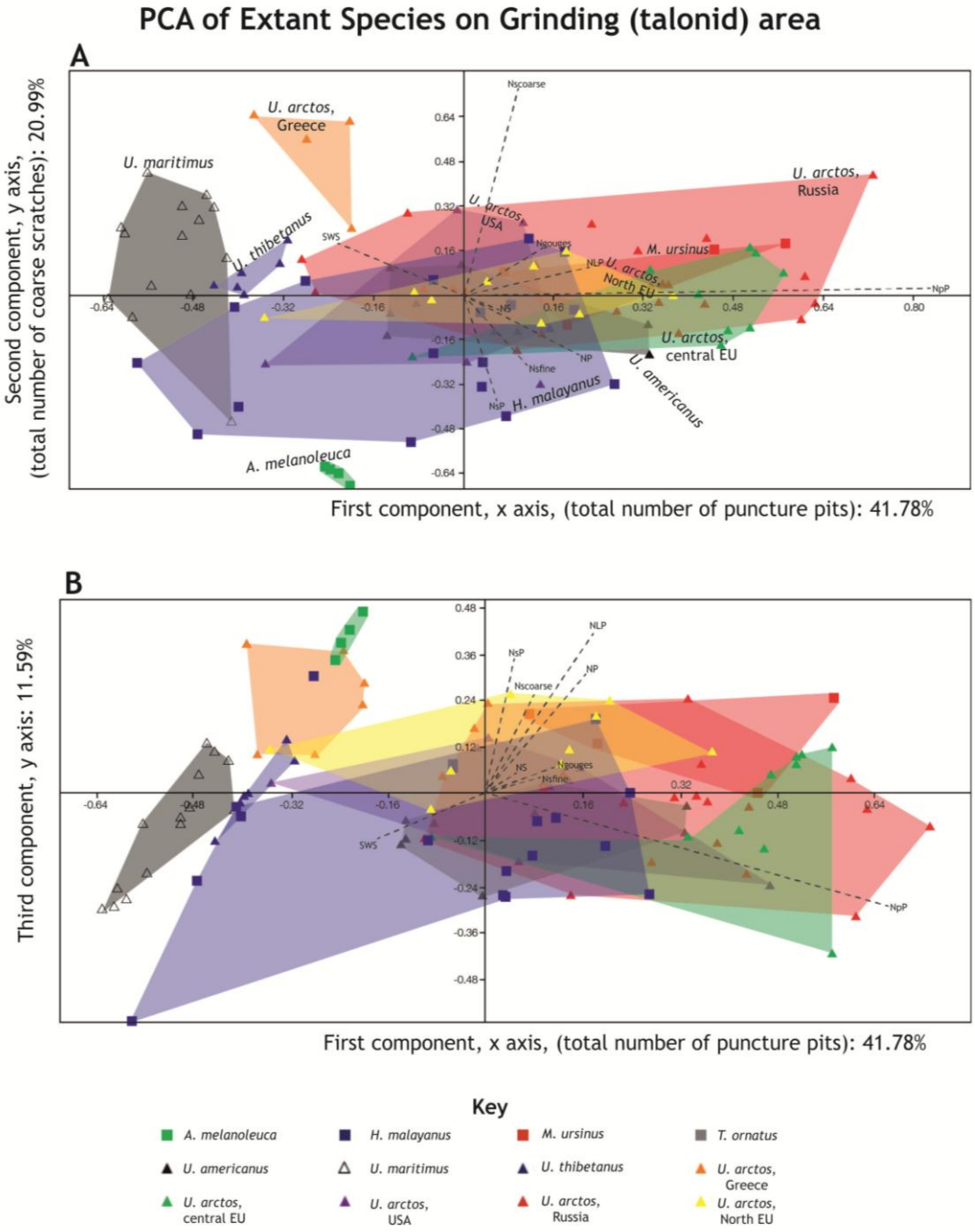

Figure 3.13. PCA plots for extant bear species on the **grinding** (talonid) area. **A**. Graph component 1 versus 2. **B.** Graph component 1 versus 3. For details of symbols, see key. Symbols of Variables as follow: NS: number of scratches; NP: number of pits; NfineS: number of fine scratches; NcoarseS: number of coarse scratches; NLP: number of large pits; NsP: number of small pits; Ngouge: number of gouges; Npp: number of puncture pits; SWS: score of wide scratches.

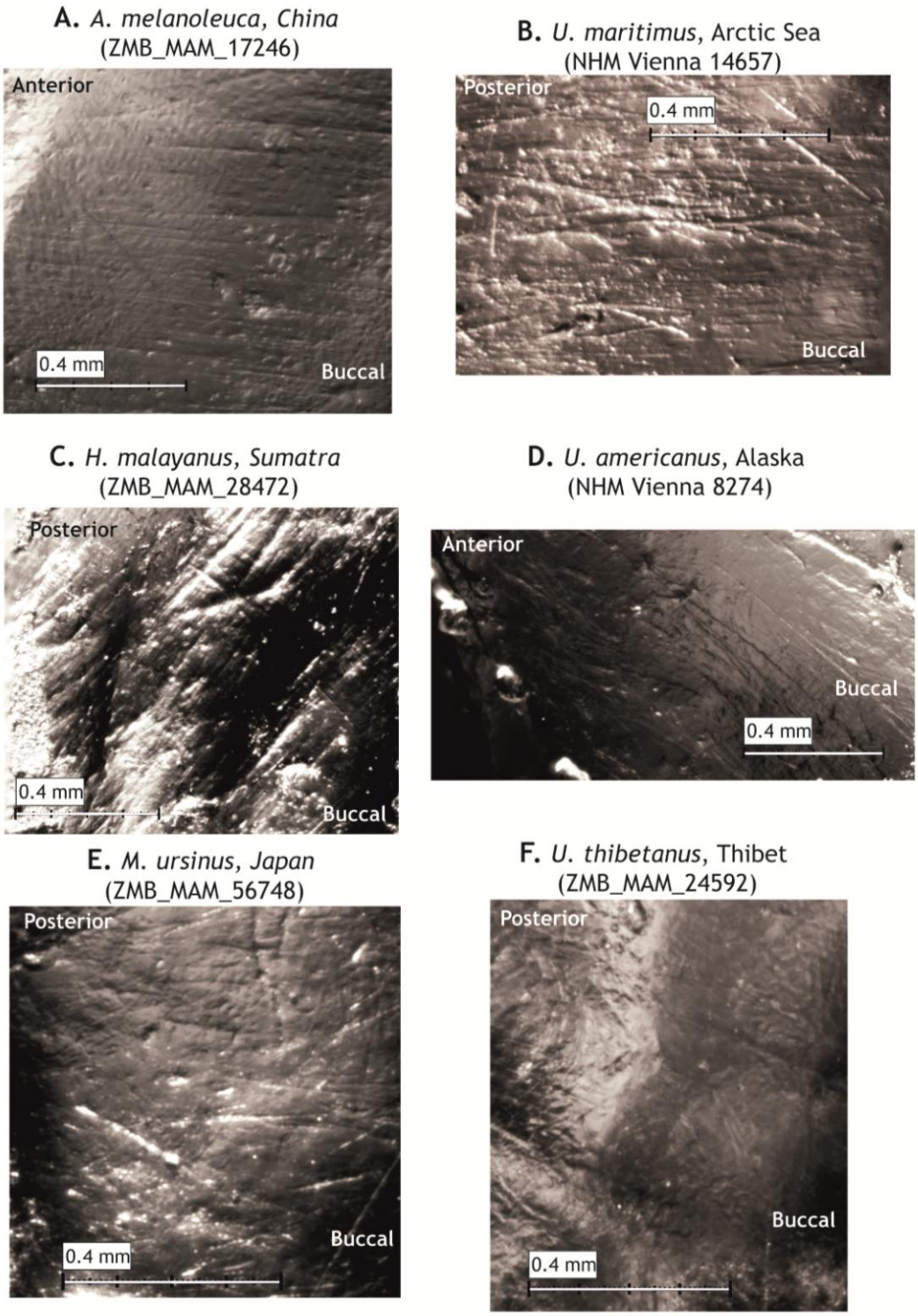

Figure 3.14. Photomicrographs of extant bear species' tooth enamel on the **grinding** (talonid) area at 35 times magnification. **A**. *A. melanoleuca*, **B.** *U. maritimus*, **C.** *H. malayanus*, **D.** *U. americanus*, **E.** *M. ursinus* and **F.** *U. thibetanus*.

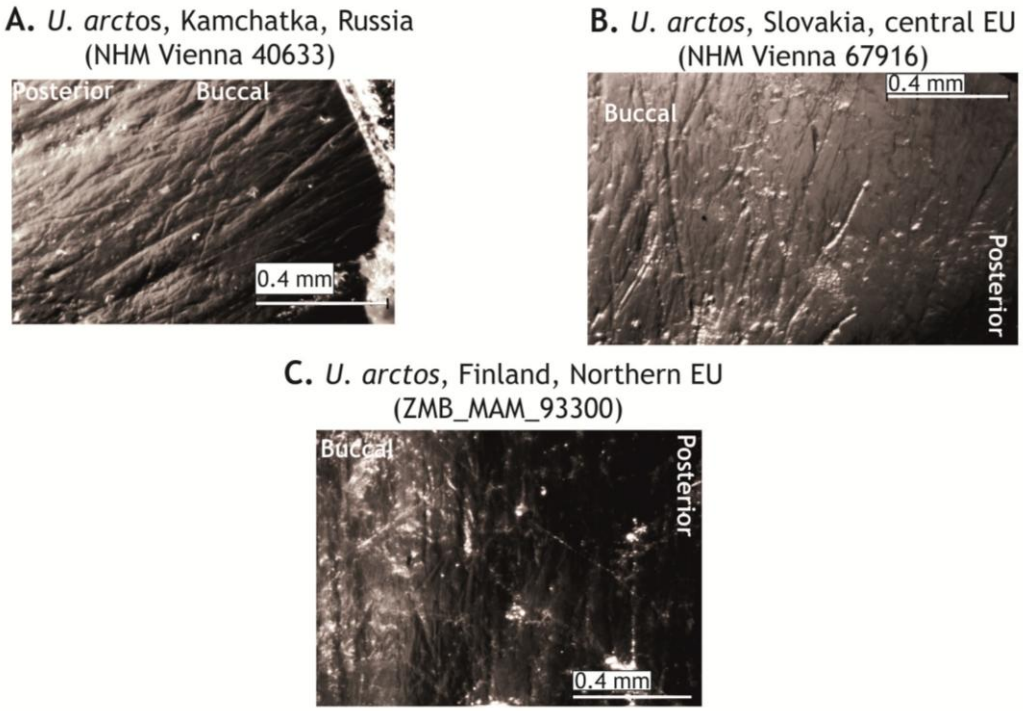

Figure 3.15. Photomicrographs of *U. arctos* (from different geographical regions) tooth enamel on the grinding (talonid) area at 35 times magnification. **A**. *U. arctos,* Kamchatka, Russia; **B.** *U. arctos,* Slovakia, central Europe and **C.** *U. arctos,* Finland, Northern Europe.

3.4.4.2. PCA - Results on the slicing (trigonid) area of m1s on extant species

Figures 3.16 A and B illustrate the distribution of extant bear samples on the first three principal components for the slicing area, using nine independent variables of dental microwear representing eight extant bear species including *U. arctos* from four different geographical regions (Greece, Russia, Central Europe and USA) (Appendix I.B table 2, score of PCA). Table 3.23 presents the summary data of the PCA on the slicing (trigonid) area with the values for each component. On the slicing area, along the first axis (x), PC1 explains 36.88% of variance and along the second axis (y), PC2 accounts for 26.25% and PC3 for 11.66% respectively (Fig. 3.16). The abbreviations of the nine independent variables are given in the caption of Figure 3.16.

Table 3.23. Extant species, analysis on the **slicing** (trigonid) area. Summary of Principal Component Analysis (PCA).

PC	Eigenvalue	% variance
1	0.1350	36.88
2	0.0961	26.25
3	0.0427	11.66
4	0.0402	10.98
5	0.0232	6.33
6	0.0151	4.12
7	0.0115	3.14
8	0.0019	0.52
9	0.0004	0.12

On the slicing area (Fig. 3.16 A and B), PC1 is heavily influenced by a positive association with the number of puncture pits (Npp) and by a negative association with scratches width score (SWS). The main variable that contributes positively to component 2 (PC2) is the number of coarse scratches (NScoarse) and negatively, the number of small pits (Nsp). Regarding PC1 and PC3, the y axis (component 3) is most heavily influenced by the number of large pits (NLp) and negatively by the number of puncture pits (NpP).

Although Figures 3.16 A and B reveal differentiation between some of the extant species such as *U. arctos* from Greece, *U. maritimus* and *A. melanoleuca*, all of which have clear microwear spectra, there are significant overlaps between the other species. The differentiation between species is more difficult to observe on PC1 and PC3 (Fig. 3.16 B).

Table 3.24 shows further information regarding the loadings of each variable of the PCA on the components for the slicing area.

Table 3.24. Extant species, analysis on **Slicing** (trigonid) area. Loadings of each variable of the PCA on the components.

	PC 1	PC 2	PC 3	PC 4	PC 5	PC 6	PC 7	PC 8	PC 9
NS	0.091	0.096	-0.077	-0.054	-0.264	0.287	0.465	0.066	-0.775
NP	0.242	-0.204	0.356	0.144	0.065	0.033	0.189	-0.843	-0.010
NSfine	0.155	-0.068	-0.119	-0.117	-0.469	0.346	0.478	0.068	0.610
NScoarse	-0.029	0.809	0.178	0.475	0.001	-0.140	0.225	-0.004	0.128
NLP	0.224	0.137	0.765	-0.519	0.043	-0.019	0.012	0.271	0.012
NsP	-0.032	-0.505	0.327	0.580	0.159	-0.058	0.299	0.427	0.001
Ngouges	0.179	0.104	0.073	0.225	0.239	0.836	-0.375	0.062	0.019
NpP	0.886	0.026	-0.300	0.046	0.210	-0.241	0.018	0.140	-0.004
SWS	-0.200	0.066	-0.182	-0.279	0.761	0.127	0.489	-0.026	0.102

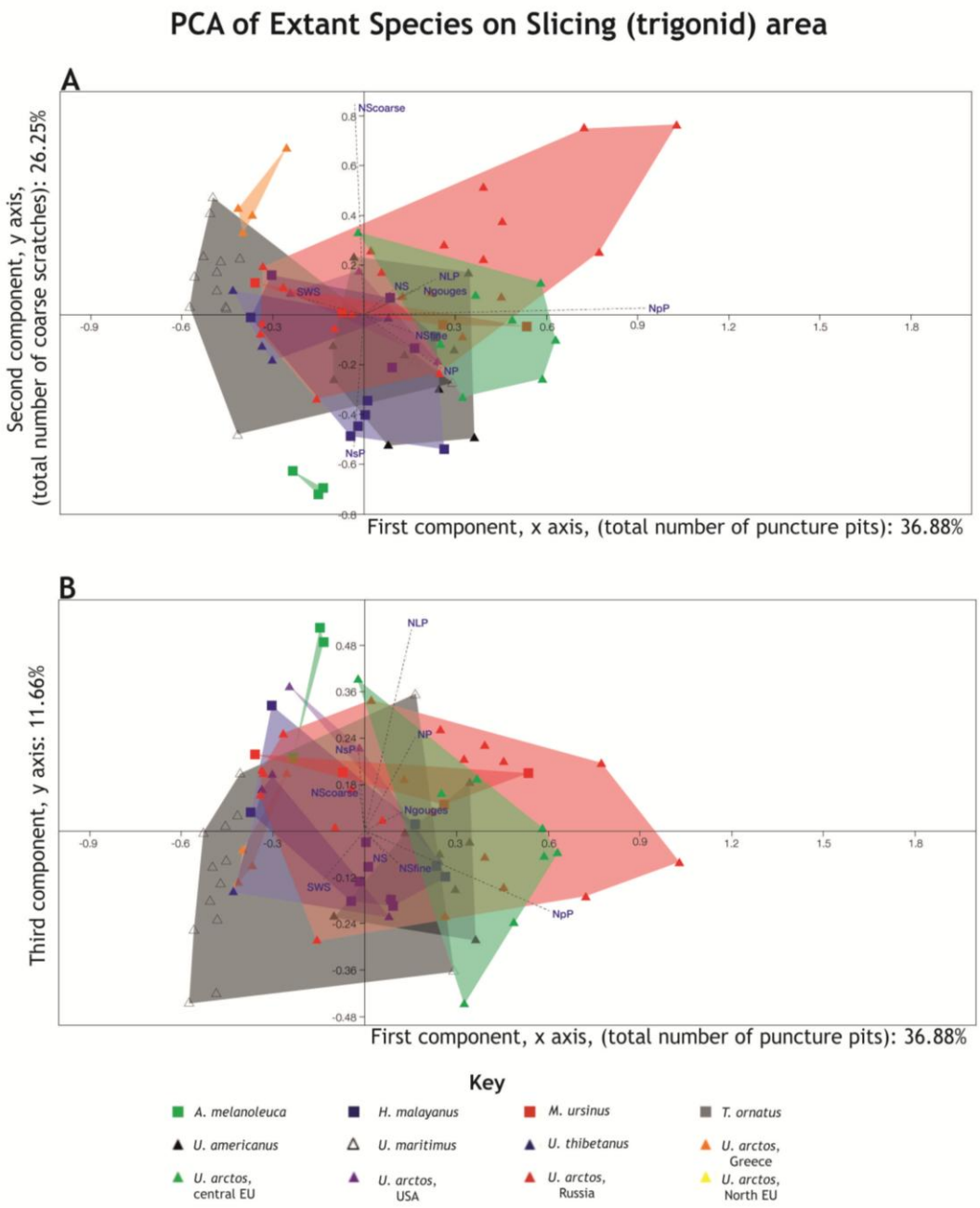

Figure 3.16. PCA plots for extant bear species on the **slicing** (trigonid) area. **A**. Graph component 1 versus 2. **B.** Graph component 1 versus 3. For details of symbols, see key. Symbols of Variables as follow: NS: number of scratches; NP: number of pits; NfineS: number of fine scratches; NcoarseS: number of coarse scratches; NLP: number of large pits; NsP: number of small pits; Ngouge: number of gouges; Npp: number of puncture pits; SWS: scratches width score.

In summary, the PCA results on the grinding area (Figs. 3.13 A and B) are notably clearer and show better the ecospace of each bear species than the PCA results on the slicing area (Figs. 3.16 A and B). Microwear differences in the grinding area of the m1s in extant ursids therefore correlate well with observed differences in their modern

diets and highlight the considerable potential for employing the method with respect to the dietary preferences of extinct bears.

3.5. Discussion

One of the main goals of this thesis was to develop and validate a comprehensive reference database of modern bear teeth related to microwear features for extant Ursidae. Throughout this Chapter, this has been successfully demonstrated. Prior studies of dental microwear on bears (e.g. Goillot *et al*., 2009; Peigné *et al*., 2009; Pinto-Llona, 2013) did not cover all modern bear species in their database. For example, neither Goillot *et al*. (2009) nor Peigné *et al*. (2009) included the omnivorous brown bear or black bears. Although Donohue *et al*. (2013) analysed five extant species, they also excluded brown bears and used a different methodology.

This Chapter has not only presented a comprehensive database for the first time but has also shown that microwear analysis can be applied successfully to most Ursidae, to reveal both inter-specific differentiation and *intra*-specific variation (the latter seen in *U. arctos* from different geographical regions). However, interpreting diet from the dental microwear of bears needs to be done very carefully as the enamel structure, tooth morphology and the wear stage present and/or the surface selected by the observer may influence the subsequent analysis. This is highlighted by the recognition that the total number of scratches and pit features in both *U. maritimus* and *U. deningeri* differs according to whether the observations are made on facet or non-facet enamel surfaces (in 3.4.1). The conclusions here follow Ungar and Teaford (1996), who proposed unworn surfaces as the most significant for the study of feeding traits in primates.

In addition, dental microwear differences on the grinding surface of bear enamel proved to be notably clearer and show better the ecospace of each species than the results on the slicing area. In their study, Donohue *et al*. (2013) also reported that the shearing facet of the m1 does not reflect the known dietary differences of modern bears and further suggested the use of the m2 hypoconulid area as a better proxy for

diet. However, it is not clear why the authors did not instead focus on the talonid area of the m1, which is used for crushing food instead of slicing. It has been repeatedly demonstrated that ursids often use their forelimbs to stabilise food items while grabbing, tearing, or cracking food with their carnassials (e.g. Davis, 1964; Ewer, 1973; Peyton, 1980), which may explain why the trigonid area of the m1 of bear species does not correlate as clearly with diet in the different species. In contrast, the ecospace of each extant bear species is revealed very clearly using the talonid area in both bivariate (section 3.4.2) and PCA (section 3.4.4.1) plots.

A. melanoleuca has a highly specialised diet consisting mainly of bamboo (e.g. Davis, 1964), which is convincingly captured in the microwear data, particularly by the presence of the highest number of fine scratches (usually with the same orientation), a high number of small pits and the absence of coarse scratches. It has been proposed from studies on herbivore species that there is an association between wide (coarse) scratches and diets rich in large phytoliths with C4 open ground grasses and between narrower (fine) scratches with smaller C3 woodland grasses (Solounias and Semprebon, 2002; Merceron *et al*., 2004a; b; Semprebon *et al*., 2004; Merceron *et al*., 2005a). Bamboo, a member of the grass Family Poaceae, is a monocotyledonous flowering C3 grass plant (Yeoh *et al*., 1981), which serves to explain the high number of fine scratches and the absence of coarse features seen in the enamel surfaces of *A. melanoleuca*. These results are also consistent with the results from the microwear texture analysis study by Donohue *et al*. (2013), which found low Asfc and high epLsar values in panda, and are also in agreement with previous optical steromicroscopic microwear studies (Goillot *et al*., 2009; Peigné *et al*., 2009), although these last also reported infrequent pitting, which contrasts with the high number of small pits found during this thesis.

U. maritimus diets are also well predicted by the microwear feature data. This species has a highly specialised hypercarnivorous diet, preying almost exclusively on seals (e.g. Rugh and Shelden, 1993; Derocher *et al*., 2002) but with occasional fish, sea birds and their eggs and carrion (Ewer, 1973), even some berries during summer months (Derocher *et al*., 2002). All polar bear individuals from this study show an absence of puncture pits, few scratches, a small number of pits and the highest scratches width

score (SWS). In addition, polar bear was the only species to show hypercoarse scratches. Few scratches and a moderate number of pits have previously reported for meat eaters (Goillot *et al*., 2009), while Van Valkenburg *et al*. (1990) demonstrated that flesh consumers that avoid any bone consumption (such as cheetahs) possess few pits but an abundance of narrow scratches. Furthermore, Bastl (2012) recorded a link between fairly coarse microwear patterns and bone crushing or shell crushing as a results of consuming tough food or ingesting grit while eating large amounts of arthropods. The size and also proportion of broad scratches found on meat eaters by Goillot *et al*. (2009) has been proposed to be a consequence of contact with the bone surface during consumption. Hence, the coarse enamel surface of *U. maritimus*, which was found to be dominated by hypercoarse scratches and small numbers of pits and scratches in this study is likely to be linked with the Arctic environment in which the species lives and hunts seals and other marine animals. Contrary to these results, the microwear texture analysis on polar bear specimens undertaken by Donohue *et al*. (2013) reported high Asfc values (i.e. heavily pitted), similar to *U. americanus*. These authors proposed that this is due to either bone consumption or freshwater fish and berries during summer, a rather unexpected conclusion for an animal that is a well established hypercarnivore.

The third extant species among the Ursidae that has a highly specialised diet is *M. ursinus*, which consumes mainly invertebrates (insects) and occasionally fruits (Joshi *et al*., 1997). Unfortunately, the ecospace of the insectivorous *M. ursinus* examined in this study plotted across a wide range on the graphs and is therefore not very well defined. This is most probably a result of the small number of individuals sampled (n = 4) and the wide distribution of *M. ursinus* suggests that the diet of these individuals was quite variable from one to another. Nevertheless, the species is clearly separated from the ecospace of both polar bear and panda and exhibits overlaps with areas of the *U. americanus*, *H. malayanus* and *U. arctos* (Russia) ecospaces. Nonetheless, some observations regarding *M. ursinus* diet can be made on the basis of the microwear features present. In particularly, this species is characterised by a high number of pits, a small number of scratches and the presence of a moderate percentage of puncture pits. Overall, species with over 30 pits (similar to *M. ursinus*) in the measured area are

interpreted as those with a considerable amount of abrasive or hard food in their diet, as has been described in other carnivore taxa (Bastl *et al*., 2012). Both shells and arthropods are part of the *M. ursinus* diet and have been shown to cause abrasive microwear patterns (Joshi *et al*., 1997).

Despite the fact that brown bears are generalists and consume a wide variety of foods, there are some very interesting patterns and differences in surface texture evident in *U. arctos* from different geographical regions and in comparison to the other omnivorous species.

For example *U. arctos* from northern Europe can be differentiated from *U. arctos* from central Europe by its evidence of an intermediate number of pits, the smallest number of scratches compared to other *U. arctos* specimens and the smallest percentage of puncture pits. These are all features that can be used to predict the diet of these bears, which is highly dominated by the consumption of "soft mast" fruits with very little or no seeds and with more a carnivorous input (flesh/meat but avoiding bone) in comparison with their southern counterparts (e.g. Persson *et al*., 2001; Vulla *et al*., 2009; Bojarka and Selva, 2012). As already mentioned, flesh eaters are expected to have few pits and narrow scratches (Van Valkenburg *et al*., 1990). In addition, according to Mainland (2003) and to Merceron *et al*. (2004a), the plucking of soft food produces small round pits on the enamel surface, whilst the tugging action on tough, woody food produces large, irregular or oval pits. Interestingly, *U. arctos* from Greece do not overlap or even plot close to *U. arctos* from northern Europe, despite the importance of "soft mast" in their respective diets. However the group from Greece occupies a separate ecospace to the other omnivorous species on account of a diet that is high in soft green vegetation and soft fruits (Giannakos, 1997; Vlachos *et al*., 2000). No flesh consumption is registered in the diet of the brown bears from Greece. The microwear features from this group show the lowest number of pits among the rest of the bears, with a relatively high scratches width score and coarse scratches. Similar patterns with more striated than pitted facets have been attributed to the ingestion of softer foods such as fruits and immature leaves by *Australopithecus africanus* (Grine, 1981; 1986).

In contrast to the “soft mast” eaters (and the more carnivorous northern European brown bears), *U. arctos* populations found in the deciduous and mixed forests of continental central Europe show the highest number of pits and the highest percentage of pits, puncture pits, gouges and large pits when compared with both *U. arctos* from northern Europe and with the rest of the omnivorous species. *U. arctos* from central Europe consume a large variety of “soft mast”, such as fleshy fruits, together with “hard mast” items (i.e. fruits and seeds with a hard outer covering or exocarp, nuts and acorns and pine seeds), the latter being dominant in the diet (Bojarska and Selva, 2012). This diet is well described by the microwear features identified here and accords well with the picture of hard and abrasive fruits with seeds or potential bone contact in their diet (e.g. Semprebon *et al*., 2004; Bastl *et al*., 2012).

Although also the predominant food of *U. thibetanus* is “hard mast”, similar to *U. arctos* from central Europe, the two species show no evidence of overlap into their ecospace and the microwear features show some clear differences. *U. thibetanus* displays the lowest percentage of puncture pits compared to the other omnivorous species, however it presents a relatively high scratches width score, resulting in a rather coarse enamel surface. Coarse microwear patterns on enamel surfaces have been identified as resulting either from the crushing of shells or other hard food including bone (Bastl, 2012). The difference between the two “hard mast” eaters can be explained first by the fact that the two species occupy different ecological zones where “hard mast” items will differ, and second because *U. thibetanus* occupies a variety of forested habitats, both broad-leaved and coniferous. In consequence, its diet shows a high seasonal variability, incorporating leaves, shoots, insects, a variety of fruits and only in some areas, meat (Huygens *et al*., 2003; Garshelis and Steinmetz, 2008; Koike *et al*., 2012).

As may be anticipated, there is overlap between the ecospaces of *U. americanus* and *U. arctos* from the USA, since both species are omnivorous, feeding on similar foods, and occupy more or less the same ecological zones. However, the predominant food type of the former is “soft mast” (Cottam *et al*., 1939; Hilderbrand *et al*., 1999; Fortin *et al*., 2007) whereas the latter has more carnivorous tendencies (Fortin *et al*., 2007). These omnivorous diets are reflected in microwear features such as an intermediate

number of pits and by the black bear having a higher percentage of puncture pits (denoting fruit and seed consumption) than the North American *U. arctos*. The brown bear, in contrast, has a higher percentage of coarse scratches and small pits on some individuals. Finally it is important to mention that the ecospaces of both *U. americanus* (mainly soft mast) and North American *U. arctos* (mainly meat from vertebrates) are clearly separated and are different from those of *U. arctos* from central Europe (mainly hard mast). Some individuals of *U. arctos* from northern Europe (predominantly soft mast) overlap with individuals of both North American species.

The two last ecospaces to be discussed are those represented by the omnivorous *H. malayanus* and *U. arctos* from Russia. Both species plot across a wide area of the graphs as such, their broad ecospaces sometimes overlap with more than one group from the other species. This implies that diet is quite variable from one individual to another within each of these two species and may reflect local dietary adaptability across geographical regions and seasons. However the majority of *H. malayanus* individuals plot very close to the ecospaces of the "soft mast" eaters (including *U. americanus*, *U. arctos* from North America and *U. arctos* from northern Europe), showing very similar microwear features (a relatively high percentage of fine scratches, small pits and small percentage of puncture pits). This is in good agreement with the established diet of this species, including insects such as bees, ants and beetles but also "soft mast" (Augeri, 2005; Fredriksson *et al*., 2006).

The wide ecospace of *U. arctos* from Russia is unsurprising, given the extensive distribution of this species there. Populations in Kamchatka are the most numerous and are widespread across the region, where food supply is extremely abundant (Bergman, 1936). Russian brown bears consume fleshy fruits, nuts, fish and vertebrates depending on season (e.g. Bergman, 1936; Krechmar, 1955; Bojarska and Selva, 2012), however the predominant food is vertebrates (Bojarska and Selva, 2012). Most individuals of Russian *U. arctos* display many similarities with of *U. arctos* from northern Europe and there is consequently a high overlap between their respective ecospaces. Some of the microwear features that the two groups share include a relatively high number of large pits, intermediate values for average number of pits and small percentages of numbers of puncture pits and gouges.

In conclusion, the establishment and testing of a dental microwear database for all modern bear species in this species lays a strong foundation for the subsequent application of this technique in order to reveal the dietary preferences of extinct species (see Chapter 4).

Chapter 4. Dental Microwear Analysis – Pleistocene Extinct Species

4.1. Introduction

Having established a set of distinct microwear characters for the various living bear species (Chapter 3), this Chapter presents the results of microwear observations on extinct bear species from eight British Pleistocene and Holocene sites of various ages, representing different palaeoenvironments, and from the Late Pleistocene site of Loutra Arideas Cave (LAC) in Greece. As previously outlined, only the grinding (talonid) area was used for analysis, since this has been demonstrated to render the clearest separation into dietary ecospace in extant species as well as within a single species (*U. arctos*) from different geographical regions. Bear remains from all palaeontological sites were compared initially with the database of extant species through simple bivariate graphs recording: a) average number of scratches versus average number of pits and b) large versus small pits. Additionally Principal Component Analysis (PCA) was employed for all sites in order to explore the dietary ecospace of extinct bear specimens from each locality.

4.2. Material

The extinct bear specimens selected for this study are housed in the following museums and universities: the Natural History Museum in London, UK (NHMUK); the Aristotle University of Thessaloniki (Geology Department) (AUThG); Loutra Aridea Museum in Greece (LAMG); Torquay Museum in Devon (TMD), UK; the Somerset Heritage Centre in Taunton, Somerset (TSHC), UK (see the complete list of specimens with raw data Appendix I.C table 1). In total, 155 specimens were examined, from the cave bears (*Ursus deningeri* and *Ursus ingressus*) and brown bears (*U. arctos*). From those, 90 specimens were used for the microwear analysis. The dental microwear analysis focused on the analysis of ursid material from a range of interglacial and cold-climate assemblages of Middle and Late Pleistocene and of Holocene age from Britain and Greece, comprising Westbury-sub-Mendip (n: 15), Kents Cavern (n: 18), Grays

Thurrock (n: 10), Tornewton Cave (n: 21), Banwell Bone Cave (n: 4), Sandford Hill (n: 4) and Cow Cave (n: 8) (for additional information for each site, see 1.3). Material from the Greek site of Loutra Arideas Cave (n: 10) was also studied for a southern European comparison.

4.3. Results of the Dental Microwear Analysis (DMA) on the extinct Ursidae from Britain

4.3.1. Results Dental Microwear Analysis (DMA) from Westbury-sub-Mendip (MIS 13)

4.3.1.1. Bivariate Analysis results from Westbury – sub - Mendip (MIS 13)

As outlined in 1.3., at the time of deposition of the early Middle Pleistocene (MIS 13) Westbury-sub-Mendip (henceforth referred to simply as Westbury) cave infill, the climate was temperate, with an intervening cool oscillation, and the reconstructed palaeoenvironment predominantly open grassland (Andrews and Cook, 1999; Schreve *et al*., 1999). From this site and after exclusion of specimens with obvious *post mortem* modification, 15 well preserved teeth were included in the Dental Microwear Analysis (DMA).

Bivariate graphs were used to compare the extinct cave bear, *Ursus deningeri*, from Westbury with the extant bear database (Fig. 4.1 A and B). Figures 4.1 A and B reveal that the Westbury bears occupy a position between *U. arctos* from Greece and *U. maritimus*, also overlapping with many *U. thibetanus* individuals. In particular, in Figure 4.1 A, the Westbury specimens clearly overlap with those of *U. thibetanus* and occupy the lower central sector of the graph, indicating an intermediate mean number of scratches and a smaller mean number of pits compared to the other extant species. The total mean values for scratches and pits for *U. deningeri* specimens from Westbury are 17.6 and 19.67 respectively (see also Table 4.1). Overall, the microwear pattern for *U. deningeri* reveals a low to intermediate number of scratches and many coarse scratches are present together with some gouge features (Table 4.1).

Figure 4.1 B reveals the total number of large pits versus small pits for *U. deningeri* from Westbury, plotted against extant species. This suggests that some individuals are

again comparable to *U. arctos* from Greece. However, *U. deningeri* is differentiated from the extant *U. arctos* populations from other geographical regions, since the latter tend to be more "hard object" specialists (as revealed by their high number of puncture pits). *U. deningeri* individuals have the lowest number of small pits (minimum 6, median 10 and maximum 22) of any species and a moderate number of large pits (median 6). Table 4.1 shows a statistical summary of eight microwear features (variables) for Westbury bears. Section 4.3.9 presents the statistical tests for *U. deningeri* from Westbury in comparison with the extant species microwear dataset and the remainder of the fossil samples from the UK.

Table. 4.1. Westbury-sub-Mendip (MIS 13), UK (n: 15) statistical summary of eight microwear features. Mean, standard deviation (SD), 95% Confidence interval (CL), 1st and 3rd quartile, minimum, maximum and median values are given.

Microwear features (variables)	Mean; SD	95% CL	1st Quartile	min	median	max	3rd quartile
Pits	19.67; 5.81	2.94	16	12	19	31	22.5
Scratches	17.6; 4.50	2.28	15.5	9	18	24	21
Fine Scratches	12.6; 4.58	2.32	10.5	4	14	19	15.5
Coarse Scratches	5; 1.81	0.92	3.5	3	5	9	6
Large Pits	5.73; 2.55	1.29	4	2	6	12	7
Small Pits	12.2; 5.43	2.75	7	6	10	22	16.5
Gouges	1.53; 1.18	0.60	1	0	1	5	2
Punctures	0.2; 0.77	0.39	0	0	0	3	0

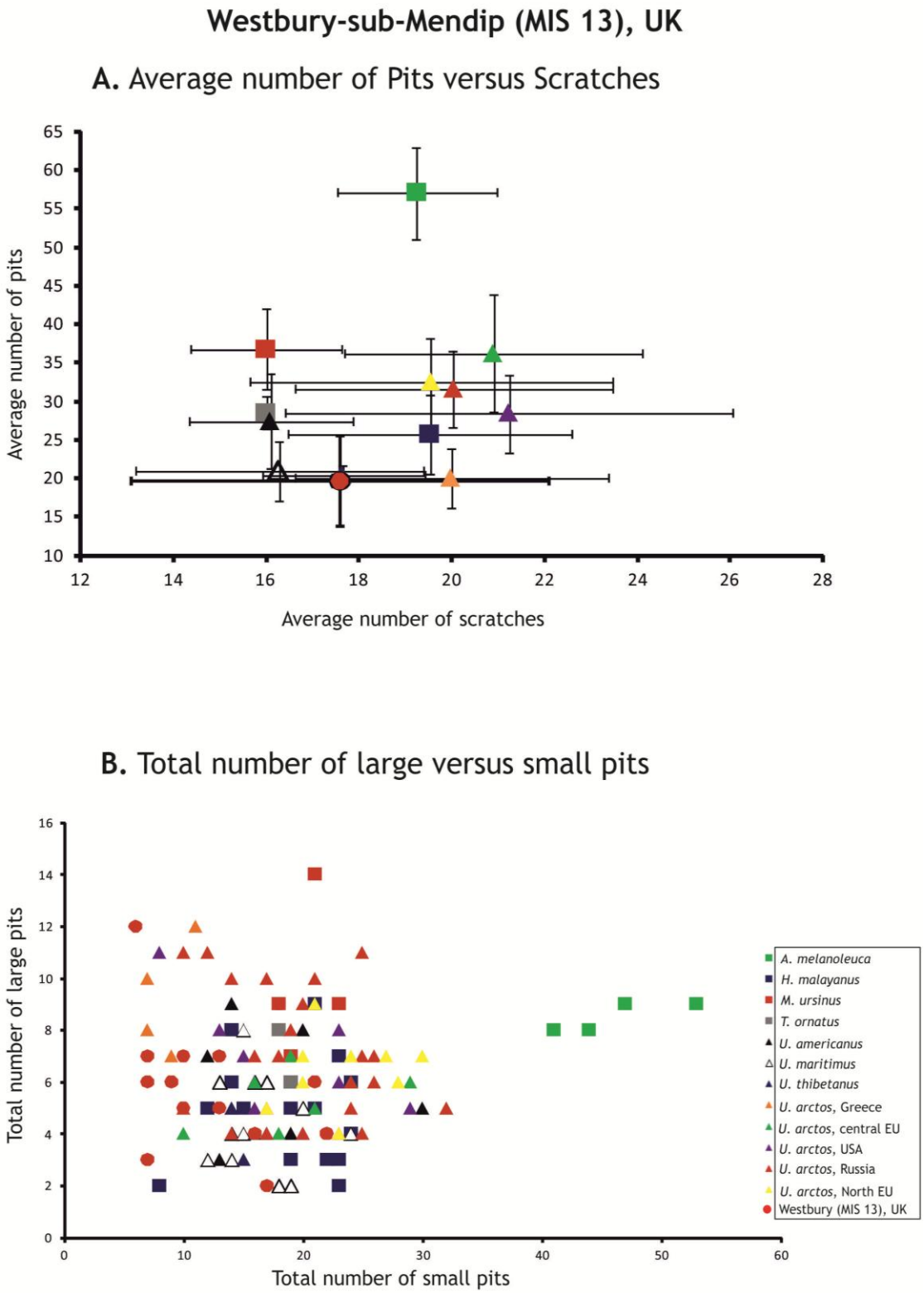

Figure 4.1. Bivariate diagrams for bears from Westbury-sub-Mendip (MIS 13), UK, in comparison with the extant bear microwear database. **A.** Plot of average number of pits versus scratches. Error bars represent the standard deviation of pits and scratches. **B.** Plot of raw data of the total number of large versus small pits.

4.3.1.2. Principal Component Analysis (PCA) results from Westbury-sub-Mendip (MIS 13)

PCA was also undertaken on the Westbury *U. deningeri* specimens. Figures 4.2 A and B show the results from observations on the grinding surfaces of m1s of Westbury cave bears, in comparison to the database of modern bear species.

The first axis (PC1) explains 40.19% of the total variance, the second (PC2) accounts for 22.24% and the third axis (PC3) for 10.61%. Abbreviations of the nine independent variables are given in the caption of Figure 4.2., while the positive and negative influence of each component has already described in 3.4.4.1 (Chapter 3).

According to components 1 and 2 on the grinding facet, *U. deningeri* from Westbury is close to *U. arctos* from Greece, with some individuals close to the *U. thibetanus* dietary ecospace and slightly overlapping with that of *U. maritimus*. Two individuals lie within *H. malayanus* ecospace and one within *U. americanus* ecospace (Fig. 4.2 A). The position of *U. deningeri* from Westbury is clearly separated from the *U. arctos* specimens from other geographical regions. Westbury's position also shows the smallest percentage of puncture pits (NpP) compared with species in the extant database (Fig. 4.2 A).

Figure 4.2 B reveals the results of components 1 and 3 for *U. deningeri* from Westbury in comparison with extant bear database. In this case, the specimens from Westbury are scattered in the left-hand side of the plot and again, there is an overlap with *U. arctos* from Greece and with the ecospace of both *U. thibetanus* and *U. maritimus*.

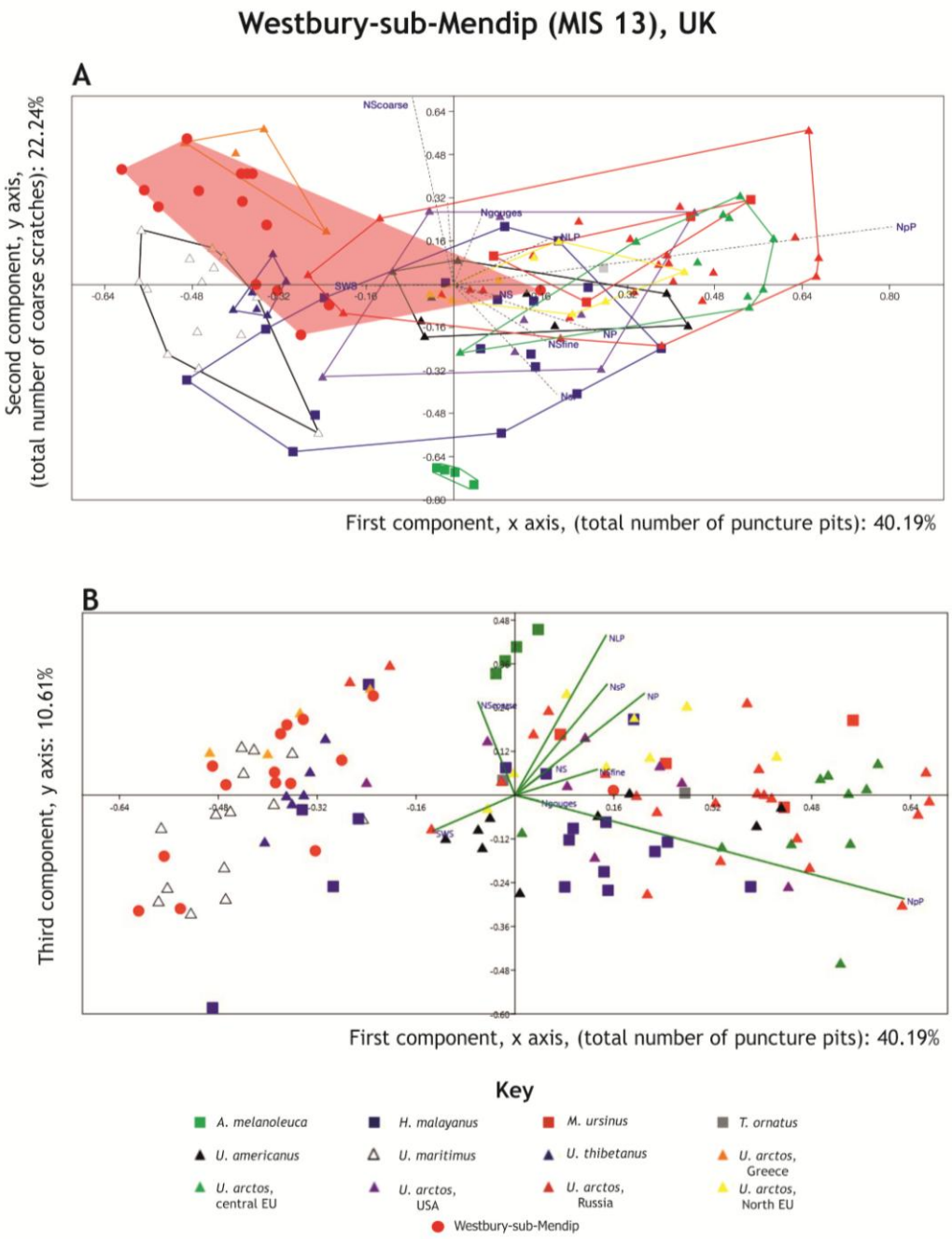

Figure 4.2. PCA plots for Westbury-sub-Mendip (MIS 13), UK in comparison with extant bear species. **A**. Graph component 1 versus 2. The shaded polygon indicates the position of the specimens from Westbury-sub-Mendip. **B.** Graph component 1 versus 3. For details of symbols, see key. Symbols of variables as follows: NS: number of scratches; NP: number of pits; NfineS: number of fine scratches; NcoarseS: number of coarse scratches; NLP: number of large pits; NsP: number of small pits; Ngouge: number of gouges; Npp: number of puncture pits; SWS: scratches width score.

4.3.2. Results of the Dental Microwear Analysis (DMA) from Kents Cavern (breccias) (early Middle Pleistocene)

4.3.2.1. Bivariate Analysis results from Kents Cavern (breccias) (early Middle Pleistocene)

A total of 25 individuals were examined from Kents Cavern, although after rejection of specimens with obvious *post mortem* modifications and/or poor preservation, only 6 were used from the breccias deposits (the results from which are presented in this section) and 12 were used from the cave earth deposits (the results from which are presented in 4.3.6). The specimens from the breccias are distinct from the Middle Devensian (MIS 3) cave earth deposits at Kent Cavern (Procter *et al*., 2005), which are described below (4.3.6). According to Procter *et al*. (2005), the bears from the Middle Pleistocene Kent Cavern breccias compare well with *U. deningeri* from Westbury. The Kents Cavern breccias have traditionally been viewed as early Middle Pleistocene (late Cromerian Complex) (e.g. Keen, 1998, Proctor *et al*., 2005), but most recently have dated to MIS 12 or early MIS 11 age (McFarlane *et al*., 2011) (see 1.3. for further details on the site).

Bivariate graphs allow comparison of the bears from the Kents Cavern breccias with the extant bear database (Fig. 4.3 A and B). Figure 4.3 A demonstrates that the Kents Cavern *U. deningeri* lie close to the *U. arctos* group and occupy the right-hand sector of the graph. This indicates a higher mean total of scratches. Kents Cavern's *U. deningeri* have an intermediate mean number of pits (32.58), similar to *U. arctos* from northern Europe (Fig. 4.3 A). However, compared to other *U. arctos* groups, *U. deningeri* from Kents Cavern have the highest mean number of scratches (24.92) (see also Table 4.2).

Figure 4.3 B compares *U. deningeri* from Kents Cavern with the extant database with reference to the total number of large pits versus small pits. In this graph, most *U. deningeri* individuals have an intermediate number of small pits (18 to 19) and an intermediate to high number of large pits (median 8 and maximum 12). Moreover, some *U. deningeri* specimens from Kents Cavern plot very close to some *U. arctos*

individuals from North Europe, while others lie closer to some *U. arctos* specimens from Russia (Fig. 4.3). The statistical tests for *U. deningeri* from Kents Cavern in comparison with extant data microwear features and the remainder of the extinct bear samples from UK are presented in 4.3.9.

Table. 4.2. Kents Cavern bear (breccias), UK (n: 6) statistical summary of eight microwear features. Mean, standard deviation (SD), 95% Confidence interval (CL), 1st and 3rd quartile, minimum, maximum and median values are given.

Microwear features (variables)	Mean; SD	95% CL	1st Quartile	min	median	max	3rd quartile
Pits	32.58; 4.18	3.34	29.25	28	32	38	35.87
Scratches	24.92; 2.65	2.12	23.87	21	25	29	25.75
Fine Scratches	18.33; 2.58	2.06	16.5	15	18.5	22	19.75
Coarse Scratches	6.58; 1.96	1.57	5.25	4	6.5	9	8.12
Large Pits	8.08; 2.97	2.38	6.25	4	8	12	10.12
Small Pits	21.5; 4.79	3.84	18.62	18	19	30	23.12
Gouges	1.58; 1.20	0.96	1	0	1.5	3.5	2
Punctures	1.58; 0.92	0.73	1.25	0	2	2.5	2

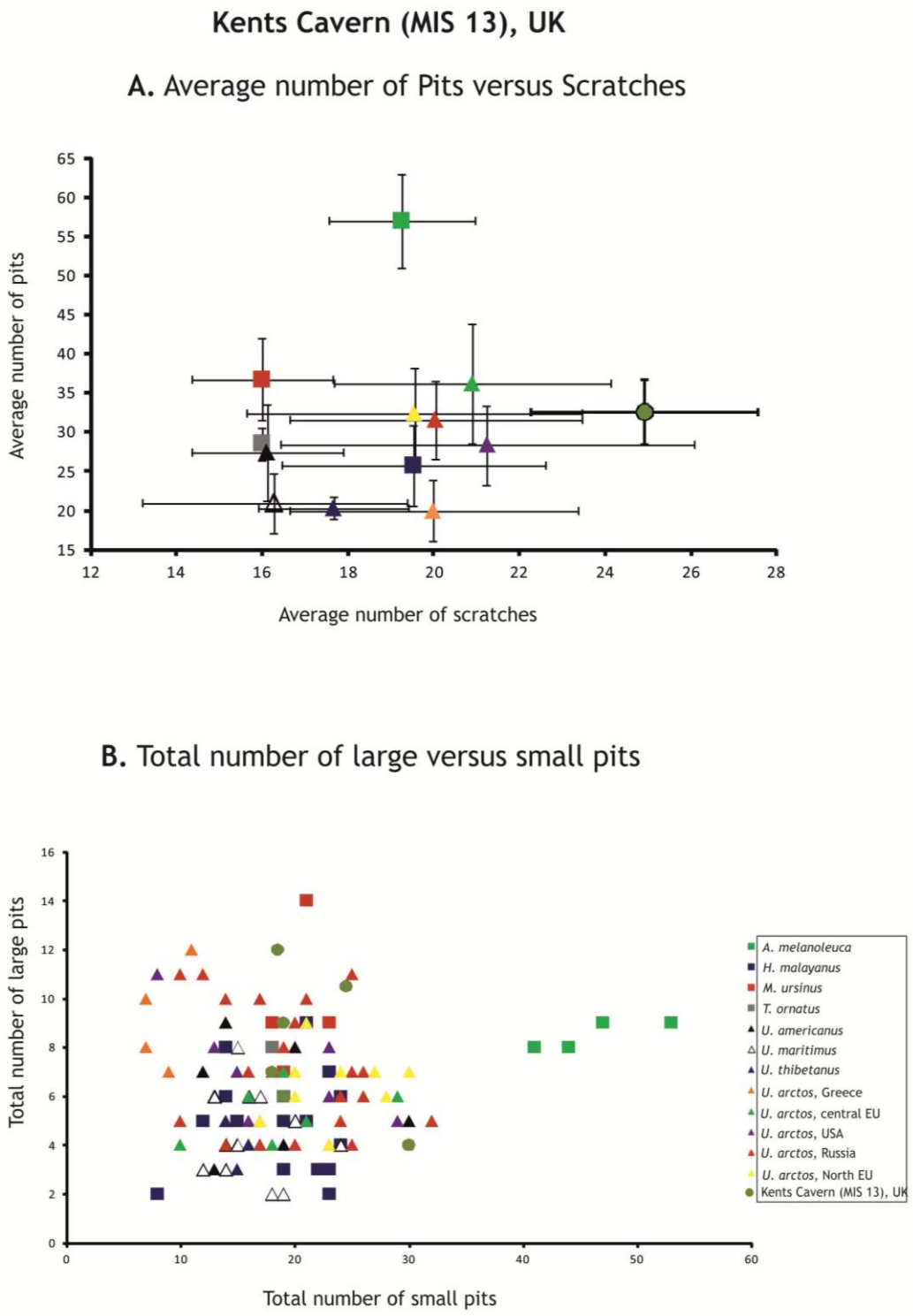

Figure 4.3. Bivariate diagrams for bears from Kents Cavern (breccias) (early Middle Pleistocene), UK, in comparison with extant bear database. **A.** Plot of average number of pits versus scratches. Error bars represent the standard deviation of pits and scratches. **B.** Plot of raw data of the total number of large versus small pits.

4.3.2.2. PCA results from Kents Cavern (breccias) (early Middle Pleistocene)

PCA was also completed for *U. deningeri* specimens from Kents Cavern. Figures 4.4. A and B show results from observations from the grinding surfaces of m1s of the extinct *U. deningeri* from Kents Cavern, in comparison with the database of modern bears. The first axis (PC1) accounts for 40.05% of the total variance, the second (PC2) for 21.15% and the third axis (PC3) explains 12.89%.

Figure 4.4 A illustrates components 1 and 2 where most of the Kents Cavern *U. deningeri* specimens occupy the top middle-right quadrant. In addition there is one individual close to *U. thibetanus* ecospace.

The position of *U. deningeri* from Kents Cavern is clearly separated from that of the hypercarnivore *U. maritimus* and from the herbivore *A. melanoleuca* (Fig. 4.4 A). The dietary ecospace of the Kents Cavern *U. deningeri* is differentiated from most extant species, but is very close to that of the omnivorous species such as *U. arctos* from USA and from Russia as well very close to *U. arctos* from northern Europe. It also shows an intermediate percentage of puncture pits (NpP), large pits (NLp) and gouges (Ngouges). Compared with the *U. arctos* groups, *U. deningeri* from Kents Cavern have a higher percentage of coarse scratches (NScoarse) and a smaller percentage of small pits (NsP) and fine scratches (NSfine) (Fig. 4.4 A).

Figure 4.4 B reveals the results of Components 1 and 3 for the Kents Cavern *U. deningeri* specimens in comparison with the extant bear database. Here, the *U. deningeri* specimens are scattered in two different areas. Two specimens lie relatively close to *A. melanoleuca* and the remaining four specimens are relatively close to the dietary ecospace of some northern European *U. arctos* specimens but remain distinct (Fig. 4.4 B).

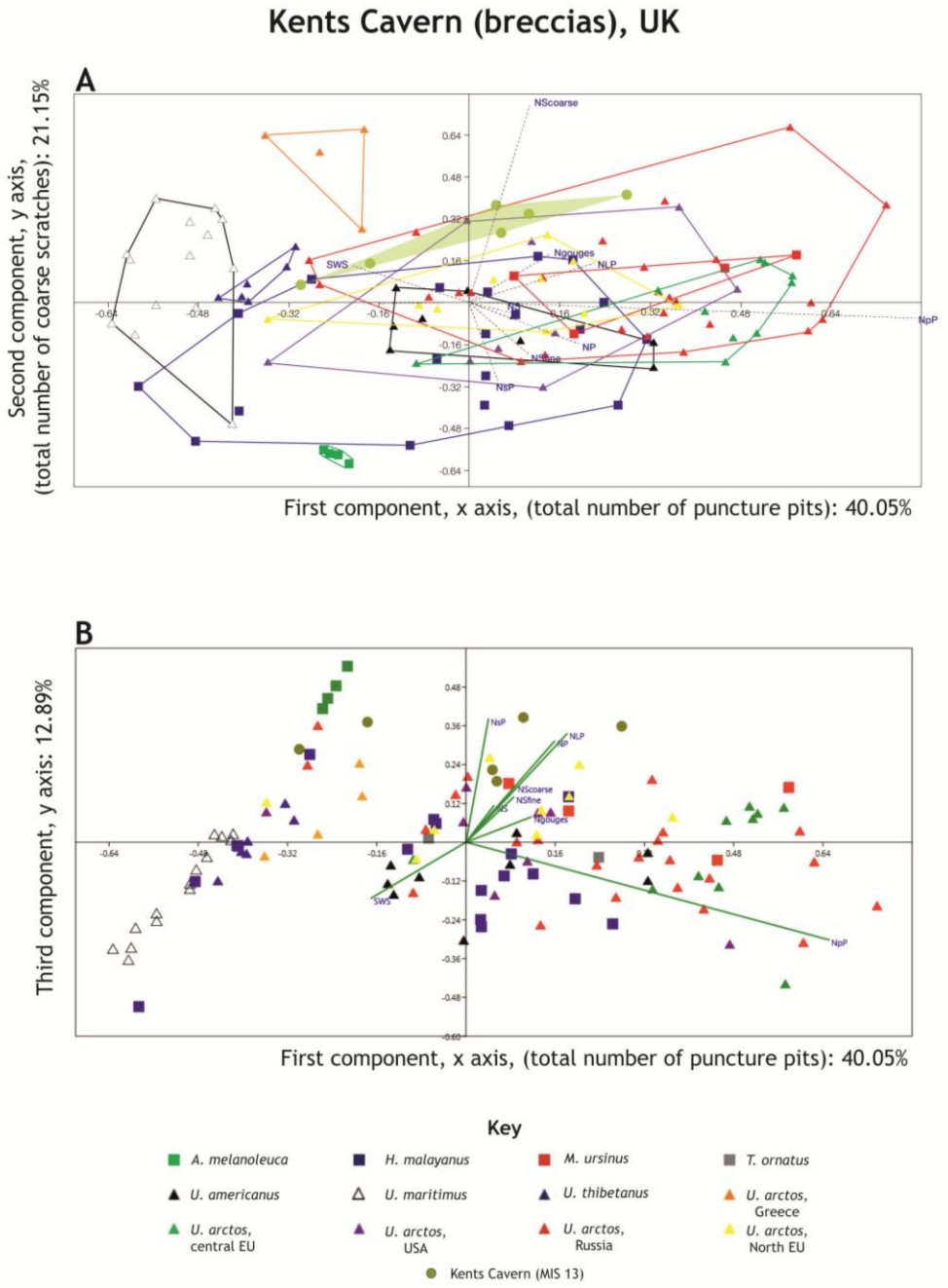

Figure 4.4. PCA plots for Kents Cavern (breccias) (early Middle Pleistocene), UK, in comparison with extant bear species. **A**. Graph component 1 versus 2. The shaded polygon indicates the position of the specimens from Kents Cavern (breccias). **B.** Graph component 1 versus 3. For details of symbols, see key. Symbols of Variable as follows: NS: number of scratches; NP: number of pits; NfineS: number of fine scratches; NcoarseS: number of coarse scratches; NLP: number of large pits; NsP: number of small pits; Ngouge: number of gouges; Npp: number of puncture pits; SWS: scratches width score.

4.3.3. Results Dental Microwear Analysis (DMA) from Grays Thurrock (MIS 9)

4.3.3.1. Bivariate Analysis results from Grays Thurrock (MIS 9)

Grays Thurrock is one of the best preserved late Middle Pleistocene assemblages, with a predominance of woodland species indicating fully temperate environmental conditions and a climate warmer than at present (Schreve, 1997). The assemblage has been attributed to MIS 9 (Schreve, 2001) (see 1.3. for further details of the site). Ten specimens were analysed for DMA.

Bivariate graphs were used to compare the bears from Grays with the extant bear database (Fig. 4.5 A and B). Figure 4.5 A reveals that *U. arctos* from Grays lies close to the modern *U. arctos* group, occupying the right-hand sector of the graph that describes a bigger total mean number of scratches. The Grays *U. arctos* have an intermediate mean number of pits (mean 31.82) and a relatively high mean number of scratches (mean 20.91). The Grays specimens occupy a position between *U. arctos* from central Europe and those from the USA, although they have a smaller mean value for pits than the former and a higher mean value than the latter. In addition, the *U. arctos* from Grays possess a lower mean value for scratches when compared with *U. arctos* from the USA, overlapping (within errors) with the values for *U. arctos* from both Russia and northern Europe (Fig. 4.5 A).

Figure 4.5 B compares *U. arctos* from Grays with the extant bear database regarding the total number of large pits versus small pits. Most *U. arctos* individuals from Grays have an intermediate to high number of small pits (median 21 and maximum 28) and an intermediate number of large pits (median 6 and maximum 8), meaning that they plot very close to some *U. arctos* individuals from central Europe, northern Europe and Russia (Fig. 4.5 B). Table 4.3 shows a statistical summary of eight microwear features (variables) for *U. arctos* from Grays Thurrock. Statistical tests for *U. arctos* from Grays in comparison with the extant bear database of microwear features and the other extinct bear samples from UK are presented in 4.3.9.

Table. 4.3. Grays Thurrock (MIS 9), UK (n: 10) statistical summary of eight microwear features. Mean, standard deviation (SD), 95% Confidence interval (CL), 1st and 3rd quartile, minimum, maximum and median values are given.

Microwear features (variables)	Mean; SD	95% CL	1st Quartile	min	median	max	3rd quartile
Pits	31.82; 3.22	1.90	29	29	32	37	33.5
Scratches	20.91; 1.92	1.13	19.5	18	21	24	22.5
Fine Scratches	17.18; 1.66	0.98	16	15	18	20	18
Coarse Scratches	3.73; 1.10	0.65	3	2	4	5	4.5
Large Pits	5.91; 1.51	0.89	5	4	6	8	7
Small Pits	22; 2.86	1.69	20	19	21	28	23
Gouges	1.54; 0.82	0.48	1	0	2	3	2
Punctures	2.36; 0.67	0.39	2	2	2	4	2.5

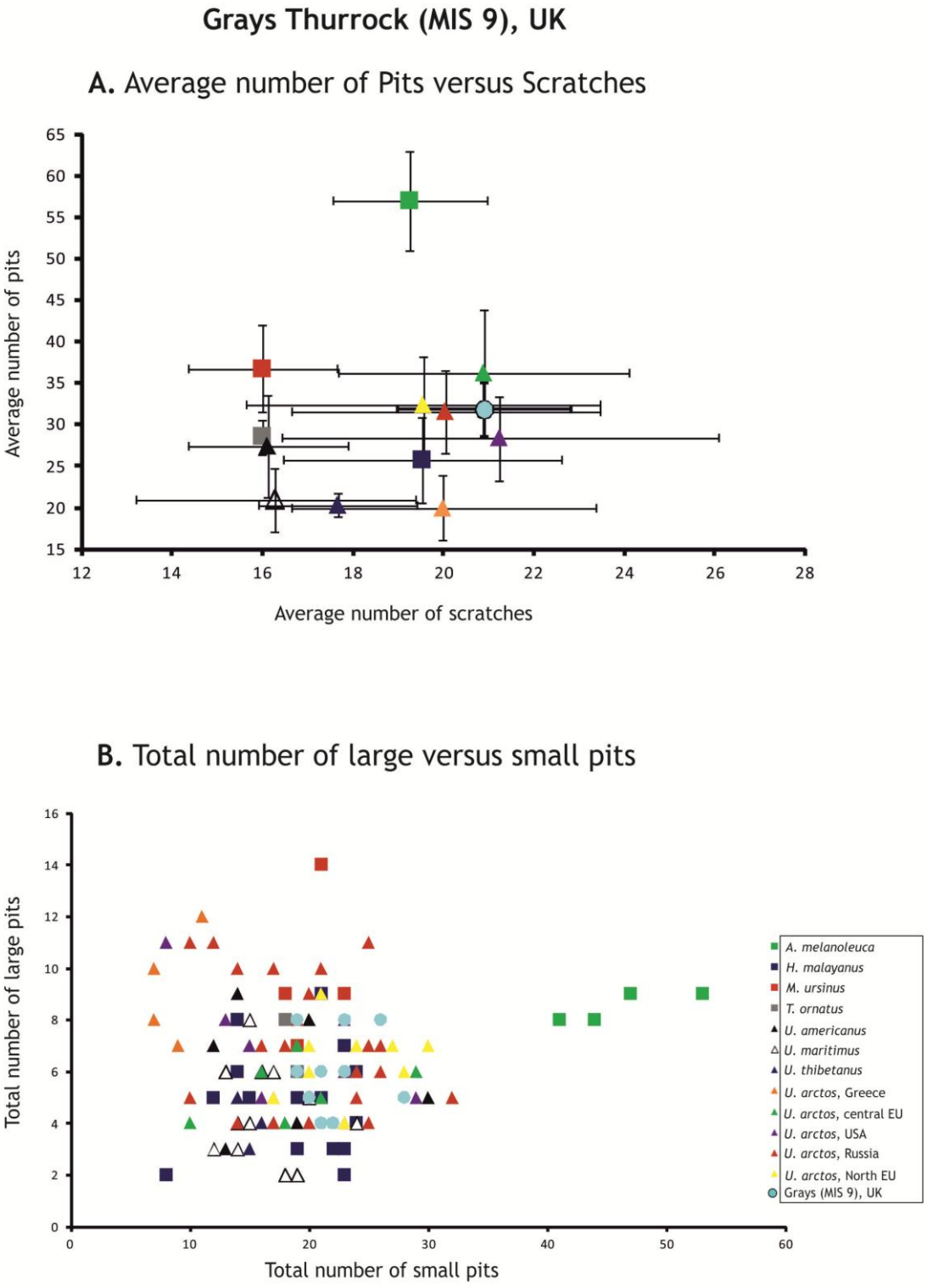

Figure 4.5. Bivariate diagrams for bears from Grays Thurrock (MIS 9), UK in comparison with the extant bear database. **A.** Plot of average number of pits versus scratches. Error bars represent the standard deviation of pits and scratches. **B.** Plot of raw data of the total number of large versus small pits.

4.3.3.2. PCA results from Grays Thurrock (MIS 9)

PCA was also undertaken on the results from the *U. arctos* specimens from Grays. Figures 4.6 A and B show the results of observations of the grinding surfaces of m1s of the extinct *U. arctos* from Grays, in comparison with the modern database of bears. The first axis (PC1) accounts for 40.59% of the total variance, the second (PC2) for 20.78% and the third axis (PC3) explains 11.94%. Abbreviations of the nine independent variables are given in the caption of Figure 4.6.

Figure 4.6 A plots Components 1 and 2, revealing that most of the *U. arctos* specimens from Grays occupy part of the central area of the graph, overlapping predominantly with the dietary ecospace of *U. arctos* from northern Europe. Moreover, as with both *U. arctos* from northern Europe and from Grays, there is noticeable overlap with the dietary ecospace of *U. americanus* and *U. arctos* from the USA. Additionally, the position of *U. arctos* from Grays is clearly separated from that of the hypercarnivore *U. maritimus* and from the herbivore *A. melanoleuca* (Fig. 4.6 A).

The position of the Grays specimens reveals that they possess the smallest percentage of puncture pits compared to any other *U. arctos* group but display an intermediate percentage for most other variables.

Figure 4.6 B plots the results of Component 1 against Component 3 for the Grays *U. arctos* specimens in comparison with the extant bear database. Most of the Grays specimens are tightly clustered and occupy the central and slightly upper part of the second quadrant. The differentiation from *U. maritimus* and *A. melanoleuca* is still clearly visible in this plot (Fig. 4.6 B).

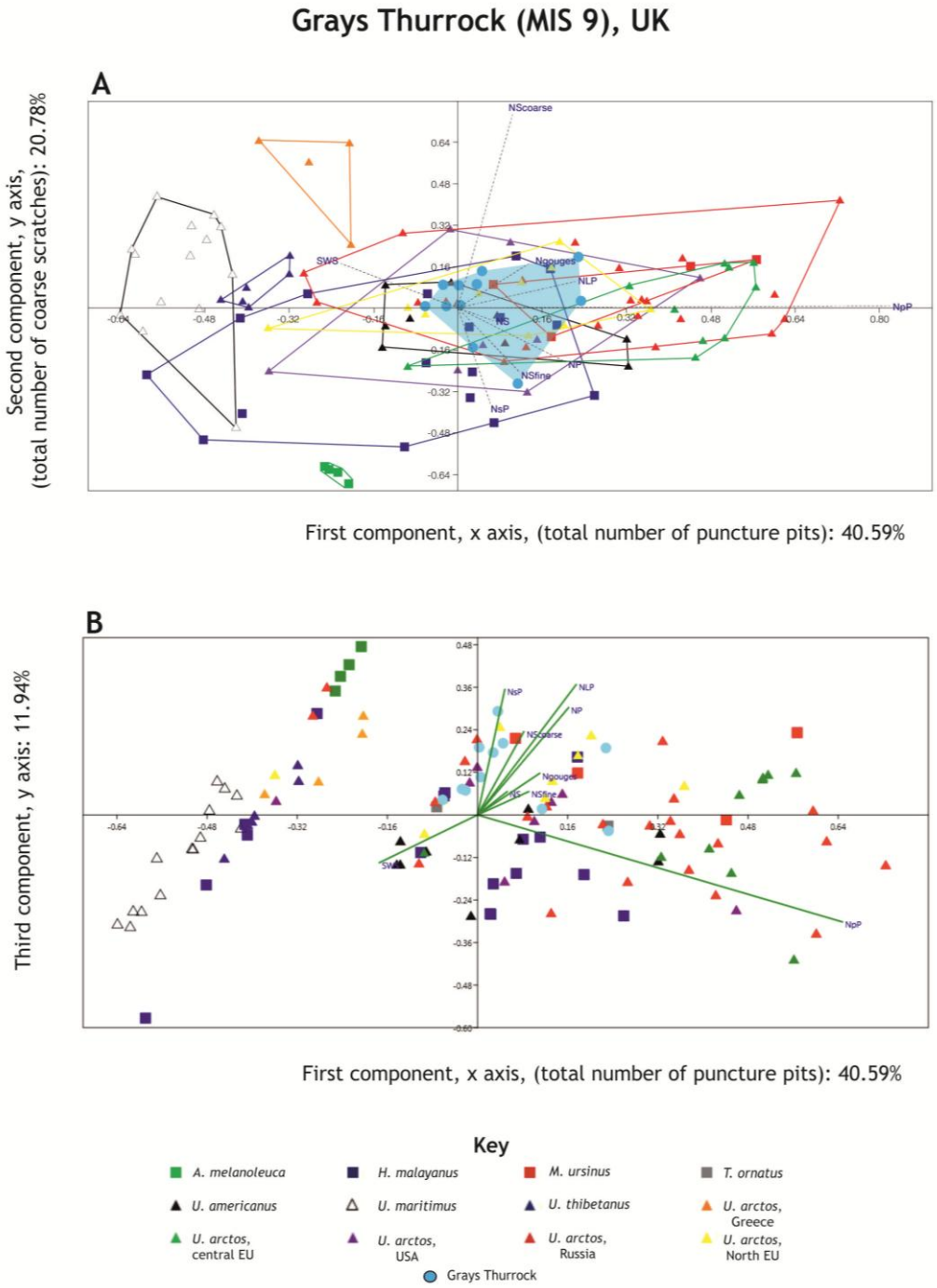

Figure 4.6. PCA plots for Grays Thurrock (MIS 9), UK, in comparison with extant bear species. **A**. Graph component 1 versus 2. The shaded polygon indicates the position of the specimens from Grays Thurrock. **B.** Graph component 1 versus 3. For details of symbols, see key. Symbols of Variable as follows: NS: number of scratches; NP: number of pits; NfineS: number of fine scratches; NcoarseS: number of coarse scratches; NLP: number of large pits; NsP: number of small pits; Ngouge: number of gouges; Npp: number of puncture pits; SWS: scratches width score.

4.3.4. Results Dental Microwear Analysis (DMA) from Tornewton Cave (MIS 5e)

4.3.4.1. Bivariate Analysis results from Tornewton Cave (MIS 5e)

As outlined in 1.3, Tornewton Cave contains one of the most complete late Middle and Late Pleistocene sequences in Britain. According to Gilmour *et al*. (2007), the deposits of both the "Hyaena" and "Bear" Strata have been attributed to difference parts of MIS 5, covering the first two temperate substages, MIS 5c and MIS 5e (=Ipswichian/Eemian interglacial) respectively, the latter characterised by the development of mixed oak woodland, elevated summer temperatures compared to today and mild winters (Candy *et al*., 2010). 41 individuals were collected from this site, of which 21 were retained for DMA, following rejection of specimens with obvious *post mortem* features and/or poor preservation. Only specimens from the MIS 5e "Bear Stratum" were chosen.

Bivariate graphs were used to compare the *U. arctos* from Tornewton Cave with the extant bear database (Fig. 4.7 A and B). Figure 4.7 A shows that the mean number of pits and scratches in *U. arctos* from Tornewton Cave is close to that seen in *M. ursinus* specimens, plotting on the left–hand side of the graph, denoting a smaller total mean number of mean values for scratches than those specimens plotting on the right-hand side. Furthermore, Tornewton Cave specimens have a relatively high mean number of pits (mean 34.48) compared to other bear species, approaching those seen in *M. ursinus* and *U. arctos* from central Europe. Moreover, *U. arctos* from Tornewton Cave have the smallest mean number of scratches (mean 15.66) compared to all other extant species (Fig. 4.7 A).

Figure 4.7 B reveals the total number of large pits versus small pits for *U. arctos* from Tornewton, plotted against the extant species. This suggests that the former occupied a position close to *M. ursinus*, although the Tornewton specimens also overlap with specimens of *U. arctos* from northern Europe and some individuals of *H. malayanus* and *U. arctos* from Russia. *U. arctos* individuals from Tornewton have an intermediate to high number of both large pits (median 7 and maximum 13) and small pits (median

24 and maximum 33) in comparison to extant species. The statistical summary of eight microwear features (variables) for the Tornewton brown bears is presented in Table 4.4. Statistical tests for *U. arctos* from Tornewton in comparison with the microwear features from the extant bear database and the other extinct bear samples from the UK are presented in 4.3.9.

Table. 4.4. Tornewton Cave bear (MIS 5e), UK (n: 21) statistical summary of eight microwear features. Mean, standard deviation (SD), 95% Confidence interval (CL), 1st and 3rd quartile, minimum, maximum and median values are given.

Microwear features (variables)	Mean; SD	95% CL	1st Quartile	min	median	max	3rd quartile
Pits	34.48; 3.16	1.35	32	29	35	40	37
Scratches	15.66; 2.21	0.94	15	10	16	19	17
Fine Scratches	12.48; 2.11	0.90	11	7	13	16	14
Coarse Scratches	3.19; 1.08	0.46	3	1	3	5	4
Large Pits	6.81; 2.23	0.95	5	4	7	13	8
Small Pits	23.71; 4.05	1.73	22	16	24	33	25
Gouges	1.76; 1.26	0.54	1	0	1	5	2
Punctures	2.19; 0.87	0.37	2	0	2	3	3

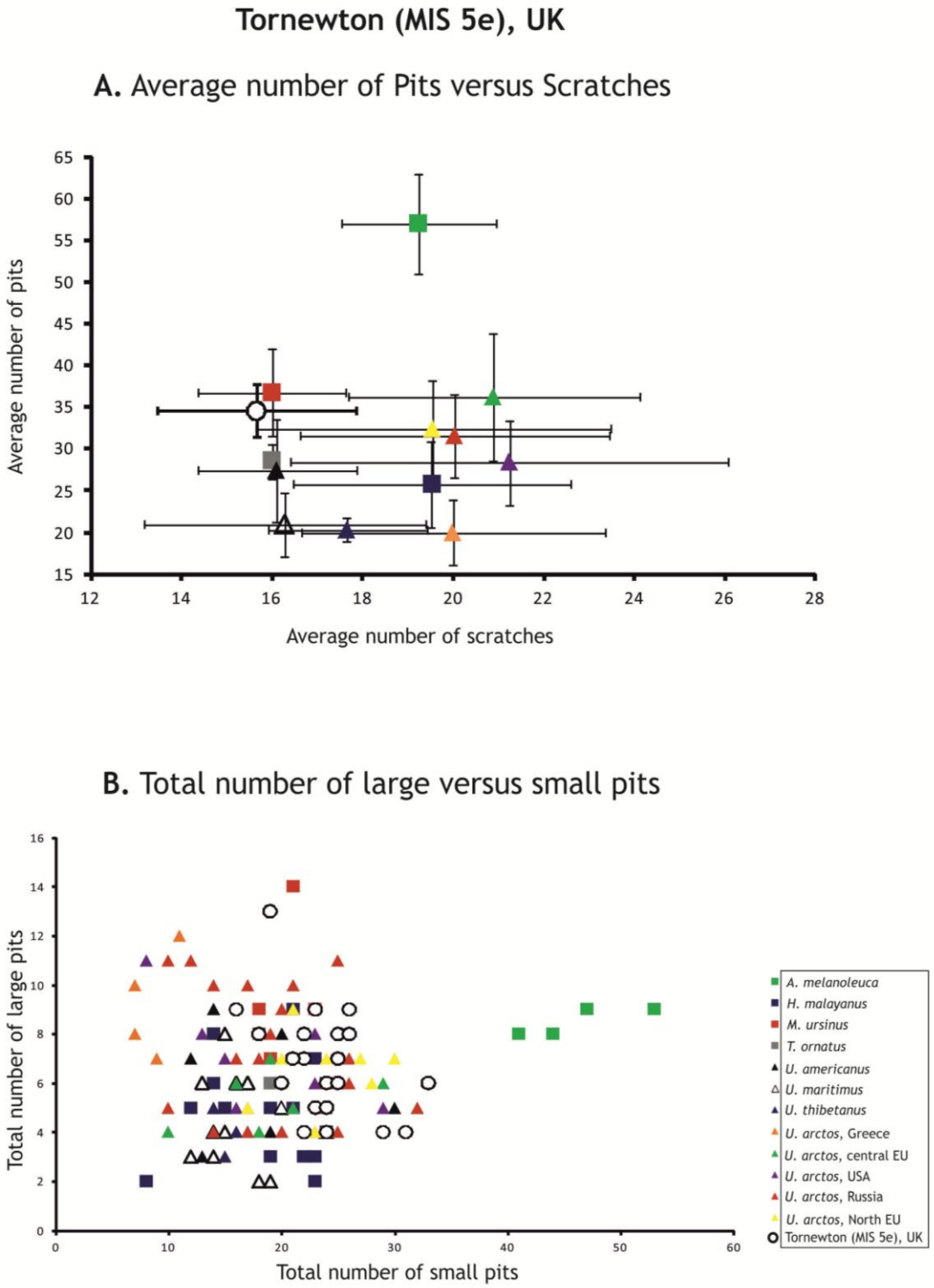

Figure 4.7. Bivariate diagrams for bears from Tornewton Cave (MIS 5e), UK, in comparison with the extant bear database. **A.** Plot of average number of pits versus scratches. Error bars represent the standard deviation of pits and scratches. **B.** Plot of raw data of the total number of large versus small pits.

4.3.4.2 PCA results from Tornewton Cave (MIS 5e)

PCA was also undertaken on the *U. arctos* specimens from Tornewton. Figures 4.8 A and B show the results from observations of the grinding surfaces of the m1s of extinct *U. arctos* from Tornewton, in comparison with the database of modern bears. The first axis (PC1) accounts for 39.05% of the total variance, the second (PC2) for 20.22% and the third axis (PC3) explains 12.61%. Abbreviations of the nine independent variables are given in the caption of Figure 4.8.

Figure 4.8 A presents Components 1 and 2. Here, the majority of the *U. arctos* specimens from Tornewton occupy the central part of the graph and clearly overlap with the dietary ecospace of *U. arctos* from northern Europe, and partially with those of *H. malayanus* and *U. americanus*.

There are four outliers from Tornewton that scatter close to *U. thibetanus* and two outliers that lie close to the dietary ecospace of *U. arctos* from Russia. Moreover, the position of *U. arctos* from Tornewton is clearly separated from that of the hypercarnivore *U. maritimus* and from the herbivore *A. melanoleuca* (Fig. 4.8 A). The majority of specimens from Tornewton display the smallest percentage of puncture pits, similar to that seen in *U. arctos* from northern Europe (in contrast to other brown bears), and display average values for most other variables.

Figure 4.8 B reveals the results of Component 1 plotted against Component 3 for the Tornewton *U. arctos* specimens in comparison with the extant bear database. Here, the Tornewton brown bears are scattered in two different areas of the graph, with the majority tightly clustered in the central and slightly upper right part of the second quadrant (Fig. 4.8 B).

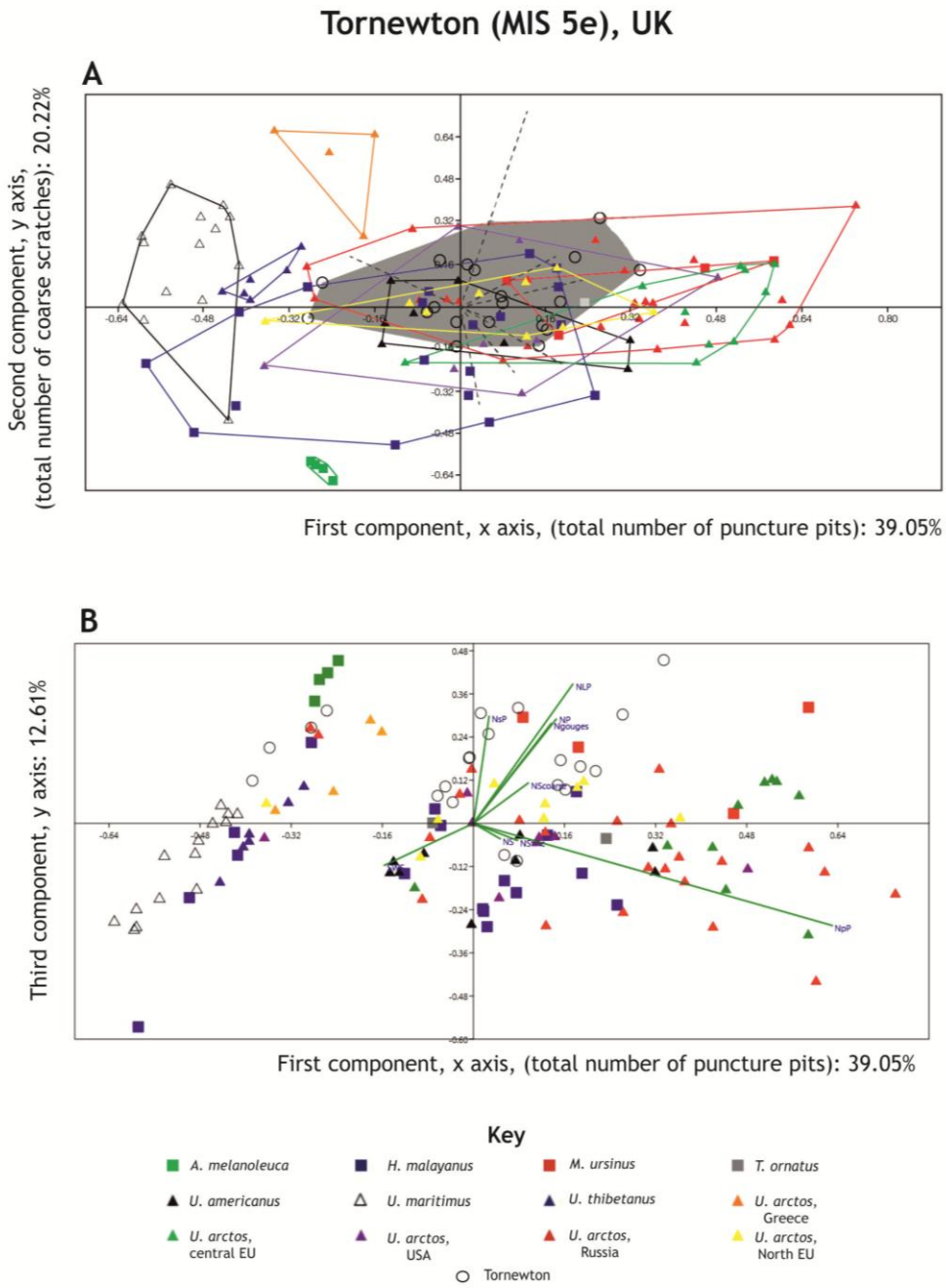

Figure 4.8. PCA plots for Tornewton Cave (MIS 5e), UK, in comparison with extant bear species. **A**. Graph component 1 versus 2. The shaded polygon indicates the position of the specimens from Tornewton Cave. **B.** Graph component 1 versus 3. For details of symbols, see key. Symbols of Variable as follows: NS: number of scratches; NP: number of pits; NfineS: number of fine scratches; NcoarseS: number of coarse scratches; NLP: number of large pits; NsP: number of small pits; Ngouge: number of gouges; Npp: number of puncture pits; SWS: scratches width score.

4.3.5. Results Dental Microwear Analysis (DMA) from Banwell Bone Cave (MIS 5a)

4.3.5.1. Bivariate Analysis results from Banwell Bone Cave (MIS 5a)

The Banwell Bone Cave mammal assemblage has been placed within the Early Devensian (last cold stage), correlated with MIS 5a (Gilmour *et al*., 2007; Currant and Jacobi, 2011). The bears from this site are particularly interesting due to their large size, with an inferred cold, open tundra environment and a fauna dominated by reindeer and bison (Currant and Jacobi, 2011) (see 1.3. for further details on the site). After exclusion of specimens with obvious *post mortem* features and/or poor preservation, four specimens were included in the analysis. The preservation of specimens from this site was generally poor and almost all specimens had heavily worn enamel (in this case, a reflection of palaeodiet and environment, as opposed to ontogenetic age), rendering observations of the microwear features quite difficult.

The mean values of pits and scratches from the Banwell Bone Cave specimens were plotted on a bivariate graph against the extant bear database (Fig. 4.9 A). The *U. arctos* specimens from Banwell Bone Cave occupy the left-hand sector of the graph, which compared with the right, denotes a smaller mean number of scratches. The Banwell Bone Cave bears plot between *U. americanus* and *U. maritimus* but lie much closer to the former. *U. arctos* from Banwell Bone Cave have slightly smaller mean numbers of scratches (mean 15.87) than *U. americanus* and a small to intermediate mean number of pits (mean 25.75) (Fig. 4.9 A) (see also Table 4.5). The absence of puncture pits and the very small number of gouges present are also identified as characteristic features in this large-bodied brown bear.

Figure 4.9 B compares the Banwell Bone Cave specimens with the extant bear database with reference to the total number of large pits versus small pits. Here, *U. arctos* from Banwell Bone Cave have an intermediate number of small (median: 18) and large (median: 6.25) pits, overlapping with some *U. maritimus* specimens and with some *U. arctos* specimens from Russia (Fig. 4.9 B). Table 4.5 shows a statistical summary of eight microwear features (variables) for *U. arctos* from Banwell Bone

Cave. Statistical tests for *U. arctos* from Banwell Bone Cave in comparison with the microwear features of extant bears and the other extinct samples from the UK are presented in 4.3.9.

Table. 4.5. Banwell Bone bear (MIS 5a), UK (n: 4) statistical summary of eight microwear features. Mean, standard deviation (SD), 95% Confidence interval (CL), 1st and 3rd quartile, minimum, maximum and median values are given.

Microwear features (variables)	Mean; SD	95% CL	1st Quartile	min	median	max	3rd quartile
Pits	25.75; 1.75	1.72	24.37	24	25.75	27.5	27.12
Scratches	15.87; 2.95	2.84	15	12	16.25	19	17.12
Fine Scratches	13.37; 2.87	2.81	12.25	10	13.35	17	14.37
Coarse Scratches	2.5; 0.71	0.69	2	2	2.25	3.5	2.75
Large Pits	6; 1.47	1.44	5.5	4	6.25	7.5	6.75
Small Pits	17.87; 1.31	1.29	16.87	16.5	18	19	19
Gouges	1.87; 1.43	1.41	1	1	1.25	4	2.12
Punctures	0	0	0	0	0	0	0

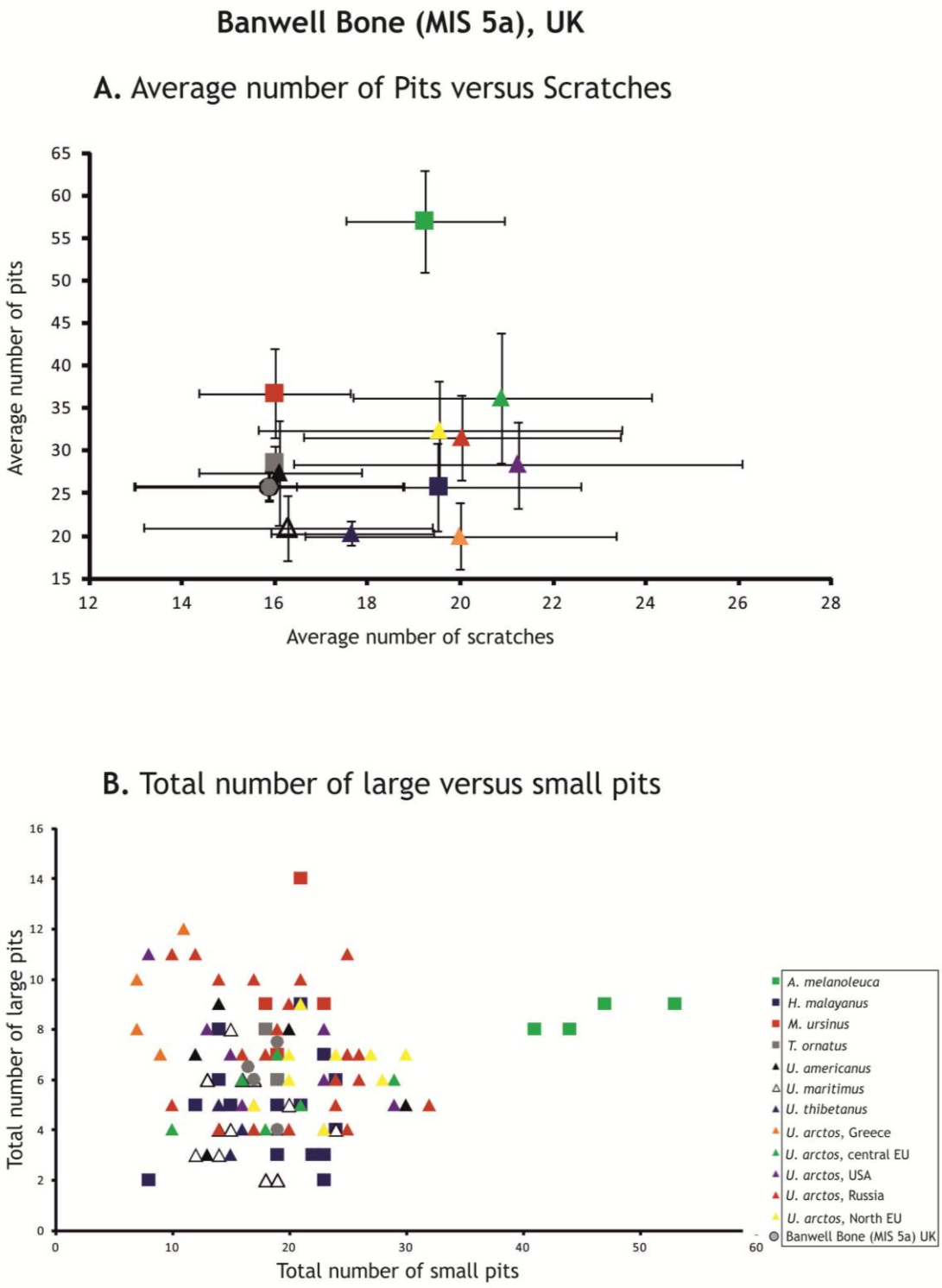

Figure 4.9. Bivariate diagrams for bears from Banwell Bone Cave (MIS 5a), UK, in comparison with the extant bear database. **A.** Plot of average number of pits versus scratches. Error bars represent the standard deviation of pits and scratches. **B.** Plot of raw data of the total number of large versus small pits.

4.3.5.2. PCA results from Banwell Bone Cave (MIS 5a)

PCA was also undertaken on the *U. arctos* specimens from Banwell Bone Cave. Figures 4.10A and B show the results from observations of the grinding surfaces of the m1s of the extinct *U. arctos* from this locality, in comparison with the modern bear database. The first axis (PC1) accounts for 41.83% of the total variance, the second (PC2) for 20.39% and the third axis (PC3) explains 11.35%. Abbreviations of the nine independent variables are given in the caption of Figure 4.10.

Figure 4.10 A illustrates Components 1 and 2, where most of the *U. arctos* specimens from Banwell Bone Cave occupy both left-hand quadrants. This position clearly shows the differentiation of the Banwell Bone Cave bears from the other *U. arctos* groups, *U. americanus* and *A. melanoleuca*. Interestingly, the Banwell Bone Cave bears are much closer to the dietary ecospace of *U. maritimus* than any other brown bears examined, overlapping with that of *U. thibetanus*.

In addition, the Banwell Bone Cave specimens also display the highest scratches width score (SWS) after *U. maritimus,* an absence of puncture pits and a moderate percentage of coarse scratches (Fig. 4.10 A).

Figure 4.10 B reveals the results of Components 1 and 3 for the Banwell Bone Cave *U. arctos* specimens in comparison with the extant bear database. Here too, the Banwell Bone Cave *U. arctos* specimens lie very close to both some *U. thibetanus* and some *U. maritimus* specimens (Fig. 4.10 B).

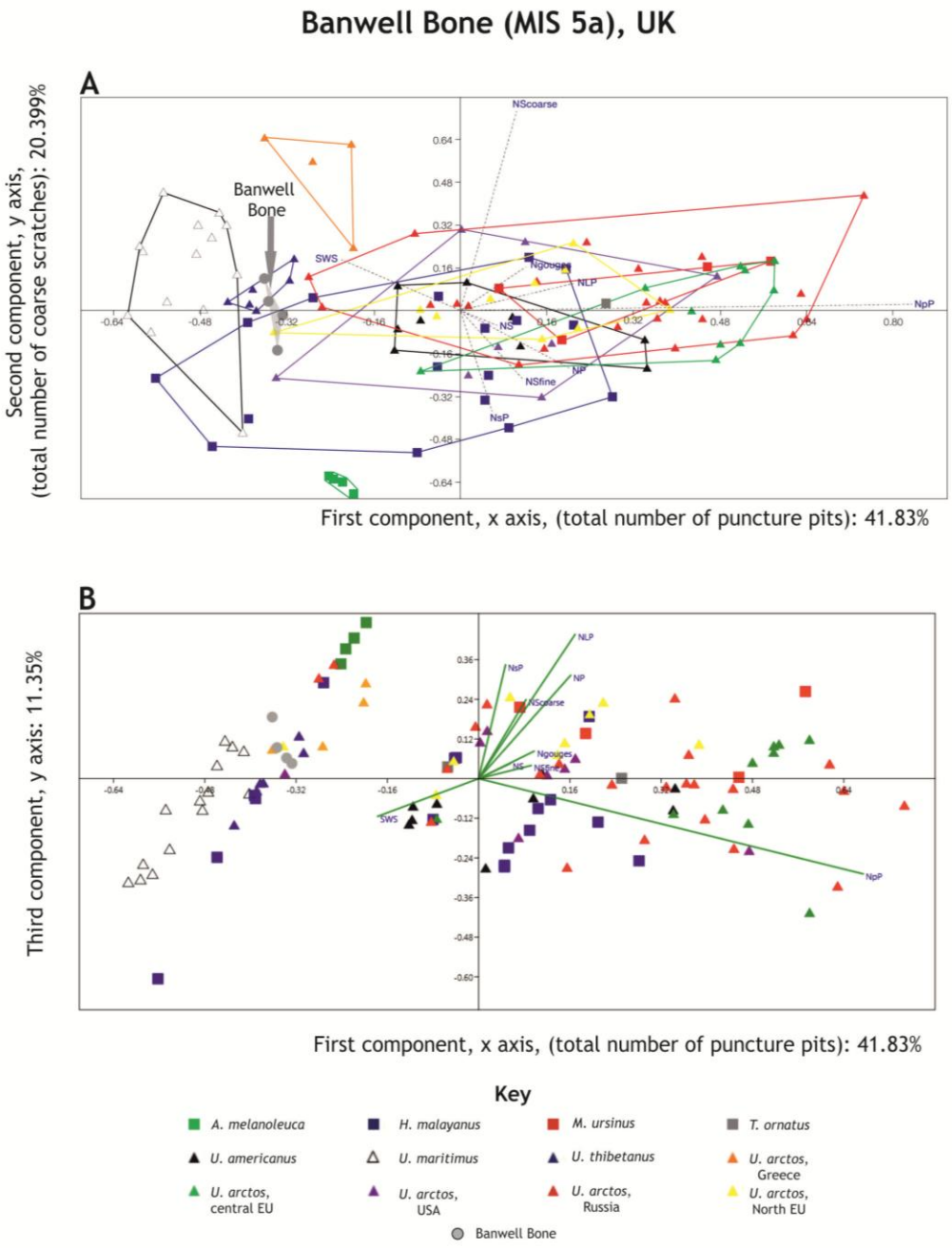

Figure 4.10 PCA plots for Banwell Bone Cave (MIS 5a), UK, in comparison with extant bear species. **A**. Graph component 1 versus 2. The shaded polygon indicates the position of the specimens from Banwell Bone Cave. **B.** Graph component 1 versus 3. For details of symbols, see key. Symbols of Variable as follows: NS: number of scratches; NP: number of pits; NfineS: number of fine scratches; NcoarseS: number of coarse scratches; NLP: number of large pits; NsP: number of small pits; Ngouge: number of gouges; Npp: number of puncture pits; SWS: scratches width score.

4.3.6. Results Dental Microwear Analysis (DMA) from Kents Cavern (cave earth) (MIS 3)

4.3.6.1. Bivariate Analysis results from Kents Cavern (cave earth) (MIS 3)

The results of dental microwear from the early Middle Pleistocene breccias at Kents Cavern were presented in 4.3.2. This section presents the results from the younger series of "cave earth" deposits at the site, attributed to MIS 3, the Middle Devensian (Currant and Jacobi, 1997, 2001; Procter *et al*., 2005). The palaeoenvironmental conditions are inferred to be steppe grassland and to reflect predominantly cold-climate conditions, notwithstanding the multiple stadial-interstadial oscillations that are noted in the Greenland ice cores for this period (e.g. Keen, 1998; Schreve *et al*., 2013) (see 1.3. for further details of the site).

After exclusion of specimens with obvious *post mortem* modifications and/or poor preservation, 12 specimens were suitable for analysis.

Bivariate graphs were used to compare the bears from this bed with the extant bear database (Fig. 4.11 A and B). Figure 4.11 A shows the *U. arctos* from Kents Cavern "cave earth" lying close to the modern *U. arctos* group on the right-hand sector of the graph. The Kents Cavern specimens have a similar mean number of pits (37.10) to *U. arctos* from central Europe (Fig. 4.11 A) but a higher mean number of scratches (24.10) than both the central European group and the other *U. arctos* groups (see also Table 4.6).

In the comparison of total number of large pits versus small pits with the extant bear database, *U. arctos* from Kents Cavern display a high number of large pits (median 10.5 and maximum 17) and an intermediate number of small pits (median 21.5 and maximum 31) (Fig. 4.11 B). Some *U. arctos* specimens from Kents Cavern plot close to some *U. arctos* individuals from Russia but in general, the former have a higher total number of large pits than most *U. arctos* groups (Fig. 4.11 B).

Table 4.6 shows a statistical summary of eight microwear features (variables) for *U. arctos* from Kents Cavern.Statistical tests for *U. arctos* from the Middle Devensian of

Kents Cavern in comparison with the microwear features for extant bears and the other extinct samples from the UK are presented in 4.3.9.

Table. 4.6. Kents Cavern bear (MIS 3), (n: 12) UK statistical summary of eight microwear features. Mean, standard deviation (SD), 95% Confidence interval (CL), 1st and 3rd quartile, minimum, maximum and median values are given.

Microwear features (variables)	Mean; SD	95% CL	1st Quartile	min	median	max	3rd quartile
Pits	37.10; 3.85	2.18	34.75	30	38	42	40.25
Scratches	24.10; 3.29	1.86	22	20	23	31	25.5
Fine Scratches	18.42; 2.71	1.53	16.75	15	17.5	24	19.5
Coarse Scratches	5.67; 2.27	1.28	4	3	5	10	6.25
Large Pits	10.33; 3.14	1.78	8	5	10.5	17	12
Small Pits	22.10; 4.27	2.42	19.75	15	21.5	31	24.5
Gouges	2; 1.13	0.64	1.75	0	2	3	3
Punctures	2.67; 0.89	0.50	2	2	2	4	3.25

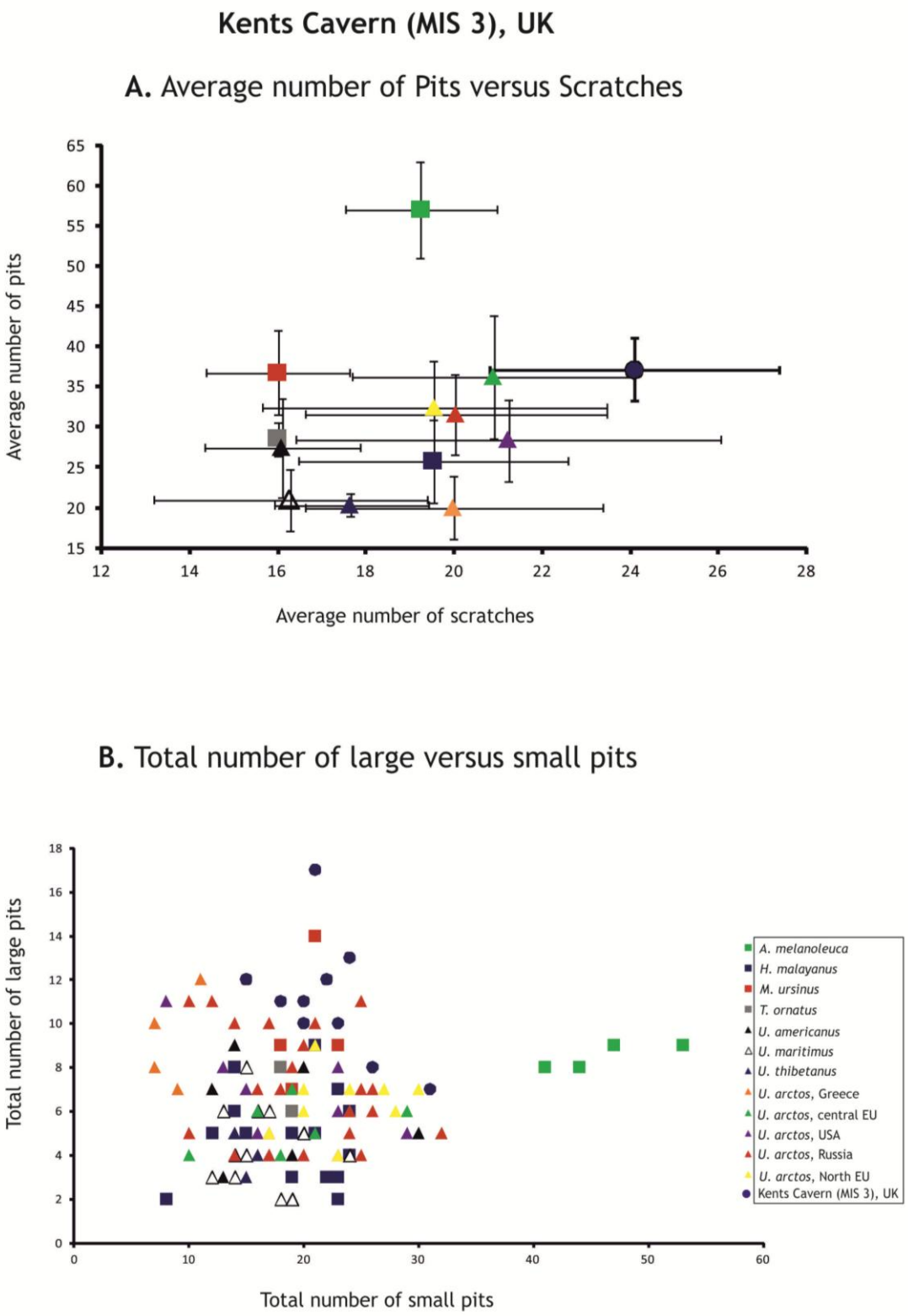

Figure 4.11. Bivariate diagrams for bears from Kents Cavern (cave earth) (MIS 3), UK, in comparison with the extant bear database. **A.** Plot of average number of pits versus scratches. Error bars represent the standard deviation of pits and scratches. **B.** Plot of raw data of the total number of large versus small pits.

4.3.6.2. PCA results from Kents Cavern (cave earth) (MIS 3)

PCA was also undertaken for *U. arctos* specimens from Kents Cavern. Figures 4.12 A and B show the results from observations of the grinding surfaces of the m1s of extinct Middle Devensian *U. arctos* from Kents Cavern, in comparison with the modern database of bears. The first axis (PC1) accounts for 39.63% of the total variance, the second (PC2) for 20.86% and the third axis (PC3) explains 13.96%. Abbreviations of the nine independent variables are given in the caption of Figure 4.12.

Figure 4.12 A illustrates Components 1 and 2, where *U. arctos* specimens from Kents Cavern cave earth occupy the top right quadrant. This position indicates a higher percentage of coarse scratches compared to the rest of the *U. arctos* group and very clear separation from both the hypercarnivore *U. maritimus* and the herbivore *A. melanoleuca* (Fig. 4.12 A).

Although the dietary ecospace of *U. arctos* from Kents Cavern is weakly differentiated from the extant species, nevertheless there is an overlap with the dietary ecospaces of the following omnivorous species: *M. ursinus*, *H. malayanus* and *U. arctos* from northern Europe and Russia. *U. arctos* from Kents Cavern also show an intermediate to high percentage of puncture pits (NpP), large pits (NLp) and gouges (Ngouges) (Fig. 4.12 A).

Figure 4.12 B reveals the results of Components 1 and 3 for the Middle Devensian Kents Cavern *U. arctos* specimens in comparison with extant bear database. In this case Kents Cavern specimens are again scattered in the top right-hand area of the graph (Fig. 4.12 B).

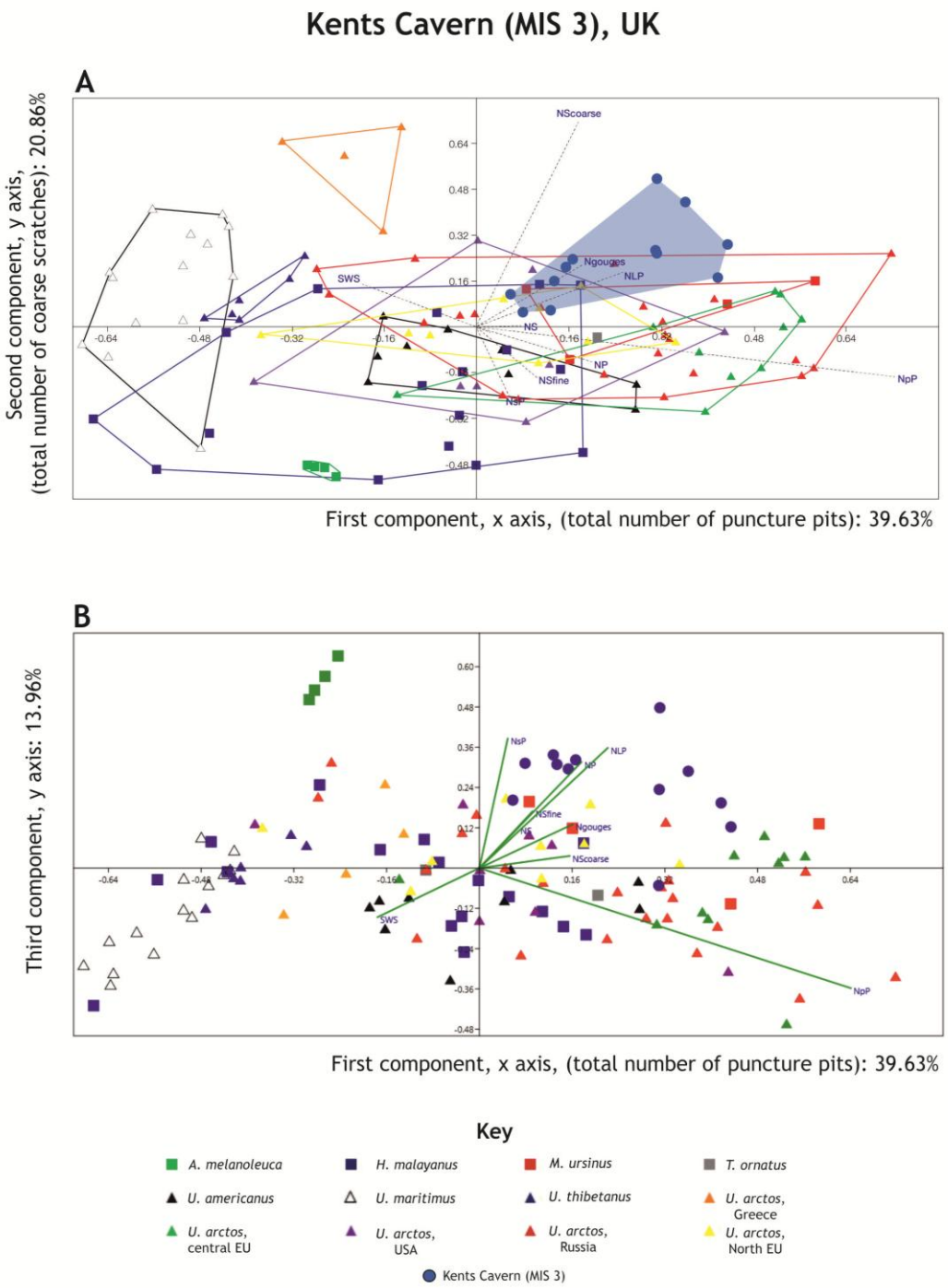

Figure 4.12. PCA plots for Kents Cavern (MIS 3), UK, in comparison with extant bear species. **A**. Graph component 1 versus 2. The shaded polygon indicates the position of the specimens from Kents Cavern (cave earth). **B.** Graph component 1 versus 3. For details of symbols, see key. Symbols of Variable as follows: NS: number of scratches; NP: number of pits; NfineS: number of fine scratches; NcoarseS: number of coarse scratches; NLP: number of large pits; NsP: number of small pits; Ngouge: number of gouges; Npp: number of puncture pits; SWS: scratches width score.

4.3.7. Results Dental Microwear Analysis (DMA) from Sandford Hill (MIS 3)

4.3.7.1. Bivariate Analysis results from Sandford Hill (MIS 3)

As outlined in 1.3., the Middle Devensian (MIS 3) site of Sandford Hill was characterized by a cool climate steppe grassland palaeoenvironment (Currant, 2004). After exclusion of specimens with obvious *post mortem* features and/or poor preservation, 4 specimens were analysed.

Bivariate graphs compared the bears from Sandford with the extant bear database (Fig. 4.13 A and B). Figures 4.13 A and B both reveal that the Sandford Hill bears lie close to *U. arctos* from northern Europe and Russia. In Figure 4.13 A, the Sandford Hill specimens are positioned close to other *U. arctos* groups and occupy the right-hand sector of the graph, which denotes a greater total number of mean values for scratches. In particular, the Sandford Hill bears plot closest to *U. arctos* from northern Europe, with which they share an intermediate mean values of pits (Fig. 4.13 A). The mean values for scratches and pits in the Sandford Hill bears are 31.37 and 19.25 respectively (see also Table 4.7).

Figure 4.13 B compares the Sandford Hill specimens with the extant database in terms of the total number of large pits versus small pits. In this graph, the Sandford Hill specimens plot closely with some *U. arctos* individuals from Russia, on account of the high number of large pits compared to the other *U. arctos* individuals from other geographical regions. Additionally the Sandford Hill specimens have an intermediate number of small pits (average number of large pits: 11.25). One individual is especially distinctive on account of the high number of large pits (14) and small pits (17) (Fig. 4.13 B).

Table 4.7 shows a statistical summary of eight microwear features (variables) for the Sandford Hill bears. Statistical tests for *U. arctos* from Sandford Hill in comparison with the microwear features recorded in the extant bear database and the other extinct bear samples from the UK are presented in 4.3.9.

Table. 4.7. Sandford Hill bears (MIS 3), UK (n: 4) statistical summary of eight microwear features. Mean, standard deviation (SD), 95% Confidence interval (CL), 1st and 3rd quartile, minimum, maximum and median values are given.

Microwear features (variables)	Mean; SD	95% CL	1st Quartile	min	median	max	3rd quartile
Pits	31.37; 3.78	3.74	29.25	27	31.25	36	33.37
Scratches	19.25; 1.89	1.85	18	18	18.5	22	19.75
Fine Scratches	15.5; 3.78	3.71	13	13	14	21	16.5
Coarse Scratches	4.25; 0.96	0.94	3.75	3	4.5	5	5
Large Pits	11.12; 2.10	2.05	10.12	9	10.45	14	11.75
Small Pits	17.12; 0.85	0.84	16.75	16	17.25	18	17.62
Gouges	2.37; 1.60	1.57	2.25	0	3	3.5	3.12
Punctures	0.75; 0.96	0.94	0	0	0.5	2	1.25

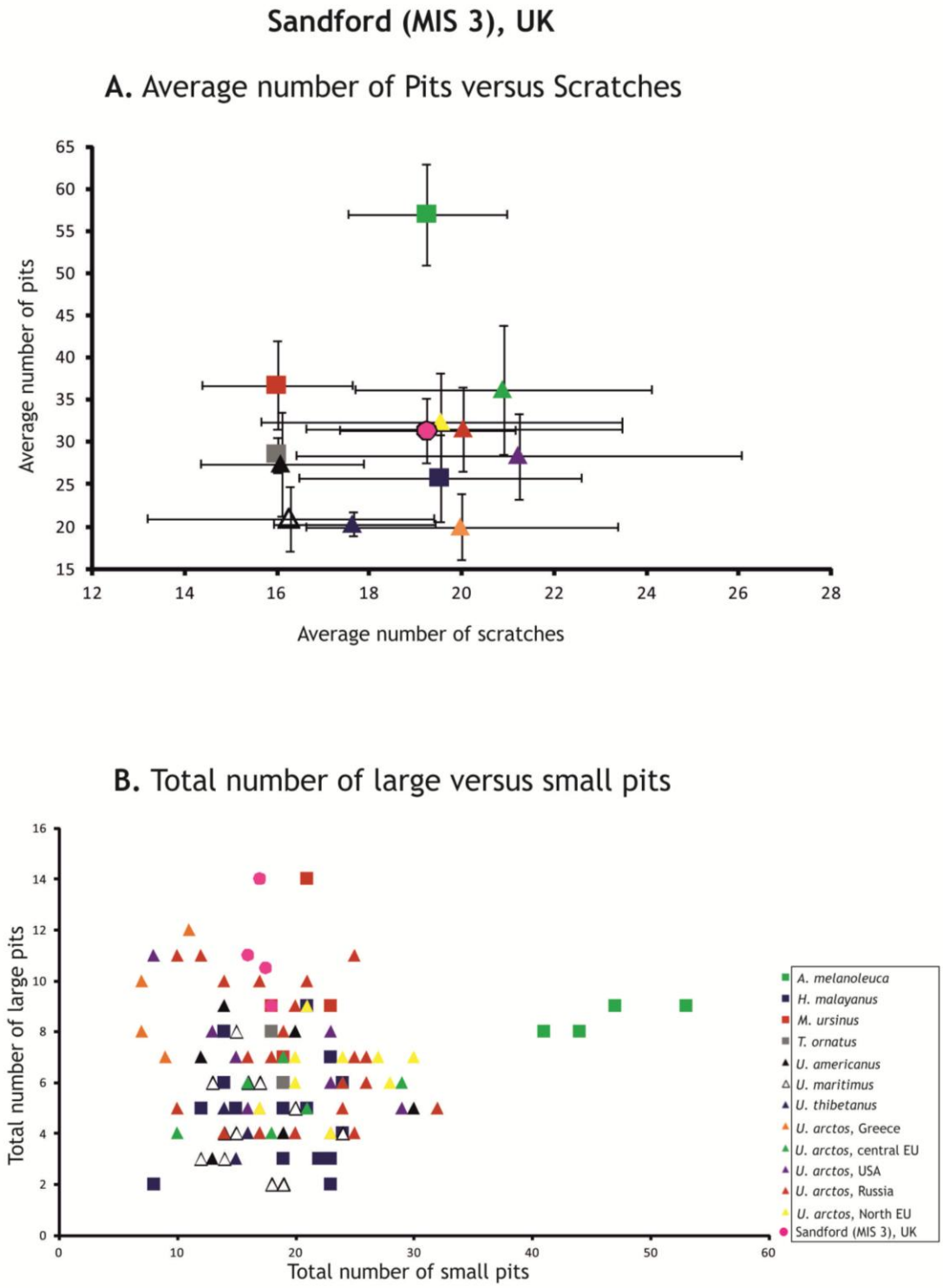

Figure 4.13. Bivariate diagrams for bears from Sandford (MIS 3), UK, in comparison with extant bear database. **A.** Plot of average number of pits versus scratches. Error bars represent the standard deviation of pits and scratches. **B.** Plot of raw data of the total number of large versus small pits.

4.3.7.2. PCA results from Sandford Hill (MIS 3)

PCA was also undertaken on the results from the Sandford Hill bears. Figures 4.14 A and B show the results from observations of the grinding surfaces of the m1s compared to the modern bear database. The first axis (PC1) explains 40.39% of the total variance, the second (PC2) accounts for 20.67% and the third axis (PC3) for 12.98%. Abbreviations of the nine independent variables are given in the caption of Figure 4.14.

Figure 4.14 A illustrates Components 1 and 2 using the grinding facet on *U. arctos* m1s from Sandford Hill. The Sandford Hill specimens are positioned between the dietary ecospaces of three different extant species: *U. arctos* from Greece, *U. thibetanus* and *U. americanus*. One outlier is located proximal to the dietary ecospace of *U. arctos* from northern Europe and *H. malayanus*. The position of *U. arctos* from Sandford Hill is clearly separated from those of the hypercarnivore *U. maritimus* and the herbivore *A. melanoleuca* (Fig. 4.14 A). It also shows very small percentage of puncture pits (NpP) and large pits (NLp) and an intermediate percentage of scratches width score. Moreover, the bears from Sandford Hill display a higher percentage of coarse scratches than seen in extant *U. arctos* specimens from central Europe, Russia and northern Europe; however they have a lower percentage than seen in *U. arctos* from Greece (Fig.4.14).

Figure 4.14 B reveals the results of Components 1 and 3 for the Sandford Hill *U. arctos* specimens in comparison with the extant bear database. In this case, the specimens from Sandford Hill are scattered across three different areas. Three specimens lie close to the ecospace of *A. melanoleuca* and *U. arctos* from Greece, showing that both species present a very small percentage of puncture pits.

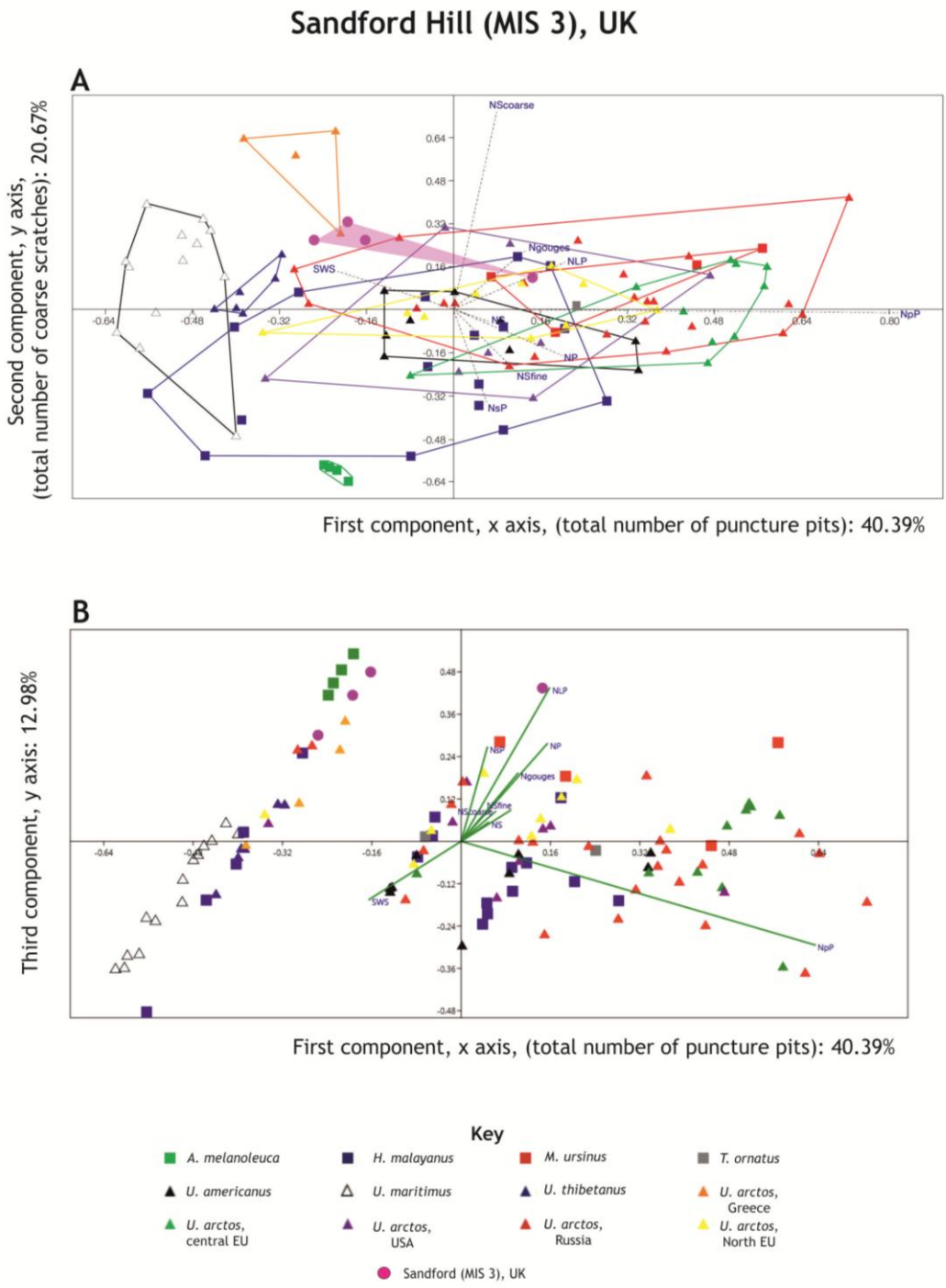

Figure 4.14. PCA plots for Sandford Hill (MIS 3), UK, in comparison with extant bear species. **A**. Graph component 1 versus 2. The shaded polygon indicates the position of the specimens from Sandford Hill. **B.** Graph component 1 versus 3. For details of symbols, see key. Symbols of Variable as follows: NS: number of scratches; NP: number of pits; NfineS: number of fine scratches; NcoarseS: number of coarse scratches; NLP: number of large pits; NsP: number of small pits; Ngouge: number of gouges; Npp: number of puncture pits; SWS: scratches width score.

4.3.8. Results Dental Microwear Analysis (DMA) from Cow Cave (Holocene?)

4.3.8.1. Bivariate Analysis results from Cow Cave (Holocene?)

As outlined in 1.3., little is known regarding the precise chronological age and paleoenvironmental conditions indicated by the Cow Cave deposits. However, the mammalian remains suggest that Sandford Hill was characterized by a cool climate steppe grassland palaeoenvironment at the time of deposition (Currant, 2004) and had similar palaeotemperatures to those reconstructed for Kents Cavern. After exclusion of specimens with obvious *post mortem* features and/or poor preservation, eight specimens were analysed.

Bivariate graphs compared the bears from Cow Cave with the extant bear database (Fig. 4.15A and B). Figure 4.15 A shows that the *U. arctos* from Cow Cave lies close to the *U. arctos* group on the right-hand sector of the graph and compare most closely with brown bears from central Europe. However, the Cow Cave bears are distinguished from all other *U. arctos* groups by their greater number of pits (mean 43.44) and scratches (mean: 22.12) (see also Table 4.8). Comparison of total number of large pits versus small pits against the extant bear database reveals that the *U. arctos* from Cow Cave show a relatively high number of large pits (median 8.5 and maximum 11) and a greater total number of small pits (median 28.5 and maximum 34) than all other extant *U. arctos* groups (Fig. 4.15 B). Some *U. arctos* specimens from Cow Cave lie close to some *U. arctos* individuals from Russia and central Europe (Fig. 4.15 B). A further interesting feature is the fact that the total number of small pits in the Cow Cave bears is similar to that seen in *A. melanoleuca*. Table 4.8 shows a statistical summary of eight microwear features (variables) for *U. arctos* from Cow Cave. Statistical tests for *U. arctos* from Cow Cave in comparison with the microwear features of extant bears and the other extinct samples from UK are presented in 4.3.9.

Table. 4.8. Cow Cave (Holocene?), UK (n: 8) statistical summary of eight microwear features. Mean, standard deviation (SD), 95% Confidence interval (CL), 1st and 3rd quartile, minimum, maximum and median values.

Microwear features (variables)	Mean; SD	95% CL	1st Quartile	min	median	max	3rd quartile
Pits	43.44; 6.32	4.38	38.62	33	45.5	52	47.25
Scratches	22.12; 3.04	2.11	19.75	18	22	26	25
Fine Scratches	15.56; 3.31	2.29	12.87	12	14.5	20	18.5
Coarse Scratches	6.44; 1.99	1.38	5	4.5	5.5	10	8
Large Pits	8.5; 1.60	1.11	7.75	6	8.5	11	9.25
Small Pits	28; 4	2.77	26	22	28.5	34	30.25
Gouges	2.31; 0.88	0.61	1.75	1	2.75	3	3
Punctures	4.62; 1.41	0.97	3.75	3	4.5	7	5.25

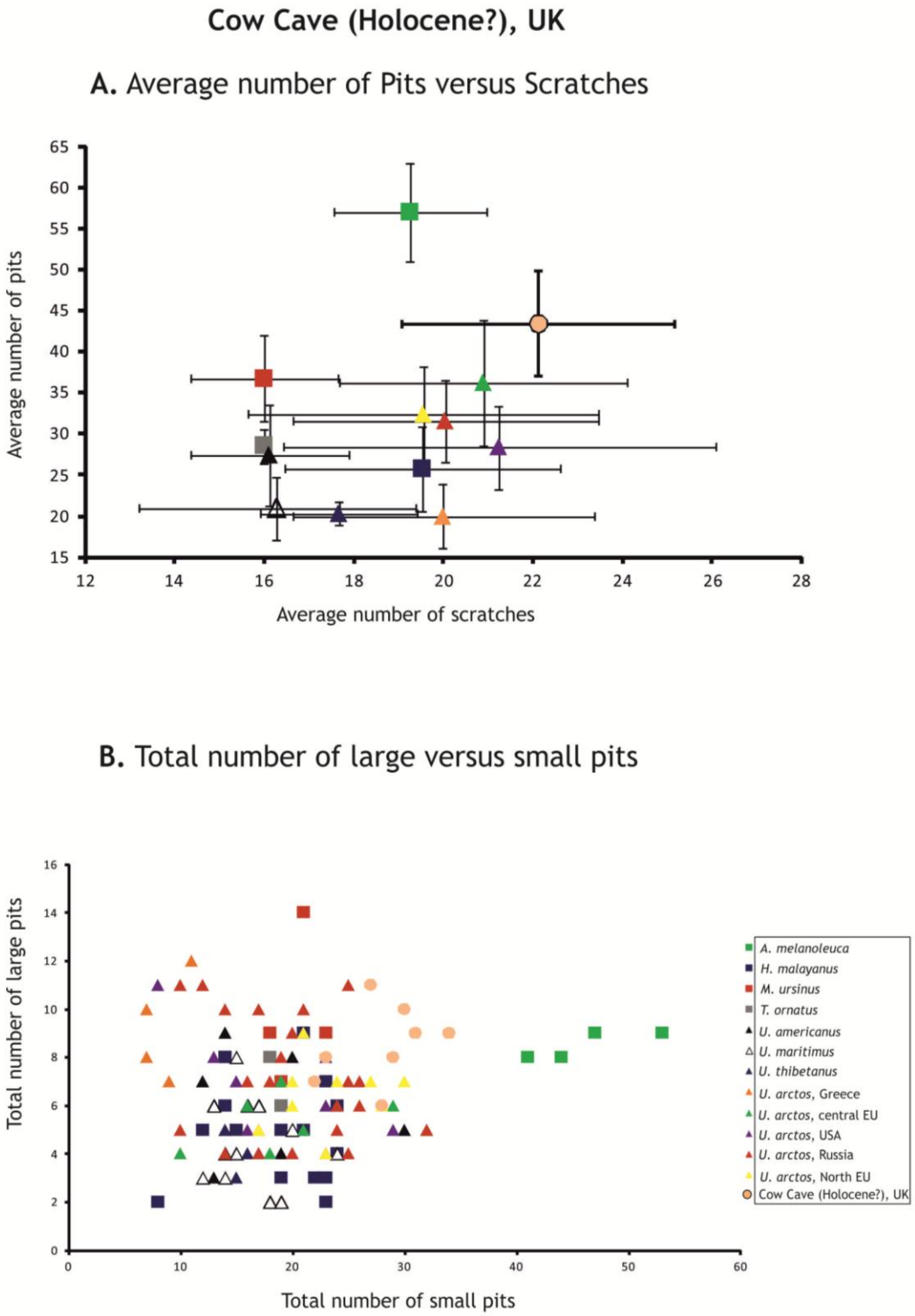

Figure 4.15. Bivariate diagrams for bears from Cow Cave (Holocene?), UK, in comparison with the extant bear database. **A.** Plot of average number of pits versus scratches. Error bars represent the standard deviation of pits and scratches. **B.** Plot of raw data of the total number of large versus small pits.

4.3.8.2. PCA results from Cow Cave (Holocene?)

PCA was also undertaken for *U. arctos* specimens from Cow Cave in comparison with the observations from the modern bear database (Fig. 4.16 A and B). The first axis (PC1) accounts for 42.74% of the total variance, the second (PC2) for 20.21% and the third axis (PC3) explains 12.23%. Abbreviations of the nine independent variables are given in the caption of Figure 4.16.

Figure 4.16 A illustrates Components 1 and 2 where the Cow Cave specimens occupy the top right quadrant of the plot. The dietary ecospace of the Cow Cave specimens partially overlaps with those of *U. arctos* from Russia and central Europe as well as with that of *U. arctos* from central Europe. This position reveals a relatively high percentage number of puncture pits, large pits and gouges (Fig. 4.16 A).

Figure 4.16 B reveals the results of Components 1 and 3 for the Cow Cave bears in comparison with the extant bear database. In this case, the specimens again plot in the top right-hand area of the graph (Fig. 4.16 B).

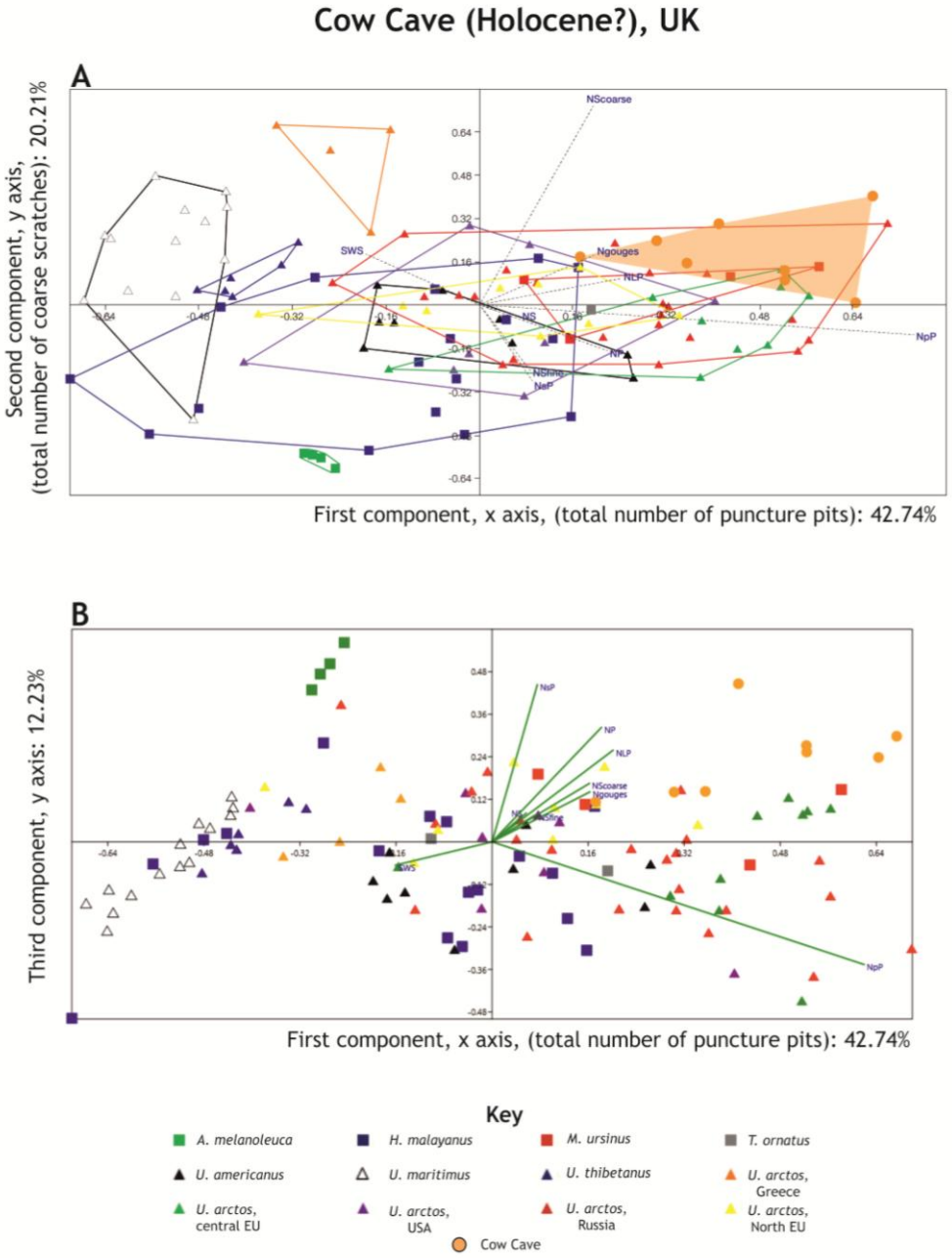

Figure 4.16. PCA plots for Cow Cave (Holocene?), UK, in comparison with extant bear species. **A**. Graph component 1 versus 2. The shaded polygon indicates the position of the specimens from Cow Cave. **B.** Graph component 1 versus 3. Details of symbols see key. Symbols of Variable as follows: NS: number of scratches; NP: number of pits; NfineS: number of fine scratches; NcoarseS: number of coarse scratches; NLP: number of large pits; NsP: number of small pits; Ngouge: number of gouges; Npp: number of puncture pits; SWS: scratches width score.

4.3.9. Statistical tests for all sites from Britain in comparison with extant species

To understand better which microwear traits differentiate the extinct species from Britain, analysis of variance (ANOVA) statistical tests were performed, along with Tukey's pairwise comparison tests. Table 4.9 presents the ANOVA tests for all extant species and extinct species from Britain using the grinding area of the m1. These revealed significant ($p<0.05$) differences for the following microwear features: scratches, pits, fine scratches, coarse scratches, large pits, small pits and puncture pits. This means that there any pair of bear species displays a significant difference in at least of the above features. Two variables, the scratches width score and the presence/absence of cross scratches were excluded from the analyses since little variation was observed between species.

The significant differences (p-values) between species as revealed by the Tukey's pairwise tests are highlighted in pink in Tables 4.10-4.13. With respect to the number of gouges present, as expected, none of the bear species differ significantly (Table 4.13 A). However, all the other microwear features show significant differences between bear species (Tables 4.10; 4.11; 4.12 A and B and 4.13 B). Thus, from these tables it is clear that there is a very good separation between species on almost all the microwear features that used and especially this is true for pits (Table 4.10B), coarse scratches (Table 4.11B) and small pits (Table 4.12B) which possess the biggest number of pairwise bear species where the p-value shows significant differences.

Table 4.9. ANOVA results for extinct species from Britain and extant species on the **grinding** area. A summary is given of the results from all the different features that were measured in each species and compared and tested between and within groups. Abbreviations as follows: Sum of sqrs is the sum of squares due to features; df is the degree of freedom in the features; Mean sqrs is the mean sum of squares duet to features; F is the *F*-statistic and p is the p-value.

		Sum of sqrs	Df	Mean square	F	p
Scratches	**Between groups:**	1271.9	18	70.66	7.177	< 0.0001
	Within groups:	1673.8	170	9.85		
	Total:	2945.6	188			
Pits	**Between groups:**	10290.9	18	571.72	24.11	< 0.0001
	Within groups:	4031.2	170	23.71		
	Total:	14322.1	188			
Fine Scratches	**Between groups:**	1111.1	18	61.73	5.905	< 0.0001
	Within groups:	1777.9	170	10.45		
	Total:	2888.3	188			
Coarse Scratches	**Between groups:**	276.8	17	16.3	8.146	< 0.0001
	Within groups:	329.8	165	1.9		
	Total:	606.6	182			
Large Pits	**Between groups:**	546.1	18	30.33	6.444	< 0.0001
	Within groups:	800.2	170	4.711		
	Total:	1346.2	188			
Small Pits	**Between groups:**	5712.5	18	317.36	14.17	< 0.0001
	Within groups:	3808.7	170	22.40		
	Total:	9521.2	188			
Gouges	**Between groups:**	10.6	10	1.06	1.147	0.341
	Within groups:	67.4	73	0.92		
	Total:	78.1	83			
Puncture Pits	**Between groups:**	198.1	12	16.51	6.858	< 0.0001
	Within groups:	284.0	118	2.41		
	Total:	482.1	130			

A. Turkey's test **scratches** for extinct species UK including all extant species.

	1	2	3	4	5	6	7	8	9	10	11	12	13	14	15	16	17	18	19
1		1	0.8991	0.9244	0.9547	1	1	1	0.9995	1	1	1	0.06386	1	0.7941	0.8648	0.251	1	0.9661
2	0.2399		0.814	0.8515	0.9007	0.9998	1	1	0.9999	1	1	0.9997	0.1061	1	0.6771	0.7664	0.3582	1	0.9883
3	2.79	3.03		1	1	1	0.6136	0.2287	0.1338	0.593	0.8045	1	< 0.0001	0.2258	1	1	0.000178	8.99E-01	0.02522
4	2.695	2.935	0.0954		1	1	0.6652	0.2666	0.16	0.6452	0.8431	1	< 0.0001	0.2633	1	1	0.000236	0.9244	0.03193
5	2.545	2.785	0.2453	0.1499		1	0.7419	0.3333	0.2085	0.7235	0.8941	1	< 0.0001	0.3296	1	1	0.000374	0.9547	0.04563
6	1.359	1.599	1.431	1.336	1.186		0.9966	0.9032	0.7941	0.9957	0.9998	1	0.001648	0.901	0.9995	0.9999	0.01317	1	0.3995
7	0.6439	0.404	3.434	3.339	3.189	2.003		1	1	1	1	0.9952	0.2234	1	0.456	0.5543	0.5741	1	0.999
8	1.417	1.177	4.207	4.112	3.962	2.776	0.7727		1	1	1	0.8862	0.6057	1	0.1375	0.1906	0.9149	1	1
9	1.717	1.477	4.508	4.412	4.262	3.077	1.073	0.3005		1	1	0.7682	0.7615	1	0.07465	0.1083	0.9707	0.9995	1
10	0.6813	0.4414	3.472	3.376	3.226	2.041	0.03733	0.7354	1.036		1	0.9941	0.2375	1	0.4361	0.5336	0.5948	1	0.9992
11	0.2623	0.02245	3.053	2.957	2.807	1.622	0.3816	1.154	1.455	0.4189		0.9997	0.111	1	0.6652	0.7559	0.3693	1	0.9895
12	1.417	1.657	1.374	1.278	1.128	0.05724	2.061	2.833	3.134	2.098	1.679		0.001379	0.8837	0.9997	0.9999	0.01129	1	0.3705
13	4.865	4.625	7.656	7.56	7.41	6.225	4.221	3.449	3.148	4.184	4.603	6.282		0.61	< 0.0001	< 0.0001	1	0.06386	0.9747
14	1.424	1.185	4.215	4.119	3.97	2.784	0.7805	0.007805	0.2927	0.7432	1.162	2.841	3.441		0.1354	0.188	0.9169	1.00E+00	1
15	3.077	3.317	0.2862	0.3816	0.5315	1.717	3.721	4.493	4.794	3.758	3.339	1.66	7.942	4.501		1	< 0.0001	0.7941	0.01197
16	2.898	3.138	0.1073	0.2027	0.3526	1.538	3.542	4.314	4.615	3.579	3.16	1.481	7.763	4.322	0.1789		0.000133	0.8648	0.01919
17	4.15	3.91	6.94	6.845	6.695	5.509	3.506	2.733	2.433	3.469	3.888	5.567	0.7155	2.725	7.226	7.048		2.51E-01	0.9996
18	0	0.2399	2.79	2.695	2.545	1.359	0.6439	1.417	1.717	0.6813	0.2623	1.417	4.865	1.424	3.077	2.898	4.15		0.9661
19	2.468	2.229	5.259	5.163	5.014	3.828	1.825	1.052	0.7513	1.787	2.206	3.885	2.397	1.044	5.545	5.366	1.681	2.468	

B. Turkey's test **pits** for extinct species UK including all extant species.

	1	2	3	4	5	6	7	8	9	10	11	12	13	14	15	16	17	18	19
1		< 0.0001	< 0.0001	< 0.0001	< 0.0001	< 0.0001	< 0.0001	< 0.0001	< 0.0001	< 0.0001	< 0.0001	< 0.0001	< 0.0001	< 0.0001	< 0.0001	< 0.0001	< 0.0001	< 0.0001	< 0.0001
2	17.31		0.00235	1	0.9361	0.8373	0.7575	0.005795	0.9999	0.7279	0.452	0.6641	0.4113	0.6424	0.06575	1	0.001326	0.767	< 0.0001
3	11.2	6.11		0.03314	< 0.0001	< 0.0001	< 0.0001	1	0.1044	0.8666	0.9763	< 0.0001	0.983	0.9161	1	0.002526	1	0.8368	0.4672
4	16.35	0.9618	5.148		0.5193	0.3465	0.2637	0.06694	1	0.9866	0.906	0.1944	0.8831	0.9722	0.3679	1	0.02092	0.9911	< 0.0001
5	19.96	2.643	8.753	3.605		1	1	< 0.0001	0.2633	0.004933	0.00104	1	0.000818	0.00304	< 0.0001	0.931	< 0.0001	0.00625	< 0.0001
6	20.29	2.972	9.082	3.934	0.3293		1	< 0.0001	0.149	0.001836	0.00037	1	0.00029	0.0011	< 0.0001	0.828	< 0.0001	0.00236	< 0.0001
7	20.47	3.157	9.267	4.119	0.5137	0.1844		< 0.0001	0.104	0.001032	0.00021	1	0.000168	< 0.0001	< 0.0001	0.746	< 0.0001	0.00133	< 0.0001
8	11.51	5.806	0.3043	4.844	8.449	8.778	8.963		0.186	0.9471	0.9947	< 0.0001	0.9966	0.9717	1	6.21E-03	1	0.903	0.3136
9	15.84	1.477	4.633	0.5148	4.12	4.449	4.633	4.329		0.9994	0.9869	0.07087	0.981	0.9982	0.6457	1	0.07087	0.9997	< 0.0001
10	14.1	3.218	2.892	2.256	5.861	6.19	6.374	2.588	1.741		1	0.00058	1	1	0.9998	0.7399	0.794	1	0.00052
11	13.59	3.728	2.382	2.766	6.371	6.7	6.885	2.078	2.251	0.5105		< 0.0001	1	1	1	0.4651	0.951	1	0.00256
12	20.65	3.341	9.451	4.303	0.6981	0.3688	0.1844	9.147	4.818	6.559	7.069		0.000104	< 0.0001	< 0.0001	0.651	< 0.0001	< 0.0001	< 0.0001
13	13.51	3.805	2.305	2.843	6.448	6.777	6.962	2.001	2.328	0.5873	0.07684	7.146		1	1	0.424	0.9632	1	0.00322
14	13.93	3.382	2.728	2.42	6.025	6.354	6.538	2.424	1.905	0.164	0.3465	6.723	0.4233		0.9999	0.6555	0.8595	1	0.00087
15	12.46	4.852	1.258	3.89	7.495	7.824	8.009	0.9537	3.375	1.635	1.124	8.193	1.047	1.471		0.06936	1	0.9995	0.05188
16	17.29	0.02441	6.086	0.9374	2.667	2.997	3.181	5.781	1.452	3.193	3.704	3.366	3.78	3.357	4.828		1.43E-03	0.7783	< 0.0001
17	11.02	6.294	0.1844	5.333	8.937	9.267	9.451	0.4887	4.818	3.077	2.566	9.636	2.49	2.913	1.442	6.27		0.7568	0.5688
18	14.18	3.136	2.974	2.175	5.779	6.109	6.293	2.669	1.66	0.08118	0.5917	6.478	0.6685	0.2452	1.716	3.112	3.158		0.0004
19	7.503	9.81	3.7	8.848	12.45	12.78	12.97	4.004	8.333	6.592	6.082	13.15	6.005	6.428	4.958	9.785	3.515	6.673	

Table 4.10. A. Results from **Tukey's test for scratches** for extinct UK species including extant species. **B.** Results from **Tukey's test for pits** for extinct UK species including extant species. Numbers linked with the following species **1:** *A. melanoleuca*; **2:** *H. malayanus*; **3:** *M. ursinus*; **4:** *U. americanus*; **5:** *U. maritimus*; **6:** *U. thibetanus*; **7:** *U. arctos*, Greece; **8:** *U. arctos*, Central Europe; **9:** *U. arctos*, USA; **10:** *U. arctos*, Russia; **11:** *U. arctos*, North Europe; **12:** Westbury-sub-Mendip (MIS 13); **13:** Kents Cavern (breccias); **14:** Grays Thurrock (MIS 9); **15:** Tornewton Cave (MIS 5e); **16:** Banwell Bone Cave (MIS 5a); **17:** Kents Cavern (MIS 3); **18:** Sandford Hill (MIS 3); **19:** Cow Cave (Holocene?). Values below the diagonal are the results of Tukey's test and those above are the p-values.

A. Turkey's test **fine scratches** for extinct species UK including all extant species.

	1	2	3	4	5	6	7	8	9	10	11	12	13	14	15	16	17	18	19
1		0.9998	0.01686	0.0829	0.00022	0.2729	0.02865	1	1	0.9576	0.8664	0.0121	1	0.9995	0.00913	0.05975	1	0.7725	0.7959
2	1.63		0.4211	0.7769	0.02614	0.9663	0.5341	1	1	1	1	0.3576	1	1	0.3089	0.7036	1	0.9999	1
3	5.416	3.786		1	1	1	1	0.3352	0.1155	0.8678	0.9582	1	0.1005	0.4711	1	1	0.08704	0.9842	0.9799
4	4.745	3.115	0.6712		0.993	1	1	0.6928	0.3575	0.9889	0.9987	1	0.3243	0.8176	1	1	0.2928	0.9998	0.9997
5	6.874	5.244	1.458	2.129		0.9028	0.9997	0.01686	0.002892	0.1799	0.3243	1	0.002344	0.03292	1	0.9971	0.001894	0.4405	0.4131
6	4.097	2.467	1.319	0.6481	2.777		1	0.9371	0.7047	0.9999	1	1	0.6684	0.9771	0.9999	1	0.6311	1	1
7	5.208	3.578	0.2083	0.4629	1.666	1.111		0.4405	0.1713	0.9277	0.9824	1	0.1509	0.586	1	1	0.1323	0.9946	0.9928
8	1.458	0.1715	3.958	3.287	5.416	2.639	3.75		1	1	1	0.2788	1	1	0.2368	0.6121	1	0.9997	0.9998
9	0.8332	0.7965	4.583	3.912	6.041	3.263	4.374	0.6249		0.9996	0.9952	0.0896	1	1	0.07194	0.2877	1	0.9842	0.9876
10	2.527	0.8972	2.889	2.218	4.347	1.57	2.681	1.069	1.694		1	0.8206	0.9993	1	0.7758	0.9776	0.9989	1	1
11	2.893	1.263	2.523	1.852	3.981	1.204	2.315	1.435	2.06	0.3663		0.9351	0.993	1	0.9102	0.9966	0.9899	1	1
12	5.541	3.911	0.125	0.7962	1.333	1.444	0.3333	4.083	4.708	3.014	2.648		0.07736	0.4047	1	1	0.06655	0.9726	0.9661
13	0.7638	0.8659	4.652	3.981	6.11	3.333	4.444	0.6944	0.06944	1.763	2.129	4.777		1	0.06177	0.2584	1	0.9783	0.9828
14	1.723	0.09357	3.693	3.022	5.151	2.373	3.484	0.2651	0.89	0.8036	1.17	3.818	0.9595		0.3529	0.7502	1	1	1
15	5.644	4.014	0.2281	0.8994	1.23	1.547	0.4365	4.186	4.811	3.117	2.751	0.1032	4.88	3.921		1	0.05283	0.9588	0.9501
16	4.895	3.266	0.5208	0.1504	1.979	0.7985	0.3125	3.437	4.062	2.368	2.002	0.6458	4.131	3.172	0.7489		0.2311	0.9993	0.999
17	0.6944	0.9353	4.722	4.05	6.18	3.402	4.513	0.7638	0.1389	1.833	2.199	4.847	0.06944	1.029	4.95	4.201		0.9709	0.9766
18	3.125	1.495	2.291	1.62	3.75	0.9721	2.083	1.666	2.291	0.5978	0.2315	2.416	2.361	1.401	2.52	1.771	2.43		1
19	3.073	1.443	2.343	1.672	3.802	1.024	2.135	1.614	2.239	0.5457	0.1794	2.468	2.309	1.349	2.572	1.823	2.378	0.05208	

B. Turkey's test **coarse scratches** for extinct species UK including all extant species.

	2	3	4	5	6	7	8	9	10	11	12	13	14	15	16	17	18	19
2		0.9993	1	0.9911	0.9979	< 0.0001	0.9954	1	0.8712	0.9004	0.03312	< 0.0001	0.926	0.9997	1	0.000838	0.4681	< 0.0001
3	1.703		1	1	1	< 0.0001	1	1	1	1	0.6013	0.00065	1	1	0.9999	0.0828	0.9965	0.001582
4	0.3514	1.352		0.999	0.9999	< 0.0001	0.9996	1	0.9571	0.9701	0.07381	< 0.0001	0.9803	1	1	0.002494	0.6597	< 0.0001
5	2.115	0.4117	1.763		1	< 0.0001	1	1	1	1	0.8065	0.00234	1	1	0.9978	0.1834	0.9998	0.005436
6	1.865	0.1622	1.514	0.2495		< 0.0001	1	1	1	1	0.6881	0.00108	1	1	0.9996	0.1152	0.9988	0.002598
7	9.002	7.299	8.651	6.887	7.137		< 0.0001	< 0.0001	0.001717	0.001282	0.3438	1	< 0.0001	< 0.0001	< 0.0001	0.934	0.01803	1
8	1.995	0.292	1.644	0.1198	0.1298	7.007		1	1	1	0.7526	0.00162	1	1	0.999	0.1477	0.9995	0.003826
9	1.217	0.4866	0.8651	0.8983	0.6488	7.786	0.7786		0.9997	0.9999	0.3438	0.00015	0.9999	1	1	0.02717	0.9631	0.000341
10	2.824	1.121	2.473	0.7096	0.9591	6.178	0.8293	1.608		1	0.9799	0.01738	1	1	0.9373	0.5045	1	0.03529
11	2.73	1.027	2.379	0.6155	0.8651	6.272	0.7353	1.514	0.09403		0.9701	0.01358	1	1	0.9548	0.4536	1	0.02809
12	5.109	3.406	4.758	2.994	3.244	3.893	3.114	3.893	2.285	2.379		0.7678	0.9564	0.5376	0.05826	1	0.9999	0.8799
13	8.191	6.488	7.84	6.076	6.326	0.811	6.196	6.975	5.367	5.461	3.082		0.01042	0.000449	< 0.0001	0.9988	0.1152	1
14	2.632	0.929	2.281	0.5172	0.7668	6.37	0.637	1.416	0.1923	0.0983	2.477	5.559		1	0.9689	0.4022	1	0.02197
15	1.587	0.1159	1.236	0.5276	0.2781	7.415	0.4078	0.3707	1.237	1.143	3.522	6.604	1.045		1	0.06455	0.9933	0.001102
16	0.2433	1.46	0.1081	1.872	1.622	8.759	1.752	0.9732	2.581	2.487	4.866	7.948	2.389	1.344		0.00179	0.6013	< 0.0001
17	6.407	4.704	6.055	4.292	4.542	2.595	4.412	5.19	3.583	3.677	1.298	1.784	3.775	4.82	6.164		0.8925	0.9999
18	3.65	1.946	3.298	1.535	1.784	5.353	1.654	2.433	0.8251	0.9191	1.46	4.542	1.017	2.062	3.406	2.757		0.1947
19	7.907	6.204	7.556	5.792	6.042	1.095	5.912	6.691	5.083	5.177	2.798	0.2839	5.275	6.32	7.664	1.5	4.258	

Table 4.11. A. Results from **Tukey's test for fine scratches** for extinct UK species including extant species. **B.** Results from **Tukey's test for coarse scratches** for extinct UK species including extant species. Numbers linked with the following species **1:** *A. melanoleuca*; **2:** *H. malayanus*; **3:** *M. ursinus*; **4:** *U. americanus*; **5:** *U. maritimus*; **6:** *U. thibetanus*; **7:** *U. arctos*, Greece; **8:** *U. arctos*, Central Europe; **9:** *U. arctos*, USA; **10:** *U. arctos*, Russia; **11:** *U. arctos*, North Europe; **12:** Westbury-sub-Mendip (MIS 13); **13:** Kents Cavern (breccias); **14:** Grays Thurrock (MIS 9); **15:** Tornewton Cave (MIS 5e); **16:** Banwell Bone Cave (MIS 5a); **17:** Kents Cavern (MIS 3); **18:** Sandford Hill (MIS 3); **19:** Cow Cave (Holocene?). Values below the diagonal are the results of Tukey's test and those above are the p-values.

A. Turkey's test **large pits** for extinct species UK including all extant species.

	1	2	3	4	5	6	7	8	9	10	11	12	13	14	15	16	17	18	19
1		0.2314	0.9999	0.4169	0.0508	0.0508	1	0.3885	0.9912	0.998	0.9534	0.613	1	0.7281	0.9941	0.7817	0.9852	0.7067	1
2	4.2		0.00675	1	1	1	0.03452	1	0.9961	0.9847	0.9997	1	0.4766	1	0.994	1	0.000747	< 0.0001	0.2314
3	1.552	5.752		0.0202	0.00065	0.000652	1	0.01751	0.4535	0.5947	0.2695	0.04845	0.995	0.07866	0.4937	0.09959	1	0.9996	0.9999
4	3.794	0.4058	5.346		1	1	0.08633	1	0.9998	0.9985	1	1	0.6978	1	0.9996	1	0.002643	0.000131	0.4169
5	4.967	0.767	6.519	1.173		1	0.00442	1	0.8981	0.8055	0.9728	0.9999	0.1493	0.9994	0.875	0.9986	< 0.0001	< 0.0001	0.0508
6	4.967	0.767	6.519	1.173	0		0.00442	1	0.8981	0.8055	0.9728	0.9999	0.1493	0.9994	0.875	0.9986	< 0.0001	< 0.0001	0.0508
7	0.9313	5.131	0.6209	4.726	5.898	5.898		0.07679	0.7817	0.8815	0.5864	0.1737	1	0.2515	0.8139	0.2994	1	0.9812	1
8	3.849	0.3506	5.402	0.05519	1.118	1.118	4.781		0.9997	0.9978	1	1	0.6689	1	0.999	1	0.002235	0.000114	0.3885
9	2.173	2.027	3.725	1.621	2.794	2.794	3.104	1.676		1	1	1	0.9997	1	1	1	0.1493	0.01615	0.9912
10	1.917	2.283	3.469	1.878	3.05	3.05	2.848	1.933	0.2564		1	0.9999	1	1	1	1	0.234	0.03096	0.998
11	2.552	1.648	4.105	1.242	2.414	2.414	3.484	1.297	0.3794	0.6359		1	0.9959	1	1	1	0.06917	0.005692	0.9534
12	3.435	0.7645	4.988	0.3587	1.531	1.531	4.367	0.4139	1.262	1.519	0.883		0.8576	1	1	1	0.007557	0.000374	0.613
13	0.5174	3.683	2.07	3.277	4.45	4.45	1.449	3.332	1.656	1.399	2.035	2.918		0.9232	0.9999	0.9473	0.8981	0.426	1
14	3.217	0.9828	4.769	0.577	1.75	1.75	4.149	0.6322	1.044	1.301	0.6648	0.2182	2.7		1	1	0.01373	0.000746	0.7281
15	2.099	2.101	3.651	1.695	2.868	2.868	3.03	1.75	0.07391	0.1825	0.4533	1.336	1.582	1.118		1	0.171	0.01957	0.9941
16	3.104	1.096	4.657	0.6899	1.863	1.863	4.036	0.745	0.9313	1.188	0.5519	0.3311	2.587	0.1129	1.005		0.01848	0.001067	0.7817
17	2.277	6.477	0.7243	6.071	7.243	7.243	1.345	6.126	4.45	4.193	4.829	5.712	2.794	5.494	4.376	5.381		1	0.9852
18	3.26	7.46	1.707	7.054	8.227	8.227	2.328	7.109	5.433	5.176	5.812	6.695	3.777	6.477	5.359	6.364	0.983		0.7067
19	0	4.2	1.552	3.794	4.967	4.967	0.9313	3.849	2.173	1.917	2.552	3.435	0.5174	3.217	2.099	3.104	2.277	3.26	

B. Turkey's test **small pits** for extinct species UK including all extant species.

	1	2	3	4	5	6	7	8	9	10	11	12	13	14	15	16	17	18	19
1		< 0.0001	< 0.0001	< 0.0001	< 0.0001	< 0.0001	< 0.0001	< 0.0001	< 0.0001	< 0.0001	< 0.0001	< 0.0001	< 0.0001	< 0.0001	< 0.0001	< 0.0001	< 0.0001	< 0.0001	< 0.0001
2	15.78		1	1	1	0.999	0.00763	0.9863	1	1	0.9146	0.5205	0.9996	0.9971	0.8455	1	0.9962	1	0.01803
3	14.8	0.9793		1	0.9837	0.8968	0.00038	1	1	1	0.9994	0.1157	1	1	0.9972	1	1	0.9993	0.1603
4	15.51	0.2678	0.7115		0.9998	0.9944	0.00351	0.9968	1	1	0.9664	0.3779	1	0.9996	0.9272	1	0.9994	1	0.03526
5	17.1	1.318	2.297	1.586		1	0.1664	0.5343	1	0.996	0.2921	0.9846	0.823	0.6894	0.2062	1	0.6644	1	0.00036
6	17.6	1.819	2.798	2.087	0.5014		0.3684	0.2804	0.9995	0.9567	0.1224	0.9992	0.5719	0.4168	0.07853	1	0.3923	1	< 0.0001
7	21.49	5.708	6.688	5.976	4.391	3.889		< 0.0001	0.00974	0.000889	< 0.0001	0.9938	< 0.0001	< 0.0001	< 0.0001	< 0.0001	< 0.0001	0.0579	< 0.0001
8	13.52	2.26	1.281	1.992	3.578	4.079	7.968		0.9795	0.9999	1	0.00491	1	1	1	0.9384	1	0.8016	0.7698
9	15.87	0.08789	1.067	0.3557	1.23	1.731	5.621	2.348		1	0.8896	0.5693	0.9993	0.9951	0.8103	1	0.9937	1	0.01431
10	15.06	0.7133	0.266	0.4454	2.031	2.532	6.422	1.547	0.8012		0.9962	0.1901	1	1	0.9877	1	1	0.9999	0.09547
11	13.04	2.734	1.755	2.466	4.052	4.553	8.443	0.4743	2.822	2.021		0.00116	1	1	1	0.7807	1	0.5587	0.9333
12	19.38	3.603	4.582	3.87	2.285	1.783	2.106	5.862	3.515	4.316	6.337		0.02312	0.01095	0.00058	0.722	0.009614	0.8954	< 0.0001
13	14.09	1.691	0.7115	1.423	3.008	3.51	7.399	0.5692	1.779	0.9775	1.043	5.293		1	1	0.9951	1	0.9631	0.4673
14	13.8	1.975	0.9961	1.708	3.293	3.794	7.684	0.2846	2.063	1.262	0.7589	5.578	0.2846		1	0.9795	1	0.9036	0.6242
15	12.83	2.951	1.972	2.683	4.269	4.77	8.66	0.6911	3.039	2.238	0.2168	6.554	1.26	0.9757		0.6734	1	0.44	0.9698
16	16.15	0.3725	1.352	0.6403	0.9452	1.447	5.336	2.632	0.2846	1.086	3.107	3.23	2.063	2.348	3.324		0.9749	1	0.00655
17	13.76	2.023	1.043	1.755	3.341	3.842	7.731	0.2372	2.111	1.31	0.7115	5.625	0.332	0.04743	0.9283	2.395		0.8896	0.6499
18	16.58	0.7994	1.779	1.067	0.5184	1.02	4.909	3.059	0.7115	1.513	3.534	2.803	2.49	2.775	3.75	0.4269	2.822		0.00184
19	10.39	5.39	4.411	5.123	6.708	7.21	11.1	3.13	5.478	4.677	2.656	8.993	3.7	3.415	2.439	5.763	3.368	6.19	

Table 4.12. A. Results from **Tukey's test for large pits** for extinct UK species including extant species. **B.** Results from **Tukey's test for small pits** for extinct UK species including extant species. Numbers linked with the following species **1:** *A. melanoleuca*; **2:** *H. malayanus*; **3:** *M. ursinus*; **4:** *U. americanus*; **5:** *U. maritimus*; **6:** *U. thibetanus*; **7:** *U. arctos*, Greece; **8:** *U. arctos*, Central Europe; **9:** *U. arctos*, USA; **10:** *U. arctos*, Russia; **11:** *U. arctos*, North Europe; **12:** Westbury-sub-Mendip (MIS 13); **13:** Kents Cavern (breccias); **14:** Grays Thurrock (MIS 9); **15:** Tornewton Cave (MIS 5e); **16:** Banwell Bone Cave (MIS 5a); **17:** Kents Cavern (MIS 3); **18:** Sandford Hill (MIS 3); **19:** Cow Cave (Holocene?). Values below the diagonal are the results of Tukey's test and those above are the p-values.

A. Turkey's test **gouges** for extinct species UK including all extant species.

	3	7	8	12	13	14	15	16	17	18	19
3		0.9983	1	0.9675	0.9923	0.924	0.9983	0.9895	1	0.983	1
7	1.25		0.998	1	1	1	1	1	0.9994	0.6074	0.9999
8	0	1.25		0.9675	0.9923	0.924	0.9983	0.9895	1	0.983	1
12	1.827	0.5768	1.827		1	1	1	1	0.9814	0.3392	0.9935
13	1.5	0.2499	1.5	0.3269		1	1	1	0.9965	0.4861	0.9992
14	2.083	0.8332	2.083	0.2564	0.5832		1	1	0.9508	0.243	0.9781
15	1.25	0	1.25	0.5768	0.2499	0.8332		1	0.9994	0.6074	0.9999
16	1.562	0.3124	1.562	0.2644	0.06249	0.5207	0.3124		0.9949	0.4565	0.9987
17	0.1389	1.111	0.1389	1.688	1.361	1.944	1.111	1.423		0.97	1
18	1.666	2.916	1.666	3.493	3.166	3.749	2.916	3.228	1.805		0.9365
19	0.3571	0.8927	0.3571	1.469	1.143	1.726	0.8927	1.205	0.2182	2.023	

B. Turkey's test **punctures** for extinct species UK including all extant species.

	2	3	4	8	9	10	11	13	14	15	17	18	19
2		0.8601	1	0.00748	1	0.544	1	0.998	1	1	1	0.9493	0.5798
3	2.504		0.9547	0.585	0.995	1	0.796	0.2121	0.5536	0.417	0.796	0.0652	1
4	0.3902	2.114		0.01866	1	0.7354	1	0.9833	0.9999	0.9991	1	0.849	0.7666
8	5.632	3.128	5.242		0.05256	0.885	0.00491	< 0.001	0.001344	0.000689	0.00491	0.00014	0.8633
9	0.8733	1.631	0.4831	4.759		0.91	0.9999	0.907	0.9965	0.985	0.9999	0.6393	0.9262
10	3.208	0.7045	2.818	2.424	2.335		0.4575	0.0617	0.2387	0.155	0.4575	0.0144	1
11	0.1734	2.677	0.5636	5.805	1.047	3.382		0.9994	1	1	1	0.9732	0.4923
13	1.47	3.974	1.86	7.102	2.343	4.678	1.296		1	1	0.9994	1	0.0708
14	0.6858	3.19	1.076	6.318	1.559	3.894	0.5124	0.784		1	1	0.9981	0.2641
15	0.9625	3.466	1.353	6.595	1.836	4.171	0.7891	0.5073	0.2767		1	0.9998	0.1739
17	0.1734	2.677	0.5636	5.805	1.047	3.382	0	1.296	0.5124	0.7891		0.9732	0.4923
18	2.146	4.65	2.536	7.778	3.019	5.355	1.973	0.6764	1.46	1.184	1.973		0.01696
19	3.138	0.6341	2.748	2.494	2.265	0.07045	3.311	4.608	3.824	4.1	3.311	5.284	

Table 4.13. A. Results from **Tukey's test for gouges** for extinct UK species including extant species. **B.** Results from **Tukey's test for puncture pits** for extinct UK species including extant species. Numbers linked with the following species **2:** *H. malayanus*; **3:** *M. ursinus*; **4:** *U. americanus*; **7:** *U. arctos*, Greece; **8:** *U. arctos*, Central Europe; **9:** *U. arctos*, USA; **10:** *U. arctos*, Russia; **11:** *U. arctos*, North Europe; **12:** Westbury-sub-Mendip (MIS 13); **13:** Kents Cavern (breccias); **14:** Grays Thurrock (MIS 9); **15:** Tornewton Cave (MIS 5e); **16:** Banwell Bone Cave (MIS 5a); **17:** Kents Cavern (MIS 3); **18:** Sandford Hill (MIS 3); **19:** Cow Cave (Holocene?). Values below the diagonal are the results of Tukey's test and those above are the p-values.

4.4. Results on extinct Ursidae from the European mainland: the example of Loutra Arideas Cave (Late Pleistocene) from Greece

The following sections present the results regarding the microwear observations on extinct bear specimens from the Late Pleistocene site of Loutra Arideas Cave (LAC) in Greece, after comparison with the modern bear dataset. As before, only the grinding (talonid) area was analysed for the LAC specimens, since this provides the clearest information regarding separation into dietary ecospace.

4.4.1. Dental Microwear Analysis (DMA) results from Loutra Arideas Cave (LAC)

As outlined in 1.3., the Late Pleistocene in the area of Loutra Arideas Cave (LAC) was characterized by a climate drier than that of today, while the palaeoenvironmental reconstruction for the species recorded indicate the presence of both coniferous and deciduous forest, as well as large areas of grassland in the vicinity (Chatzopoulou, 2014). The faunal assemblage is dominated by the cave bear species *Ursus ingressus* (Rabeder *et al*., 2004), which occupied the cave from the Middle Weichselian (42 500 BP) until the Last Glacial Maximum (Rabeder *et al*., 2006; Zacharias *et al*., 2008; Frischauf *et al*., in press) (see 1.3. for further details on the site). 25 specimens were sourced from LAC and from those, 10 specimens were included for the analysis, following rejection of specimens with obvious *post mortem* features and/or poor preservation.

The *U. ingressus* specimens from LAC were initially compared with the extant bear database through bivariate graphs (Fig. 4.17 A and B).

In Figure 4.17 A, it is clear that *U. ingressus* from LAC is distinguished from both the extant *U. arctos* group and from the rest of the extant species. *U. ingressus* shows the lowest mean number of scratches (mean 13.3) compared with the species in the extant database, and is characterised by an intermediate mean number of pits (mean 29.5), approaching the mean values of *T. ornatus*, *U. americanus* and *U. arctos* from the USA (Fig. 4.17 A).

When comparing the total number of large pits against small pits with the extant bear database, *U. ingressus* from LAC displays intermediate numbers of small pits (minimum

14, median 18, maximum 23) and small to intermediate values for large (minimum 3, median 4.5, maximum 6) (see also table 4.14) (Fig. 4.17 B). Furthermore, *U. ingressus* specimens from LAC overlap with some *H. malayanus* individuals as well as with *U. arctos* from USA and Russia (Fig. 4.17 B).

Table 4.14 shows a statistical summary of eight microwear features (variables) for *U. ingressus* from LAC.

Table. 4.14. Loutra Arideas Cave (LAC) (Late Pleistocene), Greece (n: 10) statistical summary of eight microwear features. Mean, standard deviation (SD), 95% Confidence interval (CL), 1st and 3rd quartile, minimum, maximum and median values.

Microwear features (variables)	Mean; SD	95% CL	1st Quartile	min	median	max	3rd quartile
Pits	29.5; 2.27	1.41	28	27	29	34	30.75
Scratches	13.3; 2	1.24	12.25	10	13	16	14.75
Fine Scratches	9.8; 1.13	0.70	9	8	10	12	10
Coarse Scratches	3.5; 1.43	0.89	2.25	2	3	6	4.75
Large Pits	4.6; 0.97	0.61	4	3	4.5	6	5
Small Pits	17.8; 2.44	1.51	17	14	18	23	18.75
Gouges	1.2; 1.032	0.64	0.25	0	1	3	2
Punctures	5.9; 1.66	1.03	5	3	6	8	

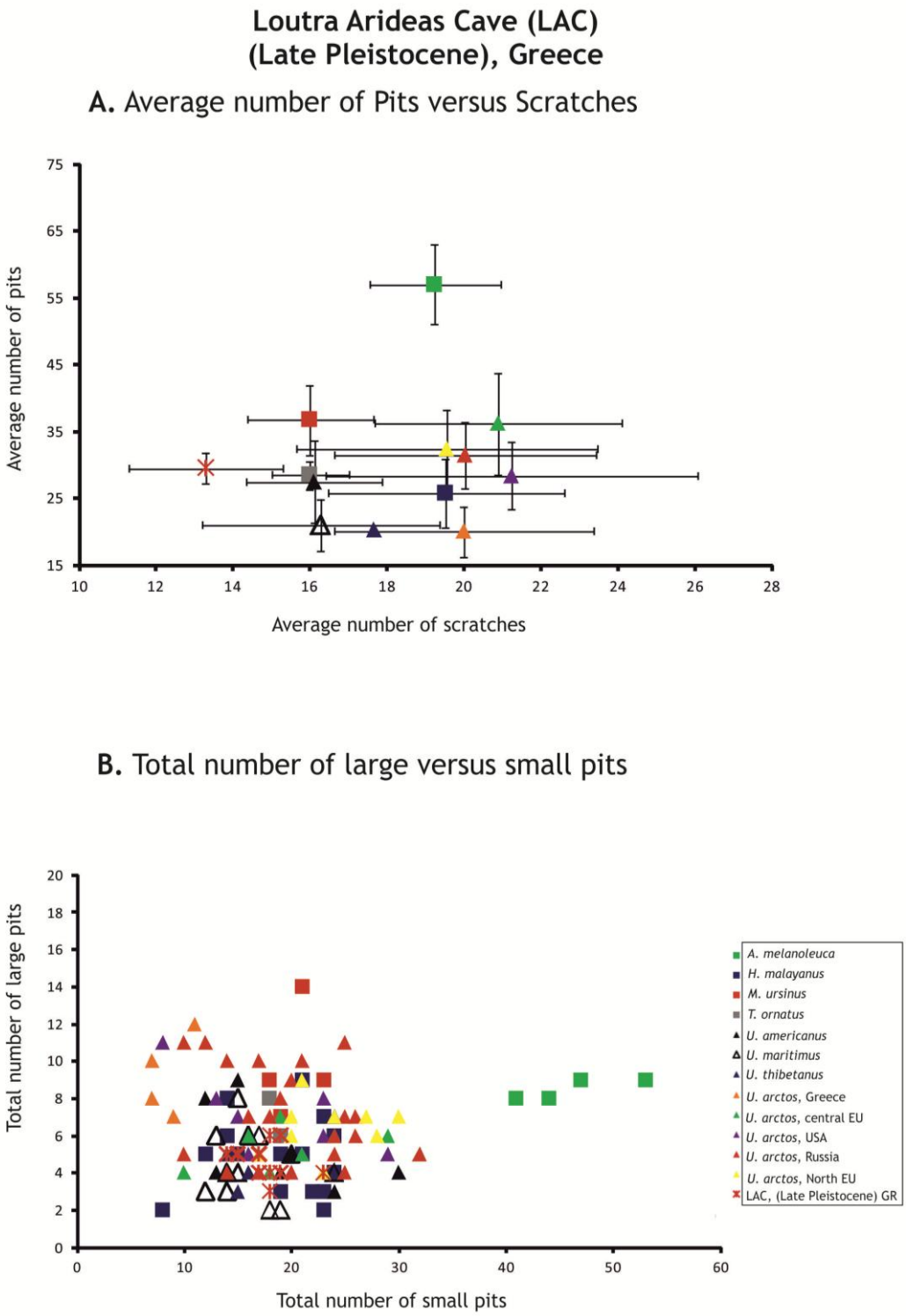

Figure 4.17. Bivariate diagrams for bears from Loutra Arideas Cave (LAC) (Late Pleistocene), Greece, in comparison with the extant bear database. **A.** Plot of average number of pits versus scratches. Error bars represent the standard deviation of pits and scratches. **B.** Plot of raw data of the total number of large versus small pits.

4.4.2. PCA results from Loutra Arideas Cave (LAC)

PCA was also completed for the Loutra Arideas bear dataset. Figures 4.18 A and B show the results from observations on the grinding surfaces of m1s of the extinct *U. ingressus* from LAC, in comparison with the modern bear database.

The first axis (PC1) explains 41.51% of the total variance, the second (PC2) accounts for 19.86% and the third axis (PC3) for 12.06%. Abbreviations of the nine independent variables are given in the caption of Figure 4.18.

In Figure 4.18 A (PC 1 and PC 2), *U. ingressus* specimens occupy the top right-hand quadrant and overlap with the dietary ecospaces of the omnivorous species *M. ursinus*, *H. malayanus* and *U. arctos* from northern Europe and Russia. Moreover, the position of *U. ingressus* from LAC denotes an intermediate to high percentage of puncture pits (NpP) and large pits (NLp) (Fig. 4.18 A). Interestingly, the position of *U. ingressus* from LAC is different to that of modern *U. arctos* from Greece. Separation from the hypercarnivore *U. maritimus* and from the herbivore *A. melanoleuca* is also readily apparent (Fig. 4.18 A).

In Figure 4.18 B (PC1 and PC3), *U. ingressus* from LAC occupy an area in the low right-hand quadrant, clearly separated from most of the extant species although some individuals are close to some *H. malayanus* individuals and to some *U. arctos* individuals from central Europe and Russia.

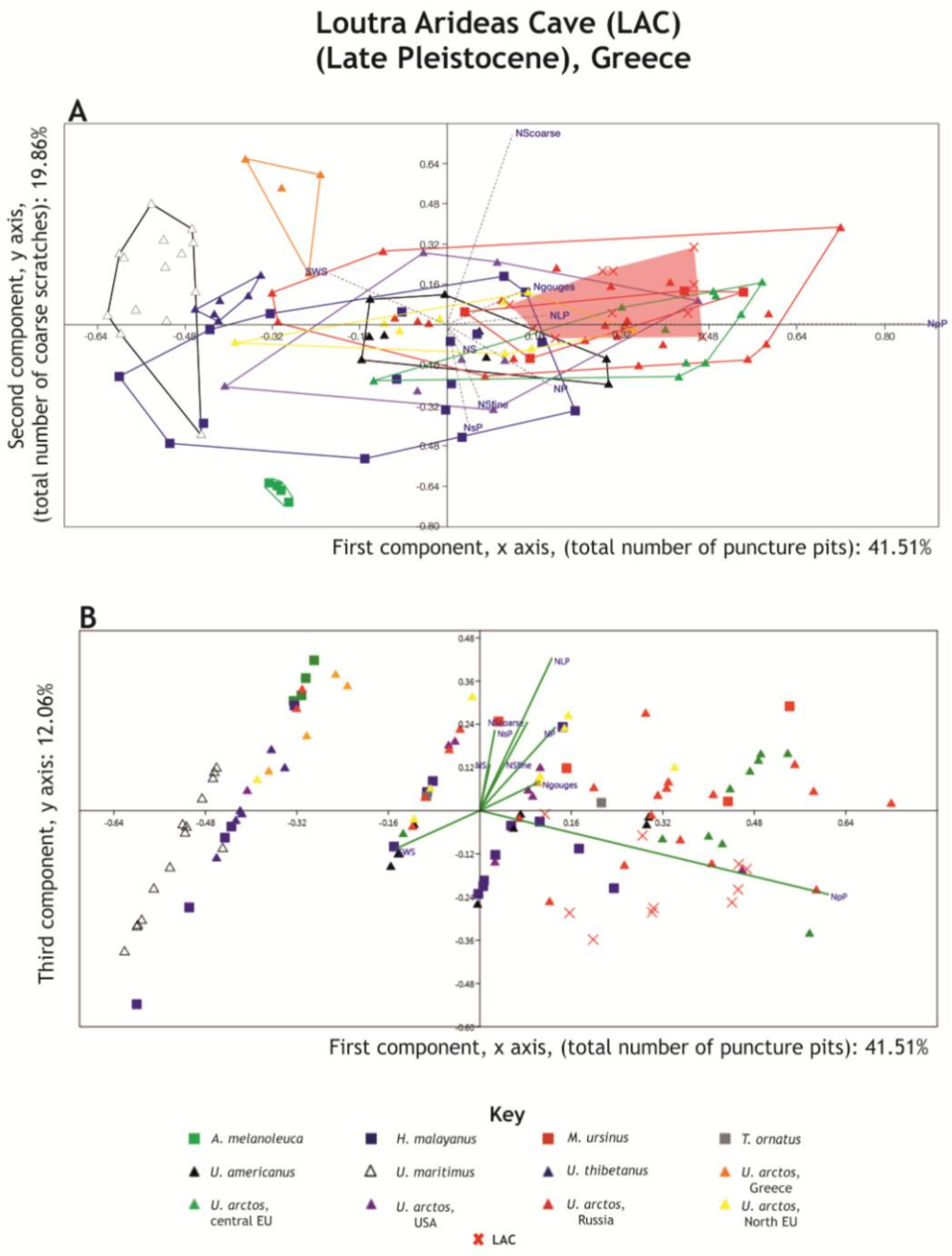

Figure 4.18. PCA plots for Loutra Arideas Cave (LAC) (Late Pleistocene), Greece, in comparison with extant bear species. **A**. Graph component 1 versus 2. The shaded polygon indicates the position of the specimens from Loutra Arideas Cave. **B.** Graph component 1 versus 3. Details of symbols see key. Symbols of Variable as follows: NS: number of scratches; NP: number of pits; NfineS: number of fine scratches; NcoarseS: number of coarse scratches; NLP: number of large pits; NsP: number of small pits; Ngouge: number of gouges; Npp: number of puncture pits; SWS: scratches width score.

4.5. Discussion

Comparison of the microwear results of fossil British and Greek bear specimens from different species and from different time periods with the modern reference database indicates pronounced dietary variability between different extinct bear species and between different age groups of extinct *U. arctos* from Britain. The differences found in the dietary ecospace of *U. arctos* extinct specimens from Britain, from MIS 3, are particularly interesting. These inter- and *intra*-specific palaeodietary trends and differences highlight important adaptations to changing environments, food availability, climates and carnivore guild composition.

The oldest bear specimens (early Middle Pleistocene) that were included in the dental microwear analysis of this thesis are the *U. deningeri* specimens found in Westbury (Calcareous Member) and the Kents Cavern bears (breccias). Although these are from the same species and some overlap between their ecospaces would therefore be expected, the results revealed that only two individuals from Kents Cavern were found to share some similarities with the Westbury bears while the rest have commonalities with the brown bear individuals from Kents Cavern from the younger cave earth.

The position occupied by *U. deningeri* from Westbury in dietary ecospace suggests that these individuals displayed many similarities in diet with modern *U. thibetanus*, *U. maritimus* and *U. arctos* from Greece. The general pattern for the microwear features for *U. deningeri* from Westbury reveals a low to intermediate number of scratches and many coarse scratches, together with some gouge features (Fig. 4.19.A). Both *U. arctos* from Greece and *U. thibetanus* include fleshy fruits, hard fruits, green vegetation and vertebrates in their diets (e.g. Vlachos *et al*., 2000; Huygens *et al*., 2003) with the former depending more on “soft mast” and the latter on “hard mast” (e.g. Mattson, 1998; Bojarska and Selva, 2012). However, *U. deningeri* from Westbury also has similarities with the hypercarnivorous polar bear (Ewer, 1973; Derocher *et al*., 2002), which implies a component of meat in the diet. This is highlighted by the few scratches present, moderate number of pits and broad scratches and the large number of broad scratches that may reflect contact with bone surfaces (Goillot *et al*., 2009).

Thus, the Westbury *U. deningeri*'s ecological niche appears to be predominantly herbivorous, reflecting seasonal availability of plant foods. Those individuals close to *U. thibetanus* ecospace consumed "hard mast" such as fruits with seeds and those close to the "soft mast" eater (*U. arctos* from Greece) feeding on fleshy fruits and green vegetation. The proximity of some individuals of *U. deningeri* to *U. maritimus* and to *U. thibetanus* indicates that meat may also have been consumed. During the period of the early Middle Pleistocene represented by the Calcareous Member, the climate was temperate (albeit with an intervening cool oscillation [Schreve *et al*., 1999; Procter *et al*., 2005]). Given the diverse carnivore guild present at Westbury and the potential high levels of competition from other carnivores, including *H. latidens, P. leo, P. gombaszoegensis, C. mosbachensis, C. (X.) lycaonoides, C. crocuta and P. brevirostris* (Turner, 1999), *U. deningeri* may have adopted a mixed dietary niche with a predominant focus on vegetation, including seasonally-available "hard mast". These findings corroborate the conclusions of Bocherens *et al*. (1994a) and García García *et al*. (2009) based on stable isotope analyses, which suggest that *U. deningeri* species displayed many similarities with the largely herbivorous *U. spelaeus*.

In contrast to *U. deningeri* from Westbury, the position that *U. deningeri* from Kents Cavern (breccias) occupies in dietary ecospace suggests that it was an animal with many similarities to individuals of *U. arctos* from Russia, the USA and northern Europe. In addition, two individuals are close to *U. thibetanus* ecospace. The general pattern for the microwear features for *U. deningeri* from Kents Cavern reveals an intermediate number of pits, and compared with *U. arctos* groups, they have a higher percentage of coarse scratches and a smaller percentage of small pits and fine scratches (Fig. 4.19.B). Although *U. arctos* from Russia, USA and northern Europe consume a wide variety of food items in their diet, studies suggest that the most consumed items are vertebrates (e.g. fish and ungulates) for Russian and North American brown bears and "soft mast" for northern European brown bears (e.g. Mattson, 1998; Vulla *et al*., 2009; Bojarska and Selva, 2012).

Hence, *U. deningeri* from Kents Cavern had most probably a broader dietary niche than *U. deningeri* from Westbury, with a diet comprising a significant proportion of soft items (e.g. soft fleshy fruits and vegetables or meat) that were at least seasonally

available. Additionally, the Kents Cavern *U. deningeri* may have either consumed more coarse vegetable matter and fruit than modern *U. arctos* from Russia, USA and northern Europe or, when consuming flesh, it possibly made more contact with the bone surface. This would explain the overall high number of scratches found in *U. deningeri* from Kents Cavern, which is paralleled by species with hard components in their diets (Bastl, 2012) and where, for example, the tugging of tough, woody food causes large irregular or oval pits (Merceron *et al*., 2004a).

In comparison to Westbury, the Kents Cavern predator guild was apparently less diverse (absence of *H. latidens, P. gombaszoegensis, C. (X.) lycaonoides and P. brevirostris*). The sites may not be precisely coeval and equally, this difference may be a taphonomic artifact. Nevertheless, it is intriguing to note that a reduction in competition from obligate carnivores may have allowed the Kents Cavern *U. deningeri* to exploit additional protein sources such as flesh. Indeed, Stiner *et al*. (1998) have suggested, on the basis of stable isotopic analysis, a more omnivorous diet for *U. deningeri* than that inferred by Bocherens *et al*. (1994a) and García García *et al*. (2009). Thus, the level of meat/bone consumption in the *U. deningeri* niche needs further careful examination in order to elucidate changes in diet in response to local environmental factors and changing levels of carnivore competition.

The ecospaces from the remaining Pleistocene *U. arctos* groups from Britain display many differences not only in comparison with *U. deningeri* but also amongst each other. For example, both *U. arctos* from Grays (MIS 9) and from Tornewton Cave (MIS 5e) share many similarities and there is overlap between their inferred ecospaces. These ecospaces are in turn clearly distinguished from the Banwell Bone Cave (MIS 5a) and Kents Cavern cave earth deposits (MIS 3), and from the Sandford Hill (MIS 3) and Cow Cave (MIS 1) brown bear individuals. Furthermore, between MIS 3 brown bear ecospaces, several interesting patterns have emerged.

Both the Late Middle Pleistocene MIS 9 and Ipswichian (MIS 5) interglacials were characterised by the development of deciduous woodland, elevated summer temperatures when compared to today and mild winters (Schreve, 1997; Candy *et al*., 2010). The dietary ecospaces of the two brown bear groups from Grays Thurrock and

from the “Bear Stratum” at Tornewton Cave are almost identical, reflecting the similarity of climatic conditions and habitats that these populations lived in. The positions occupied by both *U. arctos* groups in dietary ecospace suggest that these individuals displayed many similarities in diet with modern *U. arctos* from northern Europe, *U. americanus* and *H. malayanus*. The general pattern for the microwear features for these extinct brown bears reveals that they possessed the smallest percentage of puncture pits compared with any other modern *U. arctos* group but display an intermediate percentage for most other variables (Fig. 4.19.C and D).

The predominant food item for both *U. arctos* from northern Europe and *U. americanus* is “soft mast” (Mattson, 1998; Bojarska and Selva, 2012), and for *H. malayanus*, it is invertebrates (insects), followed by “soft mast” (Fredriksson *et al*., 2006). Hence, it can be suggested that due to the warm climatic conditions and an inferred wider availability of plants and insects during both MIS 9 and MIS 5e, brown bears populations most probably consumed fibrous food as well as soft fruits and invertebrates, together with a modest vertebrate component.

It is also worth mentioning that during both interglacials, high numbers of herbivore prey were present (e.g. *E. ferus* in MIS 9*, S. hemitoechus, C. elaphus, D. dama, C. capreolus* and large bovids in both sites). At the same time, the carnivore guild had declined dramatically by this point, with only *C. lupus*, *V. vulpes*, *C. crocuta* and rare *P. leo* noted (e.g. Currant, 1996; Schreve, 1997). This may have presented *U. arctos* with additional opportunities to include meat in its diet.

In sharp contrast, during the early part of the last cold stage (MIS 5a), the dietary pattern of the *U. arctos* population was completely different to that of the brown bears from the MIS 9 and MIS 5e interglacial stages, as seen in the clear separation of the ecospace of *U. arctos* individuals from Banwell Bone Cave. This is not surprising, given that climatic conditions were very different during MIS 5a and an open tundra environment persisted with low diversity prey (mainly reindeer and bison) (Currant and Jacobi, 2011) that may have been only seasonally available.

During this time period, brown bears grew to very large body size and became the dominant predator in Britain; *C. crocuta* is absent and only *C. lupus, A. lagopus* and

Gulo gulo were present (Currant and Jacobi, 2011). The microwear results as seen in the bivariate plots from the Banwell Bone Cave bears reveal many similarities with high-latitude species such as *U. maritimus*, *U. americanus* and *U. arctos* from Russia. In addition, the PCA revealed that the dietary ecospace of these bears had commonalities with those of *U. maritimus* and *U. thibetanus* at the present day. Some of the main microwear features noted on these large extinct brown bears are the highest score for scratches width after *U. maritimus,* an absence of puncture pits and a moderate percentage of coarse scratches (Fig. 4.19.E). The absence of puncture pits indicates that fruits with seeds did not play a part in the diet of *U. arctos* from Banwell Bone Cave (e.g. Semprebon *et al*., 2004). As well as hunting, flesh may also have been scavenged from (frozen) carcasses, as seen in modern polar bear utilisation of marine mammals (Bentzen *et al*., 2007).

Hence, during these harsh climatic conditions, the large *U. arctos* from Banwell Bone Cave most likely fed on any available hard mast items, although meat and fat played an important role into their diet and ability to reach their enormous size. The heavy tooth wear and the presence of coarse microwear patterns links clearly to the tundra-like environment inhabited and the bears may have been active in scavenging carcasses off the landscape, as well as hunting. It has been reported that remains of the other large carnivore from this time period, the wolf, also displays heavily worn teeth, suggesting an increase in bone consumption during feeding, possibly the result of dietary stress (Flower and Schreve, 2014). In addition, in a study of tooth breakage of numerous large carnivores from Rancho La Brea (USA), Van Valkenburgh and Hertel (1993) proposed that during tough times, food shortages led these animals to utilise more fully any carcasses in the vicinity, including enhanced bone consumption. In contrast, Donohue *et al*. (2013) found no support for durophagous carcass utilisation on a single *Arctodus simus* individual from Rancho La Brea using dental microwear texture analysis. Equally, DeSantis *et al*. (2012), also using texture analysis, found a lack of evidence for high levels of carcass exploitation at Rancho La Brea and suggested instead that the broken teeth seen in extinct carnivores were potentially inflicted during the hunting of diverse large prey.

The dietary ecospaces of the remaining bears, from MIS 3 and the Holocene (?) are differentiated clearly from those of both the Grays Thurrock and Tornewton Cave bears, which represent interglacials, and from that of the Banwell Bone Cave bear of the early last cold stage (MIS 5a). However, the dietary ecospace of Sandford brown bears (MIS 3) is different to that of the Kents Cavern (cave earth) bears (also MIS 3), which is more similar to the Cow Cave bears, tentatively attributed to the Holocene.

In summary, the dietary ecospace of the Kents Cavern (MIS 3) bears overlaps with the ecospaces of, and shows many similarities on the microwear patterns with *M. ursinus*, *H. malayanus* and *U. arctos* from northern Europe and Russia. In addition, the position of *U. arctos* from Cow Cave in dietary ecospace suggests that it was an animal that displayed many similarities in diet with *U. arctos* from central Europe and Russia, as well as with *M. ursinus*. The common characteristics of these two groups are the high percentage of large pits and gouges (Fig. 4.19.F). While the bears from Cow Cave show the highest percentage of puncture pits when compared to all the extant species and intermediate percentage of coarse scratches, the Kents Cavern (MIS 3) bears display a high percentage of coarse scratches and intermediate numbers of puncture pits.

In contrast, the dietary ecospace of the Sandford Hill bears is very close to that of *U. arctos* from Greece, with the exception of one individual that lies within the ecospace of *U. arctos* from northern Europe. In summary, the microwear features of the Sandford Hill bears show a low percentage of puncture pits and large pits and an intermediate percentage of coarse scratches (Fig. 4.19.G). The differences between the two MIS 3 brown bear groups most probably reflect stadial versus interstadial conditions, or interstadials of different magnitudes, where different food types would have been more readily available at one time than another.

Accordingly, both the Kents Cavern (MIS 3) and Cow Cave (Holocene?) consumed predominantly fruits and invertebrates, however the former fed mainly on “soft mast” items while the later consumed “hard mast” (reflected by the high percentage of puncture pits) and the latter “soft mast”, which would be consistent with the warmer climate and wooded conditions of the Holocene in southern England. It has been also suggested that “hard mast” would be more abundant in broad leaved forests while

"soft mast" would be more abundant in coniferous forests (Mattson, 1998). Potentially, vertebrates may also have been included in the diets of *U. arctos* from both Kents Cavern and Cow Cave whenever possible. However, the prevalence of pits over scratches seen in both Kents Cavern and Cow Cave bears is typical of more herbivorous bears (Münzel *et al*., 2014). Moreover, gouges and puncture pits reflect the consumption of small hard objects, in particular seeds from berries (Solounias and Semprebon, 2002; Merceron *et al*., 2005b)

The position and microwear features of the Sandford Hill bears indicate that these bears most probably fed exclusively on "soft mast" items, including fleshy fruits and the soft parts of green vegetation, perhaps reflecting a longer or more intense interstadial period within MIS 3.

The Pleistocene *U. ingressus* from LAC in Greece differs not surprisingly, due to its different geographical position, from nearly all *U. deningeri* and extinct *U. arctos* populations from Britain. However, it shares some similarities with the *U. arctos* from Kents Cavern (MIS 3) and most particularly with the Cow Cave (Holocene?) specimens. The key microwear features that *U. ingressus* from LAC display are a high percentage of large pits, gouges and puncture pits and an intermediate percentage of coarse scratches (Fig. 4.19 H). In contrast to the Cow Cave specimens, the LAC *U. ingressus* have a lower number of large and small pits and a smaller number of mean pits and scratches.

It is striking that the dietary ecospace of *U. ingressus* from LAC is removed from that of modern *U. arctos* from Greece. However, this could explained either by the small number of specimens examined from the modern brown bear (only 4 individuals), or because the dietary preferences of *U. ingressus* differed from those of modern brown bears from Greece. The position occupied by *U. ingressus* from LAC in dietary ecospace suggests that it was an animal that had some similarities in diet with *M. ursinus*, *U. arctos* from central and northern Europe and from Russia. This suggests that *U. ingressus* from LAC most probably consumed both "soft" and "hard mast" items, insects and potentially small portions of fish and/or flesh. These items are in accordance with the results from the isotopic analysis of *U. ingressus* bone and teeth

from LAC where it was suggested that these bears ate vegetable matter with a variable component of animal protein (terrestrial and/or aquatic) (Dotsika *et al*., 2011). In addition, the authors proposed that fish may have been an important component in the diet, since the cave is located just above the river that occupied the valley for more than 50Ka (Kabouroglou and Chatzitheodorou, 1999).

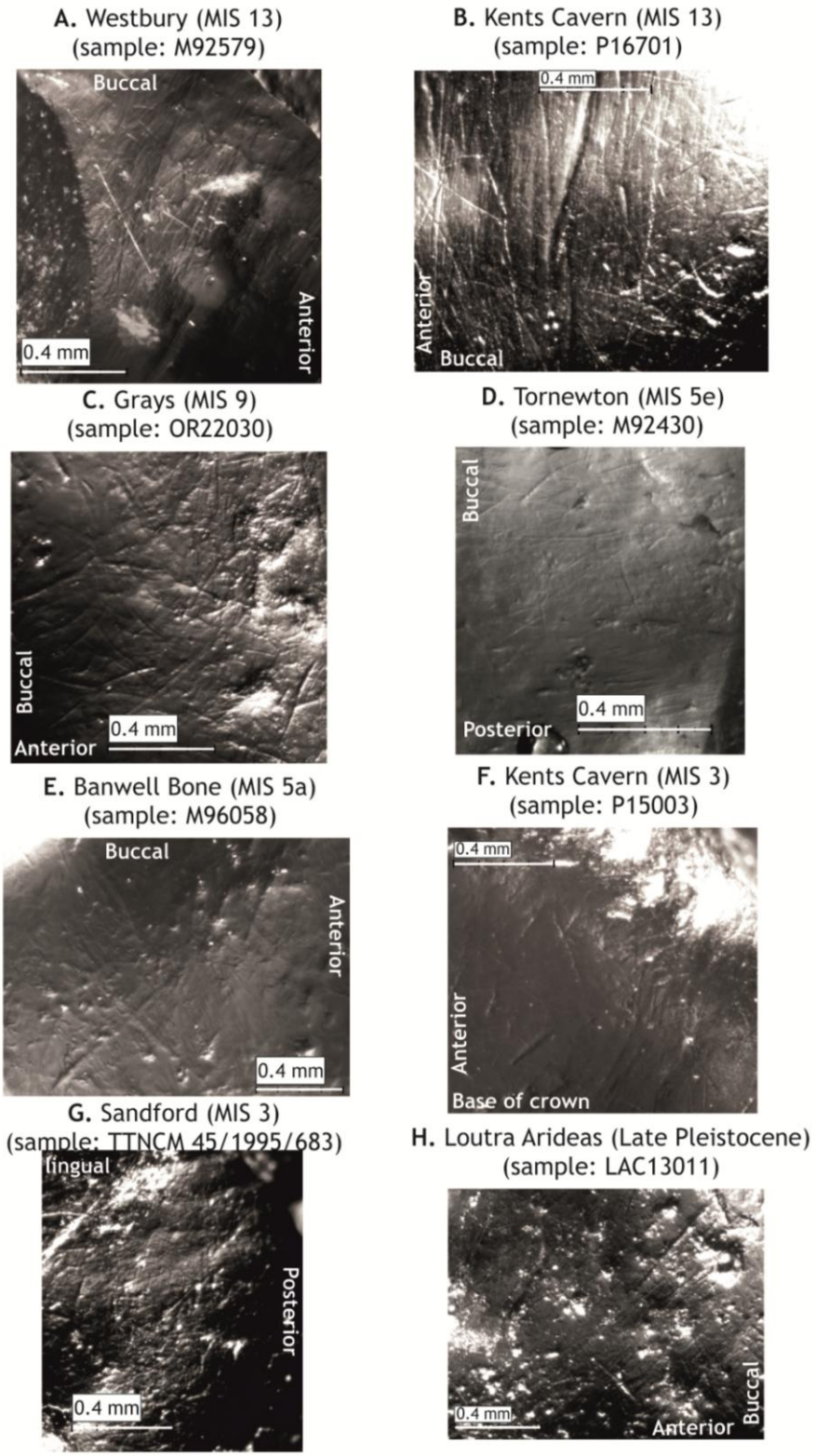

Figure 4.19. Photomicrographs of extinct bear species tooth enamel on grinding (talonid) area at 35 times magnification. **A.** *U. deningeri* from Westbury-sub-Mendip (MIS 13). **B.** *U. deningeri* from Kents Cavern (breccias) (early Middle Pleistocene). **C.** *U. arctos* from Grays Thurrock (MIS 9). **D.** *U. arctos* from Tornewton Cave (MIS 5e). **E.** *U. arctos* from Banwell Bone Cave (MIS 5a). **F.** *U. arctos* from Kents Cavern (cave earth) (MIS 3). **G.** *U. arctos* from Sandford Hill (MIS 3). **H.** *U. ingressus* from Loutra Arideas Cave (LAC) (Late Pleistocene), Greece.

In conclusion, based on the completely new modern database of extant bear species outlined in Chapter 3, it has been possible to expand this dental microwear methodology to the consideration of palaeodiet in extinct bear species. A large number of individuals from eight palaeontological sites in Britain and Greece were examined and the species' ecospaces have accordingly been reconstructed, demonstrating differences between and within species, according to geographical region and time. It is clear that in order to interpret the ecospaces of these extinct taxa correctly, it is important to establish a new protocol for these types of study. This comprises a number of key prerequisites, including the establishment of a comprehensive reference database of modern species, a relatively large number of specimens (ideally over 8 per species), careful selection and examination of the analysed enamel surface, the use of the talonid part of the m1 in preference, and the documentation and interpretation of a range of different microwear features, not just scratches or pits.

Chapter 5. Geochemical Analysis

5.1. Introduction

In addition to dental microwear analysis, further information on diet and physiology can be determined from both tooth and bone chemistry. Research has shown that molecules and minerals in bones and teeth inherit chemical signatures that reflect changes in diet and physiology occurring during the lifetime of the animal. Hence, they can provide a direct chemical means for investigating palaeodiet and palaeoecology (e.g. Richards *et al*., 2003; Sponheimer *et al*., 2003; Lee-Thorp and Sponheimer, 2006; Humphrey *et al*., 2008a; b; Ungar, 2010; Bocherens, 2015). Studies have focused either on stable isotopic or trace element analysis of bones or teeth (enamel or dentine tissue) in mammals. For example, oxygen isotope analysis has been applied to archaeological and fossil bones and teeth to enable palaeoclimatic, palaeotemperature and seasonality reconstructions (e.g. Aylifee *et al*., 1994; Bryant *et al*., 1994; Fricke and O'Neil 1996; Reinhard *et al*., 1996; Stuart-Williams and Schwarcz, 1997; Fricke *et al*., 1998a; b; Genoni *et al*., 1998; Kohn *et al*., 1998; Balasse *et al*., 2003; Grimes *et al*., 2004a; Hoppe *et al*., 2004b; Hoppe, 2006; Sharp and Cerling 1998; Bocherens *et al*., 2011a). In addition, analyses of carbon and nitrogen have been commonly used to establish palaeodiet and palaeoecology in extinct taxa (e.g. Koch *et al*., 1989; Bocherens *et al*., 1991; 1994a; 1996; Kohn *et al*., 1996; Bocherens, 2003; Bocherens and Drucker, 2003; Grimes *et al*., 2004b; Kingston and Harrison, 2007; Prevosti and Martin, 2013; Bocherens, 2015). Furthermore, trace elements (e.g. Sr/Ca and Ba/Ca ratios) in bones and teeth have also been used as biochemical indicators of trophic level and to reconstruct dietary preferences in modern and fossil mammals (e.g. Elias *et al*., 1982; Sillen, 1992; Radosevich, 1993; Gilbert *et al*., 1994; Burton *et al*., 1999; Kohn *et al*., 1999; Lee *et al*., 1999; Schutkowski *et al*., 1999; Blum *et al*., 2000; Balter *et al*., 2002; Balter, 2004; Dolphin *et al*., 2005; Sponheimer *et al*., 2005; Lee-Thorp and Sponheimer, 2006; Balter *et al*., 2008; Humphrey *et al*., 2008a; b; Jeffrey, 2010; Peek and Clementz, 2012a; b; Kohn *et al*., 2013).

However, stable isotopic and trace element analyses of fossil bones and teeth can only be carried out if several different requirements are met. For example, an understanding of the pathways of essential elements and isotopes from food to tissue is essential, irrespective of whether collagen (the main organic component of bone and dentine) or biological apatites (crystalline calcium phosphate structures forming during the mineralisation phase of bone and enamel) are analysed (Lee-Thorp and Sponheimer, 2006). It is also critical, in order to reveal and interpret as robustly as possible the "true" chemical signal that formed during the lifetime of the animal, to avoid all altered or contaminated parts (e.g. modifications due to burial conditions) (Hinz and Kohn, 2010; Bocherens, 2015). It is equally important to understand that different physiological or behavioural processes (e.g. ageing, growth rate, gestation, suckling and weaning, starvation or water stress, hibernation and/or migration [if applicable]) can lead to significant changes in diet and physiology that may ultimately alter the chemical signal (e.g. Humphrey *et al*., 2008b; Smith and Tafforeau, 2008; Peek and Clementz, 2012b; Bocherens, 2015). Last but not least, sample selection and, in the case of dental analysis, the tooth selection may also influence the results (e.g. Peek and Clementz, 2012b).

In this thesis, trace element analysis (with a focus on Sr/Ca and Ba/Ca ratios) has been applied for the first time in order to explore dietary and physiological changes within the fossil mammalian assemblage from Tornewton Cave in Devon (see 5.4. for site background and materials). The study was carried out using high resolution elemental *intra*-tooth profiles from tooth enamel via laser-ablation inductively-coupled plasma mass-spectrometry (LA-ICPMS) (see 5.4.2. for the methodology).

5.2. Geochemical Analysis Literature Review

Teeth are generally preferred to bones for chemical analysis for two important reasons. First, because they are usually well preserved in palaeontological sites and, as a result, are often more abundant than bones. Second, because the structure and chemical composition of teeth (and in particular, that of enamel) is more resistant to diagenetic alteration (see 5.2.4.) in the *post mortem* environment. Enamel is the hardest and least porous substance in the body and therefore maintains better the original chemical signal (e.g. Lee-Thorp and Van der Merwe, 1991; Ayliffe *et al*., 1994; Wang and Cerling,

1994). Porosity levels are 1% in enamel, in contrast to 40% in dentine and bone (Brudevold and Soremark, 1967; Rowles, 1967; Trautz, 1967). Additionally, the chemical and structural composition of enamel is fixed before tooth eruption, since after amelogenesis has taken place, no further exchange can occur between hydroxyapatite and the mammalian body. This therefore allows a "historical" record of, for example, trace elements absorbed during the early developmental stages to be discerned (e.g. Lee-Thorp and Van der Merwe, 1991; Wang and Cerling, 1994; Reitznerová *et al*., 2000 and references therein) (see also 5.2.1.2.). Accordingly, for the above reasons, the current analyses focussed exclusively on enamel tissue.

5.2.1. Tooth histology with an emphasis on enamel tissue

Tooth histology is the study of microscopic tooth structure, which is essential for the understanding both of tooth formation and of related aspects such as tooth function and strength, individual life history, phylogeny and evolution of mammals (Ungar, 2010).

As mentioned in 1.4. (Chapter 1), the three main components of the tooth are enamel, dentine and cement, all of which contain both organic and inorganic elements. Figure 5.1. summarises key information regarding the components of, and elements present within, dentine and enamel, and their potential applications (from Smith and Tafforeau, 2008).

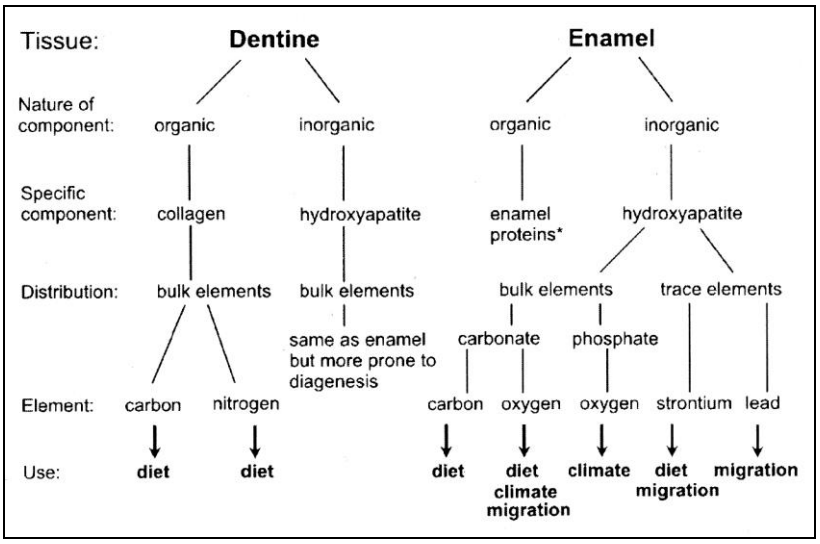

Figure 5.1. The components and elements of dentine and enamel and their potential applications (from Smith and Tafforeau, 2008).

Dentine consists of 70% apatite, 20% collagen (including some other proteins) and 10% water (Ungar, 2010), whereas cement is made up of 65% minerals (mostly hydroxyapatite, $Ca_{10}(PO_4)_6(OH)_2$, an inorganic calcium phosphate mineral), 23% organic matter and 12% water (Goldberg and Smith, 2004). In contrast, enamel consists of 96-97% (by weight) of hydroxyapatite, less than 1% organic material and the remainder (2-3%) water (Hillson, 1986). In terms of structure, enamel hydroxyapatite consists of packed crystallites (see below) approximately 50-100nm in diameter and >1000nm in length (Hillson, 1986), which bolster its resistance to diagenetic alteration (Lee-Thorp and Van der Merwe, 1991; Koch *et al*., 1994). Figure 5.2. compares the major components of apatite mineralised in human enamel, dentine and bone (from Pasteris *et al*., 2008).

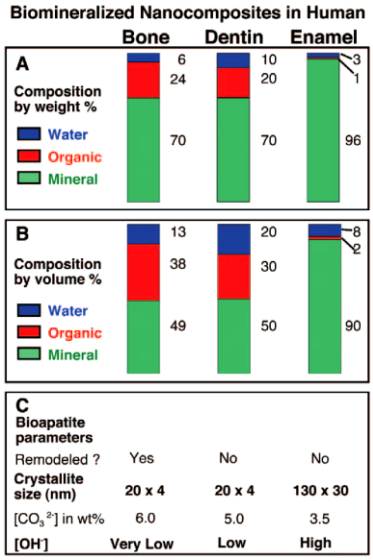

Figure 5.2. The composition by weight % of water, organic material and mineral for bone, dentine and enamel in humans (from Pasteris *et al*. [2008]).

The complex structure and formation of enamel must therefore be fully appreciated when undertaking chemical studies (especially those involving trace elements) before the choice of sampling method, materials and analysis is made.

Enamel structure can be described according to five hierarchical levels: **crystallites, prisms, enamel types, schmelzmusters** and **dentitions** (Koenigswald and Clemens, 1992). These levels are defined by the characteristics of size, structural complexity and distribution of enamel microstructures throughout the dentition (Clemens, 1997). **Crystallites** are the smallest units of enamel, ranging from 1600 to 10.000 angstroms in

length and usually reaching a maximum of about 400 angstroms in width (Clemens, 1997). With a few exceptions, crystallites radiate outward from the Enamel Dentine Junction (EDJ) (Koenigswald and Clemens, 1992). **Prisms** are bundles of crystallites bounded, at least in part, by a major discontinuity in the mineralised tissue known as the prism sheath (Clemens, 1997). The crystallites that separate the prisms are referred to collectively as the interprismatic matrix (IPM). Enamel prism or rod formation and patterns are very important in palaeontological studies and can provide much information regarding the evolutionary processes of animals (Koenigswald, 1997). The prisms are cylindrical or semi-cylindrical in shape and are organized into bundles of crystallites that expand from the EDJ to the outer enamel surface (OES); the diameter of each bundle depends on the species and tooth, varying from 2-10µm (Hillson, 1986; Ungar, 2010). The packing and orientation of the rods between the EDJ and the surface of the tooth help to prevents cracks spreading through the crown (Ungar, 2015), as well as to minimise potential damage during mastication (Young, 1975). The three different patterns of enamel prisms encountered in mammals are shown in Figure 5.3; different Orders and species within those Orders are characterised by different combinations of these patterns (Hillson, 1986).

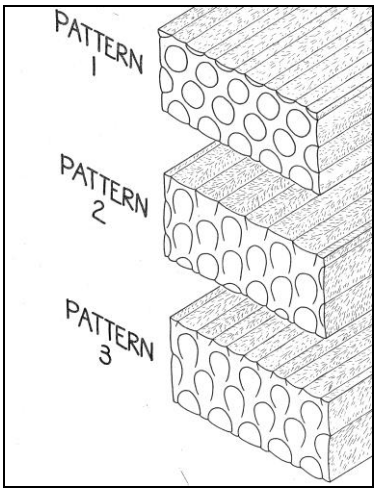

Figure 5.3. Three contrasting enamel prism patterns (after Hillson [1986]).

In the order Carnivora, for example, the main structure encountered is that seen in pattern 3 (Hillson, 1986). A very regular hexagonal pattern can be seen in the Canidae (Fig. 5.4.A) and Hyaenidae, whereas round prisms are characteristic of the Viverridae

and Phocidae (Fig. 5.4.B). For the Ursidae, a key feature is the increase of the angles between the prisms and IPM to 30-45° (Fig. 5.4.C) (Stefen, 1997).

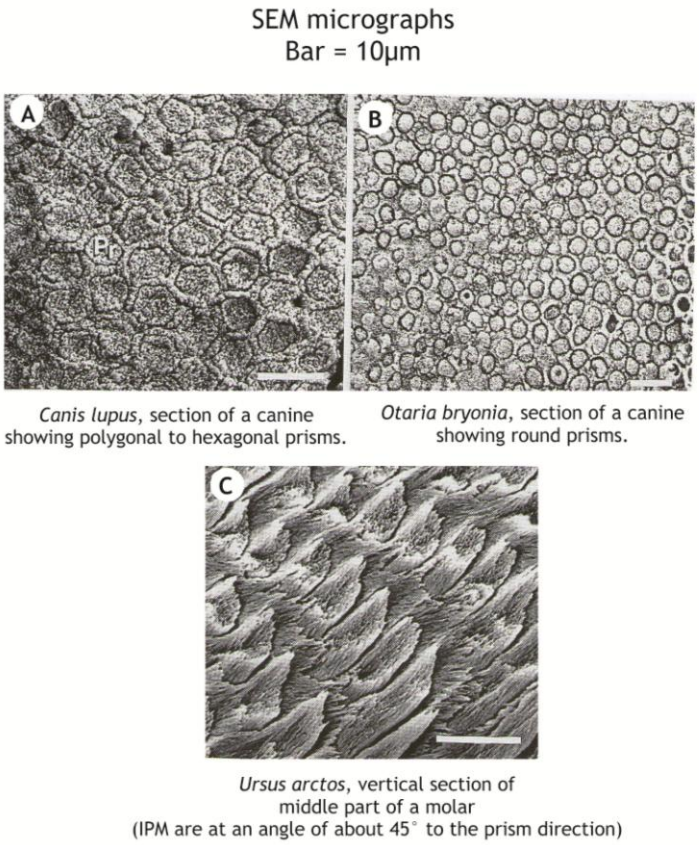

Figure 5.4. SEM micrographs showing enamel prisms for different species. **A.** *Canis lupus familiaris*. **B.** *Otaria bryonia*. **C.** *Ursus arctos* (image modified from Stefen [1997]).

The prismatic enamels are organised into two or three layers and within each layer, the prisms have similar morphologies and orientation. The individual couplets or triplets of layers are known as **enamel types** and are generally separated by well-defined boundaries (Clemens, 1997). Many enamel types have been recognized, including modified radial enamel, horizontal and vertical Hunter-Schreger bands, tangential enamel and 3-D enamel (Clemens, 1997 and references therein). Of these, the incremental Hunter-Schreger bands are the best known and most studied (e.g. Koenigswald, 1992; Stefen, 2001; 2007 Tseng, 2012). In addition, enamel types are grouped into what are referred to as **schmelzmuster** patterns (Ungar, 2015), with **dentition** denoting the highest level of enamel structural complexity (Ungar, 2010).

5.2.1.1. Incremental features of enamel

Compared to bone, enamel preserves a permanent record of its development through time, represented by incremental features. These features reflect a range of time scales, from daily (e.g. cross-striations) to longer periods (e.g. Retzius lines) (Boyde, 1989; Smith and Tafforeau, 2008). The study of these incremental features can be used to extract data regarding the life history of an individual, as well as serving as an archive of dietary development (Humphrey *et al*., 2008b). This is because these features are laid down during the secretory (matrix formation) stage of enamel and preserve an intact record of the timing of the onset of mineralisation of different areas of enamel that can be used to calibrate other events, such as suckling or weaning (Humphrey *et al*., 2008b).

The three main types of incremental features are cross-striations, Retzius lines and laminations (Smith, 2006). Figure 5.5.A. illustrates some of these features on a cross-sectioned molar tooth of chimpanzee (after Smith and Tafforeau, 2008). Cross-striations are identifiable under an optical microscope as light or bright and dark bands crisscrossing the enamel prisms (Hillson, 1986) (Fig. 5.5.A. within the bracket). They reflect daily enamel formation, with a single light/bright band deposited over a 24 hour period (Moss-Salentijn *et al*., 1997). Thus, the distance between adjacent cross-striations reveals the daily rate of enamel secretion (Smith and Tafforeau, 2008).

The arrows in Figure 5.5.A. indicate the Retzius lines on enamel. These incremental features characterise the sequential position of the matrix-forming front (Smith, 2006). In some species, Retzius lines are more obvious than cross-striations; they extend and are preserved on the surface of the tooth as wave-like bands and grooves called perikymata (Moss-Salentijn *et al*., 1997; Smith and Tafforeau, 2008; Ungar, 2010) (Fig. 5.5.B). Tafforeau *et al*. (2007) suggested that an estimation of the periodicity of Retzius lines is possible through counting of the cross-striations per Retzius line; however, this can differ between species. Laminations are the third incremental feature of enamel. These run parallel to the Retzius lines and record isochronous periods of enamel deposition. Similar to cross-striations, they have been demonstrated to be laid down on a diurnal basis in rhinoceros, humans and some other herbivores (Smith, 2006;

Tafforeau *et al*., 2007) but can be distinguished from cross-striations by their relatively oblique orientation (Smith and Tafforeau, 2008).

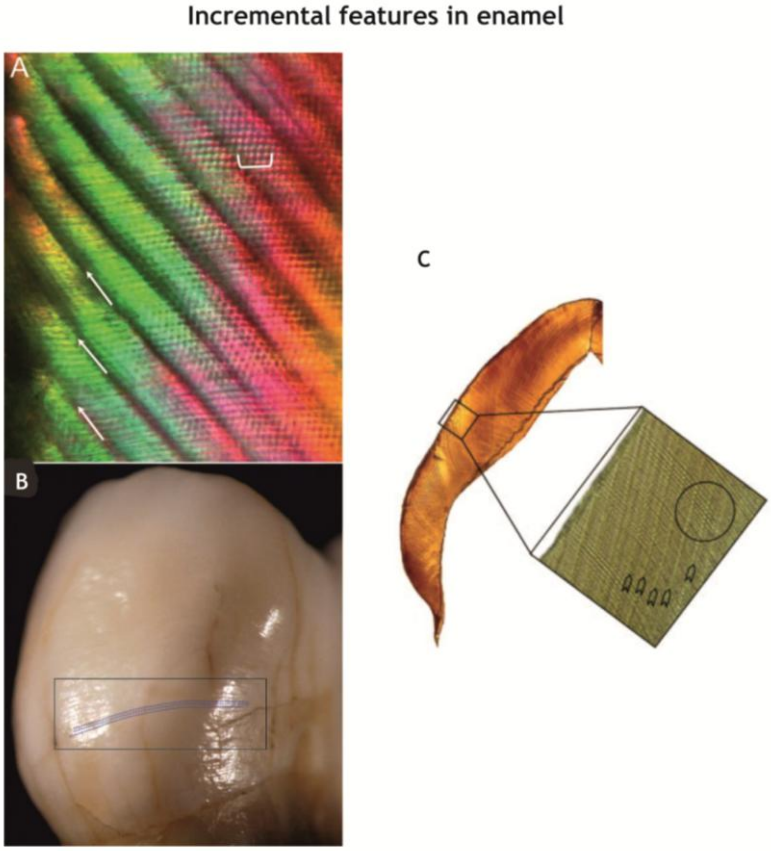

Figure 5.5. Cross-sectioned molar of chimpanzee showing incremental features in enamel. **A.** Long time periods, reflected by Retzius lines, are shown by white arrows. Diurnal cross-striations are shown in the white bracket. **B.** Blue dotted lines illustrate the perikymata of the outer layer of enamel. **C.** Molar section with enamel features under transmitted light microscopy (image modified from Smith and Tafforeau [2008]).

5.2.1.2. Amelogenesis – Enamel formation

The process of tooth formation and mineralisation is comprised of many complex stages. In order to decipher the incremental structure of mammalian enamel microstructure and to understand how calcium ions are transported across the membranes, it is important to have knowledge of how enamel is formed. Enamel is composed of a linked sheet of cells known as ameloblasts, which give their name to the process of enamel formation, 'amelogenesis'. Amelogensis has two main phases, (1) matrix production and (2) enamel maturation (Hillson, 1986; Boyde, 1989; Ungar, 2010). The first stage involves the formation of an organic, protein-rich matrix containing amelogenium and the crystallites, the former eventually being replaced by

apatite, thereby creating the heavily-mineralised mature enamel (Hillson, 1986). The structural features of the enamel are established during this initial stage (Fig. 5.6, left). The majority of mineralisation, on the other hand, occurs at the maturation stage (Ungar, 2010). At this point, high-resolution incremental features are established, with their recognised periodicity as already explained (5.2.1.1.) and visible in the fully mineralised enamel (Smith, 2006; Tafforeau *et al*., 2007). Although enamel mineralisation occurs during both the matrix formation and maturation stages, the degree of mineralisation significantly increases during the latter phase (Suga *et al*., 1970). This substantial increase in mineral content highlights the fact that the chemical composition of mature enamel at any given sampling point will reflect a time-averaged signal representing mineral deposition over a period of several months or even years (Humphrey *et al*., 2008a).

The mineralisation of enamel involves three substages: (1) secondary mineralisation from the surface enamel towards the deeper levels, (2) tertiary mineralisation from the deeper layers in the direction of the surface, and finally (3) quaternary mineralisation, when the enamel surface becomes heavily mineralised during the maturation stage (Suga, 1982). The largest amount of mineralisation takes place during the tertiary substage (Suga, 1982).

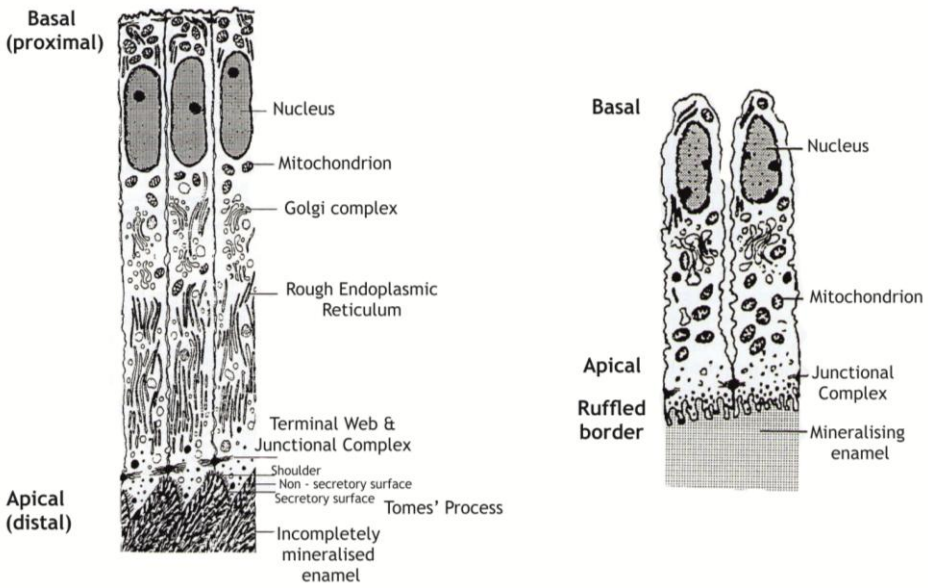

Figure 5.6. A mammalian ameloblast. **Left:** the secretory stage. **Right:** Ruffle-ended, maturation stage ameloblasts (images modified from Moss-Salentijn *et al*. [1997]).

Various studies on enamel formation in many large and small mammalian species have indicated that the degree of mineralisation varies through the enamel thickness and that the innermost enamel layer, which lies closest to the EDJ, is the most highly mineralised during matrix formation; this layer is therefore recommended for analysis (Suga *et al*., 1970; Suga 1982; 1989; Tafforeau *et al*., 2007).

The procedure of enamel formation is therefore rather prolonged and some animals need weeks or even months before their enamel is fully mineralised enamel (e.g. Hoppe *et al*., 2004b; Montgomery *et al*., 2010). This observation may have implications for high resolution *intra*-tooth chemical analysis on mammalian dentitions (e.g Passey and Cerling, 2002; Passey *et al*., 2005; Zazzo *et al*., 2005). Although many researchers have been pessimistic about the likelihood of recovering chronologically relevant isotopic and trace element sequences from enamel, according to Humphrey *et al*. (2008a), differences in strontium and calcium transportation across the ameloblast layer contribute in a predictable way to the distribution of these elements in mature enamel, thereby enhancing the physiological signal from the secretory stage of enamel formation. Humphrey *et al*. (2008a; b) further suggested that a chronological model can be recovered from enamel and discussed the different stages of this model in relation to Sr/Ca ratios preserved within (see also 5.2.3).

In addition, Tafforeau *et al*. (2007) and Zazzo *et al* (2010) stressed the importance of knowing the length of time that mineralisation takes to be completed in enamel samples. In particular, Tafforeau *et al*. (2007) reported, based on their study of rhinoceros enamel, that the innermost 20µm of the enamel near the EDJ was highly mineralised (77-90% of the final enamel mineralisation completed) during, or just after the phase of enamel matrix formation (Fig. 5.7). According to Zazzo *et al*. (2005), the chemical composition of the enamel also varies by location, with the carbonate content decreasing from 5% at the EDJ to 3% at the outer surface.

From the above observations, it is therefore clear that a micro-sampling approach, targeting the innermost part of the enamel, is essential when it comes to geochemical analyses on teeth.

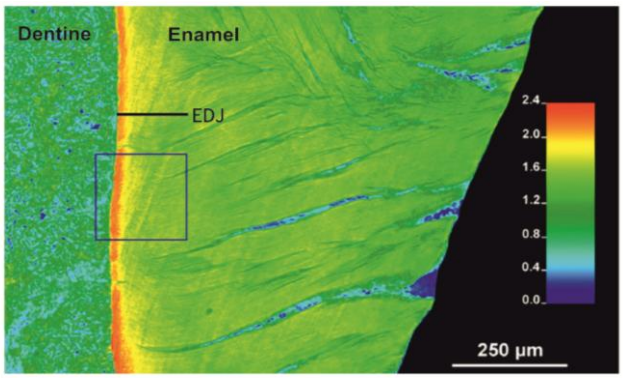

Figure 5.7. High resolution microtomographic figures showing enamel mineralisation and microstructure on a third lower molar fragment of *Rhinoceros sondaicus*. Mineral density ($g_{HA}cm^{-3}$) of enamel in cross section (red shows the densest and blue the least dense enamel) (from Tafforeau *et al*. [2007]).

5.2.2. Sampling strategies

Traditionally, chemical studies on enamel tissues used a bulk sampling approach (e.g. Glad *et al*., 2001; Peek and Clementz, 2012b) or have collected successive enamel layers by drilling or acid dissolution (e.g. Fricke and O'Neil, 1996; Reitznerova *et al*., 2000; Balasse, 2002; 2003; Zazzo *et al*., 2002; Balasse *et al*., 2003; Richards *et al*., 2008a; Britton *et al*., 2009). The drilling approach was based on the fact that enamel forms from the cusp tip to the crown base (Ungar, 2010), thereby preserving (in theory) a signal from the oldest enamel to the youngest respectively (see also Fig. 5.8). Accordingly, the drilling crosses each incremental prism of enamel and creates a time series chronology. In her study, Balasse (2002) used carbon isotope *intra*-tooth profiles on the enamel of *Bos*. Although the primary aim was to reconstruct palaeodiet (revealing a change from C_3 to C_4 plant-based diet), she further observed that the chemical input signals of enamel maturation in the lower second molar were mixed, concluding that these might be linked to the sampling procedure. Balasse (2003) subsequently used a different sampling approach by drilling the samples in an oblique direction; however the results were more or less the same as those obtained using the horizontal drilling approach. Another important aspect, especially for trace element analysis, is that previous bulk and drilling approaches have meant that the distribution of elements is averaged over relatively large areas of tooth surface (see Hinz and Kohn [2010]).

It is therefore clear that previous sampling strategies have many limitations that may adversely affect interpretation of results (Zazzo *et al*., 2005). Passey and Cerling (2002) demonstrated that the major problem with the *intra*-tooth method is that the input signals are time-averaged compared to the actual pattern of isotopic variation experienced by the animal during tooth formation. This is reflected as an attenuation of the resultant chemical signal (also the case when analysing trace elements; Kohn *et al*., 2013). Passey *et al*. (2005) and Montgomery *et al*. (2010) also stressed the time-averaging problem, with the latter authors linking this issue to either the long-term retention of strontium in the skeleton and its recirculation in the body or to the long-term maturation of enamel on a microscopic scale. Kohn (2004) concluded that the input signal will be increasingly dampened in species that have the longest period of enamel maturation.

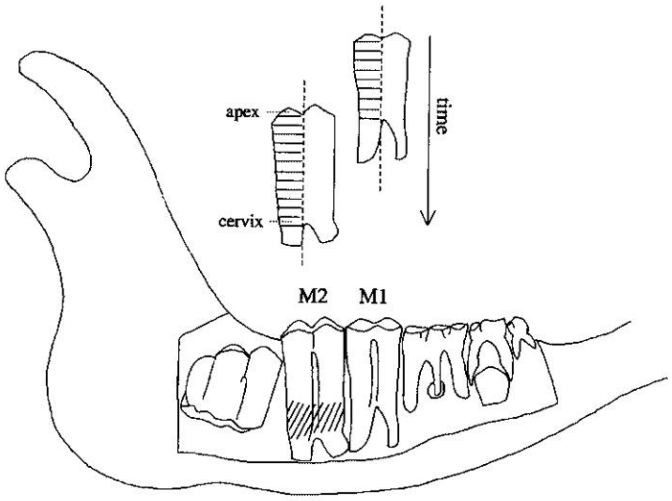

Figure 5.8. Schematic reconstruction of the *intra*-tooth sampling method. Horizontal samples were taken from the enamel cusp to the cervix of tooth (image from Balasse [2002]).

An important development is the use of LA-ICP-MS, which can be used to investigate ever-smaller compositional trends and to undertake *in situ* analysis of discrete samples from the enamel surface or from dental thin sections (Budd *et al*., 1998; Kohn, 2008; Lee *et al*., 1999; Dolphin *et al*., 2005; Kang *et al*., 2004; Sponheimer *et al*., 2006; Humphrey *et al*., 2008a; b; Hinz and Kohn, 2010; Kohn *et al*., 2013). Another advantage of LA-ICP-MS is that the technique is minimally destructive and can readily measure element concentrations along predefined tracks, repeatedly cycling through a suite of elements at a constant ablation track speed (Humphrey *et al*., 2008a; Hinz and Kohn,

2010). In addition, the results can be interpreted in relation to the sample location and incremental growth markers (Humphrey *et al*., 2008b).

In this thesis, the study of trace elements was therefore conducted by targeting the innermost enamel layer, parallel to EDJ, on all teeth sampled by utilising LA-ICPMS.

5.2.3. Trace elements - Sr/Ca and Ba/Ca ratios in food webs

The basic principle of trace elements is that since they are distributed in foodwebs, they can be used as chemical proxies for tracking past diets (Lee-Thorp and Sponheimer, 2006). More specifically, trace element studies depend principally on the different discrimination of an individual element relative to calcium (Ca) in the body (e.g. Elias *et al*., 1982; Radosevich, 1993; Kohn *et al*., 1999). Calcium (Ca), strontium (Sr) and barium (Ba) are alkaline earth metals that are widespread in the lithosphere. Ca is one of the most important elements in the Earth's crust and is involved in many biological procedures, as outlined below. In contrast, Sr and Ba are non-vital elements; however, during the process of nutrient uptake, they can mimic Ca on account of their analogous atomic properties and can therefore be used as tracers for calcium (e.g. Blum *et al*., 2000).

In the trophic pyramid at each level above the soil, there is metabolic discrimination in the epithelium of mammals against Sr, as opposed to calcium (Ca) (Radosevich, 1993). This discrimination occurs in five key areas of the mammalian body, the intestines, the kidneys, sites of bioapatite formation, the placenta and the mammary glands, and is known as biopurification of Ca (e.g. Elias *et al*., 1982; Lee-Thorp and Sponheimer, 2006; Peek and Clementz, 2012b and references therein). Theoretically, this discrimination means that as one goes up to the trophic pyramid from plant to herbivores and ultimately to carnivores, the contribution from food sources to skeletal Sr is decreased at each level (Fig. 5.9) (Radosevich, 1993).

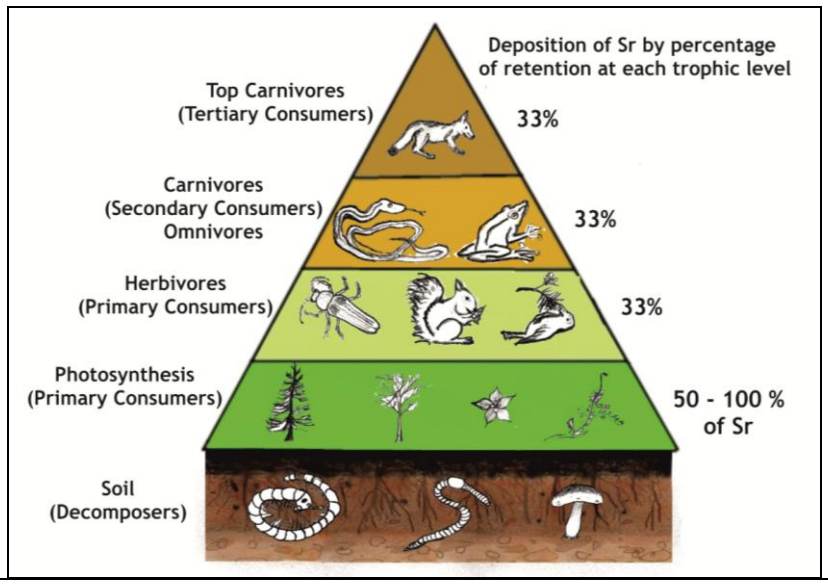

Figure. 5.9. Trophic pyramid with respect to deposition of Sr by percentage of retention at each level (data from Radosevich [1993] and image from Odum and Barrett [2005]).

As a result, herbivore tissue will have a lower Sr/Ca ratio compared to the plants they consume, while carnivores in turn will have lower Sr/Ca ratios than the herbivores they predate, likewise for the Ba/Ca ratio (Schoeninger, 1979; Elias *et al*., 1982; Sealy and Sillen, 1988; Burton *et al*., 1999). Since Sr and Ba are found in bones and teeth, where they substitute for calcium in the calcium phosphate apatite structure, they can in principle be used to investigate trophic behaviour and physiological changes of fossil fauna (Lee-Thorp and Sponheimer, 2006; Humphrey *et al*., 2008a; b) (Fig. 5.10).

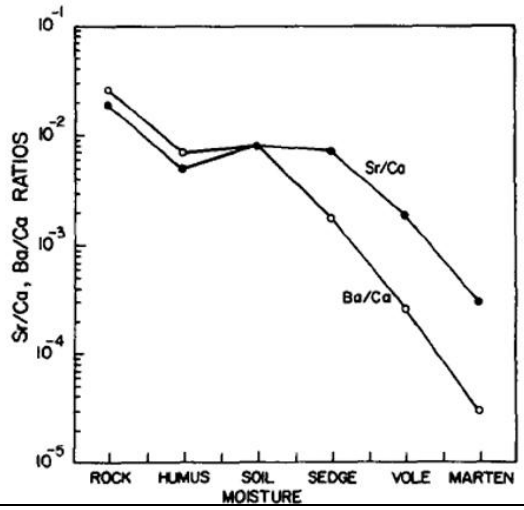

Figure. 5.10. Trace element discrimination study of a terrestrial grazing ecosystem in North America. The plant-vole-marten curves illustrate the reduction in Sr/Ca and Ba/Ca at each stage of the trophic pyramid (from Elias *et al.* [1982]).

Although other trace elements such as zinc (Zn) have been used occasionally (e.g. Safont *et al*., 1998; Lee *et al*., 1999; Sponheimer and Lee-Thorp, 2006), a lack of

knowledge regarding its distribution in foodwebs and its fixation properties in tooth and bone has limited its application (Lee-Thorp and Sponheimer, 2006). For example, Safont *et al*. (1998) found significantly higher values of Zn in carnivores compared to herbivores but did not provide any explanation as to why this occurred and what the implications for diet might be.

Initially, in order to reconstruct an animal's trophic position, previous studies used both Sr/Ca and Ba/Ca ratios (e.g. Sillen, 1992; Balter, 2004; Lee-Thorp and Sponheimer, 2006; Peek and Clementz, 2012a; b), corroborating the observation that Sr/Ca and Ba/Ca ratios decreased with each successive trophic level (e.g. Elias *et al*., 1982; Burton *et al*., 1999; Blum *et al*., 2000; Balter, 2004). Concentrations of minor and trace elements in teeth have been described in different studies (e.g. Kohn *et al*., 1999; Hinz and Kohn, 2010). Table 5.1 gives a summary of some elemental concentrations used in tooth geochemical studies (data from Kohn *et al*. [1999] and Kohn *et al*. [2013]), hereby followed in this thesis.

Table 5.1. Elements in teeth and their uses with information regarding their concentrations (data from Kohn *et al*. [1999]) and Kohn *et al*. [2013]). C and I in brackets indicate respectively concentration and isotope composition and the application of each element.

Element	Concentrations (ppm)	Uses
Li		
Mg	1000's	Diet (C)
Al	< 10-100	In this study as an additional alteration indicator
Ca	370,000	Trophic level (I) In this study used as internal standard, 37% of hydroxyapatite consists of it.
Na	1000's	Diet (C)
Mn		In this study as an additional alteration indicator
Zn	100's - 1000's	Diet (C)
Rb	>1	
Sr	100's - 1000's	Diet (C), Migration (I)
Y	<1	Diagenesis (C)
Ba	10's - 1000's	Diet (C)
Ce	<1	Diagenesis (C)
Nd	<1	Diagenesis (C)
U	<1	Diagenesis (C)
Pb	>1	In this study as an additional alteration indicator

One of the most comprehensive studies regarding trace element concentrations in teeth was carried out by Kohn *et al*. (2013) on 145 samples enamel, primary dentine and secondary dentine from herbivores, omnivores and carnivores in Idaho, USA. It was concluded that trace element concentrations differ between the three tissue types in the same tooth. Furthermore, most of the trace element concentrations were

found to be below 1ppm, except manganese (Mn), iron (Fe), zinc (Zn), mercury (Hg) and lead (Pb). It was also demonstrated that Sr and Ba biopurify with increasing trophic level but Ba shows decreasing discrimination with tissue type, having the least discrimination on enamel tissue (Kohn *et al*., 2013). However, most publications have focused on the estimation and interpretation of an average value for both the Sr/Ca and Ba/Ca signals, in order to reconstruct animal diet variability within each foodweb (e.g. Burton *et al*., 1999; Balter *et al*., 2002; 2008; Sponheimer and Lee-Thorp, 2006; Sponheimer *et al*., 2006).

Nevertheless, it must be pointed out that these studies have been constrained by the very complex pathways in foodwebs of both Sr and Ba. For example, studies on Sr/Ca and Ba/Ca ratios have shown that Sr and Ba concentrations vary between plant species and sometimes even among different parts of the same plant (Burton *et al*., 1999; Sponheimer and Lee-Thorp, 2006). Runia (1987) and Burton *et al*. (1999) observed that Sr/Ca and Ba/Ca ratios are higher in roots and stems than in leaves and fruit, which might provide differentiation between highly-selective herbivorous animals. For example Sillen (1992) and Sponheimer *et al*. (2005) have suggested that grazers have higher Sr/Ca than browsers. In addition to these complications, the bedrock and substrate may alter the results of Sr/Ca and Ba/Ca ratios in plants (and consequently in animals). It has further been observed that even geologically-similar sites can differ in the degree to which they impart certain elements (e.g. Zn) to fossils (Sponheimer and Lee-Thorp, 2006). The trace element contents in dental tissue samples can therefore vary significantly in different geographical origin (Brügman *et al*., 2012).

As well as these factors, tooth selection can have an important impact on analysis since both Sr/Ca and Ba/Ca can vary within and between teeth (e.g. Balter *et al*., 2008; Humphrey *et al*., 2008a; b; Peek and Clementz, 2012b). For example, Balter *et al*. (2008) examined herbivore enamel (selected parallel to the growth prisms, so perpendicular to the line of tooth growth) from the Kruger National Park in South Africa. Using laser ablation, these authors demonstrated that Sr/Ca profiles systematically decline from the EDJ to the enamel surface but this decrease is not linked with a change in diet. This was confirmed by Humphrey *et al*. (2008b), who suggested that one of the most critical dietary transitions experienced in the early life of most mammalian organisms is that from breast milk to food (non-milk), since the

latter has a higher Sr/Ca ratio higher than breast milk. In humans, the transfer of Sr via both the placenta and mammary glands follows a concentration gradient; however, for other elements such as Ca, Mn, Rb and Zn, the mammary glands exerting a greater transport effect than the placenta (Krachler *et al*., 1999; Rossipal *et al*., 2000). The weaning period of animal can therefore play an important role in the chemical signal of the enamel, since it is formed partially during early infancy (Sponheimer *et al*., 2005). Metcalfe *et al*. (2010) demonstrated that unborn and nursing infants have lower Sr/Ca ratios than their mother. Analysis from Dolphin *et al*. (2005) on human milk teeth further revealed differences in normalised trace elements intensities between enamel samples taken on either side of the neonatal line. The importance of the weaning signal should therefore be taken into account when high resolution profiles are examined.

One of the first studies to develop a chronological model taking into account the different dietary and physiological parameters that contribute to Sr/Ca changes during different dietary phases of an individual's life was undertaken by Humphrey *et al*. (2008b), comparing deciduous and permanent teeth of baboons (*Papio hamadryas anubis*) from Uganda. This study demonstrated that it is indeed possible to track retrospectively dietary development during weaning from Sr/Ca ratios in tooth enamel. According to this model, there are four distinct stages of dietary development, during which different dietary and physiological parameters contribute to the Sr/Ca content of tissues forming at those times. Changes in Sr/Ca during each dietary phase and at the transitions between phases should therefore be predictable. These stages comprise: prenatal (stage 1), where nutritional requirements are obtained directly from the mother via the placenta, exclusive suckling (stage 2), where nutritional requirements are obtained from the mother in the form of breast milk; mixed suckling and independent feeding (stage 3), the first stage of the weaning process where non-milk food is introduced to the infant's diet, and dietary maturity (stage 4), marked by a complete cessation of suckling (Humphrey *et al*., 2008b).

During these stages, the Sr/Ca values were predicted to fall between stages 1 and 2, due to a difference in the transport of calcium and strontium across the placenta and via the mammary glands (Humphrey *et al*., 2008a; b and references therein). During stage 2 of exclusive milk feeding, a gradual fall in Sr/Ca ratios was predicted, followed

by a rise in Sr/Ca marking the transition between stages 2 and 3. The highest Sr/Ca ratio occurs when suckling stops marking the transition between stage 3 and 4 and after this age the Sr/Ca ratio is expected to fall as the infant's ability to discriminate against strontium in the gastrointestinal tract continues to develop. According to Humphrey *et al*. (2008b), the transition between stages 3 and 4 may be complex because during this period, a wide range of adult food sources may be involved. In addition, periodic fluctuations in Sr/Ca ratios due to seasonal patterns of resources should also be anticipated with respect to enamel forming during stage 4 (Sponheimer *et al*., 2006).

Given the complexities and difficulties in interpreting dietary variability through Sr/Ca and Ba/Ca ratios, the aim of this thesis was to consider as far as possible the various influencing factors and to model, following Humphrey *et al*. (2008b), the different stages along the Sr/Ca and Ba/Ca profiles within each tooth and species analysed. In addition, in order to recreate the trophic levels of the Tornewton Cave assemblage, the average values of both Sr/Ca and Ba/Ca ratios were calculated from tooth profiles that most likely represented stage 4, dietary maturity.

5.2.4. Diagenesis

As already alluded to, diagenesis of zooarchaeological and palaeontological material may also impact on these types of study. Athough enamel is more resistant to chemical alterations than other parts of the teeth (or indeed bone), the original Sr/Ca and Ba/Ca ratios may become altered (Balter *et al*., 2002) as the chemical state of the fossil tooth is affected by precipitation of secondary minerals and chemical alteration of biogenic apatatite (Kohn *et al*., 1999). The following sections present a review of different diagenetic situations, illustrated by examples from previous studies.

Diagenesis denotes any chemical alteration to either the protein or mineral fractions of bones and teeth that may occur in the burial environment (Britton, 2009). As previously discussed, tooth enamel is generally more resistant to diagenetic alteration than bone (e.g. Ayliffe *et al*., 1994; Wang & Cerling, 1994; Budd *et al*., 2000; Hoppe *et al*., 2003; Lee-Thorp and Sponheimer, 2003). The larger amounts of organic matter and smaller crystals in bone, when compared to enamel, favour ionic exchange within the

burial environment (Lee-Thorp *et al*., 1989; Lee-Thorp and Van der Merwe, 1991; Wang and Cerling, 1994; Budd *et al*., 2000; Hoppe *et al*., 2003). Several studies have documented the more resistant nature of enamel to diagenetic changes. For example, Bocherens *et al*. (1994b) studied fossil dinosaur teeth and revealed that enamel tissue was more resistant than dentine to trace element contamination, even in material more than 100 million years old. Moreover, Budd *et al*. (2000), in a study of prehistoric and medieval human teeth from four different UK sites, suggested that dentine (as a more porous material) exhibited the same behaviour as bone in terms of contamination, documenting significant differences between enamel and dentine and minor differences between dentine and soil. Kohn *et al*. (1999) investigated modern and fossil teeth from northern and central Kenya at a micrometre to sub-micrometre scale, revealing physical contamination of enamel by a number of elements (Fe, Mn, Si, Al, Ba and possibly Cu) and chemical alteration of U, REE, F and possibly Sr. They further documented concentrations of secondary minerals, ranging from ~0.3% in enamel and ~5% in dentine, thereby proving the more resistant nature of enamel.

However, although enamel has more resistance to diagenetic alteration than bone and dentine, such modification can still occur (Kohn *et al*., 1999; Sponheimer and Lee-Thorp, 1999; Lee-Thorp and Sponheimer, 2003; Zazzo *et al*., 2004). Hydroxyapatite, the major mineralised component of enamel, can become unstable after death and undergo ionic substitution such as Ca^{2+}, with or without fundamental structure change (e.g. Zazzo *et al*., 2004). This process leads to higher concentrations of trace elements in the altered enamel (Trueman and Tuross, 2002). In addition, increases in concentrations of some trace elements in fossil versus modern teeth indicate a growth of secondary minerals after burial (e.g. Kohn *et al*., 1999). In some cases, enamel may become enriched in rare-earth elements (REE) (e.g. Kohn *et al*., 1999) during the fossilisation process, possibly entering through cracks on the apatite surface (Reynard *et al*., 1999). Alteration also occurs through the filling of cracks by secondary minerals, reflected by increases in Fe, Mn and Al concentrations. The presence of Fe and Mn indicates contamination by oxyhydroxides, commonly forming dark stains on the surface (Jaques *et al*., 2008), while Al increases are produced by the presence of clay in the depositional environment (Kohn *et al*., 1999). Since U and the REEs occur in very low concentrations in modern apatite tissue, increases in their concentrations suggest

post-mortem alteration in fossil teeth (Kohn *et al*., 1999), allowing the identification of chemical alteration when comparing fossil with modern specimens.

Enamel can be also affected by biological and enzymatic attack (e.g. Turner-Walker, 2008), although this is usually detectable via light microscopy. Dauphin and Williams (2004) studied fossil rodent tooth enamel, noting that it was enriched in Sr and Fe compared to modern enamel, whereas Kohn *et al*. (1999) identified diagenetic-related enrichment of Ba and potentially Sr in early hominin enamel from Kenya. An analysis carried out on fossil and modern enamel from sites located on both dolomitic and granitic bedrocks was carried out by Sponheimer and Lee-Thorp (2006). Although these authors demonstrated that Sr/Ca, Ba/Ca and Pb/Ca ratios in enamel had not been significantly increased during fossilisation at three of their study sites, Zn/Ca ratios were highly altered in the material from the fourth. The study stressed the importance of comparing material from the same geological substrates and always approaching carefully the potential problem of enamel diagenesis, following Kohn *et al*. (1999), should enrichment in Sr, Ba, Fe, Zn, Al, Mn, U and the REEs be found. Additional screening procedures may therefore prove helpful in future for the evaluation of enamel chemistry, such as virtual sectioning and quantitative mineralisation mapping. An example of diagenetic patterns of enamel and dentine in fossil primate teeth is shown in Fig. 5.11 (after Smith and Tafforeau, 2008).

Thus, it is important to consider a multiplicity of factors when employing chemical analysis, since the taphonomic history of an individual specimen could substantially affect the results produced (Sponheimer and Lee-Thorp, 2006). Using trace element analysis, a further aim of this thesis is to establish potential diagnosis in the Tornewton Cave sample. This was achieved by observing the patterns of behaviour of U, Al, Mn, Pb and REEs along each enamel track and also by comparing the concentrations of these elements with the concentrations of the same elements for published modern enamel data (see 5.5.2.).

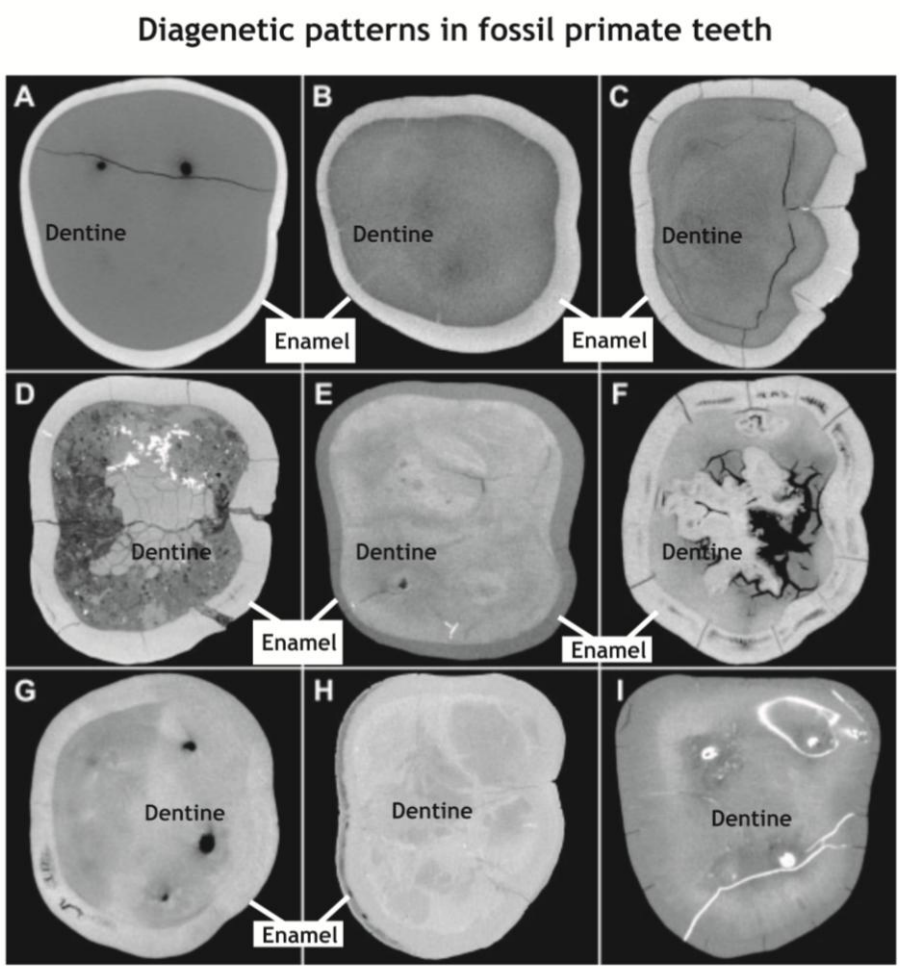

Figure. 5.11. Fossil primate tooth images with monochromatic absorption synchrotron micro-CT showing examples of diagenetic patterns. **A.** Modern human tooth with normal (homogenous) tissue. **B.** Pleistocene human tooth demonstrating slight tissue heterogeneity. **C.** Miocene hominoid tooth (slight heterogeneity). **D.** Miocene hominoid tooth with good preservation of enamel but poor preservation of dentine. **E.** Eocene primate with inverse contrast between tissues. **F.** Pleistocene hominin tooth with strong alteration of both enamel and dentine. **G.** Same tooth as F with moderate contrast of tissues. **H.** Miocene hominoid with de-mineralised enamel. **I.** Eocene primate with no tissue contrast and metallic oxides (image and information from Smith and Tafforeau [2008]).

5.3. Ecology and dental development in modern analogue taxa

The following section introduces some ecological and biological characteristics (with a focus on dental development) of five living species including *U. arctos*, *C.crocuta*, *E. ferus* and *C. elaphus*. These animals were selected as they represent the closest living relatives of the extinct species on which geochemical analyses were performed in this thesis. Knowledge of the biological traits of the mammals in question is an essential precursor to a robust interpretation of their geochemistry, as is the detailed understanding of dental development in each species.

5.3.1. Bears

5.3.1.1. Ecology

Many aspects concerning the ecology of the various bear species, including their dietary preferences, have been presented in Chapter 2. This section therefore focuses on other biological and social behavioural traits that may be of relevance to the geochemical analysis. The Chapter begins with a literature review of the dental development and eruption sequence in extant *U. arctos* and other living bear species, followed by a consideration of winter lethargy, otherwise known as the hibernation mechanism.

5.3.1.2. Dental development

Although members of the Order Carnivora, most bear species are omnivores with a frequently large proportion of plant matter in their diet. This generalist behaviour is reflected in bear teeth, which are large and robust with bunodont molars (Hillson, 1986). As in all carnivores, the carnassial teeth comprise the last (fourth) premolar in the upper jaw (P4) and the first molar in the lower jaw (m1). These are adapted for cutting through meat with a scissor-like action, although in bears, there is more emphasis on the crushing and grinding function of the dentition than in other carnivores (Ewer, 1973). The teeth are therefore broader, with somewhat more rounded ends to the cusps, in comparison with other carnivores. Figure 5.12 shows the permanent upper and lower dentition from an extant brown bear.

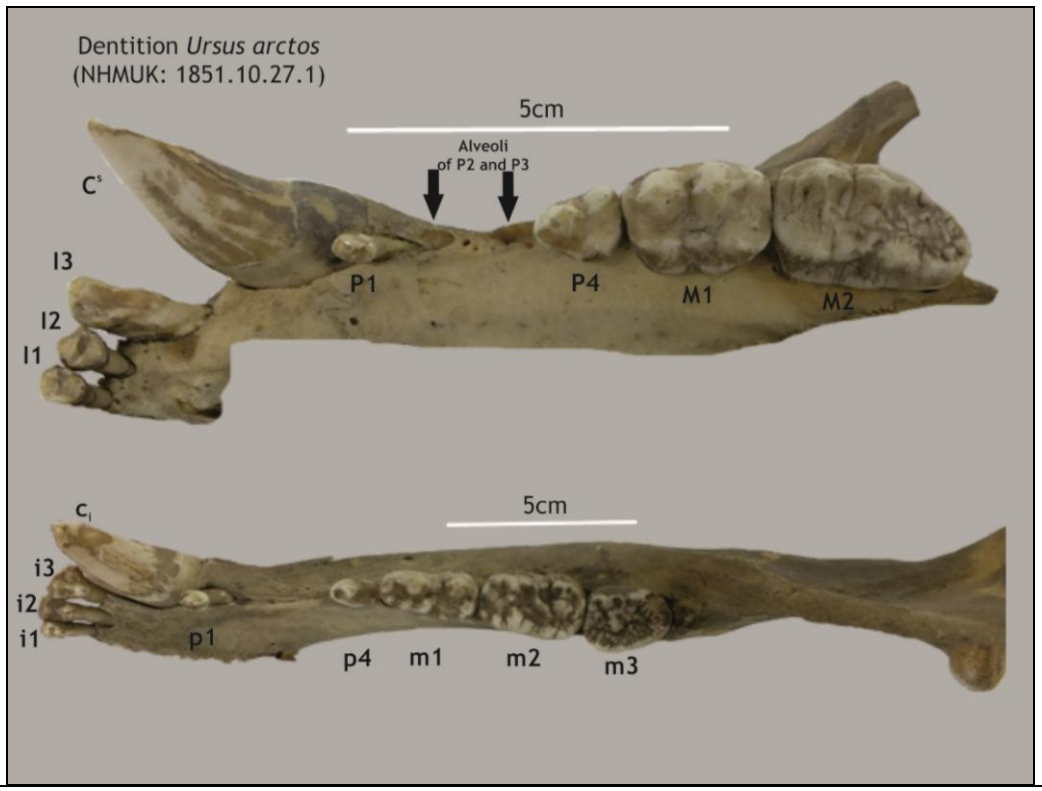

Figure 5.12. *Ursus arctos* dentition (NHM, London, Life Sciences collections 1851.10.27.1). Top: Upper left side dentition with near complete dentition (missing 2nd and 3rd premolars). Below: Lower right side with complete dentition. Upper case denotes upper teeth, lower case denotes lower teeth. ^{s} denotes superior (upper), ^{i} denotes inferior (lower).

As in most mammals, bears are diphyodont, meaning that the first dentition (deciduous or milk teeth) is replaced by a second set, the permanent dentition (Hillson, 1986). Knowledge of the ontogenetic progress and most particularly, of enamel formation and mineralisation in the teeth of each species is very important for reconstructing a detailed profile of an individual's life through geochemical analysis. Although for many herbivore species, the timing of tooth formation and mineralisation has been studied, for carnivores, such resources are limited. An exhaustive search of the literature revealed no publications on enamel mineralisation in bears, although information is available regarding the timing of weaning and of appearance or eruption of different teeth in various extant bear species (e.g. Dittrich, 1960; Rausch, 1961; Marks and Erickson, 1966), as well as for some extinct bear species (e.g. Ehrenberg, 1931; Debeljak, 1996). The dental formula in the permanent teeth for each extant bear species has been outlined in detail in Chapter 2 but follows the general pattern of: I3/3; C1/1; P4/4 and M2/3 (Hillson, 1986). For the deciduous dentition in bears, the following formula applies: dI 3/3; dC 1/1 and dP 3/3 (Rausch, 1961).

All cubs are born toothless and the first milk teeth start erupting during the second month of life, coming into position during the third month (Dittrich, 1960). The eruption of permanent teeth begins late in the third month of life, when a small part of the P1 crown and of the first and second incisors first appears (Rausch, 1961). Deciduous and partially-erupted permanent teeth co-exist in the mouth during the fourth month of a bear's life, as illustrated in Figure 5.13 by Debeljak (1996). Here, the permanent dentition is developing in the jaws beneath the deciduous teeth, prior to progressive replacement.

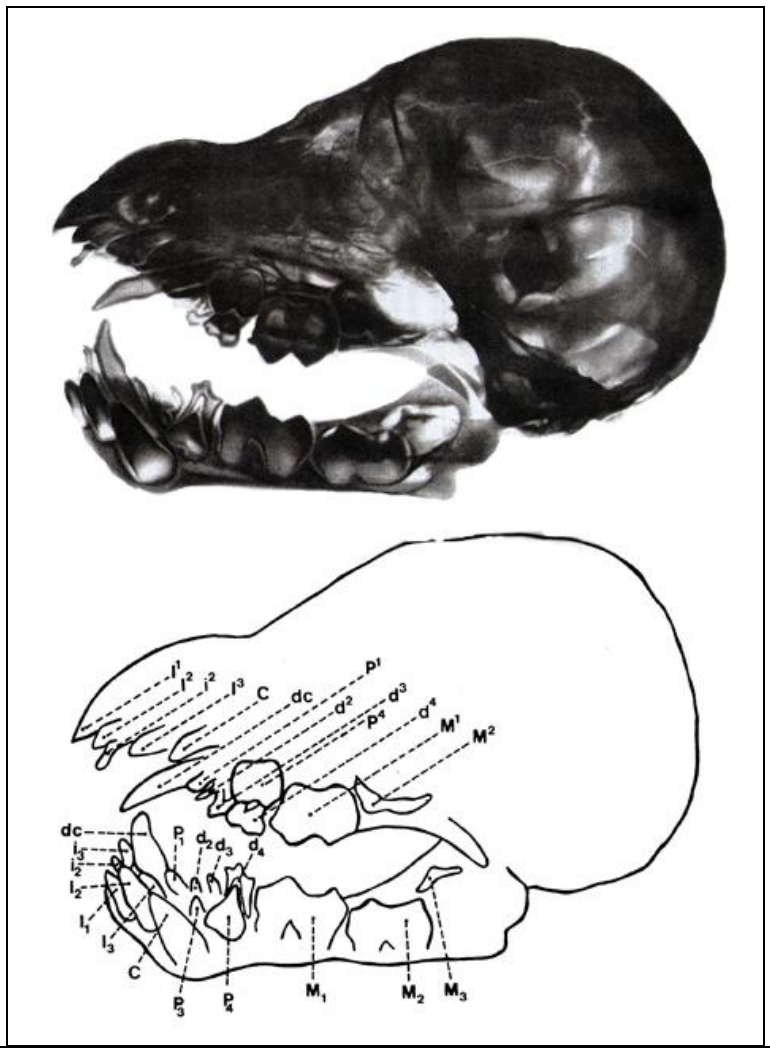

Figure 5.13. Cranium and mandible of a four month old individual of *Ursus arctos* from the Pyrenees. The upper image shows an X-ray photograph of the cranium, deciduous and partially-erupted permanent dentition and the lower image present a schematic illustration (modified after Debeljak [1996]).

Similar ontogenetic development has been reported in *U. arctos*, *U. americanus* and *U. maritimus* (Rausch, 1961). The bears are normally born at the beginning of February and the permanent teeth (except the canines) start erupting between May and September

(Marks and Erickson, 1966) (Table 5.2). The first permanent tooth to erupt is the first molar (m1/M1), followed by (in order) the first premolar (p1/P1), the fourth premolar (p4/P4), the second molar (m2/M2) and finally, the third molar (m3/M3) and the canine (c/C) (Dittrich, 1960; Marks and Erickson, 1966; Debeljak, 1996). From X-ray images made by Dittrich (1960) and Debeljak (1996), the following assumptions can be made regarding enamel formation on each tooth: enamel formation is initiated approximately one month after birth in the first molar (which is also the first tooth to erupt at 4th month after birth), in the canine at two months and in the third molar four months after birth. Unfortunately the end of each period of tooth enamel formation is not clear.

Table 5.2. Weaning and tooth eruption times (in months) from black and brown bear (from Dittrich [1960]; Rausch [1961]; Marks and Erickson [1966]; Ewer [1973]; Debeljak [1996]). I = incisors, Ci = canine initial eruption, Cf = canine final eruption, P = premolars, M = molars.

Species	Weaning	I1/I2	Ci	Cf	P1	P2	P3	P4	M1	M2	M3
Ursus americanus (Black bear)	6	4-5/ 5-7	8-10		5-7	7-8	7-8	5-7	4-5	5-7	7-8
Ursus arctos (Brown bear)	24		8	54	12-24	12-24	12-24	12-24	12-24	12-24	Last erupt

In carnivores, the exact termination of suckling by young is difficult to estimate. In principle, the ontogenetic shift from nursing to consuming a solid diet can alter geochemical signatures both within teeth that mineralise over a significant period as well as among teeth that mineralise at different times (Kohn and McKay, 2012). Bears begin weaning close to two years of age (Ewer, 1973). According to the eruption sequence of bear teeth, this means that weaning occurs after the initial eruption of the canines (at 8 months) and the cheek teeth (at 12-24 months). Therefore, milk consumption has the potential to influence the geochemical signature of bear teeth.

5.3.1.3. Hibernation

One of the most interesting physiological aspects of the ursids is the hibernation process and many studies have explored this biological mechanism in bears (e.g. Folk *et al*., 1972; 1976; Nelson *et al*., 1983; Hilderbrand *et al*., 2000; Seger *et al*., 2011; López-Alfaro *et al*., 2013).

Usually a hibernating animal remains inactive for a period over winter, during which normal physiological processes (e.g. maintenance of body temperature, heart and respiratory rates) are greatly reduced, thereby reducing the energy requirements of the animal. However, some mammals may periodically awaken and warm up, even drink or eat (Macdonald, 2009). Classic hibernation, with body temperature and metabolic rate remaining low for long periods over winter is characteristic of many small herbivores such as rodents, predominantly because of limited food resources during this season (Ewer, 1973).

Since bears consume a large quantity of plant matter, including some fruits rich in protein that are not available during winter, they experience greater difficulties finding food than many other carnivores during harsh weather and therefore opt to hibernate. However, the main difference in bears' dormancy patterns, compared to the other deep hibernators, is that both black and grizzly bears are reported to hibernate continuously from 3 to 7 months at a near-normal body temperature (31-35 °C), although a large reduction in heart rate has been observed (Folk *et al*., 1972). Nelson *et al*. (1983) proposed four annual physiological stages for black and brown bears as follows: I – hibernation, in which lean body mass is preserved and body fat supplies energy; II – walking hibernation, in which the biochemistry of hibernation is integrated with physical activity, but food and water intake are minimal; III – normal activity of the animal; IV – hyperphagia, in which bears increase fat reserves before hibernation.

During hibernation, bears survive without eating, drinking, urinating or defecating (Macdonald, 2009). Interestingly, although these animals can remain inactive for such a long period and would be expected to experience loss of bone mass, bears possess an osteoregulatory mechanism that protects them from osteoporosis during hibernation (Floyd *et al*., 1990). In their study, Floyd *et al*. (1990) studied calcium levels and bone metabolism in black bears during summer, winter and spring, revealing that the calcium concentration in serum did not change over the course of the year, nor did bone mass, bone formation or mineral apposition rates differ from summer values, even after four months of inactivity.

It is equally notable that female bears give birth and nurse their cubs during the hibernation period. Cubs are born very small compare to their mother's size (less than

1 percent); however they can absorb fat from their mother's milk and therefore gain weight rapidly (Macdonald, 2009). Grizzly bear milk has 4.5 times more fat and 17 times more protein than human milk (Robbins *et al*., 2006), whereas average fat content in polar bear milk is 33%, similar to that of marine mammals (Derocher *et al*., 1993). On the other hand, although bone density does not reduce, many studies have reported that body mass loss occurs on a daily basis during hibernation in adult female nursing bears (e.g. Hilderbrand *et al*., 2000).

Thus, during the dormancy period, bears use up the body reserves (both fat and lean mass) that they accumulated during their active period, in order to support the energetic and protein costs of hibernation and reproduction (Macdonald, 2009; López-Alfaro *et al*., 2013). Hence, bears consume high-protein diets in order to regain lean mass (mainly after hibernation), while bears on low-protein diets gain primarily fat (Felicetti *et al*., 2003). Dietary composition is therefore vital, particularly for bears in northern areas, which hibernate for twice as long as those in more southern areas and lose relatively more weight (Swenson *et al*., 2007). Brown bears in areas with longer winters therefore need to select a protein-rich diet in order to make best use of energetic resources and to promote mass growth (Swenson *et al*., 2007; Vulla *et al*., 2009; Bojarska and Selva, 2012).

Previous studies concerning geochemical analysis in the Ursidae have been highlighted (2.4.2.) but little attention has been given in the literature to the potential effects of hibernation and growth patterns on the geochemical signatures of fossil remains. Chemical studies on trace elements linked with observations on hibernation for bear species are not available, however the mechanism has been explored with stable isotopic analysis. Analysis of bear blood revealed that the $\delta^{13}C$ values during hibernation decrease, while the $\delta^{15}N$ increases (Lohuis *et al*., 2007). In addition, in the same study, the authors observed that the $\delta^{15}N$ values of skeletal muscle increases at the beginning of hibernation but stay stable afterwards.

According to Lidén and Angerbjörn (1999), dormancy and hibernation are examples of catabolic states where nitrogen (N) can be recycled in the body. On the one hand, this will cause isotopic fractionation during winter but on the other, during periods of growth and protein turnover, the isotopic value will be diluted in relation to the

concomitant change in diet. Furthermore, it has been observed that there is a variable increase in the isotopic signature of N due to the continued re-use of urea for protein and bone collagen synthesis during hibernation (e.g. Fernández Mosquera *et al*., 2001). With specific reference to cave bears, Nelson *et al*. (1998) and Pérez-Rama *et al*. (2011a; b) have further suggested that due to metabolic recycling of the mother's proteinaceous tissue, cave bear cubs were born with $\delta^{15}N$ values 5% higher that of their mother. In addition, a decrease in the carbon (C) isotopic signature of bears was linked by Bocherens *et al*. (1994a) to the processes of hibernation and, most particularly, to the use of lipids during dormancy.

It is therefore clear that bear species have an interesting and complex metabolism (aspects of which remain poorly understood), combined with a long weaning period and timing of eruption for almost all permanent teeth. In view of the potential impact of these factors on the geochemistry of their teeth, the conclusions from the pilot study presented in this thesis must be viewed as a first step towards better understanding of this topic.

The following sections present information on the ecology and dental development of the other large mammal species that were geochemically analysed in this study.

5.3.2. *Crocuta crocuta* (Spotted hyaena) Erxleben, 1777

5.3.2.1. Ecology

The spotted hyaena is nowadays restricted to sub-Saharan Africa but during the Pleistocene, this species had a much wider distribution in Asia, Europe and Africa (Werdelin and Solounias, 1991). Remains of hyaenas are plentiful in the British Pleistocene, especially from cave sites (Reynolds, 1902). Such remains have often been referred to in the literature as 'cave hyaena' (*Crocuta crocuta spelaea*), largely because of their abundance in cave sites, which hyaenas occupied as dens (evident from the frequent presence of coprolites, of characteristically-gnawed bones and of abundant deciduous teeth from young individuals [Reynolds 1902]). A close relationship between modern spotted hyaena and Pleistocene 'cave hyaena' has always been accepted and indeed, although there are some morphological differences between the two (e.g.

Nagel *et al*., 2004), there is no molecular basis for a phylogenetic division (Rohland *et al*., 2005).

Today, although the Hyaenidae family consists of only four species in three genera (*Crocuta crocuta*, *Hyaena hyaena*, *Hyaena brunnea* and *Proteles cristata*) (Wilson and Reeder, 2005), they show a remarkable diversity of ecological adaptation and social behaviour (Macdonald, 2009). Figure 5.14 presents information for *C. crocuta* regarding taxonomy, distribution, biology and size.

Systematics

Order: Carnivora Bowdich, 1821
Suborder: Feliformia Kretzoi, 1945
Family: Hyaenidae Gray, 1821
Genus: *Crocuta* Kaup, 1828
Species:

Crocuta crocuta Erxleben, 1777
(Spotted hyaena)

Additional information

Dental Formula of Spotted Hyaena: I/i 3/3; C/c 1/1; P/p 4/3 and M/m 1/1.

Geographic distribution (after Wilson & Reeder [2005], Macdonald [2009] and Bohm & Höner [2015]): Spotted hyaenas are widely distributed in Africa, south of the Sahara, except the Congo. There is also no confirmed evidence of their presence in Egypt, Lesotho, Liberia, Libya, Tunisia or Morocco and no recent records from Togo.

Biological information (after Law [2004] and Macdonald [2009]): *Crocuta crocuta* has a short-haired sandy, ginger or grey to brown coat with dark brown spots that are usually absent in very old animals. Females are heavily built and their sexual organs are almost indistinguishable from those of males, meaning that males and females look very similar. The clitoris is large and penis-like and the vaginal labiae are fused to form pseudotestes. Females give birth through the clitoris. Spotted hyaenas live in clans, with members sharing a territory and defending it against neighbours. All females are dominant to all males and females remain in their natal clan for their entire lives. Males leave their clan at subadulthood. Females are sexually mature at 2 to 3 years and males at less than 2 years. Mating is polygynous and aseasonal. The gestation period is approximately 4 months. Usually twins are born, but up to 4 offspring is known. Spotted hyaenas can live in the wild for up to 25 years and in captivity for up to 40 years.

Size (after Macdonald [2009]): Spotted hyaena head to tail length ranges from 1.3-1.85m and shoulder height is from 0.7-0.95m. The males weigh between 45-62 kg and females from 55-82.5kg.

Figure 5.14. Systematics and geographic distribution, biology and body size in *Crocuta crocuta*. Image from http://images.fineartamerica.com/images-medium-large/spotted-hyena-crocuta-crocuta-portrait-pete-oxford.jpg

Spotted hyaenas are a medium- to large-sized animal with relatively large and robust heads and forequarters heavier than their hindquarters (Ewer, 1973). The distinctive morphological features of the cranium and dentition reveal a top predator specialized for crushing large bones and cutting thick hides and tendons (e.g. Ewer, 1973; Wilson and Reeder, 2005; Macdonald, 2009). Some of these features include exceptionally robust teeth, strong muscles and a strong sagittal crest on the skull for attachment of

the temporalis muscle (Fig. 5.15) (Ewer, 1973). The relatively short jaws have a powerful grip, while the premolars are large and conical for effective bone crushing and the carnassials are specialised for slicing and shearing (Fig. 5.15 B and D) (Macdonald, 2009). Spotted hyaenas are not only scavengers but also very efficient at hunting (especially nocturnally) and making their own kills (Ewer, 1973).

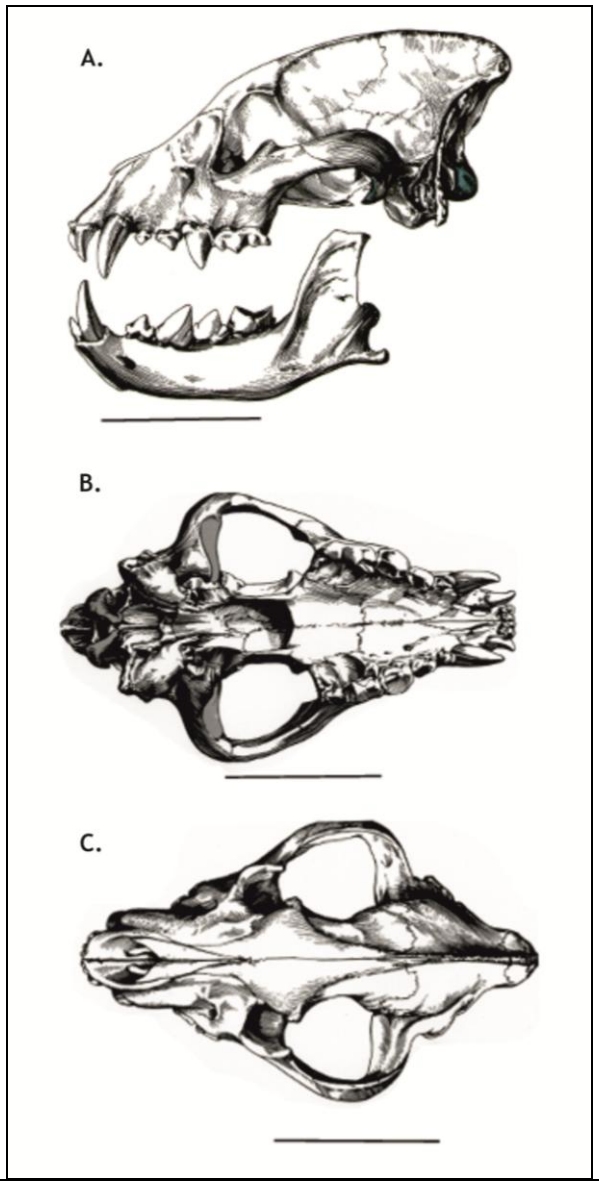

Figure 5.15. Cranium and mandible of spotted hyaena **A**. Lateral view (left side) of cranium and mandible ramus. **B.** Ventral view of cranium. **C.** Dorsal view of cranium. Scale 10cm (image modified from Pales and Lambert [1971]).

C. crocuta has been observed to eat a wide variety of prey, including wildebeest, zebra, Thompson's gazelle, other carnivores such as bat-eared fox, golden jackal and even other hyaenas, but also termites and birds (e.g. Ewer, 1973; Law, 2004). Hence, *C. crocuta* are the most abundant African large mammalian predator and are present

today in many different open, dry habitats such as semi-desert, savannah (where they occur at their highest densities) and acacia scrub, as well as mountainous forest (e.g. Law, 2004; Macdonald, 2009; Bohm and Höner, 2015). They are absent or occur only at low density in extreme desert conditions, at very high altitudes in mountain zones and in tropical rainforests (Bohm and Höner, 2015).

5.3.2.2. Dental development

Hyaenas are true predators. Their major dental specialisation concerns their ability to break up large bones, something that sets them apart from other carnivores (Ewer, 1973). Bone eating species experience the highest dental stress of any mammal (Rensberger, 1999). Certain structural features of the hyaena skull reveal their adaptations to the high stress caused by bone consumption, such as a vaulted forehead and broad palate (Werdelin and Solounias, 1991). Nevertheless, the most important specialisation in hyaenas is the shape of the teeth and, more specifically, the pyramidal shape of the premolars (Rensberger, 1999).

Although many studies have focused on the structure and particularly on the Hunter – Schreger bands in hyaena tooth enamel (e.g. Rensberger, 1999; Tseng, 2011), very little is known about the dental eruption sequence in hyaena (e.g. Van Horn *et al*., 2003) and indeed, more widely for other carnivores. Carnivore dentition is highly complex as each tooth performs a different function. Thus, the transition from milk to permanent dentition must take place without disrupting the functionality of the dentition as a whole (Ewer, 1973). According to Slaughter *et al*. (1974), carnivores can be separated in two types regarding their eruption sequences; these types can be considered as 'primitive' or 'advanced', according to the level of carnassial development for efficient meat shearing. Hyaenas are grouped with felids and canids in sharing a more specialised carnassial apparatus (Slaughter *et al*., 1974).

Van Horn *et al*. (2003) estimated the ages of spotted hyaena based on a tooth wear model. Their results regarding the tooth eruption are in agreement with those of Slaughter *et al*. (1974), specifically that deciduous incisors and canines erupt by birth and deciduous cheek teeth erupt by 2 months of age. Replacement of deciduous teeth begins with the incisors (1^{st}, 2^{nd} and 3^{rd} upper and 1^{st}, 2^{nd} and 3^{rd} lower in that order),

followed by the eruption of cheek teeth (1st, 4th, 3rd and 2nd upper premolars and 1st lower molar, 2nd, 4th and 3rd lower premolar in that order). The last teeth to emerge are the canines. Although Van Horn *et al*. (2003) established these data for hyaena teeth, details regarding the timing of individual tooth eruption were, however, limited. These authors stated that the permanent 1st incisor is present between 6.5 and 9 months of age, whereas the remainder of the permanent incisors erupt between 7.8 and 12 months, the permanent cheek teeth erupt between 10 and 15 months and all adult teeth are present by 13 to 18 months.

However, in order to interpret the geochemical data, more information is needed regarding enamel tooth formation and further details on the timing of eruption in the teeth. As neither of these details are available for hyaenas, similar information regarding eruption timing were gathered for *Canis lupus* and *Panthera leo.* These are deemed to be the closest appropriate comparators since both share the same specialised carnassial apparatus with hyaenas (Slaughter *et al*. (1974). Table 5.3 outlines the eruption sequence in *C. lupus* and *P. leo*.

Table. 5.3. Timing of birth and tooth eruption sequence in months of *Canis lupus* and *Panthera leo* (from Kohn and McKay [2012]). I = incisors, Ci = canine initial eruption, Cf = canine final eruption, P = premolars, M = molars, X = normally absent.

Species	Birth	I1/I2	Ci	Cf	P1	P2	P3	P4	M1	M2	M3
Canis lupus (Grey wolf)	**late-Apr**	3-4/4	4	6-7	3-4	5	5	5	4-5	5	5
Panthera leo (African lion)	**Apr-Jun**	8-13	11-15	28-36	X		15-20	15-20	11-15	X	X

According to the above table and the tooth eruption model suggested by Van Horn *et al*. (2003) for hyaenas, the African lion is most comparable in terms of the timing of tooth eruption to hyaenas and this sequence will therefore be adopted for all hyaena samples in this study. Hyaena cubs, in contrast to lion cubs, are weaned at 12 to 16 months (e.g. Pusey Packer, 1994; Macdonald, 2009; Law, 2004), so the enamel formed before that period would be expected to influence the geochemical signature. In hyaena tooth samples, the nursing signal would therefore be anticipated to have a modest effect on canines, premolars and molars.

5.3.3. *Cervus elaphus* (Red deer)

5.3.3.1. Ecology

Red deer (*Cervus elaphus*) is a member of the Cervidae Family. Fossil remains of red deer were abundant in Britain from the early Middle Pleistocene Cromer Forest-bed Formation onwards and are linked with a range of palaeoenvironmental conditions, from relatively warm and wooded to cool and open habitats (Reynolds, 1933; Lister, 1992). This ecological flexibility means that today, red deer has a wide global distribution (see also Figure 5.16. for further details on biology and body size).

At the present day, red deer inhabit open deciduous woodland, upland moors and open mountainous areas, natural grasslands, pastures and meadows (Lovari *et al*., 2008). Seasonal movements also take place (Figure 5.16), resulting in a seasonally varied diet. Red deer are generally regarded as mixed feeders and prefer fresh shoots, forbs and grasses (Senseman, 2002; Lovari *et al*., 2008). During summer, red deer feed on grasses, sedges and forbs, whereas during the winter months, they consume woody plants including shrubs and tree shoots, as well as occasionally mushrooms and lichens that are rich in protein (Senseman, 2002; Lovari *et al*., 2008). This seasonality in red deer diet should therefore be expected to be reflected in their geochemical signatures.

Systematics

Order: Artiodactyla Owen, 1848
Family: *Cervidae* Goldfuss, 1820
Genus: *Cervus* Linnaeus, 1758
Species:
Cervus elaphus Linnaeus, 1758
(Red Deer)

Additional information

Dental Formula of Red Deer: I/i 0/3; C/c 0-1/1; P/p 3/3 and M/m 3/3.

Geographic distribution (after Wilson & Reeder [2005] & Lovari *et al*. [2008]): Red deer has a wide global distribution extending from Europe and North Africa through central Asia, Siberia, the far East and North America. It has also been deliberately reintroduced to several countries where it had gone extinct including Belorussia, Estonia, Kaliningrad, Lithuania, Greece and Portugal.

Biological information (after Senseman [2002], Lovari *et al*. [2008] and Macdonald [2009]): Red deer are social animals and live in groups. Females and young individuals live in small herds and form larger groups during summer. Males are more solitary but also join herds during summer. Red deer frequently migrate to higher elevations during summer, returning to lower ground during winter. Mating occurs in late September or early October each year. During this period, stags vigorously defend their "harem" of hinds from rivals. The sexes separate before the calves are born. Individuals are sexually mature at about 1.5-2.5 years. Gestation ranges from 8-8.73 months and females give birth in June - July. In the wild, red deer live to about 15 years and in captivity until 27 years.

Size (after Senseman [2002]): Red deer have slender legs and a short tail, a long head and large. Males have branching antlers that reach a maximum width of 1.1-1.5m. Red deer body length ranges from 1.6-2.7m from nose to tail. Females weigh 171-292kg and males 178-497kg.

Figure 5.16. Systematics and geographic distribution, biology and body size in *Cervus elaphus*. Image from http://fc04.deviantart.net/fs23/f/2007/339/9/d/Red_Deer___Stock_by_Sassy_Stock.jpg

5.3.3.2. Dental development

Dental eruption in *Cervus elaphus* has been the subject of previous study (see Mitchell, 1967; Hillson, 1986; Brown and Chapman, 1991a; Azorit *et al*., 2002).

Red deer are born toothless and between 2 to 5 months, the deciduous premolars all erupt (Hillson, 1986). For the permanent dentition, according to Azorit *et al.* (2002),

based on their studies of red deer populations from southern Spain, the eruption sequence is as follows for the lower dentition: m1, i1, m2, i2, c, i3, premolars and finally, the m3. The m1 erupts at 6 months. By the age of 14 to 15 months, the m2 and i1 have also emerged. By 17 to 18 months, i2 and c erupt and between 19 to 25 months, i3 is fully erupted. Between 27 to 30 months, all the permanent premolars have come into wear. The sequence is completed by the m3, erupting between 31 to 32 months. (see Table 5.4.).

Table 5.4. Eruption sequence and age (in months) of permanent dentition of *Cervus elaphus* (adjusted from Hillson [1986], Brown and Chapman [1991a] and Azorit *et al*. [2002]).

m1	i1	m2	i2	c	i3	premolars	m3	References
6	14-15	15-16	17-18	17-18	19-25	27-30	31-32	Azorit *et al*., 2002
4-6	12-15	12-15	19	21		21-28	33	(in Azorit *et al*. [2002] from Mitchell [1967])
5-12		12-24				27-	23-	(in Hillson [1986] from Habermehl [1961])
0-5		13				26	26	Brown & Chapman (1991a)

However, as already discussed, since the geochemical signal is fixed during the matrix formation or mineralization, it is important to know the timing of enamel formation, in order to understand any potential influence on the results. Currently, there is no available published data on red deer enamel formation, however a study on fallow deer (*Dama dama*), based on radiographs of developing permanent molars was undertaken by Brown and Chapman (1991b) and may be used to interpret the same process in red deer (Table 5.5.).

Table 5.5. Eruption sequence (gingival emergence) in fallow deer (*Dama dama*) (from Brown and Chapman [1991a]).

m1	Erupted by 5 to 6 months
m2	Erupted by 13 to 16 months
m3	Erupting by 21 to 24 months, but not fully completed until 50 months

In their study, Brown and Chapman (1991b) calculated that formation of the m1 crown in fallow deer begins *in utero* and is completed at less than 4 months of age. m2 crown formation starts at 3.5 months and finishes at 9 months, whereas the formation of the m3 crown commences at 9 months of age and terminates before 18 months.

It is known that *C. elaphus* calves are weaned within the first 60 days of life (Senseman, 2002). Thus, the enamel formed before that period is expected to affect the geochemical signature but any enamel formed subsequently will reflect the plant

matter that the animal consumed during its life. Little if any geochemical influence from nursing is therefore expected in the enamel of both m2 and m3 in *C. elaphus*, since these teeth are formed after the weaning period.

5.3.4. *Equus* (Horse)

5.3.4.1. Ecology

Horses belong to the Order Perissodactyla. Equids first evolved in North America during the early Eocene, developing modifications for a cursorial mode and a progressive tendency for limb elongation and reduction in the lateral digits (Macdonald, 2009). During the Pleistocene, horses were present on all continents except Australia and Antarctica (Wilson and Reeder, 2005) and have generally been interpreted as reflecting open vegetation conditions (Stuart, 1976).

With the exception of rare wild populations such as the Przewalski's horse (*Equus ferus przewalskii*) of central Asia, modern equids are largely the product of anthropogenic domestication. All are specialist grazers with an elongated skull, long neck, high-crowned (hypsodont) cheek teeth and an extremely deep and massive lower jaw. Further information on the biology, body size and geographical distribution of modern horses is presented in Figure 5.17.

The extensive geographic range and the ecological success of equids are attributed to four key characteristics: their cursorial and springy gait; their grinding teeth, their large size and the lock position in their legs that enables them to rest (Macdonald, 2009).

Horses can adapt in a wide variety of habitats, however they favour cool, temperate grasslands, steppes and savannahs and occasionally semi-deserts (Clement, 2015). Equids consume mainly fibrous food. Their diet includes grasses and sedges; however they will also eat bark, leaves, buds, fruits and roots (Macdonald, 2009). There is a degree of dietary plasticity noted, with up to 50% browse taken during the winter season when grasses are less available (Rivals *et al*., 2010). The role of water is very important as they need to drink at least once a day.

Systematics

Order: Perissodactyla Owen, 1848
Family: *Equidae* Gray, 1821
Genus: *Equus* Linnaeus, 1758
Species:

Equus ferus ssp. przewalskii Poliakov, 1881
(wild horse)

Additional information

Dental Formula of Equid: I/I 3/3; C/c 0-1/0-1; P/p 3-4/3-4 and M/m 3/3.

Geographic distribution (after King *et al*. [2015]): The Przewalksii horse is the nearest modern analogue to the Pleistocene *Equus ferus*. Until the late 18th century, it was distributed from the Russian steppes east to Kazakhstan, Mongolia and northern China, but has suffered a dramatic decline in numbers since as a result of anthropogenic pressure. The last wild population survived until the mid-20th century in southwestern Mongolia and adjacent Gansu, Xinjiang and Inner Mongolia (China).

Biological information (after Luu [2002], Macdonald [2009] and Clement [2015]): The Przewalskii is the last true wild horse and the sole surviving ancestor of the modern domestic horse. In general, equids are highly social animals. They live in groups with a permanent membership consisting of a male and a few females that remain in the same "harem" throughout their adult lives. Females disperse when they become sexually mature at about 2 years old and males disperse by their fourth year to form bachelor associations. Females can breed annually (males sire foals in April to June) but most miss a year because of the physical effort to raise a foal. Mating and birth occur during the same season, since females come on heat 7-8 days after giving birth. The gestation period is from 11-12 months one foal is born during April or May. Young individuals start grazing within a few weeks after birth but are generally not weaned until 8-13 months.

Size (after Luu [2002]): The Przewalskii horse has a stocky body with robust short legs and a short neck. The head is very big with a long face and a powerful jaw. Nose to tail length is 210cm and to the shoulder 120cm. Weight ranges from 200-300kg.

Figure 5.17. Systematics and geographic distribution, biology and body size in *Equus przewalskii*. Image from http://animaldiversity.org/accounts/Equus_caballus_przewalskii/pictures/

5.3.4.2. Dental development

The sequence and timing of tooth mineralisation and eruption in modern equids are well documented (e.g. Penzhorn, 1982). The deciduous premolars are present at birth or appear within a couple of weeks afterwards (Hillson, 1986). As seen in Figure 5.18,

the first permanent tooth to erupt is the first upper premolar (P1) at 5 to 6 months, although this tooth is not always present (Bryant *et al*., 1996a; b). The first upper molar (M1) emerges at 7 to 12 months of age (e.g. Hillson, 1986; Bryant *et al*., 1996a; b), followed by the M2 at about 16 to 24 months, the P2 and P3 at 2.5 to 3.5 years (see also Fig. 5.18). The last to erupt are the P4 and M3 between the ages of 3 to 5 years. The sequence of eruption in the lower teeth is similar to that in the upper teeth, although slightly delayed by several weeks to months (Bryant *et al*., 1996b).

Some months or even years before tooth eruption, the mineralisation of the enamel takes place (Bryant *et al*., 1996a; b). The weaning period in horses starts at 9 to 15 months of age. Almost all permanent teeth should therefore be free from the effects of nursing in terms of their geochemical signatures, since they mineralise well after weaning. The only exceptions are the M1 and M2, which are wholly or partially mineralised before weaning (Bryant *et al*., 1996b).

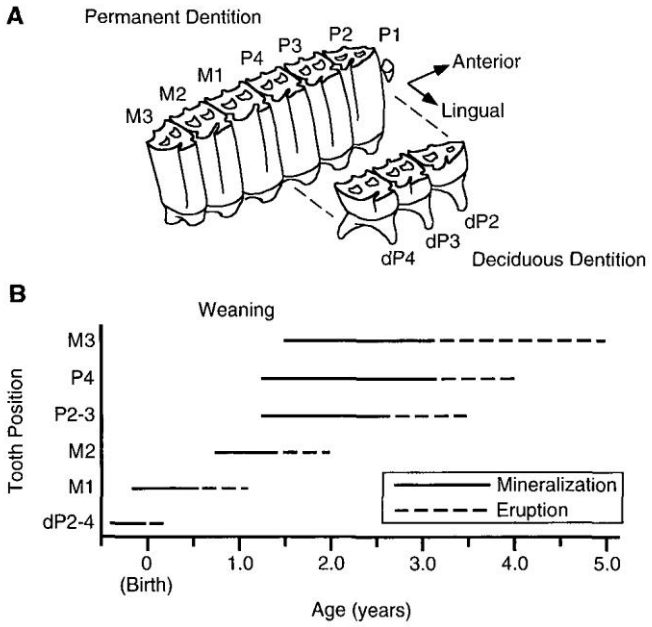

Figure 5.18. A. Permanent and deciduous right upper dentition (after Hillson [1986]). **B.** Timing and sequence of tooth eruption and mineralization (modified from Hillson [1986]; Bryant *et al*. [1996b]).

5.4. Materials and Methods

5.4.1. Case study: Tornewton Cave, Devon, UK

Fossil remains of brown bear and other mammalian species from Tornewton Cave in Devon (see 1.3 for location) were studied in this thesis in order to explore their geochemistry and to understand further aspects of the palaeoecology and trophic levels of these animals.

5.4.1.1. Site History – stratigraphy and palaeoenviromental summary

History

Tornewton Cave, which lies on the southwest side of the Torbryan Valley, near Ipplepen, Devon (grid ref: SX 81726737), has been put forward as a site with one of the most complete late Middle and Late Pleistocene sequences in Britain, spanning from MIS 7 through multiple phases of MIS 5 to MIS 2 (Currant, 1998; Schreve, 2001; Gilmour *et al*., 2007). James Lyon Widger was the first to discover the Torbryan Caves and the first to excavate Tornewton Cave around 1877 (Currant, 1998). Parts of Widger's collections are figured in Reynolds (1902, 1906, 1909, 1922). Further excavations were carried out by the Torquay Natural History Society between 1924-1926 and 1936-1939, following the evaluation by the archaeologist Dorothy Garrod of the many caves within the valley, amongst which Tornewton Cave was selected for further study (Garrod, 1924). From 1944 until the 1960s, further excavations were conducted at the site and Sutcliffe and Zeuner (1962) provide the most substantial account of the cave and its assemblages.

The most recent excavations were led by Andrew Currant from 1990–1992, on behalf of the Natural History Museum. These were the first systematic excavations, resulting in a comprehensive description of the stratigraphy that combined all of the previous stratigraphic descriptions and an up-to-date list of the faunal assemblages preserved within the cave (Currant, 1998). More recently, Gilmour *et al*. (2007) produced a number of U-series dates from an *in situ* stalagmite in the Main Chamber of the cave,

which extended from the cemented Bear Stratum (see below for description of the stratigraphic sequence), up through the Hyaena and Dark Earth Strata, thereby providing a geochronological framework for the deposition of the bone assemblages (Gilmour *et al*., 2007).

Stratigraphy

The cave consists of two sub-vertical phreatic rifts with associated horizontal passages (Fig. 5.19). The Main Chamber is the biggest one and has three separate connections to the outside: the Upper, Middle and Lower entrances. The connection of the Main Chamber with the Middle Entrance is through a narrow passage (the Middle Tunnel), whereas the Lower Entrance is an artificial one and has been enlarged to give access to both the Lower Tunnel and the Main Chamber. The smaller sub-vertical rift is known as Vivian's Vault (Currant in Roberts [1996]) (Fig. 5.19, top).

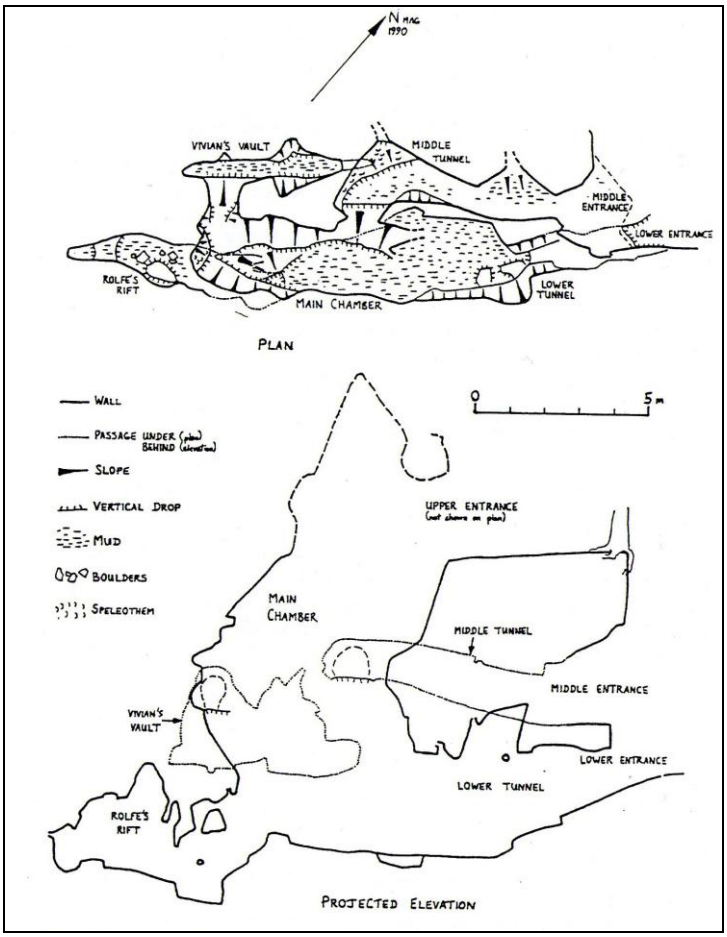

Figure 5.19. Tornewton Cave top: plan of the cave and below: projected elevation of the cave (after Proctor [1994]).

Tornewton Cave has a complex stratigraphy and undoubtedly, its interpretation is all the more complicated because of the different excavators involved and the use of different names for the various stratigraphic beds. A schematic profile of Tornewton Cave showing the stratigraphy of both internal and external deposits (from Sutcliffe and Zeuner [1962]), together with supplementary information regarding the nomenclature of different beds, is presented in table 5.6 and Figure 5.20. The faunal list from the cave is presented in table 5.7.

Table 5.6. Stratigraphy of Tornewton Cave (after Sutcliffe and Zeuner [1962]; Currant in Roberts [1996]). Description from base upwards (see also Fig. 5.20 and table 5.7 and text for supplementary information and details regarding the Otter Stratum).

Unit		Brief description
1	**Laminated clay**	Sterile water-lain clays and silts.
2	**Stalagmite formation**	Broken stalagmite clasts in the overlying Unit 3 were interpreted as representing a floor that had previously sealed Unit 1.
3	**Glutton Stratum**	A heavily-disturbed, compact cave earth containing abundant teeth and bone fragments of a variety of species (see table 5.7). Interpreted by Sutcliffe and Zeuner (1962) as accumulating under periglacial conditions.
4	**Bear Stratum**	Overlying Unit 3 and extending for the full length of the Main Chamber and Lower Tunnel. According to Sutcliffe and Zeuner (1962), there was no faunal distinction between this and the underlying Glutton Stratum, although the sediments of the former were distinctive in showing signs of internal stratigraphy and containing rock clasts of limestone rather than stalagmite.
5	**Stalagmite floor**	A thin and continuous sheet across the Main Chamber with individual stalagmites in the Lower Tunnel.
6	**Hyaena Stratum**	This deposit is interpreted as the product of a prolonged period of denning by spotted hyaena (*C. crocuta*). This bed is present throughout the Main Chamber and Lower Tunnel and consists mostly of teeth, bones and bone debris, hyaena coprolites and fragmented coprolitic material. Hyaena remains of all ages are abundant, comprising mainly teeth and metapodial elements. Other species were also found in this deposit (see table 5.7), the remains of many of which are heavily gnawed.
7	**Stalagmite floor**	Initially reported by Widger as 0.6m thick, re-examination of the remaining part of stalagmite by Sutcliffe and Zeuner (1962) suggested a thickness of 0.05m.
8	**Head** (presents only outside the cave)	A talus deposit that accumulated outside the Lower Entrance and which was considered to post-date Unit 6 by Sutcliffe & Zeuner (1962). Near the mouth of the cave, these deposits rested directly on top of Unit 1, with the remainder of the sequence apparently missing.
9	**Elk Stratum**	A thin deposit lying immediately on top of Unit 8 outside the Middle Entrance. This produced a rich fauna assemblage (see table 5.7). Lister (1994) later re-identified the cervid in this deposit, after which it was originally named, as red deer.
10	**Grey Loam**	A thin deposit overlying Unit 9 outside the Middle Entrance and in turn overlain by the "Reindeer Stratum" containing an assemblage attributed to an interstadial phase within the Last Glaciation.

Sutcliffe and Zeuner (1962) originally attributed the Hyaena Stratum (Unit 6) to the Ipswichian Interglacial and the Glutton and the Bear Strata (Units 3 and 4 respectively) were consequently assigned to the penultimate cold stage (MIS 6), on account of their positions below the Hyaena Stratum. Further excavations by Antony Sutcliffe in Vivian's Vault (Fig. 5.19, top) revealed a previously unrecorded deposit containing

abundant microvertebrate remains including white-toothed shrew (*Crocidura* sp., Rzebik, 1968), abundant bird bones, and teeth and bones of the clawless otter (*Cyrnaonyx antiqua*) (Currant, in Roberts [1996]). Sutcliffe and Kowalski (1976) referred to this Unit as the Otter Stratum and listed a number of other species (see table 5.7). According to them, this assemblage included two discrete faunal groups, the temperate elements belonging to the Ipswichian Interglacial (correlated with MIS 5e) and the cold-climate ones associated with the penultimate cold stage (MIS 6).

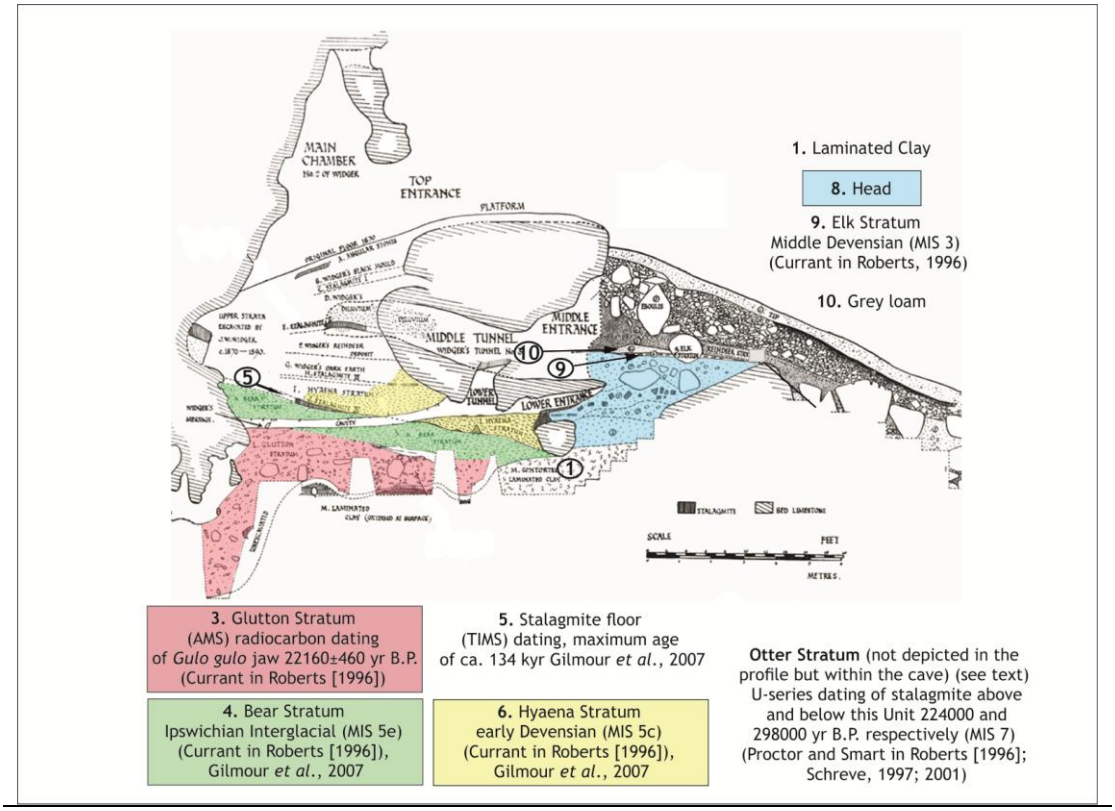

Figure 5.20. Tornewton Cave stratigraphical profile with dates where available (modified from Sutcliffe and Zeuner [1962]) (see also table 5.6 and 5.7 and text for supplementary information).

However, subsequent reappraisal of the collections from Sutcliffe's excavations has led to the partial reinterpretation of the Tornewton Cave sequence (Currant, in Roberts [1996]). The Glutton Stratum (Unit 3) assemblage was found to contain a much wider range of species than originally reported by Sutcliffe and Zeuner (1962) adding a strongly "temperate" aspect to what was supposed to be a cold-climate MIS 6 assemblage (Currant, in Roberts [1996]). The Glutton Stratum fauna was described by Currant and an admixture of temperate and boreal indicators and was re-assigned an age in MIS 2 (the Devensian/Weichselian Last Glacial Maximum, LGM). This was based

on direct radiocarbon dating of a wolverine (*Gulo gulo*) jaw, although the unit also contains material reworked from older deposits and appears to have been emplaced as a debris flow beneath the older Bear Stratum (Unit 4) some time around the LGM (Currant, in Roberts [1996]). Hence, it is likely that a major part of the cave became filled during the early part of the Devensian (MIS 5d-4 inclusive) and that the cave was largely sealed during the Middle Devensian (MIS 3). At this access point, appears to have been via the Middle Tunnel, where the "Elk Stratum" and its associated deposits have yielded the only characteristically Middle Devensian assemblage from the cave (Currant, in Roberts [1996]).

Further re-examination of *in situ* Bear and Hyaena Stratum deposits in a small cavern space at the back of the Main Chamber led to the recovery of large numbers of *Microtus oeconomus* (northern vole) molars in the Hyaena Stratum (Currant, in Roberts [1996]). This species would be unusual in an assemblage of Ipswichian age (see Sutcliffe and Zeuner, 1962). Furthermore, a microvertebrate fauna of clear interglacial character was subsequently recovered from the Bear Stratum (Cornish in Roberts [1996]). This led Currant (in Roberts [1996]) to suggest that the Bear Stratum should be attributed to MIS 5e (Ipwsichian Interglacial) and the overlying Hyaena Stratum to MIS 5c (early Devensian). This was subsequently supported by U-series dating of stalagmite deposits in Hyaena Stratum that have yielded age-estimates of ca. 134kyr (Gilmour *et al*., 2007) (see also Fig. 5.20).

During 1991 and 1992, new excavations in Vivian's Vault revealed a small remnant of *in situ* Hyaena Stratum, overlying a large fragment of *in situ* Bear Stratum against the wall of the Vault (Currant, in Roberts [1996]). Immediately beneath the Bear Stratum, a thin unit of barren clay was found to overlie a partly broken stalagmite floor containing pockets of sediments rich in *Crocidura* remains (the Otter Stratum). This demonstrated that the Otter Stratum was the oldest of the deposits within the cave and must therefore represent a pre-Ipswichian temperate episode (Currant, in Roberts [1996]). Schreve (2001) subsequently attributed the Otter Stratum to the Ponds Farm MAZ of early MIS 7. The Otter Stratum is overlain by deposits attributed to a debris flow during MIS 6 and containing species with cold-climate affinities such as *Lagurus* and *Cricetus* (Currant, 1998).

The material selected for the geochemical analysis (see also 5.4.1.3) in this study came mostly from the deposits of the two temperate sub-stages of MIS 5, namely MIS 5e (Ipswichian interglacial) and MIS 5c. The former is characterised by the development of mixed oak woodland and elevated summer temperatures, at least 2°C warmer mean summer temperatures than today (Candy *et al*., [2010] and references therein). Terrestrial evidence from deposits of MIS 5c age is very rare, however Currant and Jacobi (2001, 2011) and Gilmour *et al*. (2007) assigned faunal assemblages from parts of Bacon Hole and Minchin Hole (Gower peninsula, South Wales) to this interstadial. The faunal evidence indicates a transition from woodland to a more open grassland environment during this period with conditions still warm, although lacking the most thermophilous elements such as *Hippopotamus*. In addition, some specimens were also selected from the Elk Stratum, attributed to MIS 3 (Currant, 1998; Gilmour *et al*., 2007). This period is characterised by predominantly cold (but rapidly oscillating) climatic conditions and a steppe grassland environment with *Mammuthus primigenius*, *Coelodonta antiquitatis* and *Equus ferus* as typical elements of Currant and Jacobi's (2001, 2011) Pin Hole MAZ.

Table 5.7. Age and associated mammalian elements of the fossiliferous horizons (Units) from Tornewton Cave (see also Fig. 5.20 and text for supplementary information).

Units	**Age**	**Associated Fauna**	**References**
Otter Stratum	MIS 7 (Ponds Farm MAZ)	*Crocidura sp* *Crocidura cf. russula* *Sorex araneus* *Erinaceus europaeus* *Cyrnaonyx antiqua* *Apodemus sylvaticus* *Vulpes vulpes* *Meles meles*	Currant, in Roberts 1996; Proctor and Smart in Roberts 1996; Schreve, 1997; Currant, 1998; Schreve, 2001.
Bear Stratum	MIS 5e (Ipswichian Interglacial)	mainly *Ursus arctos*	Sutcliffe and Zeuner, 1962; Gilmour *et al*., 2007; Pappa *et al*., 2013
Hyaena Stratum	MIS 5c (early Devensian)	*Crocuta crocuta* *Canis lupus* *Panthera leo* *V.vulpes* *U. arctos* *Stephanorhinus hemitoechus* *Dama dama* *Cervus elaphus* A large bovid *Lepus sp* *Arvicola sp.*	Sutcliffe and Zeuner, 1962; Currant, in Roberts 1996; Currant, 1998; Gilmour *et al*., 2007
Head deposits		*Rangifer tarandus*	Sutcliffe and Zeuner, 1962; Currant,

			in Roberts 1996; Currant, 1998
Elk Stratum	MIS 3 (Middle Devensian)	*Equus ferus* *Coelodonta antiquitatis* *C. crocuta* *C. elaphus*	Sutcliffe and Zeuner, 1962; Lister, 1994; Currant, in Roberts 1996; Currant, 1998;
Glutton Stratum	MIS 2 (22160±460yrBP dates from *G. gulo* jaw)	*Gulo gulo* *R. tarandus* *U. arctos* *C. lupus* *P. leo* *V. vulpes*	Sutcliffe and Zeuner, 1962; Currant, in Roberts 1996; Currant, 1998

5.4.1.2. Site geology

A geological map of Tornewton Cave is shown below (Fig. 5.21).

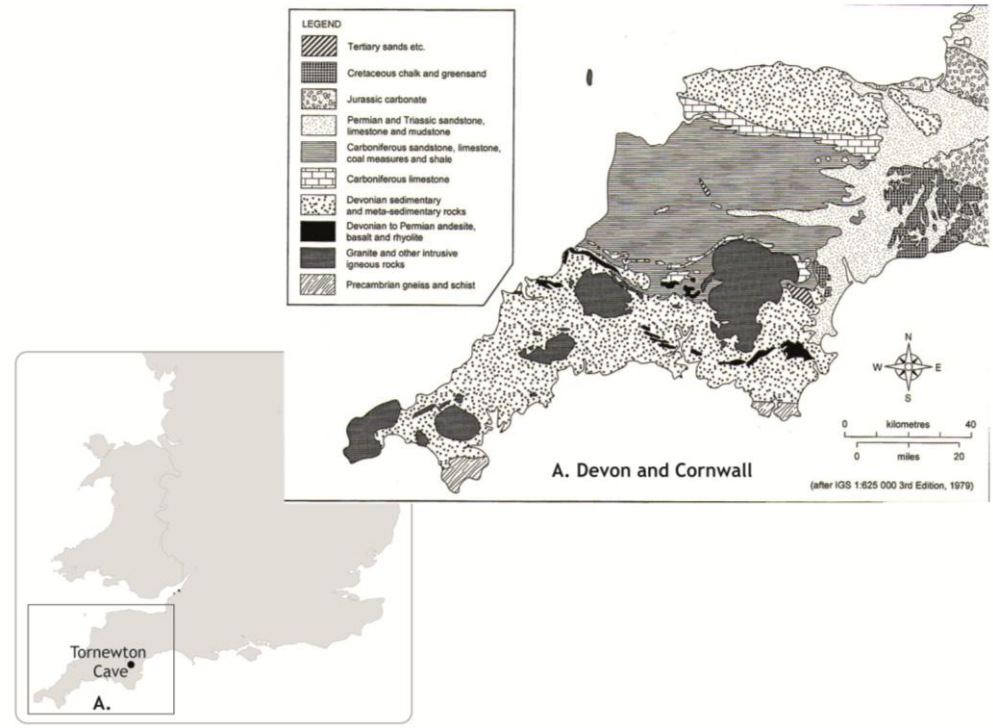

Figure 5.21. Map with Tornewton Cave and additional geological map (simplified) (A) for Devon and Cornwall (after Charman and Newnham [1996]).

The oldest rocks in the region form the basic igneous complex of the Lizard Peninsula, which may be of Pre-Cambrian age (Charman and Newnham, 1996; Campbell, 1998). According to Charman and Newnham (1996), during the Ordovician and Silurian, the region lay beneath a fairly shallow but extensive warm sea, as evidenced by the relatively small masses of exotic Ordovician quartzite and Silurian limestone, which occur within Devonian Beds at Meneage and Nare Head. The subsequent Caledonian

orogeny raised land to the north of the present peninsula, which drained southwards through swamps and deltas to the geosynclinal basin of the Devonian Sea. Lower Devonian sandstones, shales, conglomerates and some calcareous beds accumulated in this sea and at its margins, while the finer-grained deposits that form the succeeding Middle and Upper Devonian slates and mudstones reflect denudation of the northern landmass down to a low rolling plain (Charman and Newnham, 1996). In addition, locally, clear shallow water permitted the formation of coral banks as indicated by the numerous limestone outcrops between Plymouth and Torquay. The coral formation during the Devonian appears to have been interrupted at times by volcanic activity. These volcanic rocks are well exposed around Pentire on the north coast of Cornwall and they also outcrop intermittently between south-eastern Cornwall and Torbay. Volcanic activity subsequently accompanied formation of the silts and muds of the Lower Carboniferous (Charman and Newnham, 1996). During the Armonican orogeny at the end of the Carboniferous, the thick Devonian-Carboniferous sediments were folded along east and west axes together with faulting and thrusting and the development of slaty cleavages. Metamorphic activity resulted in the presence of granite, bosses of which (of late Carboniferous to Permian age) are the most distinguishing characteristics of the regional geomorphology. In the Torbryan Valley, the local bedrock comprises Lower Devonian slates and sandstones, Devonian limestones and Permian breccias, sandstones, mudstones and volcanics (Campbell, 1998).

5.4.1.3. Material

Fourteen of the 26 teeth that were initially selected from Tornewton Cave (housed in the Department of Earth Sciences in the Natural History Museum in London) were analysed by LA-ICPMS. The specimens are presented in Table 5.8, including additional information such as stratigraphic provenance. Images of each tooth prior to analysis are shown in Figure 5.22.

Table 5.8. Specimens from Tornewton Cave included in the present geochemical analysis (lower case letters denote lower teeth and upper case denote upper teeth) (see also photographs Fig. 5.22).

Registered number	**Species**	**Stratum info**	**Description**	**Side**	**Stage of wear** for bear specimens (after Stiner, 1998)
M92408	*E. ferus*	Reindeer/Elk Stratum (Stratum 5-6)	m3	Left	
M 92410	*C. crocuta*	Elk Stratum (Str. 6) coll. 1960	m1	Right	
M 38994	*C. crocuta*	Hyaena Stratum (UHS 2) coll. 1945	m1	Left	
M 41530	*C. elaphus*	Hyaena Stratum (UHS 2) coll. 1945	mandible with m3-m1	Right	
M 92414	*U. arctos*	Bear Stratum (BS/SB TN XVIIC) coll. 1960	m3	Right	IV
M 40750	*U. arctos*	Bear Stratum (BS3) coll. 1948	m3	Left	IV
M 41097	*U. arctos*	Bear Stratum (BS3/4) coll. 1945	m1	Left	IV
M 41397	*U. arctos*	Bear Stratum (BS9/LHS3) coll. 1948	m1	Left	III
M 40646	*U. arctos*	Bear Stratum (BS2) coll. 1949	C	Left	Unworn tip fully formed crown
M 40688	*U. arctos*	Bear Stratum (BS3) coll. 1948	C	Left	Unworn tip fully formed crown
M 41389	*U. arctos*	Hyaena Stratum coll. 1945	m1	Right	III
M 92417	*U. arctos*	Glutton Stratum (XVII) coll. 1959	m3	Left	IV

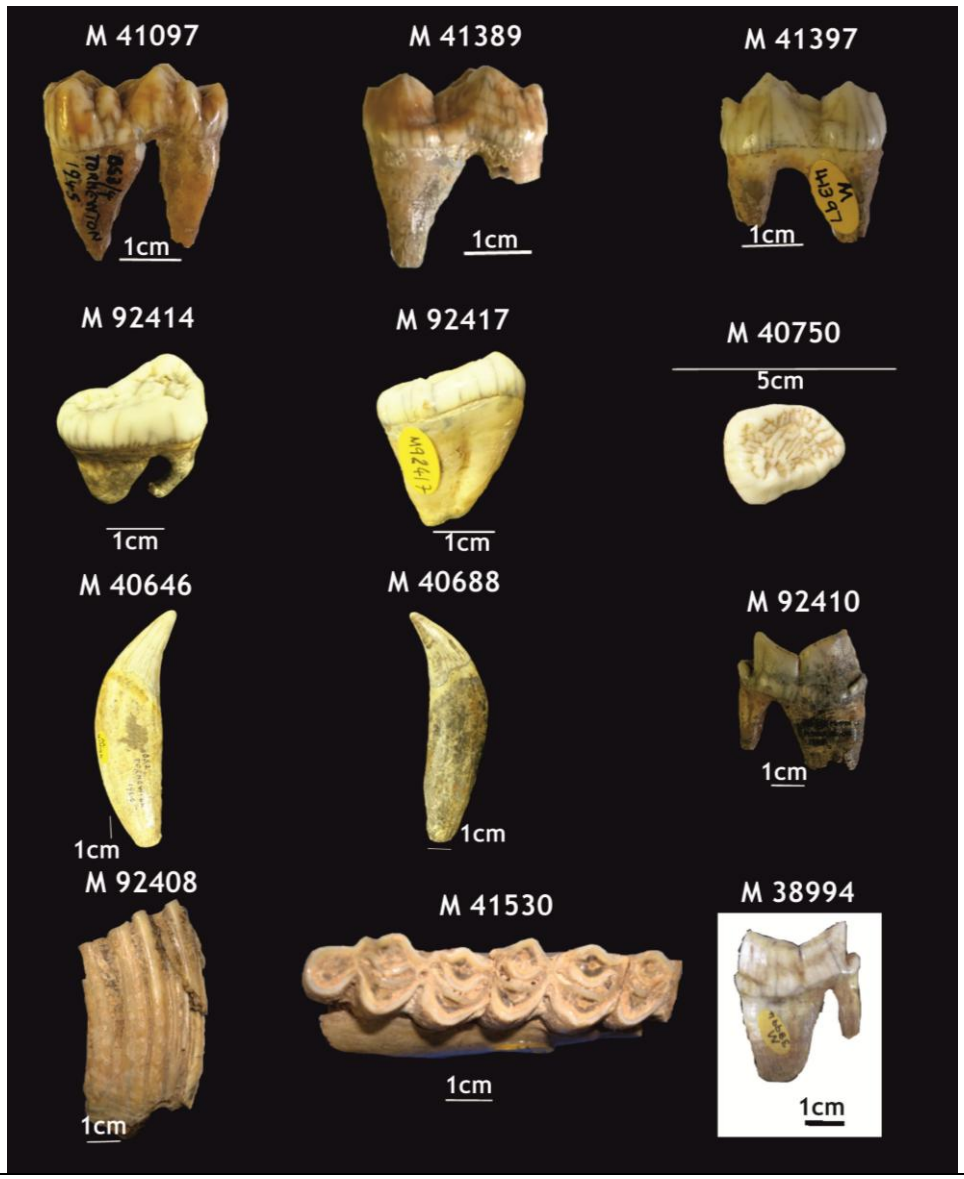

Figure 5.22. Photographs of the teeth from Tornewton Cave that were sampled by LA-ICP-MS (see also table 5.8 for supplementary information).

5.4.2. Methodology

5.4.2.1. Sample preparation

The technique followed in this study is a destructive sampling technique and as a result, part of each specimen was unavoidably destroyed during its preparation and analysis. However, efforts were taken to section the teeth in a way that would allow for them to be reconstructed after analysis. The sample was first cleaned with acetone, prior to preparation for a longitudinal section and the position of the section marked. The sample was then encased in Crystalbond^{TM}, a dissolvable resin that breaks down in acetone, ideal for temporary mounting. The mounting was done by melting small

pieces of Crystalbond onto aluminium foil (Fig. 5.23.A) and moulding it around the tooth until a thin layer of resin was created around the specimen (Fig. 5.23.B). This resin layer also enhanced stabilisation during the cross-sectioning of the tooth with a water-cooled diamond rotary saw, using a blade thickness of ~100-150 µm (Fig. 5.23. C and D). A thicker saw was used for bigger specimens such as the high crowned teeth of horse) (Fig. 5.23.E). By developing this method, the entire tooth, with the exception of the cross-sectioned surface, was protected. Cuts were placed so as to ensure the best inner enamel exposure, generally through the tips of the cusps and the thickest sections of enamel (Fig. 5.23.F).

After sectioning of the tooth, one half of it was embedded into epoxy resin blocks prior to LA-ICPMS analysis and the other half was retained (Fig. 5.23.G). Tooth cross sections selected for trace element analysis smaller than 5cmx2.5cm were embedded in epoxy resin blocks measuring approximately 5cm x 2.5cm (one or two teeth per block depending on tooth cross-section size) (Fig. 5.23.G). Tooth cross sections larger than 5cm x 2.5cm were stable enough to be placed into the laser sample holder without being mounted in epoxy and so were simply cut and polished. Each tooth cross-section was hand polished using wet 120, 600, 1200 and 2500 silicon carbide grinding paper to ensure that the EDJ was clearly visible when carrying out the LA-ICPMS (Fig. 5.23.H and I). Samples were then washed twice with de-ionised water in an ultrasonic bath for a total of 60 minutes before trace element analysis took place.

The LA-ICPMS causes minimum loss of material (~100 µm being the thickness for each cut), thereby allowing the specimen to be reconstructed afterwards for later study. After LA-ICPMS analysis, the polished tooth section that is encased in a block of combined Crystalbond and epoxy glue/resin can then be extracted by simply dissolving the Crystalbond with acetone. Reconstruction of the tooth can then be effected by simply gluing the two halves back together, thus allowing the specimen to be used for future metrical or morphological studies, for example.

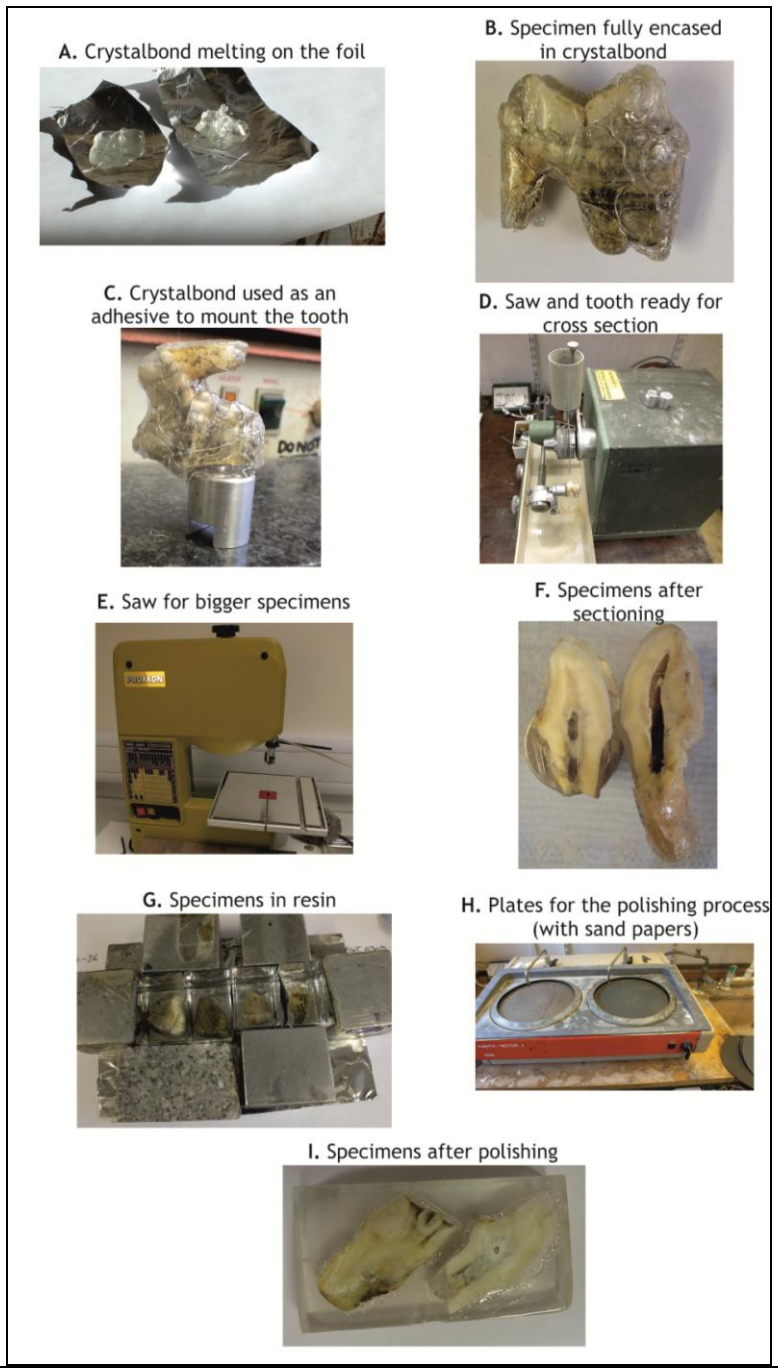

Figure 5.23. Specimen preparation for the LA-ICP-MS (see also text for supplementary information).

5.4.2.2. Analytical methodology

Solution Inductively-Coupled Plasma Mass-Spectrometry (ICP-MS) was, until recently, the most common way of introducing samples into the inductively-coupled plasma for elemental analysis. However, the development of laser ablation methods has yielded new opportunities for such analyses (e.g. Dolphin *et al*., 2005; Humphrey *et al*., 2008a). LA-ICPMS includes introduction (LA), ionisation (ICP) and detection (MS) steps. LA-

ICPMS was used here first for the analysis of trace elements in the teeth and eventually, to determine Sr/Ca ratios from sectioned enamel. The rationale for the choice of technique is summarized below in Table 5.9.

Table 5.9. Rationale for selection of the LA-ICPMS technique.	
1	Enamel thickness varies on each animal and is usually difficult to remove. This is rendered much easier using LA-ICPMS.
2	Teeth are the most informative and important elements from zooarchaeological and palaeontological collections but represent a finite resource. An analytical technique that gives accurate and reliable results and simultaneously uses the smallest amount of sample is therefore preferable.
3	LA-ICPMS is especially useful because it provides elemental concentrations within the sample and not just molecular information. This allows the analysis of trace elements.
4	Small amounts of certain elements that can be detected by LA-ICPMS may provide important information on animal physiology and life history (e.g. Humphrey *et al*., 2008b).

The laser ablation system in the Department of Earth Sciences at Royal Holloway University of London features the RESOlution M-50 prototype laser-ablation system (193 nm ArF excimer) coupled to an Agilent 7500ce/cs quadrupole ICPMS (Müller *et al*., 2009) (see also Fig. 5.24). Samples were placed on the sample holder (Fig. 5.24.D), cleaned with methanol, and then introduced into the LA chamber. At the beginning of each day of the analysis, the mass spectrometer was tuned using NIST 610 and 612 (US National Institute of Standards and Technology [NIST]) glasses to optimise the peak to background ratio, minimise noise and to calibrate the pulse and analogue detectors to ensure smooth transition between high and low concentrations.

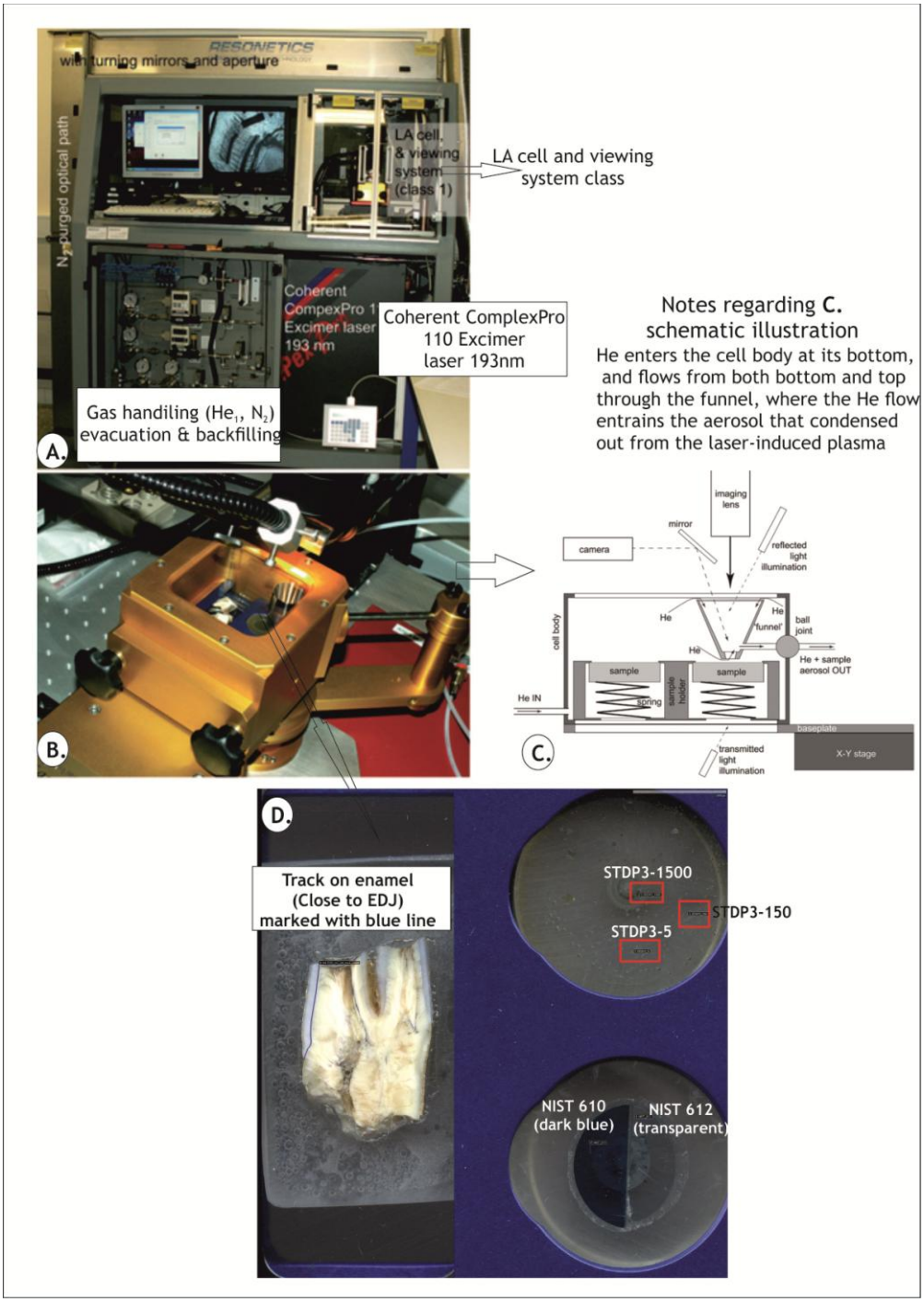

Figure 5.24. Photo of laser ablation unit A. (ICPMS not shown) showing photograph B. and schematic C. details of Laurin two-volume laser–ablation cell (modified from Müller *et al*. [2009]). D. Details of sample holder showing sample (M41530, *C. elaphus*, m2)), NIST 610 and 612 and STDP3-5, STDP3-150 and STDP3-1500 (see also text for supplementary information and appendix IIB folder 1 video 1 showing an example of the running procedure).

Tracks were created on the enamel surface close to the EDJ on each sample, without causing ablation of the dentine (Fig. 5.24.D). Table 5.10 presents the laser parameters that were followed on each tooth sample and on standards during the analysis.

Table 5.10. Details of the settings used for the LA-ICPMS.			
	Speed	**Repetition rate**	**Spot Size**
Cleaning	6mm/min	30Hz	74μm
Tooth Sample	1mm/min	15Hz	44μm
NIST 610 & 612 glass standards	Same as tooth sample	Same as tooth sample	Same as tooth sample
Phosphate glass international standards: STDP3-5, STDP3-150 & STDP3-1500	Same as tooth sample	Same as tooth sample	Same as tooth sample
MACs-3	Same as tooth sample	Same as tooth sample	Same as tooth sample

Standardisation of LA-ICPMS data is complicated by the control of the sample matrix in response to laser energy. Hence it is important to try to use matrix-matched standards where possible (Cucina *et al*., 2007). Phosphate glass international standards, STDP3-5, STDP3-150 and STDP3-1500 (values from Klemme *et al*., 2008) (see also Fig. 5.24.D) and pressed synthetic calcium carbonate pellet MACs-3 (values from Jochum *et al*., 2012) were used as matrix-matched standards in selected runs to allow the assessment of long-term precision and reproducibility (see also summary of settings table 5.10).

Calcium (^{43}Ca) was used as the internal standard as 37% of hydroxyapatite consists of calcium. Uranium (^{238}U) and the REEs - neodymium (^{146}Nd), cerium (^{140}Ce) and yttrium (^{89}Y) - were analysed as indicators of diagenetic alteration, since these are known to occur in very low concentrations in modern teeth. Lead (^{208}Pb), aluminium (^{27}Al) and manganese (^{55}Mn) were also analysed as additional alteration indicators, whereas measurements of Strontium (^{88}Sr), Barium (^{138}Ba) and Zinc (^{65}Zn) were made as indicators of palaeodiet variability.

Data reduction and the calculation of each element concentrations (in ppm) were completed using IGOR software and the Iolite plug-in with respect to Ca. Concentrations were normalised to Ca assuming a concentration of 37%, which implicitly assumes that all trace elements are hosted in bioapatite rather than in other tissue components. This assumption is accurate for enamel, which is c. 98% mineralised, but for dentine, which contains substantial water and protein, total tissue-normalised concentrations would be lower in the proportion of mineral mass to

total tissue mass (Kohn *et al*, 2013). In addition, in IGOR, the new reference values for NIST SRM 610 and 612 glasses were used, published by Jochum *et al*. (2011).

All data from each sample were then exported by using the NIST 612 (this was preferred to 610 because the recommended standard should be characterised by values close to sample values) to a Microsoft Excel spreadsheet where further data processing was carried out, including the creation of graphs, calculation of distance on each track (Table 5.11), comparison with modern published data and calculation of Sr/Ca, Ba/Ca and Zn/Ca ratios. For the precision and accuracy of the ICPMS, tables and graphs were produced in Excel showing results regarding STDP3 -5; 150 & 1500 and MACS-3 and the results compared with published data from Klemme *et al*. (2008) and from Jochum *et al*., 2011 respectively (see 5.5.1).

Table 5.11. Details of the steps used to calculate the distance on each sample (in mm).	
1	Find the last record in seconds from elapsed time (sec) on each sample
2	Find the scan speed of the main ablation (mm/sec) on each sample
3	Note the total number of points on each sample
4	Multiple step 1 x step 2
5	Divide step 4/3 This is the starting point in mm for the sample.

The limit of detection (LOD) or Limit of Blank (LOB) and Limit of Quantitation (LOQ) are terms used to describe the smallest concentration of a measurand that can be reliably measured by an analytical procedure (Armbruster and Pry, 2008). In this study, the Limit of Blank (LOB) was calculated for each sample by using Equation 1. The LOB of elements such as ^{238}U, ^{146}Nd, ^{140}Ce, ^{89}Y, ^{7}Li and ^{85}Rb are presented in Appendix IIA. According to Armbruster and Pry (2008), LOB is the highest *apparent* analyte concentration expected to be found when replicates of a blank sample containing no analyte are tested.

Equation 1: $LOB = mean_{blank} + 1.645(SD_{blank})$

5.5. Results of the Geochemical Analyses

This Chapter introduces the results of the geochemical analyses of fossil mammalian species from Tornewton Cave, Devon. For each sample, element concentration variations along the tracks are presented, together with variations in Sr/Ca, Ba/Ca and Zn/Ca.

5.5.1. Precision and accuracy of trace element analysis

In order to allow the precision and accuracy of the ICP-MS to be calculated, phosphate glass international standards (STDP3-5, STDP3-150 & STDP3-1500) and MACs-3 were analysed daily alongside the tooth samples.

The phosphate glasses were selected because (1) they encompassed the range of concentrations that are expected to occur in the analysed tooth samples and (2) they have the same matrix as the enamel so are expected to respond in a similar way to the laser energy (Klemme *et al*., 2008). On occasions when the phosphate glasses were not available, pressed synthetic calcium carbonate pellets (in this case MACs-3) were used for the same purpose (Jochum *et al*, 2011). In this study, international phosphate glass standards (STDP3-5, STDP3-150 & STDP3-1500) were used seven times during three days of analysis. Figures 5.25 to 5.27 present the performance of the ICP-MS calculated from the international phosphate glasses run throughout the tooth analyses. In addition, table 5.12 shows that relative two standard deviations (2 RSD) and averages for STDP3-5, STDP3-1500 and STDP3-150 for most elements (in bold) are within the acceptable limits of published data. The precision of Nd is poor within all STDP3 glasses, due to extremely low concentration of this element within these standards, as can be observed from the published data (Klemme *et al*., 2008) Nd: 0.04ppm; 0.02ppm and 0.01ppm respectively for STDP3-1500 and STDP3-150 and STDP3-5 (table 5.12). Additionally, Zn shows high 2 RSD on all standards and should therefore be treated with caution. Unfortunately, there are no published Zn values for the STDP glasses. Pb also shows high variability with double the acceptable limit 2 RSD value, which is 0.6ppm (Klemme *et al*., 2008).

Figures 5.25 to 5.27 illustrate the accuracy of the ICP-MS by comparing the known average element concentrations within the international phosphate standards (Klemme *et al*., 2008) with the concentrations obtained by the ICP-MS during the different time/day of analysis. For Mn and Zn there are no available published data from Klemme *et al*. (2008). In general, the accuracy of the remaining elements varies between each of the standards. It is also important to mention that on the second day of analysis (31/03/13), the tracks obtained from the STDP3s were shorter than on the other days because the surface of the standard was not sufficiently polished; this potentially influenced the performance of some elements (e.g. Zn, Fig. 5.26).

More precisely, Figures 5.25. A and B illustrate the performance of elements against STDP3-1500. The accuracy of the elements during the first day (12/03/13) of analysis is considered to be high; there is minimal variability and most of the elements present highly stable concentrations throughout the day, with the sole exception of Zn concentrations around noon. The values obtained from both the second (31/03/14) and third days (01/04/14) of analysis are similar to those of the first day. In summary, the average concentrations obtained by ICPMS for STDP3-1500 are very close, for most elements (excluding Rb and Pb), to those published by Klemme *et al*. (2008), indicating very good performance of the equipment.

Figures 5.26. A and B display the performance of elements for STDP3-150. The only outlier is the average Zn concentrations on day two of the analysis, as previously mentioned. As for STDP3-1500, Rb average values in STDP3-150 were slightly lower on the second and third days in comparison to the first day. Most elements are within or close to international standards (Klemme *et al*. [2008]) with Rb and Pb average values being slightly lower.

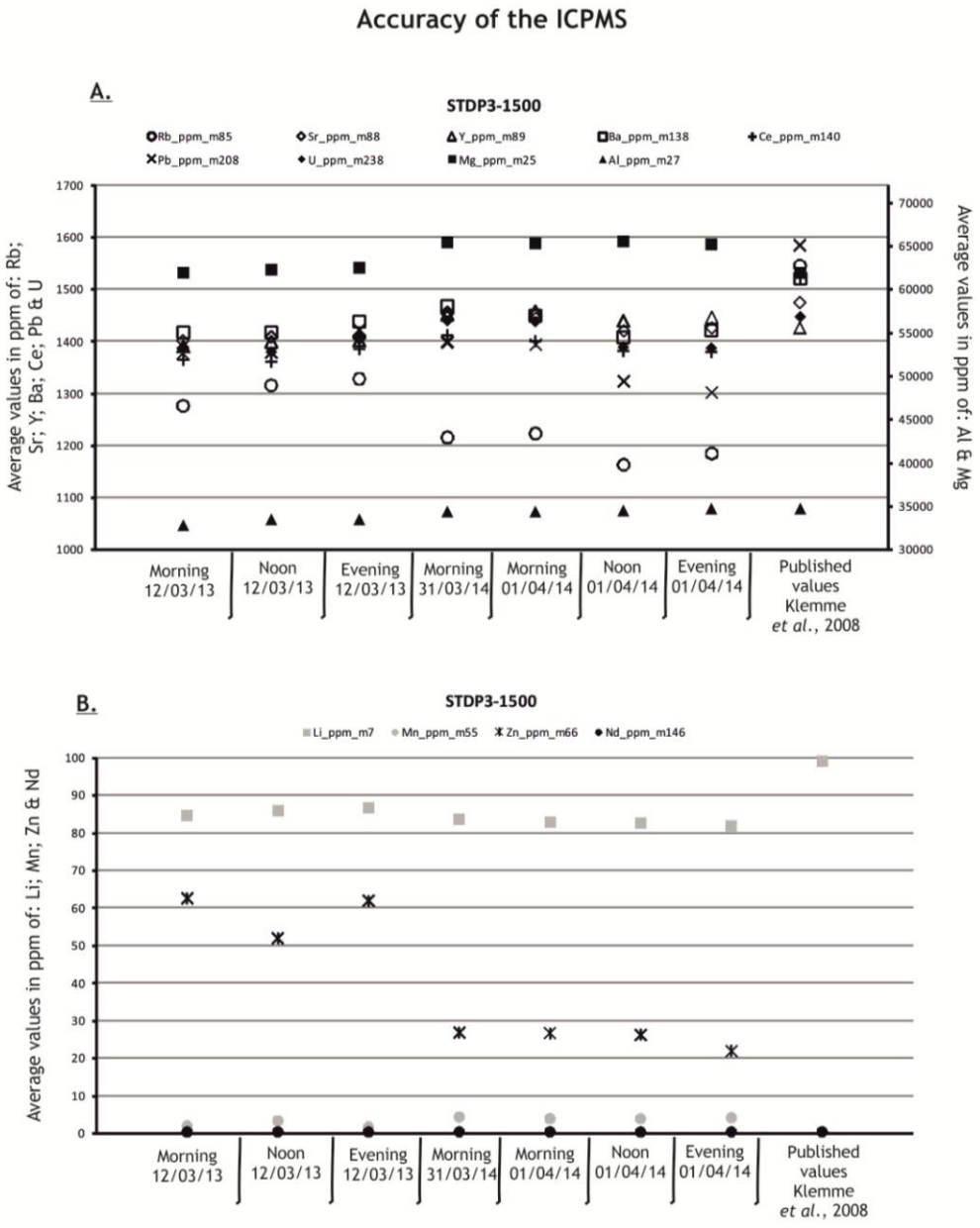

Figure 5.25. Accuracy of the ICP-MS demonstrated through average values of all element concentrations included in the **STDP3-1500** phosphate glass across different days and times of analysis, compared to average published values of elements from Klemme *et al*. (2008).

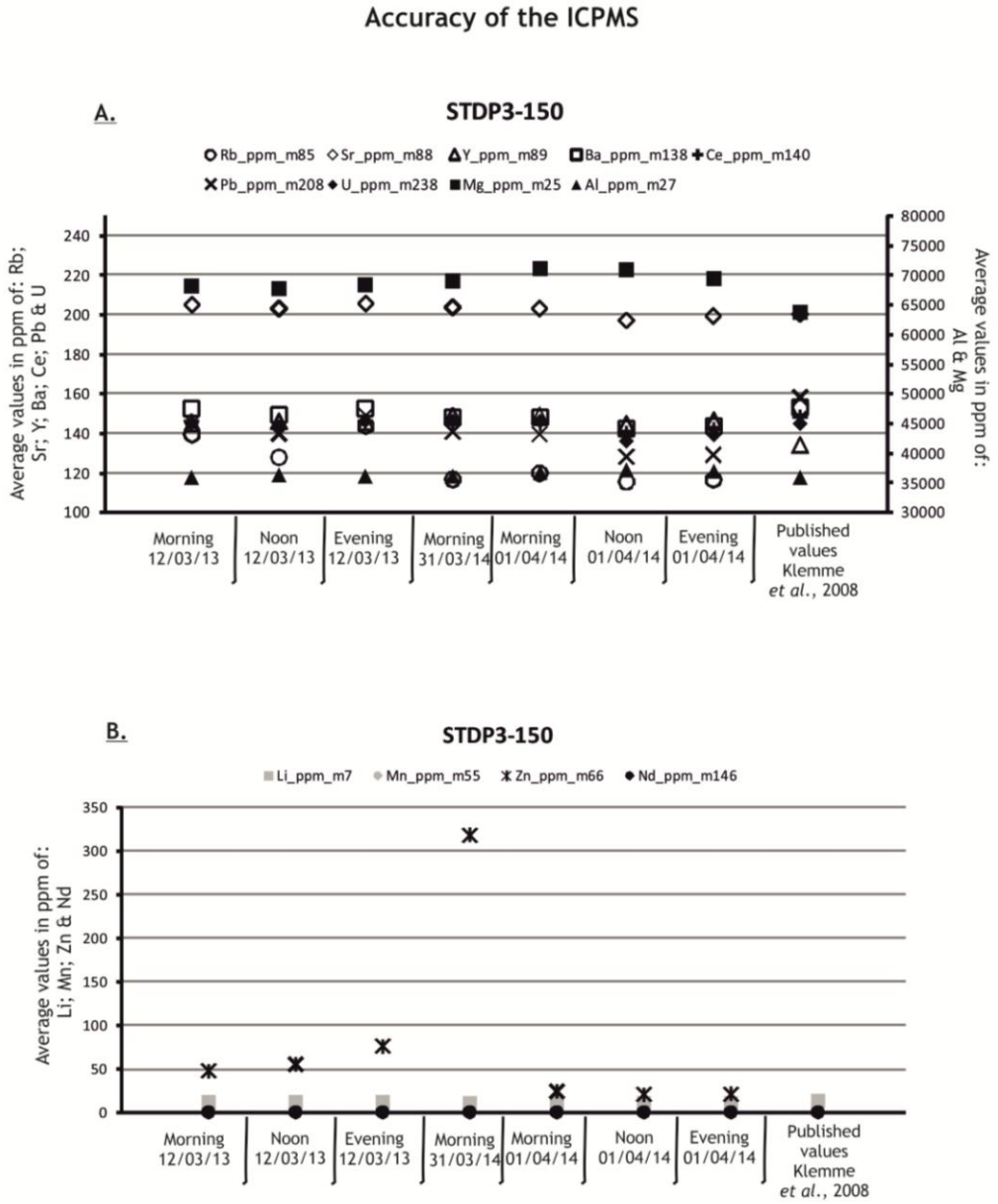

Figure 5.26. Accuracy of the ICP-MS demonstrated through average values of all element concentrations included in the **STDP3-150** phosphate glass across different days and times of analysis, compared to average published values of elements from Klemme *et al*. (2008).

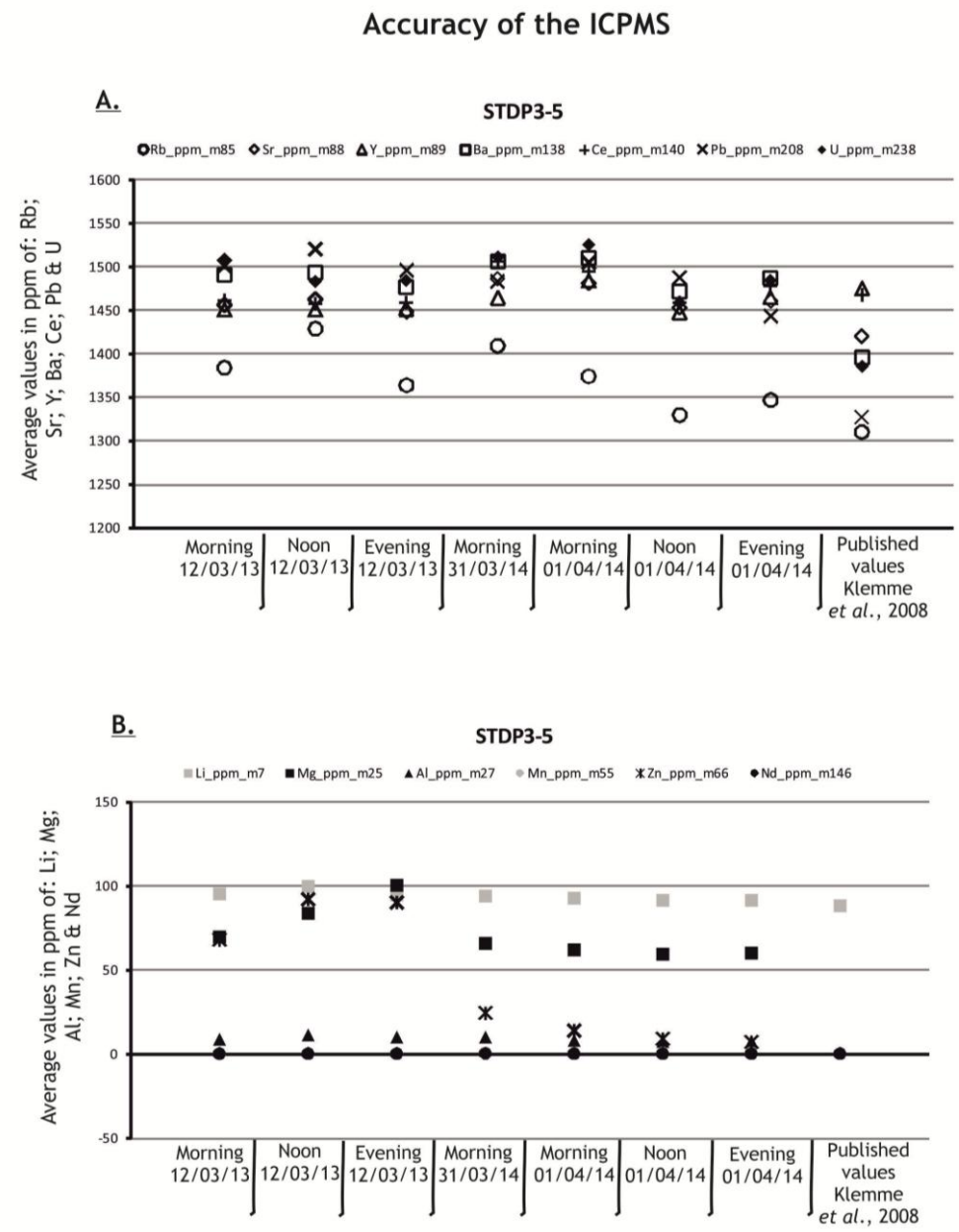

Figure 5.27. Accuracy of the ICP-MS demonstrated through average values of all element concentrations included in the **STDP3-5** phosphate glass across different days and times of analysis, compared to average published values of elements from Klemme *et al*. (2008).

Table. 5.12. Precision of ICP-MS for the three phosphate glasses analysed (STDP3-1500, STDP3-150, STDP3-5) in comparison with the relative two standard deviations (2 RSD and average) data from Klemme *et al*. (2008). In bold black type are all values within accepted and published values and in red bold type, those that are slightly higher.

		^{7}Li	^{85}Rb	^{86}Sr	^{89}Y	^{138}Ba	^{140}Ce	^{146}Nd	^{208}Pb	^{238}U
STDP3-1500	Values from this analysis									
	Average	**84**	**1238**	**1420**	**1427**	**1426**	**1380**	**0.38**	**1360**	**1400**
	2 RSD	**0.08**	**0.11**	**0.05**	**0.05**	**0.04**	**0.05**	**0.59**	**0.08**	**0.05**
	Values from Klemme *et al*. (2008)									
	Average	99	1545	1474	1426	1520	1522	0.40	1584	1446
	2 RSD	1	12	6	7	5	6	0.04	13	7
STDP3-150	Values from this analysis									
	Average	**11**	**127**	**202**	**146**	**148**	**144**	**0.17**	**138**	**142**
	2 RSD	**0.20**	**0.19**	**0.05**	**0.04**	**0.07**	**0.05**	**0.96**	**0.13**	**0.0705**
	Values from Klemme *et al*. (2008)									
	Average	12.8	153	200	134	153	148	0.19	158	145
	2 RSD	0.2	1.4	0.6	0.8	0.7	0.9	0.02	0.6	1.0
STDP3-5	Values from this analysis									
	Average	**95**	**1377**	**1461**	**1458**	**1489**	**1468**	**0.27**	**1494**	**1492**
	2 RSD	**0.09**	**0.06**	**0.04**	**0.04**	**0.04**	**0.05**	**0.44**	**0.06**	**0.06**
	Values from Klemme *et al*. (2008)									
	Average	88	1310	1420	1475	1396	1468	0.25	1327	1385
	2 RSD	1	8	4	3	10	12	0.01	15	21

Figures 5.27 A and B present the average element concentrations in comparison with published data from Klemme *et al*. (2008]) for STDP3-5 glass. Most average values on STDP3-5 from the ICP-MS are very close with the published values (from Klemme *et al*. [2008]) with the exception of Pb and Rb, which are higher than the published values. Thus, Pb data should be treated with caution while Rb is not considered in this thesis as an important element. Additionally Mg and Zn display lower values during the second and third day in comparison with the first day of analysis.

During the fourth and final day of samples analysis, an additional phosphate glass standard, the MACs-3, was included in order to check the performance of the ICP-MS. Table 5.13 reports all the elements that were analysed against the MACs-3 and their average and standard deviation values in comparison with published data from

Jochum *et al*. (2011). Concentrations of most elements are well within acceptable limits in comparison with the published data Jochum *et al*. (2011).

Table. 5.13. Precision of ICP-MS of MACs-3 element values (average and standard deviation [STDEV]) analysed in comparison with average and standard deviations (STDEV) element values from Jochum *et al*. (2011).

	^{7}Li	^{25}Mg	^{27}Al	^{55}Mn	^{66}Zn	^{85}Rb	^{86}Sr	^{89}Y	^{138}Ba	^{140}Ce	^{146}Nd	^{208}Pb	^{238}U
Values from this analysis													
average	62.62	1895	168	512	132	0.07	6268	19.0	53.4	10.3	9.7	60.0	1.17
STDEV	7.09	214	18	64	23	0.05	735	1.6	5.4	1.1	0.9	7.3	0.25
Values from Jochum *et al*. (2011)													
average		1880	403	532			6570	22.9	58.9	11.5	11.5		1.38
STDEV		70	48	23			170	0.6	1.9	0.4	0.4		0.05
Values from this analysis													
average	63.76	1851	183	512	138	0.10	6399	20.2	56.4	10.8	10.4	67.7	1.24
STDEV	7.15	147	25	44	20	0.14	619	1.3	5.6	0.9	0.9	6.6	0.21
Values from Jochum *et al*. (2011)													
average		1880	403	532			6570	22.9	58.9	11.5	11.5		1.38
STDEV		70	48	23			170	0.6	1.9	0.4	0.4		0.05
Values from this analysis													
average	63.18	1909	173	530	142	0.10	6551	19.1	55.2	10.5	9.9	64.6	1.26
STDEV	8.16	228	30	60	24	0.07	946	1.6	6.8	1.0	1.0	8.4	0.26
Values from Jochum *et al*. (2011)													
average		1880	403	532			6570	22.9	58.9	11.5	11.5		1.38
STDEV		70	48	23			170	0.6	1.9	0.4	0.4		0.05
Values from this analysis													
average	61.75	1910	180	517	130	0.09	6562	19.4	55.3	10.2	9.8	70.1	1.24
STDEV	5.48	164	27	44	16	0.16	1050	1.2	7.6	0.9	0.9	40.4	0.38
Values from Jochum *et al*. (2011)													
average		1880	403	532			6570	22.9	58.9	11.5	11.5		1.38
STDEV		70	48	23			170	0.6	1.9	0.4	0.4		0.05

5.5.2. Results high-resolution trace element analysis for each species from Tornewton Cave

This section presents the high-resolution LA-ICP-MS trace element data from all samples studied from Tornewton Cave.

The individual species are considered in turn. The first section for each species presents the element variations expressed as concentrations (ppm) along each track from the cusp (tip of the profile, oldest enamel) to the base of the crown (end of the profile, youngest enamel) in each tooth sample (subsequent analysis follows the same pattern, from the oldest to the youngest enamel). Sr, Ba and Zn concentrations are presented first, followed by U and Mg concentrations and then finally, the Rare Earth Elements (REE) and Al, Mn, Pb and U patterns are presented in order to identify any potential diagenesis. Elements with similar behaviour are plotted together in order to observe more readily those that bioaccumulate together, those that do not and those that are good indicators of diagenesis.

This is followed by an assessment of REE in each sample in comparison with published data (e.g. Kohn *et al*., 1999; Kohn *et al*., 2013) in order to provide a second test of *post mortem* diagenesis.

The Chapter concludes with a discussion of within-tooth variation in the high-resolution Sr/Ca, Ba/Ca and Zn/Ca ratios in order to explore the diet variation for each species and finally, to reconstruct the food web from Tornewton Cave.

5.5.2.1. Results for *U. arctos* teeth

5.5.2.1.1. Element profiles of *U. arctos* samples

A single track from each of the eight bear teeth from Tornewton Cave was analysed, with the exception of one sample (an m3, registered number M40750), in which representative elemental behaviour (Sr, Ba, U and Al) were examined across two tracks, in order to enable comparison of elemental behaviour in both anterior (left track) and posterior (right track) parts of the tooth.

Representative laser ablation tracks from each of three different sectioned bear teeth from Tornewton Cave are shown in Figure 5.28.

Figures 5.29 to 5.33 reveal the different element concentrations in each sample. The Y-axis shows different elemental concentrations in parts per million (ppm), whereas the X-axis records distance (in mm) from the oldest enamel (tip of cusp/start of profile) to the newest (base of crown/end of profile) on each tooth. Lines from each element connect consecutive measurements along the track (following the profile of each tooth), making it easier to observe short- and long-term trends within the data for each tooth.

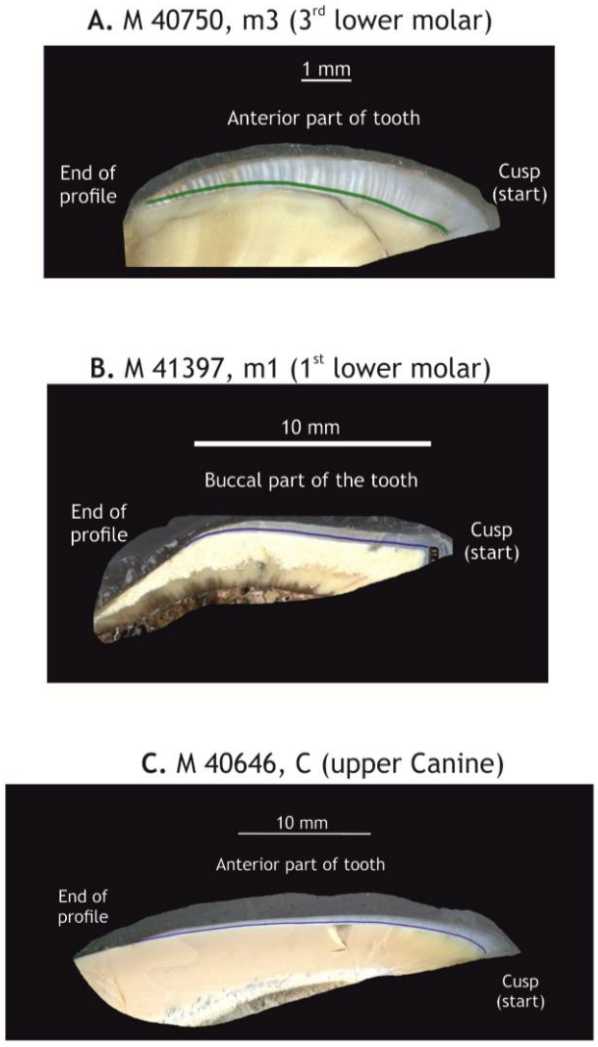

Figure 5.28. Representative laser ablation tracks marked with green or blue lines on each of three bear tooth samples from Tornewton Cave (NHM specimens). The start and end of each profile are located close to the EDJ.

In Figure 5.29, several different patterns are apparent in the Sr, Ba and Zn concentrations of each sample. In general, Sr covaries with Ba, whereas Zn does not. However, in some samples, peaks in Ba and Zn are synchronous, for example Figure 5.29.B at 0.2mm and approximately 3mm, Figure 5.29.C at 1mm and 4.5mm, Figure 5.29.D at 8.2mm, Figure 5.29.E at 2mm and Figure 5.29.H at 4.8mm, 8mm, 8.5mm, 11mm and 28mm. These peaks may therefore be linked to cracks or other post-depositional alterations. This will be discussed further with reference to other elemental behaviour such as that of Al, Mg, U and the REE. The results from each tooth will be described below.

Both M40750 and M92414 (m3s) show broadly similar patterns variability in Sr, Ba and Zn (Fig. 5.29.A and 5.29.B). Initial Sr and Ba concentrations remain relatively flat for the first ~2mm while both samples show a decrease in Sr and Ba at around 2mm. Whereas in M40750, the concentrations continue to decrease until the end of the track, in M92414, the Sr concentration rises slowly back up to its initial levels and Ba concentration plateaus. In addition, both concentrations of Sr and Ba are higher in M92414 (260ppm and 170ppm, respectively) than in M40750 (200ppm and 155ppm, respectively). Both samples have Zn concentrations that are initially flat but which become significantly higher in concentration and with greater variation from about 3mm to the end of the track.

Furthermore Figure 5.29.A compares Sr and Ba elements between the right (posterior part of the tooth) and left (anterior part of the tooth) tracks in M40750. In general, there is a decrease in Sr concentration from older to newer enamel along both tracks, with Sr values in the left track being slightly higher (ranging from a maximum of 208ppm to a minimum of 138ppm) than in the right track (declining from 90ppm to 173ppm) (Fig. 5.29.A). Ba shows more variability on the left track in comparison with the right, however there are some overlaps between them at 0.5mm, 4-4.6mm and 5.7-6mm. Moreover, on the right track, Ba displays three distinct peaks that are missing from the left track, at 1.3mm, 3mm and 4.9mm, and which might be linked to the presence of cracks.

In M92417 (m3, Fig. 5.29.C), there is a general decline in both Sr and Ba concentrations along the track, with both elements displaying a relatively similar trend. This specimen, in comparison with the two other third molars, displays lower Sr concentrations (between 120ppm to 160ppm) (Fig. 5.29.C) and the pattern is slightly different from the other two. At 0.7mm, there is a sharp dip in concentrations of both elements, followed by a levelling-out for both and then a progressive decline (Sr from 165ppm to 129ppm and Ba from 17ppm to 8ppm) (Fig. 5.29.C). The decrease in both elements is interrupted at 4.4mm by a brief peak, in which Ba concentrations are stronger than for Sr. In contrast to Ba and Sr, Zn concentrations show an increase after 1mm, with values going from 18ppm to over 30ppm. Similar to the Sr and Ba patterns, Zn also shows a spike at 4.4mm, most probably related to the presence of a crack.

The results of Sr and Ba concentrations for all m1 bear samples, M41097 (Fig. 5.29.D), M41397 (Fig. 5.29.E) and M41389 (Fig. 5.29.F) display generally very similar patterns. Sr levels remain almost flat in all samples until 8mm, after which they present a small increase for sample M41097, while for M41397 and M41389, they continue almost unchanged. In addition, M41097 exhibits higher Sr concentrations (between 190 and 230ppm) than both M41397 and M41389 (around 110ppm and 130ppm respectively). The patterns in Ba reveal some differences in each m1 samples.

For example Ba in M41097 displays a gradual small increase until approximately 8mm, after which it fluctuates until almost the end of the profile where it reaches its maximum concentration (above 35ppm). While Ba concentrations are less variable in both M41397 and M41389, in the former, it peaks early in the profile, at 2mm, and in the latter, it increases slowly after 1.4mm until 6.2mm (from 14.6ppm to a maximum 18.9ppm) and then gradually decreases until 8.9mm, after which it shows a slight increase until the end of the profile. Zn-concentrations display high variability along the tracks with a cyclical pattern of rise-fall-rise in both M41097 and M41389, while in M41397, it shows a very similar pattern to Ba in this sample.

The last two Figures, 5.29. G and H, depict elemental patterns for two canine teeth. In general, all elements in both teeth show similar variability, with Zn fluctuating more than both Sr and Ba and presenting several peaks along both sample tracks. Sr

demonstrates minor variability at the start in both samples until 15mm in M40646 (Fig. 5.29.G) and until 11mm in M40688 (Fig. 5.29.H). After those points, there is a progressive increase in Sr in both tracks until almost the end, with concentrations reaching as high as 262ppm on M40646 and 350ppm on M40688. The latter, however, demonstrates slightly higher variability with some narrow peaks in the last 3mm. Ba trends are slightly different across the two samples. For example in M40646, variability is minimal until 22.8mm and Ba then fluctuates between 12ppm and 15ppm before continuously increasing from 22.8mm onwards. On the other hand, in M40688, Ba concentrations are highly variable until 10mm, with multiple narrow peaks co-varying with some in Zn. After 10mm, there is an increase until the end of the track, with the highest levels of Ba in the last 3mm of the profile (44ppm).

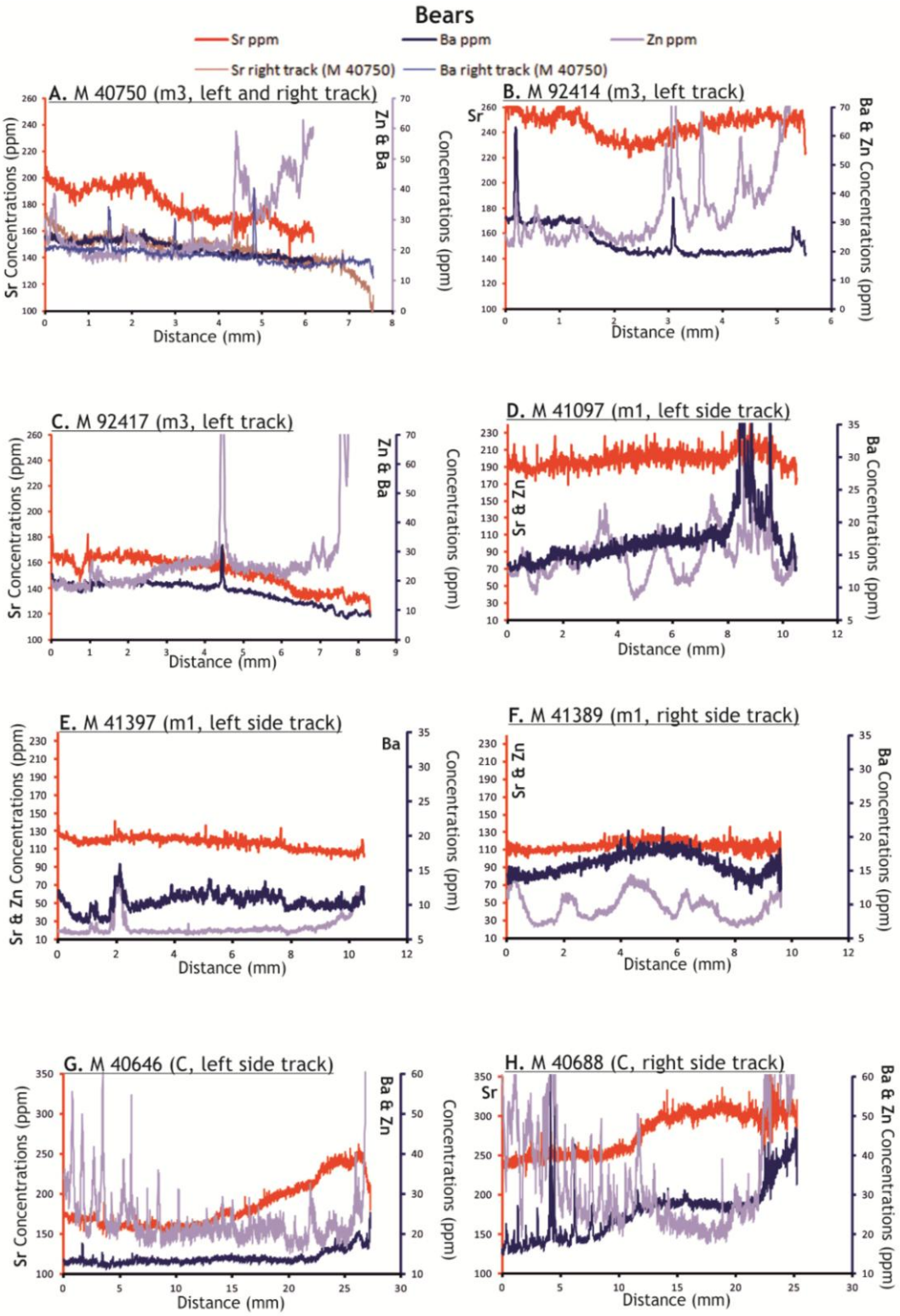

Figure 5.29. Sr, Ba and **Zn** concentrations (in ppm) from laser ablation profiles in Tornewton Cave bear samples, shown against distance (in mm) down the profile. 0 on the X –axis marks the oldest enamel and the starting point for analysis.

Figure 5.30. presents the Mg concentrations for bear teeth shown against U concentrations. As already stated, increases in U result from chemical alteration to apatite. Therefore, Figures 5.30 A to H present the trends in U in order to identify potential diagenetically altered areas on the sample (for the limit of blank (LOB) values see Appendix II.A), and to document how Mg behaves as a result. Finally, U concentrations for each sample are plotted against the REEs in Figures. 5.31 and 5.32, since these are also indicative of chemical alteration (for the limit of blank (LOB) values see Appendix II.A).

In general, for some bear samples, the Mg pattern is very similar along the track to the observed Sr pattern in Figure 5.29. This is the case for samples M40750 (Fig. 5.30.A, left track), M92414 (Fig. 5.30.B), M41097 (Fig. 5.30.D), M41389 (Fig. 5.30.F) and M40688 (Fig. 5.30.H). In all samples, Mg concentrations generally vary between 1200ppm to 2100ppm, with occasional deviation from this pattern denoted by individual peaks in M92417 (Fig. 5.30.C) from 6.5mm to 7mm, M41097 (Fig. 5.30.D) at the end of the profile, M41397 (Fig. 5.30.E) between 5.5mm and 6.5mm and at the end of the profile, M40646 (Fig. 5.30.G) from 25mm to 26mm, and M40688 (Fig. 5.30.H) close to 5mm.

U concentrations are relatively high in some parts of some samples but in most cases, these peaks are not aligned with those of Mg. U peaks are apparent in M40750 between 0.5mm and 2mm. It is also clear that until 3.5mm, U on the right-hand track shows higher concentrations than that on the left track, reaching as high as 2.5ppm at 1.5mm, whereas in M92414, there are multiple narrow peaks between 3mm until the end of the profile, nevertheless all these are below 1ppm. In M92417, U shows an extended peak between 3mm and 5mm with values reaching as high as 3ppm indicating an area of chemical alteration. In general, therefore, all m3 samples appear to show little correlation between U and Mg. In the m1s (M41097 and M41397) and the canines (M40646 and M40688), all show increases in U at the end of the tracks, which appear to be broadly associated with an increase in Mg. In the m1s, M41097 and M41397, U concentrations are generally very low (less than 1ppm) and show very little variability. In contrast, the m1 M41389 displays a peak in U concentration between 0.5mm and 5.7mm and peaks over 1ppm are also apparent in the two canine

teeth, M40646 and M40688, from 22.5mm to 26mm and from 22mm to 24mm respectively.

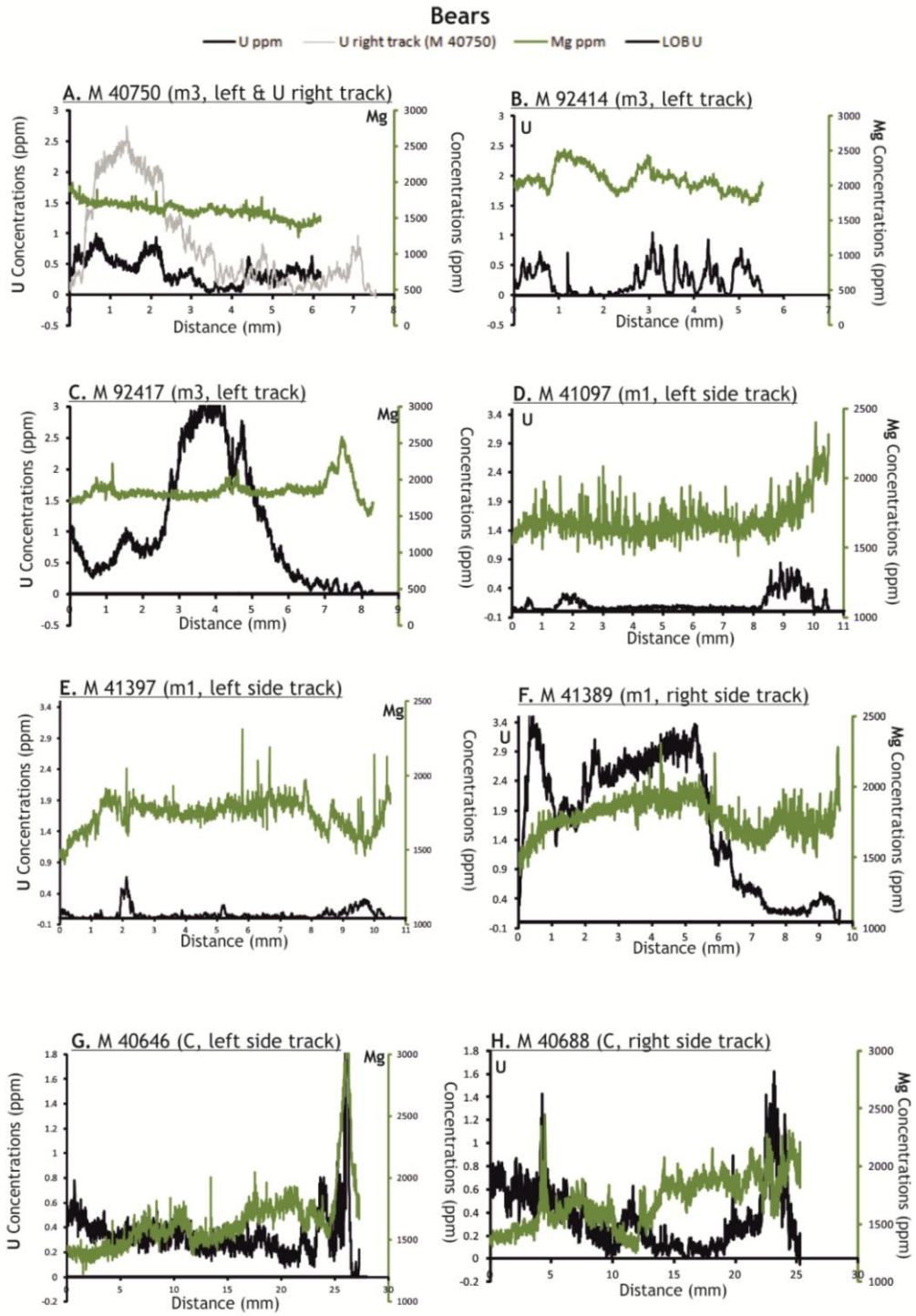

Figure 5.30. Mg and **U** concentrations (in ppm) from laser ablation profiles in Tornewton Cave bear samples, shown against distance (in mm) down the profile. 0 on the X –axis marks the oldest enamel and the starting point for analysis.

Before discussing the Sr/Ca, Ba/Ca and Zn/Ca ratios, it is essential to examine the profiles of the geochemical alteration indicators in each sample. As previously explained above, Y, Ce, Nd and U are used in this study as primary indicators of enamel alteration, supplemented by information from Al, Mn and Pb. Figures 5.31 and 5.32 demonstrate the trends in those elements along the profile for each sample, accompanied by images of the sample taken subsequent to analysis and in which the laser ablation tracks can be seen.

In the m3 M40750 (Fig. 5.31.A.1 and A.2), most of the elements in question present relatively low concentrations. For example, all REEs and U display concentrations lower than 1ppm along the track, as does Pb. However, at 4.3mm, Al, U, Mn, Pb, Y, Ce and Nd show a peak in values and then level off after 4.8mm. This is paralleled by a change in the physical preservation of the sample (notably a change in colour) and the presence of a small crack (Fig. 5.31.A.1, image). Some early peaks in Mn are also apparent at 0.2mm and 2mm, over which distance from the cusp, there is also an apparent darkening of the enamel.

The patterns of Al, U, Mn, Pb and REEs for the m3 M92414 show relatively little variability with concentrations remaining below 1ppm until approximately 3mm. Pb, Y, Ce and Nd profiles show similar muted variability (Fig. 5.31.B.1 and B.2). However, from that point onwards until the end of the profile, the trends become very “noisy” and highly variable, with concentrations for some elements reaching as high as 1000ppm for Al, 2500 for Mn and 14ppm for Y. Ce, Nd, Pb and U maximum values are 4ppm, 6ppm, 4ppm and 1ppm respectively.

Al, U, Mn, Pb (Fig. 5.31.C.1), Y, Ce and Nd (Fig. 5.31.C.2) concentrations in the m3 M92417 display spikes between 4.2mm and 4.7mm down the profile. Over the same area, there is a visible change in the physical preservation of the sample (Fig. 5.31.C.1, image), denoted both by the black colour and the clear crack. Along the remainder of the profile, however, most elements present very little variability except U and Mn. The former shows a large peak between 3mm and 5.4mm, with concentrations higher than 1ppm, whereas in the latter, there is a peak at the end of the profile.

In M41097 (m1) (Fig. 5.31.D.1 and D.2) most of the elements present very little variability. However, at the end of the profile, at 8.2mm, trends in all elements show spikes, coincident with a visible change in the preservation of the sample (Fig. 5.31.D.1, image). Additionally, at 2mm, U, Pb, Al, Y, Ce and Nd display a modest rise in concentrations although the values remain below 1ppm for U, Pb, Y, Ce and Nd and below 100ppm for Al.

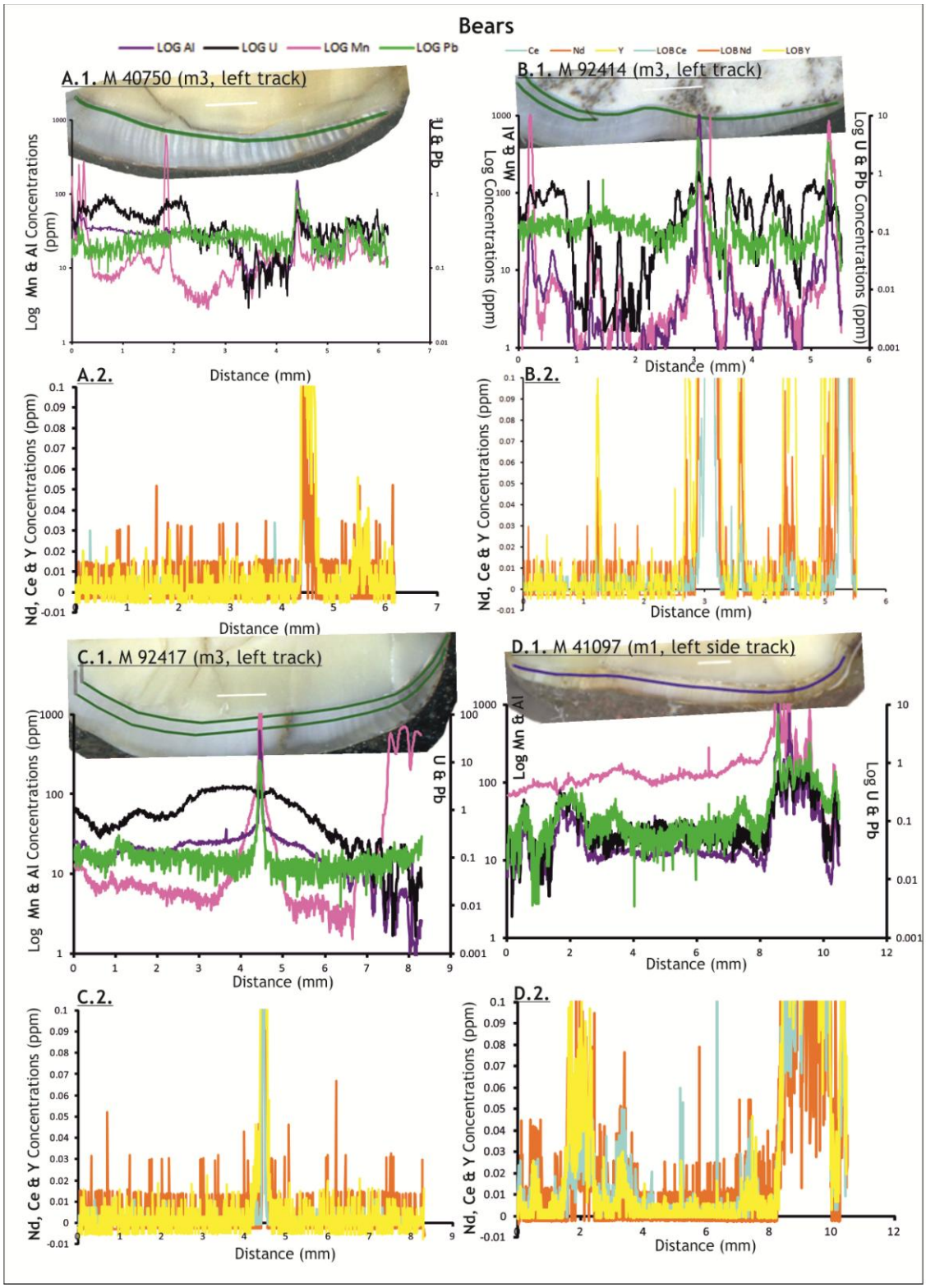

Figure 5.31. Al, **U**, **Mn**, **Pb** and **REE** concentrations (in ppm) from laser ablation profiles of M 40750 (A1 & A2), M 92414 (B1 & B2), M 92417 (C1 & C2) and M 41097 (D1 & D2) bear teeth from Tornewton Cave, shown against the distance (in mm) down the profile. 0 on the X –axis marks the oldest enamel and the starting point for analysis. Sectioned teeth and laser ablation tracks are also shown.

M41397 (m1) (Fig. 5.32. A.1 and A.2) and M41389 (m1) (Fig. 5.32. B.1 and B.2) similarly display very little variability along the profile for most elements. In general, Al concentrations are below 100ppm and Pb below 1ppm. Y, Ce and Nd also remain below 1ppm along the profile. The pattern of U concentrations in M41389 differs, since it remains above 1ppm from the beginning of profile until 5.7mm, and then drops below 1ppm (Fig. 5.32.B.1). In contrast, U concentrations in M41397 (Fig. 5.32. A.1) are below 1ppm along the whole profile. It is also important to note the presence, at 2mm on this sample, of narrow peaks in all elements, followed by a second rise in concentrations close to the end of the profile (Fig. 5.32.A.1 and A.2). Spikes on Y, Ce and Nd concentrations are also apparent between 6.7mm and 7.7mm in M 41389 (Fig. 5.32.B.2).

The last two samples, M40646 (Fig. 5.32.C.1 and C.2) and M40688 (Fig. 5.32. D.1 and D.2) exhibit very different patterns in almost all elements along their profiles. This is to be anticipated since M40688 is visibly very poorly preserved (Fig. 5.32.D.1 image), in comparison with that seen in M40646 (Fig. 5.32.C.1 image). This is reflected across all elements by multiple peaks along most of the profile (Fig. 5.32.D.1 and D.2). Variability is more muted between 16mm and 22mm. On the other hand, in M40646 (Fig. 5.32.C.1 and C.2), most elements show very little variability and along the profile, REEs remain below 1ppm. U and Pb concentrations remain below 1ppm for almost the entire profile except for a slight increase after 24mm until the end of the track. Moreover, Al concentrations are below 100ppm along the whole profile and only a narrow peak is evident at the end of the profile (Fig. 5.32.C.1). Finally, Mn shows general concentrations below 10ppm, except for two very narrow peaks between 2mm and 4mm and a final spike at the end of the profile, coincident with that seen for the other elements (Fig. 5.32.C.1).

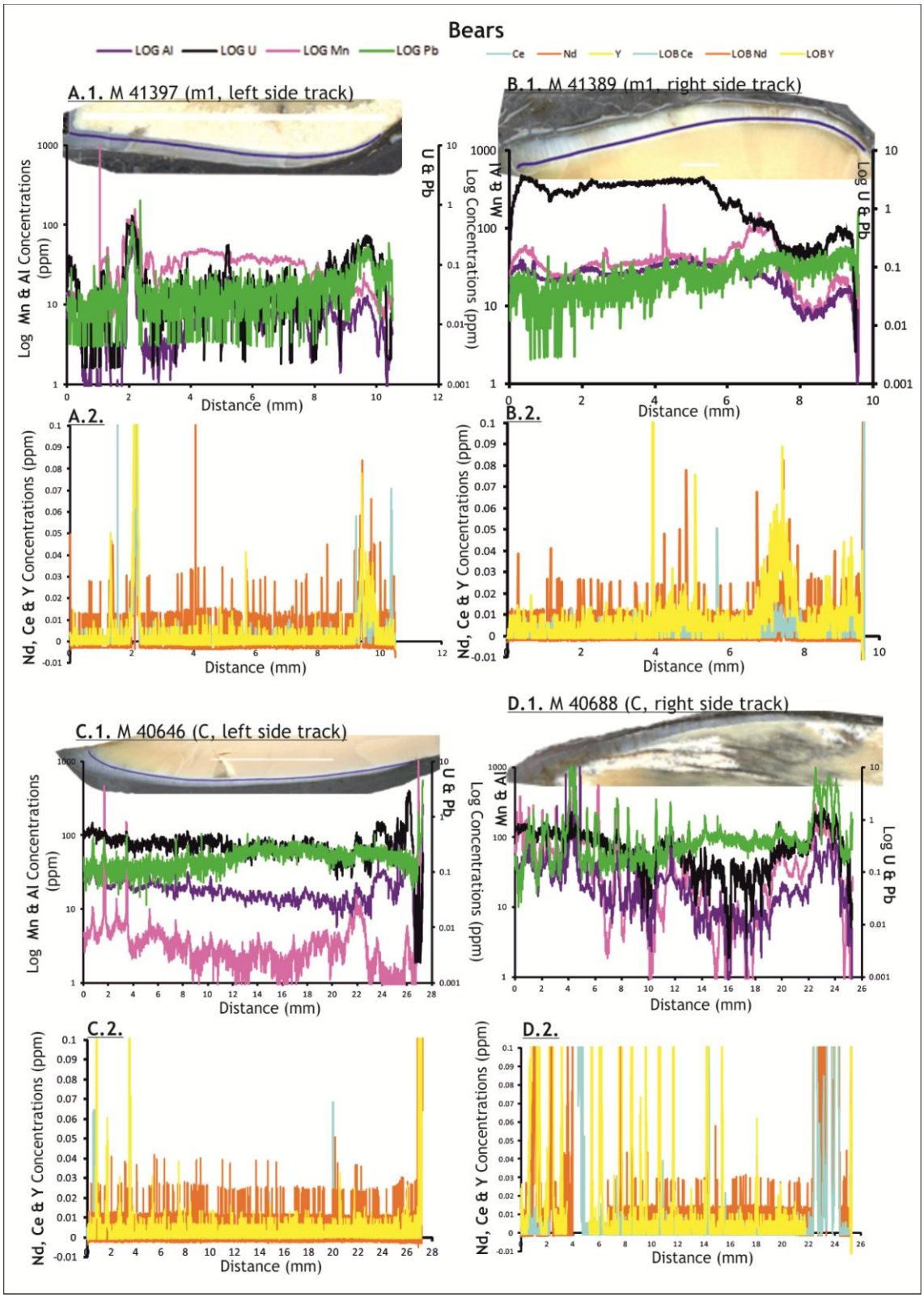

Figure 5.32. Al, **U**, **Mn**, **Pb** and **REE** concentrations (in ppm) from laser ablation profiles of M 41397 (A1 & A2), M 41389 (B1 & B2), M 40646 (C1 & C2) and M 40688 (D1 & D2) bear teeth from Tornewton Cave, shown against distance (in mm) down the profile. 0 on the X –axis marks the oldest enamel and the starting point for analysis.. Sectioned teeth and laser ablation tracks are also shown.

5.5.2.1.2. Examination of diagenesis on *U. arctos* samples through comparison with modern published data

This section assesses the REE, U, Al and Mn values by comparing medians, average, 1st and 3rd quartile and 10th and 90th percentiles from each fossil bear tooth with published concentrations of the same element on modern species, in order to reveal potential diagenetic alteration in the post-mortem environment of Tornewton Cave. The boxplots in Figure 5.33 (Ce, Nd and U) and Figure 5.34 (Al and Mn) illustrate concentrations of each bear specimen from Tornewton Cave analysed in comparison with values of the same elements from modern species (data from Kohn *et al*. [1999] and Kohn *et al*. [2013]). As already explained in 5.2.4., increases in U and REEs in fossil enamel are a result of chemical alteration to the apatite crystallites, since U and the REEs have strongly affinity for the Ca and OH sites in the apatite (Kohn *et al*., 1999). In addition, increases in Al and Mn, along with Ba, are indicative of contamination by diagenetic oxyhydroxides and clay (Kohn *et al*., 1999).

The majority of U and REE concentration data of the fossil bear teeth fall within or close to recorded concentrations in modern enamel (Fig. 5.33). Most teeth from Tornewton Cave have low concentrations of both Ce and Nd and fall within the range covered by concentrations of modern species, the exceptions being the average values of M92414 and M40688 (Ce) that lie outside these ranges. Interestingly, the reported concentration values for modern black bear teeth published by Kohn *et al*. (2013) for Ce is significantly higher than the values of fossil bear teeth and also fall outside the range marked by the published data of recent enamel species from Kohn *et al*. (1999) (the pink rectangle in Fig. 5.33). This can be explained by the exclusion of bear teeth from the range of modern mammals analysed by Kohn *et al*. (1999).

The majority of the fossil bear teeth have higher U-concentrations than the modern teeth (Fig. 5.33). Extremely high U-values are seen in M92417 (m3) and M41389 (m1). In addition, M40750 also shows higher U values than modern teeth, while M41097 and M41397 are within the reported ranges for modern teeth (Fig. 5.33).

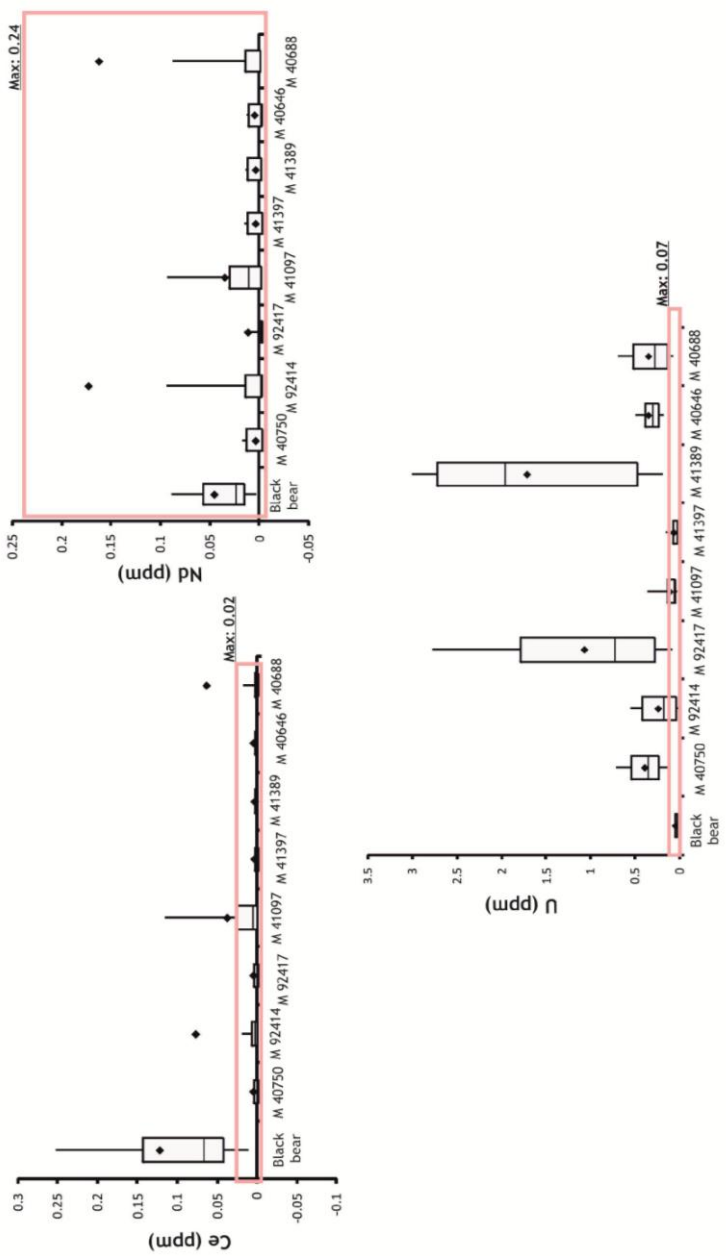

Figure 5.33. Box plots showing **Ce, Nd** (top) and **U** (below) concentrations (in ppm) data for bear samples from Tornewton Cave in comparison with concentrations reported for extant black bear teeth (1st box plot on each graph) (Kohn *et al*., 2013). The pink rectangles represent concentration ranges reported on modern enamel (Kohn *et al*., 1999). The boxes represent 1st and 3nd quartiles, the medians (horizontal line), averages are represented by diamonds and the whiskers show the 90th and 10th percentiles.

In addition, Al and Mn concentrations of most fossil bear teeth have higher values than the values recorded on modern enamel from Kohn *et al*. (1999) (Fig. 5.34). However, Al concentration values reported on modern black bear from Kohn *et al*. (2013) show higher values from some of the fossil bear teeth (M92414, M41397 and M 40646). Values of Al are low and fall within the modern reported concentrations for M92414 and M 41397. Mn values of M40750, M92414, M41397, M40646 and partly of M92417

and M40688 are also low and within the reported ranges of modern teeth, while Mn concentrations in M41389 are extremely high reaching over 1000ppm (Fig. 5.34).

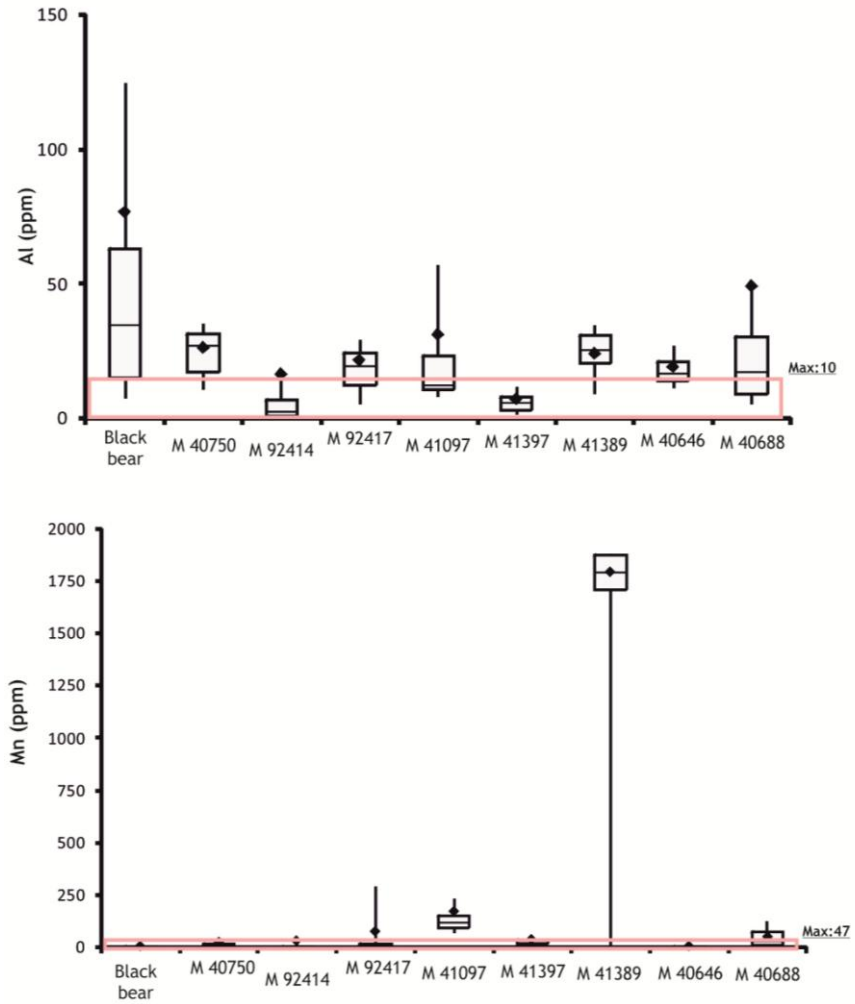

Figure 5.34. Box plots showing **Al** (top) and **Mn** (below) concentrations (in ppm) data for each bear sample from Tornewton Cave in comparison with concentrations reported for extant black bear teeth (1st box plot on each graph) (Kohn *et al*., 2013). The pink rectangles represent concentration ranges reported on modern enamel (Kohn *et al*., 1999). The boxes represent 1st and 3nd quartiles, the medians (horizontal line), averages are represented by diamonds and the whiskers show the 90th and 10th percentiles.

5.5.2.2. Results of *C. crocuta* teeth

5.5.2.2.1. Element profiles of *C. crocuta* samples

Two hyaena first lower molars (m1) were analysed from Tornewton Cave (see 5.4). A single track from each tooth was analysed and these are shown in Figure 5.35.

Figure 5.36. displays the different element concentrations in each sample. The Y-axis shows different elemental concentrations in ppm, whereas the X-axis records distance (in mm) from the oldest enamel (tip of cusp/start of profile) to the newest (base of crown/end of profile) on each tooth. Lines from each element connect consecutive measurements along the track (following the profile of each tooth), making it easier to observe long and short-term trends within the data for each tooth.

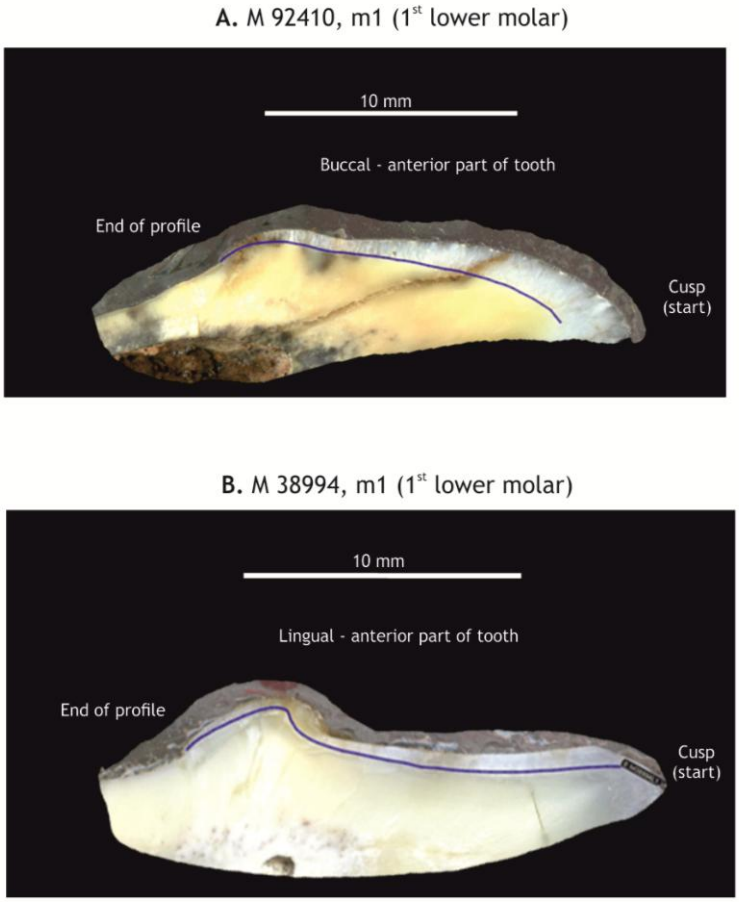

Figure 5.35. Laser ablation tracks marked with blue lines on each hyaena tooth sampled from Tornewton Cave (NHM specimens). The start and end of each profile are located close to the EDJ.

In general, some differences between the patterns in the Sr, Ba, Zn, U, Pb, Mn and REE concentrations of both hyaena samples are apparent (Figs. 5.36. A.1, A.3, A.4, B.1, B.3 and B.4). There is also a clear difference between the physical preservation of each sample with M92410 displaying slightly poorer preservation with a big crack at the

beginning of the enamel profile, coinciding with a notable change in colour (Fig. 5.36 A.1, image). In addition all elements in this sample have a gap between 3.5mm and 4.5mm because of the presence of resin. A second gap at the end of the profile between 12.6mm and 13.7mm is because element concentrations in this area exceeded the plot area of the graph (Fig. 5.36 A.1 – A.4).

With respect to M92410, similar covariance between Sr, Ba and Zn can be seen with the last presenting a slightly more variable pattern especially from 8mm onwards. Sr and Ba exhibit very similar patterns with minor variability until approximately 12mm. After 11mm and until almost the end of the profile, there is high fluctuation with peaks where both Sr and Ba as well as Zn reach their maximum concentrations of 4500ppm, 18000ppm and 7000ppm respectively, strongly suggesting diagenetic alteration (Fig. 5.36.A.1). On these parts of the track, both Sr and Ba display a positive correlation with U and Mn (especially at 4mm and after 12mm until the end of the profile) and therefore in these areas, it is proposed that alteration has occurred through secondary mineral formation. In particular, an increase in Mn suggests contamination by oxyhydroxides, leading to the presence of dark stains on the enamel (Jaques *et al*., 2008; see Fig. 5.36.A.2.), also coincident with peaks in U values (Fig. 5.36.A.3) (Millard and Hedges, 1996; Kohn *et al*., 1999). For M92410, minor diagenetic alteration may occur between 10mm and 14mm, where both Sr and Ba values co-vary with peaks in Al and Mn. In addition, Ba displays two distinct peaks that are missing from the Sr pattern at 7.5mm and 9.8 mm (Fig. 5.36.A.1), which correlate positively with U and Mn peaks (Fig. 5.36.A.3) and suggest additional diagenetic alteration. This is also confirmed by analysis of the remaining elements such as Al and Pb (Fig. 5.36.A.3) as well as REEs (Fig. 5.36.A.4).

Finally, in M92410, the Mg pattern is very similar along the track to the observed Ba pattern, with the difference that in the former, no additional peaks are displayed in 7.5mm and/or in 9.8mm and the pattern is smoother (Fig. 5.36.A.2). It is worth mentioning that the U pattern shows intensive peaks along almost the entire track and in comparison with M38994 (Fig. 5.36.B.2), it displays much higher concentrations. Again, this is linked with chemical alteration of the apatite (Fig. 5.36.A.2).

In M38994, trends in both Sr and Ba show higher variability (Fig. 5.36.B.1) than in M92410 (Fig. 5.36.A.1) and interestingly, the Sr values are much higher in the former than in latter. Sr displays minor variability for the first 4.2mm and then shows a continuous drop in concentration until 12mm, followed by a small increase and a leveling-off of values until the end of the profile (Fig. 5.36.B.1). Sr concentrations range between 900ppm and 700ppm (Fig. 5.36.B.1). Ba concentrations in M38994 show little variability until 12mm and reach 13ppm, while after 12mm and until the end of the profile, there is a small increase in concentrations (up to a maximum of 20ppm) (Fig. 5.36.B.1). Between 10mm to 14mm, both Sr and Ba co-vary with peaks recorded in Al and Mn, suggesting contamination of the enamel by fine sediments and this is also associated with some change in enamel (colour) preservation (Fig. 5.36.B.1. graph and image and B.3). In contrast, Zn concentrations are very different from both Sr and Ba especially after 5.8mm (Fig. 5.36.B.1). Zn concentrations remain almost flat until the 5.8mm point, after which they fluctuate between 25ppm to over 65ppm until the end of the track. All the alteration indicators, such as Mn, Al, U, Pb and REEs, show very little variability and generally occur in very low concentrations (Fig. 5.36. B.3 and B.4) (details regarding the limit of blank (LOB) please see Appendix II.A). In addition, Mg varies in a similar way to Sr and fluctuates between 1600 to 2400ppm (Fig. 5.36.B.2).

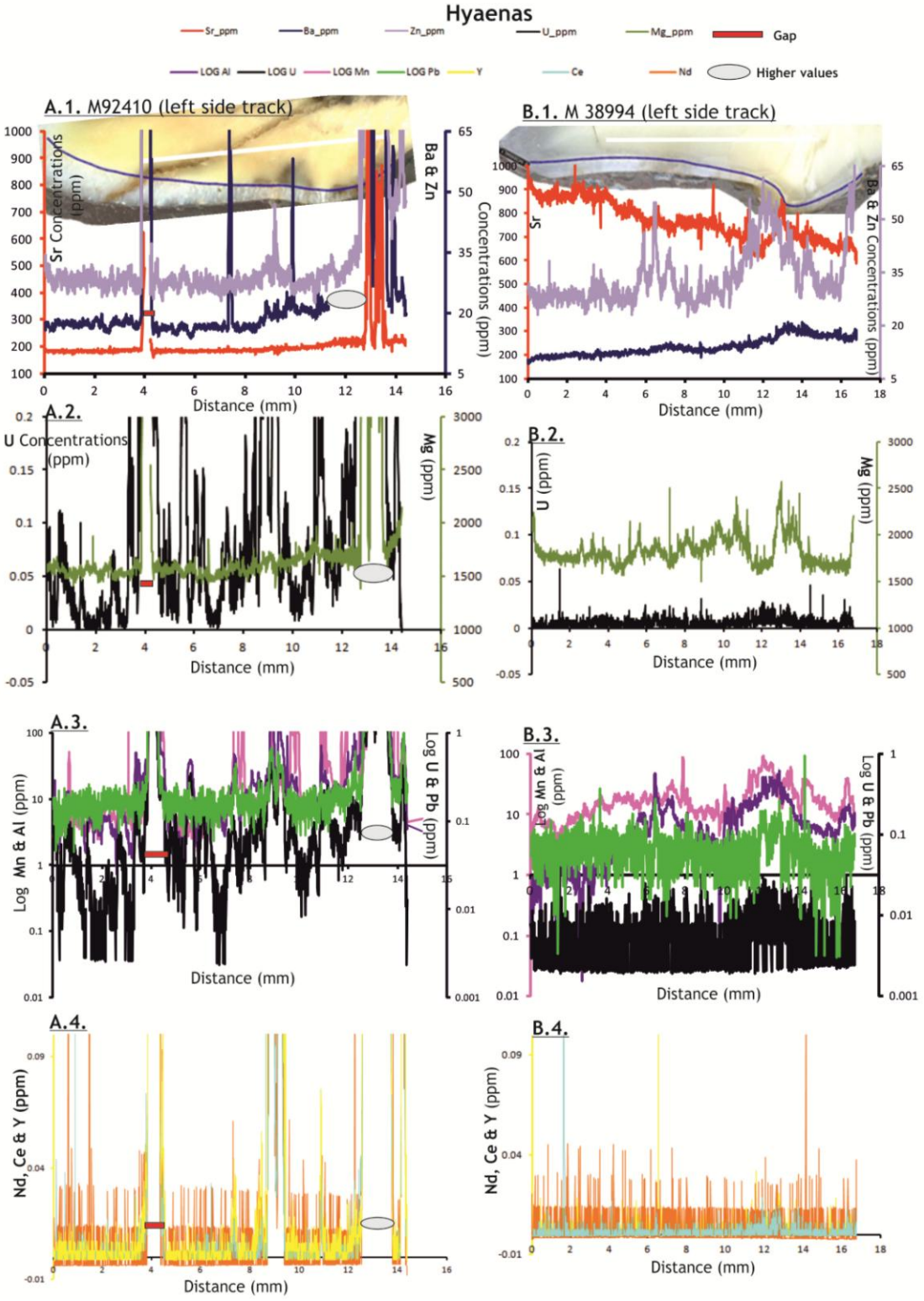

Figure 5.36. Sr, **Ba**, **Zn** (A.1 & B.1); **Mg** and **U** (A.2 & B.2); **Al**, **U**, **Mn**, **Pb** (A.3 & B.3) and **REE** (A.4 & B.4) concentrations (in ppm) from laser ablation profiles of M92410 (A1 - A4) and M38994 (B1 – B4) hyaena teeth from Tornewton Cave, shown against distance (in mm) down the profile. 0 on the X –axis marks the oldest enamel and the starting point for analysis. Sectioned teeth and laser ablation tracks are also shown.

5.5.2.2.2. Examination of diagenesis examination in *C. crocuta* samples through comparison with modern published data

Medians, average, 1st and 3rd quartile and 10th and 90th percentiles of REE, U, Al and Mn from each fossil hyaena tooth are compared below with published concentrations of the same element on modern species. The boxplots in Figure 5.37 (Ce, Nd and U) and Figure 5.38 (Al and Mn) illustrate the concentrations for each hyaena specimen from Tornewton Cave, in comparison with values of the same elements from modern species (data from Kohn *et al*. [1999] and Kohn *et al*. [2013]).

U and REE concentrations data of both hyaena teeth fall within or close to recorded concentrations in modern enamel (Fig. 5.37). Both teeth from Tornewton Cave have low concentrations of both Ce and Nd and fall within the range covered by concentrations of modern species, exceptions being the 90th percentile of M92410 (Ce), which lie outside these ranges. Interestingly, the reported concentration values for modern carnivore (wolf and puma) enamel (data from Kohn *et al*. [2013]) for Ce is significantly higher than the values of fossil hyaena teeth and also falls outside the range established for recent enamel by Kohn *et al*. (1999) (pink rectangles in Fig. 5.37). This can be explained by the exclusion of hyaena teeth from the range of modern mammals analysed by Kohn *et al*. (1999). Obvious is also the smaller values of Ce, Nd and U that display the M38994 sample in comparison with the M92410 (Fig. 5.37). In addition, the latter displays also higher 90th percentiles, average and 1st quartile than the values reported in modern animals for U (Fig. 5.37).

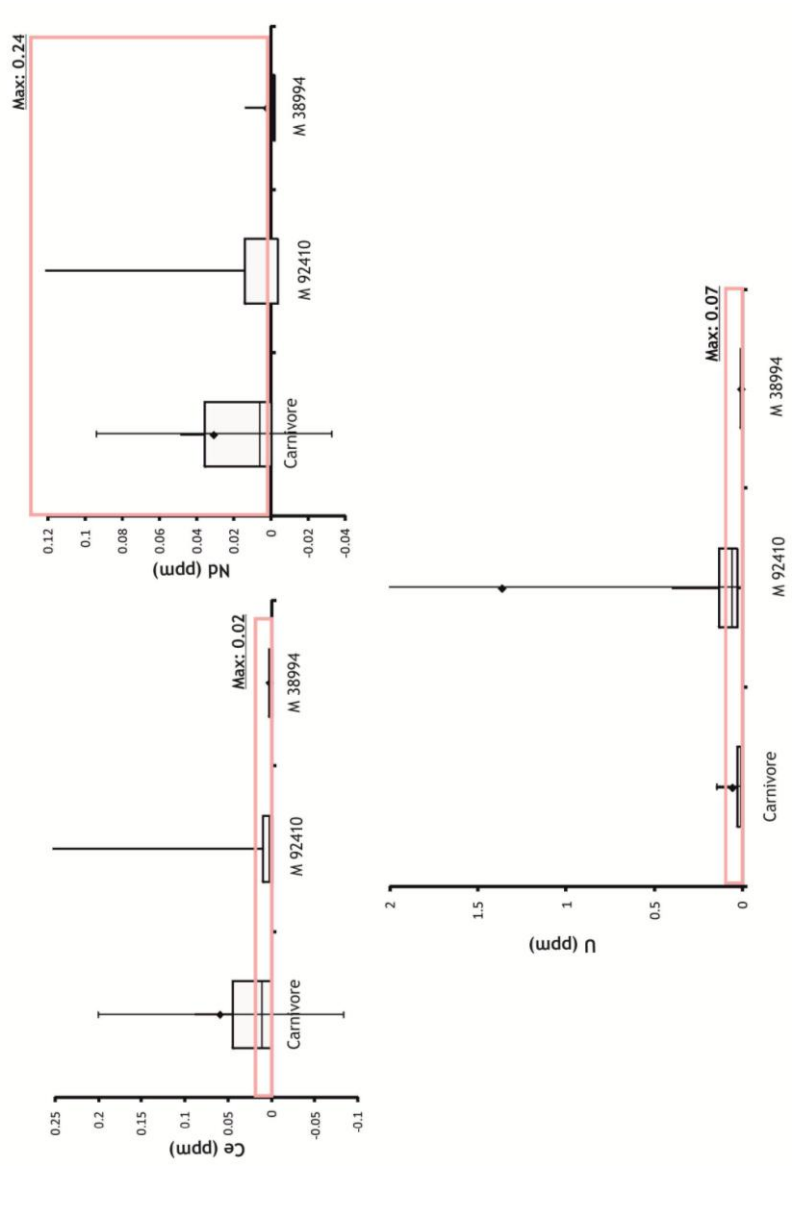

Figure 5.37. Box plots showing **Ce, Nd** (top) and **U** (below) concentrations (in ppm) for each hyaena sample from Tornewton Cave in comparison with concentrations reported for extant carnivore teeth (1st box plot on each graph) (Kohn *et al.*, 2013). The pink rectangles represent concentration ranges reported on modern enamel (Kohn *et al.*, 1999). The boxes represent 1st and 3nd quartiles, the medians (horizontal line), averages are represented by diamonds and the whiskers show the 90th and 10th percentiles.

Most Al and Mn values in both hyaena fossil teeth are within the reported values of modern enamel (Fig. 5.38). However, Al concentrations of the modern carnivores considered by Kohn *et al*. (2013) display higher values than those reported on modern specimens by Kohn *et al*. (1999). Thus, although M92410 is not within the reported values from Kohn *et al*. (1999), it falls within the revised values for modern carnivore enamel of Kohn *et al*. (2013) (Fig. 5.38).

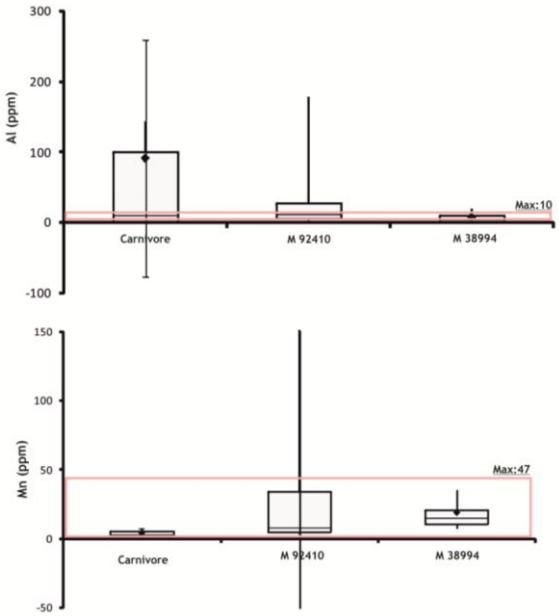

Figure 5.38. Box plots showing **Al** (top) and **Mn** (below) concentrations (in ppm) for each hyaena sample from Tornewton Cave in comparison with concentrations reported on carnivore teeth (1st box plot on each graph) (Kohn *et al*., 2013). The pink rectangles represent concentration ranges reported on modern enamel (Kohn *et al*., 1999). The boxes represent 1st and 3nd quartiles, the medians (horizontal line), averages are represented by diamonds and the whiskers show the 90th and 10th percentiles.

5.6.2.3. Results of *C. elaphus* samples

5.6.2.3.1. Element profiles of *C. elaphus* samples

A single track was analysed on each of the three molar teeth in a red deer mandible (M41530) from Tornewton Cave (Fig. 5.39). Figures 5.40 and 5.41 illustrate the different element concentrations in each tooth. The Y-axis shows different elemental concentrations in parts per million (ppm), whereas the X-axis records distance (in mm) from the oldest enamel (tip of cusp/start of profile) to the newest (base of crown/end of profile) on each tooth. Lines from each element connect consecutive measurements along the track (following the profile of each tooth), making it easier to observe long and short-term trends within the data for each tooth.

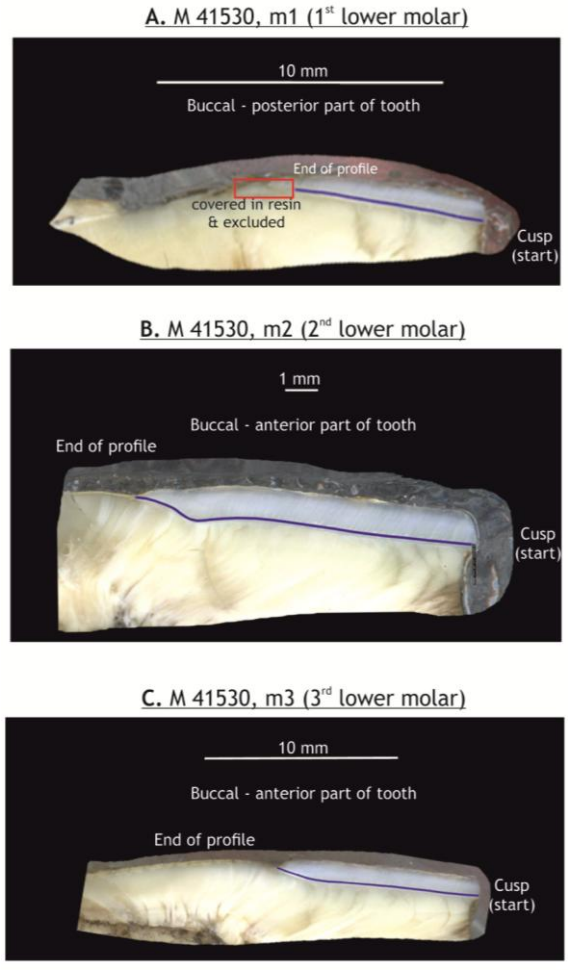

Figure. 5.39. Laser ablation tracks marked with blue lines on each of three red dear tooth samples from Tornewton Cave (NHM specimens). The start and end of each profile are located close to the EDJ. In m1 (A), part of the enamel at the end of the profile was covered with resin, thus this profile is expected to be shorter than the other two teeth (m2 and m3, B and C respectively).

In general Sr covaries with Ba in all three molars of M41530, whereas Zn does not (Fig. 5.40 A.1, B.1 and C.1). Figure 5.40 A.1 illustrates the trends of Sr, Ba and Zn for each of the three teeth, together with the profiles of the geochemical alteration indicators such as Mn, Al, U and Pb (Fig. 5.40 A.2, B.2 and C.2) and Nd, Ce and Y (REEs) (Fig. 5.40 A.3, B.3 and C.3) for each tooth.

With respect to the m1, Sr and Ba show minor variability until 1mm, followed by a progressive increase for both Sr (from 200ppm to 247ppm) and Ba (from 54ppm to 74ppm) and then a leveling-out with small fluctuations (between 230 and over 255ppm for Sr and 70 and over 80ppm for Ba) until the end of the profile (Fig. 5.40 A.1). In contrast to Ba and Sr, Zn concentrations show very little variability until 4.7mm (between 12 and 24ppm), then a peak is present from 4.7 to 6mm where values reach as high as 30ppm, after which there is a gradual decrease until the end of the profile (Fig. 5.40 A.1).

The m2 (Fig. 5.40 B.1) shows generally slightly higher Sr and Ba concentrations than the m1. Trends in both Sr and Ba display some minor variability until 8.2mm, with values fluctuating between 230 to over 253ppm and 80 to over 100ppm respectively, followed by a drop in concentrations (Sr: 199ppm and Ba: 77ppm) until 9mm. From that point until the end of the profile, there is high variability in both Sr and Ba (Fig. 5.40 B.1). Zn concentrations in the m2 (Fig. 5.40 B.1) are similar to those in the m1, varying little until 7.7mm (between 13 and 18ppm), then a peak is present (7.7 to 9mm) when values reach as high as 28ppm, followed by a leveling-out until the end of the profile.

Patterns of Sr and Ba in the m3 illustrate pronounced variability especially after 4mm. Both elements display a cyclical pattern of rise-fall-rise, with high values in Sr and Ba (236ppm and 92ppm respectively) until 0.8mm, after which there is progressive decrease in the values of both elements (below 195ppm for Sr and 75ppm for Ba) until 2.8mm. This is followed by a short zone (from 2.7 to 3.8mm) of minor variability and then a peak at approximately 4mm (up to 220ppm for [Sr] and 90ppm [Ba]). After 4.7mm and until the end of the profile, even higher variability is present with peaks and troughs where both Sr and Ba reach as high as 247ppm and 100ppm and drop up

to 192ppm and 62ppm respectively. The Zn pattern in the m3 is similar to that of the other two molars.

The patterns of Mn, Al, U, Pb (Fig. 5.40 A.2, B.2 and C2), Nd, Ce and Y (Fig. 5.40 A.3, B.3 and C.3) vary little across all samples, suggesting that the enamel is not diagenetically alterered (details regarding the limit of blank (LOB) are given in Appendix II.A). All the REEs (Fig. 5.40 A.3, B.3 and C.3) display concentrations lower than 1ppm along the tracks. This is echoed by the visibly very good physical preservation of each sample (Fig. 5.40, sample images). In most parts of the tracks for all samples, U and Pb remain below 1ppm however in the m1, U levels are slightly over 1ppm from 0 until 0.7mm and from 5mm until the end of the profile, whereas Pb is over 1ppm along the whole track. In addition, some peaks in Mn and Al are apparent at 5mm onwards in the m1 and at 9mm onwards in the m3. In the m2, both Al and Mn are slightly higher than in the other two samples but are nevertheless still in low concentrations (below 10ppm) and, more importantly for the purposes of eliminating diagenesis, do not co-vary with either Sr or Ba.

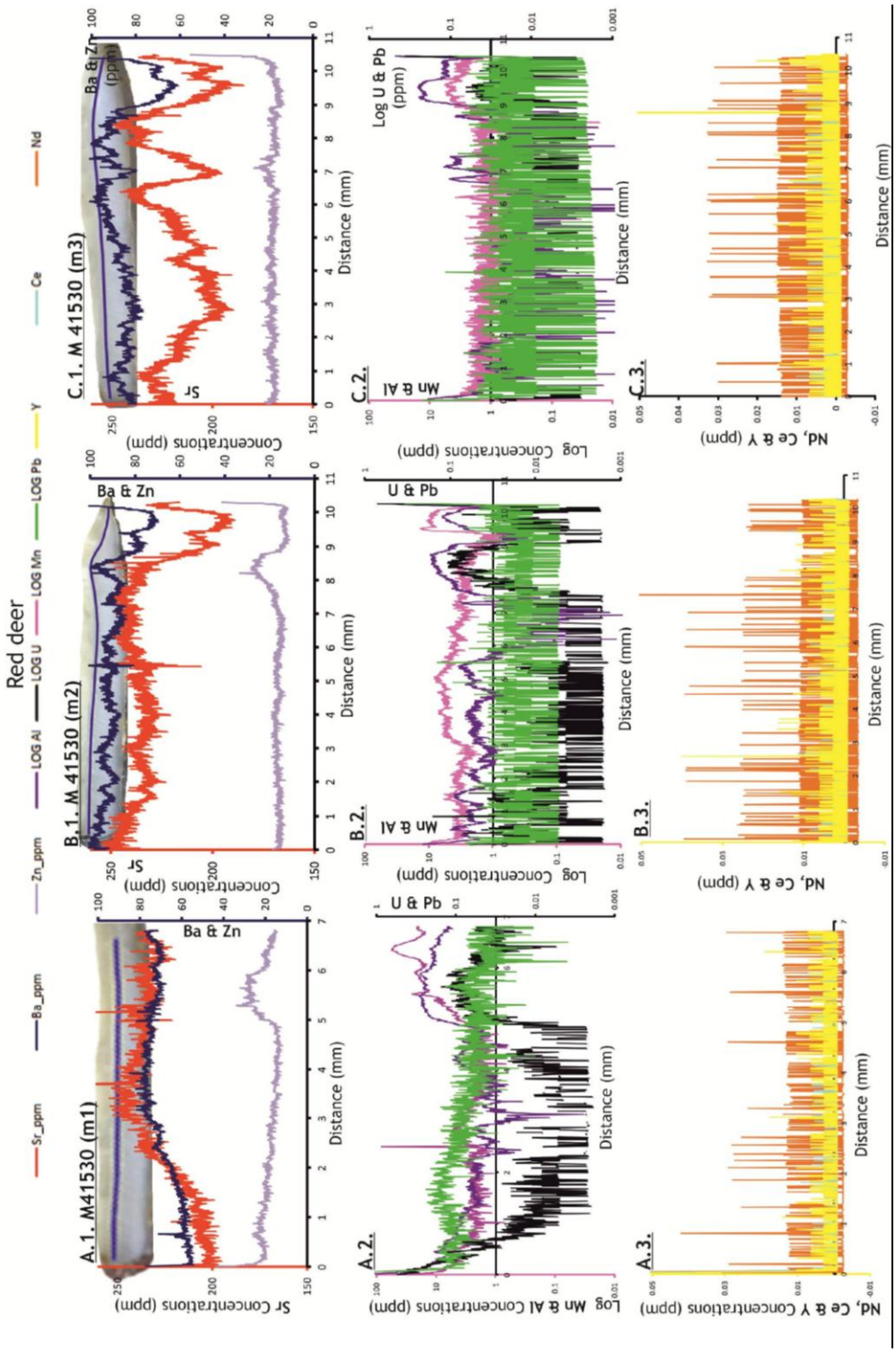

Figure. 5.40. Ba, Zn (A.1, B.1 & C.1); **Al, U, Mn, Pb** (A.2, B.2 &C.2) and **REE** (A.3, B.3 & C.3) concentrations (in ppm) from laser ablation profiles of M 41530 m1 (A.1 – A.3), M41530 m2 (B.1 – B.3) and M41530 m3 (C.1 – C.3) red deer teeth from Tornewton Cave, shown against distance (in mm) down the profile. 0 on the X –axis marks the oldest enamel and the starting point for analysis. Sectioned teeth and laser ablation tracks are also shown.

Figures 5.41 A.1, B.1 and C.1 present the Mg concentrations for red deer teeth shown against U concentrations. In all samples, Mg concentrations show very little variability at the beginning of the tracks and until 3mm in the m1 (Fig. 5.41 A.1), 6mm for the m2 (Fig. 5.41 B.1) and 4mm for the m3 (Fig. 5.41 C.1). After these points in each sample,

there is a zone of increased variability until the end of each profile, where Mg values vary between 1800 and 2500ppm. Interestingly, in the m2 and m3, peaks in U close to the end of each profile correspond with lower concentration values of Mg, while in the m1, they correlate with higher values.

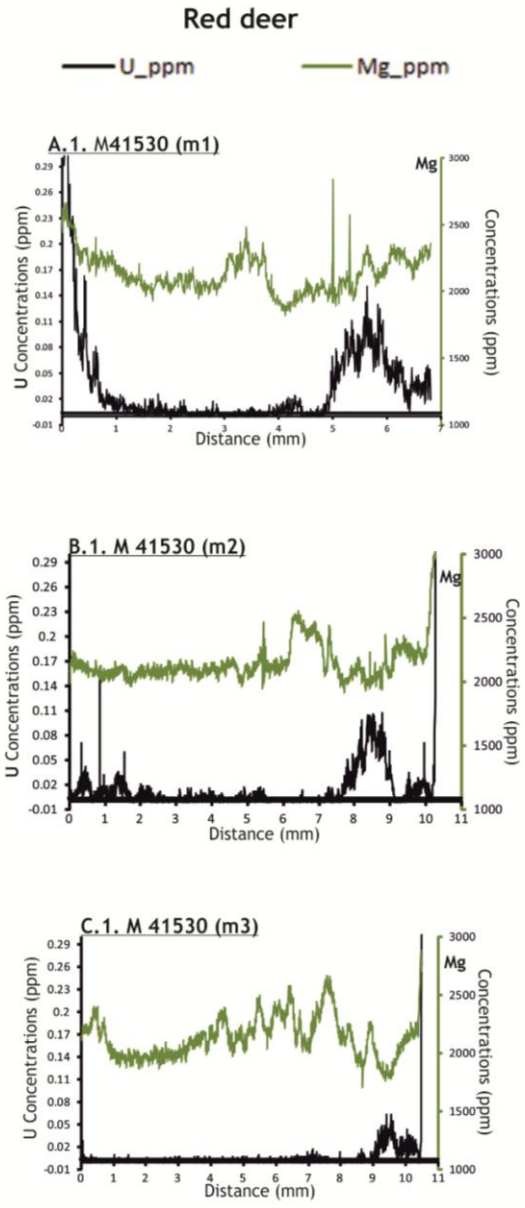

Figure. 5.41. Mg and **U** (A.1, B.1 & C.1) concentrations (in ppm) from laser ablation profiles of red deer teeth from Tornewton Cave, shown against distance (in mm) down the profile. 0 on the X –axis marks the oldest enamel and the starting point for analysis.

5.5.2.3.2. Examination of diagenesis on *C. elaphus* samples through comparison with modern published data

Before the examination of Sr/Ca, Ba/Ca and Zn/Ca, REE, U, Al and Mn must be assessed by comparing medians, average, 1st and 3rd quartile and 10th and 90th percentiles from each red deer tooth with published concentrations of the same element on modern species, in order to reveal potential diagenetic alteration in the post-mortem environment of Tornewton Cave. The boxplots in Figure 5.42 (Ce, Nd and U) and Figure 5.43 (Al and Mn) illustrate concentrations of each of the three red deer teeth compared to with values of the same elements from modern species (data from Kohn *et al*. [1999] and Kohn *et al*. [2013]). All the elements in the fossil red deer samples present low concentrations and fall within the reported concentrations in modern enamel.

Concentrations of U (Fig. 5.42) and Al and Mn (Fig. 5.43) in the m1 are slightly higher than for the other two fossil teeth, however still within the accepted values. Thus, it can be assumed that for these teeth, the enamel has not been affected by the burial conditions and the ratios of both Sr/Ca and Ba/Ca are expected to represent true signals.

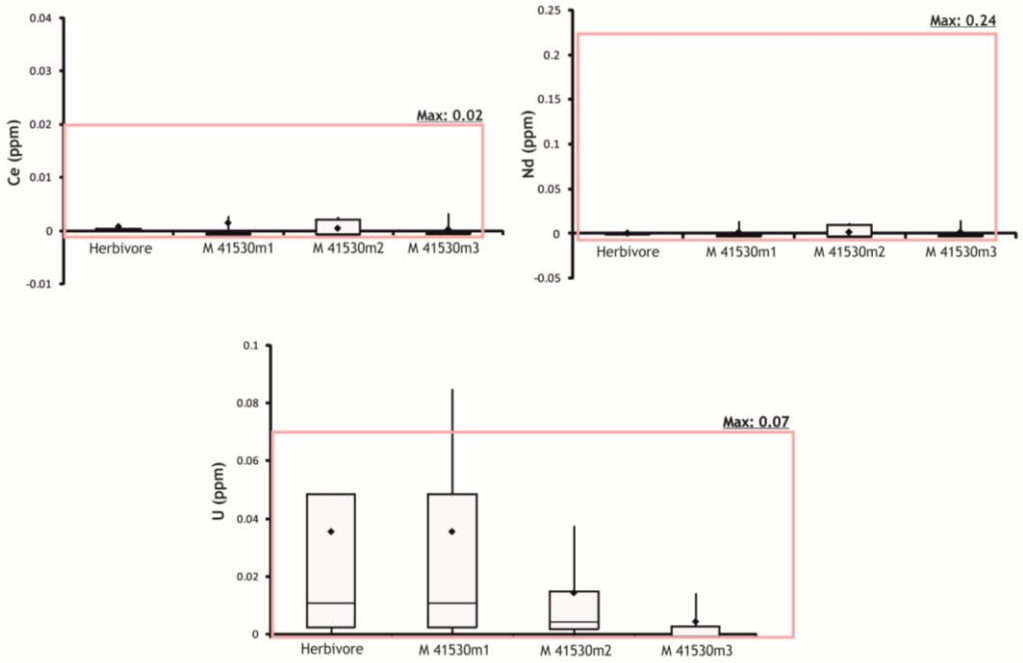

Figure. 5.42. Box plots showing **Ce, Nd** (top) and **U** (below) concentrations (in ppm) data of each red deer tooth from Tornewton Cave in comparison with concentrations reported on extant herbivore teeth (1st box plot on each graph) (Kohn *et al*., 2013). The pink rectangles represent concentration ranges reported on modern enamel (Kohn *et al*., 1999). The boxes represent 1st and 3nd quartiles, the medians (horizontal line), averages are represented by diamonds and the whiskers show the 90th and 10th percentiles.

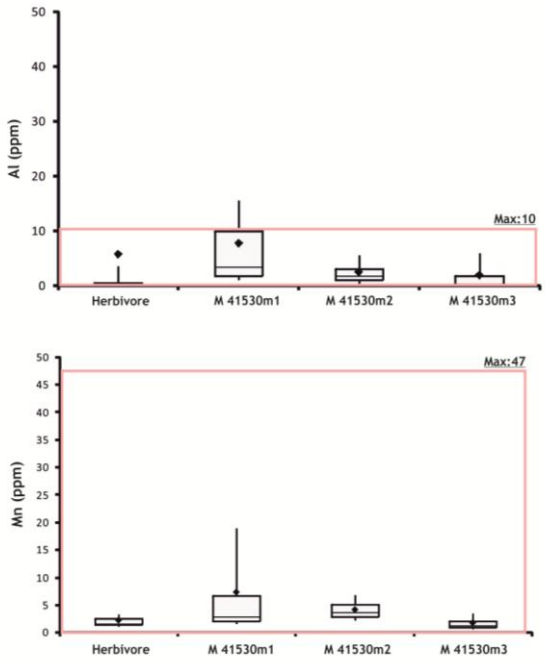

Figure. 5.43. Box plots showing **Al** (top) and **Mn** (below) concentrations (in ppm) data of each red deer tooth from Tornewton Cave in comparison with concentrations reported on extant herbivore teeth (1st box plot on each graph) (Kohn *et al*., 2013). The pink rectangles represent concentration ranges reported on modern enamel (Kohn *et al*., 1999). The boxes represent 1st and 3nd quartiles, the medians (horizontal line), averages are represented by diamonds and the whiskers show the 90th and 10th percentiles.

5.5.2.4. Results of the *Equus* sample

5.5.2.4.1. Element profiles of the *Equus* sample

A single track on a horse m3 (M92408) from Tornewton Cave was analysed (Fig. 5.44). Figures 5.45 and 5.46 present the different element concentrations in this tooth. The Y-axis shows different elemental concentrations in parts per million (ppm), whereas the X-axis records distance (in mm) from the oldest enamel (tip of cusp/start of profile) to the newest (base of crown/end of profile) on each tooth. Lines from each element connect consecutive measurements along the track (following the profile of each tooth), making it easier to observe long and short-term trends within the data for each tooth.

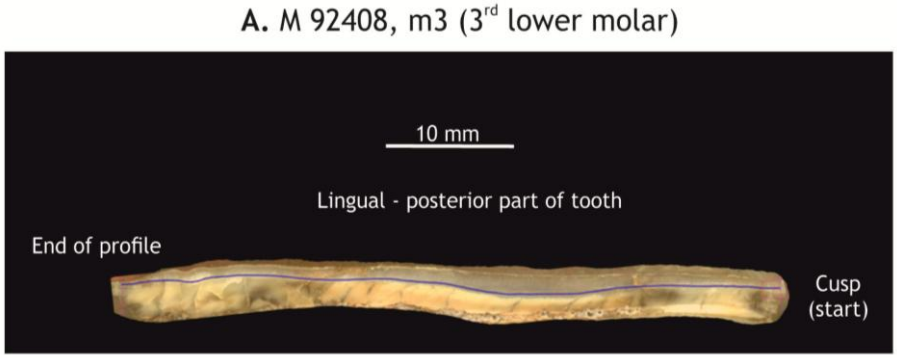

Figure 5.44. Laser ablation track marked with a blue line on the horse tooth sample from Tornewton Cave (NHM specimen). The start and end of each profile are located close to the EDJ.

Figure 5.45 illustrates the trends of Sr, Ba and Zn (A.1) in M92408 and the profiles of the geochemical alteration indicators Mn, Al, U and Pb (A.2) and Nd, Ce and Y (REEs) (A.3). In general, Sr, Ba and Zn exhibit different patterns, with Sr showing greater fluctuations than both Ba and Zn and presenting several peaks along the track (Fig. 5.45 A.1). Sr ranges between 390ppm and 460ppm until approximately 7.5mm, followed by a period of higher variability with three distinct spikes at 8.5mm (620ppm), 14.2mm (686ppm) and 16mm (543ppm) until 16.8mm, after which there is more minor variability and Sr fluctuations 330ppm and up to 477ppm until 42mm. From then until the end of the profile, the pattern displays similarities to that observed in

the first 7.5mm of the track. Ba presents minor variability until 8.5mm (between 12ppm and 17ppm), after which there are multiple broad peaks and troughs between 10.3mm and 34.2mm and between 35.5 and 43mm, with values varying between 9ppm and 16ppm. In addition, two narrow peaks are clear at 10mm (up to 106ppm) and at 35mm (up to 106ppm), which correlate with Zn peaks at the same point (up to 99ppm and 94ppm respectively). At 43mm, a sharp increase in Ba occurs (up to 20ppm), with minor variation until 48mm and a final high peak between 48.5mm and the end of the profile where values reach 50ppm. In Zn, the background concentrations vary between 11ppm and 35ppm, with the exception of the two spikes mentioned above, and a further final peak close to the end of the profile (47.5mm until the end) where the concentrations reach as high as 120ppm.

The patterns for Mn, Al, U, Pb (Fig. 5.45 A.2), Nd, Ce and Y (Fig. 5.45 A.3) in the horse sample show several peaks along the track but also parts where the concentrations are below 1ppm (for details regarding the limit of blank (LOB), please see Appendix II.A). Mn and Al present both narrow and wide peaks along the track with very high values at 0.5mm (Mn: 2570ppm and Al: 980ppm), 10mm (Mn: 888ppm and Al: 913ppm), 35mm (Mn: 960ppm and Al: 1460ppm) and 48mm (Mn: 906ppm and Al: 420ppm). At the same points, both Pb and U also show spikes although these are mainly below 1ppm, with the exception of the peaks at 10mm (Pb: 23ppm and U: 4ppm) and 35mm (Pb: 30ppm and U: 7.3ppm). Most of the peaks correspond with visible discoloration and small cracks in the sample (Fig. 5.45, sample images).

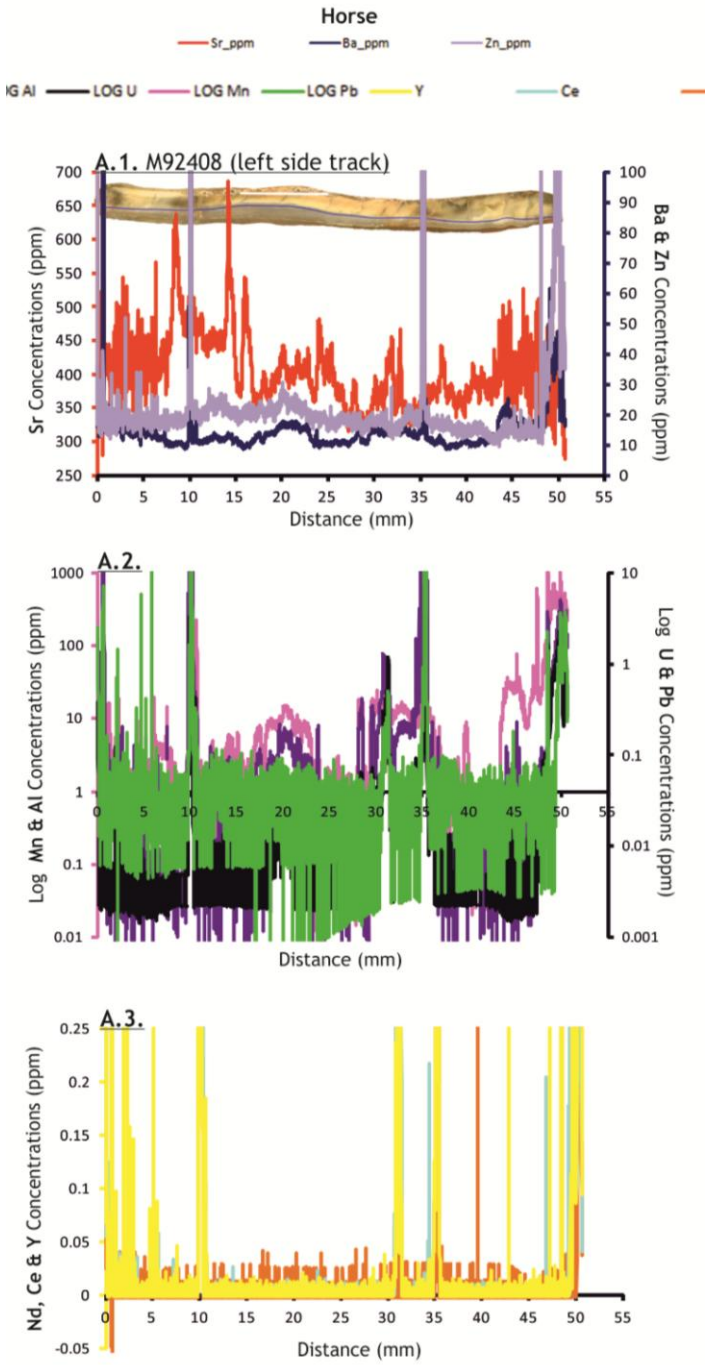

Figure 5.45. Sr, **Ba**, **Zn** (A.1); **Al**, **U**, **Mn**, **Pb** (A.2) and **REE** (A.3) concentrations (in ppm) from the laser ablation profile of M92408 horse tooth from Tornewton Cave, shown against distance (in mm) down the profile. 0 on the X –axis marks the oldest enamel and the starting point for analysis. The sectioned tooth and laser ablation track are also shown.

Furthermore, the peaks on all REEs (Fig. 5.45 A.3) display concentrations lower than 1ppm along the track with the exception of a spike in Y at 39mm up to 1.4ppm, correlating with the U peaks from 30mm onwards. Usually, the exposed parts of the

tooth where the enamel is thinner (i.e. close to the tip or base, here at 0-0.5mm and from 48mm onwards) offer entry points for diagenetic factors (Hinz and Kohn, 2010), as do fractures (here at 10mm and 35mm), which become filled by secondary minerals. The latter is highlighted by an increase in Mn values, which indicate contamination by oxyhydroxides, commonly forming dark stains on the tooth (Jaques *et al*., 2008), of Al suggesting the presence of clay (Kohn *et al*., 1999) and of REE and U values forming sharp peaks (Millard and Hedges, 1996; Kohn *et al*., 1999).

Figure 5.46 A.1 displays the Mg concentrations for the horse tooth shown against U concentrations a larger scale. These show high variability along the track and fluctuate between 1800 and 3200ppm. In addition, similar to the other elements, Mg presents two spikes at 10mm and 35mm where the concentrations reach as high as 4700ppm. Peaks in U around 20mm, between 30mm and 35mm and close to the end of the profile correspond with lower Mg concentration values.

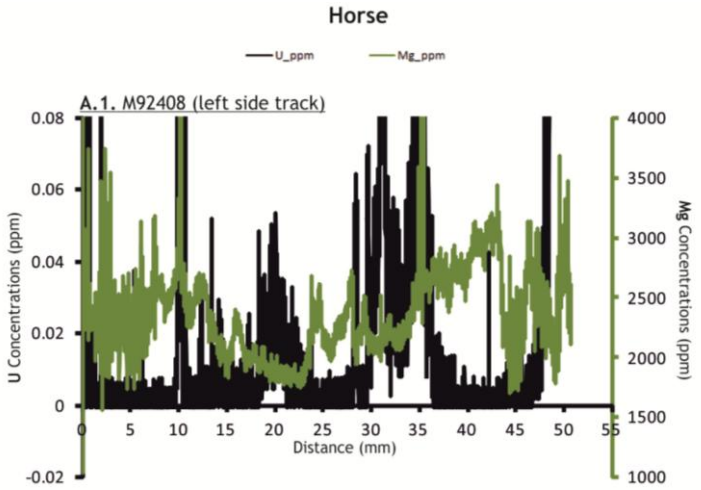

Figure 5.46. Mg and **U** (A.1) concentrations (in ppm) from the laser ablation profile of M92408 horse tooth from Tornewton Cave, shown against distance (in mm) down the profile. 0 on the X –axis marks the oldest enamel and the starting point for analysis.

5.5.2.4.2. Examination of diagenesis in the *Equus* sample through comparison with modern published data

REE, U, Al and Mn are evaluated by comparing medians, average, 1st and 3rd quartile and 10th and 90th percentiles from the horse tooth with published concentrations of

the same element on modern species, in order to reveal potential diagenetic alteration in the post-mortem environment of Tornewton Cave. The boxplots in Figure 5.47 (Ce, Nd and U) and Figure 5.48 (Al and Mn) illustrate concentrations for M92408, shown against values of the same elements from modern species (data from Kohn *et al*. [1999] and Kohn *et al*. [2013]). Although the detailed examination above (5.5.2.4.1) revealed peaks in the alternation indicators, these elements fall within the range of modern published enamel data. Nevertheless, the signal of Sr/Ca and Ba/Ca in M92408 must be treated with caution and the reasons for the high concentrations of U, Al, Mn and REEs displayed along the enamel profile must be considered.

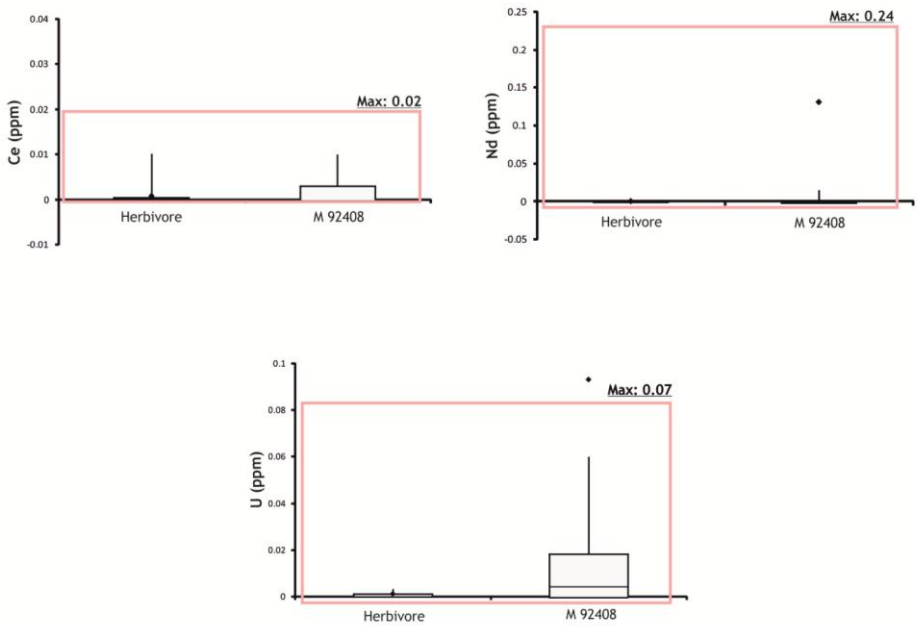

Figure 5.47. Box plots showing **Ce, Nd** (top) and **U** (below) concentrations (in ppm) of the horse tooth from Tornewton Cave in comparison with concentrations reported on extant herbivore teeth (1st box plot on each graph) (Kohn *et al*., 2013). The pink rectangles represent concentration ranges reported on modern enamel (Kohn *et al*., 1999). The boxes represent 1st and 3nd quartiles, the medians (horizontal line), averages are represented by diamonds and the whiskers show the 90th and 10th percentiles.

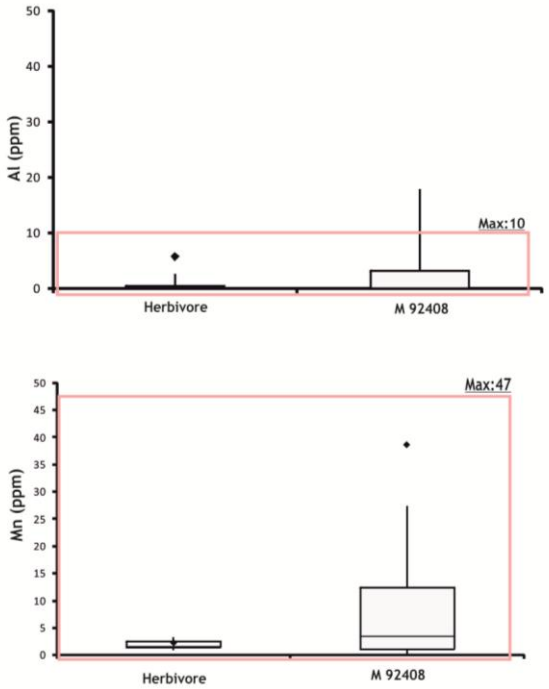

Figure 5.48. Box plots showing **Al** (top) and **Mn** (below) concentrations (in ppm) in the horse tooth from Tornewton Cave in comparison with concentrations reported on extant herbivore teeth (1st box plot on each graph) (Kohn *et al*., 2013). The pink rectangles represent concentration ranges reported on modern enamel (Kohn *et al*., 1999). The boxes represent 1st and 3nd quartiles, the medians (horizontal line), averages are represented by diamonds and the whiskers show the 90th and 10th percentiles.

5.6. Discussion

Sr/Ca, Ba/Ca and Zn/Ca ratios have been used throughout the literature as proxies for dietary variability, based on the fact that the elemental variation observed in terrestrial plants can be passed up the foodchain to consumers (in this case, mammals) (e.g. Burton *et al*., 1999; 2002; Sponheimer *et al*., 2005; Peek and Clementz, 2012a;b). As previously stated, the biopurification process results in a decrease of Sr/Ca and Ba/Ca with every increase in trophic position in a foodweb (Burton *et al*., 1999). In most publications, average values for both the Sr/Ca and Ba/Ca signals have been used to reconstruct dietary variability (e.g. Burton *et al*., 1999; 2002; Balter *et al*., 2002; 2008; Sponheimer and Lee-Thorp, 2006; Sponheimer *et al*., 2006) but despite many studies acknowledging the complexities of calculating these values, very few have actually pinpointed the importance of analysing only samples where "true" values can be obtained, i.e. where the mature diet is fully displayed (notably Humphrey *et al*., 2008a; b and Peek and Clementz, 2012b). Where this has not been done previously, therefore, the use of average values may grossly skew the results and analysis for each sample.

As outlined by Humphrey *et al*. (2008b), the different dietary and physiological parameters that contribute to the Sr/Ca content of tissues can be subdivided into four distinct stages of dietary development, for which the changes in Sr/Ca during and between them can be predicted: 1) prenatal; 2) exclusive suckling; 3) mixed suckling and independent feeding and 4) dietary maturity. Tooth selection, sampling strategy, physiological processes and geological factors also play an important roles in governing the type and reliability of any information gathered (e.g. Sponheimer and Lee-Thorp, 2006; Humphrey *et al*., 2008a; Brügman *et al*., 2012; Peek and Clementz, 2012b), as does the possibility of diagenetic alteration through the precipitation of secondary minerals and chemical alteration of biogenic apatite (Kohn *et al*., 1999; Balter *et al*., 2002). Before any interpretation of dietary variability using Sr/Ca and Ba/Ca ratios can be made, it is therefore worth reminding oneself of the complexities involved and the need to proceed with caution in interpretation.

In this section, the high resolution Sr/Ca and Ba/Ca profiles from the Tornewton Cave sample dataset will therefore be considered against the Humphrey *et al*. (2008b) model. It must be stressed from the outset that this is the first attempt to recognise these particular stages and transitions in individuals from fossil species and the conclusions should therefore be regarded as provisional, pending the future availability of more detailed histological studies, such as calculation of age at death for individual animals and further information on the timing of enamel formation in particular groups. Even for modern bears, no such study has apparently yet been carried out.

Prior to the generation of high resolution Sr/Ca and Ba/Ca profiles (Fig. 5.49 -5.54), all samples were evaluated as to whether their enamel had undergone chemical alteration in order to exclude any affected parts (see 5.5.2.). This was not only important for the accurate identification of the different dietary development stages but also essential for the calculation of the average Sr/Ca and Ba/Ca values needed for the Tornewton Cave foodweb reconstruction (see 5.6.5). Furthermore, although Zn/Ca ratios were calculated, the dearth of knowledge regarding the relationship with diet means that these ratios are not interpreted further here. Preferentially, only the fourth stage (the mature diet stage of Humphrey *et al*., 2008b) should be used for the calculation of Sr/Ca and Ba/Ca average values. In some samples, however, the third stage could also be considered.

5.6.1. Sr/C, Ba/Ca and Zn/Ca ratios of *U. arctos* samples

The variability in both Sr/Ca and Ba/Ca ratios seen in the brown bear samples from Tornewton Cave can now be linked with key stages in the life of each individual. The majority of the bear samples came from the Last Interglacial (Ipswichian, MIS 5e) deposits of the "Bear Stratum", with the exception of M41389, an m1 from the "Hyaena Stratum" (MIS 5c, Early Devensian interstadial) and M92417, an m3 from the "Glutton Stratum", MIS 2, Last Glacial Maximum). For the "Bear Stratum" samples, the background climatic and environmental conditions indicate temperate conditions, with elevated summer temperatures compared to today and mild winters and predominant mixed oak woodland habitats (Candy *et al*., 2010).

In total, 8 samples were analysed, representing a minimum number of 8 individuals. For the interpretation and the discussion of Sr/Ca and Ba/Ca profiles, the bear samples were grouped by individual tooth, so all m1s (Fig. 5.49), C (Fig. 5.50) and m3s (Fig. 5.51) will be approached separately.

In general, the Sr/Ca and Ba/Ca profiles from the bear teeth examined (Fig. 5.49 - 5.51) display variability in line with what would be expected for an omnivorous species with a seasonal diet that includes varying levels of meat, and soft and hard mast items (Mattson, 1998; Persson *et al*., 2001; Bojarska and Selva, 2012). The results are consistent with those from the dental microwear (4.3.4.), which demonstrates that the Tornewton Cave bears occupied the same eco-space as *U. arctos* from northern Europe, *U. americanus* and *H. malayanus*. This suggests that these bears were most probably consuming mainly soft mast (such as fleshy fruits, fibrous foods such as leaves and flowers) and invertebrates, taking vertebrates (fish and ungulates) only occasionally.

Despite the fact that the timing of mineralisation in bear teeth has not been fully studied, it is nevertheless possible to map the dietary stages of Humphrey *et al*. (2008b) onto X-ray images of living brown bear and fossil cave bear teeth from Slovenia (Dittrich, 1960; Debeljak, 1996) in order to explore further certain physiological processes in bears. It is clear from the Sr/Ca and Ba/Ca profiles generated from the Tornewton Cave sample that some variation in the signal must be attributed to the weaning effect. This is the first time that the influence of milk consumption in fossil bears has been demonstrated through geochemistry.

As might be anticipated, the m1 samples analysed display a similar pattern along their Sr/Ca and Ba/Ca profiles (Fig. 5.49.A.1 –C.1). All presented very low concentrations of almost all alteration indicators (see 5.5.2.1.2) and it can therefore be concluded that the geochemical signals have not been affected by diagenesis. The exceptions are certain parts of the M41097 and M41397 profiles, for which the data have been excluded (Fig. 5.49A.1 and B.1.).

The first 0.6mm of the enamel profile of the m1 samples (Fig. 5.49.A.1 –C.1) is considered here to record the suckling period (stage 2 of Humphrey *et al*. [2008b]), on

account of the higher Sr/Ca signals at this point. At 0.6mm distance, the ratios drop slightly and then increase again, also becoming more variable. This is interpreted here as reflecting the introduction of complementary food in addition to milk (the mixed suckling and independent feeding period, stage 3 of the Humphrey *et al*., [2008b] model). In contrast, the final phase (stage 4, dietary maturity) is not consistently recognisable in the m1s because of the apparent variability between the teeth. However, in M41389 (Fig. 5.49.C.1), which also appears to be the best preserved m1, an increase at 3.3mm in both Sr/Ca and Ba/Ca ratios may mark the transition between dietary stages 3 and 4. If this is the case, it may be hypothesized that the transition occurs at a similar point along the profile for the other teeth. In M41097 (Fig. 5.49.A.1), a small increase Sr/Ca and Ba/Ca ratios may mark the onset of stage 4, although the likelihood of diagenetic alteration from 8.2mm until the end of the profile means that the later phases of this stage cannot be documented on this specimen. In M41397, (Fig. 5.49.B.1), the Sr/Ca and Ba/Ca profiles are clearly different to those of the other two specimens at both key points, after 0.6mm and after 3.3mm. Alteration indicators are in low concentrations and there is no apparent diagenesis of the enamel, except around 2mm. It may therefore be tentatively concluded that this individual exploited different resources to the other two after the transition to independent feeding.

With respect to the canine teeth, the Sr/Ca and Ba/Ca profiles on both samples (Fig. 5.50.A.1 and B.1) are similar but M40688 has clearly been diagenetically affected on account of the presence of alteration indicators and the physical condition of the sample. In contrast, Sr/Ca and Ba/Ca signals in M40646 may be considered to be faithfully reproduced, since alteration indicators remain low throughout (see 5.5.2.1.2.).

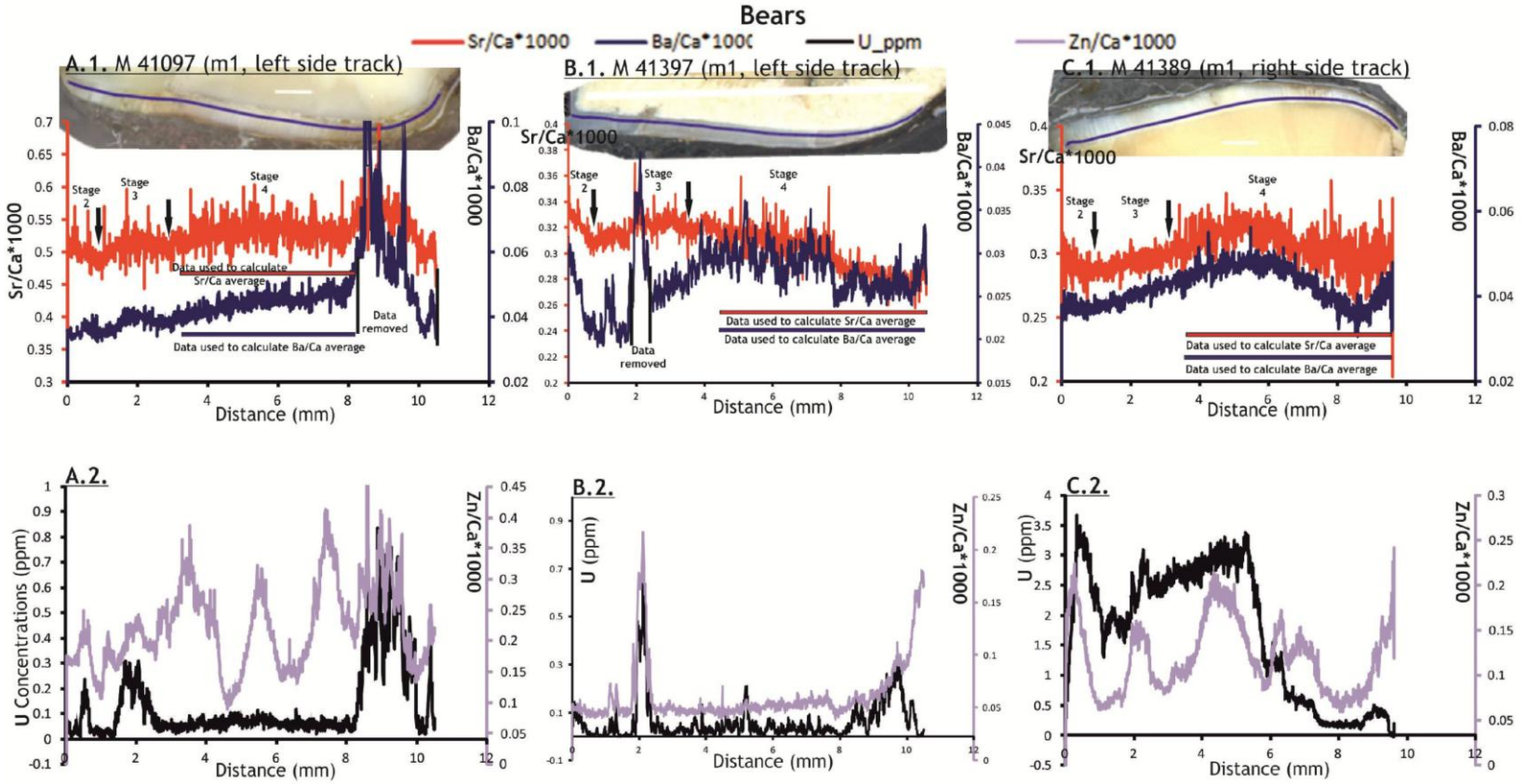

Figure 5.49. Graphs showing high resolution **Sr/Ca and Ba/Ca** (A.1, B.1, C.1) and **Zn/Ca ratios and U-concentrations** (A.2, B.2, C.2) of bear m1s from Tornewton Cave, shown against distance (in mm). The oldest enamel is at the cusp of the tooth (0 on the X -axis), whilst the youngest is at the end of profile. Sectioned teeth and laser ablation tracks are also shown. Red and blue lines mark the Sr/Ca and Ba/Ca areas that most probably represent unaltered dietary signals and were used for the calculation of average values (see section 5.6.5). The different dietary stages according to Humphrey *et al.* (2008b) are also indicated (arrows mark the start of each stage).

The first 2.5mm of the enamel profile in M40646, where Sr/Ca and Ba/Ca ratios are relatively high, is considered to represent the suckling phase (stage 2 of Humphrey *et al*. [2008b]). This is followed by a small decrease and then increase again in the ratios until 6.3.mm, this period most probably reflecting the introduction of complementary food in addition to milk, (stage 3 of Humphrey *et al*., 2008b). The last part of the record, from 6.3mm until the end of the profile, therefore potentially reflects the "true" adult diet of the individual.

With respect to the Sr/Ca and Ba/Ca profiles on the m3, the evidence for alteration indicators implies that these samples have undergone some degree of chemical alteration (see 5.5.2.1.2.); these parts were accordingly excluded from the calculation of the average values of Sr/Ca and Ba/Ca. In addition, the Sr/Ca and Ba/Ca profiles in M92417 are difficult to interpret because of the high U values (higher than in modern enamel) throughout the tooth, which differ from those seen in the other two m3 samples. For this reason, this tooth was excluded from the calculations of average Sr/Ca and Ba/Ca values.

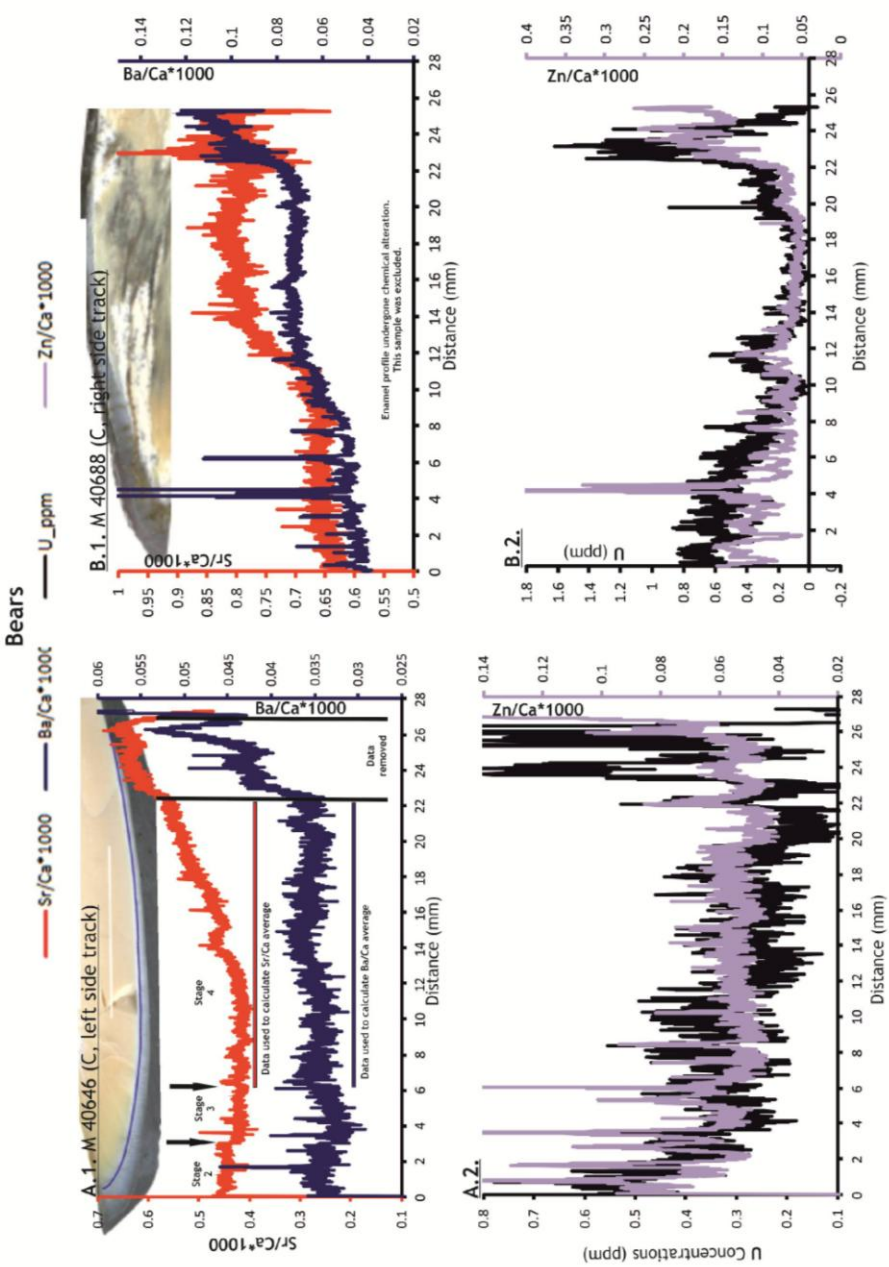

Figure 5.50. Graphs showing high resolution **Sr/Ca and Ba/Ca** (A.1, B.1) and **Zn/Ca ratios and U-concentrations** (A.2, B.2) of bear canine teeth from Tornewton Cave, shown against distance (in mm). The oldest enamel is at the cusp of the tooth (0 on the X -axis), whilst the youngest is at the end of profile. Sectioned teeth and laser ablation tracks are also shown. Red and blue lines mark the Sr/Ca and Ba/Ca areas that most probably represent unaltered dietary signals and were used for the calculation of average values (see section 5.6.5). The different dietary stages according to Humphrey *et al.* (2008b) are also indicated (arrows mark the start of each stage).

On M40750 (Fig. 5.51.A.1) and M92414 (Fig. 5.51.B.1), from the beginning of the profile until 0.7mm of enamel, the stage 2 suckling period is indicated by relatively high Sr/Ca signals. At 0.7mm, the ratios drop slightly and then increase again with the introduction of complementary food in addition to milk. This is considered to reflect the mixed suckling and independent feeding period of the bears (stage 3 of Humphrey *et al*., 2008b) until the 1.3mm point, although this is tentative (see below). The last

stage, which is thought here to record the “true” signal of dietary maturity, is therefore inferred to start from 1.3mm onwards in each sample. Both the Sr/Ca and Ba/Ca signals are more variable from this point onwards, reflecting dietary variability in these individuals. Of note in both samples is the sudden decrease in both Sr/Ca and Ba/Ca values, at 2.3mm in M40750 and at 1.6mm in M92414. This could be interpreted as either (1) reflecting a major change in diet due to seasonal availability, although none of the samples display clear sinusoidal signals that might uphold this suggestion; or (2) marking the real onset of dietary stage 4 (as opposed to 1.3mm onwards, as previously inferred above). This would indicate that differences are present within the same element in two individuals with respect to the timing of the onset of each stage; or (3) reflecting a stress-related event that impacted on the animals’ physiology, for example hibernation. These hypotheses must, for the time being, remain speculative until future timing of enamel formation and histological studies are carried out.

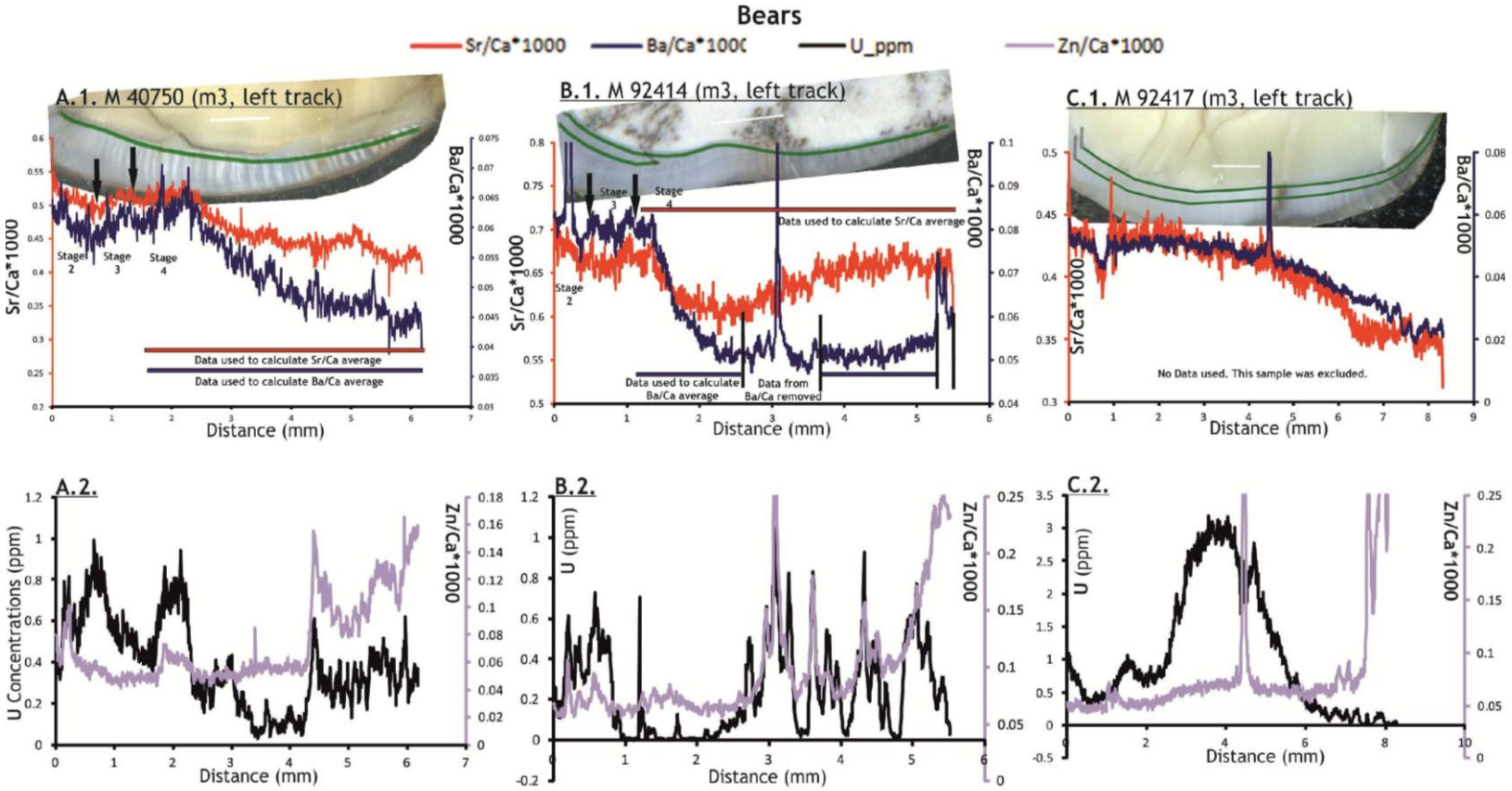

Figure 5.51. Graphs showing high resolution **Sr/Ca and Ba/Ca** (A.1, B.1, C.1) and **Zn/Ca ratios and U-concentrations** (A.2, B.2, C.2) of bear m3 teeth from Tornewton Cave, shown against distance (in mm). The oldest enamel is at the cusp of the tooth (0 on the X -axis), whilst the youngest is at the end of profile. Sectioned teeth and laser ablation tracks are also shown. Red and blue lines mark the Sr/Ca and Ba/Ca areas that most probably represent unaltered dietary signals and were used for the calculation of average values (see section 5.6.5). The different dietary stages according to Humphrey *et al*. (2008b) are also indicated (arrows mark the start of each stage).

5.6.2. Sr/Ca, Ba/Ca and Zn/Ca ratios of *C. crocuta* samples

The two hyaena samples (both m1s) discussed in this section were found in different strata within Tornewton Cave. M92410 (Fig. 5.52.A.1 and A.2) was reportedly found in the "Elk Stratum", attributed to MIS 3 (Currant, in Roberts [1996]; Currant, 1998; Gilmour *et al*., 2007) and M38994 (Fig. 5.52.B.1 and B.2) was recovered from the "Hyaena Stratum", attributed to MIS 5c (Gilmour *et al*., 2007). The climate in southern Britain during MIS 3 was overall cooler than present, although subject to rapid and abrupt oscillations, and the environment was predominantly treeless steppe grassland (Currant and Jacobi 2001; 2011), whereas during MIS 5c, an interstadial within the Early Devensian, a transition from woodland to more open grassland conditions has been suggested (Currant and Jacobi, 2001; 2011; Gilmour *et al*., 2007).

Within the wider carnivore guild, it is to be anticipated that the obligate meat-eaters will have the highest Sr/Ca ratios. For example, studies on *Homotherium*, the extinct sabre-tooth, from the Omo Shungura Formation in Ethiopia have revealed that this hypercarnivore had elevated Sr/Ca ratios when compared to other carnivores (Sillen, 1992). However, unexpectedly for the Tornewton *Crocuta*, given that this is a wholly carnivorous species (Kruuk, 1972), the results from the two teeth have different Sr/Ca and Ba/Ca ratios. In M92410 (Fig. 5.52.A.1), the Sr/Ca and Ba/Ca ratios are around of around 0.5 and 0.04 respectively until 8.5mm and then increase up to 0.6 in Sr/Ca and to 0.06 in Ba/Ca, becoming increasingly "noisy", with very high values indicating alteration towards the end of the profile. In contrast, M38994 (Fig. 5.52.B.1) is more variable throughout, with higher Sr/Ca and Ba/Ca ratios than M92410, and a decrease in Sr/Ca along the growth profile, from 2.5 to approximately 1.5, whereas the Ba/Ca ratios increase from 0.02 to 0.05.

The differences between the two hyaena samples are most probably not due to chemical alteration, since neither specimen displays significant evidence of alteration (see 5.5.2.2.2.).

Currently, there is no published information available on the timing of tooth mineralisation in hyaenas so it is unclear what time period the enamel profile in the m1s covers. However, it is known that the approximate eruption time of the

permanent cheek teeth is between 10 and 15 months (Van Horn *et al*., 2003). The nursing period lasts for the first 12-16 months of the animal's life (Kruuk, 1972; Law, 2004), although the young can process solid food as early as 3 months of age (Kruuk, 1972). Therefore, it is most likely that the two Tornewton samples cover three of the four dietary stages of Humphrey *et al*. (2008b), although the beginning and end of each stage, and indeed the evidence for dietary maturity, may be difficult to pinpoint because of the lack of information on mineralisation. In M92410, it can be inferred that the minor decrease observed in both Sr/Ca and Ba/Ca ratios at approximately 2mm indicates the onset of a different dietary stage, most likely the introduction of non-milk foods alongside suckling (stage 3 of Humphrey *et al*., 2008b). The end of this stage and the cessation of suckling (stage 4 of Humphrey *et al*., 2008b) is suggested to be either at 6mm or close to 8.5mm, where the ratios slightly decrease and increase in both profiles (Fig. 5.52.A.1). In M38994, the end of stage 2 and beginning of stage 3 could potentially lie close to 4mm, with the transition from stage 3 to 4 at 8mm (Fig. 5.52.B.1).

The differences in the ratios between the two samples may be a reflection of their different stratigraphical provenance and age. M38994 (from the "Hyaena Stratum", MIS 5c) has overall higher Sr/Ca ratios and therefore most probably represents a hyaena that consumed prey species with higher Sr/Ca ratios than those eaten by the individual represented by M92410 (from the "Elk Stratum", MIS 3). The herbivore prey available to large carnivores during MIS 3 included woolly mammoth, woolly rhinoceros, bison, wild horse, red deer, giant deer and reindeer, whereas during MIS 5c, a different range of more temperate-adapted taxa is noted, including straight-tusked elephant, red deer, bison and roe deer, although occasional woolly mammoth has also been noted (Turner, 2009). Since prey availability was therefore likely to be similar for the carnivores between both stages, the differences are probably related to the type and availability of plant species for the herbivores. During times of relatively higher productivity, such as interglacials or interstadials, a greater range of roots and stems (with higher Sr/Ca and Ba/Ca ratios) will be also available and animals may have bigger choices. In addition to this it has been reported that Sr/Ca and Ba/Ca ratios are

higher in roots and stems than in leaves and fruits (e.g. Runia, 1987; Burton *et al*., 1999).

However, this interpretation must be seen as tentative, since other explanations such as tooth mineralisation chronology, metabolic responses to a specialist flesh diet and migration need to be considered. Given that the Tornewton Cave specimens are unlikely to have become mixed with those of another fossil locality, it is more likely that M38994 represents an individual that may have spent its early years in an area with a different geological background, one with higher Sr/Ca ratios.

Figure 5.52 shows the parts of the Sr/Ca and Ba/Ca profiles from which the average values for both ratios were calculated.

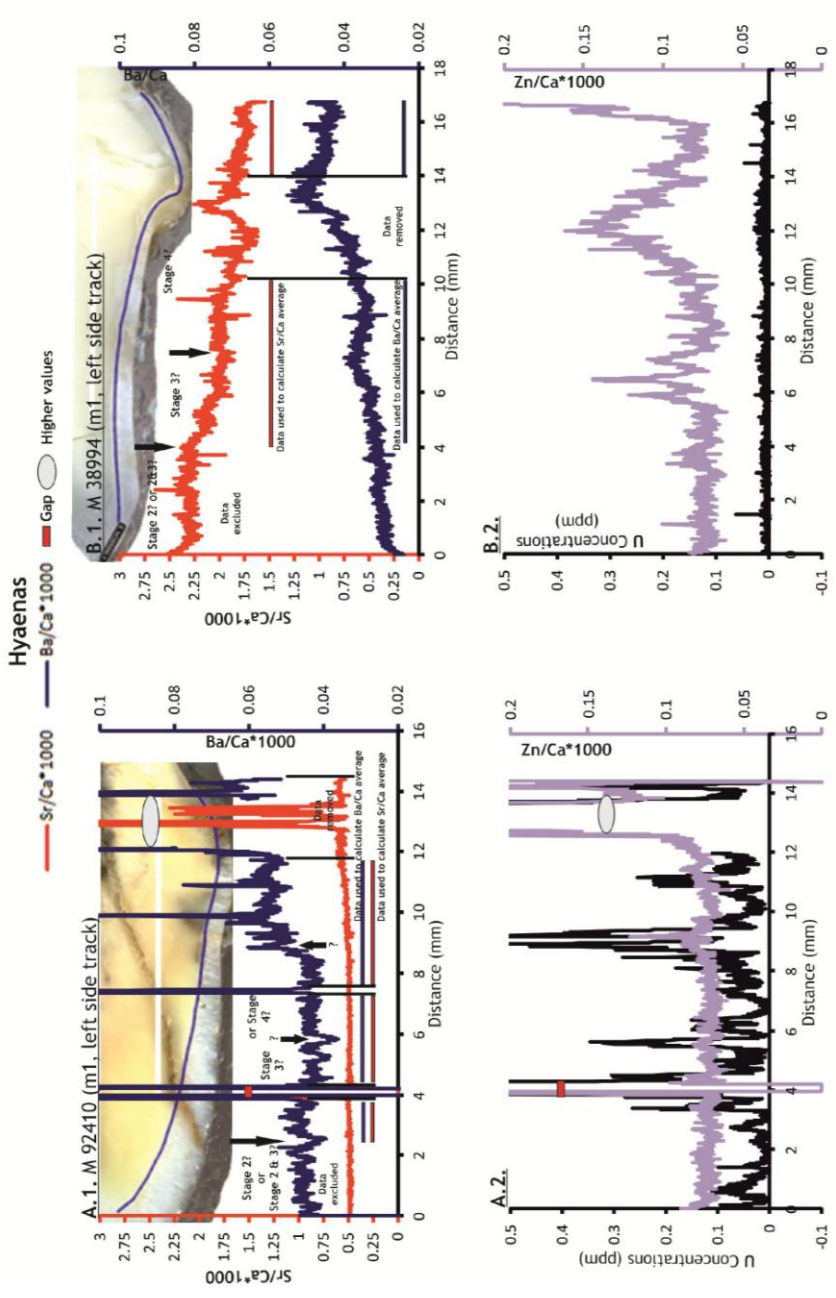

Figure 5.52. Graphs showing high resolution **Sr/Ca and Ba/Ca** (A.1 and B.1) and **Zn/Ca ratios and U-concentrations** (A.2 and B.2) in m1 hyaena teeth from Tornewton Cave, shown against distance (in mm). The oldest enamel is at the cusp of the tooth (0 on the X - axis), whilst the youngest is at the end of the profile. Sectioned teeth and laser ablation tracks are also shown. Red and blue lines mark the Sr/Ca and Ba/Ca areas that most probably represent unaltered dietary signals and were used for the calculation of average values (see section 5.6.5). The different dietary stages according to Humphrey *et al.* (2008b) are also indicated (arrows mark the start of each stage).

5.6.3. Sr/Ca, Ba/Ca and Zn/Ca ratios of *C. elaphus* samples

The patterns noted in both Sr/Ca and Ba/Ca ratios in the m1 (Fig. 5.53.A.1), m2 (Fig. 5.53.B.1) and m3 (Fig. 5.53.C.1) of the sampled red deer specimen (M41530) from Tornewton Cave (from the "Hyaena Stratum, MIS 5c) reveal much important information regarding the physiology and dietary parameters during the life history of this animal. Examination of the alteration indicators in these samples reveals very low concentrations, well below modern published enamel values, suggesting that both Sr/Ca and Ba/Ca ratios are unaltered. Compared to the hyaena samples discussed

above, the red deer would be expected to present a more variable Sr/Ca profile, since they are mixed feeder herbivores. Red deer are ruminants with foregut microbial fermentation and as a mixed feeder, they should also present lower Sr/Ca ratios than grazers (see comparison with horse in 5.6.4).

Variations observed in the Sr/Ca and Ba/Ca ratios reflect the different stages in the early development and later life of the animal (Fig. 5.53.A.1-C.1), changes that can be linked to the four dietary stages of Humphrey *et al*. (2008b). In the m1, all four stages are apparent, since mineralisation in this tooth begins *in utero* and is completed 4 months after birth (Brown and Chapman, 1991a). Red deer give birth in spring to early summer (June or July) and calves are weaned within the first 60 days of life (Senseman, 2002). Both the Sr/Ca and Ba/Ca profiles of the m1 show similar variability. It is therefore inferred here that the first 1mm of the enamel profile (Fig. 5.53.A.1) is recording the placental and nursing signals (stages 1 and 2 of Humphrey *et al*., [2008b]), with little internal variability apparent. After 1mm and until 3mm, the increase in Sr/Ca (from 0.57 to 0.61) and Ba/Ca (from 0.15 to 0.17) ratios may indicate the introduction of complementary foods in addition to milk (stage 3). The highest Sr/Ca ratios, when suckling ceases, mark the transition between dietary stages 3 and 4 and this is visible in the m1 from approximately 3mm (Fig. 5.53.A.1). After this point, the young red deer begins to discriminate fully against Sr and Ba in the digestive tract, which is reflected in the small decrease in values and subsequent minor oscillations in the ratios (around 0.6 in Sr/Ca and 0.2 in Ba/Ca). For the m1, only the last part of the Sr/Ca and Ba/Ca profiles was therefore used for average calculation of values, since this is most probably the period when the animal had reached dietary maturity.

In the red deer m2 (Fig. 5.53.B.1), it is also possible to discern the effect of the weaning signal, since this tooth mineralises between 3.5 and 9 months (Brown and Chapman, 1991a). Both Sr/Ca and Ba/Ca ratios of the enamel from the crown to the base of the m2 reveal substantial changes, notably the transition between dietary stages 3 and 4 (indicated by a decrease in values) after the first 1.5mm of the profile. In addition, from 3mm and until the end of both Sr/Ca and Ba/Ca profiles, a more variable, possibly sinusoidal, signal develops; this is especially visible after 6mm in Ba/Ca. This is echoed by the Zn/Ca profile (Fig. 5.53.B.2). This sinusoidal signal is interpreted here as

reflecting seasonal variation in diet and is also apparent in the Sr/Ca, Ba/Ca and Zn/Ca ratios in the m3 (Fig. 5.53.C.1 and C.2). The m3 is the only tooth in this individual to be completely unaffected by the weaning signal, since the m3 mineralises between 9 and 26 months (Brown and Chapman, 1991a), well after the cessation of suckling. It can therefore be assumed that the Sr/Ca and Ba/Ca profiles in the m3 (Fig. 5.53.C.1) recording dietary maturity (stage 4 of Humphrey *et al*., 2008b) and furthermore, reflect seasonal variation in diet. Although red deer are highly adaptable, they are generally regarded as mixed feeders that prefer fresh shoots, forbs and browse, with grasses making up a lesser part of the diet (Gebert and Verheyden-Tixier, 2001; Lovari *et al*., 2008; Storms *et al*., 2008). During summer, red deer feed on forbs, sedges and grasses, whereas during the winter months, they consume woody plants including shrubs and tree shoots, as well as occasionally mushrooms and lichens that are rich in protein (Senseman, 2002; Lovari *et al*., 2008). Studies on grazer versus browser species have revealed that the former have higher Sr/Ca ratios than the latter (e.g. Sillen, 1992; Sponheimer *et al*., 2005; Sponheimer and Lee-Thorp, 2006). This ultimately could potentially also be linked with small variations in Sr/Ca and Ba/Ca ratios during different seasons when the animals consume different food items. For example, it is expected that during periods when the red deer from Tornewton Cave consumed grasses and sedges (in summer); will have higher values than when feeding on shrubs and tree shoots (in winter). In addition, such variations may be also enhanced by any seasonal migration that the animal undertook on an annual basis. For example it has been documented that red deer spends summers at higher elevation, migrating to lower elevations during winter (Senseman, 2002). Figure 5.53 reveals the areas on each sample that were used for average value calculations. In summary, the three teeth provide complementary lines of evidence that together reveal the dietary history of the first 1.5 years of life of the individual. All four dietary stages of Humphrey *et al*. (2008b) have been mapped for the first time in a Pleistocene mammal and secondly, a sinusoidal signal has been detected in the m3, which is interpreted as reflecting seasonal dietary changes where most probably the areas of Sr/Ca and Ba/Ca profiles with higher ratios reflecting summer and those with lower ratios winter.

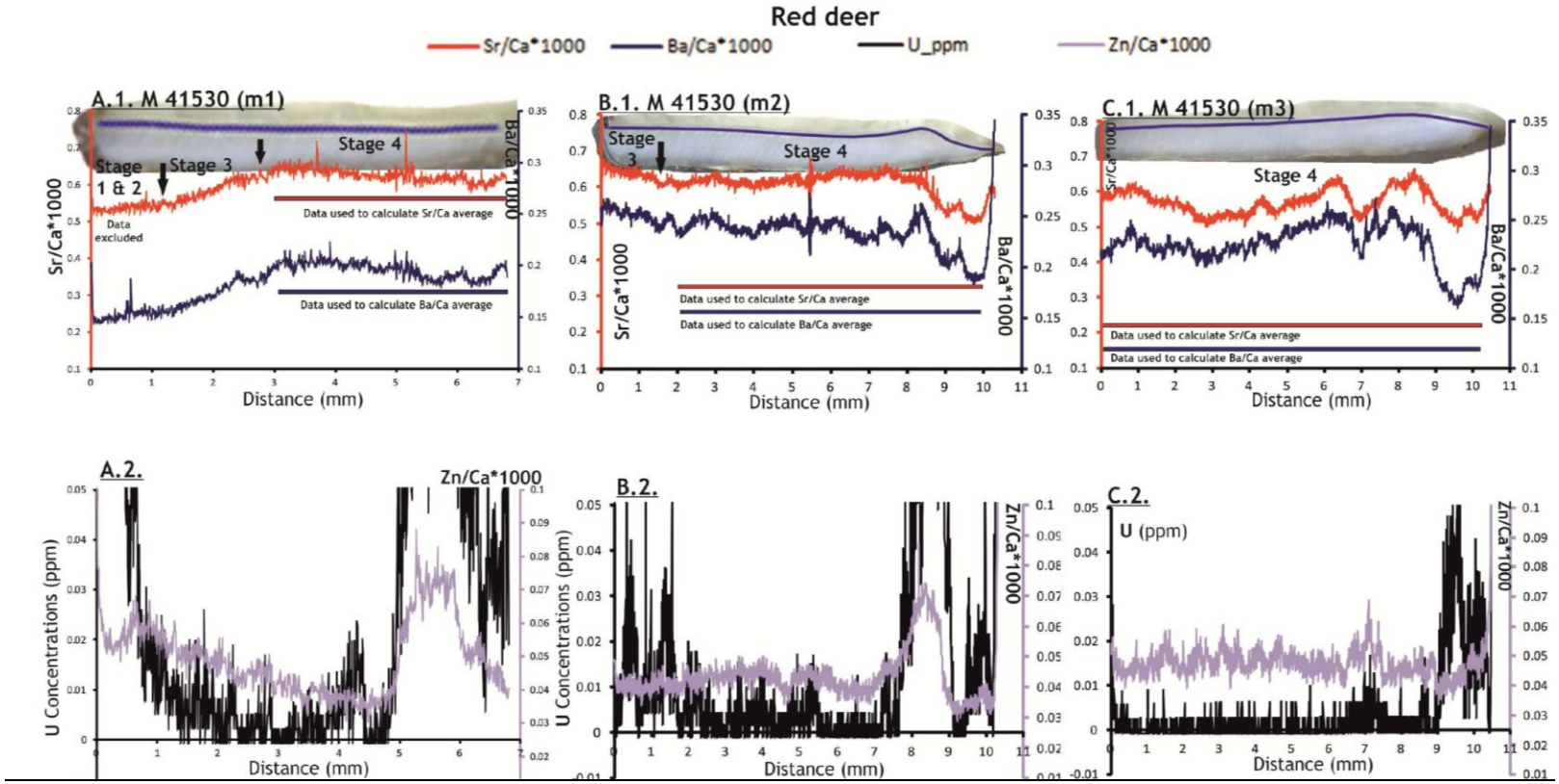

Figure 5.53. Graphs showing the high resolution **Sr/Ca and Ba/Ca** (A.1, B.1, C.1) and **Zn/Ca ratios and U-concentrations** (A.2, B.2, C.2) of M41530 m1 (A.1 and A.2), M41530 m2 (B.1 and B.2) and M41530 m3 (C.1 and C.2) red deer teeth from Tornewton Cave, shown against distance (in mm). The oldest enamel is at the cusp of the tooth (0 on the X -axis), whilst the youngest is at the end of the profile. Sectioned teeth and laser ablation tracks are also shown. Red and blue lines mark the Sr/Ca and Ba/Ca areas that most probably represent unaltered dietary signals and were used for the calculation of average values (see section 5.6.5). The different dietary stages according to Humphrey *et al*. (2008b) are also indicated (arrows mark the start of each stage).

5.6.4. Sr/Ca, Ba/Ca and Zn/Ca ratios of *Equus* samples

The horse specimen, an m3 (M92408), was recorded from the "Elk Stratum" (Middle Devensian, MIS 3; Currant, in Roberts [1996]; Currant, 1998; Gilmour *et al*., 2007). As stated above, the climate of this time was predominantly cool and the environment characterised by a treeless steppe grassland (Currant and Jacobi 2001; 2011]). The high hypsodonty of equid teeth, as well as the evidence from dental microwear indicate a highly abrasive diet based on grasses (e.g. Rivals *et al*., 2010).

A particular point of note is that the Sr/Ca and Ba/Ca profiles from the horse sample record high amplitude variation (Fig. 5.54.A.1). Examination of the alteration indicators reveals that there are parts of the signal that have been chemically altered and although also the photograph of the m3 (Fig.5.54.A.1.image) hints a poor preservation and highlights the possibility of U uptake through the side of the dentine (Hoffman *et al*., 2008), the alteration indicators for the remainder of the profile are relatively low and within modern published enamel values (section 5.5.2.4.2).

Figure 5.54.A.1 shows and highlights in the sections of the Sr/Ca and Ba/Ca profiles the areas that most likely reflect the "true" unaltered dietary values and where average values for both ratios were calculated. As mentioned above, grazers have higher Sr/Ca and Ba/Ca ratios than browsers because although there is a great deal of inter- and *intra*-specific variation in plant ratios, grasses have higher Sr/Ca and Ba/Ca ratios than browse (forbs and trees) (e.g. Sponheimer and Lee-Thorp, 2006). The horse sample from Tornewton Cave would therefore be expected to have higher average ratios than all the other species from the site, as will be seen in the trophic level graph (see 5.6.5).

Enamel mineralisation in the m3 of horse begins at 21 months and ends at 55 months (Hoppe *et al*., 2004), thus the enamel profile records approximately 2.5 years of the animal's life. The nursing period ends by 9 months (e.g. Bryant *et al*., 1996b; Hoppe *et al*., 2004) so by the onset of enamel mineralisation in this tooth, the wild horse would have developed the ability to discriminate against Sr and Ba in the digestive tract. Neither the Sr/Ca, nor the Ba/Ca ratios are therefore affected by the weaning signal. Thus, any variability identified in this unaltered signal must relate either to the diverse nature of the grasses consumed, and/or to mobility, where the animal moves to a

different location with a different geology and plant types. However, similar to the patterns observed for red deer above, both the Sr/Ca and the Ba/Ca ratios display some sinusoidal signal that may be interpreted as a seasonal pattern diet. Horses are known to be grazing specialists based on their morphology, recent habitat selection and dietary choices (e.g. Eisenmann, 1998; Macdonald, 2009) but will sometimes browse especially during winter (5.3.4) This can be observed on the pattern of both Sr/Ca and Ba/Ca ratios in the Tornewton horse specimen and as with the red deer (5.6.3), lower ratios are considered to reflect the winter period and higher ratios the summer (Fig. 5.54.A.1).

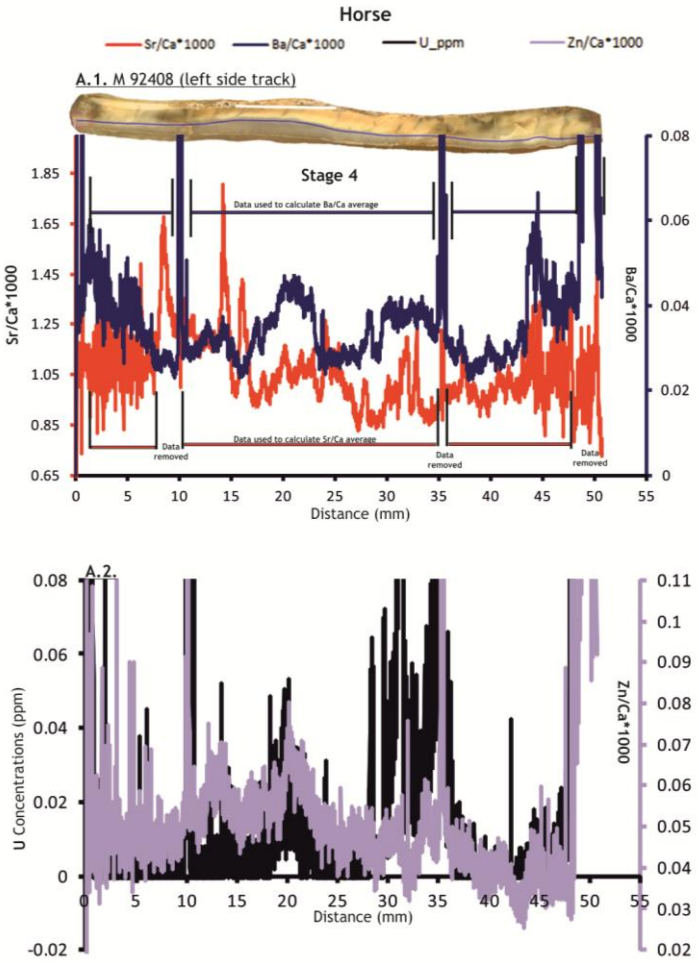

Figure 5.54. Graphs showing high-resolution **Sr/Ca and Ba/Ca** (A.1) and **Zn/Ca ratios and U-concentrations** (A.2) in a horse m3 from Tornewton Cave, shown against distance (in mm). The oldest enamel is at the cusp of the tooth (0 on the X -axis), whilst the youngest is at the end of the profile. Sectioned teeth and laser ablation tracks are also shown. Red and blue lines mark the Sr/Ca and Ba/Ca areas that most probably represent unaltered dietary signals and were used for the calculation of average values (see section 5.6.5). The different dietary stages according to Humphrey *et al*. (2008b) are also indicated (arrows mark the start of each stage).

5.6.5. Average Sr/Ca and Ba/Ca values and food web reconstruction from Tornewton Cave

Previous studies have demonstrated that the Ca biopurification process results a decrease of Sr/Ca and Ba/Ca with increasing trophic level in a foodweb (e.g. Elias *et al*., 1982; Burton *et al*., 1999; Blum *et al*., 2000). With respect to the pilot study conducted here from Tornewton Cave, the hypothesis would therefore be that the obligate carnivore (spotted hyaena) samples should demonstrate lower Sr/Ca and Ba/Ca ratios than the herbivore taxa, with the omnivorous bear samples lying in between. Average Sr/Ca and Ba/Ca values were calculated from sections of enamel that were considered unaltered (or where alteration indicators were present in low concentrations) and for those parts, the dietary maturity of each individual could be recognised with reasonable confidence. Table 5.14 presents the raw averages from the whole tracks as well as the re-calculated averages (from stage 4 only) for each tooth profile. From these results, it is clear that bulk ratios used in previous studies as palaeodietary proxies may not be appropriate, since they fail to take account of the variation along the profile that can affect the average results for Sr/Ca and Ba/Ca values. The variability around the mean values is displayed with the errors for each sample in Figure 5.55.

Table 5.14. Sr/Ca and Ba/Ca averages from each tooth from Tornewton Cave.

Tooth/Sample	Average calculated with reference to alteration indicators and dietary maturity (stage 4 after Humphrey *et al*. [2008b])		Raw average	
	Sr/Ca	Ba/Ca	Sr/Ca	Ba/Ca
Hyaena M92410	0.494	0.049	0.569	0.403
Hyaena M38994	1.956	0.038	2.016	0.037
Red deer M41530m1	0.624	0.196	0.600	0.182
Red deer M41530m2	0.605	0.233	0.610	0.236
Red deer M41530m3	0.570	0.225	0.570	0.225
Bears M40750	0.462	0.053	0.472	0.054
Bears M92414	0.639	0.056	0.646	0.062
Bears M41097	0.528	0.044	0.524	0.047
Bears M41389	0.307	0.043	0.301	0.042
Bears M40646	0.462	0.035	0.484	0.036
Horse M92408	1.025	0.034	1.062	0.041

It is now possible to make some observations regarding the food web at Tornewton Cave. Figure 5.55 supports the aforementioned hypothesis, confirming that the herbivorous species from Tornewton Cave have higher Sr/Ca and Ba/Ca ratios than the carnivorous hyaena M92410 from the MIS 3 "Elk Stratum". However, an important point is that the hyaena M38994, from the MIS 5c "Hyaena Stratum" exhibits the highest Sr/Ca ratio of any species sampled from the cave. The differences between the two hyaena signals have already been discussed in 5.6.2. but after plotting this sample against the other species from Tornewton Cave, the most plausible explanation (having eliminated any possibility of diagenetic contamination) is that the geographical origin of this specimen is different to that of the other species, i.e. that this animal spent the first year(s) of its life elsewhere before moving to the Tornewton area. Further investigation using strontium isotopic analysis could be used to support or reject this explanation (e.g. Brügman *et al*., 2012).

Another interesting aspect of Figure 5.55 is the position of the omnivorous brown bear. As hypothesised, this species would be expected to have Sr/Ca and Ba/Ca ratios intermediate between those of herbivores and carnivores. The bears examined have lower values than the herbivore species but when compared to the hyaena M92410, most samples show very similar ratios. This similarity between the hyaena and bear ratios could be explained by the fact that some bears from Tornewton Cave may have included large portions of meat into their diet. The conclusions of the dental microwear study of the Tornewton bears (see 4.3.4 and 4.5) do not rule out the consumption of meat, however it suggests that these bears were most probably consuming soft mast (such as flesh fruits, including fibrous food such as leaves and flowers) and invertebrates and only very occasionally vertebrates (fish and ungulates).

With respect to the bear samples, one specimen (M92414) has Sr/Ca average ratios slightly above 0.5, which lie very close to the values of the mixed feeder, red deer, while one specimen (M41389) shows lower average ratios than the majority of the bears (Fig. 5.55). This could potentially reflect *intra*-species variability, with one individual exploiting either a different kind of plant matter to the other, or more meat than the other (M41389 being more carnivorous).

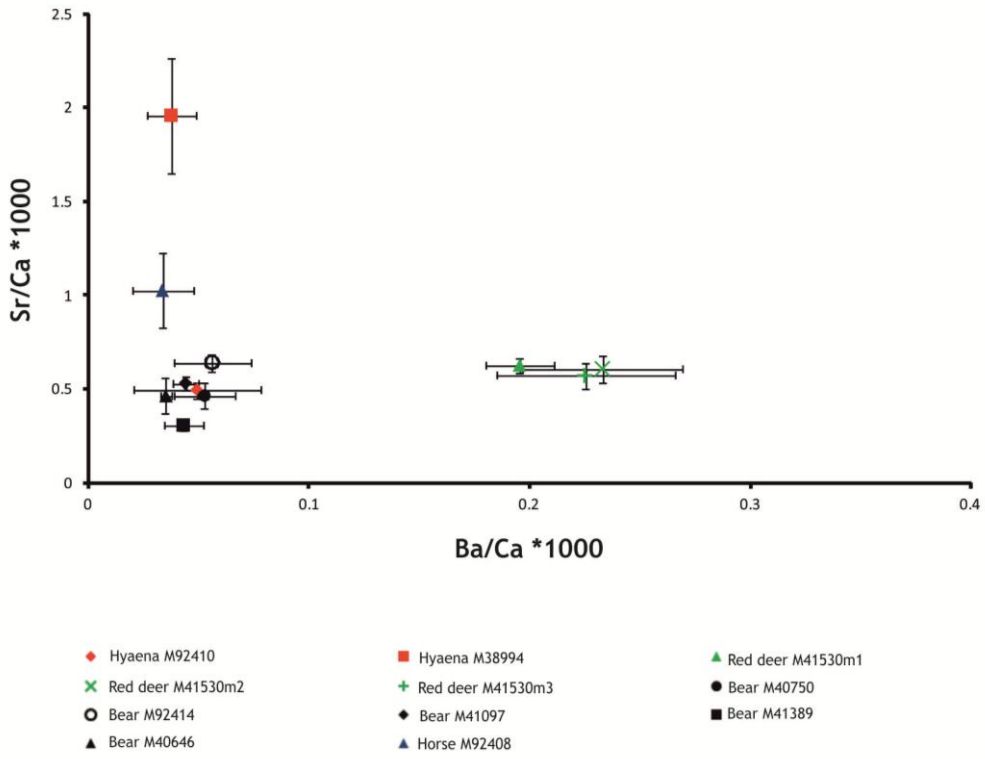

Figure 5.55. Graph showing the average **Sr/Ca and Ba/Ca** ratios from each tooth from Tornewton Cave. Errors denote 2 standard deviations.

Differences between Sr/Ca and Ba/Ca ratios have been recorded on plant matter with roots, edible grass parts (notably seeds) and stems, for example, having higher Sr/Ca and Ba/Ca ratios than leaves and fruits (Runia, 1987; Burton *et al*., 1999). Comparison of the Sr/Ca and Ba/Ca ratios with the results from the dental microwear reveal that M41389 is closely comparable to the other bear specimens from Tornewton in terms of its microwear features, i.e. the features do not reveal a particularly carnivorous tendency. Thus, the simplest explanation for the geochemical differences between M41389 and M92414 is that they were consuming different plant species. This is consistent with the fact that the two specimens are from different stratigraphical levels; the former is from the "Hyaena Stratum" (MIS 5c), whereas the latter is from the "Bear Stratum" (MIS 5e). The individual from the "Hyaena Stratum" may therefore have been preferentially consuming plants such as roots and grasses (which have higher Sr/Ca ratios) in an interstadial environment, whereas the individual from the "Bear Stratum" was exploiting more fruit and leaves, consistent with a fully interglacial environment. This does not preclude a meat component in the diet of both bears,

particularly since the geochemical composition of the prey consumed will itself be influenced by the nature of the available vegetation.

In terms of future work, more hyaena samples need to be analysed in order first to clarify the carnivorous position of this animal within the Tornewton Cave ecosystem and to provide a more detailed point of comparison with the potentially highly carnivorous tendencies of some of the bears. In addition, investigation of the timing of enamel mineralisation in both hyaenas and bears would also help to establish whether the low Sr/Ca and Ba/Ca ratios of the hyaena M92410 result from the weaning signal, and how the changes within Sr/Ca and Ba/Ca signals in the bears reflect variations in diet.

The horse sample M92408 yielded the highest Sr/Ca ratios (Fig. 5.55) compared to the other herbivores from Tornewton Cave. While this might (in part) result from the diagenetic alteration that is apparent on some parts of the specimen, the higher Sr/Ca ratio is to be expected for a grazing animal, as opposed to a browser (e.g. Sponheimer and Lee-Thorp, 2006). As a mixed feeder, the red deer from Tornewton Cave has lower Sr/Ca ratios but higher Ba/Ca ratios than the grazing horse. A possible explanation for the enrichment of Ba/Ca ratios in red deer might result from differences caused by the digestive apparatus, since in a study of MIS 3 mammal assemblages from western Europe, Balter *et al*. (2002) found that Ba/Ca ratios were elevated in ruminant bovines and reindeer compared to monogastric rhinoceros and horse.

In general, the Ca biopurification signal seems to be better preserved in the Sr/Ca as opposed to the Ba/Ca ratios in all specimens. This is to be anticipated because the Ba/Ca signal along the profiles appears to have been more subject to chemical alteration than Sr/Ca. Again, the results highlight the need for supplementary information on the timing of enamel formation and the consideration of many different factors in order to interpret palaeodiet.

Chapter 6. Conclusions

The overarching aim of this thesis is to investigate the palaeodietary and palaeoecological niches, together with aspects of the physiology, of different fossil bears in the Middle to Late Pleistocene in Britain and Greece. Throughout this thesis, this has been successfully demonstrated through the combined application of dental microwear and novel geochemical analysis and the subsidiary aims identified in Chapter 1 are considered to be met in full.

This thesis has been the first study to develop and validate a robust database of dental microwear features for extant Ursidae, revealing features that reflect dietary variability not only *between* species but also *within* an individual species (*U. arctos* specimens from different geographical regions). Furthermore, this is the first time that a single study has attempted to reconstruct the palaeodietary adaptations of various fossil bear species from different palaeontological sites of diverse ages, using the evidence from the extant species database as a template for interpretation.

The key findings in terms of dietary differentiation between fossil bears are as follows:

- Identification of differences between the species: *U. deningeri*, *U. arctos* and *U. ingressus*.
- Identification of differences within the same species (e.g. *U. deningeri* from Westbury and from Kents Cavern).
- Identification of differences across contrasting warm and cold-climate episodes in Britain (e.g. *U. arctos* specimens from MIS 9 and 5e versus MIS 5a sites).
- Identification of stadial-interstadial variation during MIS 3 (e.g. *U. arctos* specimens from Kents Cavern “Cave earth deposits” versus those from Sandford Hill) and

- Identification of variation between different geographical regions (specimens within British sites and British versus Greek sites).

In addition to dental microwear analysis, the present study also undertook new high-resolution Sr/Ca and Ba/Ca intra-tooth profiles on four different mammalian taxa from Tornewton Cave, in order to explore evidence for dietary and physiological parameters present in their dental enamel tissues. In all specimens, the concentrations of alteration indicators (such as Mn. Al, Pb, U and REE) were rigorously assessed in order to identify changes that linked with diagenetic alteration of tooth chemistry in burial environment. The parts that had undergone diagenesis were removed from the analysis, thereby allowing the average values of the Sr/Ca and Ba/Ca profiles to be confidently calculated for each animal and the trophic level of each to be determined within the Tornewton Cave foodweb. This has revealed some very significant new patterns, as well as evidence for distinct stages of dietary development in bear, spotted hyaena, red deer and horse, the first time that this has been realised for fossil mammals.

6.1. Dental Microwear Analysis method and database of extant bear specimens

A key component of the thesis was to establish a robust methodology for the application of dental microwear to extant bear specimens and to erect a comprehensive database of microwear features, both of which have been successfully achieved.

Of particular importance was the question of enamel surface selection in DMA. This has been resolved through statistical testing of observations of scratch and pit features from selected extant species (e.g. polar bear) and extinct (e.g. *Ursus deningeri*) specimens on both facet and non-facet tooth surfaces, with the conclusion that the “unworn” enamel surface should be the focus of investigation (e.g. similar Münzel *et al*. [2014]).

DMA of bear samples in this study used nine different variables to quantify microwear features. However, non-microwear features that link to enamel structure (e.g. Hunter-Schreger bands) or to the complex occlusal surface (e.g. small ridges) were also identified for the first time in this study (and subsequently excluded from the counted features). The results highlight the importance of correctly observing and identifying such features when applying DMA on bears.

In addition, the nine variables were statistically tested on both the trigonid and talonid areas of the studied m1 specimens in extant bears, thereby confirming that results from the talonid area are most effective in the differentiation of ursid dietary ecospaces. It is consequently suggested here that this should be adopted in future studies as the most appropriate area for DMA study in bears (*contra* Donohue *et al*., 2013.

A clear conclusion to emerge from this study is that dental microwear features convincingly capture the diets of most extant Ursidae and that even *intra*-specific variation in dietary ecospace can be discerned, something noted for the first time here, through a combination of bivariate and PCA analysis on the talonid observations.

This study has demonstrated that the dietary ecospace of *U. maritimus* and *A. melanoleuca* can be clearly differentiated using dental microwear features from the rest of the omnivorous species. The former is the only species to display hypercoarse scratches, which are a reflection of both diet and the extreme Arctic environment in which it lives, whereas the latter has the highest number of fine scratches of all species, usually aligned in the same orientation and again, a direct reflection of a diet consisting mainly of bamboo.

Since most of the remaining bear species studied are generalists and exploit a wide variety of food items, it is unsurprising that some overlaps between dietary ecospaces were noted. However, this thesis has revealed additional interesting differences between them. For example, *U. arctos* from northern Europe (a “soft mast” eater) can be differentiated from *U. arctos* from central Europe (a “hard mast”

eater), with the latter preserving a more pitted enamel surface with many puncture pits and gouges compared to the former, where such features are rare or even absent. Furthermore, *U. thibetanus* specimens are clearly differentiated from the other omnivorous species and their dietary ecospace is even different to that of the other "hard mast" (*U. arctos* from central Europe). The conclusions that can be drawn from this are that the two species inhabit different ecological zones where "hard mast" items will vary. *U. thibetanus* occupies a wider range of forested habitats (both broad-leaved and coniferous) than central European *U. arctos* and may have been able to exploit different food resources. In addition, this study has shown that the dietary ecospace of *U. arctos* from Greece (a "soft mast" eater) can be distinguished from those of the other "soft mast" eaters because of an absence of flesh consumption and a diet rich in soft green vegetation and fruit.

As may be expected, the analysis has also documented similarities in the microwear features between "soft mast" eaters and vertebrate eaters (the latter comprising individuals that avoid bone consumption) (e.g. *U. arctos* from Russia and *U. arctos* from northern Europe, *U. arctos* from USA and *U. americanus*). This is because all consume "soft" items, either fruit with no hard seeds on the one hand, or flesh and fat on the other hand. Nevertheless, it is still possible to identify differences between them (see below for a summary of the key features), which can allow them to be separated according to diet.

Last but not least, broad dietary ecospaces have been observed for both *U. arctos* from Russia and *H. malayanus*. This signifies that the diet in these species is rather variable from one individual to another in both species and may reflect local dietary adaptability across geographical regions and seasons.

A summary of the main microwear characteristics of each extant species is presented below:

Species	**Term-Group** (based on the most consumed items)	**Symbols**

A. melanoleuca Foliage-Herbivore 

Microwear characteristics:

1) The highest number of fine scratches

2) The highest number of small pits

3) The highest average number of pits

4) Most scratches have the same orientation

5) Absence of coarse scratches

U. thibetanus Hard mast-Omnivore 

Microwear characteristics:

1) High scratches width score (2nd after *U. maritimus*)

2) The lowest percentage of puncture pits in comparison with the other extant species

3) The smallest average number of pits and an intermediate average number of scratches

M. ursinus Invertebrates-Insectivore 

Microwear characteristics:

1) High number of pits

2) Small number of scratches

3) Moderate percentage of puncture pits

H. malayanus Invertebrates-Omnivore 

Microwear characteristics:

1) Relatively high percentage of fine scratches

2) Relatively high percentage of small pits

3) Relatively small average number of pits and intermediate to high average number of scratches

4) Small percentage of puncture pits

U. maritimus Vertebrates-Hypercarnivore

Microwear characteristics:

1) Few scratches

2) Small number of pits

3) The highest scratches width score of any extant bear species

4) Absence of puncture pits

5) Presence of hypercoarse scratches

U. americanus Soft mast-Omnivore

Microwear characteristics:

1) Intermediate percentage of fine scratches

2) Intermediate number of pits

3) Higher percentage of puncture pits than *U. arctos* from USA

4) Small average number of scratches

***U. arctos,* USA**	Vertebrates-Omnivore	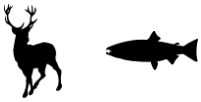
Microwear characteristics:	1) Intermediate number of pits 2) Small percentage of puncture pits 3) Higher percentage of coarse scratches than *U. americanus* 4)Smaller percentage of pits than *U. americanus* 5) The highest average number of scratches	
***U. arctos,* Russia**	Vertebrates-Omnivore	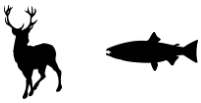
Microwear characteristics:	1) Low to intermediate percentage of puncture pits and gouges 2) Relatively high number of large pits 3) Small number of scratches 4) Intermediate values of average number of pits	
***U. arctos,* North Europe**	Soft mast-Omnivore	
Microwear characteristics:	1) Small percentage of puncture pits and gouges 2) Intermediate number of scratches 3) Intermediate to high number of pits	

***U. arctos,* central Europe**	Hard mast-Omnivore	
Microwear characteristics:	The highest percentage in comparison to other *U. arctos* of: 1) Pits 2) Puncture pits 3) Gouges 4) Large pits	
***U. arctos,* Greece**	Soft mast-Omnivore	
Microwear characteristics:	1) The lowest percentage of pits and of puncture pits in comparison to the other omnivorous species 2) Intermediate scratches width score 3) High coarse scratches 4) Relatively high average number of scratches	

6.2. Palaeodietary and palaeocological niches of extinct bear species.

Knowledge and understanding of microwear patterns and dietary ecospaces of extinct species are important for the reconstruction of palaeodietary niches, since they directly reflect both the food consumed and the local environment. The large number of bear specimens and the range of sites that were analysed in this thesis have therefore created an opportunity to compare patterns between the different extinct bear populations and the palaeoecological conditions that they inhabited.

One of the important achievements of this study has been to highlight adaptations to changing environments, climates and carnivore guild composition between fossil

bear species such as *U. deningeri*, *U. arctos* and *U. ingressus.* It has also revealed dietary differentiation between fossil bear specimens of the same species from different geographical regions.

During the early Middle Pleistocene, the inferred ecospaces of *U. deningeri* from Westbury and Kents Cavern reveal some interesting differences. For both populations, it is suggested that their diet comprised a significant proportion of soft items that were at least seasonally available, however *U. deningeri* from Kents Cavern appears to have had a broader dietary niche and included some hard components in its diet (see also Table 6.1). The early Middle Pleistocene is characterised by a number of climatic oscillations and although both localities are tentatively attributed to MIS 13, they may not be exactly coeval. Furthermore, although the herbivore prey base appears to be similar at both sites, the differences between Kents Cavern and Westbury *U. deningeri* may be related to a reduction in competition from carnivores at the former site that potentially allowed the *U. deningeri* from there to utilise additional protein sources such as flesh (and to some extent, bone). Alternatively, in the Kents Cavern area, the availability of plant food may have been slightly more diverse than at Westbury, allowing individuals from the former to incorporate "hard mast" such as fruits with seeds into their diet. These findings echo the contrasting interpretations put forward regarding *U. deningeri* diet by Stiner *et al*. (1998) Bocherens *et al*. (1994a) and García García *et al*. (2009).

The palaeodiet of most Pleistocene *U. arctos* specimens from Britain can be distinguished from that of the early Middle Pleistocene *U. deningeri.* It is significant that major similarities in dietary ecospace (and hence, in their microwear patterns) between *U. arctos* from MIS 9 and MIS 5e sites. These brown bears demonstrate the consumption of fibrous food as well as soft fruits and invertebrates, together with a modest vertebrate component (see also Table 6.1). Both interglacials (MIS 9 and MIS 5) were characterised by the development of deciduous woodland, elevated summer temperatures when compared to today and mild winters. Thus, the ecospaces and the palaeodietary niches that both brown bear populations adopted during these periods are in agreement with the inferred similarity in climatic conditions and

habitats. The post-Anglian (MIS 12) reduction in large carnivore competitors in Britain may also have allowed these bears more opportunities to include flesh in their diets compared to older time periods, although this remains a subsidiary component.

In contrast, *U. arctos* specimens from the early part of the last cold stage (MIS 5a, as exemplified by Banwell Bone Cave) displayed very different dietary preferences to those from the MIS 9 and MIS 5e interglacials. The dietary ecospace of the large-bodied brown bears from MIS 5a implies that they most probably fed on any available "hard mast" items, while meat and fat played an important role into their diet (see also Table 6.1). Furthermore, the intensive and coarse microwear patterns observed on the enamel surfaces of their teeth may be linked to the open, tundra-like environment in which they lived. *U. arctos* was the dominant predator in Britain at this time, likely facilitated by the absence of spotted hyaena during MIS 5a. In view of the obstacles it may have faced during a period of cold climate (enhancing the importance of herbivore prey – perhaps only seasonally available - for calorific return, combined with lower general availability of fruit and soft vegetation), these bears would have readily exploited any available protein sources from flesh and bone, thereby potentially developing a more specialised hypercarnivorous diet.

Another new finding of the microwear analysis in this thesis is the identification of different dietary ecospaces in brown bears from MIS 3 sites (Sandford Hill and Kents Cavern "Cave earth deposits") in Britain. These populations are distinguished from both the brown bears from the early last cold stage (MIS 5a) and the interglacial sites (Grays and Tornewton Cave). The dietary ecospace and the microwear features of brown bears from Sandford Hill (see also Table 6.1) demonstrates that these bears consumed mainly soft mast items (very close to modern *U. arctos* from Greece), while the patterns and dietary ecospace of *U. arctos* from Kents Cavern (cave earth deposits) (see also Table 6.1) reveal that this population consumed not only soft mast but also invertebrates and potentially some vertebrates. Even though Middle Devensian (MIS 3) represents a period of elevated climatic warmth when compared with MIS 4 and MIS 2, it is characterised by multiple millennial to sub-millenial-scale

climatic oscillations between stadials and interstadials that could explain this difference between the two MIS 3 brown bear populations. In addition, this dietary difference could also reflect interstadials of different magnitudes, where different food types would have been more readily available at one time than another.

The brown bear population from the probable Holocene locality, Cow Cave, differs clearly from all the rest of the extinct brown bear groups from Britain, although some individuals have shown a small overlap with the dietary ecospace of *U. arctos* from Kents Cavern (cave earth deposits). Both the dietary ecospaces (see also Table 6.1) and the microwear patterns of Cow cave bears suggest that this population had more herbivorous tendencies and consumed both "soft" and "hard mast" items, which is also consistent with the inferred warmer climate and wooded conditions of the Holocene in southern England.

As a point of comparison, *U. ingressus* specimens from Loutra Arideas Cave (LAC) (Late Pleistocene) in Greece were also analysed in this thesis. The dietary ecospace and the microwear patterns of this bears separate, not surprisingly due to its different geographical position, from most extinct *U. deningeri* and *U. arctos* groups from Britain. However, some *U. ingressus* individuals were found to overlap with some individuals from Pleistocene interglacial sites (Grays and Tornewton Cave) and from the Holocene (Cow Cave) site. *U. ingressus* dietary ecospace (see also Table 6.1) therefore reflects a predominately herbivorous bear that consumed both "soft" and "hard mast" items, insects and probably some relatively soft animal protein such as fish.

Table 6.1. Similarities and overlaps between extinct bear population dietary ecospaces (from PCA) and extant species ecospaces.

Extant/Extinct ecospaces	*U. deningeri* (early Middle Pleistocene) Westbury	*U. deningeri* (early Middle Pleistocene) Kents Cavern	*U. arctos* (MIS 9)	*U. arctos* (MIS 5e)	*U. arctos* (MIS 5a)	*U. arctos* (MIS 3) Kents Cavern	*U. arctos* (MIS 3) Sandford Hill	*U. arctos* (Holocene) Cow Cave	*U. ingressus* (Late Pleistocene) LAC
A. melanoleuca									
U. maritimus	X				X				
M. ursinus						X			X
U. thibetanus	X	X			X				
H. malayanus			X	X		X			
U. americanus			X	X					
U. arctos, USA		X							
U. arctos, Greece	X						X		
U. arctos, central Europe								X	X
U. arctos, North Europe		X	X	X		X	X		
U. arctos, Russia		X						X	X

6.3. Palaeodietary and physiological remarks on carnivore and herbivore species from Tornewton Cave

This thesis has demonstrated that although the interpretation of dietary variability using high-resolution Sr/Ca and Ba/Ca ratios is a very complex process, nevertheless some very important information can be derived regarding palaeodietary and physiological constraints.

The high-resolution method (LA-ICP-MS) employed here has allowed detail observations to be made along the enamel profiles of all specimens from the tip to the base of the tooth crown, thereby allowing the patterns of different elements from the oldest to the youngest enamel tissues to be observed and measured.

For the first time, the present study focused also on to the rigorous evaluation of post-depositional diagenesis of enamel tissues of all analysed specimens. This is vital for the correct recovery of a “clean” signal from the enamel tissues. The results have shown that most parts of the 14 dental enamel tissues from Tornewton Cave specimens were generally well preserved. However, alterations were seen at the cracks and in some cases, at the beginning or end of the traverse, where brown or grey staining was noted. Here, alteration occurred as filling of fractures by secondary minerals, reflected by an increase of Al, Mn and REE concentrations. In addition,

alteration of the apatite crystallites was observed on specimens with high concentrations of U and REE. Interestingly, elevated U concentrations were recognised in two bear samples (M92417 and M41389) that did not match variations in either the REE or in any other alteration indicator and which was consequently difficult to explain. It is concluded that in the majority of cases, high concentrations of Al and Mn affect more the Ba/Ca ratios than the Sr/Ca ones. The results suggest that the Sr/Ca ratios have been less chemically altered in comparison to the Ba/Ca ratios. Furthermore, usually the type of alteration that was observed on profiles reflects the slow diffusion of secondary elements. However, the majority of U, Al, Mn and REE concentrations of the specimens, when compared with published values on modern animals, were low or within accepted ranges, with the exception of most U and Al concentrations on bears. It must be highlighted that the method used in this thesis allows averages to be calculated from sections of enamel that appear to be unaltered by diagenesis and contain low concentrations of alteration indicators, thereby enabling the extraction of only the cleanest parts of the signal.

This thesis has demonstrated that the use of this method, in conjunction with knowledge of the timing of mineralisation of the teeth and additional ecological information from modern analogue taxa, allows the different dietary stages in the early life of each animal to be recognised in the enamel profile. This in turn allows the section of enamel that contains the “true” chemical signal of dietary maturity to be identified in each animal.

For all specimens, the four dietary stages were mapped along the Sr/Ca and Ba/Ca profiles. This is the first time that this has been attempted in fossil species. The study has revealed that these stages can be unequivocally recognised in individuals where all the molars are present (for example, in the red deer individual M41530 with m1-m3 - the first time that a mandible with all three molars has been analysed for the recovery of the dietary history of the first 1.5 years of life of this individual) but can also be established in isolated teeth belonging to other animals. The results have shown that the canine, m1 and m3 of bears most probably preserve three of the four dietary stages (2, 3 and 4), as does the m1 in spotted hyaena. The identification of

the influence of milk consumption in fossil bears through chemical analysis is entirely new. In addition, the m3 of horse covered only the fourth stage (dietary maturity), whereas in the red deer, the m1 covers stages 1, 2, 3 and 4, the m2 stages 3 and 4 and the m3 only stage 4.

Undoubtedly, Tornewton Cave has a complex stratigraphy including fossiliferous horizons associated with MIS 7, 5e, 5c, 3 and 2. The majority of the specimens selected for the geochemical analysis were from MIS 5e and 5c, however the horse specimen and the hyaena M92410 came from levels assigned to MIS 3 and the M92417 bear specimen from MIS 2.

The results indicate that there was some variability in almost all Sr/Ca and Ba/Ca bear teeth profiles. This was even noticed within the parts where the stage 4 (dietary maturity) was mapped. This might be expected as bears from Tornewton Cave would have exploited a high diversity of fruit and plant taxa and possibly invertebrates during the MIS 5e interglacial. However, the consumption of meat cannot be ruled out on the basis of this study, since comparison of their relative position with the obligate carnivore, the spotted hyaena, proved complex (see below). Interestingly, this thesis found no clear evidence of stress-related events that might impact on the bear's physiology, such as hibernation. This is true both for m1 and canine tooth profiles. This does not mean definitively that these bears did not hibernate but further analysis is needed to explore this subject more fully. On the other hand, if indeed these bears did not hibernate, it might be explained by the fact that MIS 5e was characterised by very mild winters. In contrast, the sudden decrease in both Sr/Ca and Ba/Ca ratios in the m3 samples (e.g. M40750 and M92414) might hint instead a hibernation period, rather than marking the onset of dietary stage 4 as suggested in this thesis. Again, this requires further investigation.

With respect to the bears' average Sr/Ca and Ba/Ca values, all specimens have shown lower values from both the horse (grazer) and the red deer (mixed feeder). In addition, although almost all bear average Sr/Ca and Ba/Ca values lie very close to one another, one specimen (M41389) has slightly lower values. This may be a result of *intra*-species variability, with this individual consuming either a different kind of

plant matter to the others or more meat than the others. This can be further explained by the fact that M41389 is from a different stratigraphic horizon (MIS 5c) than the rest bear specimens (MIS 5e). Hence, M41389 may have adopted a diet of plants such as roots and grasses in an interstadial environment, whereas the individuals from the Last Interglacial "Bear Stratum" were exploiting more fruit and leaves, consistent with a fully interglacial environment. The geochemical results for bear specimens from Tornewton Cave are also in agreement with the microwear patterns observed on bear enamel surfaces from this site and with the dietary ecospace inferred for these bears.

A relatively flat signal was displayed by the two hyaena individuals in terms of their Sr/Ca and Ba/Ca high-resolution profiles. This was to be expected as these are carnivorous animals and probably consumed very similar prey species throughout the annual cycle. Nevertheless, an interesting difference was revealed between these two specimens. M38994 had overall higher average Sr/Ca ratios than M92410. This might be explained by the fact that the latter is from different horizon (MIS 3), so most probably consumed prey that fed on different type of plant species than the former. It might also suggest that M38994 (MIS 5c) with the higher Sr/Ca values preyed on species with higher Sr/Ca values. However, it would be anticipated that the two hyaena specimens should both have lower average Sr/Ca and Ba/Ca values than all the other species from Tornewton Cave but this was not the case. This was especially noticeable in the case of the M38994 specimen, which displayed higher average Sr/Ca ratios than the herbivore species from the site. This emphasizes the importance of analyzing larger numbers of teeth from single species from multiple horizons in future studies. The most likely explanation for the results (given that there is no evidence for diagenesis) is that this particular individual may have spent its early years in an area with a different geology and moved later to the Tornewton Cave area. However, additional strontium isotope analysis would be needed to support this assumption as well as knowledge of the exact duration of the m1 mineralisation in modern hyaena.

In the red deer, high-resolution Sr/Ca and Ba/Ca profiles representing the dietary maturity (stage 4) phase on both the m2 and m3 appear to display a sinusoidal signal. Based on modern ecological behaviour in red deer, this most likely reflects seasonal variation in diet and might be linked with periods of consumption of grasses and sedges (in summer), which would lead to higher values, compared to the winter period when shrubs and tree shoots would be consumed. Additional future strontium isotope analysis might shed light on whether this variation includes a seasonal migratory component. As to be expected, the average Sr/Ca values of the mixed feeder red deer from Tornewton were lower than the grazer, the horse, and higher than the values of the bears and one hyaena. This thesis has also revealed that the red deer, in comparison with the horse and with the other specimens from the site, had higher average Ba/Ca values, possibly a reflection of ruminant digestion.

The high-resolution Sr/Ca and Ba/Ca ratios in the horse specimen recorded high amplitude variation and had the highest average Sr/Ca ratios of all other species from the site, with the exception of the M38994 hyaena specimen. The Tornewton Cave horse may have consumed a diverse range of grass species in the steppe-tundra environment of MIS 3. In addition the great variability in both the Sr/Ca and Ba/Ca profiles of this specimen may reflect periodic consumption of browse plants, especially during the winter when grass was less widely available.

In summary, the results from this thesis have revealed the great potential of this method for extracting palaeodietary information from fossil specimens, as well as highlighting for the first time, the need to consider both the different metabolic processes and ecological information in order to interpret these ratios.

6.4. Future work

The establishment here of a robust dental microwear database for all modern species will be of use in the future for many different applications. For example, it can be employed for the better understanding of the nature of bear diets and

habitats of other extinct bear species from other localities within Britain and from other European sites. In addition, it can be also used as a base for testing and comparing these results with results that will be extracted from the same specimens using 3D dental microwear texture analysis. It would be very helpful for the future to include some more extant specimens of both *U. arctos* from Greece and *M. ursinus* in order to explore better their dietary ecospace.

In addition, a number of non-microwear features were identified on both extant and extinct specimens, although further investigation was beyond the scope of the present study. Nevertheless, these could be explored in depth in the future, as they may reveal new information about species' diet.

It is also suggested that examination of additional brown bear specimens of MIS 3 age might provide further information on the dietary patterns and differences that have been described in this thesis between stadials and interstadials, if chronological support can be obtained. Although the availability of radiocarbon dates on ultrafiltered collagen has improved the reliability of the ages generated, the error ranges on the dates currently make it difficult to isolate material from individual stadials or interstadials; nevertheless, future improvements in resolution of the technique may allow greater insight. More specimens of cave bear species from different geographical sites should also be examined in the future with dental microwear analysis in order to determine their dietary ecospaces.

Additional screening procedures may be also used in the future for the evaluation and the better understanding of all enamel chemistry, such as virtual sectioning and quantitative mineralisation mapping.

It is also strongly suggested that further isotopic analysis on bear samples from all the sites that were included in microwear analysis should be undertaken in order to allow comparison of the results from the two methods. While isotopic analysis on the Tornewton specimens can clarify the palaeodiet and trophic level status of the animals, oxygen isotope analysis could shed light on seasonal palaeoclimate. Furthermore, strontium isotope analysis could help to determine the mobility of

each species in the landscape of Tornewton Cave and importantly, clarify the position of the hyaena sample and whether the sinusoidal signal observed in red deer reflect seasonal migration that the animal undertook on an annual basis.

Moreover, more hyaena samples should be analysed from Tornewton Cave in the future so that reconstruct clearly the carnivorous position of this animal in this ecosystem and also provide a more clear point of the comparison with the potentially highly carnivorous tendencies of some of the bear individuals.

It is also proposed that in the future, the study of enamel thin sections on bear teeth could potentially give the answer to better understanding of these animals physiology and reveal important patterns related to hibernation.

Finally, a critical aspect of the better understanding of Sr/Ca and Ba/Ca profiles in both hyaenas and bears is knowledge of the timing of enamel mineralisation in modern species, information that is currently unavailable.

Bibliography

Adam, K. D., 1975. Die mittelpleistozäne Säugetier-Fauna aus dem Heppenloch bei Gutenberg (Württemberg). Abhandlungen zur Karst- und Höhlenkunde Reihe D, Paläontologie, Zoologie (Heft 1). München.

Agustí, J. and Antón, M., 2002. Mammoths, Sabertooths, and Hominids. Columbia University Press, New York. p.313.

Akhtar, N., Bargali, H. S. and Chauhan, N. P. S., 2007. Characteristics of sloth bear day dens and use in disturbed and unprotected habitat of North Bilaspur Forest Division, Chhattisgarh, Central India. *Ursus*. **18**(2):203-208.

Andrews, P., 1990. Owls, Caves and Fossils. –Natural History Museum Publications. London. p. 231.

Andrews, P. and Cook, J., 1999. Description of the sedimentary sequence in Westbury Cave. pp 19-57 in: Andrews, P., Cook, J., Currant., A. and Stringer, C. (Eds.), *Westbury Cave. The Natural History Museum Excavations 1976 - 1984*. Western Academic & Specialist Press, Bristol. p. 309.

Andrews, P. and Turner, A., 1992. Life and death of the Westbury bears. *Annales Zoologici Fennici*. **28**: 139-149.

Andrews, P., Cook, J., Currant, A. and Stringer, C. 1999. Westbury Cave. The Natural History Museum Excavations 1976-1984. Western Archaeological and Specialist Press. University of Bristol.

Anyonge, W., 1996. Microwear on Canines and Killing Behavior in Large Carnivores: Saber Function in *Smilodon fatalis. Journal of Mammalogy*. **77**(4): 1059-1067.

Argant, A. 1991. Carnivores quaternaires de Bourgogne. Documents des Laboratoires de Géologie Lyon. **115**: 1–301.

Argant, A., 1996. B. Sous – famílie des Ursínae- In: Guérin, C. & Patou – Mathis, M. (Eds.): Les grand mammiferes Plio-Pléistocenes d' Europe, 167-177; Paris, Milano & Barcelona (Masson).

Argant, A., 2001. Cave bear ancestors. Cadernos do Laboratorio Xeolòxico de Laxe. **26:** 341–348.

Argant, A., 2009. Biochronologie et Grands Mammifères au Pléistocène Moyen et Supérieur en Europe Occidentale: L'Apport des Canidés, des Ursidés et des Carnivores en Général. *Quaternaire*. **20**(4): 467-480.

Argant, A. and Argant, J., 2002. Die Bären von Château (Burgund, Frankreich). In W. Rosendahl, M. Morgan & M. López Correa (Eds.), Cave Bear Researches/Höhlen-Bären-Forrschungen. Abhandlung zur Karst – und Höhlenkunde, Heft 34, 112 S, München. p. 57-63.

Argant, A. and Crégut-Bonnoure, E., 1996. III. Famille des Ursidae, 167–179. In Guérin, C. and Patou-Mathis, M. (Eds) *Les Grands mammifères plio-pléistocènes d'Europe*. Masson, Paris.

Argant, A. and Philippe, M., 1997. Les ours et leur évolution.- In "Coll. Int. : L'Homme et l'Ours", Auberives en Ryans, Isè. p. 8.

Augeri, D. M., 2005. On the biogeographic ecology of the Malayan sun bear. PhD Thesis, Cambridge: University of Cambridge. p. 331.

Aylifee, L. K., Chivas, A. R. and Leakey, M. G., 1994. The retention of primary oxygen isotope compositions of fossil elephant skeletal phosphate. *Geochimica et Cosmochimica Acta.* **58** (23): 291-529.

Azorit, C., Analla, M., Carrasco, R., Calvo, J. A. and Mupoz-Cobo, J. 2002. Teeth eruption pattern in red deer (*Cervus elephus hispanicus*) in southern Spain. *Anales de Biología*. **24**: 107-114.

Baca, M., Mackiewicz, P., Stankovic, A., Popović, D., Stefaniak, K. Czarnogórska, K., Nadachowski, A., Gąsiorowski, M., Hercman, H. and Weglenski, P., 2014. Ancient DNA and dating of cave bear remains from Niedźwiedzia Cave suggest early appearance of Ursus ingressus in Sudetes. *Quaternary International*. **339–340:** 217-223.

Baker, G., Jones, L. H. P. and Wardrop, I. D., 1959. Cause of wear in sheeps' teeth. *Nature*. **184**: 1583-1584.

Balasse, M., 2002. Reconstructing Dietary and Environmental History from Enamel Isotopic Analysis: Time Resolution of Intra-tooth Sequential Sampling. *International Journal Osteoarchaeology.* **12**: 155–165.

Balasse, M., 2003. Potential Biases in Sampling Design and Interpretation of Intra-tooth Isotope analysis. *International Journal Osteoarchaeology.* **13**: 3–10.

Balasse, M., Smith, B., Ambrose, S. H. and Leigh, S., 2003. Determining sheep birth seasonality by analysis of tooth enamel oxygen isotope ratios: the Late Stone Age site of Kasteelberg (South Africa). *Journal of Archaeological Science*. **30:** 205-215.

Ballenger, L., 2002. "Ursus arctos" (On-line), Animal Diversity Web. Accessed December 19, 2015 at http://animaldiversity.org/accounts/Ursus_arctos/

Balter, V., 2004. Allometric Constraints on Sr/Ca and Ba/Ca Partitioning in Terrestrial Mammalian Trophic Chains. *Oecologia*. **139** (1): 83-88.

Balter, V., Telouk, P., Reynard, B., Braga, J., Thackeray, J. and Albare, F., 2008. Analysis of coupled Sr/Ca and $^{87}Sr/^{86}Sr$ variations in enamel using laser-ablation tandem quadrupole-multicollector ICPMS. *Geochimica et Cosmochimica Acta***. 72**: 3980–3990.

Balter, V., Bocherens, H., Person, A., Labourdette, N., Renard, M. and Vandermeersch, B., 2002. Ecological and physiological variability of Sr/Ca and Ba/Ca in mammals of West European mid-Würmian food webs. *Palaeogeography, Palaeoclimatology, Palaeoecology*. **186** (1–2): 127-143.

Bargali, H. S., Akhtar, N. and Chauhan, N. P. S., 2004. Feeding ecology of sloth bears in a disturbed area in central India. *Ursus*. **15** (2): 212-217.

Barnes, I., Matheus, P., Shapiro, B., Jensen, D. and Cooper, A., 2002. Dynamics of Pleistocene population extinctions in Beringian brown bears. *Science***. 295:** 2267-2270.

Barnosky, A. D., Koch, P. L., Feranec, R. S., Wing, S. L. and Shabel, A. B., 2004. Assessing the causes of Late Pleistocene extinctions on the continents. *Science***. 306** (5693): 70–75.

Baryshnikov, G. F., 2006. Morphometrical Variability of Cheek Teeth of Cave Bears. In: *Scientific Annals* School of Geology. Aristotle University of Thessaloniki. **98**: 81-102.

Baryshnikov, G. F., 2007. Fauna of Russia and neighbouring countries. Mammals. Ursidae*,* Nauka, Saint Petersburg, p. 541.

Baryshnikov, G. F. and Foronova, I., 2001. Pleistocene small cave bear (*Ursus rossicus*) from the South Siberia, Russia. *Cadernos do Laboratorio Xeolo´xico de Laxe*. **26**: 373–398.

Baryshnikov, G. F. and Lavrov, A., 2013. Pliocene bear *Ursus minimus* Devèze de Chabriol et Bouillet, 1827 (Carnivora, Ursidae) in Russia and Kazakhstan. *Russian* Journal of Theriology. **12** (2): 107-118.

Baryshnikov, G. F. and Puzachenko, A. Yu., 2011. Craniometrical variability in the cave bears (Carnivora, Ursidae): Multivariate comparative analysis. *Quaternary International***. 245**: 350-368.

Baryshnikov, F. G and Tsoukala, E., 2010. New analysis of the Pleistocene carnivores from Petralona Cave (Macedonia, Greece) based on the Collection of the Thessaloniki Aristotle University. *Geobios.* **43**: 389–402.

Baryshnikov, G. F., Germonpré, M. and Sablin, M., 2003. Sexual dimorphism and morphometric variability of cheek teeth of the cave bear (*Ursus spelaeus*). *Belgian Journal of Zoology*. **133**(2): 111-119.

Bastl, K., 2012. Ecomorphology of the European *Hyaenodon.* PhD Thesis. Doktorin der Naturwissenschaften Wien, p. 297.

Bastl, K., Semprebon, G. and Nagel, D., 2012. Low-magnification microwear in Carnivora and dietary diversity in Hyaenodon (Mammalia: Hyaenodontidae) with additional information on its enamel microstructure. *Palaeogeography, Palaeoclimatology, Palaeoecology.* **348–349:** 13–20.

Bennett, L. J., English, P. F. and Watts. R. L., 1943. The Food Habits of the Black Bear in Pennsylvania. *Journal of Mammalogy*. **24** (1): 25-31.

Bentzen, T. W., Follmann, E. H., Amstrup, S. C., York, G. S., Wooller, M. J. and O'Hara, T. M., 2007. Variation in winter diet of southern Beaufort Sea polar bears inferred from stable isotope analysis. *Canadian Journal of Zoology*. **85**: 596–608.

Bergman, S., 1936. Observations on the Kamchatkan Bear. *Journal of Mammalogy*. **17**(2): 115-120.

Bies, L., 2002. "Ailuropoda melanoleuca" (On-line), Animal Diversity Web. Accessed December 19, 2015 at http://animaldiversity.org/accounts/Ailuropoda_melanoleuca/

Bies, L., 2002. "Melursus ursinus" (On-line), Animal Diversity Web. Accessed December 19, 2015 at http://animaldiversity.org/accounts/Melursus_ursinus/

Bies, L., 2007. "Helarctos malayanus" (On-line), Animal Diversity Web. Accessed December 19, 2015 at http://animaldiversity.org/accounts/Helarctos_malayanus/

Bishop, M. J., 1974. A preliminary report on the Middle Pleistocene mammal bearing deposits of Westbury-sub-Mendip, Somerset. *UBSS Proceedings*. **13** (3):301-318.

Bishop, M.J., 1982. The Mammal fauna of the early Middle Pleistocene cavern *mull* site of Westbuxy-sub-Mendip, Somerset. *Special Papers of the Palaeontographical Association, 26.*

Blockley, S., Bourne, A., Brauer, A., Davies, S., Hardiman, M., Harding, P., Lane, C., MacLeod, A., Matthews, I., Pyne-O'Donnell, S., Wulf, S. and Zanchetta, G. 2014. Tephrochronology and the extended intimate (integration ice-core, marine and terrestrial records) event stratigraphy 8-128Ka b2k. *Quaternary Science Reviews*. **106:** 88-100.

Blum, J. D., Taliaferro, E. H., Weisse, M. T. and Holmes, R. T., 2000. Changes in Sr/Ca, Ba/Ca and $^{87}Sr/^{86}Sr$ ratios between two forest ecosystems in the northeastern USA. *Biogeochemistry*. **49**: 87-101.

Bocherens, H., 1998. Comments on: 'Use of stable isotopes to determine diets of living and extinct bears' by Hilderbrand *et al*.(1996). *Canadian Journal of Zoology*. **76:** 2299–2300.

Bocherens, H., 2003. Isotopic biogeochemistry and the paleoecology of the mammoth steppe fauna - in: Reumer, J.W.F., De Vos, J. & Mol, D. (Eds.) - Advances in mammoth research (*Proceedings of the Second International Mammoth Conference*, Rotterdam, May 16-20 1999) – Deinsea. **9:** 57-76.

Bocherens, H., 2009. Dental microwear of cave bears: The missing temperate/boreal vegetarian ‘‘carnivore’’ *Proceedings of the National Academy of Sciences*. **106** (48): E133.

Bocherens, H., 2015. Isotopic tracking of large carnivore palaeoecology in the mammoth steppe. *Quaternary Science Reviews*. **117**: 42-71.

Bocherens, H. and Drucker, D., 2003. Trophic level isotopic enrichment of carbon and nitrogen in bone collagen: case studies from recent and ancient terrestrial ecosystems. *International Journal Osteoarchaeology.* **13:** 46–53.

Bocherens, H., Fizet, M. and Mariotti, A., 1994a. Diet, physiology and ecology of fossil mammals as inferred by stable carbon and nitrogen isotopes biogeochemistry: implications for Pleistocene bears. *Palaeogeography, Palaeoclimatology, Palaeoecology*. **107**: 213-225.

Bocherens, H., Brinkman, D. B., Dauphin, Y. and Mariotti, A., 1994b. Microstructural and geochemical investigations on Late Cretaceous archaeosaur teeth from Alberta, Canada, *Canadian Journal of Earth Science*. **31:** 783–92.

Bocherens, H., Pacaud, G., Lazarev, P. and Mariotti, A., 1996. Stable isotope abundances (^{13}C, ^{15}N) in collagen and soft tissues from Pleistocene mammals from Yakutia. Implications for the paleobiology of the mammoth steppe. *Palaeogeography Palaeoclimatology Palaeoecology*. **126:** 31-44.

Bocherens, H., Drucker, D. G., Billiou, D., Geneste, J.-M. and van der Plicht, J., 2006. Bears and humans in Chauvet Cave (Vallon-Pont-d'Arc, Ardeche, France): insights from stable isotopes and radiocarbon dating of bone collagen. *Journal of Human Evolution*. **50:** 370-376.

Bocherens, H., Billiou, D., Patou-Mathis, M., Bonjean, D., Otte, M. and Mariotti, A., 1997. Paleobiological Implications of the Isotopic Signatures (^{13}C, ^{15}N) of Fossil

Mammal Collagen in Scladina Cave (Sclayn, Belgium). *Quaternary Research*. **48** (3): 370-380.

Bocherens, H., Fizet, M., Mariotti, A., Lange-Badre, B., Vandermeersch, B., Borel, J. P. and Bellon, G., 1991. Isotopic biogeochemistry (^{13}C, ^{15}N) of fossil vertebrate collagen: application to the study of a past food web including Neandertal man. *Journal of Human Evolution*. **20** (6): 481-492.

Bocherens, H., Argant, A., Argant, J., Billiou, D., Cregut-Bonnoure, E., Donat-Ayache, B., Philippe, M. and Thinon, M., 2004. Diet reconstruction of ancient brown bear (Ursus arctos) from Mont Ventoux (France) using bone collagen stable isotope biogeochemistry (^{13}C, ^{15}N). *Canadian Journal of Zoology*. **82:** 576-586.

Bocherens, H., Stiller, M., Hobson, K. A., Pacher, M., Rabeder, G., Burns, J. A., Tütken, T. and Hofreiter, M. 2011a. Niche partitioning between two sympatric genetically distinct cave bears (*Ursus spelaeus* and *Ursus ingressus*) and brown bear (*Ursus arctos*) from Austria: Isotopic evidence from fossil bones. *Quaternary International.* **245**: 238-248.

Bocherens, H., Drucker, D. G., Bonjean, D., Bridault, A., Conard, N. J., Cupillard, C., Germonpré, M., Höneisen, M., Münzel, S. C., Napierala, H., Patou-Mathis, M., Stephan, E., Uerpmann, H.-P. and Ziegler, R., 2011b. Isotopic evidence for dietary ecology of cave lion (Panthera spelaea) in North-Western Europe: Prey choice, competition and implications for extinction. *Quaternary International*. **245** (2, 6): 249-261.

Bohm, T. and Höner, O.R., 2015. *Crocuta crocuta*. The IUCN Red List of Threatened Species. Version 2015.2. <www.iucnredlist.org>. Downloaded on **05 August 2015**.

Bojarska, K. and Selva, N., 2012. Spatial patterns in brown bear *Ursus arctos* diet: the role of geographical and environmental factors. *Mammal Review*. **42** (2): 120–143.

Bond, G., Showers, W., Cheseby, M., Lotti, R., Almasi, P., deMenocal, P., Priore, P., Cullen, H., Hajdas, I. and Bonani, G., 1997. A pervasive millennial-scale cycle in North Atlantic Holocene and glacial climates. *Science*. **278:** 1257-1266.

Bowen, D. Q., Phillips, F. M., McCabe, A. M., Knutz, P. C. and Sykes, G. A., 2002. New data for the Last Glacial Maximum in Great Britain and Ireland. *Quaternary Science Reviews*. **21:** 89–102.

Boyde, A., 1989. Enamel. *Handbook of Microscopic Anatomy: Teeth*, Eds Oksche A, Vollrath L (Springer, Berlin). **6**: 309–473.

Britton, K. H., 2009. Multi-isotope analysis and the reconstruction of prey species palaeomigrations and palaeoecology. PhD theses.Durham University. Available at Durham E-Theses Online: http://etheses.dur.ac.uk/216/

Britton, K. V., Grimes, J. D. and Richards, M. P., 2009. Reconstructing faunal migrations using intra-tooth sampling and strontium and oxygen isotope analyses: a case study of modern caribou. *Journal of Archaeological Science.* **36**: 1163-1172.

Brown, W. A. B. and Chapman, N. G., 1991a. The dentition of red deer (*Cervus elaphus*): a scoring scheme to assess age from wear of the permanent molariform teeth. *Journal of Zoology.* **224:** 519-536.

Brown, W. A. B. and Chapman, N. G., 1991b. Age assessment of fallow deer (*Dama dama)*: from a scoring scheme based on radiographs of developing permanent molariform teeth. *Journal of Zoology.* **224:** 367-379.

Brudevold, F. and Soremark, R. 1967. Chemistry of the mineral phase of enamel—Crystalline organization of dental mineral. *In* A.E.D. Miles (Eds.) Structural and Chemical Organization of Teeth. Academic Press, London. **2**: 247-277.

Brügmann, G., Krause, J., Brachert, T. C., Stoll, B., Weis, U., Kullmer, O. and Mertz, D. F., 2012. Chemical composition of modern and fossil hippopotamid teeth and implications for paleoenvironmental reconstructions and enamel formation–Part 2: Alkaline earth elements as tracers of watershed hydrochemistry and provenance. *Biogeosciences.* **9** (11): 4803-4817.

Bryant, J. D., Luz, B. and Froelich, P. N., 1994. Oxygen isotopic composition of fossil horse tooth phosphate as a record of continental paleoclimate. *Palaeogeography, Palaeoclimatology, Palaeoecology.* **107**: 303-316.

Bryant, J. D., Froelich, P. N., Showers,W. J. and Genna, B. J., 1996. Biologic and climatic signals in the oxygen isotopic composition of Eocene–Oligocene equid enamel phosphate. *Palaeogeography Palaeoclimatology Palaeoecology*. **126:** 75–89.

Budd, P., Montgomery, J., Barreiro, B. and Thomas, R.G., 2000 Differential diagenesis of strontium in archaeological human dental tissues. *Applied Geochemistry*. **15**: 687-694.

Budd, P., Montgomery, J., Cox, A., Krause, P., Barreiro, B. and Thomas, R.G., 1998. The distribution of lead within ancient and modern human teeth: implications for long-term and historical exposure monitoring. *The Science of the Total Environment*. **220:** 121-136.

Burton, J. H. Price, T. D. and Middleton, W. D., 1999. Correlation of Bone Ba/Ca and Sr/Ca due to Biological Purification of Calcium. *Journal of Archaeological Science*. **26**: 609–616.

Campbell, J. B. and Sampson, C. G., 1971. A new analysis of Kent's Cavern, Devonshire, England. University of Oregon Anthropological Papers. **3:** 1-40.

Campbell, S. and Collcutt, S. N., 1998. Chudleich Caves. pp 145-149 in: Campbell, S., Hunt, C. O., Scourse, J.D. and Keen, D.H., *Quaternary of South-West England.* Chapman & Hall, London. p. 439.

Candy, I., Coope, G. R., Lee, J. R., Parfitt, S. A., Preece, R. C., Rose, J. and Schreve, D. C. 2010. Pronounced warmth during early Middle Pleistocene interglacials: investigating the Mid-Brunhes Event in the British terrestrial sequence. *Earth Science Reviews*. **103**: 183-196.

Cerling, T. E., Harris, J. M., MacFadden, B. J., Leakey, M. G., Quade, J., Eisenmann, V. and Ehleringer, J. R., 1997. Global vegetation change through the Miocene/Pliocene boundary. *Nature*. **389:** 153–158.

Charles, C., Jaeger, J-J., Michaux, J. and Viriot, L., 2007. Dental microwear in relation to changes in the direction of mastication during the evolution of Myodonta (Rodentia, Mammalia). *Naturwissenschaften***. 94**: 71–75.

Charman, D. and Newnham, R., 1996. Introduction. In: Devon and East Cornwall Field Guide, Charman, D. J. et al. (Eds.). *Quarternary Research Association London*. p. 1-13.

Chatzopoulou, K., 2003. The Late Pleistocene small mammal fauna from Loutra Aridea Bear-Cave (Pella, Macedonia, Greece). Additional Data. –Atti Mus. Civ. Stor. Nat., Trieste **49** (Suppl.): 35-45.

Chatzopoulou, K., 2005a. The stratigraphy from the Loutra Aridéas Bear-Cave (Pella, Macedonia, Greece) with emphasis on two new chambers. –Proceed. Of The 14th Intern. Congr. Of Speleology (Kalamos/Athens, 21-28 August 2005). **1**: 49-51.

Chatzopoulou, A., 2014. The micromammals of the Quaternary deposits from Cave A, Loutra Almopias (Pella, Northern Greece). Stratigraphy-Taphonomy-Paleoenvironment. PhD Thesis. Aristotle university of Thessaloniki School of Geology Department of Geology. (in Greek).

Chatzopoulou, K., Vasileiadou, A., Koliadimou, K., Tsoukala, E., Rabeder, G. and Nagel, D., 2001. Preliminary report on the Late Pleistocene small mammal fauna from Loutraki Bear-cave (Pella, Macedonia, Greece). –Cadernos Lab. Xeolóxico de Laxe, Coruña. **26**: 485-495.

Christiansen, P., 1999a. What size were Arctodus simus and Ursus spelaeus (Carnivora: Ursidae)? *Annales Zoologici Fennici*. **36:** 93-102.

Christiansen, P., 1999b. On the head size of sauropodomorph dinosaurs: implications for ecology and physiology. *Journal of History of Biology.* **13**: 269–297.

Christiansen, P., 2007b. Evolutionary implications of bite mechanics and feeding ecology in bears. *Journal of Zoology*. **272**: 423–443.

Clemens, W. A., 1997 Characterization of enamel microstructure terminology and application of the origins of prismatic structures in systematic analyses. In: Koengiswald, W.v., Sander, P.M. (Eds.), Tooth enamel microstructure. Balkema, Rotterdam. p.85–112.

Clement, C., 2015. "Equus caballus" (On-line), Animal Diversity Web. Accessed August 04, 2015 at http://animaldiversity.org/accounts/Equus_caballus/

Coope, G.R., 2010. Coleopteran faunas as indicators of interglacial climates in central and southern England. *Quaternary Science Reviews.* **29:** 1507-1514.

Cottam, C., Nelson, A. L. and Clarke, T. EE., 1939. Notes on Early Winter Food Habits of the Black Bear in George Washington National Forest. *Journal of Mammalogy*. **20**(3): 310-314.

Crégut-Bonnoure, E., 1996: A review of small Middle Pleistocene bears from France. – *Acta Zoologica Cracoviensia*. **39**: 89-101.

Currant, A. P., 1989. The Quaternary origins of the modern British mammal fauna. *Biological Journal of the Linnean Society*. **38:** 23-30.

Currant, A. P., 1996. Tornewton Cave and the palaeontological succession. In Devon & East Cornwall Field Guide, Charman DJ, Newnham RM, Croot DG (Eds), London. *Quaternary Research Association.* 174–180.

Currant, A. P., 1998. Tornewton Cave. pp 138-145 in: Campbell, S., Hunt, C. O., Scourse, J.D. and Keen, D.H., *Quaternary of South-West England.* Chapman & Hall, London. p. 439.

Currant, A. P., 2000. The Quaternary Mammal Collections at the Somerset County Museum, Taunton. pp 39-44 in: Webster, C. J. (Eds.) *Somerset Archaeology*. Somerset County Council, Taunton.

Currant, A. P., 2004. The Early Devensian mammalian fauna of Banwell Bone Cave, Banwell, Somerset. in Schreve, D.C. (Eds.) *The Quaternary Mammals of Southern and Eastern England. Field Guide*.

Currant, A. P., and Jacobi, R., 1997. Vertebrate faunas of the British Late Pleistocene and the chronology of human settlement. *Quaternary Newsletter.* **82:** 1-8.

Currant, A. P., and Jacobi, R., 2001. A formal mammalian biostratigraphy for the Late Pleistocene of Britain. *Quaternary Science Reviews.* **20**: 1707-1716.

Currant, A. P., and Jacobi, R., 2011. The mammalian faunas of the British Late Pleistocene. In: Ashton, N.M., Lewis, S.G. and Stringer, C.B. (Eds), The Ancient Human Occupation of Britain. Dev. *Quaternary Science*. **14:** 165-180.

Dansgaard, W., Johnsen, S. J., Clausen, H. B., Dahljensen, D., Gundestrup, N. S., Hammer, C.U., Hvidberg, C.S., Steffensen, J.P., Sveinbjörnsdóttir, A. E., Jouzel, J.

and Bond, G., 1993. Evidence for general instability of climate from a 250 kyr ice core record. *Nature*. **264:** 218-220.

Dauphin, Y. and Williams, C. T., 2004. Diagenetic trends of dental tissues. *Comptes Rendus Palevol.* **3**(6–7): 583-590.

Davis, D. D., 1964. The Giant Panda. A morphological study of Evolutionary mechanism. Fieldiana: Zoology memoirs **3:** 1 – 340. Chicago Natural History Museum.

Debeljak, I., 1996. Ontogenetic development of dentition in the cave bear. Ljubljana *Geologija*. **39**: 13-77.

Debeljak, I., 2011. Determination of Individual Age and Season at Death in Cave Bear from Ajdovska jama near. Krško (Slovenia). — *Mitt. Komm. Quartarforsch. Osterr. Akad. Wiss*. **20**:51–63, Wien.

Delson, E., Thomas, H. and Spassov, N., 2005. Fossil Old World monkeys (Primates, Cercopithecidae) from the Pliocene of Dorkovo, Bulgaria. *Geodiversitas.* **27:** 159-166.

Derocher, A. E., Andriashek, D. and Arnould, J. P. Y., 1993. Aspects of milk composition and lactation in polar bears. *Canadian Journal Zoology*. **71:** 561-567.

Derocher, A. E., Wiig, Ø. and Andersen, M., 2002. Diet composition of polar bears in Svalbard and the western Barents Sea Polar. *Biology*. **25** (6): 448-452.

DeSantis, L. R. G., Schubert, B. W., Scott, J. R. and Ungar., P. S., 2012. Implications of Diet for the Extinction of Saber-Toothed Cats and American Lions. *PLoS ONE*. **7**(12): e52453. doi:10.1371/journal.pone.0052453.

Dewar, E. W., 2004. Microwear of carnivorous mammals described with low-magnification dental stereomicroscopy. *Journal of Vertebrate Paleontology***. 24** (3): 52A.

Dittrich, L., 1960. Milchgebibentwicklung und Zahnwechsel beim Braunbären (Ursus arctos L.) und anderen Ursiden, - Morh. Jb. 101/1, 1-141, Leipzig.

Dobey, S., Masters, D. V., Scheick, B. K., Clark, J. D., Pelton, M. R. and Sunquist, M. E., 2005. Ecology of Florida Black Bears in the Okefenokee-Osceola Ecosystem. *Wildlife Monographs*. **158:** 1-41.

Dolphin, A. E., Goodman, A. H. and Amarasiriwardena, D., 2005. Variation in elemental intensities among teeth and between pre- and postnatal regions of enamel. *American Journal of Physical Anthropology*. **128**: 878-888.

Donohue, S. L., DeSantis, L. R. G., Schubert, B. W. and Ungar, P. S., 2013. Was the Giant Short-Faced Bear a Hyper-Scavenger? A New Approach to the Dietary Study of Ursids Using Dental Microwear Textures. *PLoS ONE.* **8** (10): e77531.

Döppes, D. and Pacher, M., 2005. Brown bear Finds from Caves in the Alpine region. – In: Ambros, D., Gropp, C., Hilpert, B. and Kaulich, B. (Eds): Neue Forschungen zum Höhlenbären in Europa. – *Abhandlungen der Naturhistorischen Gesellschaft in Nürnberg*. **45**: 91-104.

Dotsika, E., Zisi, N., Tsoukala, E., Poutoukis, D., Lykoudis, S. and Giannakopoulos, A., 2011. Palaeoclimatic information from isotopic signatures of Late Pleistocene Ursus ingressus bone and teeth apatite (Loutra Arideas Cave, Macedonia, Greece). *Quaternary International*. **245** (2): 291-301.

Doupe, J. P., England, J. H., Furze, M. and Paetkau, D., 2006. Most Northerly Observation of a Grizzly Bear (Ursus arctos) in Canada. Photographic and DNA evidence from Melville Island, Northwest Territories. *Arctic*. **60:** 271–276.

Dumond, E. R., 1995. Enamel thickness and dietary adaptation among extant primates and chiropterans. *Journal of Mammalogy*. **76**: 1127-1136.

Durner, G. M., Douglas, D. C., Nielson, R. M., Amstrup, S. C., Mcdonald, T. L., Stirling, I., Mauritzen, M., Born, E. W., Wiig, Ø., Deweaver, E., Serreze, M. C., Belikov, S. E., Holland, M. M., Maslanik, J., Aars, J., Bailey, D. A. and Derocher, A. E., 2009. Predicting 21st-century polar bear habitat distribution from global climate models. *Ecological Monographs*. **79** (1): 25–58.

Ehrenberg, K., 1929. Die Ergebnisse der Ausgrabungen in der Schreiberwandhöhle am Dachstein. – *Paläont. Z*. **11** (3):261–268.

Ehrenberg, K., 1931. Über die ontogenetische Entwicklung des Höhlenbären. In: O. Abel and G. Kyrte (Eds.), Die Drachenhöhle bei Mixnitz – *Speläolog. Monogr*. **7 – 9**: 624-710.

Eisenmann, V., 1998. Folivores et tondeurs d'herbe : forme de la symphyse mandibulaire des ıquidıs et des tapiridıs (Perissodactyla, Mammalia). *Geobios*. **31:** 113–123.

Elgmork, K. and Kaasa, J., 1992. Food habits and foraging of the brown bear *Ursus arctos* in central south Norway. *Ecography.* **15:** 101–110.

Elias, S. and Schreve, D., 2007. Late Pleistocene Megafaunal Extinctions. Encyclopedia of Quaternary Science. Elias, S. A. (Eds.). 4. Amsterdam : Elsevier Science Publishers B.V. (North-Holland) p. 3202-3217.

Elias, R. W., Hirao, Y. and Patterson, C. C., 1982. The circumvention of the natural biopurification of calcium along nutrient pathways by atmospheric inputs of industrial lead. *Geochimica et Cosmochimica Acta*. **46** (12): 2561-2580.

El-Zaatari, S., Grine, F. E., Teaford, M. F. and Smith, H. F., 2005. Molar microwear and dietary reconstructions of fossil Cercopithecoidea from the Plio-Pleistocene deposits of South Africa. *Journal of Human Evolution.* **49:** 180-205.

Enserink, M. and Vogel, G., 2006. The carnivore comeback. *Science*. **314:** 746–9.

Erdbrink, D. P., 1953. A review of fossil and recent bears of the old world. British Museum, Natural History. Two Volumes, p. 597.

Ewer, R.F., 1973. The Carnivores. The World Naturalist. Great Britain by Cox amd Wyman Ltd., London Fakenham and Reading. Cornell Univ. Press, Ithaca, NY. P. 494.

Felicetti, L. A., Robbins, C. T. and Shipley, L. A., 2003. Dietary protein content alters energy expenditure and composition of mass gain in grizzly bears (*Ursus arctos horribilis*). *Physiological and Biochemical Zoology.* **76:** 256–261.

Fernández-Mosquera, D., Vila-Taboada, M. and Grandal-d'Anglade, A., 2001. Stable isotopes data ($\delta^{13}C$, $\delta^{15}N$) from cave bear (*Ursus spelaeus*). A new approach to its paleoenvironment and dormancy. Proceedings of the Royal Society of London. Series B, Containing papers of a Biological character. *Royal Society* **268:** 1159-1164.

Figueirido, B., Palmqvist, P. and Pérez-Claros, J. A., 2009. Ecomorphological correlates of craniodental variation in bears and palaeobiological implications for extinct taxa: an approach based on geometric morphometrics. *Journal of Zoology.* **277**: 70–80.

Flower, L. O.H. and Schreve, D. C., 2014. An investigation of palaeodietary variability in European Pleistocene canids. *Quaternary Science Reviews*. **96:** 188-203.

Floyd, T., Nelson, R. A. and Wynne, G. F., 1990. Calcium and bone metabolic homeostasis in active and denning black bears (*Ursus americanus*). *Clinical Orthopaedics and Related Research*. **255:** 301-309.

Folk, G. E., Folk, M. A. and Minor, J. J., 1972. Physiological Condition of Three Species of Bears in Winter Dens. *Bears: Their Biology and Management* Vol. 2, A Selection of Papers from the Second International Conference on Bear Research and Management, Calgary, Alberta, Canada, 6-9 November 1970. IUCN Publications New Series no. **23:** 107-124

Folk, G. E., Larson, A. and Folk, M. A., 1976. Physiology of Hibernating Bears *Bears: Their Biology and Management* Vol. 3, A Selection of Papers from the Third International Conference on Bear Research and Management, Binghamton, New York, USA, and Moscow, U.S.S.R., June 1974. IUCN Publications New Series no. **40**: 373-380.

Fortelius, M. and Solounias, N., 2000. Functional characterization of ungulate molars using the abrasion-attrition wear gradient: a new method for reconstructing paleodiets. *American Museum Novitates*. **3301:** 1-36

Fortin, J. K., Farley, S. D., Rode, K. D. and Robbins, C. T., 2007. Dietary and spatial overlap between sympatric ursids relative to salmon use. *Ursus*. **18** (1): 19-29.

Frary, V. J., Duchamp, J., Maehr, D. S. and Larkin, J. L., 2011. Density and distribution of a colonizing front of the American black bear *Ursus americanus. Wildlife Biology.* **17:** 404-416.

Fredriksson, G. M., Wich, S. A. and Trisno, 2006. Frugivory in sun bears (*Helarctos malayanus*) is linked to El Niño-related fluctuations in fruiting phenology, East Kalimantan, Indonesia. *Biological Journal of the Linnean Society*. **89** (3):489-508.

Fredriksson, G., Steinmetz, R., Wong, S. and Garshelis, D. L. (IUCN SSC Bear Specialist Group) 2008. *Helarctos malayanus*. In: IUCN 2013. IUCN Red List of Threatened Species. Version 2013.2. <www.iucnredlist.org>.

Fricke, H. C. and O'Neil, J. R., 1996. Inter- and intra-tooth variation in the oxygen isotope composition of mammalian tooth enamel phosphate: implications for palaeoclimatological and palaeobiological research. *Palaeogeography, Palaeoclimatology, Palaeoecology*. **126**: 91-99.

Fricke, H. C., Clyde, W. C. and O'Neil, J. R., 1998a. Intra-tooth variations in $\delta^{18}O$ (PO_4) of mammalian tooth enamel as a record of seasonal variations in continental climate variables. *Geochimica et Cosmochimica Acta*. **62** (11): 1839–1850.

Fricke, H. C., Clyde, W. C., O'Neil, J. R. and Gingerich, P. D., 1998b. Evidence for rapid climate change in North America during the latest Paleocene thermal maximum: oxygen isotope compositions of biogenetic phosphate from Bighorn Basin (Wyoming). *Earth and Planetary Science Letters.* **160:** 193-208.

Frischauf, C., Rabeder, G. and Withalm, G. (in press). Chronology of the Loutra Almopia Cave (Macedonia, Greece). -*Mitt. Komm. Quartärforsch. Österr. Akad. Wiss, Wien*.

Fulton, T. L. and Strobeck, C., 2006. Molecular phylogeny of the Arctoidea (Carnivora): Effect of missing data on supertree and supermatrix analyses of multiple gene data sets. *Molecular Phylogenetics and Evolution*. **41** (1):165-181.

Galbany, J., Martinez, L. and Amor, H.L., 2005. Error rates in buccal-dental microwear quantification using scanning electron microscopy. *Scanning*. **27**: 23-29.

García, N., 2003. Revisión de los úrsidos pleistocenos en Europa: relaciones filogené ticas entre los úrsidos del último millón de años; pp. 414–468, Osos y otros arnívoros de la Sierra de Atapuerca. Fundacio´n Oso de Asturias, Oviedo.

García, N., 2004. New results on the remains of Ursidae from Untermaβfelt: comparisons with *Ursus dolinensis* from Atapuerca and other Early and Middle Pleistocene sites. 18th International Senckenberg Conference in Weimar.

García, N. and Arsuaga, J. L., 2001. *Ursus dolinensis*: a new species of Early Pleistocene ursid from Trinchera Dolina, Atapuerca (Spain). *Comptes rendus de*

l'Académie des sciences, Série II, Sciences de la Terre et des planets. ***332:*** 717–725.

García, N., Santos, E., Arsuaga, J. L. and Carretero, J. M., 2006. High-Resolution X-Ray computed tomography applied to the study of some endocranial traits in cave and brown bears. Proceedings of the 12th International Cave bear Symposium, Thessaloniki/ Aridea, 2-5 November 2006. *Scientific Annals*, school of Geology, Aristotle University, Thessaloniki. **98**: 141-146.

García, N., Feranec, R. S., Arsuaga, J. L., Bermúdez de Castro, J. M. and Carbonell, E., 2009. Isotopic analysis of the ecology of herbivores and carnivores from the Middle Pleistocene deposits of the Sierra De Atapuerca, northern Spain. *Journal of Archaeological Science.* **36** (5): 1142-1151.

Garrod, D.A.E., 1924. Excavations at Tor Bryan, 1924. Unpublished report to the Torquat Natural History Society dated 12/4/24.

Garshelis, D. L. and Steinmetz, R. (IUCN SSC Bear Specialist Group) 2008. *Ursus thibetanus*. In: IUCN 2013. IUCN Red List of Threatened Species. Version 2013.2. <www.iucnredlist.org>.

Garshelis, D. L., Crider, D. and van Manen, F. (IUCN SSC Bear Specialist Group) 2008a. *Ursus americanus*. In: IUCN 2013. IUCN Red List of Threatened Species. Version 2013.2. <www.iucnredlist.org>.

Garshelis, D. L., Ratnayeke S. and Chauhan, N. P. S. (IUCN SSC Bear Specialist Group) 2008b. *Melursus ursinus*. In: IUCN 2013. IUCN Red List of Threatened Species. Version 2013.2. <www.iucnredlist.org>.

Gebert, C. and Verheyden-Tixier, H., 2001. Variation of diet composition in red deer (Cervus elaphus L.) in Europe. *Mammal Review*. **31:** 189–201.

Genoni, L., Iacumina, P., Nikolaev, V., Gribchenko, Yu. and Longinelli, A., 1998. Oxygen isotope measurements of mammoth and reindeer skeletal remains: an archive of Late Pleistocene environmental conditions in Eurasian Arctic. Earth and Planetary Science Letters. **160**: 587 – 592.

Gentry, A. W., 1999. Fossil ruminants (mammalian, Artiodactyla) from Westbury Cave. pp 139-174 in: Andrews, P., Cook, J., Currant, A. and Stringer, C. (Eds.),

Westbury Cave. The Natural History Museum Excavations 1976 - 1984. Western Academic & Specialist Press, Bristol. p.309.

Geraads, D., 1997. Carnivores du Pliocène terminal de Ahl al Oughlam (Casablanca, Maroc). *Géobios*. **30**: 127-164.

Giannakos, P., 1997. Frugivory and seed dispersal by carnivores in the Rhodopi mountains of northern Greece. PhD Thesis. Durham University, Department of Biological Sciences.

Gilmour, M., Currant, A., Jacobi, R. and Stringer, C., 2007. Recent TIMS dating results from British Late Pleistocene vertebrate faunal localities: context and interpretation. *Journal of Quaternary Science*. **22** (8): 793-800.

Glab, H., Szostek, K. and Kaczanowski, K., 2001. Trace element concentrations from *Papio hamadryas* teeth sequences. *Journal of Trace Elements in Medicine and Biology.* **15**: 59-61.

Goillot, C., Blondel, C. and Peigne, S., 2009. Relationships between dental microwear and diet in Carnivora (Mammalia) – Implications for the reconstruction of the diet of extinct taxa. *Palaeogeography, Palaeoclimatology, Palaeoecology*. **271:** 13-23.

Goldberg, M. and Smith, A. J., 2004. Cells and extracellular matrices of dentin and pulp: a biological basis for repair and tissue engineering. *Critical Reviews in Oral Biology and Medicine.* **15** (1):13-27.

Goldstein, I., Velez-Liendo, X., Paisley, S. and Garshelis, D.L. (IUCN SSC Bear Specialist Group) 2008. *Tremarctos ornatus*. In: IUCN 2013. IUCN Red List of Threatened Species. Version 2013.2. <www.iucnredlist.org>.

Goodall, R. H., Darras, L. P. and Purnell, M. A., 2015. Accuracy and precision of silicon based impression media for quantitative areal texture analysis. *Scientific Reports* **5**: 10800.

Goodness, T., 2004. "Ursus thibetanus" (On-line), Animal Diversity Web. Accessed December 19, 2015 at http://animaldiversity.org/accounts/Ursus_thibetanus/

Gordon, K. D., 1984a. Orientation of occclusal contacts in the chimpanzee, Pan troglodytes verus, deduced from scanning electron microscopic analysis of dental microwear patterns. *Archives of Oral Biology*. **29**: 783–787.

Gordon, K. D., 1984b. The assessment of jaw movement direction from dental microwear. *American Journal of Physical Anthropology*. **63**: 77–84.

Gordon, K. D., 1984c. Taphonomy of dental microwear, II. *American Journal of Physical Anthropology.* **64**: 164–165.

Grandal D'Anglade, A., 1993. Sexual dimorphism and interpopulation variability in the Lower Carnassial of the Cave Bear, *Ursus spelaeus* ROS.-HEIN. *Cuadernos do Laboratorio XeolSxico de Laxe.* **18**: 231-239.

Grandal D'Anglade, A. and López González, F., 2004. A study of the evolution of the pleistocene Cave Bear by a morphometric analysis of the lower carnassial. *Oryctos*. **5:** 83–94.

Grandal D'Anglade, A. and López-González, F., 2005. Sexual dimorphism and ontogenetic variation in the skull of the cave bear (*Ursus spelaeus* Rosenmüller) of the European Upper Pleistocene. *Geobios*. **38**: 325–337.

Grandal D'Anglade, A. and Mosquera, D. F., 2008. Hibernation can also cause high $d^{15}N$ values in cave bears: a response to Richards *et al*. *Proceedings of the National Academy of Sciences of the U. S. A*. **105**: E14.

Grandal D'Anglade, A. and Vidal Romani, J. R., 1997. A population study on the Cave Bear *(Ursus spelaeus* ROS.-HEIN.) from Cova Eirós (Triacastela, Galicia, Spain). [Étude de populations sur l'ours des cavernes *(Ursus spelaeus* ROS.-HEIN) de Cova Eirós (Triacastela, Galice, Espagne)]. G*eobios*. **30** (5): 723-731.

Grandal D'Anglade, A., Pérez-Rama, M. and Fernández-Mosquera, D., 2011. Diet, physiology and environment of the cave bear: a biogeochemical study. In: Toskan, B. (Ed.), Fragments of Ice Age Environments. *Proceedings in Honour of Ivan Turk's Jubilee, Opera Instituti Archaeologici Sloveniae*. **21:** 111-125.

Green, J. L., Semprebon, G. M. and Solounias, N., 2005. Reconstructing the palaeodiet of Florida *Mammut americanum* via low-magnification stereomicroscopy. *Palaeogeography, Palaeoclimatology, Palaeoecology*. **223:** 34– 48.

Grimes, S. T., Mattey, D. P., Collinson, M. E. and Hooker, J. J., 2004a. Using mammal tooth phosphate with freshwater carbonate and phosphate palaeoproxies to

obtain mean paleotemperatures. *Quaternary Science Reviews*. **23** (7–8)**:** 967-976.

Grimes, S. T., Collinson, M. E., Hooker, J. J., Mattey, D. P., Grassineau, N. V. and Lowry, D., 2004b. Distinguishing the diets of coexisting fossil theridomyid and glirid rodents using carbon isotopes. *Palaeogeography, Palaeoclimatology, Palaeoecology*. **208** (1–2): 103-119.

Grine, F. E., 1981. Trophic differences between 'gracile' and 'robust' australopithecines: a scanning electron microcope analysis of occlusal events. *South African Journal of Science.* **77:** 203–230.

Grine, F. E., 1986. Dental evidence for dietary differences in *Australopithecus* and *Paranthropus*: A quantitative analysis of permanent molar microwear. *Journal of Human Evolution*. **15:** 783–822.

Grine, F. E., Ungar, P. S. and Teaford, M. F., 2002. Error rates in dental microwear quantification using scanning electron microscopy. *Scanning*. **24:** 144–153.

Guérin, C., 2002. Conclusion générale sur la faune du Pléistocéne supérieur de la grotte de Jaurens (commune de Nespouls, Corréze, France). *Cahiers scientifiques Muséum d' Histoire naturelle de Lyon*. **1**: 55-66.

Gunderson, A., 2009. "Ursus maritimus" (On-line), Animal Diversity Web. Accessed December 19, 2015 at http://animaldiversity.org/accounts/Ursus_maritimus/

Guthrie, R. D., 2001. Origin and causes of the mammoth steppe: a story of cloud cover, woolly mammal tooth pits, buckles, and inside-out Beringia. *Quaternary Science Reviews*. **20:** 549-574.

Hilderbrand, G. V., Farley, S. D. and Robbins, C. T., 1998. Predicting body condition of bears via two field methods. *Journal of Wildlife Management*. **62:** 406-409.

Hilderbrand, G. V., Schwartz, C. C., Robbins, C. T. and Hanley, T. A., 2000. Effect of Hibernation and Reproductive Status on Body Mass and Condition of Coastal Brown Bears. *The Journal of Wildlife Management*. **64** (1): 178-183

Hilderbrand, G. V., Farley, S. D., Robbins, C. T., Hanley, T.A., Titus, K. and Servheen, C., 1996. Use of stable isotopes to determine diets of living and extinct bears. *Canadian Journal of Zoology.* **74:** 2080 -2088.

Hilderbrand, G. V., Schwartzc, C. C., Robbins, T., Jacoby, M. E., Hanley, T. A., Arthur, S. M. and Servheen, C., 1999. Importance of dietary meat, particularly salmon, to body size, population productivity, and conservation of North American brown bears. *Canadian Journal of Zoology*. **77:** 132-138.

Hillson, S., 1986. Teeth. Cambridge Mannuals in Archaeology. Cambridge University p. 376.

Hinz, E. A., and Kohn, M. J., 2010. The effect of tissue structure and soil chemistry on trace element uptake in fossils. *Geochimica et Cosmochimica Acta*. **74** (11): 3213-3231.

Hirata, D., Mano, T., Abramov, A. V., Baryshnikov, G. F., Kosintsev, P. S., Vorobiev, A. A., Raichev, E. G., Tsunoda, H., Kaneko, Y., Murata, K., Fukui, D. and Masuda, R., 2013. Molecular phylogeography of the brown bear (*Ursus arctos*) in Northeastern Asia based on analyses of complete mitochondrial DNA sequences. *Molecular Biology and Evolution.* **30**: 1644-1652.

Hoffmann, D. L., Paterson, B. A., and Jonckheere, R., 2008. Measurements of the uranium concentration and distribution in a fossil equid tooth using fission tracks, TIMS and laser ablation ICPMS: Implications for ESR dating. *Radiation Measurements*. **43** (1): 5-13.

Hofreiter, M. and Stewart, J., 2009. Ecological Change, Range Fluctuations and Review Population Dynamics during the Pleistocene. *Current Biology*. **19:** R584–R594.

Hofreiter, M., Rabeder, G., Jaenicke-Despres, V., Withalm, G., Nagel, D., Paunovic, M., Jambresic, G. and Pääbo, S., 2004a. Evidence for Reproductive Isolation between Cave Bear Populations. *Current Biology*. **14**: 40–43.

Hofreiter, M., Serre, D., Rohland, N., Rebeder, G., Nagel, D., Conrad, N., Münzel, S. and Pääbo, S., 2004b. Lack of phylogeography in European mammals before the

last glaciation. *Proceedings of the National Academy of Sciences USA*. **101:** 12963-12968.

Hoppe, K. A., 2006. Correlation between the oxygen isotope ratio of North American bison teeth and local waters: implication for palaeoclimatic reconstructions. *Earth and Planetary Science Letter.* **244**: 408-417.

Hoppe, K. A., Koch, P. L. and Furutani, T. T., 2003. Assessing the Preservation of Biogenic Strontium in Fossil Bones and Tooth Enamel. *International Journal of Osteoarchaeology.* **13**: 20–28.

Hoppe, K. A., Stover, S. M., Pascoe, J. R. and Amundson, R., 2004. Tooth enamel biomineralization in extant horses: implications for isotopic microsampling. *Palaeogeography, Palaeoclimatology, Palaeoecology*. **206** (3–4): 355–365.

Humphrey, L. T., Dean, M. C., Jeffries, T. E. and Penn, M., 2008a. Unlocking evidence of early diet from tooth enamel. *Proceedings of the National Academy of Sciences.* **105** (19): 6834-6839.

Humphrey, L. T., Dirks, W., Dean, M. C. and Jeffries, T. E., 2008b. Tracking dietary transitions in weanling baboons *(Papio hamadryas anubis) u*sing strontium/calcium ratios in enamel. *Folia Primatol***. 79**: 197–212.

Huygens, O. C., Miyashita, T., Dahle, B., Carr, M., Izumiyama, S., Sugawara, T. and Hayashi, H., 2003. Diet and Feeding Habits of Asiatic Black Bears in the Northern Japanese Alps. *Ursus*. **14** (2): 236-245.

Jacobi, R. M., Higham, T. F. G. and Bronk Ramsey, C., 2006. AMS radiocarbon dating of Middle and Upper Palaeolithic bone in the British Isles: improved reliability using ultrafiltration. *Quaternary Science Reviews*. **21:** 557-573.

Jacobi, R. M., Rose, J., MacLeod, A. and Higham, T. F.G., 2009. Revised radiocarbon ages on woolly rhinocerous (Coelodonta antiquitatis) from western central Scotland: significance from timing the extinction of woolly rhinoceros in Britain and the onset of the LGM in central Scotland. *Quaternary Science Reviews*. **28:** 2551-2556.

Jacques, L., Ogle, N., Moussa, I., Kalin, R., Vignaud, P., Brunet, M., and Bocherens, H., 2008. Implications of diagenesis for the isotopic analysis of Upper Miocene large

mammalian herbivore tooth enamel from Chad. *Palaeogeography, Palaeoclimatology, Palaeoecology*. **266** (3): 200-210.

Jeffrey, A., 2010. Exploring seasonal dietary variability in a Late Pleistocene mammalian ecosystem using trace element ratios from high-resolution LA-ICPMS. Dissertation in Royal Holloway University of London,

Jochum, K. P., Weis, U., Stoll, B., Kuzmin, D., Yang, Q., Raczek, I., Jacob, D. E., Stracke, A., Birbaum, K., Frick, D. A., Günther, D. and Enzweiler, J., 2011. Determination of Reference Values for NIST SRM 610–617 Glasses Following ISO Guidelines. *Geostandards and Geoanalytical Research*. **35**: 397–429.

Joshi, A. R., Garshelis, D. L. and Smith, J. L. D., 1997. Seasonal and Habitat-Related Diets of Sloth Bears in Nepal. *Journal of Mammalogy*. **78** (2): 584-597.

Kabouroglou, E. and Chatzitheodorou, Th., 1999. Γεωμορφολογικές μεταβολές και ιζηματογένεση σπηλαίου Α (Αγίασμα) Λουτρακίου Ν. Πέλλας (Μακεδονία). - Πρακτικά 5ου Πανελληνίου Γεωγραφικού Συνεδρίου, 83-93, Αθήνα. In Greek

Kahlke, R. D., 1994. Die Entstehungs-, Entwicklungs- und Verbreitungsgeschichte des oberpleistozänen Mammuthus-Coelodonta- Faunenkomplexes in Eurasien (Grossäuger). Abhandlungen der Senckenbergischen naturforschenden Gesellschaft. **546**: 1‑164.

Kahlke, R. D., 1999. The History of the Origin, Evolution and Dispersal of the Late Pleistocene Mammuthus-Coelodonta Faunal Complex in Eurasia (Large Mammals). Fenske Companies, Rapid City. p.219

Kahlke, R. D., García, N., Kostopoulos, D. S., Lacombat, F., Lister, A. M., Mazza, P. P. A., Spassov, N. and Titov, V. V., 2011. Western Palaearctic palaeoenvironmental conditions during the Early and early Middle Pleistocene inferred from large mammal communities, and implications for hominin dispersal in Europe. *Quaternary Science Reviews*. **30** (11–12): 1368-1395.

Kang, D., Amarasiriwardena, D. and Goodman, A. H., 2004. Application of laser ablation-inductively coupled plasma-mass spectrometry (LA–ICP-MS) to investigate trace metal spatial distributions in human tooth enamel and dentine growth layers and pulp. *Analytical and Bioanalytical Chemistry*. **378**: 1608–1615.

Karamanlidis, A. A., de Gabriel Hernando, M., Krambokoukis, L. and Gimenez, O., 2015. Evidence of a large carnivore population recovery: Counting bears in Greece. *Journal for Nature Conservation*. **27:** 10-17.

Kay, R. F., 1981. The nut-crackers: a new theory of the adaptations of the Ramapithecinae. *American Journal of Physical Anthropology*. **55**: 141–151.

Keen, D. H., 1998. Kent's Cavern. In: Quaternary of South-West England. Geological Conservation Reviews Series, No 14, Campbell, S., et al (Eds.), Kluwer: London. p. 134-138.

Kempe, S., Rosendahl, W. and Döppes, D., 2005. The making of the cave bear – Die wissenschaftliche Entdeckung des, *Ursus spelaeus'.* In Nagel, D. (Eds.): Festschrift Gernot Rabeder, 89–106. Mitteilungen der Kommission für Quart ärfrschung der Österreichischen Akademie der Wissenschaften 14.

King, T., Andrews, P. and Boz, B., 1999. Effect of taphonomic processes on dental microwear. *American Journal of Physical Anthropology*. **108**: 359-373.

King, S. R. B., Boyd, L., Zimmerman, W. and Kendall, B. E., 2015. *Equus ferus ssp. przewalskii*. The IUCN Red List of Threatened Species 2015: e.T7961A45172099. http://dx.doi.org/10.2305/IUCN.UK.2015-2.RLTS.T7961A45172099.en. Downloaded on **30 November 2015**.

Kingston, J. D. and Harrison, T., 2007. Isotopic dietary reconstructions of Pliocene herbivores at Laetoli: Implications for early hominin paleoecology. *Palaeogeography, Palaeoclimatology, Palaeoecology*. **243**: 272–306.

Kistchinski, A. A., 1972. Life history of the brown bear (*Ursus arctos* L.) in northeast Siberia. Pages 67–73. In S. Herrero, editor. Bears, their biology and management. IUCN Publisher, Morges, Switzerland.

Klemme, S., Prowatke, S., Münker, C., Magee, C. W., Lahaye, Y., Zack, T., Kasemann, S. A., Cabato, E. J. A. and Kaeser, B., 2008. Synthesis and preliminary

characterization of new silicate, phosphate and titanite reference glasses. *Geostandards and Geoanalytical Research*. **32:** 39-54.

Koch, P. L., Fisher, D. C. and Dettman, D. L., 1989. Oxygen isotope variation in the tusks of extinct proboscideans: A measure of season of death and seasonality. *Geology.* **17:** 515-519.

Koch, P. L., Fogel, M. L. and Tuross, N., 1994. Tracing the diets of fossil animals using stable isotopes. In stable isotopes and ecology and environmental Science. Blackwell Scientific Publications, Oxford. p. 63-92.

Koenigswald, W. and Clemens, W. A., 1992. Levels of complexity in the microstructure of mammalian enamel and their application in studies of systematics. *Scanning Microscopy*. **6**(1): 195–218.

Koenigswald, W.v., 1992. The enamel of the cave bear (*Ursus spelaeus*) and the relationship between diet and enamel structures. *Annales Zoologici Fennici*. **28**: 21-227.

Koenigswald, W.v., 1997. Evolutionary trends in the differentiation of mammalian enamel ultrastructure. In: Koengiswald, W.v., Sander, P.M. (Eds.), Tooth enamel microstructure. Balkema, Rotterdam. p.203–235.

Koenigswald, W. v. and Heinrich, W. D., 1999. Mittelpleistozäne Säugetierfaunen aus Mitteleuropa – der Versuch einer biostratigraphischen Zuordnung. – *Kaupia*. **9**: 53-112.

Koenigswald, W. V, Kalthoff, D. C. and Semprebon, G. M., 2010. The microstructure of enamel, dentine and cementum in advanced Taeniodonta (Mammalia) with comments on their dietary adaptations. *Journal of Vertebrate Paleontology.* **30**: 1797–1804.

Kohn, M., 2004. Comment: tooth enamel mineralization in ungulates: implications for recovering a primary isotopic time-series, by B. H. Passey and T. E. Cerling 2002. *Geochimica et Cosmochimica Acta*. **68:** 403 – 405.

Kohn, M. J., 2008. Models of diffusion-limited uptake of trace elements in fossils and rates of fossilization. *Geochimica et Cosmochimica Acta*. **72:** 3758-3770.

Kohn, M. J. and McKay, M. P., 2012. Paleoecology of late Pleistocene-Holocene faunas of eastern and central Wyoming, USA, with implications for LGM climate models. *Palaeogeography Palaeoclimatology Palaeoecology*. **326-328:** 42-53.

Kohn, M. J., Morris, J. and Olin, P., 2013. Trace element concentrations in teeth–a modern Idaho baseline with implications for archeometry, forensics, and palaeontology. *Journal of Archaeological Science*. **40** (4): 1689-1699.

Kohn, M. J., Schoeninger, M. J. and Barker, W. W., 1999. Altered states: effects of diagenesis on fossil tooth chemistry. *Geochimica et Cosmochimica Acta*. **63** (18): 2737-2747.

Kohn, M. J., Schoeninger, M. J. and Valley, J. W., 1996. Herbivore tooth oxygen isotope compositions: effects of diet and physiology. *Geochimica et Cosmochimica Acta.* **60:** 3889-3896.

Kohn, M. J., Schoeninger, M. J. and Valley, J. W., 1998. Variability in oxygen isotope compositions of herbivore teeth: reflections of seasonality or developmental physiology? *Chemical Geology*. **152:** 97-112.

Koike, S., Morimoto, H., Kozakai, C., Arimoto, I., Yamazaki, K., Iwaoka, M., Soga, M. and Koganezawa, M., 2012. Seed removal and survival in Asiatic black bear *Ursus thibetanus* faeces: effect of rodents as secondary seed dispersers. *Wildlife Biology.* **18:** 24-34.

Korotkevič, M. L., 1967. Fauna krupnyh mlekopitaûŝih iz pliocenovyh otloženij doliny r. Kyčurgana [Large mammals from the Pliocene layers of Kučurgan River]. – In: Mesto i značenie iskopaemyh mlekopitaûŝih Moldavii v kajnozoe SSSR [Position and importance of fossil mammals from the territory of Moldova in the Quaternary of USSR]. 77-84. Kišinev: Šiinca. [In Russian.]

Krachler, M., Rossipal, E. and Micetic-Turk, D., 1999. Trace element transfer from the mother to the newborn – investigations on triplets of colostrum, maternal and umbilical cord sera. *European Journal of Clinical Nutrition*. **53**: 486–494.

Krause, J., Unger, T., Nocon, A., Malaspinas, A-S., Kolokotronis, S-O, Stiller, M., Soibelzon, L., Spriggs, H., Dear, P. H., Briggs, A. W., Bray, S.-CE., O'Brien, S. J., Rabeder, G., Matheus, P., Cooper, A., Slatkin, M., Pääbo, S. and Hofreiter, M.,

2008. Mitochondrial genomes reveal an explosive radiation of extinct and extant bears near the Miocene-Pliocene boundary. *BMC Evolutionary Biology*. **8:** 220.

Krechmar, M. A., 1995. Geographical aspects of the feeding of the brown bear (*Ursus arctos* L.) in the extreme northeast of Siberia. *Russian Journal of Ecology.* **26**: 436–443.

Kronk, C., 2007. "Ursus americanus" (On-line), Animal Diversity Web. Accessed December 19, 2015 at http://animaldiversity.org/accounts/Ursus_americanus/

Kruuk, H., 1972. The spotted hyaena: a Study of predation and social behavior. The University Chicago. p. 335.

Kurtén, B., 1955. Sex dimorphism and size trends in the cave bear. *Acta Zoologica Fennica*. **90**: 1-47

Kurtén, B., 1958. Life and death of the Pleistocene cave bear: a study in paleoecology. *Acta Zoologica Fennica*. **95**: 4–59.

Kurtén, B., 1959. On the Bears of the Holsteinian Interglacial. *Stockholm Contributions to Geology*. **2**: 73-102.

Kurtén, B., 1960. Rates of evolution in fossil mammals. *Cold Spring Harbor Symposium on Quantitative Biology*. **24:** 205-215.

Kurtén, B., 1966. The Pleistocene bears of North America, I: Genus Tremarctos, spectacled bears. *Acta Zoologica Fennica*. **115:** 1- 120.

Kurtén, B., 1968. Pleistocene Mammals of Europe. -Aldine Publishing Company, Chicago. P. 317.

Kurtén, B., 1969. Cave Bears. Studies in Spelaeology. **2**: 13-24.

Kurtén, B., 1975. Fossile Reste von Hyänen und Bären (Carnivora) aus den Travertinen von Weimar-Ehringstdorf. III. Internationales Paläontologisches Kolloquium 1968. Das Pleistozän von Weimar- *Ehringstdorf. Teil II. Abhandlung des Zentralen Geologischen Instituts*. **23**: 465-484.

Kurtén, B., 1976. The Cave Bear Story. Life and Death of a Vanished Animal. New York: Columbia University Press. p. 1-163.

Kurtén, B. and Anderson, E., 1980. Pleistocene Mammals of North America. Columbia University Press, New York.

Kurtén, B. and Poulianos, A. N., 1977. New Stratigraphic and faunal Material from Petralona Cave with special reference to the Carnivora. – *Anthropos.* **4:** 47-130.

Kurtén, B. and Poulianos, A. N., 1981. Fossil carnivore of Petralona cave: status of 1980. *Anthropos.* **8**: 9–56.

Law, J., 2004. "Crocuta crocuta" (On-line), Animal Diversity Web. Accessed August 05, 2015 at http://animaldiversity.org/accounts/Crocuta_crocuta/

Lebel, S., Trinkaus, E., Faure, E., Fernandez, Ph., Guérin, C., Richter, D., Mercier, M., Valladas, H. and Wagner, G. A., 2001. Comparative morphology and paleobiology of Middle Pleistocene human remains from the Bau de l' Aubesier, Vaucluse, France. – *Proceedings of the National Academy of Sciences of the United States of America*. **98** (20): 11097-11102.

Lee, K. M., Appleton, J., Cooke, M., Keenan, K. and Sawicka-Kapusta, K., 1999. Use of laser ablation inductively coupled plasma mass spectrometry to provide element versus time profiles in teeth. *Analytica Chimica Acta*. **395:** 179-185.

Lee-Thorp, J. A. and Sponheimer, M., 2003. Three case studies to reassess the reliability of fossil bone and enamel isotope signals for paleodietary studies. *Journal of Anthropological Archaeology*. **22**: 208-216.

Lee-Thorp, J. A. and Sponheimer, M., 2006. Contributions of biogeochemistry to understanding hominin dietary ecology. *Yearbook of Physical Anthropology*. **49:** 131-148.

Lee-Thorp, J. A. and van der Merwe, N. J., 1989. Stable carbon isotope ratio differences between bone collagen and bone apatite, and their relationship to diet. *Journal of Archaeological Science*. **16**: 585-599.

Lee-Thorp, J. A. and van der Merwe, N. J., 1991. Aspects of the chemistry of modern and fossil biological apatites. *Journal of Archaeological Science*. **18**: 343-354.

Leonard, J. A., Wayne, R. K. and Cooper, A., 2000. Population genetics of ice ages brown bears. *Proceedings of the National Academy of Sciences USA*. **97**: 11651-11654.

Lidén, K. and Angerbjörn, A., 1999. Dietary change and stable isotopes: a model of growth and dormancy in cave bears. *Proceedings of the Royal Society: Biological Sciences*. **266:** 1779-1783.

Lister, A. M., 1992. Mammalian Fossils and Quaternary Biostratigraphy. *Quaternary Science Reviews.* **11:** 329-344.

Lister, A. M., 1994. The evolution of the giant deer, *Megaloceros giganteus* (Blumenbach). *Zoological Journal of the Linnean Society.* **112:** 65-100.

Lister, A. M. and Bahn, P., 2007. Mammoths. Giants of the Ice Age. University of California Press. p.192.

Liu, X., Skidmore, A. K., Wang, T., Yong, Y. and Prins, H. H. T., 2002. Giant panda movements in Foping Nature Reserve, China. *Journal of Wildlife Management*. **66:** 1179-1188.

Lohuis, T. D., Harlow, H. J. and Beck, T. D. I., 2007. Hibernating black bears (Ursus americanus) experience skeletal muscle protein balance during winter anorexia. *Comparative Biochemistry and Physiology.* B **147**: 20-28.

López-Alfaro, C., Robbins, C. T., Zedrosser, A. and Nielsen, S. E., 2013. Energetics of hibernation and reproductive trade-offs in brown bears. *Ecological Modelling*. **270**: 1-10.

Lovari, S., Herrero. J., Conroy, J., Maran, T., Giannatos, G., Stubbe, M., Aulagnier, S., Jdeidi, T., Masseti, M., Nader, I., de Smet, K. and Cuzin, F., 2008. *Cervus elaphus*. The IUCN Red List of Threatened Species. Version 2015.2. <www.iucnredlist.org>. Downloaded on **04 August 2015**.

Lucas, P., Constantino, P., Wood, B. and Lawn, B., 2008. Dental enamel as a dietary indicator in mammals. *Bioessays*. **30**: 374–385.

Lü, Z, Wang, D. and Garshelis, D.L. (IUCN SSC Bear Specialist Group) 2008. *Ailuropoda melanoleuca*. In: IUCN 2013. IUCN Red List of Threatened Species. Version 2013.2. <www.iucnredlist.org>.

Luu, J., 2002. "Equus caballus przewalskii" (On-line), Animal Diversity Web. Accessed November 30, 2015 at http://animaldiversity.org/accounts/Equus_caballus_przewalskii/

Macdonald, D. W., 2009. The Encyclopedia of mammals. OUP Oxford.

MacFadden, B. J., Solounias, N. and Cerling, T. E., 1999. Ancient diets, ecology, and extinction of 5-million-year-old horses from Florida. *Science*. **283:** 824-827.

Maddy, D., Lewis, S.G., Scaife, R.G., Bowen, D.Q., Coope, G.R., Green, C.P., Hardaker, T., Keen, D.H., Rees-Jones, J., Parfitt, S. and Scott, K., 1998. The Upper Pleistocene deposits at Cassington, near Oxford, England. *Quaternary Science Reviews.* **13** (3): 205-231.

Maier von Mayerfels S., 1929. Zur Stammesgeschichte der europäischen Bären. *Neues Jahrbuch für Mineralogie, Geologie und Paläontologie*, Beilagen-Band. **62:** 325-332.

Mainland, I. L., 2003. Dental microwear in grazing and browsing Gotland sheep (*Ovis aries*) and its implications for dietary reconstruction. *Journal of Achaeological Science.* **30**: 1513-1527.

Marks, S. A. and Erickson, A. W., 1966. Age Determination in the Black Bear. *The Journal of Wildlife Management* **30** (2): 389-410.

Marra, A. C., 2003. *Ursus arctos* from selected Pleistocene sites of Eastern Sicily. *Bollettino della Societá Paleontologica Italiana*. **42** (1-2): 145-150.

Martinez-Perez, C., Rayfield, E. J., Purnell, M. A. and Donoghue, P. C. J., 2014. Finite element, occlusal, microwear and microstructural analyses indicate that conodont microstructure is adapted to dental function. *Palaeontology*. **57**(5): 1059-1066.

Matheus, P. E., 1995. Diet and Co-ecology of Pleistocene Short-Faced Bears and Brown Bears in Eastern Beringia. *Quaternary Research*. **44** (3): 447-453.

Mattson, D. J., 1998. Diet and morphology of extant and recently extinct northern bears. *Ursus*. **10:** 479-496.

Mazza, P., and Rustioni, M., 1992. Morphometric revision of the Eurasian species *Ursus etruscus* Cuvier. *Palaeontolgraphica Italica*. **79:** 101-146.

Mazza, P. and Rustioni, M., 1994. On the phylogeny of Eurasian bears. *Palaeontographica Abteilung* (A). **230**: 1–38.

McFarlanea, D. A., Sabol, M. and Lundberg, J., 2011. A unique population of cave bears (Carnivora: Ursidae) from the Middle Pleistocene of Kents Cavern, England, based on dental morphometrics.*Historical Biology*. **23** (2–3): 131–137.

McLellan, B., and Reiner, D. C., 1994. A review of bear evolution. *International Conference on Bear Research and Management*. **9:** 85-96.

McLellan, B. N., Servheen, C. and Huber, D., (IUCN SSC Bear Specialist Group), 2008. *Ursus arctos*. In: IUCN 2013. IUCN Red List of Threatened Species. Version 2013.2. <www.iucnredlist.org>.

Merceron, G., Viriot, L. and Blondel, C., 2004b. Tooth microwear pattern in roe deer (*Capreolus capreolus*, L.) from Chize (Western France) and relation to food composition. *Small Ruminant Research*. **53** (1): 125-132.

Merceron, G., Bonis, L de, Viriot, L. and Blondel, C., 2005a. Dental microwear of fossil bovids from northern Greece: paleoenvironmental conditions in the eastern Mediterranean during the Messinian. *Palaeogeography, Palaeoclimatology, Palaeoecology*. **217:** 173–185.

Merceron, G., Blondel, C., Bonis, L de., Koufos, G. D. and Viriot, L., 2005b. A new method of dental microwear analysis: Application to extant primates and *Ouranopithecus macedoniensis* (Late Miocene of Greece). *Palaios*. **20:** 551–561.

Merceron, G., Taylor, S., Scott, R., Chaimanee, Y. and Jaeger, J. J., 2006. Dietary characterization of the hominoid *Khoratpithecus* (Miocene of Thailand): evidence from dental topographic and microwear texture analyses. *Naturwissenschaften*. **93:** 329–333.

Merceron, G., Blondel, C., Brunet, M., Sen, S., Solounias, N., Viriot, L. and Heintz, E., 2004a. The Late Miocene paleoenvironment of Afghanistan as inferred from dental microwear in artiodactyls. *Palaeogeography, Palaeoclimatology, Palaeoecology*. **207:** 143–163.

Metcalfe, J. Z., Longstaffe, F. J. and Zazula, G. D., 2010. Nursing, weaning, and tooth development in woolly mammoths from Old Crow, Yukon, Canada: Implications for Pleistocene extinctions. *Palaeogeography, Palaeoclimatology, Palaeoecology*. **298**: 257–270.

Meurman, J. H. and Frank, R. M., 1991a. Progression and Surface Ultrastructure of in vitro Caused Erosive Lesions in Human and Bovine Enamel. *Caries Res*earch. **25**: 81-87.

Meurman, J. H. and Frank, R. M., 1991b. Scanning Electron Microscopic Study of the Effect of Salivary Pellicle on Enamel Erosion. *Caries Res*earch. **25**: 1-6.

Millard, A. R., and Hedges, R. E., 1996. A diffusion-adsorption model of uranium uptake by archaeological bone. *Geochimica et Cosmochimica Acta*. **60** (12): 2139-2152.

Miller, G. S., 1912. Catalogue of the Mammals of Western Europe (Europe exclusive of Russia) in the Collection of the British Museum. London. Ursidae: p. 284-303.

Miller, C.R., Waits, L.P. and Joyce, P., 2006. Phylogeography and mitochondrial diversity of extirpated brown bear (*Ursus arctos*) populations in the contiguous United States and Mexico. *Molecular Ecology*. **15**: 4477–4485.

Miller, S. D., White, G. C., Sellers, R. A., Reynolds, H. V., Schoen, J. W., Titus, K., Barnes, V. G., Jr., Smith, R. B., Nelson, R. R., Ballard, W. B. and Schwartz, C. C., 1997. Brown and black bear density estimation in Alaska using radiotelemetry and repiicated mark-resight techniques. *Wildlife Monographs*. **133**: 1-55.

Miller, W., Schuster, S. C., Welch, A. J., Ratan, A., Bedoya-Reina, O. C., Zhao, F., Kim, H. L., Burhans, R. C., Drautz, D. I., Wittekindt, N. E., Tomsho, L. P., Ibarra-Laclette, E., Herrera-Estrella, L., Peacock, E., Farley, S., Sage, G. K. Rode, K., Obbard, M., Montiel, M. R., Bachmann, L., Ingólfsson, Ó., Aars, J., Mailund, Th., Wiig, Ø., Talbot, S. L. and Lindqvist, Ch., 2012. Polar and brown bear genomes reveal ancient admixture and demographic footprints of past climate change. *Proceedings of National Academy of Science USA*. **109:** E2382–90.

Mitchell, B., 1967. Growth layers in dental cement for determining the age of red deer (*Cervus elaphus* L.). *Journal Animal Ecology*. **36**: 279-293.

Montgomery, J., Evans, J. A. and Horstwood, M. S. A., 2010. Evidence for long-term averaging of strontium in bovine enamel using TIMS and LA-MC-ICP-NS strontium isotope intra-molar profiles. *Environmental Archaeology*. **15** (1): 32-42.

Montoya, P., Ginsburg, L., Alberdi, M. T., van der Made, J., Morales, J. and Soria, M. D., 2006. Fossil large mammals from the early Pliocene locality of Alcoy (Spain) and their importance in biostratigraphy. *Geodiversitas.* **28:** 137-173.

Morris, J., 1836. On a freshwater deposit containing mammalian remains, recently discovered at Grays, Essex. *Magazine ofNatural History*. **9** (1): *261-264.*

Moss-Salentijn, L., Moss, M. L. and Yuan, M. S., 1997. The ontogeny of mammalian enamel. In: Koengiswald, W.v., Sander, P.M. (Eds.), Tooth enamel microstructure. Balkema, Rotterdam. p. 5–30.

Mottl, M., 1964. Bärenphylogenese in Südost-Österreich.Mitteilungen des Museums für Bergbau, Geologie und Technik am Landesmuseum Joanneum. **26**: 1–55.

Mowat, G., and Heard, D.C., 2006. Major components of grizzly bear diet across North America. *Canadian Journal of Zoology.* **84** (3): 473–489.

Müller, W., Shelley, M., Miller, P. and Broude, S., 2009. Initial performance metrics of a new custom-designed ArF excimer LA-ICPMS system coupled to a two-volume laser-ablation cell. *Journal Analytical Atomic Spectrometry*. **24:** 209-214.

Münzel, S.C., Stiller, M., Hofreiter, M., Mittnik, A., Conard, N.J. and Bocherens, H., 2011. Pleistocene bears in the Swabian Jura (Germany): Genetic replacement, ecological displacement, extinctions and survival. *Quaternary International*. **245**: 225-237.

Münzel, S. C., Rivals, F., Pacher, M., Döppes, D., Rabeder, G., Conard, N. J. and Bocherens, H., 2014. Behavioural ecology of Late Pleistocene bears (Ursus spelaeus, Ursus ingressus): Insight from stable isotopes (C, N, O) and tooth microwear. *Quaternary International*. **339-340:** 148-163.

Nagel, D. and Rabeder, G., 1997. Chronologie de L' ours des caverns en Autriche "MAN and BEAR».- International Meeting, Auberives-en-Royans, 4-6 November 1997, France.- Eraul- *Etudes et Recherches Archéologiques de L'Université de Liège*. **100:** 265-287.

Nagel, D., Rohland, N. and Hofreiter, M., 2004. Phylogeography of the cave hyena (Crocuta crocuta spelaea) -morphology versus genetics. *18th International Conference Senckenberg 2004 in Weimar. Abstract Volume,* http://www.senckenberg.de/fis/doc/abstracts/75_Nagel_etal.pdf

Nelson, S., Badgley, C. and Zakem, E., 2005. Microwear in Modern Squirrels in Relation to Die. *Palaeontologia Electronica*. **8** (1): 2 – 15.

Nelson, R. A., Folk, G. E., Jr., Pfeiffer, E. W., Craighead, J. J., Jonkel, C. J. and Steiger, D.L., 1983. Behavior, biochemistry, and hibernation in black, grizzly, and polar bears. *International Conference on Bear Research and Management.* **5**: 284 – 290.

Odum, E. P. and Barrett, G. W., 2005. Fundamentals of Ecology, 5th edn. Thomson Brooks/Cole, Belmont.

Pacher, M., 1997. Der Höhlenbärenkult aus ethnologischer Sicht. *Wissenschaftliche Mitteilungen aus dem Niederösterreichischen Landesmuseum*. **10:** 251–375.

Pacher, M., 2000. Höhlenbäre und Mensch: Tatsachen und Vermutungen. In Rabeder, G., Nagel, D. & Pacher, M. (Eds.): Der Höhlenbär. *Species*. **4:** 82–104. Thorbecke Verlag, Stuttgart.

Pacher, M., 2002. Polemique autour d'un culte de l'Ours des Cavernes. In Tillet, T. & Binford, L. R. (Eds.): L'ours et L'homme, 235–246. Etudes et Recherches Arche´ologiques de l'Universite´ de Liège 100.

Pacher, M., 2004. Taphonomic analyses of cave bear remains from Potoèka zijalka (Slovenia): Further analyses and conclusion. In Pacher, M., Pohar, V. & Rabeder, G. (eds.): Potoèka zijalka – Paleontological and archaeological results of the campaigns 1997–2000, 97–114. *Mitteilungen der Kommission für Quartärforschung der Österreichischen Akademie der Wissenschaften* 13.

Pacher, M., 2007. The type specimen of Ursus priscus Goldfuss, 1818 and the uncertain status of Late Pleistocene brown bears. *N. Jb. Geol. Paläont. Abh. Stuttgart*. **245/3:** 331-339.

Pacher, M. and Stuart, J. S., 2007. European Cave Bears and Brown Bears in the Late Pleistocene. Proceedings 13th International Cave Bear Symposium (ICBS), Brno, Czech Republic, in Scripta Fac. Sci. Nat. Univ. Masaryk. Brun. **35:** 139-140.

Pacher, M. and Stuart, A. J., 2009. Extinction chronology and paleoecology of the cave bear *Ursus spelaeus*. *Boreas*. **38** (2): 189-206.

Pales, L. and Lambert, C., 1971. Atlas ostéologique pour servir à l'identification des Mammifères du Quaternaire. Éditions du C. N. R. S., Paris.

Palombo, M. R., Filippi, M. L., Iacumin, P., Longinelli, A., Barbieri, M. and Maras, A., 2005. Coupling tooth microwear and stable isotope analyses for palaeodiet reconstruction: the case study of Late Middle Pleistocene Elephas (*Palaeoloxodon*) *antiquus* teeth from Central Italy (Rome area). *Quaternary International*. **126–128:** 153–170.

Pappa, S., Pacher, M. and Schreve, D., 2013. Preliminary morphological results on Bear specimens from Tornewton Cave, Devon, England. Abstract book 19th International Cave Bear Symposium (ICBS), Semriach, Styria, Austria.

Paralikidis, N. P., Papageorgiou, N. K., Kontsiotis, V. J. and Tsiompanoudis, A. C., 2010. The dietary habits of the Brown bear (*Ursus arctos*) in western Greece. *Mammalian Biology*. **75:** 29-35.

Passey, B. H. and Cerling, T. E., 2002. Tooth enamel mineralization in ungulates: implications for recovering a primary isotopic timeseries. *Geochimica et Cosmochimica Acta.* **66** (18): 3225–3234.

Passey, B. H., Cerling, T. E., Schuster, G. T., Robinson, T. F., Roeder, B. L. and Krueger, S. K., 2005. Inverse methods for estimating primary input signals from time-averaged isotope profiles. *Geochimica et Cosmochimica Acta.* **69** (16): 4101–4116.

Pasteris, J. D., Wopenka, B. and Valsami-Jones, E., 2008. Bone and Tooth mineralization: Why Apatite? *Elements*. **4**: 97-104.

Paunović, M., 1988. Morphometrische und Morphogenetische untersuchungen der Ursidenzähne aus den Höhlen Nordwestkroatiens. *Palaeont. Jugosl. Jugosl. Akad., Zagreb.* **36**: 1-40.

Peek, S. and Clementz, M. T., 2012a. Sr/Ca and Ba/Ca variations in environmental and biological sources: A survey of marine and terrestrial systems. *Geochimica et Cosmochimica Acta*. **95**: 36-52.

Peek, S. and Clementz, M. T., 2012b Ontogenetic variations in Sr/Ca and Ba/Ca ratios of dental bioapatites from Bos taurus and Odocoileus virginianus. *Journal of Trace Elements in Medicine and Biology.* **26** (4): 248-254.

Pei, W.C., 1934. On the Carnivora from Locality 1 of Choukoutien. *Palaeontologia Sinica* (C). **8**: 1-216.

Peigné, S., Goillot, C., Germonpré, M., Blondel, C., Bignon, O. and Merceron, G., 2009. Predormancy omnivory in European cave bears evidenced by a dental microwear analysis of Ursus spelaeus from Goyet, Belgium. *Proceedings of the National Academy of Sciences*. **106** (36): 15390-15393.

Pengelly, W., 1884. The literature of Kent's Cavern, Part V. Transactions of the Devonshire Association for the Advancement of Science, Literature and Art. **14:** 189-434.

Penzhorn, B.L., 1982. Age determination in Cape Mountain Zebras *Equus Zebra Zebra* in the Mountain Zebra National Park. *Koedoe*. **25** (1): 89-102.

Pérez-Rama, M., Fernández-Mosquera, D. and Grandal-d'Anglade, A., 2011a. Recognizing growth patterns and maternal strategies in extinct species using stable isotopes: the case of the cave bear *Ursus spelaeus* ROSENMÜLLER. *Quaternary International*. **245:** 302-306.

Pérez-Rama, M., Fernández-Mosquera, D. and Grandal-d'Anglade, A., 2011b. Effects of hibernation on the stable isotope signatures of adult and neonate cave bears. *Quaternaire, Hors-série*. **4:** 79-88.

Persson, I-L., Wikan, S., Swenson, J. E. and Mysterud, I., 2001. The diet of the brown bear *Ursus arctos* in the Pasvik Valley, northeastern Norway. *Wildlife Biology*. **7:** 27-37.

Peyton, B., 1980. Ecology, distribution, and food habits of spectacled bears, *Tremarctos ornatus*, in Peru. *Journal of Mammalogy*. **61:** 639–652.

Pinto-Llona, A. C., 2006. Comparative dental microwear analysis of cave bears. Proceedings of the 12th International Cave Bear Symposium, Thessaloniki/ Aridea, 2-5 November 2006. *Scientific Annals*, School of Geology, Aristotle University, Thessaloniki. **98:** 103 - 108

Pinto-Llona, A. C., 2013. Macrowear and occlusal microwear on teeth of cave bears Ursus spelaeus and brown bears *Ursus arctos*: Inferences concerning diet. *Palaeogeography, Palaeoclimatology, Palaeoecology*. **370**: 41–50.

Pinto-Llona, A. C. and Andrews, P., 2001. Dental wear and grit ingestion in extant and extinct bears from N. Spain. *Cadernos del Laboratorio de Xeoloxia de Laxe*. **26:** 423–429.

Pinto Llona, A. C. and Andrews, P. J., 2003. Scavenging behaviour patterns in cave bears *Ursus spelaeus*. In Brugal, J. Ph. & Fosse, P. (eds.): Hommes et carnivores au Paléolithique. Hommage à Philippe Morel, 845–853. Actes du XIVe Congrès UISPP, Univ. de Liège, Belgique 2–8 Septembre 2001. Revue de Paléobiologie 23.

Pinto Llona, A. C., Andrews, P. and Etxeberría, P., 2005. Taphonomy and Palaeoecology of Cave Bears from the Quaternary of Cantabrian Spain. 680 pp. Fondación de Asturias/Du Pont Ibérica/The Natural History Museum, Grafinsa, Oviedo.

Prevosti, F. J. and Martin, F. M., 2013. Paleoecology of the mammalian predator guild of Southern Patagonia during the latest Pleistocene: Ecomorphology, stable isotopes, and taphonomy. *Quaternary International*. **305**: 74-84.

Proctor, C. J., 1994. A British Pleistocene chronology based on uranium series and electron spin resonance dazing of speleothems. Unpublished PhD Thesis: University of Bristol.

Proctor, C. J., 1996. Kent's Cavern. In: Devon and East Cornwall Field Guide, Charman, D. J. et al. (Eds.). *Quarternary Research Association London*. p. 163-167.

Proctor, C. J. and Smart, P. L., 1996. Uranium Series and ESR Dating of speleothems from Three Holes and Tornewton Cave. In: Devon and East Cornwall Field Guide, Charman, D. J. et al. (Eds.). *Quarternary Research Association London*. p. 181-186.

Proctor, C. J., Berridge, P. J., Bishop, M. J. Richards, D. A. and Smart, P.L., 2005. Age of Middle Pleistocene fauna and Lower Palaeolithic industries from Kent's Cavern, Devon. *Quaternary Science Reviews*. **24**: 1243-1252.

Purnell, M. A., Hart, P. J. B., Baines, D. C. and Bell, M. A., 2006. Quantitative analysis of dental microwear in threespine stickleback: a new approach to analysis of trophic ecology in aquatic vertebrates. *Journal of Animal Ecology.* **75**: 967–977.

Purnell, M. A. Crumpton, N., Gill, P. G., Jones, G. and Rayfield, E. J., 2013. Within-guild dietary discrimination from 3-D textural analysis of tooth microwear in insectivorous mammals. *Journal of Zoology*. **291** (4): 249-257.

Pusey, A. E. and Packer, C., 1994. Non-offspring nursing in social carnivores: minimizing the costs. *Behavioral Ecology*. **5**: 362-374.

Quilès, J., 2003. Les Ursidae du Pléistocène moyen et supérieur en Midi méditerranéen: Apports paléontologiques, biochronologiques et archéozoologique [PhD Thesis]. Paris: Museum National d'Histoire Naturelle. p.322.

Quilès, J., Monchot, H. and Pacher, M., 2005. Mixture analysis: Application to cave bear sex-ratio determination. *Bulletin de Societé d'Histoire Naturelle Toulouse*. **141**: 29–37.

Rabeder, G., 1983. Neues vom Höhlenbären. Zur Morphogenetik der Backenzähne. *Die Höhle*, H., Wien. **2** (34): 67-85.

Rabeder, G., 1989. Modus und Geschwindigkeit der Höhlenbären-Evolution.- Schriftenreihe d. Vereins zur Verbreitung naturwiss. *Kenntnisse in Wien*. **127**: 105-126.

Rabeder, G., 1995. Die Gamssulzenhöhle imToten Gebirge. –Mitt. Komm. Quartärforsch. Österr. Akad. Wiss. **9**: 1–133.

Rabeder, G., 1999. Die Evolution des Höhlenbärengebisses. – *Mitt. Quartärkomm. Österr. Akad.Wiss.,* Wien. **11**: 1–102.

Rabeder, G. and Hofreiter, M., 2004. Der neue Stammbaum der alpinen Höhlenbären. *Die Höhle*. **55**: 1-19.

Rabeder, G. and Tsoukala, E., 1990. Morphodynamic analysis of some cave-bear teeth from Petralona cave (Chalkidiki, N. Greece). *Beitrage zur Paläont. von Österreich, Wien*. **16**: 103-109.

Rabeder, G. and Withalm, G., 2006. Brown Bear remains (Ursidae, Mammalia) from Early Pleistocene cave fillings of Deutsch-Altenburg (Lower Austria). – Abstract Book 12th International Cave Bear Symbosium, Aridea, Macedonia, Greece, 2-5 November 2006.

Rabeder, G., Hofreiter, M. and Withalm, G., 2004b. The Systematic position of the cave bear from Potocka zijalka (Slovenia). *Mitt. Quartärkomm. Österr. Akad.Wiss.,* Wien. **13**: 197-200.

Rabeder, G., Nagel, D. and Pacher, M., 2000. Der Höhlenbär. Thorbecke Verlag, Stuttgart. Species 4. p. 111.

Rabeder, G., Pacher, M. and Withalm, G., 2010. Early Pleistocene bear remains from Deutsch-Altenburg (Lower Austria). – *Mitt. Quartärkomm. Österr. Akad.Wiss.,* Wien. **17**: 1-135.

Rabeder, G., Tsoukala, E. and Kavcik, N., 2006. Chronological and systematic position of cave Bears from Loutra Arideas (Pella, Macedonia, Greece).- Proceedings of the 12th International Cave bear Symposium, Thessaloniki/ Aridea, 2-5 November 2006. *Scientific Annals*, school of Geology, Aristotle University, Thessaloniki. **98**: 69-73.

Rabeder, G., Hofreiter, M., Nagel, D. and Withalm G., 2004a. New Taxa of Alpine Cave Bears (Ursidae, Carnivora). Cahiers scientifiques - Département du Rhône – Muséum, Lyon, Hors. **2**: 49-67.

Radosevich, S. C., 1993. The six deadly sins of trace element analysis: a case of wishful thinking in science. In: Sandford, M.K. (Eds.), Investigations of Ancient Human Tissue: Chemical Analyses in Anthropology. Food and Nutrition in History and Anthropology. Gordon and Breach, Langhorne, UK. **10**: 269 – 332.

Ramesh, T., Sankar, K. and Qureshi, Q., 2009. Additional notes on the diet of sloth bear *Melursus ursinus* in Mudumalai Tiger Reserve as shown by scat analysis. *The Journal of the Bombay Natural History Society.* **106** (2): 204-206.

Rasmussen, S. O., Andersen, K. K., Svensson, A. M., Steffensen, J. P., Vinther, B. M., Clausen, H. B., Siggaard-Andersen, M.-L., Johnsen, S. J., Larsen, L. B., Dahl-Jensen, D., Bigler, M., Röthlisberger, R., Fischer, H., Goto-Azuma, K., Hansson, M. E. and Ruth, U., 2006. A new Greenland ice core chronology for the last glacial termination. *Journal of Geophysical Research*. **111**: D06102, doi:06110.01029/02005JD006079.

Rausch, R. L., 1961. Notes on the black bear, *Ursus americanus*, Pallas, in Alaska, with particular reference to dention and growth. *Z. Saeugetierkd.* **26**: 77 – 107.

Reichenau, W. v., 1906. Beiträge zur näheren Kenntnis der Carnivoren aus den Sanden von Mauer und Mosbach. *Abhandlungen der Grossherzoglichen Hessischen Geologischen Landesanstalt*. **4**: 1–313.

Reinhard, E., Torres, T. and O'Neil, J., 1996. $^{18}O/^{16}O$ ratios of cave bear tooth enamel: a record of climate variability during the Pleistocene. *Palaeogeography, Palaeoclimatology, Palaeoecology*. **126**: 45-59.

Reitznerova, E., Amarasiriwardena, D., Kopcakova, M. and Barnes, R.M., 2000. Determination of some trace elements in human tooth enamel. *Fresenius Journal of Analytical Chemistry*. **367**: 748-754.

Rensberger, J. M., 1999. Rensberger Enamel microstructural specialization in the canine of the spotted hyena, *Crocuta crocuta. Scanning Microscopy*. **13** (2-3): 343-361.

Reynard, B., Lécuyer, C. and Grandjean, P., 1999. Crystal-chemical controls on rare-earth element concentrations in fossil biogenic apatites and implications for paleoenvironmental reconstructions. *Chemical Geology*. **155** (3): 233-241.

Reynolds, S. H., 1902. A monograph of the British Pleistocene Mammalia Vol. II Part I The Cave Hyaena. London: Palaeontographical Society.

Reynolds, S. H., 1906. A monograph of the British Pleistocene Mammalia. Vol. II Part II. The Bears. London: Palaeontographical Society.

Reynolds, S. H., 1906. A monograph on the British Mammalia. Vol. II. British Pleistocene Hyaenidae, Ursidae, Canidae and Mustelidae. – *Monographs of the Palaeontographical Society of London*. **2**: 1-35.

Reynolds, S. H., 1909. A monograph of the British Pleistocene Mammalia Vol. II Part III. The Canidae. London: Palaeontographical Society.

Reynolds, S. H., 1922. A monograph of the British Pleistocene Mammalia. Vol. III, Part I. Hippopotamus. London: Palaeontographical Society.

Reynolds, S. H., 1933. A monograph of the British Pleistocene Mammalia. Vol. III, Part IV The Red Deer, Reindeer, and Roe. London: Palaeontographical Society for 1931.

Richards, M. P., Fuller, B. T., Sponheimer, M., Robinson, T. and Ayliffe, L., 2003. Sulphur isotopes in palaeodietary studies: a review and results from a controlled feeding experiment. *International Journal of Osteoarchaeology*. **13**: 37-45.

Richards, M. P., Pacher, M., Stiller, M., Quilès, J., Hofreiter, M., Constantin, S., Zilhao, J. and Trinkaus, E., 2008b. Isotopic evidence for omnivory among European cave bears: late Pleistocene Ursus spelaeus from the Pestera cu Oase, Romania. *Proceedings of the National Academy of Sciences USA*. **105**: 600-604.

Richards, M. P., Harvati, K., Grimes, V., Smith, C., Smith, T., Hublin, J., Karkanas, P. and Panagopoulou, E., 2008a. Strontium isotope evidence of Neanderthal mobility at the site of Lakonis, Greece using laser-ablation PIMMS. *Journal of Archaeological Science*. **35**: 1251-1256.

Rigg, R. and Gorman, M., 2005. Diet of brown bears (*Ursus arctos*): new results from the Tatras region and a comparison of research methods. *Výskum a ochrana cicavcov na Slovensku.* **7**: 61–79.

Rivals, F. and Athanassiou, A., 2008. Dietary adaptations in an ungulate community from the late Pliocene of Greece. *Palaeogeography, Palaeoclimatology, Palaeoecology*. **265**: 134–139.

Rivals, F. and Deniaux, B., 2003. Dental microwear analysis for investigating the diet of an argali population (*Ovis ammon antiqua*) of mid-Pleistocene age, Caune de

l'Arago cave, eastern Pyrenees, France. *Palaeogeography, Palaeoclimatology, Palaeoecology*. **193**: 443–455.

Rivals, F. and Semprebon, G. M., 2011. Dietary plasticity in ungulates: Insight from tooth microwear analysis. *Quaternary International*. **245**: 279-284.

Rivals, F., Semprebon, G. M. and Lister, A., 2012. An examination of dietary diversity patterns in Pleistocene proboscideans (Mammuthus, Palaeoloxodon, and Mammut) from Europe and North America as revealed by dental microwear. *Quaternary International*. **255**: 188-195

Rivals, F., Solounias, N. and Mihlbachler, M. C., 2007. Evidence for geographic variation in the diets of late Pleistocene and early Holocene Bison in North America, and differences from the diets of recent Bison. *Quaternary Research*. **68**: 338–346.

Rivals, F., Mihlbachler, M. C., Solounias, N., Mol, D. Semprebon, G. M., de Vos, J. and Kalthoff, D.C., 2010. Palaeoecology of the Mammoth Steppe fauna from the late Pleistocene of the North Sea and Alaska: Separating species preferences from geographic influence in paleoecological dental wear analysis. *Palaeogeography, Palaeoclimatology, Palaeoecology.* **286** (1–2): 42-54.

Robbins, C. T., Schwartz, C. C. and Felicetti, L. A., 2004. Nutritional ecology of bears: the review of newer methods and management implications. *Ursus*. **15**: 161–171.

Robbins, C. T., Schwartz, C. C., Gunther, K. A. and Servheen, C., 2006. Grizzly Bear Nutrition and Ecology Studies in Yellowstone National Park. *Yellowstone Science*. **14** (3): 19 – 26.

Rohland, N., Pollack, J. L., Nagel, D., Beauval, C., Airvaux, J., Pääbo, S. and Hofreiter, M., 2005. The Population History of Extant and Extinct Hyenas. *Molecular Biology*. **22**: 2435-2443.

Rosendahl, W. and Grupe, G., 2001. Mittelwürmzeitliche Höhlenbären und ihre Nahrungspräferenz – Forschungen aus der Neuen Laubenstein–Bärenhöhle/Chiemgau. *Mitteilungen der Bayerischen Staatssammlung für Paläontologie und historische Geologie*. **41**: 85–94.

Rosendahl, W. and Kempe, S., 2005. *Ursus spelaeus* Rosenmüller 1794 and not Rosenmüller and Heinroth- Johann Christian Rosenmüller, his life and the *Ursus spelaeus*. – In: Ambros, D., Gropp, C., Hilpert, B. & Kaulich, B. (Eds): Neue Forschungen zum Höhlenbären in Europa. – *Abhandlungen der Naturhistorischen Gesellschaft in Nürnberg.* **45**: 191-198.

Rossipal, E., Krachler, M., Li, F. and Micetic-Turk, D., 2000. Investigation of the transport of trace elements across barriers in humans: studies of placental and mammary transfer. *Acta Paediatrica*. **89**: 1190–1195.

Rowles, S.L. 1967. Chemistry of the mineral phase of dentine. *In* A.E.D. Miles (ed.) Structural and Chemical Organization of Teeth. *Academic Press*, London. **2**: 201-245.

Runia, L.T., 1987. Strontium and calcium distribution in plants: effect on palaeodietary studies. *Journal of Archaeological Science*. **14**: 599–608.

Rugh, D. J. and Shelden, K. E. W., 1993. Polar Bears, *Ursus maritimus*, feeding on Beluga Whales, *Delphinapterus leucas*. *Canadian Field-Naturalist*. **107** (2): 235-237.

Rustioni, M. and Mazza, P., 1993. The genus *Ursus* in Euarsia: Dispersal events and stratigraphical significance. *Rivista Italiana di Paleontologia e Stratigrafia.* **98**: 487-494.

Ryan, A.S., 1979. A preliminary scanning electron microscope examination of wear striation direction on primate teeth. *Journal of Dental Research*. **58**: 525–530.

Sabol, M., 2001. Fossil Brown Bears of Slovakia. Los osos pardos fósiles de Eslovaquia. Cadernos Lab. *Xeolóxico de Laxe*, Coruña. **26**: 311-316.

Sacco, T. and Van Valkenburgh, B., 2004. Ecomorphological indicators of feeding behaviour in the bears (*Carnivora: Ursidae*). *Journal of Zoology (London)* **263**: 41–54.

Safont, S., Malgosa, A., Subira, M. E. and Gibert, J., 1998. Can Trace Elements in Fossils Provide Information about Palaeodiet? *International Journal of Osteoarchaeology*. **8**: 23–37.

Santos, E., Garcia, N., Carretero, J. M., Arsuaga, J. L. and Tsoukala, E., 2014. Endocranial traits of the Sima de los Huesos (Atapuerca, Spain) and Petralona (Chalkidiki, Greece) Middle Pleistocene ursids. Phylogenetic and biochronological implications. *Annales de Paléontologie*. **100** (4): 297-309.

Schliebe, S., Wiig, Ø., Derocher, A. and Lunn, N. (IUCN SSC Polar Bear Specialist Group) 2008. *Ursus maritimus*. In: IUCN 2013. IUCN Red List of Threatened Species. Version 2013.2. <www.iucnredlist.org>.

Schoeninger, M. J., 1979. Diet and status at Chalcatzingo: some empirical and technical aspects of strontium analysis. *American Journal of Physical Anthropology*. **51:** 295-310.

Schreve, D. C., 1997. Mammalian biostratigraphy of the later Middle Pleistocene in Britain. PhD Thesis. University of London.

Schreve, D. C., 2001. Differentiation of the British late Middle Pleistocene interglacials: the evidence from mammalian biostratigraphy. *Quaternary Science Reviews*. **20**: 1693-1705.

Schreve, D. C. and Bridgland, D. R., 2002. Correlation of English and German Middle Pleistocene fluvial sequences based on mammalian biostratigraphy. *Geologie en Mijnbouw.* **81:** 357-373.

Schreve, D. C. and Currant A. P., 2003. The Pleistocene history of the Brown Bear with particular reference to the western Palaearctic. In: Living with Bears. A large European Carnivore in a Shrinking World. Edited by B. Kryštufek, B. Flajšman and H. I. Griffiths, Ljubjana, Slovenia. 27-39.

Schreve, D. C., Currant, A. P. and Stringer, C., 1999. Conclusion: correlation of the Westbury Cave deposits. pp 275-284 in: Andrews, P., Cook, J., Currant, A. and Stringer, C. (eds.), *Westbury Cave. The Natural History Museum Excavations 1976 - 1984.* Western Academic & Specialist Press, Bristol. p.309.

Schreve, D., Howard, A., Currant, A., Brooks, S., Buteux, S., Coope, G. R., Crocker, B., Field, M., Greenwood, M., Greig, J. and Toms, P., 2013. A Middle Devensian woolly rhinoceros from Whitemoor Haye Quarry, Staffordshire (UK):

palaeoenvironmental context and significance. Journal of Quaternary Science. **28**(2): 118-130.

Schubert, B. W., Ungar, P. S. and DeSantis, L. R. G., 2010. Carnassial microwear and dietary behaviour in large carnivorans. *Journal of Zoology*. **280**: 257–263.

Schutkowski, H., Herrmann, B., Wiedemann, F., Bocherens,H. and Grupe, G., 1999. Diet, status and decomposition at Weingarten: trace element and isotopic analyses on Early Medieval skeletal material. *Journal of Archaeological Science*. **26**: 675–685.

Scott, R. S., Ungar, P. S., Bergstrom, T. S., Brown, C. A., Grine, F. E., Teaford, M. F. and Walker, A., 2005. Dental microwear texture analysis shows within-species diet variability in fossil hominins. *Nature*. **436**: 693-695.

Scott, R. S., Ungar, P. S., Bergstrom, T. S., Brown, C. A., Childs, B. E., Teaford, M.F. and Walker, A., 2006. Dental microwear texture analysis: technical considerations. *Journal of Human Evolution*. **51**: 339-349.

Scott, R. S., Godfrey, L. R., Jungers, W. L., Scott, R. S., Simons, E. L., Teaford, M. F., Ungar, P. S. and Walker, A., 2009. Dental microwear texture analysis of two families of subfossil lemurs from Madagascar. *Journal of Human Evolution*. **56**: 405–416.

Sealy, J. C. and Sillen, A., 1988. Sr and Sr/Ca in Marine and Terrestrial Foodwebs in the Southwestern Cape, South Africa. *Journal of Archaeological Science*. **15**: 425-438.

Seger, R. L., Cross, R. A., Rosen, C. J., Causey, R. C., Gundberg, C. M., Carpenter, T. O., Chen, T. C., Halteman, W. A., Holick, M. F., Jakubas, W. J., Keisler, D. H., Seger, R. M. and Servello, F. A., 2011. Investigating the mechanism for maintaining eucalcemia despite immobility and anuria in the hibernating American black bear (*Ursus americanus*). *Bone*. **49** (6): 1205-1212.

Semprebon, G. M. and Rivals, F., 2006. A comparison of the dietary habits of a large sample of the Pleistocene pronghorn Stockoceros onusrosagris from the Papago springs cave in Arizona to the modern Antilocapra Americana. *Journal of Vertebrate Paleontology*. **26**(2):495–500.

Semprebon, G. M. and Rivals, F., 2007. Was grass more prevalent in the pronghorn past? An assessment of the dietary adaptations of Miocene to Recent Antilocapridae (Mammalia: Artiodactyla). *Palaeogeography, Palaeoclimatology, Palaeoecology*. **253:** 332-347.

Semprebon, G. M. and Rivals, F., 2010. Trends in the paleodietary habits of fossil camels from the Tertiary and Quaternary of North America. *Palaeogeography, Palaeoclimatology, Palaeoecology*. **295:** 131–145.

Semprebon, G. M., Godfrey, L. R., Solounias, N., Sutherland, M. R. and Jungers, W. L., 2004. Can low-magnification stereomicroscopy reveal diet? *Journal of Human Evolution*. **47:** 115-144.

Semprebon, G. M., Rivals, F., Fahlke, J. M., Sanders, W. J., Lister, A., M. and Göhlich, U. B., (in press). Dietary reconstruction of pygmy mammoths from Santa Rosa Island of California. *Quaternary International*.

Senseman, R., 2002. "Cervus elaphus" (On-line), Animal Diversity Web. Accessed August 04, 2015 at http://animaldiversity.org/accounts/Cervus_elaphus/

Sharp, Z. D. and Cerling, T. E., 1998. Fossil isotope records of seasonal climate and ecology: straight from the horse's mouth. *Geology*. **26:** 219-222.

Shipman, P., 1981. Life history of a fossil. An introduction to Taphonomy and Paleoecology. –Harvard University Press: 1-222.

Sillen, A., 1992. Strontium-calcium ratios (Sr/Ca) of *Australopithecus robustus* and associated fauna from Swartkrans. *Journal of Human Evolution*. **23:** 495-516.

Silva, M. and Downing, J. A., 1995. The allometric scaling of density and body mass: a non-linear relationship for terrestrial mammals. *American Naturalist*. **145**: 704–727.

Slaughter, B. H., Pine, R. H. and Pine, N. E., 1974. Eruption of cheek teeth in insectivora and carnivora. *Journal of Mammalogy*. **55:** 115–125.

Smith, T. M., 2006. Experimental determination of the periodicity of incremental features in enamel. *Journal of Anatomy.* **208**: 99–113.

Smith, T. M. and Tafforeau, P., 2008. New visions of dental tissue research: Tooth development, chemistry, and structure. *Evolutionary Anthropology*. **17**: 213–226.

Soibelzon, L. H. and Schubert, B. W., 2011. The Largest Known Bear, *Arctotherium angustidens*, from the Early Pleistocene Pampean Region of Argentina: With a Discussion of Size and Diet Trends in Bears. *Journal of Paleontology*. **85** (1): 69–75.

Solounias, N. and Hayek, L-A., 1993. New methods of tooth microwear analysis and application to dietary determination of two extinct antelopes. *Journal of Zoology London*. **229**: 421-445.

Solounias, N. and Semprebon, G., 2002. Advances in the Reconstruction of Ungulate Ecomorphology with Application to Early Fossil Equids. *American Museum Novitates*. **3366**: 1-49.

Solounias, N., Teaford, M. F. and Walker, A., 1988. Interpreting the diet of extinct ruminants: the case of a non-browsing giraffid. *Paleobiology*. **14**: 287–300.

Sponheimer, M. and Lee-Thorp, L., 1999. Alteration of enamel carbonate environments during fossilization. *Journal of Archaeological Science*. **26**: 143-150.

Sponheimer, M. and Lee-Thorp, L., 2006. Enamel diagenesis at South African Australopith sites: Implications for paleoecological reconstruction with trace elements. *Geochimica et Cosmochimica Acta.* **70**: 1644–1654.

Sponheimer, M., de Ruiter, D., Lee-Thorp, L. and Späth, A., 2005. Sr/Ca and early hominin diets revisited: new data from modern and fossil tooth enamel. *Journal of Human Evolution*. **48**: 147-156.

Sponheimer, M., Passey, B. H., de Ruiter, D. J., Guatelli-Steinberg, D., Cerling, T. E. and Lee-Thorp, J. A., 2006. Isotopic evidence for dietary variability in the early hominin *Paranthropus robustus*. *Science* **314**: 980–982.

Sponheimer, M., Robinson, T., Ayliffe, L., Roeder, B., Hammer, J., Passey, B., West, A., Cerling, T., Dearing, D. and Ehleringer, J., 2003. Nitrogen Isotopes in Mammalian Herbivores: Hair $\delta^{15}N$ Values from a Controlled Feeding Study. *International Journal of Osteoarchaeology*. **13**: 80-87.

Stefen, C., 1997a. Differentiations in Hunter-Schreger bands of carnivores. In: Koengiswald, W.v., Sander, P.M. (Eds.), Tooth enamel microstructure. Balkema, Rotterdam, p. 123–136.

Stefen, C., 1997b. The enamel of Creodonta, Arctocyonidae, and Mesonychidae (Mammalia), with special reference to the appearance of Hunter–Schreger bands. *Paläontologische Zeitschrift.* **71** (3/4), 291–303.

Stefen, C., 1999. Enamel structure of Recent and fossil Canidae (Carnivora, Mammalia). *Journal of Vertebrate Paleontology*. **19**: 576–588.

Stefen, C., 2001. Enamel structure of arctoid carnivora: amphicyonidae, ursidae, procyonidae, and mustelidae. *Journal of Mammalogy*. **82** (2): 450-462.

Stiner, M. C., 1998. Mortality analysis of Pleistocene bears and its paleoanthropological relevance. *Journal of Human Evolution*. **34**: 303-326.

Stiner, M. C., Achyuthan, H., Arsebük, G., Howell, F. C., Josephson, S., Juell, K., Pigati, J. and Quade, J., 1998. Reconstructing cave bear paleoecology from skeletons: a cross-disciplinary study of Middle Pleistocene bears from Yarimburgaz Cave, Turkey. *Paleobiology*. **24** (1): 74–98.

Stiller, M., Baryshnikov, G., Bocherens, H., Grandal d'Anglade, A., Hilpert, B., Munzel, S. C., Pinhasi, R., Rabeder, G., Rosendahl, W., Trinkaus, E., Hofreiter, M. and Knapp, M., 2010. Withering Away—25,000 Years of Genetic Decline Preceded Cave Bear Extinction. *Molecular Biology and Evolution.* **27**(5):975–978.

Stirling, J., 1993. Bears, Majestic Creatures of the Wild. Emmaus, Pennsylvania: Rodale Press,. pages 240. *http://www.bearbiology.com/index.php?id=41*

Stirling, I. and Derocher, A. E., 1990. Factors Affecting the Evolution and Behavioral Ecology of the Modern Bears. *Bears: International Conference on Bear Research and Management.* **8:** 189-204.

Storms, D., Aubry, P., Hamann, J.-L., Saïd, S., Fritz, H., Saint-Andrieux, C. and Klein, F., 2008. Seasonal variation in diet composition and similarity of sympatric red and roe deer. *Wildlife Biology*. **14**. 237–250.

Stringer, C., Andrews, P. and Currant, A., 1999. Introduction to the site and previous work. pp 1-12 in: Andrews, P., Cook, J., Currant., A. and Stringer, C. (Eds.), *Westbury Cave. The Natural History Museum Excavations 1976 - 1984*. Western Academic and Specialist Press, Bristol.

Stuart, A. J., 1976. The History of the Mammal Fauna During the Ipswichian/Last Interglacial in England. *Philosophical Transactions of the Royal Society of London*. B 1976. **276**: 221-250.

Stuart, A. J., 1982. Pleistocene vertebrates in the British Isles. London and New York: Longman.

Stuart, A. J., 1996. Vertebrate faunas from the early Middle Pleistocene of East Anglia. In Turner, C. (Eds.): The Early Middle Pleistocene in Europe, 9–24. A. A. Balkema, Rotterdam.

Stuart, A. J., 2005. The extinction of woolly mammoth (Mammuthus primigenius) and straight-tusked elephant (Palaeoloxodon antiquus) in Europe. *Quaternary International*. **126–128**: 171–177.

Stuart, A. J. and Lister, A. M., 2007. Patterns of Late Quaternary megafaunal extinctions in Europe and northern Asia. *Courier Forschungsinstitut Senckenberg*. **259**: 287–297.

Stuart, A. J. and Lister, A. M., 2012. Extinction chronology of the woolly rhinoceros Coelodonta antiquitatis in the context of late Quaternary megafaunal extinctions in northern Eurasia. *Quaternary Science Reviews*. **51:** 1-17

Stuart, A. J., Kosintsev, P. A., Higham, T. F. G. and Lister, A. M., 2004. Pleistocene to Holocene extinction dynamics in giant deer and woolly mammoth. *Nature*. **431**: 684–689.

Stuart-Williams, H. L. Q. and Schwarcz, H. P., 1997. Oxygen isotopic determination of climatic variation using phosphate from beaver bone, tooth enamel, and dentine. *Geochimica et Cosmochimica Acta.* **61:** 2539-2550.

Stynder, D. D., Ungar, P. S., Scott, J. R. and Schubert, B. W., 2012. A Dental Microwear Texture Analysis of the Mio-Pliocene Hyaenids from Langebaanweg, South Africa. *Acta Palaeontologica Polonica.* **57**(3): 485-496.

Suga, S., 1982. Progressive mineralization pattern of developing enamel during the maturation stage. *Journal of dental Research*. **61**: 1532-1542.

Suga, S., 1989. Enamel hypomineralisation viewed from the pattern of progressive mineralization of human and monkey developing enamel. *Advances in Dental Research*. **2**: 188-198.

Suga, S., Murayma, Y. and Musashi, T., 1970. A study of the mineralization progress in the developing enamel of guinea pigs. *Archives of Oral Biology*. **15**: 597-612.

Sutcliffe, A. J. and Kowaiski, K., 1976. Pleistocene Rodents of the British Isles. Bulletin of the British Museum (Natural History), Geology, 27/2.

Sutcliffe, A.J. and Zeuner, F.E., 1962. Excavations in the Torbryan Caves. Devonshire I. Tornewton Cave. *Proceedings of the Devon Archaeological Exploration Society*. **5–6**: 127–145.

Svensson, A., Andersen, K. K., Bigler, M., Clausen, H. B., Dahl-Jensen, D., Davies, S. M., Johnsen, S. J., Muscheler, R., Parrenin, F., Rasmussen, S. O., Röthlisberger, R., Seierstad, I., Steffensen, J. P. and Vinther, B. M., 2008. A 60,000 year Greenland stratigraphic ice core chronology. *Climate of the Past*. **4:** 47-57.

Swenson, J. E., Adamič, M., Huber, D. and Stokke, S., 2007. Brown bear body mass and growth in northern and southern Europe. *Oecologia* **153:** 37–47.

Taberlet, P. and Bouvet, J., 1994. Mitochondrial DNA polymorphism, phylogeography, and conservation genetics of the brown bear *Ursus arctos* in Europe. *Proceedings of Royal Society of London* B. **255:** 195- 200.

Tafforeau, P., Bentaleb, I., Jaeger, J-J. and Martin, C., 2007. Nature of laminations and mineralization in rhinoceros enamel using histology and X-ray synchrotron microtomography: Potential implications for palaeoenvironmental isotopic studies. *Palaeogeography, Palaeoclimatology, Palaeoecology*. **246**: 206–227.

Talbot, S.L. and Shields, G.F., 1996a. Phylogeography of brown bears (Ursus arctos) of Alaska and paraphyly within the Ursidae. *Molecular Phylogenetics and Evolution*. **5**: 477-494.

Talbot, S.L. and Shields, G.F., 1996b. A phylogeny of the bears (Ursidae) inferred from complete sequences of three mitochondrial genes. *Molecular Phylogenetics and Evolution.* **5**: 567-575.

Teaford, M.F. and Glander, K.E. 1991. Dental microwear in live, wild-trapped *Alouatta palliata* from Costa Rica. *American Journal of Physical Antropology*. **85**: 313–319.

Teaford, M. F. and Robinson, J. G., 1989. Seasonal or ecological differences in diet and molar microwear in *Cebus nigrivittutus*. *American Journal of Physical Anthropology*. **80**:391-401.

Teaford, M. and Walker, A., 1984. Quantitative differences in dental microwear between primate species with different diets and a comment on the presumed diet of Sivapithecus. *American Journal of Physical Anthropology*. **64**: 191-200.

Todd, N. E., Falco, N., Silva, N. and Sanchez, C., 2007. Dental microwear variation in complete molars of *Loxodonta africana* and *Elephas maximus. Quaternary International*. **169–170**: 192–202.

Torres Pérez-Hidalgo, T., 1988. Osos (Mammalia, Carnivora, Ursidae) del Pleistoceno Ibérico: I. Filogenia; Distribución estratigráfica y geográfica. Estudio anatómico y métrico del cráneo [Bears (Mammalia, Carnivora, Ursidae) from Pleistocene of the Iberian peninsula: I. Phylogeny; Stratigraphical and geographical distribution; Morphometrical studies on the skull]. *Boletín Geológico y Minero* **99**: 3-46. [In Spanish.]

Torres Pérez-Hidalgo, T., 1992. The European descendants of *Ursus etruscus* C. Cuvier (Mammalia, Carnivora, Ursidae). *Boletín Geológico y Minero.* **103**: 12–22.

Trautz, O. R., 1967. Crystalline organization of dental mineral. In A.E.D. Miles (Eds.) Structural and Chemical Organization of Teeth. Academic Press, London. **2**: 165-200.

Trueman, C.N. and Tuross, N., 2002. Trace elements in recent and fossil bone apatite. *Reviews in Mineralogy and Geochemistry*. **48:** 489-521.

Tseng, Z. J., 2011. Variations and implications of intra-dentition Hunter Schreger band pattern in fossil hyaenids and canids (Carnivora, Mammalia). *Journal of Vertebrate Paleontology.* **31**: 1163–1167.

Tseng, Z. J., 2012. Connecting Hunter-Schreger Band Microstructure to Enamel Microwear Features: New Insights from Durophagous Carnivores. *Acta Palaeontologica Polonica*. **57**(3):473-484.

Tsoukala, E., 1991: Contribution to the study of the Pleistocene fauna of large mammals (Carnivora, Perissodactyla, Artiodactyla) from Petralona Cave (Chalkidiki, N. Greece). Preliminary report. – *Comptes Rendus de l'Académie des Sciences. Série II, Mecanique, Physique, Chimie, Sciences de la Terre, Sciences de l'Univers*. **312**: 331-336.

Tsoukala, E., 1994. Bärenreste aus Loutraki (Mazedonien, Griechenland)-"*Ursus spelaeus*". -2nd Höhlenbären Symposium (Corvara, 15-18 September), Italy.

Tsoukala, E., 2006. Paleontological research and excavations - Cave-bears and Late Pleistocene associated fauna. In: A Guide to Almopia Speleopark- Geology-Paleontology-Speleology, edit. Municipality of Aridea, Greece, 62-81 and 104-105.

Tsoukala, E. and Rabeder, G., 2005. Cave bears and Late Pleistocene associated faunal remains from Loutra Arideas (Pella, Macedonia, Greece). 15 years of research. -In: Neue Forschungen zum Höhlenbären in Europa. *Abhandlung Band, Naturhistorische Gesellschaft Nürnberg.* **45**: 225-236.

Tsoukala, E., Rabeder, G. and Verginis, S., 1998. *Ursus spelaeus* and associated faunal remains from Loutraki (Pella, Macedonia, Greece) - Excavations of 1996. Geological and geomorphological approach". -4th International Höhlenbären - Symposium, 17-19 September, Velenje, Slovenia.

Tsoukala E., Rabeder, G. and Verginis, S., 2001. *Ursus spelaeus* and Late Pleistocene associated faunal remains from Loutraki (Pella, Macedonia, Greece) - Excavations of 1999. -*Cadernos Lab. Xeolóxico de Laxe*. **26:** 441-446.

Tsoukala, E., Chatzopoulou, K., Rabeder, G., Pappa, S., Nagel, D. and Withalm, G., 2006. «Paleontological and stratigraphical research in Loutra Arideas bear cave

(Almopia Speleopark, Pella, Macedonia, Greece)».- Proceedings of the 12th International Cave bear Symposium, Thessaloniki/ Aridea, 2-5 November 2006. *Scientific Annals*, school of Geology, Aristotle University, Thessaloniki. **98**: 41-67.

Turner, A., 1999. Large Carnivores (Mammalia, Carnivora) from Westbury Cave. pp 175-193 in: Andrews, P., Cook, J., Currant., A. and Stringer, C. (Eds.), *Westbury Cave. The Natural History Museum Excavations 1976 - 1984*. Western Academic & Specialist Press, Bristol. p. 309.

Turner, A., 2009. The evolution of the guild of large Carnivora of the British Isles during the Middle and Late Pleistocene. *Journal of Quaternary Science.* **24**: 991–1005.

Turner, A. and Antón, M., 1997. The Big Cats and their Fossil Relatives. Columbia University Press: New York.

Turner, A. and Antón, M., 2004. Evolving Eden: An Illustrated Guide to the Evolution of the African Large-Mammal Fauna. Columbia University Press: New York.

Turner, E., 2000. Miesenheim I. Excavations at a Lower Palaeolithic site in the Central Rhineland of Germany.*Monographien des Römisch-Germanischen Zentralmuseums.* **44**: 1-151.

Turner-Walker G., 2008. The Chemical and Microbial Degradation of Bones and Teeth . New York: Wiley. p. 389.

Ungar, P.S., 1996. Dental microwear of European Miocene catarrhines: evidence for diets and tooth use. *Journal of Human Evolution*. **31**: 335–366.

Ungar, P.S., 2010. Mammal Teeth: Origin, Evolution, and Diversity, Johns Hopkins University Press, Baltimore, USA.

Ungar, P. S., 2015. Mammalian dental function and wear: A review. *Biosurface and Biotribology*. **1**: 25–41.

Ungar, P. S., and Lucas, P. W., 2010. Tooth Form and Function in Biological Anthropology, in A Companion to Biological Anthropology (ed C. S. Larsen), Wiley-Blackwell, Oxford, UK.

Ungar, P. S. and Teaford, M. F., 1996. A preliminary examination of non-occlusal dental microwear in anthropoids: Implications for the study of fossil primates. *American Journal of Physical Anthropology.* **100**: 101–113.

Ungar, P. S., Simons, J. C. and Cooper , J. V., 1991. A semiautomated image analyses procedure for the quantification of dental microwear. *Scanning.* **13**: 31-36.

Ungar, P. S., Brown, C. A., Bergstrom, T. S. and Walker, A. 2003. Quantification of Dental Microwear by Tandem Scanning Confocal Microscopy and Scale-Sensitive Fractal Analyses. *Scanning*. **25**: 185–193.

Ungar, P. S., Scott, J. R., Schubert, B. W. and Stynder, D. D., 2010. Carnivoran dental microwear textures: comparability of carnassial facets and functional differentiation of postcanine teeth. *Mammalia*. **74**: 219-224.

Valdiosera, C. E., Garcia-Garitagoitia, J. L., Garcia, N., Doadrio, I., Thomas, M. G., Hänni, C., Arsuaga, J-L., Barnes, I., Hofreiter, M., Orlando, L. and Götherström, A., 2008. Surprising migration and population size dynamics in ancient Iberian brown bears (*Ursus arctos*). *Proceedings of the National Academy of Sciences of USA*. **105**: 5123-5128.

Valli, A. M. F. and Palombo, M.R., 2008. Feeding behaviour of middle-size deer from the Upper Pliocene site of Saint-Vallier (France) inferred by morphological and micro/mesowear analysis. *Palaeogeography, Palaeoclimatology, Palaeoecology.* **257**: 106–122.

Van Horn, R. C., Mcelhinny, T. L. and Holekamp, K. E., 2003. Age estimation and dispersal in the spotted hyena (*Crocuta crocuta*). *Journal of Mammalogy.* **84** (3):1019–1030.

Van Valkenburgh, B. and Hertel, F. 1993. Tough Times at La Brea: Tooth Breakage in Large Carnivores of the Late Pleistocene. *Science*. **261** (5120): 456-459.

Van Valkenburgh, B., Teaford, M. F. and Walker, A., 1990. Molar microwear and diet in large carnivores: inferences concerning diet in the sabretooth cat, Smilodon fatalis. *Journal of Zoology, London*. **222**: 319-340.

Vereshchagin, N. K. and Baryshnikov, G. F., 1983. Quaternary Mammalian Extinctions in Northern Eurasia. In Martin, P. J. & Klein, R. G. (Eds.): Quaternary Extinctions, 483–517. University of Arizona Press, Tucson.

Vila Taboada, M., Fernández Mosquera, D. and Grandal d'Anglade, A., 2001. Cave bear's diet: A new hypothesis based on stable isotopes. *Cadernos do Laboratorio Xeolóxico de Laxe*. **26**: 431–439.

Vlachos, C. G., Bakaloudis, D. E., Dimitriou, M., Kritikou, K. and Chouvardas, D., 2000. Seasonal food habits of the European brown bear (*Ursus arctos*) in the Pindos Mountains, Western Greece. *Folia Zoo*. **49**(1): 19-25.

Vulla, E., Hobson, K. A., Korsten, M., Leht, M., Martin, A-J., Lind, A., Männil, P., Valdmann, H. and Saarma, U., 2009. Carnivory is positively correlated with latitude among omnivorous mammals: evidence from brown bears, badgers and pine martens. *Annales Zoologici Fennici*. **46**: 395–415.

Wagner, J. 2010. Pliocene to early Middle Pleistocene ursine bears in Europe: a taxonomic overview. *Journal of the National Museum (Prague), Natural History Series* **179**(20): 197–215.

Wagner, J. and Čermák, S., 2012. Revision of the early Middle Pleistocene bears (Ursidae, Mammalia) of Central Europe, with special respect to possible co-occurrence of spelaeoid and arctoid lineages. *Bulletin of Geosciences.* **87**(3): 461–496.

Waits, L. P., Sullivan, J., O'Brien, S. J. and Ward, R. H., 1999. Rapid radiation events in the family Ursidae indicated by likelihood phylogenetic estimation from multiple fragments of mtDNA. *Molecular Phylogenetics and Evolution.* **13**: 82–92.

Williams, F.L. and Geissler, E., 2014. Reconstructing the Diet and palecology of Plio-Pleistocene *Cercopithecoides williamsi* from Sterkfontein, South Africa. *Palaios*. **29**: 483-494.

Walker, A., Hoeck, H. N. and Perez, L., 1978. Microwear of mammalian teeth as an indicator of diet. *Science*. **201**: 908-910.

Walker, M. and Lowe, J., 2007. Quaternary science 2007: a 50-year retrospective. *Journal of Geological Society*. **164**: 1073-1092.

Wang, Y. and Cerling, T.E., 1994. A model of fossil tooth and bone diagenesis: implications for paleodiet reconstruction from stable isotopes. *Palaeogeography, Palaeoclimatology, Palaeoecology.* **107**: 281-289.

Weinstock, J., 2000. Cave bears from southern Germany: Sex ratios and age structure. A contribution towards a better understanding of the paleobiology of *Ursus spelaeus*. *Archaeofauna*. **9**: 165–182.

Werdelin, L. and Solounias, N., 1991. The Hyaenidae: Taxonomy, systematics and evolution. *Fossils and Strata*. **30**: 1-104.

Wiig, Ø., Amstrup, S., Atwood, T., Laidre, K., Lunn, N., Obbard, M., Regehr, E. and Thiemann, G., 2015. *Ursus maritimus*. The IUCN Red List of Threatened Species 2015: e.T22823A14871490. http://dx.doi.org/10.2305/IUCN.UK.2015-4.RLTS.T22823A14871490.en. Downloaded on **08 December 2015**.

Williams, V. S., Barrett, P. M. and Purnell, M. A., 2009. Quantitative analysis of dental microwear in hadrosaurid dinosaurs, and the implications for hypotheses of jaw mechanics and feeding. *Proceedings of the National Academy of Sciences*. **106** (27): 11194–11199.

Wilson, D. E. and Reeder D. M., 2005. Mammal Species of the World. A Taxonomic and Geographic Reference (3rd Eds), Johns Hopkins University Press. **2**. p.142.

Wright, W., Sanson, G. D. and MacArthur, C., 1991. The diet of the extinct bandicoot Chaeropus ecaudatus. p. 229-245 In Rich, P. V., Monaghan, J. M., Baird, R. F. and Rich, T. H., (Eds.) Vertebrate Palaeontology of Australasia. Monash University Publications Committee, Melbourne, Australia.

Yalden, D., 1999. The History of British Mammals. London: Poyser Natural History.

Yeoh, H.-H., Badger, M. R. and Watson, L., 1981. Variations in kinetic properties of Ribulose-1,5-bisphosphate carboxylases among plants. *Plant Physiology*. **67**: 1151–1155.

Young, J. Z., 1975. The life of Mammals. Oxford University Press.

Yu, L., Li, Y. W., Ryder, O. A. and Zhang, Y. P., 2007 Analysis of complete mitochondrial genome sequences increases phylogenetic resolution of bears (Ursidae), a mammalian family that experienced rapid speciation. *BMC Evolutionary Biology.* **7**: 198.

Zacharias, N., Kabouroglou, E., Bassiakos, Y. and Michael, C.T., 2008. Dating and analysis of speleosediments from Aridaia at Macedonia, Greece. - *Radiation Measurements*. **43**: 791-796.

Zachos, J., Pagani, M., Sloan, L., Thomas, E., and Billups, K., 2001. Trends, rhythms, and aberrations in global climate 65 Ma to present. *Science*. **292**: 686–693.

Zazzo, A., Balasse, M. and Patterson, W. P., 2005. High-resolution $\delta^{13}C$ intratooth profiles in bovine enamel: Implications for mineralization pattern and isotopic attenuation. *Geochimica et Cosmochimica Acta*. **69** (14): 3631-3642.

Zazzo, A., Mariotti, A., Lécuyer, C. and Heintz, E., 2002. Intra-tooth isotope variations in late Miocene bovid enamel from Afghanistan: paleobiological, taphonomic, and climatic implications. *Palaeogeography, Palaeoclimatology, Palaeoecology***. 186** (1–2): 145-161.

Zazzo, A., Lécuyer, C., Sheppard, S. M. F., Grandjean, P. and Mariotti, A., 2004b. Diagenesis and the reconstruction of paleoenvironments: A method to restore original $\delta^{18}O$ values of carbonate and phosphate from fossil tooth enamel. *Geochimica et Cosmochimica Acta*. **68** (10): 2245-2258.

Zazzo, A., Balasse, M., Passey, B. H., Moloney, A. P., Monahan, F. J. and Schmidt, O., 2010. The isotope record of short- and long-term dietary changes in sheep tooth enamel: Implications for quantitative reconstruction of paleodiets. *Geochimica et Cosmochimica Acta.* **74**: 3571–3586.

Appendix IA. Dental Microwear Analysis

Table 1. Microwear features raw results for extant bear species on the grinding area. Abbreviations for museums: NHMV: the Natural History Museum in Vienna, Austria; NHMP: the Natural History Museum in Paris, France (Department of Comparative Anatomy); NHMB: the Natural History Museum in Berlin, Germany; AUThG: the Aristotle University of Thessaloniki (Geology Department), Greece and AUThW: Aristotle University of Thessaloniki (Laboratory of Wildlife and freshwater Fisheries of the School of Forestry and Natural Environment), Greece. Abbreviations for features: S: Scratches; P: Pits; Fs: Fine scratches; Cs: Coarse scratches; SWS: Scratches width score; Lp: Large pits; Sp: Small pits; G: gouges and Pp: puncture pits.

Museum code	Species	Number	S	P	Fs	Cs	SWS	Lp	Sp	G	Pp
ZMB	*A. melanoleuca*	17246	21	62	21	0	0	9	53	0	0
ZMB	*A. melanoleuca*	17246	17	61	17	0	0	8	44	0	0
ZMB	*A. melanoleuca*	17542	19	56	19	0	0	9	47	0	0
ZMB	*A. melanoleuca*	85761	20	49	20	0	0	8	41	0	0
NHMP	*H. malayanus*	1899-193	22	10	21	1	1	2	8	0	0
NHMP	*H. malayanus*	1913-505	22	28	21	1	1	6	19	0	3
NHMP	*H. malayanus*	1913-72	26	30	25	1	1	4	24	0	2
NHMP	*H. malayanus*	1932-3197	19	25	19	0	0	2	23	0	0
NHMP	*H. malayanus*	1901.652	21	28	19	2	1	3	22	0	3
NHMP	*H. malayanus*	1919-62	17	27	16	1	1	8	14	0	5
NHMP	*H. malayanus*	A2132	19	20	17	2	1	5	12	0	3
NHMP	*H. malayanus*	1971-188	19	22	16	3	1	3	19	0	0
ZMB	*H. malayanus*,Thailand	17531	17	24	16	1	1	5	19	0	0
ZMB	*H. malayanus*,Borneo	17245	26	29	22	4	1	3	23	0	3
ZMB	*H. malayanus,*Thailand	105707	19	28	15	4	1	5	21	0	2
ZMB	*H. malayanus*, Sumatra	28472	17	32	15	2	1	6	24	0	2
ZMB	*H. malayanus*,Thailand	17533	18	23	17	1	1	6	14	0	3
ZMB	*H. malayanus*,Thailand	17533	15	26	13	2	1	8	14	1	4
ZMB	*H. malayanus*,Thailand	34002	20	30	15	5	1	9	21	0	3
ZMB	*H. malayanus*, Sumatra	85771	17	25	13	4	1	5	15	2	3
ZMB	*H. malayanus*,Thailand	17532	18	30	14	4	1	7	23	0	0
NHMP	*M. ursinus*	1883-59	14	37	12	2	1	9	23	2	3
ZMB	*M. ursinus*, Kaulas, India	44144	16	34	12	4	1	7	19	2	6
ZMB	*M. ursinus*, Japan	56748	18	32	15	3	1	9	18	3	2
ZMB	*M. ursinus*, Kaulas, India	44143	16	44	12	4	1	14	21	3	6
NHMP	*T. ornatus*	1848-	16	27	13	3	1	6	19	0	2

		369									
ZMB	*T. ornatus*, Venezouela	6121	16	30	13	3	1	8	18	0	4
NHMV	*U. americanus*, Alaska	63555	15	29	12	3	1	3	24	0	2
NHMV	*U. americanus*, Alaska	64947	14	20	11	3	1	4	13	0	3
NHMV	*U. americanus*, Alaska	8269	18	36	16	2	1	7	24	0	5
NHMV	*U. americanus*, Alaska	8273	16	22	14	2	1	8	12	0	2
NHMV	*U. americanus*, Alaska	8271	17	28	14	3	1	5	20	0	3
NHMV	*U. americanus*, Alaska	8270	17	37	14	3	1	4	30	0	3
NHMV	*U. americanus*, Alaska	8272	15	25	13	2	1	4	19	0	2
NHMV	*U. americanus*, Alaska	8274	19	29	17	2	1	9	15	0	5
NHMV	*U. americanus*, Alaska	8275	14	21	11	3	1	5	14	0	2
NHMV	*U. maritimus*	7140	14	29	14	0	0	4	24	1	0
NHMV	*U. maritimus*	13176	18	23	12	2	3	6	16	0	1
NHMV	*U. maritimus*	7150	19	23	13	2	3	2	18	0	0
NHMV	*U. maritimus*	7139	14	21	8	2	3	2	19	0	0
NHMV	*U. maritimus*	7149	12	17	8	3	3	3	14	0	0
NHMV	*U. maritimus*	7141	19	23	16	3	3	8	15	0	0
NHMV	*U. maritimus*	7148	14	15	9	3	3	3	12	0	0
NHMV	*U. maritimus*	7143	16	22	10	4	3	6	16	0	0
NHMV	*U. maritimus*	14657	16	25	9	6	3	5	20	0	0
NHMV	*U. maritimus*	7794	15	19	11	3	3	6	13	0	0
NHMV	*U. maritimus*	7144	19	23	11	5	3	6	17	0	0
NHMV	*U. maritimus*	7142	17	18	12	2	3	4	14	0	0
NHMV	*U. maritimus*	7147	23	16	16	5	3	4	14	0	0
NHMV	*U. maritimus*	7138	12	19	5	5	3	4	15	0	0
NHMP	*U. thibetanus*	2006-415	17	20	14	3	1	4	16	0	0
ZMB	*U. thibetanus*, Japan	56747	20	22	16	4	1	6	16	0	0
ZMB	*U. thibetanus*, Japan	69401	15	20	12	3	1	5	14	1	0
ZMB	*U. thibetanus*, Thibet	24592	17	18	14	3	1	3	15	0	0
ZMB	*U. thibetanus*, Japan	69400	19	21	15	4	1	5	14	2	0
ZMB	*U. thibetanus*, Thibet	69396	18	21	15	3	1	4	17	0	0
AUThG	*U. arctos*, Greece	Skull 1	22	25	18	4	1	12	11	2	0
AUThG	*U. arctos*, Greece	Skull 1	21	17	14	7	1	8	7	2	0
AUThW	*U. arctos*, Greece	Skull 2	15	17	6	9	1	7	9	1	0
AUThW	*U. arctos*, Greece	Skull 3	22	21	14	8	1	10	7	3	1
NHMV	*U. arctos*, Slovakia, central EU	52	17	27	14	3	1	4	10	3	10
NHMV	*U. arctos*, Ukraine,	21491	16	29	13	3	1	6	16	2	5

	central EU										
NHMV	U. arctos, Slovakia, central EU	51	21	45	18	3	1	5	32	2	6
NHMV	U. arctos, central EU	7146	23	44	18	5	1	6	29	2	7
NHMV	U. arctos, Romania, central EU	67919	23	39	18	5	1	6	24	3	6
NHMV	U. arctos (Europe)	4220	24	46	21	3	1	5	32	3	6
NHMV	U. arctos, Bosnia, central EU	7396	21	39	16	5	1	6	24	3	6
NHMV	U. arctos, Bulgaria, central EU	55276	20	34	18	2	1	7	19	1	7
NHMV	U. arctos, Slovenia, central EU	67301	18	34	15	3	1	5	21	2	6
NHMV	U. arctos, Romania, central EU	46465	26	25	24	2	1	4	18	0	2
NHMV	U. arctos, Canada, N. America	7793	13	28	11	2	1	11	8	2	7
ZMB	U. arctos, America	87110	16	25	11	5	1	7	15	0	3
ZMB	U. arctos, America	87110	22	23	16	6	1	8	13	0	2
ZMB	U. arctos, Middle Creek, USA	43592	25	37	23	2	1	5	29	0	3
ZMB	U. arctos, Alaska, N. America	37701	26	25	24	2	1	4	20	0	0
ZMB	U. arctos, Alaska, N. America	43593	26	32	23	3	1	6	23	0	3
ZMB	U. arctos, Alaska	87132	23	33	21	2	1	8	23	0	2
ZMB	U. arctos, Alaska, N. America	69342	19	24	17	2	1	5	16	0	3
NHMV	U. arctos,Kamtchatka, Russia	40624	14	35	12	2	1	6	26	0	3
NHMV	U. arctos,Kamtchatka, Russia	40633	19	40	15	4	1	11	25	0	4
NHMV	U. arctos,Kamtchatka, Russia	40635	19	32	15	4	1	6	24	0	2
NHMV	U. arctos,Kamtchatka, Russia	40608	27	30	23	4	1	4	14	1	11
NHMV	U. arctos,Kamtchatka, Russia	40607	25	34	21	4	1	5	24	0	5
NHMV	U. arctos,Kamtchatka, Russia	40613	20	29	17	3	1	4	20	0	5
NHMV	U. arctos,Kamtchatka, Russia	40625	21	30	18	3	1	10	14	1	5
NHMV	U. arctos,Kamtchatka, Russia	40616	22	29	19	3	1	5	17	0	7
NHMV	U. arctos,Kamtchatka, Russia	40628	24	36	21	3	1	10	17	0	9
NHMV	U. arctos,Kamtchatka, Russia	40615	18	29	14	4	1	11	12	0	6
NHMV	U.	40611	24	30	20	4	3	7	16	3	4

	arctos,Kamtchatka, Russia										
NHMV	U. arctos,Kamtchatka, Russia	40645	19	29	15	4	1	4	23	0	2
NHMV	U. arctos,Kamtchatka, Russia	40640	19	34	13	6	1	4	25	0	5
NHMV	U. arctos,Kamtchatka, Russia	40636	17	25	15	2	1	4	17	0	4
NHMV	U. arctos,Kamtchatka, Russia	40630	18	35	14	4	1	7	26	0	2
NHMV	U. arctos,Kamtchatka, Russia	40609	19	27	16	2	1	8	19	1	6
NHMV	U. arctos,Kamtchatka, Russia	40648	18	28	14	4	1	7	18	0	3
NHMV	U. arctos,Kamtchatka, Russia	40634	26	39	23	3	1	10	21	0	8
NHMV	U. arctos,Kamtchatka, Russia	40643	21	18	16	5	1	5	10	1	2
NHMV	U. arctos,Kamtchatka, Russia	40605	19	33	13	7	1	11	10	1	12
NHMV	U. arctos,Kamtchatka, Russia	40626	21	37	16	5	1	5	32	0	0
NHMV	U. arctos,Kamtchatka, Russia	40642	14	29	10	4	1	9	20	0	0
NHMV	U. arctos,Kamtchatka, Russia	40638	17	37	13	4	1	7	25	0	5
ZMB	U. arctos, Lithuania, N. Europe	14425	28	32	23	5	1	7	24	0	2
ZMB	U. arctos, Lithuania, N. Europe	14414	16	30	12	4	1	7	20	0	3
ZMB	U. arctos, Lithuania, N. Europe	14423	24	41	20	4	1	7	30	1	3
ZMB	U. arctos, Lithuania, N. Europe	14422	18	28	15	3	1	4	23	0	1
ZMB	U. arctos, Lithuania, N. Europe	14404	17	38	14	3	1	6	28	1	3
ZMB	U. arctos, Lithuania, N. Europe	14408	18	24	15	3	1	5	17	0	2
ZMB	U. arctos, Lithuania, N. Europe	14403	17	28	14	3	1	6	20	0	2
ZMB	U. arctos, Lithuania, N. Europe	14402	19	39	15	4	1	7	27	0	5
ZMB	U. arctos, Finland, N. Europe	93300	19	32	14	5	1	9	21	0	3

Table 2. Microwear features raw results for extant bear species on the slicing area. Abbreviations for museums as following: NHMV: the Natural History Museum in Vienna, Austria; NHMP: the Natural History Museum in Paris, France (Department of Comparative Anatomy); NHMB: the Natural History Museum in Berlin, Germany; AUThG: the Aristotle University of Thessaloniki (Geology Department), Greece and AUThW: Aristotle University of Thessaloniki (Laboratory of Wildlife and freshwater Fisheries of the School of Forestry and Natural Environment), Greece. Abbreviations for Features: S: Scratches; P: Pits; Fs: Fine scratches; Cs: Coarse scratches; SWS: Scratches width score; Lp: Large pits; Sp: Small pits; G: gouges and Pp: puncture pits.

Museum code	Species	Number	S	P	Fs	Cs	SWS	Lp	Sp	G	Pp
ZMB	A. melanoleuca	17246	17	62	17	0	0	11	51	0	0
ZMB	A. melanoleuca	17542	20	58	20	0	0	11	47	0	0
ZMB	A. melanoleuca	85761	19	40	19	0	0	6	34	0	0
NHMP	H. malayanus	1899-193	21	25	20	1	1	5	18	0	2
NHMP	H. malayanus	1913-505	20	26	19	1	1	4	20	0	2
NHMP	H. malayanus	1913-72	19	34	18	1	1	5	25	0	4
NHMP	H. malayanus	1932-3197	19	26	17	2	1	8	15	0	3
NHMP	H. malayanus	1901.65	20	29	17	3	1	5	20	0	4
NHMP	H. malayanus	1919-62	22	22	22	0	0	7	13	0	2
NHMP	H. malayanus	A2132	19	25	18	1	1	7	16	0	2
ZMB	H. malayanus,Borneo	17425	16	25	12	4	1	4	21	0	0
ZMB	H. malayanus,Thailand	105707	19	25	17	2	1	4	18	0	3
ZMB	H. malayanus,Thailand	34002	22	23	18	4	1	4	16	0	3
ZMB	H. malayanus, Sumatra	85771	15	26	10	5	1	9	17	0	0
NHMP	M. ursinus	1883-59	16	44	11	5	1	4	34	2	4
ZMB	M. ursinus, Kaulas, India	44144	14	25	9	5	1	6	18	0	1
ZMB	M. ursinus, Japan	56748	17	38	14	3	1	11	19	1	7
ZMB	M. ursinus, Kaulas, India	44143	11	25	8	3	1	8	15	0	2
ZMB	T. ornatus, Venezouela	6121	13	17	10	3	1	3	14	0	0
NHMV	U. americanus, Alaska	63555	13	29	13	0	0	4	22	0	3
NHMV	U. americanus, Alaska	64947	20	25	14	6	1	7	16	0	2
NHMV	U. americanus, Alaska	8269	18	32	15	3	1	4	23	0	5

NHMV	U. americanus, Alaska	8273	15	30	14	1	1	4	20	0	6
NHMV	U. americanus, Alaska	8271	18	34	16	2	1	5	25	0	4
NHMV	U. americanus, Alaska	8270	18	25	16	2	1	3	20	0	2
NHMV	U. americanus, Alaska	8272	16	26	14	2	1	7	16	0	3
NHMV	U. americanus, Alaska	8274	19	25	15	4	1	8	12	0	5
NHMV	U. americanus, Alaska	8275	17	19	15	2	1	4	13	0	2
NHMV	U. maritimus	7140	13	29	10	1	3	6	23	0	0
NHMV	U. maritimus	13176	19	23	13	1	3	6	11	0	6
NHMV	U. maritimus	7150	18	15	12	3	3	2	13	0	0
NHMV	U. maritimus	7139	15	16	9	4	3	3	13	0	0
NHMV	U. maritimus	7149	19	16	13	4	3	5	11	0	0
NHMV	U. maritimus	7148	15	19	10	5	1	2	17	0	0
NHMV	U. maritimus	7143	20	15	13	7	3	4	11	0	0
NHMV	U. maritimus	14657	14	21	10	3	3	6	15	0	0
NHMV	U. maritimus	7145	12	44	9	3	1	10	31	0	3
NHMV	U. maritimus	7794	15	13	8	5	3	7	6	0	0
NHMV	U. maritimus	7144	13	19	6	5	3	5	14	0	0
NHMV	U. maritimus	7142	18	23	11	5	3	8	15	0	0
NHMV	U. maritimus	7147	19	12	15	4	1	2	10	0	0
NHMV	U. maritimus	7138	17	20	13	3	3	5	15	0	0
NHMP	U. thibetanus	2006-415	17	22	19	3	1	4	14	1	3
ZMB	U. thibetanus, Japan	69401	15	19	11	4	1	3	13	0	0
ZMB	U. thibetanus, Japan	69400	13	21	11	2	1	7	14	0	0
ZMB	U. thibetanus, Thibet	69396	15	25	13	2	1	7	17	1	0
AUThG	U. arctos, Greece	Skull 1	27	16	19	8	1	4	12	0	0
AUThW	U. arctos, Greece	Skull 2	20	14	13	7	1	4	9	1	0
AUThW	U. arctos, Greece	Skull 3	22	17	13	9	1	9	6	2	0
AUThW	U. arctos, Greece	Skull 5	20	17	13	7	1	4	13	0	0

NHMV	U. arctos, Ukraine, central EU	21491	21	32	19	2	1	2	24	0	6
NHMV	U. arctos, Slovakia, central EU	51	15	41	12	3	1	5	24	3	9
NHMV	U. arctos, central EU	7146	15	31	7	8	1	11	18	0	2
NHMV	U. arctos, Romania, central EU	67919	17	35	13	4	1	7	20	4	4
NHMV	U. arctos (Europe)	4220	15	35	12	3	1	7	23	1	4
NHMV	U. arctos, Bosnia, central EU	7396	14	41	12	2	1	5	25	3	8
NHMV	U. arctos, Bulgaria, central EU	55276	23	37	18	5	1	6	21	3	7
NHMV	U. arctos, Slovenia, central EU	67301	24	39	19	5	1	3	27	1	8
NHMV	U. arctos, Canada, N. America	7793	17	28	15	2	1	6	17	1	4
ZMB	U. arctos, America	87110	22	36	16	6	1	8	27	0	1
ZMB	U. arctos, Canada, N. America	43594	17	27	12	5	1	9	16	0	2
NHMV	U. arctos,Kamtchatka, Russia	40650	17	29	13	4	1	6	21	0	2
NHMV	U. arctos,Kamtchatka, Russia	40624	19	25	15	4	1	9	15	0	1
NHMV	U. arctos,Kamtchatka, Russia	40633	16	35	12	4	1	11	18	0	6
NHMV	U. arctos,Kamtchatka, Russia	40635	17	31	12	5	1	6	21	0	4
NHMV	U. arctos,Kamtchatka, Russia	40608	20	36	17	3	1	10	22	0	4
NHMV	U. arctos,Kamtchatka, Russia	40607	24	24	18	6	1	6	10	2	6
NHMV	U. arctos,Kamtchatka, Russia	40613	15	39	13	2	1	10	24	2	3
NHMV	U. arctos,Kamtchatka, Russia	40616	18	20	13	5	1	5	10	0	5

NHMV	U. arctos,Kamtchatka, Russia	40649	24	39	20	4	1	19	9	1	10
NHMV	U. arctos,Kamtchatka, Russia	40628	34	26	26	8	1	12	3	1	10
NHMV	U. arctos,Kamtchatka, Russia	40615	15	19	11	4	1	8	11	0	0
NHMV	U. arctos,Kamtchatka, Russia	40611	23	27	18	5	1	6	14	2	5
NHMV	U. arctos,Kamtchatka, Russia	40645	15	30	11	4	1	4	24	0	2
NHMV	U. arctos,Kamtchatka, Russia	40640	16	29	12	4	1	5	23	0	1
NHMV	U. arctos,Kamtchatka, Russia	40636	18	30	14	4	1	4	26	0	0
NHMV	U. arctos,Kamtchatka, Russia	40630	15	28	9	6	1	5	19	1	3
NHMV	U. arctos,Kamtchatka, Russia	40609	14	29	12	2	1	2	24	0	2
NHMV	U. arctos,Kamtchatka, Russia	40644	14	28	11	5	1	14	12	0	2
NHMV	U. arctos,Kamtchatka, Russia	40634	28	38	22	6	1	18	2	2	16
NHMV	U. arctos,Kamtchatka, Russia	40605	27	34	15	12	1	8	18	4	4
NHMV	U. arctos,Kamtchatka, Russia	40626	15	29	11	4	1	8	17	1	3

Appendix IB. Dental Microwear Analysis

Table 1. Dental microwear PCA score results for extant bear species on grinding area.

Species	PC 1	PC 2	PC 3	PC 4	PC 5	PC 6	PC 7	PC 8	PC 9
A. melanoleuca	-0.202	-0.685	0.471	-0.062	0.124	0.034	0.032	-0.033	0.011
A. melanoleuca	-0.238	-0.627	0.391	-0.085	0.154	0.017	-0.071	-0.076	-0.016
A. melanoleuca	-0.223	-0.640	0.423	-0.103	0.132	0.018	-0.008	-0.023	0.004
A. melanoleuca	-0.247	-0.615	0.346	-0.105	0.084	0.033	0.019	-0.018	0.008
H. malayanus	-0.581	-0.242	-0.597	-0.177	-0.342	0.140	0.077	0.043	0.027
H. malayanus	0.076	-0.433	-0.162	-0.175	0.002	0.001	0.096	0.014	0.034
H. malayanus	-0.094	-0.529	-0.122	-0.008	-0.085	0.087	0.128	-0.009	0.039
H. malayanus	-0.474	-0.504	-0.227	0.118	-0.136	0.148	-0.072	-0.032	-0.006
H. malayanus	0.034	-0.240	-0.201	0.180	-0.095	0.031	0.001	-0.011	0.000
H. malayanus	0.269	-0.319	-0.263	-0.323	0.109	-0.091	0.011	0.003	0.016
H. malayanus	0.029	-0.061	-0.266	-0.136	-0.102	-0.044	0.039	0.014	-0.002
H. malayanus	-0.408	-0.041	-0.034	0.141	-0.208	0.043	-0.050	0.000	-0.014
H. malayanus,Thailand	-0.401	-0.401	-0.060	-0.204	-0.033	0.035	-0.051	0.015	0.012
H. malayanus,Borneo	0.085	-0.035	-0.074	0.329	-0.205	0.025	0.096	-0.016	-0.003
H. malayanus,Thailand	-0.054	0.056	0.075	0.116	-0.100	-0.054	-0.028	0.006	-0.007
H. malayanus, Sumatra	-0.054	-0.208	0.064	-0.027	0.021	-0.046	-0.060	0.008	-0.006
H. malayanus,Thailand	0.032	-0.331	-0.270	-0.271	0.016	-0.032	0.018	0.015	0.019
H. malayanus,Thailand	0.197	-0.052	-0.138	-0.222	0.069	-0.134	-0.061	0.009	-0.010
H. malayanus,Thailand	0.181	0.156	0.193	0.012	-0.040	-0.139	0.038	0.044	0.010
H. malayanus, Sumatra	0.116	0.203	-0.063	-0.003	-0.045	0.185	-0.116	0.015	-0.002
H. malayanus,Thailand	-0.281	0.050	0.301	0.005	-0.088	-0.060	-0.040	0.006	-0.008
M. ursinus	0.184	-0.108	0.125	-0.185	0.183	0.148	-0.178	0.030	-0.003
M. ursinus, Kaulas, India	0.447	0.165	-0.001	0.004	0.102	0.114	-0.141	0.015	0.003
M. ursinus, Japan	0.072	0.083	0.207	-0.209	0.031	0.343	-0.068	0.026	0.001
M. ursinus, Kaulas, India	0.572	0.185	0.247	-0.185	0.213	0.214	-0.124	0.025	0.010
T. ornatus	-0.067	0.007	0.041	-0.025	-0.024	-0.082	-0.087	0.013	-0.011
T. ornatus, Venezouela	0.238	0.027	0.000	-0.079	0.056	-0.144	-0.059	0.014	-0.008
U. americanus, Alaska	-0.131	-0.062	-0.069	0.231	-0.040	-0.020	-0.198	-0.018	-0.019
U. americanus, Alaska	-0.005	0.112	-0.264	-0.003	-0.049	-0.091	-0.163	0.012	-0.015
U. americanus, Alaska	0.331	-0.212	-0.031	-0.015	0.094	-0.096	-0.016	0.013	0.002
U. americanus, Alaska	-0.084	-0.026	-0.077	-0.298	-0.029	-0.094	-0.016	0.007	-0.011
U. americanus, Alaska	0.081	-0.020	-0.052	0.067	-0.023	-0.074	-0.071	0.011	-0.009
U. americanus, Alaska	0.095	-0.129	0.027	0.243	0.017	-0.044	-0.122	-0.013	-0.012
U. americanus, Alaska	-0.137	-0.142	-0.131	0.013	-0.020	-0.030	-0.141	0.008	-0.014
U. americanus, Alaska	0.328	-0.104	-0.101	-0.206	0.040	-0.120	0.068	0.003	0.001
U. americanus, Alaska	-0.131	0.100	-0.117	-0.067	-0.047	-0.091	-0.152	0.016	-0.015
U. maritimus	-0.412	-0.451	-0.041	-0.084	0.028	0.041	-0.169	-0.011	-0.025

U. maritimus	-0.486	0.006	-0.037	-0.093	0.299	-0.005	0.169	-0.012	0.024
U. maritimus	-0.590	-0.076	-0.274	0.258	0.190	0.115	0.100	-0.078	0.006
U. maritimus	-0.631	-0.013	-0.299	0.241	0.302	0.057	-0.098	-0.040	0.037
U. maritimus	-0.604	0.224	-0.246	0.104	0.270	-0.015	-0.067	0.012	-0.030
U. maritimus	-0.422	0.136	0.087	-0.111	0.225	-0.025	0.292	0.012	-0.051
U. maritimus	-0.609	0.246	-0.292	0.070	0.209	0.000	0.012	0.016	-0.007
U. maritimus	-0.471	0.273	0.049	0.019	0.269	-0.057	0.106	0.005	-0.003
U. maritimus	-0.458	0.364	0.130	0.203	0.261	-0.061	0.052	-0.008	0.001
U. maritimus	-0.501	0.216	-0.061	-0.091	0.258	-0.044	0.128	0.017	-0.034
U. maritimus	-0.445	0.320	0.109	0.086	0.222	-0.048	0.169	-0.002	0.018
U. maritimus	-0.556	0.037	-0.207	-0.024	0.236	0.026	0.136	0.012	0.007
U. maritimus	-0.501	0.323	-0.078	0.151	0.053	0.024	0.299	0.053	-0.007
U. maritimus	-0.563	0.445	-0.079	0.127	0.339	-0.101	-0.166	-0.009	0.065
U. thibetanus	-0.403	0.030	-0.023	0.004	-0.171	-0.005	-0.073	0.020	-0.014
U. thibetanus, Japan	-0.327	0.119	0.142	-0.046	-0.195	-0.036	0.036	0.019	-0.007
U. thibetanus, Japan	-0.395	0.085	-0.003	-0.100	-0.123	-0.047	-0.115	0.009	-0.018
U. thibetanus, Thibet	-0.444	0.039	-0.123	0.066	-0.212	0.021	-0.091	0.017	-0.015
U. thibetanus, Japan	-0.314	0.201	0.086	-0.077	-0.182	0.253	-0.049	0.021	-0.005
U. thibetanus, Thibet	-0.391	0.006	0.002	0.025	-0.179	0.005	-0.047	0.016	-0.012
U. arctos, Greece	-0.200	0.242	0.287	-0.365	-0.156	0.192	0.117	-0.020	-0.009
U. arctos, Greece	-0.279	0.563	0.105	-0.282	-0.275	0.175	0.052	-0.029	0.006
U. arctos, Greece	-0.374	0.653	0.104	-0.125	-0.140	-0.188	-0.221	-0.037	0.096
U. arctos, Greece	-0.202	0.629	0.233	-0.334	-0.238	0.319	0.048	-0.068	0.010
U. arctos, Slovakia, central EU	0.569	0.193	-0.415	-0.043	0.025	0.330	-0.123	-0.058	-0.016
U. arctos, Ukraine, central EU	0.332	0.094	-0.111	-0.060	0.062	0.153	-0.124	0.014	-0.005
U. arctos, Slovakia, central EU	0.470	-0.123	0.048	0.208	0.074	0.215	-0.045	0.008	0.006
U. arctos, central EU	0.569	0.080	0.120	0.234	0.030	0.171	0.007	0.011	0.011
U. arctos, Romania, central EU	0.519	0.155	0.102	0.148	0.008	0.340	-0.008	0.023	0.014
U. arctos (Europe)	0.510	-0.115	0.075	0.191	0.052	0.399	-0.003	0.018	0.016
U. arctos, Bosnia, central EU	0.510	0.171	0.096	0.142	0.038	0.325	-0.060	0.023	0.014
U. arctos, Bulgaria, central EU	0.457	-0.177	-0.140	-0.048	0.061	-0.100	0.056	-0.008	0.003
U. arctos, Slovenia, central EU	0.417	0.004	-0.096	0.083	0.059	0.185	-0.095	0.011	-0.001
U. arctos, Romania, central EU	-0.090	-0.217	-0.112	0.037	-0.188	0.050	0.150	-0.009	0.011
U. arctos, Canada, N. America	0.468	0.136	-0.239	-0.466	0.167	0.066	-0.127	-0.063	-0.025
U. arctos, America	0.106	0.263	0.018	-0.020	-0.032	-0.156	-0.091	0.008	0.005
U. arctos, America	-0.011	0.310	0.121	-0.063	-0.185	-0.111	0.104	0.002	0.003
U. arctos, Middle	0.136	-0.319	0.037	0.125	-0.051	0.011	0.112	-0.003	0.014

Creek, USA									
U. arctos, Alaska, N. America	-0.353	-0.243	0.028	0.027	-0.229	0.085	0.140	-0.010	0.008
U. arctos, Alaska, N. America	0.155	-0.117	0.068	0.083	-0.112	-0.026	0.160	0.010	0.008
U. arctos, Alaska	0.004	-0.237	0.147	-0.098	-0.044	-0.030	0.124	0.010	0.011
U. arctos, Alaska, N. America	0.055	-0.130	-0.176	-0.058	-0.060	-0.039	0.017	0.015	0.000
U. arctos,Kamtchatka, Russia	0.095	-0.196	0.016	0.004	0.124	-0.092	-0.169	0.011	-0.011
U. arctos,Kamtchatka, Russia	0.333	0.034	0.244	-0.016	0.067	-0.160	0.023	0.013	0.001
U. arctos,Kamtchatka, Russia	-0.018	0.027	0.169	0.102	-0.060	-0.069	-0.024	0.005	-0.006
U. arctos,Kamtchatka, Russia	0.607	0.070	-0.320	0.201	-0.138	-0.063	0.176	-0.068	-0.008
U. arctos,Kamtchatka, Russia	0.346	-0.023	-0.004	0.223	-0.092	-0.054	0.115	0.001	0.003
U. arctos,Kamtchatka, Russia	0.272	-0.054	-0.177	0.170	-0.053	-0.052	-0.001	-0.002	-0.005
U. arctos,Kamtchatka, Russia	0.365	0.040	-0.020	-0.172	-0.014	-0.137	0.124	-0.016	-0.005
U. arctos,Kamtchatka, Russia	0.429	-0.027	-0.208	0.091	-0.053	-0.078	0.081	-0.008	-0.002
U. arctos,Kamtchatka, Russia	0.625	-0.027	-0.041	-0.077	0.021	-0.142	0.182	-0.016	0.004
U. arctos,Kamtchatka, Russia	0.432	0.209	-0.034	-0.188	0.021	-0.198	0.047	-0.026	-0.009
U. arctos,Kamtchatka, Russia	0.227	0.259	-0.025	0.021	0.296	0.387	0.313	0.020	-0.032
U. arctos,Kamtchatka, Russia	-0.071	0.026	0.046	0.204	-0.109	-0.031	-0.053	-0.005	-0.009
U. arctos,Kamtchatka, Russia	0.310	0.162	-0.009	0.349	-0.039	-0.102	-0.090	-0.014	0.009
U. arctos,Kamtchatka, Russia	0.138	-0.134	-0.265	0.030	-0.018	-0.046	-0.065	0.007	-0.006
U. arctos,Kamtchatka, Russia	0.003	0.021	0.235	0.078	-0.014	-0.091	-0.048	0.005	-0.005
U. arctos,Kamtchatka, Russia	0.382	-0.135	-0.127	-0.115	0.068	-0.123	0.031	0.075	0.032
U. arctos,Kamtchatka, Russia	0.127	0.112	0.052	-0.001	-0.037	-0.117	-0.018	0.014	-0.004
U. arctos,Kamtchatka, Russia	0.600	-0.086	0.040	-0.024	0.014	-0.122	0.209	-0.001	0.011
U. arctos,Kamtchatka, Russia	-0.100	0.297	-0.117	-0.038	-0.248	-0.065	0.072	-0.010	-0.008
U. arctos,Kamtchatka, Russia	0.730	0.435	-0.084	-0.086	0.016	-0.256	0.058	-0.092	-0.012

U. arctos,Kamtchatka, Russia	-0.265	0.013	0.365	0.242	-0.133	-0.011	-0.021	-0.023	-0.007
U. arctos,Kamtchatka, Russia	-0.288	0.135	0.312	-0.120	0.003	-0.127	-0.155	0.006	-0.006
U. arctos,Kamtchatka, Russia	0.354	0.042	0.077	0.114	0.072	-0.145	-0.076	0.009	-0.001
U. arctos, Lithuania, N. Europe	0.041	0.052	0.260	0.123	-0.183	-0.039	0.194	0.016	0.006
U. arctos, Lithuania, N. Europe	0.125	0.108	0.078	0.019	0.017	-0.134	-0.094	0.013	-0.003
U. arctos, Lithuania, N. Europe	0.205	-0.064	0.240	0.161	-0.050	-0.063	0.100	-0.004	0.001
U. arctos, Lithuania, N. Europe	-0.355	-0.076	0.114	0.113	-0.128	0.013	-0.073	-0.016	-0.017
U. arctos, Lithuania, N. Europe	0.138	-0.101	0.115	0.111	0.050	-0.085	-0.084	-0.003	-0.009
U. arctos, Lithuania, N. Europe	-0.089	0.010	-0.039	0.003	-0.098	-0.049	-0.028	0.014	-0.009
U. arctos, Lithuania, N. Europe	-0.056	-0.016	0.062	-0.006	-0.036	-0.072	-0.057	0.012	-0.010
U. arctos, Lithuania, N. Europe	0.372	0.004	0.109	0.143	0.047	-0.126	-0.019	0.009	0.000
U. arctos, Finland, N. Europe	0.182	0.159	0.201	0.012	-0.017	-0.146	0.006	0.021	0.006

Table 2. Dental microwear PCA score results for extant bear species on slicing area.

Species	PC 1	PC 2	PC 3	PC 4	PC 5	PC 6	PC 7	PC 8	PC 9
A. melanoleuca	-0.148	-0.720	0.525	-0.069	-0.065	0.110	0.130	-0.069	0.001
A. melanoleuca	-0.136	-0.695	0.490	-0.106	-0.124	0.156	0.181	-0.050	-0.010
A. melanoleuca	-0.235	-0.627	0.189	-0.071	-0.152	0.150	0.084	-0.049	-0.008
H. malayanus	-0.020	-0.447	-0.131	-0.210	-0.172	0.109	-0.001	0.031	-0.029
H. malayanus	-0.044	-0.487	-0.180	-0.127	-0.151	0.095	-0.006	0.007	-0.027
H. malayanus	0.264	-0.539	-0.118	-0.087	-0.044	0.004	0.030	0.015	-0.025
H. malayanus	0.165	-0.133	0.018	-0.198	-0.093	-0.011	-0.002	0.054	0.002
H. malayanus	0.235	-0.086	-0.088	0.076	-0.058	-0.061	0.094	0.030	0.004
H. malayanus	0.013	-0.345	-0.092	-0.382	-0.216	0.132	-0.023	0.061	-0.017
H. malayanus	0.004	-0.402	-0.027	-0.308	-0.141	0.081	-0.057	0.043	-0.021
H. malayanus,Borneo	-0.373	-0.010	0.050	0.183	-0.093	-0.016	-0.013	-0.034	0.005
H. malayanus,Thailand	0.091	-0.211	-0.193	0.002	-0.094	-0.011	0.015	0.020	-0.001
H. malayanus,Thailand	0.085	0.070	-0.176	0.104	-0.133	-0.024	0.102	0.034	0.003
H. malayanus, Sumatra	-0.305	0.162	0.324	0.007	-0.046	-0.065	-0.062	0.000	-0.005
M. ursinus	0.258	-0.038	0.069	0.486	0.173	0.061	-0.003	-0.052	-0.005
M. ursinus, Kaulas, India	-0.359	0.129	0.199	0.117	-0.022	-0.088	-0.096	-0.028	-0.012
M. ursinus, Japan	0.536	-0.047	0.151	-0.073	0.070	-0.171	0.045	0.038	0.009
M. ursinus, Kaulas, India	-0.072	0.008	0.153	-0.074	0.086	-0.175	-0.236	0.005	0.010

T. ornatus, Venezouela	-0.453	-0.009	-0.169	0.077	-0.076	-0.044	-0.207	-0.013	0.010
U. americanus, Alaska	0.080	-0.520	-0.168	-0.059	0.022	-0.059	-0.147	-0.014	0.016
U. americanus, Alaska	-0.034	0.237	0.123	0.073	-0.095	-0.059	0.076	0.034	-0.005
U. americanus, Alaska	0.294	-0.137	-0.147	0.181	0.008	-0.117	0.073	0.001	0.004
U. americanus, Alaska	0.362	-0.490	-0.276	-0.074	0.048	-0.100	-0.107	0.004	-0.014
U. americanus, Alaska	0.245	-0.294	-0.057	0.064	-0.014	-0.062	0.062	0.009	0.000
U. americanus, Alaska	-0.101	-0.256	-0.216	0.089	-0.110	0.016	0.000	-0.022	0.000
U. americanus, Alaska	0.131	-0.157	-0.002	-0.138	-0.031	-0.062	-0.070	0.039	0.008
U. americanus, Alaska	0.344	0.172	-0.026	-0.097	-0.037	-0.120	0.011	0.053	0.007
U. americanus, Alaska	-0.102	-0.121	-0.218	-0.097	-0.123	0.003	-0.102	0.029	0.005
U. maritimus	-0.417	-0.478	0.043	-0.281	0.349	0.072	0.031	-0.045	-0.001
U. maritimus	0.291	-0.268	-0.358	-0.468	0.358	-0.013	0.061	0.030	-0.061
U. maritimus	-0.574	0.034	-0.441	-0.009	0.196	0.088	0.108	-0.026	-0.004
U. maritimus	-0.558	0.154	-0.253	-0.018	0.285	0.002	0.047	-0.016	-0.001
U. maritimus	-0.472	0.220	-0.133	-0.199	0.181	0.087	0.152	0.030	0.019
U. maritimus	-0.484	0.100	-0.224	0.326	-0.083	-0.057	-0.096	-0.062	-0.012
U. maritimus	-0.506	0.412	-0.176	-0.039	0.170	0.060	0.210	0.028	0.032
U. maritimus	-0.456	0.033	0.015	-0.184	0.302	0.021	0.071	-0.006	0.037
U. maritimus	0.166	-0.184	0.356	0.095	0.159	-0.201	-0.049	-0.011	0.010
U. maritimus	-0.498	0.475	-0.090	-0.364	0.266	-0.019	-0.069	0.012	-0.015
U. maritimus	-0.527	0.238	-0.003	-0.033	0.404	-0.094	-0.018	-0.022	-0.046
U. maritimus	-0.409	0.229	0.151	-0.148	0.262	0.035	0.200	0.003	0.007
U. maritimus	-0.485	0.177	-0.417	0.091	-0.242	0.054	-0.092	0.027	0.005
U. maritimus	-0.454	0.027	-0.073	-0.164	0.222	0.086	0.160	0.003	0.040
U. thibetanus	0.079	-0.010	-0.219	0.011	-0.125	-0.028	0.012	0.020	0.089
U. thibetanus, Japan	-0.432	0.102	-0.150	0.116	-0.114	-0.026	-0.131	-0.061	0.003
U. thibetanus, Japan	-0.336	-0.122	0.109	-0.189	-0.074	-0.009	-0.205	0.013	0.017
U. thibetanus, Thibet	-0.304	-0.179	0.150	-0.142	-0.106	0.031	-0.102	-0.006	0.012
U. arctos, Greece	-0.369	0.404	-0.086	0.122	-0.297	0.085	0.146	0.053	-0.009
U. arctos, Greece	-0.415	0.430	-0.128	0.040	-0.209	0.004	-0.055	0.029	-0.016
U. arctos, Greece	-0.256	0.674	0.152	-0.116	-0.156	0.258	-0.156	-0.001	-0.025
U. arctos, Greece	-0.400	0.333	-0.046	0.145	-0.178	-0.003	0.009	0.026	-0.017
U. arctos, Ukraine, central EU	0.324	-0.329	-0.444	0.252	-0.051	-0.052	0.117	-0.050	-0.012
U. arctos, Slovakia, central EU	0.631	-0.100	-0.053	0.291	0.256	0.165	-0.157	-0.003	0.015
U. arctos, central EU	-0.021	0.335	0.395	0.128	0.115	-0.175	-0.083	0.004	-0.074
U. arctos, Romania, central EU	0.366	0.082	0.138	0.224	0.171	0.364	-0.175	0.025	0.016
U. arctos (Europe)	0.250	-0.115	0.100	0.071	0.067	-0.153	-0.001	0.008	0.009

U. arctos, Bosnia, central EU	0.587	-0.256	-0.060	0.217	0.256	0.192	-0.206	-0.003	0.016
U. arctos, Bulgaria, central EU	0.581	0.132	0.010	0.280	0.093	0.275	0.036	0.040	0.008
U. arctos, Slovenia, central EU	0.487	-0.017	-0.233	0.394	-0.018	-0.124	0.270	-0.033	-0.005
U. arctos, Canada, N. America	0.241	-0.182	-0.076	-0.082	-0.023	-0.074	-0.028	0.027	0.004
U. arctos, America	-0.244	0.091	0.378	0.175	-0.147	0.036	0.216	-0.023	-0.002
U. arctos, Canada, N. America	-0.016	0.179	0.218	-0.005	-0.038	-0.093	0.001	0.026	-0.001
U. arctos,Kamtchatka, Russia	-0.043	0.008	0.111	0.110	-0.041	-0.070	0.035	0.005	0.006
U. arctos,Kamtchatka, Russia	-0.267	0.112	0.254	-0.099	-0.166	0.041	0.028	0.010	0.010
U. arctos,Kamtchatka, Russia	0.453	0.074	0.183	-0.026	0.088	-0.203	0.013	0.042	0.005
U. arctos,Kamtchatka, Russia	0.222	0.091	0.052	0.178	0.041	-0.167	0.051	0.020	-0.005
U. arctos,Kamtchatka, Russia	0.323	-0.085	0.189	-0.043	-0.032	-0.066	0.127	0.050	0.007
U. arctos,Kamtchatka, Russia	0.454	0.379	-0.142	0.060	-0.031	0.151	-0.004	0.041	0.003
U. arctos,Kamtchatka, Russia	0.249	-0.230	0.265	-0.017	0.109	0.163	-0.123	0.023	0.016
U. arctos,Kamtchatka, Russia	0.262	0.284	-0.217	0.004	-0.029	-0.157	-0.052	0.039	-0.002
U. arctos,Kamtchatka, Russia	0.774	0.256	0.176	-0.343	-0.050	-0.114	0.127	-0.004	0.005
U. arctos,Kamtchatka, Russia	0.724	0.756	-0.167	-0.420	-0.239	-0.048	0.141	-0.097	-0.005
U. arctos,Kamtchatka, Russia	-0.334	0.197	0.153	-0.147	-0.107	-0.030	-0.147	0.024	0.008
U. arctos,Kamtchatka, Russia	0.392	0.226	-0.065	0.112	-0.016	0.169	0.021	0.049	0.007
U. arctos,Kamtchatka, Russia	-0.097	-0.048	0.013	0.248	0.010	-0.110	-0.007	-0.038	0.001
U. arctos,Kamtchatka, Russia	-0.337	-0.030	0.160	0.165	-0.078	-0.018	0.012	-0.045	0.005
U. arctos,Kamtchatka, Russia	-0.342	-0.073	0.097	0.238	-0.118	0.020	0.085	-0.054	0.005
U. arctos,Kamtchatka, Russia	0.058	0.175	0.032	0.237	0.074	-0.204	-0.040	-0.012	-0.029
U. arctos,Kamtchatka, Russia	-0.156	-0.336	-0.278	0.257	-0.014	-0.058	-0.077	-0.106	0.006
U. arctos,Kamtchatka, Russia	0.022	0.260	0.340	-0.165	-0.008	-0.126	-0.088	0.003	0.044
U. arctos,Kamtchatka, Russia	1.029	0.768	-0.078	-0.559	-0.078	0.136	-0.089	-0.226	0.006
U.	0.392	0.517	0.225	0.374	0.083	0.378	0.040	0.047	-0.040

arctos,Kamtchatka, Russia									
U. arctos,Kamtchatka, Russia	0.127	0.076	0.137	0.011	0.035	-0.150	-0.048	0.016	0.004

Appendix IC. Dental Microwear Analysis

Table 1. Microwear features raw results for extinct bear species from Britain and Greece on the grinding area. Abbreviations Museums: NHMUK: the Natural History Museum in London, UK; TMD: Torquay Museum in Devon, UK; TSHC: the Somerset Heritage Centre in Taunton, Somerset, UK; AUThG: the Aristotle University of Thessaloniki (Geology Department), GR and LAMG: Loutra Aridea Museum, GR. Abbreviations Sites: WS: Westbury-sub-Mendip (MIS 13), UK; KC13: Kents Cavern (MIS 13), UK; GT: Grays Thurrock (MIS 9), UK; TC: Tornewton Cave (MIS 5e), UK; BBC: Banwell Bone Cave (MIS 5a), UK; KC3: Kents Cavern (MIS 3), UK; SH: Sandford Hill (MIS 3), UK; CC: Cow Cave (Holocene?), UK and LAC: Loutra Arideas Cave (Late Pleistocene), GR. Abbreviations Features: S: Scratches; P: Pits; Fs: Fine scratches; Cs: Coarse scratches; SWS: Scratches width score; Lp: Large pits; Sp: Small pits; G: gouges and Pp: puncture pits.

Museum	Species	Number	S	P	Fs	Cs	SWS	Lp	Sp	G	Pp
NHMUK	WS	47439	18	21	14	4	1	4	16	1	0
NHMUK	WS	92578	9	13	5	4	1	6	7	0	0
NHMUK	WS	92580	15	12	11	4	1	3	7	2	0
NHMUK	WS	33844	22	24	19	3	1	2	17	5	0
NHMUK	WS	47351	20	17	15	5	1	6	9	2	0
NHMUK	WS	47449	24	16	18	6	1	7	7	2	0
NHMUK	WS	92448	11	12	6	5	1	3	7	2	0
NHMUK	WS	47438	22	18	16	6	1	12	6	0	0
NHMUK	WS	34941	20	21	14	6	1	7	13	1	0
NHMUK	WS	92445	17	16	10	7	1	5	10	1	0
NHMUK	WS	33848	11	19	4	7	1	7	10	2	0
NHMUK	WS	92579	22	20	13	9	1	5	13	2	0
NHMUK	WS	292	18	28	15	3	1	9	18	1	0
NHMUK	WS	293	16	31	13	3	1	6	21	1	3
NHMUK	WS	294	19	27	16	3	1	4	22	1	0
TMD	KC13	P14116	24	38	15	9	1	11	25	1	2
TMD	KC13	P14352	29	28	20	9	1	7	18	1	2
TMD	KC13	P8665	25	37	18	7	1	12	19	4	3
TMD	KC13	P16701	25	29	19	6	1	6	19	2	2
NHMUK	KC13	M92441	21	34	16	5	1	4	30	0	0
NHMUK	KC13	M1030	26	30	22	4	1	9	19	2	1
NHMUK	GT	20260	24	29	20	4	1	5	20	0	4
NHMUK	GT	95990	23	32	18	5	1	8	19	2	3

NHMUK	GT	95989	20	29	16	4	1	4	21	2	2
NHMUK	GT	OR22030	23	32	18	5	1	6	23	1	2
NHMUK	GT	22029	20	37	15	5	1	8	26	1	2
NHMUK	GT	22029	22	29	18	4	1	4	22	1	2
NHMUK	GT	96013	19	32	15	4	1	6	21	3	2
NHMUK	GT	96012	18	35	16	2	1	8	23	2	2
NHMUK	GT	96011	19	29	16	3	1	5	20	2	2
NHMUK	GT	95998	21	37	19	2	1	5	28	1	3
NHMUK	GT	96010	21	29	18	3	1	6	19	2	2
NHMUK	TC	M41097	14	32	11	3	1	7	22	1	2
NHMUK	TC	M41397	12	35	10	2	1	8	22	2	3
NHMUK	TC	M92438	16	38	12	4	1	4	31	1	2
NHMUK	TC	M41095	12	30	10	2	1	5	23	1	1
NHMUK	TC	M41093	15	32	12	3	1	4	24	1	3
NHMUK	TC	M92430	16	34	12	4	1	9	23	1	1
NHMUK	TC	M92420	16	37	11	5	1	9	26	0	2
NHMUK	TC	M92427	18	30	14	4	1	4	22	1	3
NHMUK	TC	M92419	16	35	14	2	1	6	24	2	3
NHMUK	TC	M92436	10	33	7	3	1	7	21	3	2
NHMUK	TC	M92433	18	30	14	4	1	9	16	2	3
NHMUK	TC	M41088	18	37	15	3	1	7	25	3	2
NHMUK	TC	M92440	19	37	16	3	1	8	25	1	3
NHMUK	TC	M92416	16	37	13	3	1	8	26	1	2
NHMUK	TC	M92426	17	29	12	5	1	6	20	1	2
NHMUK	TC	M92425	17	36	14	3	1	4	29	2	1
NHMUK	TC	M41103	16	35	14	2	1	6	25	2	2
NHMUK	TC	M41102	15	39	14	1	1	6	33	0	0
NHMUK	TC	M41396	15	33	10	5	1	8	18	4	3
NHMUK	TC	M41395	16	40	13	3	1	13	19	5	3
NHMUK	TC	M41389	17	35	14	3	1	5	24	3	3
TSHC	BBC	40/1995/182	17	28	13	4	2	7.5	19	1	0
TSHC	BBC	40/1995/183	16	25	14	3	1.5	6.5	17	2	0
NHMUK	BBC	M96058	19	24	17	2	1	6	17	1	0
NHMUK	BBC	M96059	12	27	10	2	1	4	19	4	0
TMD	KC3	P14319	25	41	15	10	1	17	21	0	3
TMD	KC3	P15003	31	42	21	10	1	13	24	3	2
TMD	KC3	P14323	23	30	16	7	1	5	19	2	4
TMD	KC3	P14878	23	38	17	6	1	10	23	2	3
TMD	KC3	P8646	23	32	19	4	1	11	18	1	2
TMD	KC3	P14315	29	40	24	5	1	7	31	0	2
TMD	KC3	P14322	22	41	17	5	1	8	26	3	4
TMD	KC3	P8664	27	35	22	5	1	11	20	2	2
TMD	KC3	P8625	22	34	17	5	1	12	15	3	4
NHMUK	KC3	M1121	20	39	16	4	1	8	26	3	2
NHMUK	KC3	M1011	22	38	19	3	1	12	22	2	2

NHMUK	KC3	M590	22	35	18	4	1	10	20	3	2
TSHC	SH	44/1995/304a	19	33	15	4	1	11	18	4	1
TSHC	SH	44/1995/304b	18	27	13	5	1	11	16	0	0
TSHC	SH	45/1995/683	22	36	21	3	1	14	17	3	2
TSHC	SH	45/1995/681	18	30	13	5	1	9	18	3	0
TMD	CC	P32013.2	23	47	13	10	1	11	27	3	6
TMD	CC	P31806	18	38	13	5	1	8	23	3	4
TMD	CC	P31761	26	46	18	8	1	10	30	3	3
TMD	CC	P32010	21	33	15	6	1	7	22	1	3
TMD	CC	P32012	20	39	12	8	1	6	28	1	4
TMD	CC	P31807	25	45	20	5	1	8	29	3	5
TMD	CC	P31804	19	48	14	5	1	9	31	3	5
TMD	CC	P32013.1	25	52	20	5	1	9	34	2	7
AUThG	LAC	5145d	13	31	10	3	1	5	17	1	8
AUThG	LAC	14530	12	29	9	3	1	4	19	0	6
AUThG	LAC	5063	14	29	9	5	1	5	15	2	7
AUThG	LAC	13011	13	34	11	2	1	6	18	3	7
LAMG	LAC	8517	16	32	10	6	1	4	23	0	5
AUThG	LAC	6735	15	27	10	5	1	3	18	0	6
LAMG	LAC	8798	16	28	12	4	1	5	14	1	8
LAMG	LAC	11830	13	30	10	3	1	6	19	2	3
LAMG	LAC	11339	11	27	9	2	1	4	17	2	4
LAMG	LAC	12492	10	28	8	2	1	4	18	1	5

Appendix IIA. Geochemical Analysis

Limit of Blank (LOB) values calculated for all specimens.

	M40750	M92414	M92417	M41097	M41397	M41389	M40646	M40688	M92410	M38994	M92408	M41530 (m3)	M41530 (m2)	M41530 (m1)	M92406	M92409
Li	0.352	0.381	0.594	1.141	0.791	1.126	0.700	0.981	1.271	0.168	0.974	1.284	0.789	1.086	1.272	0.593
Mg	0.705	0.734	1.220	7.392	5.573	6.227	5.238	6.610	8.509	5.699	4.669	6.065	5.973	5.146	9.725	4.546
Al	360.017												782.975			
Mn					27.695				46.610				0.561			26.513
Zn	1.046	1.261	2.229	0.675	0.449	0.601	0.596	0.763	0.725	0.617	0.704	0.698	0.475	0.665	1.023	0.443
Rb	0.093	0.099	0.150	0.091	0.080	0.091	0.071	0.085	0.135	0.844	0.086	0.083	0.086	0.086	0.154	0.096
Sr	0.009	0.009	0.018	0.022	0.013	0.015	0.010	0.018	0.022	0.019	0.026	0.023	0.013	0.015	0.047	0.011
Y	0.017	0.018	0.033	0.006	0.005	0.007	0.005	0.004	0.009	0.007	0.004	0.007	0.005	0.006	0.010	0.005
Ba	0.005	0.006	0.007	0.031	0.012	0.014	0.010	0.038	0.015	0.015	0.010	0.036	0.009	0.021	0.013	0.005
Ce	0.003	0.003	0.004	0.003	0.004	0.004	0.003	0.004	0.005	0.004	0.003	0.004	0.003	0.004	0.005	0.003
Nd	0.012	0.013	0.018	0.015	0.012	0.017	0.012	0.016	0.028	0.017	0.016	0.014	0.016	0.015	0.025	0.012
Pb	0.037	0.042	0.071	0.053	0.049	0.054	0.050	0.059	0.075	0.058	0.062	0.065	0.046	0.058	0.095	0.035
U	0.003	0.003	0.005	0.006	0.003	0.004	0.003	0.005	0.006	0.004	0.004	0.003	0.003	0.004	0.006	0.003